Sterol Biomarker Discovery in Neurodegenerative Diseases

Student:

Manuela Pacciarini

Supervisor:

Professor Yuqin Wang

Professor William J. Griffiths

Professor Michael Gravenor

Swansea University
Prifysgol Abertawe

Submitted to Swansea University in fulfilment of the requirements for the Degree of Doctor of Philosophy

Swansea University

2023

Summary

Neurodegenerative diseases (ND) are age-related heterogeneous disorders leading to uncontrollable neuroneal cell death. Nowadays, there is no cure or specific diagnostic biomarkers for ND. However, much evidence links disrupted brain cholesterol metabolism with the development of Alzheimer's (AD) and Parkinson's (PD) diseases, the two most common ND. Cholesterol is the most abundant sterol lipid in the human brain, the main component of myelin and a modulator of many neuroneal pivotal pathways. Several attempts have been made to understand the role and the entity of the sterol variations over PD and AD, highlighting modifications in the plasma and CSF content of the main brain cholesterol metabolite (24S)-hydroxycholesterol, (24S)-HC, and cholesterol itself but no conclusive results are yet reported. This thesis has been designed to study the plasma and CSF cholesterol and cholesterol metabolite variations in AD and PD, evaluating the ability of the discriminating sterols to be putative biomarkers. Our findings report a complete sterolome profile for AD CSF and PD plasma/CSF, identifying up to 21 different sterols. The results show an increase in the plasma levels of (24S)-HC and of 7α-hydroxy-3-ketone-cholestenoic acids in PD patients with respect to healthy controls. A decrease in plasma cholesterol is also observed in the PD group. However, (24S)-HC is the only sterol to also discriminate between males and females affected by PD and to demonstrate a diagnostic ability to predict PD. CSF and plasma sterols have also been screened in progressive PD, resulting in no significant variation, making them unsuitable prognostic biomarkers. In AD CSF, a positive correlation between the level of extracerebral 26-hydroxycholesterol, (24S)-HC and disease severity is reported. In conclusion, the results reported in this thesis support

the use of cholesterol metabolites as diagnostic biomarkers for ND. However, validation studies on different cohorts of patients are needed.

Declaration

This work has not previously been accepted in substance for any degree and is not being concurrently submitted in candidature for any degree.

Signed 

Date…03/08/2023……..

Statement 1

This thesis is the result of my own investigations, except where otherwise stated. Other sources are acknowledged by footnotes giving explicit references. A bibliography is appended.

Signed… 

Date…03/08/2023……..

Statement 2

I hereby give consent for my thesis, if accepted, to be available for photocopying and for inter-library loan, and for the title and summary to be made available to outside organisations.

Signed… 

Date…03/08/2023……..

Statement 3

The University's ethical procedures have been followed and, where appropriate, that ethical approval has been granted.

Signed.. 

Date..... 03/08/2023.....

Table of Contents

Acknowledgements

"Questo cuore sparpagliato per il mondo se ne va. Questo cuore disperato e delicato".

What a journey.

The last four years have been the most adventurous, creative, explorative, fearful, inspirational, laborious, and meaningful of my life. Many times, the doctorate is considered just as an obligate step of the scientist career path but for me it has been much more. The PhD, my PhD, has represented my rebirth, my evolution towards a new me. During the PhD years I acquired much more self-awareness, which did help to build what I do hope is a better human being, but also a decent scientist. Oh, and be much more PATIENT.

HOWEVER, this is not a solo story. This Doctor of Philosophy looks much more like a big and harmonic orchestra, where every single participant contributes to the final, marvellous, harmony we called music. Now I will take the occasion to express my gratitude to all the musicians which have contributed to the Manuela's PhD opera.

First thing first, I would like to acknowledge my supervisors Professor Yuqin Wang and Professor William J. Griffiths for being a guide through all over these years. They not only showed me what a life dedicated to the academic research means, with all the pros and cons, but they also taught me that the whatsoever is your research interest/aim, the harmony of your research group should be the priority. Experiments can fail or simply reject your hypothesis. There will be always time to repeat them or change ideas if you have motivated and enthusiastic scientist on your side. Labs are made of people, brilliant people, we must take care of them.

As we have introduced the lab environment, I will now spend one word or two on my colleagues, or better FRIENDS.

I will be always grateful to Doctor Eylan Yutuc, the senior post doc of our group. Eylan, if today I can run 3 orbitraps in a row is only because of you! Everything that I know about mass spectrometry of sterols, and RP HPLCs I have learnt from you. So, thank you for your time spent in deliriant discussion on contaminants, run failures, internal standards management (you know) and LC methods. But most of all, thank you showing me other point of view, thank you for stopping me to be "too passionate" about my experiments, thank you for teaching me how to best cooperate with people, thank you for always having a good word in my worst moments. Thank you for letting me be a better human. You are one of the best people I have ever met, you deserve the world. Have trust in you (especially as an analytical chemist). I DO.

Thanks to my PhD mate Doctor Lauren Griffiths. Lauren, you have shared this journey with me and, honestly, I couldn't ask for anything better than you. Thank you for our brainstorming on mass spec and MALDI (why you were trusting me on this I still don't know as YOU are the imaging expert, certainly not me) issues, thank you for calm me down and getting me reflect on the best way to address the issues. Thank you for trusting me so much to let me give you an hand in your experiment, I have learnt a lot because of that. Thank you being the shoulder I need in my worst moments, you are great (human + scientist), please always remind it to yourself.

Marti do you really think I wouldn't have spent a paragraph or two on you? AHAHAHAHAH NO. I would like to acknowledge, thank, be grateful, adore, prostrate to Doctor Martina Sassi(y). Marti for me represent the personification of a real research scientist. Passionate,

dedicated to her job, resilient, crazy ("hi Manu, today I am running 287493784294 ELISA at the same time 😊), patient, thoughtful, knowledgeable, always, and when I say always, I mean ALWAYS, there to give you a hand, even when she has no idea of what you are doing. Respectful, leader, perfect lab manager, cooperative, marvellous writing editor, holidays-guided spirt, obsessed life organiser. But she also has downsides. I have never met a person so similar to me but much much much better. I don't even know where to start with the acknowledgment thing so I will only tell you this. Marti, thank you for always telling me the truth, your opinion and point of views but without dragging me down. Thank you for letting me reflect more on things, to give a hand in understanding my intricated worries. Thank you for being so supportive but most of all for don't let me to destroy myself. You have been and still are the only human being to have changed my mind and letting me embrace my weaknesses. You made me the person I am today, which I do hope is a bit better than yesterday and a less than tomorrow. I will be always here for you, that's a promise.

Thanks to Robbi, Doctor Roberto Angelini. Robbi is the perfect example of the crazy/autistic/genius scientist stereotype. He is that kind of person you really want by your side when you are hopeless about your experiments (or about life expectations, I leave the choice to you). He can start an intricated monologue about your problems which will end in 2-3 days but at the end will come up with a brilliant idea which will save your life (and your experiments). Thank you, Robbi, for always pushing me to be a better scientist, for our chemistry-oriented conversation and for being a good friend (when you remember :P). Obviously, you won't be as you are without Claudia, also known as Robbi's wife. Cla, thank you for keeping Robbi

with the feet anchored in this world and not on a parallel universe of his. But most of all thank you for being a very good friend to us all. Thank you for showing me what supporting a person means.

Many many thanks to Amanda, Doctor Amanda Hornsby. Amanda, you showed me what perseverance is. You taught me that feeling low is okay, life is difficult, and we can't deny it. However, you also taught me that I can changed it. I am the maker of rules (dealing with foooools I can cheat you blind, ops sorry 80's baby). Thank you for letting me learn one of the best life's hacks, and thank you for being how you are, fantastic friend, great cooker, brilliant scientist. Can't wait to try your new kitchen!

Thank to our little Beth, soon to be doctor Bethan Davies. Beth, you remind me of a younger version of myself, but much more conscious and wiser (but not less chatty, actually, we think about opening a podcast, it might be an unbeatable success ahahahah). Thank you for showing me that one of the most powerful resources we have are resilience and willingness. Believe in yourself, you have all the instruments to be a very good scientist, better than me for sure.

Thanks to Jeff, Professor Jeffrey Davies, and Owain, doctor Owain Howell. You two resembles the two best example to aspire in the academic career path. I admire you for have being tremendous scientists but also smart, accountable, dedicated, supportive, focused leaders. If at some point I will change my mind and decide to be a PI, I will take your example!

Obviously, I would like to thank all the people who passed by the lab, form Post docs to PhDs to undergrads and masters. All of them have left something to me and have contributed to my personal growing as a mentor, scientist, and person. Thak you guys!

I would like to thank all the new friends I made here, which have been an invaluable source of laugh and life. Thank you taking care of me, especially when no one else would have done it (yes, I can be terrible sometime, I am working on it). So, thank you Manu1, Nav, Carla, Simo, Kristen, Ben, Justine, Alice, Benoit, Hugo & Noemi. I love you all, you will never be forgotten (and you are all invited to my bakery/pizzeria when I'll decide to open one).

Finally, I would like to spend two words on my beloved ones. For this I will turn Italian to let anyone understand it.

Grazie mamma Angelica e papà Simone. Se oggi posso scrivere queste 500 pagine di delirio è solo grazie a Voi. Vi ringrazio per avermi permesso di studiare ciò che mi rendeva più felice, anche se non era esattamente ciò che avreste voluto per me. Penso di avervi dimostrato che, se sono veramente appassionata di qualcosa, non ci sarà nulla al mondo ad impedirmi di provare ad ottenerla. Io sono una guerriera, io lotto per ciò che ritengo giusto. Ma ho imparato anche ad accettare le sconfitte. Non sempre si può ottenere ciò che si vuole, magari è un segno per dirci di cambiare strada e non dobbiamo ignorarlo. Magari tra dieci anni faro un altro lavoro e sarò un'altra persona chi lo sa. Certamente continuerò a lottare sempre per una cosa: aiutare gli altri. Grazie per tutto quello che avete fatto per me, ve ne sarò sempre grata. Vi voglio tanto bene.

Grazie a mia sorella Cristina e mio fratello Manuel . Loro sono stati i miei primi amici e saranno sempre la mia ancora di salvezza quando vedrò tutto buio. Sono molto orgogliosa di voi e delle vostre carriere, siete delle persone straordinarie ed estremamente creative, vi ammiro molto. Cercate sempre di non farvi sopraffare dai vostri impegni, ricordatevi che di vita ne esiste una sola e che la vostra priorità deve essere Voi e solo Voi. Non io, ne mamma e papà, e

nemmeno amici o fidanzati. L'unica persona con cui dovrete convivere per tutta la vita siete voi e se non vi sopportate la devo dura ahahhaah. Grazie per essermi stati accanto, mi mancate davvero molto. Vi voglio davvero un mondo di bene anche se non ve lo dico quasi mai. Questa tesi è anche per Voi.

Infine, vorrei ringraziare chi mi sopporta da 12 anni suonati, il mio fidanzato Luca. Luca, non ho mai incontrato una persona come te, ed io di persone ne ho viste veramente tante ed in tutto il mondo! Ti prego, non perdere mai la gentilezza che ti contraddistingue, la tua genuinità, la tua ingenuità, la tua forza d'animo, la tua solarità'. Tu riesci ad illuminare una stanza con la tua simpatia e permetti alle persone di far entrare un raggio di luce nelle loro corazze di odio e cattiveria. Io non ti posso garantire come andrà il futuro ma quello che posso prometterti e che cercherò di afre sempre di tutto per rendere la tua permanenza su questa terra un po' più accettabile. Ti meriti il mondo e non lo sai. Ti Amo.

Here we are, back to the mainland English language. As you could have appreciated, many people guided me through my PhD journey and have contributed to the formation of this thesis. Clearly, I must thank myself for being through all the experiments hereby reported. However, it is always good to remember that you are the result of your choices and the people that surrounds you.

Have a great time in reading this masterpiece (I had fun in making it true!)

"Tu lo sai che non è la fine, si che lo sai. Che viene maggio e sciolgo le brine, si che lo sai. Resti d'inverno, persi nel vento, io non mi stanco, no no. E vengo a cercarti in un sogno amaranto".

List of Figures

List of Tables

Abbreviations

ABC- adenosine triphosphate (ATP) -binding cassette
ACAT- acyl-coenzyme A-cholesterol acyltransferase
Acetyl-CoA- acetyl-Coenzyme A
ACN- acetonitrile
AD- Alzheimer's disease
ALS- amyotrophic lateral sclerosis AP- atmospheric pressure
APO- apolipoprotein
APO-A1-apolipoprotein A1
APOE-apolipoprotein E
APP- amyloid precursor protein Aß- amyloid beta
Aß- amyloid ß
BA- bile acid
BBB- blood-brain barrier
CA- cholestenoic acid
CE- cholesteryl esters
CHO- cholesterol oxidase
CI- chemical ionisation
CID- collision induced dissociation
CNS- central nervous system
CYP- cytochrome P450
DA- dopamine
EADSA- enzyme assisted derivatisation for sterol analysis
EBI2- Epstein-Barr virus induced receptor 2
EC- epoxycholesterol
ER- endoplasmic reticulum
ESI- electrospray ionisation
FA- fatty acids
FAS-FA synthase
FT-MS- Fourier transform MS
FWHM- full width half maximum
GBA- glucocerebrosidase
GC- gas chromatography
GP- Girard P hydrazine
GPR183- G protein coupled receptor 183
HC- hydroxycholesterol
HDL-high density lipoprotein
HLB-hydrophilic lipophilic balance
HMG-CoA-R- 3-Hidroxymethylglutayl-CoA reductase
HPLC- high-performance liquid chromatography

HSD-hydroxysteroid dehydrogenase
ID- isotope dilution
INSIG- Insulin-induced gene 1 protein
iPSCs- induced pluripotent stem cells
iSTDs- internal standard
IT- ion trap
LAS-lysosomal autophagy system
LC- liquid chromatography
LCAT- lecithin-cholesterol acyltransferase
LDL r - low density lipoprotein receptor
LDL-low density lipoprotein
LIT- linear ion trap
LLE-liquid-liquid extraction
LOD- limit of detection
LOQ-
LRRK2-Leucine-rich repeat kinase 2
LXR- liver X receptor
m/z- mass-to-charge ration
MAPK- mitogen-activated protein kinase
MCI- mild cognitive impairment
MRI- magnetic resonance imaging
MRM- multiple reaction monitoring
MS- mass spectrometry
MS^n- tandem mass spectrometry
MUS- multiple sclerosis
NADPH- nicotinamide adenine dinucleotide phosphate
ND- neurodegenerative diseases
NES- neuroepithelial stem cells
NFT- neurofibrillary tangles
NMDA- N-methyl-D-aspartate
NP- normal phase
NPC-1- Niemann-Pick-C1
NPC-2-Niemann-Pick C 2
p- τ- phosphorylated τ
PARK2- parkin gene
PD- Parkinson's disease
PPAR-γ-Peroxisome proliferator-activated receptor gamma
RCT- reverse cholesterol transport
RF- radio frequency
RIC- reconstructed ion chromatogram
ROR- retinoic acid receptor (RAR)-related orphan receptor
ROS- reactive oxygen species

RP- Reversed Phase
RXR- retinoid X receptor
SCI- subjective cognitive impairment
SERM- selective estrogen receptor modulator
SM- squalene monooxygenase
SMO- smoothened protein
SNCA- α synuclein gene
SPE- solid phase extraction
SRE- sterol regulatory element
SREBP- sterol regulatory binding element
SRM- selected reaction monitoring
ST- sterol lipids
TLC- thin layer chromatography
TMS- trimethylsilyl
TOF- time of flight
UHPLC- ultra high-performance liquid chromatography
UPS-Ubiquitin-proteasome system
α-syn- α synuclein
τ - protein tau
(24S)-HC- (24S)-hydroxy cholesterol

Chapter 1 – Introduction

1.1 Sterol lipids

The term sterols refer to a broad class of amphipathic lipid molecules originated from the carbocation condensation of the isoprene units dimethylallyl pyrophosphate and isopentenyl pyrophosphate. The sterols' structure is characterised by a 4 fused ring assembly called cyclopentanoperhydrophenanthrene, which is made of three cyclohexane rings, A, B and C, and a cyclopentane one, the D ring. This arrangement confers to the lipid a quasi-rigid conformation, see figure 1.1. Bound to carbon 17, C17, is a hydrocarbon side chain whose length varies depending on the sterol subclass. The amphipathic nature is given through the presence of an oxygenated function, usually represented by a hydroxyl group at carbon 3, C3.

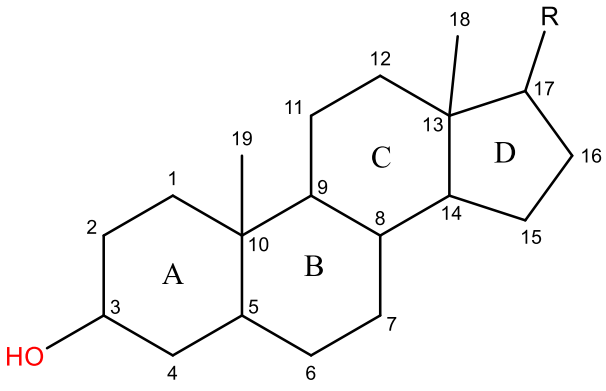

Chemical Formula: $C_{19}H_{31}OR$

Figure 1.1 General sterol structure.

Sterols are fundamental structural components of vertebrate, plant, and bacterial membranes, critical for maintaining adequate membrane fluidity and in the formation of organised pool of membrane lipids called lipid rafts (McNamara, 2013; Mouritsen & Zuckermann, 2004; Sathitnaitham *et al.*, 2021; Schade *et al.*, 2020a; Sezgin *et al.*, 2017; Simons & Ehehalt, 2002; Valitova *et al.*, 2016; Yeagle, 1991). This ordered membrane states are believed to take part into pivotal biological process such as cell growth and cell signalling (Sezgin *et al.*, 2017; Simons & Ehehalt, 2002). Moreover, sterol lipids have several biological functions. For instance, in plants cholesterol can regulate the stress response, (Valitova *et al.*, 2016). In eukaryotic cells, especially in mammals sterol lipids represent the scaffold for steroid hormone synthesis (Holst *et al.*, 2004), regulate dietary fats absorption (Staels & Fonseca, 2009), and act as signalling molecules in many different physiological and pathological pathways such as aging, inflammation, and immune response (Mutemberezi *et al.*, 2016a). The contribution of sterol molecules to the maintenance of a healthy and functional environment for cellular growth and survival has pushed researchers into a deeper study of this class of lipids and their contribution to human health (W. J. Griffiths & Wang, 2019a).

In humans, cholesterol is the most represented sterol and along with its precursors and metabolites constitutes the third most abundant lipid class (Schade *et al.*, 2020a). The hydrophobicity, the relative non-volatile nature and the huge chemical diversity of cholesterol precursors and metabolites introduces many challenges in their precise identification. However, recent developments in analytical techniques have helped in deciphering their chemical structure as

well as in their quantification (W. J. Griffiths & Wang, 2019a). In this thesis the focus will be on cholesterol, its precursors and a specific subclass of sterol lipids, the 27-carbon oxygenated cholesterol metabolites called oxysterols.

1.1.1 Cholesterol

Cholesterol, cholest-5-en-3ß-ol, is the most abundant sterol lipid found in eukaryotic cells with a concentration of 10-20 fmol per cell. (Infante & Radhakrishnan, 2017a). Its chemical structure was first identified in 1953 by Woodward and Bloch (Woodward R. B. & Konrad Bloch, 1953) and it is characterised by a cholestane nucleus with a trans junction between rings A and B, B and C and C and D, figure 1.2. The main body structure is completed by a C5 unsaturation and two angular methylene (ß configuration) at C10 and 13. All the above characteristics confer planarity and rigidity to the molecule. The flexible part of cholesterol is the aliphatic iso-octyl side chain bonded to C17. The amphipathic nature is given by the hydroxyl group bonded to C3, which also presents with ß stereochemistry.

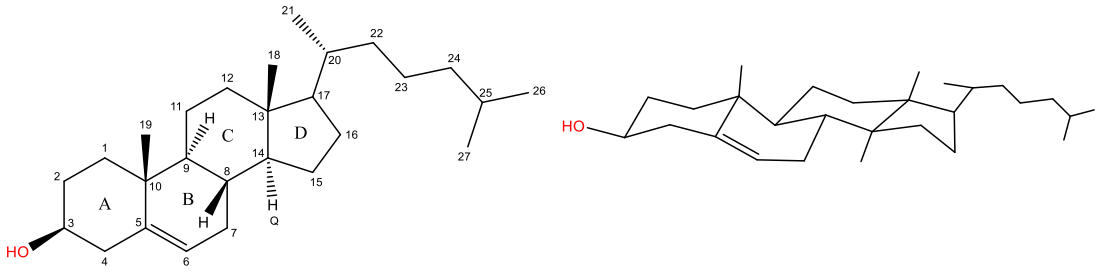

Chemical Formula: $C_{27}H_{46}O$
Exact Mass: 386.35
Molecular Weight: 386.66

Figure 1.2 Cholesterol general and planar structure.

Cholesterol is a relatively hydrophobic and neutral molecule synthesized by almost all types of human cell at the endoplasmic reticulum level (Cerqueira *et al.*, 2016). Once synthesised, it is transported to other organelles, cell compartments and the plasma membrane, which accounts for 60-90% of whole cellular cholesterol, and where cholesterol makes up 45 moles % of the total lipid content (Lange *et al.*, 1989a)(Cerqueira *et al.*, 2016).

At the membrane surface, the cholesterol 3ß-hydroxyl group interacts with the polar head of membrane phospholipids, letting the sterol intercalate into the bilayer. The cholesterol-membrane lipid interaction is stabilised through non-polar-electrostatic bonds between the tetracyclic cholestane body and aliphatic chains of phospholipids (Mouritsen & Zuckermann, 2004). The plasma membrane is a dynamic environment and site of several fundamental biochemical processes (Marguet *et al.*, 2006). The maintenance of the right degree of order and correct fluidity allows the cell to exchange information with the surrounding milieu, through cell signalling, important also for cell survival. Being a regulator of plasma membrane fluidity, cholesterol percentage varies between different cell types and within the same cell, as it determines membrane biophysical properties. For this reason, cholesterol homeostasis is tightly regulated in human cells, creating an intricate communication between its uptake, biosynthetic machinery and metabolism.

1.1.1.2 Cholesterol biosynthesis and homeostasis

Cholesterol can be present in two different forms in the human body: the active free form and the inactive esterified form. The main source of cholesterol comes from endogenous *de novo* synthesis, which accounts for almost 70% of pooled body cholesterol.(Kapourchali *et al.*, 2016). The remaining 30% come from recycling of circulating cholesterol and from the diet. Cholesterol uptake, synthesis and metabolism is finely regulated to maintain its appropriate physiological level. Cholesterol homeostasis is also guaranteed through the regulation of its excretion and re-absorption, by means of a process called reverse cholesterol transport (Gliozzi *et al.*, 2021).

Cholesterol *de novo* synthesis is a long-multi-step pathway. It starts with a series of carbocation condensations, known as the mevalonate pathway (Cerqueira *et al.*, 2016; Nes, 2011), figure 1.3. In the cytosol, an initial condensation of two units of Acetyl-Coenzyme A (Acetyl-CoA) gives Acetoacteyl-CoA, through thiolase enzyme catalysis. Acetoacteyl-CoA passively diffuses from the cytosol to the ER where it is converted by the enzyme 3-Hydroxymethylglutayl-CoA synthase (HMG-CoA-S) into 3-Hydroxymethylglutayl-CoA (HMG-CoA) through another carbocation condensation with Acetyl-CoA. Subsequent reduction catalysed by HMG-CoA reductase (HMG-CoA-R) converts HMG-CoA to mevalonate. This is the rate limiting step in the mevalonate pathway and constitutes an important check point in the synthesis of cholesterol but also of important isoprenoid units (Cerqueira *et al.*, 2016; Nes, 2011). HMG-CoA-R is therefore heavily regulated: translational control is operated through a negative feedback mechanism depending on dietary cholesterol level (Chambers & Ness, 1998)(Ness, 2015) but is also subjected to

transcriptional and activity modulation (Chambers & Ness, 1997; Osborne *et al.*, 1988), as well as regulation of enzyme elimination (Faust *et al.*, 1982). The importance of HMG-CoA-R made it a feasible drug target and one the most effective classes of cholesterol synthesis inhibitors for lowering high plasma cholesterol has been developed to target the enzyme: the statins.

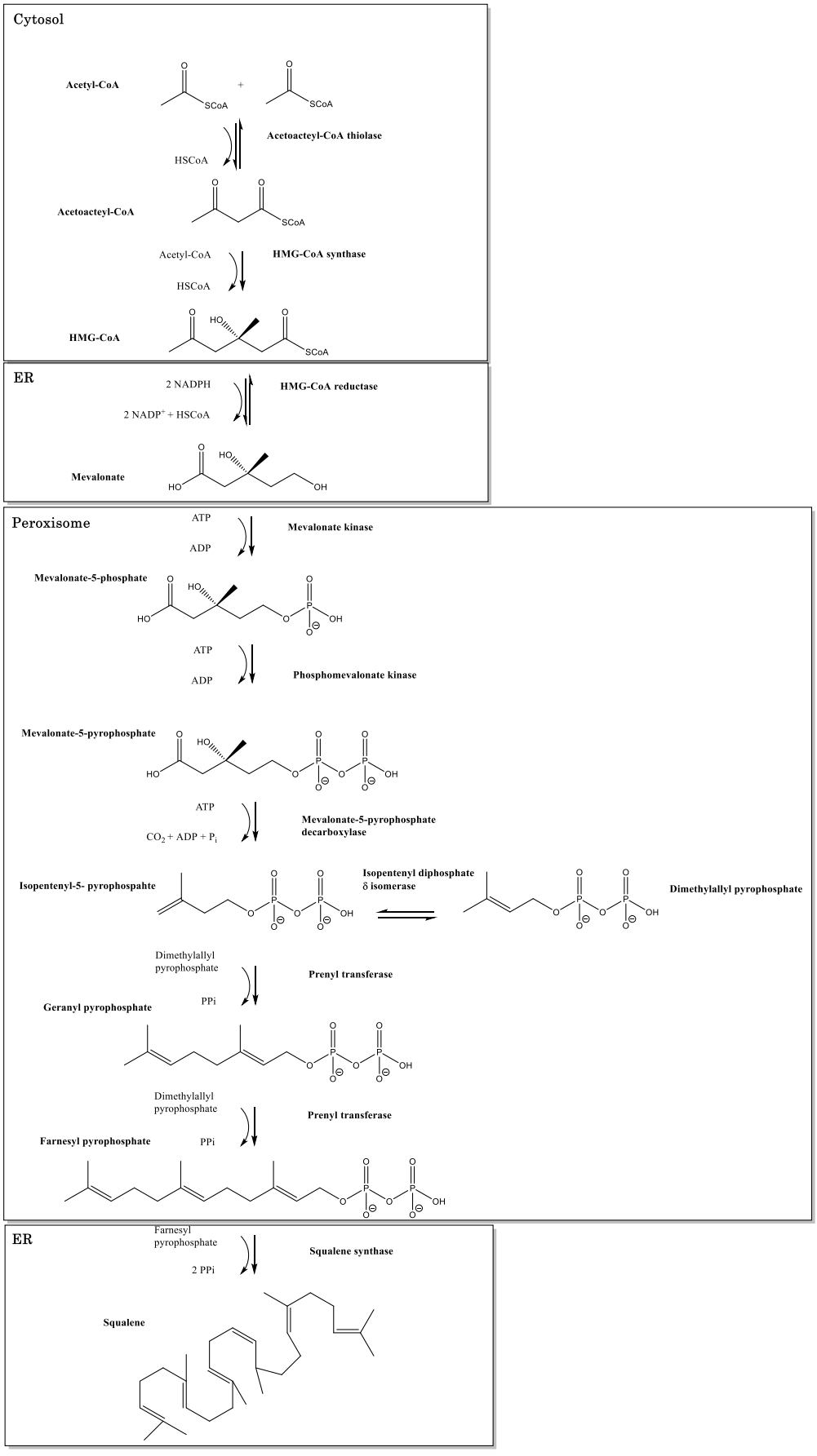

Figure 1.3 The mevalonate pathway.

The next step in the synthesis of cholesterol comprises the generation of activated isoprene structures, which constitute the backbone structure of the cholesterol body. Mevalonate first passes into the peroxisome, where one phosphate unit is added to carbon 5 thanks to the action of mevalonate kinase and mevalonate-5-phospate is thus formed. Another phosphate unit is then added to form mevalonate-5-pyrophosphate, catalysed by phosphomevalonate kinase. Finally, mevalonate-5-pyrophosphate decarboxylase catalyses a decarboxylation reaction required to form the isoprene unit isopentenyl-5-pyrophosphate. Isopentenyl-5-pyrophosphate is then converted into its active form, the electrophile isomer dimethylallyl pyrophosphate by isopentyl-diphosphate δ-isomerase. Isoprene units are fundamental building blocks for the creation of more than 20,000 compounds called isoprenoids. These molecules are involved in many essential cell pathways, one of which is the formation of cholesterol (Sarah A. Holstein & Raymond J. Hohl, 2004). The active dimethylallyl pyrophosphate is fused to isopentenyl-5-pyrophosphate through the catalytic action of prenyl transferase to form geranyl pyrophosphate. Geranyl pyrophosphate reacts with another unit of dimethylallyl pyrophosphate to form farnesyl pyrophosphate. Farnesyl pyrophosphate diffuses back to the ER. The next step in the isoprenoid pathway involves a squalene synthase reductive dimerization of two farnesyl pyrophosphate units to form squalene. This dimerization establishes another important check point as it brings to the formation of an intermediate that exclusively belongs to the sterol biosynthesis (Cerqueira *et al.*, 2016). From now on the biosynthetic pathway focuses on the cyclisation of the planar squalene hydrocarbon structure.

Squalene monooxygenase (SQLE) is a NADPH dependent monooxygenase that catalyses the oxidation of the squalene Δ2 double bond to form 2,3-oxidosqualene, also called squalene epoxide. The following reaction is a cyclisation of the acyclic 2,3-oxidosqualene to the first polycyclic cholesterol precursor lanosterol. 2,3-oxidosqualene cyclase or lanosterol synthase, is the enzyme involved in this conversion.

The last part in the cholesterol biosynthesis involves more than 19 different steps and their relative enzymes. Two different pathways have been proposed for the conversion of lanosterol to cholesterol, see figure 1.4: the classical and first to be discovered is the Bloch pathway (Bloch, 1965) while the second one is the Kandutsch-Russel pathway (Kandutsch & Russell, 1960). The two processes share the same series of reactions, from demethylation to reduction and isomerisation, but differs in the substrates. An unsaturation at the C24 side chain carbon is present in all the Bloch pathway compounds while in the Kandutsch-Russel pathway the unsaturation is immediately reduced. The conversion of lanosterol starts with the C14α-demethylase demethylation of C14, followed by a reduction step, catalysed by a Δ14-desaturase. Two demethylations catalysed by C14α-demethylase form the intermediate Zymosterol. At this point, the two synthetic pathways diverge: a Δ24-desaturase can catalyse the shift from the Bloch pathway to the Kandutsh-Russel pathway, forming Zymostenol. All the following reactions are shared between Bloch and Kandutsh-Russel ways, what distinguish one from the other is the presence of a side chain Δ24 olefin. The next reaction, shared by the two pathways, consists in an isomerisation of Δ8-double bond to a Δ7 double bond through the action of a Δ8-Δ7-isomerase forming lathosterol, in the Kandustsh-Russel, and

cholesta-7,24-dien-3ß-ol, in the Bloch. The two intermediates undergo to a desaturation catalysed by Δ5-desaturase, which introduce a new olefin at C5, forming 7-dehydrocholetserol and cholesta-5,7,24-trien-3ß-ol, respectively. The ultimate reaction is a reduction of the C7 double bond, by a Δ7-desaturase to form cholesterol and desmosterol, respectively. Therefore, the Bloch pathway requires one final step to form cholesterol: the reduction of the desmosterol Δ24 double bond by Δ24-desaturase.

The huge complexity of the entire cholesterol synthesis pathway makes it a high energy consuming pathway, which requires one hundred ATP molecules and eleven oxygen molecules (Nes, 2011). Consequently, its production is circumscribed to metabolically active tissues, with liver as the main producer, but also brain, adrenal glands, testis, and skin. The Bloch pathway is usually the preferred path for *de novo* synthesis of the cholesterol, but tissue/cell specific stimuli can determine a switch to the Kandutsh-Russel pathway (Ačimovič & Rozman, 2013; Bae & Paik, 1997). In the brain cells of Central Nervous System (CNS) the Kandutsh-Russel way is supposedly preferred (Gliozzi *et al.*, 2021). The considerable energy consumption required for the synthesis along with the importance of the sterol for cell physiology results in a strict, complex, and multi-level homeostasis regulating machinery, which also include cholesterol compartmentalisation.

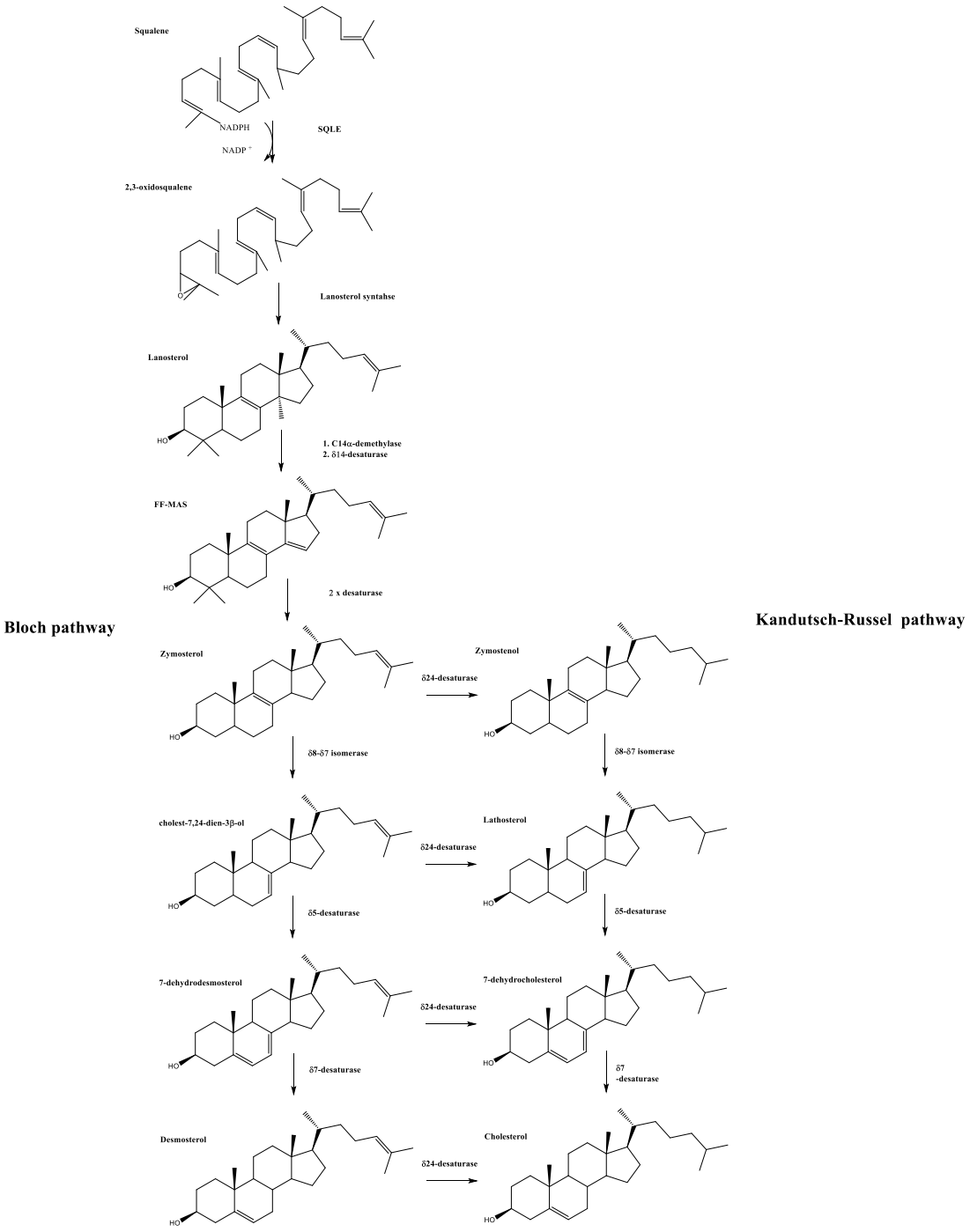

Figure 1.4 Bloch and Kandutsh-Russel pathways: the mammalian dichotomy in cholesterol synthesis.

Cellular cholesterol distribution varies a lot depending on the cellular compartments: even if synthesised in the ER, here it accounts for only 0.5-1% of the total cellular cholesterol (Lange *et al.*, 1999). Once the synthesis is completed, free cholesterol leaves the ER almost

immediately to reach the plasma membrane and other organelles to meet the cell's need. Fast passive transmembrane diffusion represents one of the possible ways to mobilise intracellular cholesterol, which usually occurs through the passage between membrane junctions (DeGrella & Simoni, 1982). However, other two mechanism for the mobilisation of cholesterol are known: vesicular and non-vesicular modes. The former fashion seems to involve the vesicle-mediated protein secretory pathway, but suppression of this way has only minorly affected cholesterol transport from the ER (Urbani & Simoni, 1990). Non-vesicular modes include cytosolic protein mediated transport involving caveolin proteins. Caveolins are integral membrane proteins involved in the receptor independent endocytosis (Tang *et al.*, 1996). The mechanism by which caveolins assist cholesterol transport remains uncertain, however one of the possible hypotheses suggests a complex formation with chaperon proteins to aid the cholesterol transport from ER bypassing the Golgi apparatus (Heino *et al.*, 2000). To note, the caveolin transporter presents cholesterol binding sites (Ikonen & Parton, 2000) but suppression of this pathway has not deeply affected cholesterol intracellular trafficking, confounding the findings (Heino *et al.*, 2000).

As mentioned above, cholesterol levels are constantly monitored to maintain physiological levels. Excess of free cholesterol is detrimental for the cell: from loss of membrane fluidity (Milhiet *et al.*, 2002) and, consequently, its properties, to cholesterol crystals formation and damage of organelles (Kellner-Weibel *et al.*, 1999). Abnormal sterol level has a substantial cytotoxic effect (Tabas, 2002). On the other side, low sterol levels can also deeply affect cellular well-being and survival. Increased membrane fluidity, diminished

cholesterol-derived product, like steroid hormones, oxysterols and bile acids, and loss of cholesterol as bioactive compound significantly affect many essential biological pathways (Duan *et al.*, 2022). The maintenance of cholesterol homeostasis is, therefore, exerted through multiple mechanisms, which usually occurs simultaneously, see figure 1.5. These pathways involve:

1. Cholesterol esterification and storage into cytosolic lipid droplets.
2. Control of its biosynthesis and uptake.
3. Import and export from/to external tissues.
4. Metabolism.

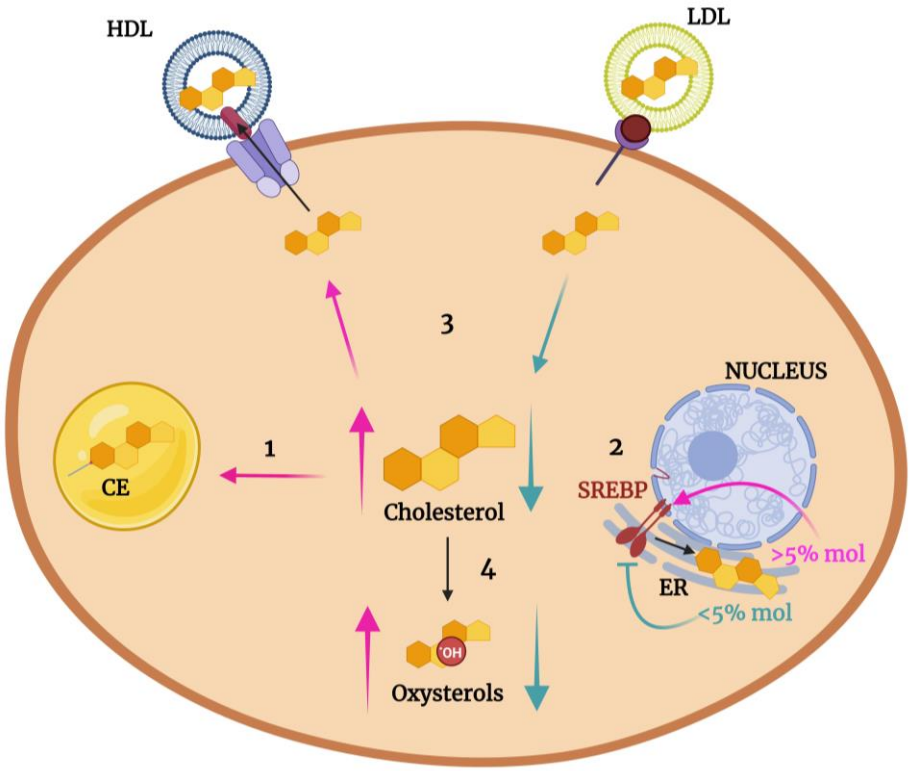

Figure 1.5 Cellular cholesterol homeostasis.
Several different pathways are involved in the preservation of cholesterol physiological levels, including accumulation as cholesteryl esters (1), concentration dependent control of its biosynthesis and uptake (2), redistribution to peripheral accumulation sites or uptake form external sources (3) and metabolism (4).

One of the first mechanism activated by steroidogenic cells to get rid of excess sterol is the formation of cholesterol esters (CE). This type of cells relies on cholesterol *de novo* biosynthesis, uptake, and storage to produce cholesterol derived products. When cholesterol levels are high, the ER-enzyme acyl-coenzyme A: cholesterol acyltransferase (ACAT, also called Sterol O-acyltransferase) is activated and catalyses the esterification of the 3ß-hydroxyl moiety with long chain fatty acids (Uittenbogaard *et al.*, 2002). CE are thus formed and stored along with triglycerides in the cytosolic lipid droplets. Simultaneously to the CE formation, surplus of free cholesterol inhibits its *de novo* synthesis through a negative feedback mechanism.

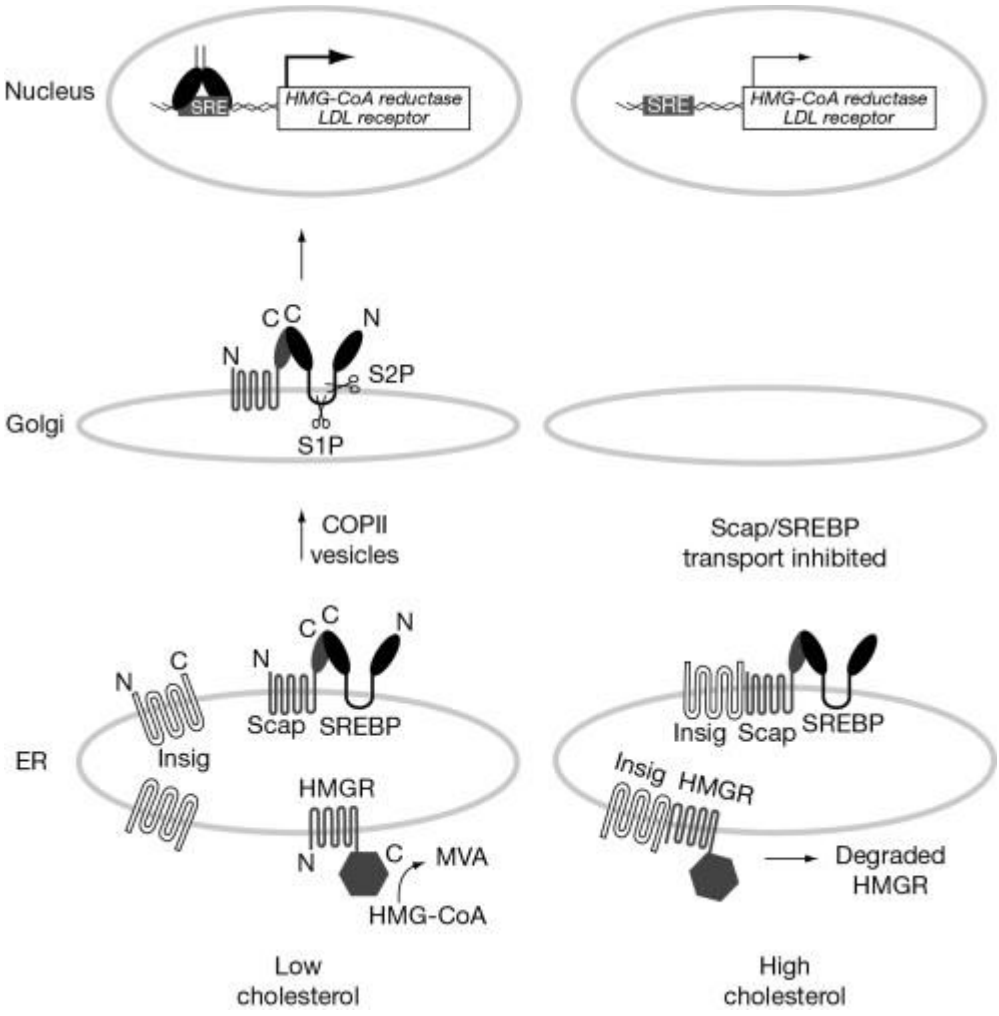

Figure 1.6 Regulation of cholesterol biosynthesis through SREBP2/SCAP mechanism.
SREBP2 is a transcription factor able to induce cholesterol biosynthesis rate limiting enzymes like HMG-CoA to replenish cellular cholesterol needs in an ER cholesterol concentration dependent manner. Figure taken from (Espenshade, 2013).

This mechanism requires sterol regulatory binding element proteins (SREBP), a class of membrane proteins located at the outer surface of ER membrane which controls lipid homeostasis (Eberlé *et al.*, 2004). There are three isoforms of SREBP: SREBP-1c, which controls the expression of genes involved in fatty acid and triglycerides synthesis and SREBP-1a and SREBP-2, which regulates genes involved in the sterol synthesis. The SREBPs are transcription factors composed of three domains:

- A **NH_2 terminal domain**, which contains the catalytic active site made of proline and serine residues along with the DNA binding and dimerization region (Eberlé *et al.*, 2004)
- A **hydrophobic transmembrane domain** made of two subunits which project into the ER membrane and are connected through a short loop which extrude into the ER lumen (Eberlé *et al.*, 2004)
- A **carboxy-terminal end** which constitute the regulatory domain (Eberlé *et al.*, 2004)

SREBPs are produced as inactive proteins, anchored to the ER membrane, where they are bonded to the SREBP-cleavage-activating protein SCAP (SREBP cleavage activated protein), figure 1.6 (Rawson *et al.*, 1997). SCAP transports SREBP from the ER to the Golgi, see figure 1.6. Activation of SREBPs in the Golgi requires a double cleavage operated by site-1 and site-2 proteases (Rawson *et*

al., 1997). These proteases activate SREBP through the hydrolysis of transcription factor specific amide bonds, which are exposed to cleavage only when SREBP interacts with SCAP. The proteolysis of the transcription factor determines the release of the NH2-terminal, the active form of SREBP called SREBPn. SREBPn translocases to the nucleus to promote the expression of lipogenic and steroidogenic genes like HMG-CoA-R and the low-density lipoprotein receptor (LDLr) (Nohturfft *et al.*, 1998). Tissue distribution of the three different isoforms differs: SREBP-1a is very abundant in the spleen (Shimomura *et al.*, 1997) while SREBP-1c is highly expressed in metabolic non dividing tissues such as adipose and liver. SREBP-2 is also very abundant in liver and is considered one of the main regulators of the cholesterol homeostasis (Eberlé *et al.*, 2004). The transcription regulation of all the SREBPs protein respond to variation of the intracellular cholesterol content but with different extent. For example, SREBP-2 is the most sensitive to the intracellular sterol content (Eberlé *et al.*, 2004). When there is an excess of cholesterol in the ER, more than 5 mole % of total ER lipids, the sterol binds to the cholesterol binding domain of the SCAP protein. This binding induces conformational changes in the SCAP, allowing the protein insulin induced gene (Insig) to bind the SCAP-SREBP-2 complex, stabilising it and anchoring it to the ER membrane and preventing its transport to the Golgi (Horton *et al.*, 2002a). The Insig-SCAP-SREBP-2 complex abolish the cleavage of SREBP-2 to SREBP-n therefore reducing the expression of cholesterol producing enzymes like HMG-CoA-R as well as of cholesterol uptake receptors like LDLr (M. S. Brown *et al.*, 2018; Goldstein *et al.*, 2006; Horton *et al.*, 2002b). As a result, cholesterol levels decrease by means of reduced endogenous synthesis and uptake, reaching back again the physiological level. Considered as

the sensor of cholesterol levels, SREBP-2 is also engaged in restoring the sterol levels when they are below the physiological threshold in the ER, < 5% mol of ER lipids. Without conformational changes dictated by cholesterol binding, the SCAP-SREBP-2 complex is transported to Golgi where SREBP-2 proteolysis and activation to SREBP-n occurs. Then SREBP-n translocases to the nucleus, where it binds to sterol regulatory element (SRE) DNA sequences, activating gene expression and inducing cholesterol synthesis (M. S. Brown *et al.*, 2018; Goldstein *et al.*, 2006; Horton *et al.*, 2002b). Cholesterol in the ER constitutes only 1% of total cell cholesterol l(Radhakrishnan *et al.*, 2008) while the majority, between 60 and 90*%*, is confined in the plasma membrane (Lange *et al.*, 1989b). However, it is ER cholesterol that regulates SREBP-2 activity. This can be explained by the fact that levels of ER cholesterol depend on cholesterol in the plasma membrane which is in particular highly thermodynamic energetic environment, termed accessible cholesterol which can be sampled by to the ER (Ferrari *et al.*, 2020; Sandhu *et al.*, 2018). Cholesterol exists in three forms in the plasma membrane:

- The free-accessible form, which by means of its high energetic environment can readily interact with receptors and chaperon proteins to be transferred to the ER (Das *et al.*, 2014)
- The sphingomyelin sequestered pool, which can be released only upon sphingomyelin hydrolysis by the enzyme sphingomyelinase (Das *et al.*, 2014)
- The residual pool essential for membrane integrity (Das *et al.*, 2014)

Excess cholesterol can be stored in the plasma membrane as accessible cholesterol. As a consequence of its high energy environment, accessible cholesterol can be easily transported to the

ER, where it increases its levels. When it crosses the threshold of 5 % mol, ER cholesterol inhibits SREBP-2 machinery. On the contrary, when ER cholesterol is below 5 mole%, SREBP-2 is activated, and sterol synthesis induced.

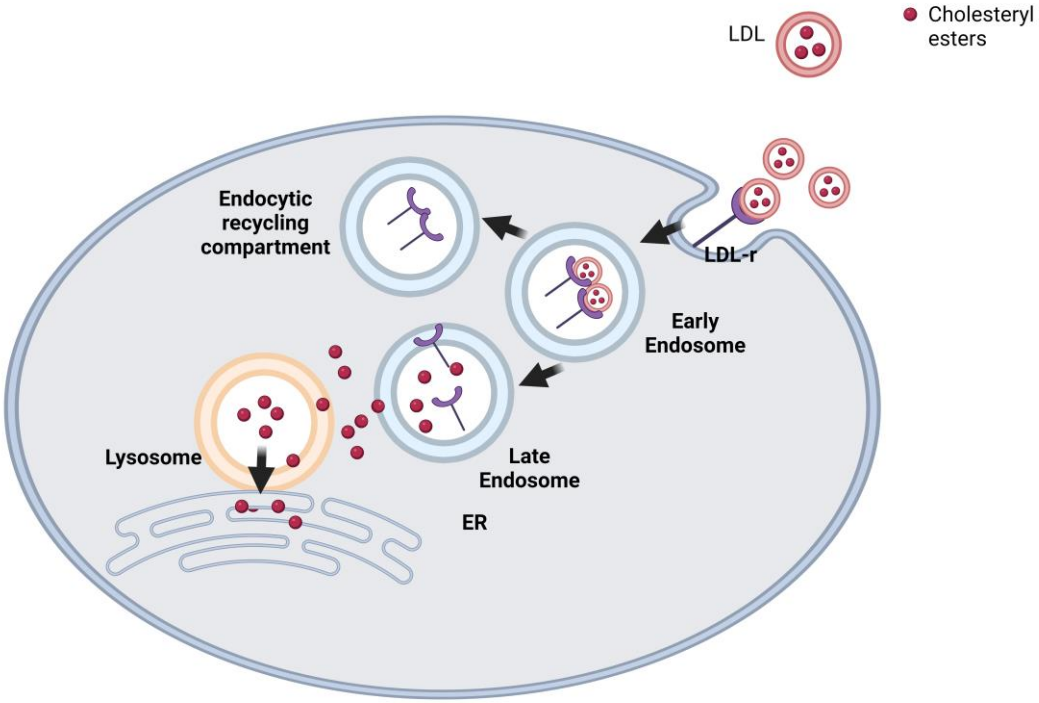

Figure 1.7 Uptake of LDL-cholesterol.
Circulating LDL-cholesterol is up taken by the cell through an LDL-LDLr endocytic mechanism which ultimately leads to the release of free cholesterol into the ER, replenishing the cell's needs.

Another way the cell uses to maintain cholesterol homeostasis is its export or import into/from circulation. Cholesterol being a neutral and hydrophobic molecule, it is mainly found in plasma internalised in circulating lipoproteins. Lipoproteins are a specific type of particles made of a hydrophobic core made of triglycerides and cholesterol esters, surrounded by a monolayer of phospholipids and free cholesterol, along with apolipoproteins (L. C. Smith *et al.*, 1978). The function of lipoproteins is to carry water-insoluble lipids through

the blood stream (McNamara, 2013; L. C. Smith *et al.*, 1978). Seven classes of lipoprotein exist, based on size, lipid composition or apolipoprotein content (L. C. Smith *et al.*, 1978). The most represented in human blood are chylomicrons, which serve as carriers for diet derived lipid, very low-density lipoprotein (VLDL), intermediate density lipoprotein (IDL) and low-density lipoprotein (LDL), for transport of liver-derived cholesterol to peripheral tissues. The last type of lipoproteins is the high-density lipoprotein (HDL), used for reverse cholesterol transport, from peripheral tissues to the liver (L. C. Smith *et al.*, 1978). When cholesterol levels are low, especially in steroidogenic cells, the uptake of circulating LDL increases. Low levels of plasma membrane cholesterol cause an ER cholesterol reduction, which induces the activation of the SREBP-2 pathway. Active SREBP-2 increases the expression of the low-density lipoprotein receptor, LDL-r found on the outer plasma membrane leaflet (Das *et al.*, 2014; Radhakrishnan *et al.*, 2008). Circulating LDL binds to LDL-r and is being internalised in the cell through receptor-mediated-endocytosis, see figure 1.7 (M. S. Brown & Goldstein, 1986). The endocytosis is generally composed of 7-step in which (Soccio & Breslow, 2004):

1. After LDL-LDL-r biding, the LDL is firstly internalised in the receiving cell trough the formation of an early endosome.
2. By means of low pH in the endosomal-lysosome compartment, which induces the dissociation of LDL from LDL-r, cholesterol esters are released and then hydrolysed by the enzyme lysosomal acid lipase.
3. A proportion of the cholesterol and LDL-r are transported to the endocytic recycling compartment (ERC) and brought back to the plasma membrane.

4. Free cholesterol moves to the late endosome-lysosome.
5. Once in the late endosome-lysosomal compartment, cholesterol moves across the organelle upon binding to the soluble cholesterol binding protein Niemann-Pick C 2 (NPC-2). NPC-2 aids the transport of the sterol between the intra organelle compartments to reach the limiting membrane. At the limiting membrane, cholesterol is flushed outside the endosome through Niemann-Pick C 1 (NPC-1) binding. NPC-1 is another isoform of the Niemann-Pick protein family and is an integral membrane protein which acts as a pump for cholesterol.
6. Ultimately cholesterol reaches the ER. Multiple mechanisms have been proposed for the mobilisation of cholesterol from late endosome to ER: the first involves a vesicular transport to the Golgi, to further move to the plasma membrane and back to the ER. The second mechanism involves a direct diffusion after NPC-1 secretion, from late endosome to the ER via membrane contact sites. A more recently uncovered mechanism involves transport first to the plasma membrane and then on to the ER (Trinh *et al.*, 2020, 2022).
7. Once in the ER, free cholesterol is then redistributed to other cellular compartments for production of steroid-based hormones, bile acids, oxysterols or internalised in the membrane compartment for structural purpose.

Thank to LDL, cellular cholesterol needs are replenished, along with the other mechanisms described above.

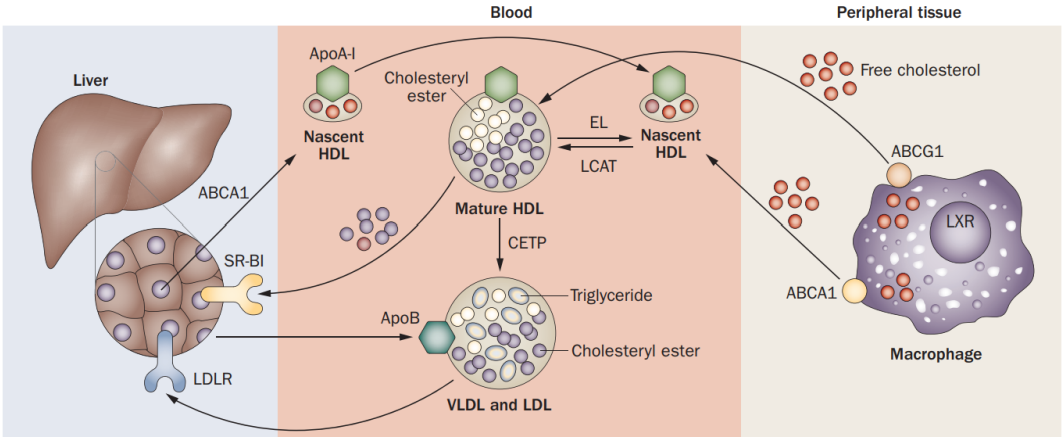

Figure 1.8 Reverse cholesterol transport (RCT).
Reverse cholesterol transport is the mechanism through which peripheral cells eliminate the excess of intracellular cholesterol upon the formation of a HDL-cholesterol loaded lipoprotein. In the blood stream, the HDL reaches the liver where it is internalised through SR-BI-HDL binding and cholesterol released into the hepatocytes for metabolism to bile acids. Figure taken from (Duffy & Rader, 2009).

On the other side, excess of cellular cholesterol induces a process called reverse cholesterol transport or RCT. RCT lowers the intracellular free sterol levels through its efflux back to the liver in a new HDL particle, see figure 1.8 (Ouimet *et al.*, 2019). The process starts with the liver secretion of the apolipoprotein A1 (Apo A-1) into the blood stream. Apo A-1 is a lipid binding protein which constitutes almost 70% of the HDL protein content (X. Xu *et al.*, 2022). Apo A-1 reaches cholesterol overloaded tissues. ABCA-1 is an integral membrane protein of ABC-transporter family. The protein possesses two characteristic extracellular domains (ECDs) that binds to cholesterol and phosphatidyl choline when an excess of cholesterol is present (Ishigami *et al.*, 2018). Through the lipid binding, ABCA-1 undergoes to conformational changes and dimerises. Apo A-1 recognises ABCA-1 dimers and binds to cholesterol and phosphatidyl choline rich ECDs (Ishigami *et al.*, 2018). Cholesterol-loaded Apo A-1 forms the so called pre ß-HDL, with a typical discoidal shape and

cholesterol molecules at the surface. Whereupon the pre ß-HDL interacts with another ABC-transporter, ABCG1, and more cholesterol is loaded into the pre-HDL (Feingold, 2000; Ouimet *et al.*, 2019). At this point, the enzyme lecithin-cholesterol acyltransferase or LCAT catalyses the formation of a mature α-HDL through the remodelling of pre ß-HDL, esterifying cholesterol and moving it from the surface to the core of the particle (Ouimet *et al.*, 2019; X. Xu *et al.*, 2022). α-HDL is then secreted into the blood stream. Once in the circulation, the lipoprotein can have two different destinies, which will both bring to the release of extrahepatic cholesterol for elimination or metabolism. In the first way, α-HDL cholesterol is transferred to a circulating LDL trough the action of the enzyme cholesteryl ester transferase protein (CETP) (Feingold, 2000). The LDL goes then back to the liver where it binds to hepatic cells LDL-r. In the hepatocytes, LDL-derived cholesterol is released upon CE hydrolysis, which can be then further metabolised for elimination, esterified for accumulation, converted to bile acids, or redistributed to extra hepatic tissues (Feingold, 2000). On the other side, circulating α-HDL can directly reach the liver where it binds to the hepatocyte's scavenger receptor class B type 1 (SR-B1) and releases extrahepatic cholesterol (Ouimet *et al.*, 2019).

The last mechanism throughout which cell maintains cholesterol homeostasis consist of regulation of its metabolism. Sterol metabolites of cholesterol consist of a vast family of steroid-base molecules including bile acids, steroid hormones, and oxysterols, oxygenated form of cholesterol, see figure 1.9. Considering the chemical diversity of these molecules, their biological functions are very broad, from emulsion and subsequent internalisation of dietary lipids into enterocytes, control of the reproductive system, glucose

metabolism, blood pressure and water/salt balance, to the modulation of immune response (J. Hu *et al.*, 2010)(W. J. Griffiths & Wang, 2019b, 2022; Y. Wang, Yutuc, *et al.*, 2021).

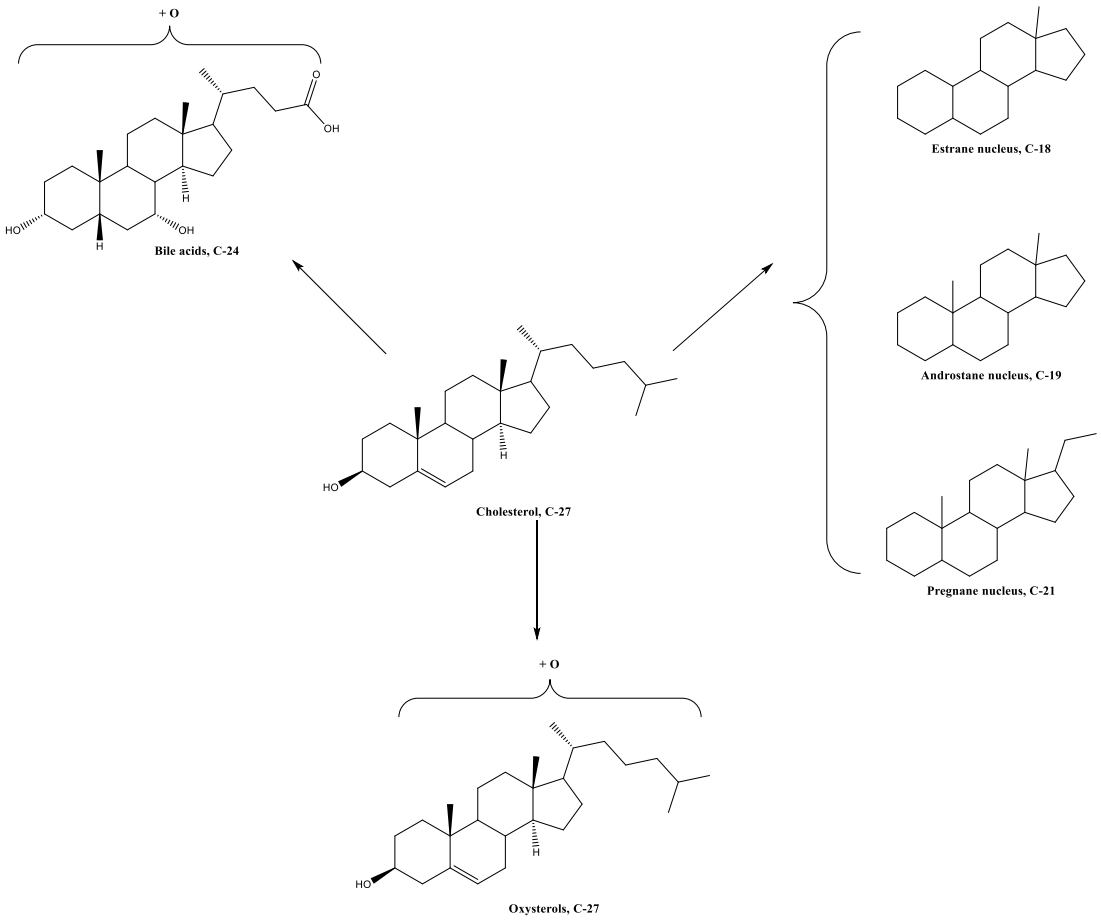

Figure 1.9 Main human cholesterol metabolites.
Human cholesterol metabolites can be classified into 3 different categories, based on the number of carbons composing the tetrahydro cyclopentane phenanthrene and/or the number and type of substituents. The three main classes are: C-24 bile acids, composed of a cholane nucleus, steroid hormones, which can be made of a C-18 estrane, C-19 androstane or C-21 pregane nucleus, or C-27 oxysterols.

Bile acids are molecules belonging to the family of sterol lipids, characterised by a C-24-5ß-cholanoic nucleus. Their structure is like the parent cholesterol one, but presents several differences like:

- A **3α-hydroxyl** group, consequence of cholesterol 3ß-OH epimerisation
- An A-B ring **cis** junction, different from the trans of the cholestane structure, which introduces a 5ß-hydrogen. This configuration constrains the steroid nucleus to assume a chair-gauche conformation.
- Additional **hydroxyl** groups
- A C24 **carboxylic** group

In the cholanoic molecules, the hydroxyl and carboxyl moieties face the same side of the plane, forming a hydrophilic region which is opposed to the very hydrophobic one represented by the hydrocarbon chain and the 4-fused-ring nucleus. This specific spatial arrangement of the cholanoic nucleus substituents is a direct consequence of the chair conformation. The differences between cholesterol and its end-products bile acids reflect the complex architecture of the acids endogenous biosynthesis.

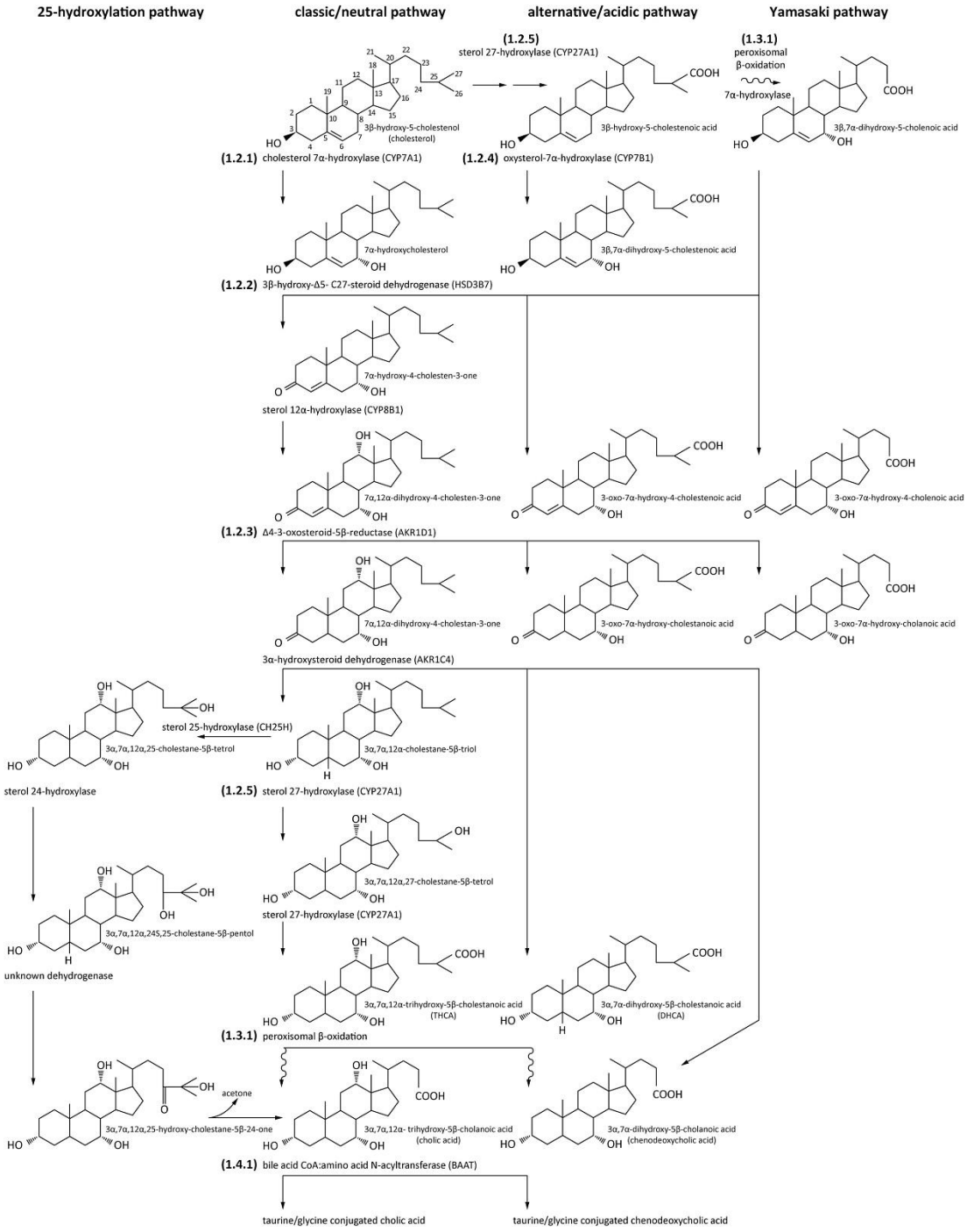

Figure 1.10 Bile acids biosynthetic pathways in humans.
Figure taken from (Vaz & Ferdinandusse, 2017)

Bile acid biosynthesis is a multi-step process involving the conversion of the cholesterol C27 carbon cholestane nucleus into the C24 carbon cholanoic one, figure 1.10. The main site of cholanoic acid production is the liver. Two main synthetic pathways have been identified for

bile acids *de novo* generation in human: the neutral and the acidic pathway, see figure 1.10 (Chiang, 1998). Being first one to have been discovered, the neutral pathway is also the predominant in the human hepatocytes. The classical neutral pathway starts with **ring** modifications through the oxidation of cholesterol C7 position by the enzyme cytochrome P450 7A1, CYP7A1 (Chiang, 1998). In the ER of the hepatocyte, a hydroxyl moiety with a 7α configuration is introduced and 7α-hydroxycholesterol (7α-HC) is thus formed. This is the rate limiting step in the bile acid synthesis through the neutral pathway. Cellular cholesterol levels are believed to be the driving force and the limiting factor of the enzymatic reaction catalysed by CYP7A1, (Staels & Fonseca, 2009). When cholesterol levels exceed the baseline ER concentration, bile acid synthesis is stimulated (Staels & Fonseca, 2009). On the contrary, minimum ER sterol levels avoid bile acid formation (Staels & Fonseca, 2009). In the second step of classical bile acid synthesis the enzyme 3β-hydoxy-Δ5-C27-oxidoreducatse (HSD3B7) converts the 3β-hydoxy-Δ5 function of 7α-HC into a 3-oxo-Δ4 arrangement, forming the 7α-hydroxycholest-4-en-3-one (7α-HCO). In this step, the 3β-OH is oxidised to 3-keto group and the Δ5 double bond is epimerised into a Δ4 bond. At this point, 7α-HCO is transported in the cytosol for further modifications. The Δ4 double bond is now reduced by the enzyme Δ4-3-oxosteroid-5β-reductase (AKR1D1), followed by a final reduction step, involving the conversion of the 3-oxo ketone into a 3α-OH by the 3α-hydroxysteroid dehydrogenase (AKR1C4). 5β-cholstan-3α,7α-diol is thus formed. 7α-HCO might also undergo to a further oxidative step before AKR1D1 enzymatic reduction. This additional step involves the sterol 12α-hydroxylase (CYP8B1) to introduce a 12α-OH group into 7α-HCO and form 7α,12α-dihydroxycholest-4en-3-one (7α,12α-diHCO), precursor of the cholic acid (CA). Hereinafter, 7α,12α-diHCO goes through the

same set of reduction and dehydrogenation steps promoted by AKR1D1 and AKR1C4, to form 5ß-cholestan-3α,7α,12α-triol (3α,7α,12α-triHC). In the neutral pathway **side chain** modifications starts only after the steroid-body alterations are completed, with the hydroxylation of the C26 carbon by CYP27A1 in the mitochondria. From the cytosol 5ß-cholstan-3α,7α-diol and 3α, 7α,12α-triHC moved to the mitochondria where they are subjected to a first C26 hydroxylation by CYP27A1 and a second oxidative step to form a C26 carboxylic group, also catalysed by CYP27A1. The cholestanoic-based intermediates 3α,7α-dihydroxy−5ß-cholestanoic acid (DHCA) and 3α,7α,12α-trihydroxy−5ß-cholestanoic acid (THCA) are formed. The following steps see a reduction in length of the side chain and the subsequent transportation of DHCA and THCA. This process requires the precursors THCA and DHCA to be first activated into the corresponding coenzyme A (CoA) esters. Bile acid-CoA synthetase (BACS) and very long chain acyl-CoA synthase catalyse the esterification reaction at the carboxyl C26 group. Activated C26 cholestanoic esters are then transported to the peroxisome by the peroxisomal membrane protein 70 (PMP 70 or ABCD3) where they are subjected to a C25 isomerisation from R- to S-configuration by the enzyme α-methyl acyl CoA racemase (AMACR), followed by a sidechain shortening through peroxisomal ß-oxidation. The peroxisomal ß-oxidation is made of 4 reactions that includes:

- Double bond formation at C-4 position by acyl CoA oxidase-2 (ACOX-2).
- Hydration step of the Δ24 double bond into a 24-OH by D-bifunctional protein (DBP) .
- A second oxidative step to convert 24-OH to 24-keto by DBP.
- Loss of the propionyl group at C24 give the C-24 COOH group.

Cholic and chenodeoxycholic acid (CDCA) are thus formed. Lastly, the cytosolic or peroxisomal bile acid: amino-acid transferase (BAAT) conjugates the amino acids glycine or taurine to the C24 carboxylic group to give tauro- and glycol- cholic -or chenodeoxycholic conjugates.

The acidic pathway starts in a different way respect to the neutral one: cholesterol in the ER is converted into the oxysterols (25R)26-hydroxycholesterol (26-HC), also commonly called 27-hydroxycholesterol, by the mitochondrial enzyme CYP27A1. As for the neutral pathway, the rate limiting substrate in this synthesis is represented by the cholesterol availability for the enzyme CYP27A1. Excess of plasma membrane accessible cholesterol causes the mobilisation of the sterol to the mitochondria inner membrane through the action of the steroidogenic regulatory protein (StarD1) (Pandak *et al.*, 2002). The rise in ER cholesterol stimulates bile acid synthesis (Pandak *et al.*, 2002). A shunt pathway of the acidic bile acid biosynthesis involves a further oxidation of 26-HC to the bile acid precursor 3ß-hydroxy-5-cholestenoic acid (CA) by CYP27A1. However, the general acidic pathway continues with 26-HC and 25-hydroxycholesterol, 25-HC, C7 oxidation by oxysterol 7α-hydroxylase (CYP7B1) to form 7α,26-dihydroxycholesterol (7α,26-diHC) and 7α,25-dihydroxycholesterol (7α,25-diHC). The introduction of a 7α-OH moiety into the oxysterols 26- and 25-HC structure represents also a fundamental metabolic step in the reduction of their biological activity, except as EBI2 ligands. This argument is extensive described in the section 1.2. The 7α-hydroxylated sterols are further metabolised to 7α,26-dihydroxy-3-ketocholest-4-ene and 7α,25-dihydroxy-3-ketocholest-4-ene by HSD3B7, followed by a further oxidation at the C26 to give 26-COOH, and the related cholestenoic

acids. At this point a side chain cleavage occurs at C24 and CDCA is thus formed (Jp, 2006). CDCA can be also made through the shunt pathway, where CA is hydroxylated by CYP7B1 to give the relative 7α-hydroxylated form and side chain-cleaved to C24-Δ5-3β,7α-cholanic acid. C24-Δ5-3β,7α-cholanic acid is then subjected to a reduction and dehydrogenation step by AKR1D1 and AKR1C4, to finally give CDCA (Pandak & Kakiyama, 2019). CDCA is then esterified to form tauro- and glyco-conjugates. At this point, all the tauro and glyco- cholic acid and CDCA conjugates are secreted into the bile via bile salt export pump (BSEP) and the bile secreted into the intestine. In the colon, conjugated BAs are hydrolysed to cholic acid and CDCA and 7α-dehydroxylated by bacterial bile salt hydroxylase (BSH) to give 3α-hydroxy-5β-cholanoic acid commonly called lithocholic acid (LCA) and 3a,12a-dihydroxy-5b-cholanoic acid called deoxycholic acid (DCA), respectively. As mentioned above, one of the pathways to control cholesterol levels and maintain its homeostasis is the induction or the inhibition of its metabolism to bile acids. In the liver, increased cholesterol levels due to the reverse cholesterol transport (RCT) and HDL endocytosis stimulates CYP7A1 synthesis and cholesterol elimination via the neutral BA pathway (Jp, 2006). Moreover, elevated intracellular cholesterol induces the sterol metabolism to the other cholesterol metabolites: the oxysterols. Oxysterols are ligands of the nuclear receptors called Liver X receptors. Upon LXRs activation, the expression of CYP7B1 gene is induced, and oxysterols further metabolised to BA though the acidic pathway (Pandak *et al.*, 2002).

Cholesterol is also the precursor of steroid hormones. Steroid hormones are referred to a broad class of mostly planar compounds possessing a tetracyclic structure, like cholesterol. In mammalian

cells are derived from cholesterol but, often possess different substituents on the A and C rings as well as a shorter side chain. They are classified based on their chemical structure and function into mineralocorticoids, glucocorticoids, androgens, and oestrogens (Schiffer *et al.*, 2019). Corticosteroids (mineral- and glucocorticoids) are synthesised in the adrenal cortex while androgens and oestrogens are produced in the gonads and in the placenta (Schiffer *et al.*, 2019). However, they all share the same precursor, pregnenolone, that is a direct cholesterol metabolite. The importance of steroid hormones in the regulation of water/salt equilibrium, energetic metabolism, and response to stress as well as sexual system development, differentiation, and pregnancy, requires a constant supply of these molecules (Schiffer *et al.*, 2019). It is immediately evident how cholesterol constitutes a vital compound for steroidogenic tissues, cholesterol must always encounter the need for the synthesis of new steroids therefore its physiological levels are constantly maintained upon threshold through *de novo* cholesterol synthesis and uptake from circulation.(Schiffer *et al.*, 2019)

It becomes evident that not just cholesterol itself, but its end-products constitute key mediators and essential components of several biological pathways, which greatly contributes to the well-being of mammalian organism. Human cells can regulate cholesterol metabolism based on different series of stimuli, including feedback mechanism based on cholesterol and steroid metabolites concentrations. The control of cholesterol metabolism to bile acids and steroid hormones can be cell or system specific. The extensive and detailed description of this mechanisms is out of the scope of this thesis and the reader is reminded to several reviews where it has been discussed (Schiffer *et al.*, 2019; Staels & Fonseca, 2009).

Oxysterols complete the range of cholesterol metabolites produced in eukaryotic cells. Oxysterols are oxidised form of cholesterol and represents intermediates in the bile acid synthesis, end products of cholesterol metabolism and bioactive molecules involved in the modulation of several pivotal pathways. In the next section of this thesis, this class of sterol lipids will be deeply described.

1.1.2 Oxysterols

Oxysterols are C_{27} oxygenated intermediates in cholesterol catabolism composed of a cyclopentane peridrophenanthrene body and a 17ß- isooctyl side chain, figure 1.9. The four fused ring structure possess a Δ^5 double bond at the A-B ring junction and *trans* junctions between B-C and C-D rings. This arrangement of the cholestane body forces the oxysterol to assume a planar, half-chair conformation. The other common features of oxysterols family are represented by a 3ß-hydroxyl moiety and two angular ß-methylene at C10 and C13. All these characteristics are inherited from the common precursor cholesterol but respect to the highly hydrophobic parent sterol, oxysterols possess additional oxygenated functions like hydroxyl, ketone, epoxide, or carboxylic groups on A- B ring or the side chain, which increased their hydrophilicity. Thanks to this characteristic, oxysterols can freely pass across cellular membranes and easily reach different cellular compartments or be excreted extracellularly, making them the perfect way for the cells to control cholesterol homeostasis (Lange *et al.*, 1995; Meaney *et al.*, 2002). Moreover, depending on the position of the additional oxygenated functions, oxysterols can modulate membrane dynamics and

properties as well as their orientation in the bilayer (Olsen *et al.*, 2008). Oxysterols were firstly identified in the late 50's as intermediates in the bile acids synthesis (Fredrickson & Ono, 1956) and further on as autoxidation products of cholesterol (L. L. Smith, 1987). Over the last twenty years oxysterols research has been focusing on structural elucidation, physiological formation and biological functions in healthy and disease states of human being (Björkhem, 2009; Brzeska *et al.*, 2016; de Medina *et al.*, 2022; Janowski, B. A.; Grogan, M. J.; Jones, S. A.; Wisely, G. B.; Kliewer, S. A.; Corey, E. J.; Mangelsdorf, 1999; Mutemberezi *et al.*, 2016a; Schroepfer, 2000a; Zmysłowski & Szterk, 2019).

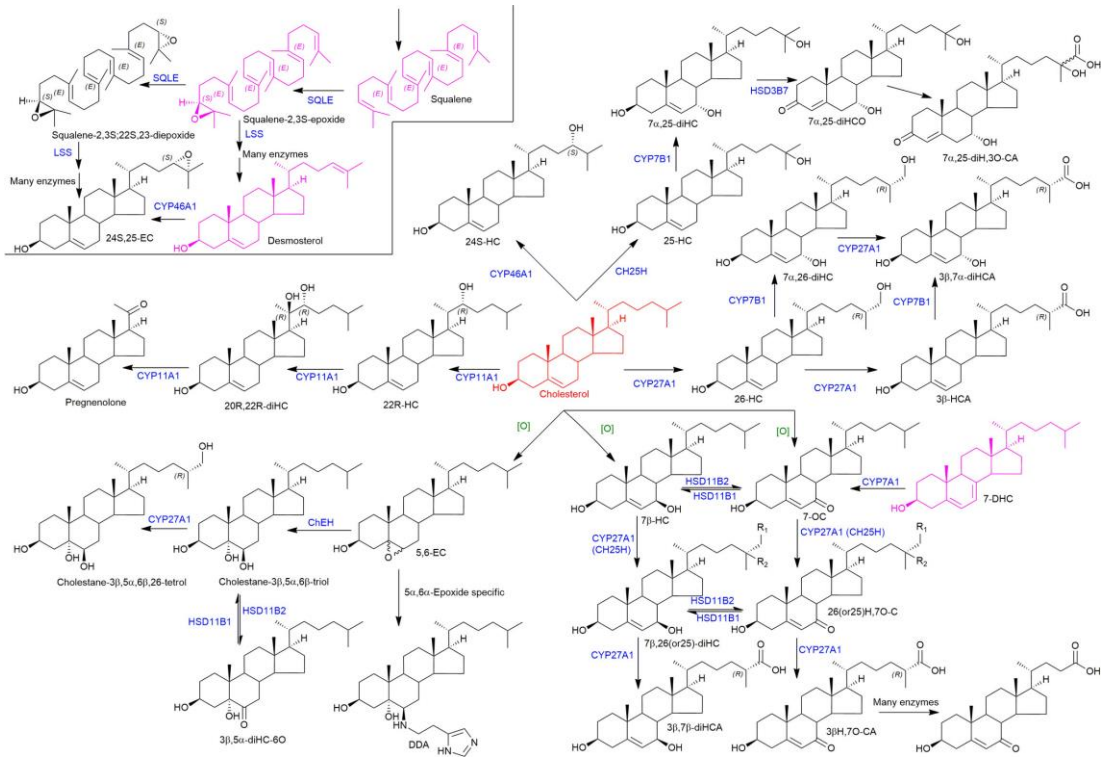

Figure 1.11 Cholesterol metabolism to oxysterols.
In this figure are presented the main, and known, metabolic ways to convert human cholesterol (in red) to its oxygenated form, the oxysterol (in black). The principal enzymes responsible for cholesterol metabolism are reported in blue while its precursors in pink. Autoxidation products of cholesterol are highlighted by the green oxygen molecule [O]. For the compounds 7ß,26-diHC and 26-HC,7O-

C, the substituents R1 and R2 are OH and H, respectively, while for compounds 7β,25-diHC and 25H,7O-C are H and OH, respectively. Figure taken from (Y. Wang, Yutuc, *et al.*, 2021)

Among the oxysterols found in human plasma, the monohydroxy sterols are usually the most represented ones, alongside cholestenoic acids. In the following sections are reported the most common and abundant monohydroxy sterols, their hydroxylation products and cholestenoic acids found in human. The attention will be focused on oxysterols formation, their biochemical function, and their involvement in certain illness. Note that other oxygenated cholesterol-derived products complete the human sterolome, however, their very low abundance united to the poor ionisable nature of these neutral molecules constitute a big challenge for their identification and quantification.

1.1.2.1 Monohydroxy and dihydroxy sterols

Most of the oxysterols found in human body are formed via enzymatic reactions catalysed by three main classes of enzymes: the cytochrome P 450 family, other the sterol hydroxylases, and hydroxysteroid dehydrogenases, see figure 1.11 (Y. Wang, Yutuc, *et al.*, 2021). However, some of them can also be formed through autoxidation process in tissue/cell compartments rich in reactive oxygen species (ROS) (L. L. Smith, 1987). The active form of this class of sterol lipids is the free-non esterified form, while inactivation is made through an Lecithin cholesterol acyl transferase LCAT-mediated esterification of the free hydroxyl function with fatty acids (Szedlacsek *et al.*, 1995a). Most circulating oxysterols are present as esters, while intracellular

oxysterols are usually abundant as un-esterified forms. The reason for the site-specific structure of these sterol lipids might reflect their role in the living organism: oxysterols are regulators of the intracellular cholesterol homeostasis and bioactive molecules involved in many cellular biochemical pathways. In the human cells, they exert their function, which is stimuli and cell/tissue specific, in their un-esterified form. Their activity is subsequently switched off upon esterification and excretion into the blood for elimination (Brzeska *et al.*, 2016).

The most abundant monohydroxy oxysterols found in human body fluids is the sterol 26-HC, also commonly known as 27-hydroxycholesterol (27-HC). 26-HC possess an additional OH group at C26 position of the sterol side chain. As discussed in the section 1.1.1.2, 26-HC is formed though CYP27A1 hydroxylation of cholesterol and represents the first metabolite in the alternative or acidic pathway of the bile acid formation. 26-HC has been extensively studied in the last decades because of its role in several pathological conditions, which arise from the many biological pathways in which it is involved (Y. Wang, Yutuc, *et al.*, 2021).

Firstly, 26-HC can regulate cholesterol intracellular levels through the induction of its metabolism to bile acids and by inhibiting SREBP-2 regulated *de novo* cholesterol synthesis in an INSIG-mediated manner (Radhakrishnan *et al.*, 2007). Moreover, the oxysterol is also a weak agonist of Liver X receptors LXRs (Janowski, B. A.; Grogan, M. J.; Jones, S. A.; Wisely, G. B.; Kliewer, S. A.; Corey, E. J.; Mangelsdorf, 1999; Janowsky, Bethany A.; Willy, P. J.; Rama Devi, T.; Falck, J. R.; Mangelsdorf, 1996). Upon LXRs activation, the expression of LXRs target genes, and cholesterol transporters, the ATP binding cassette A1 and G1 (ABCA1 and ABCG1), is induced

and cholesterol efflux promoted through RCT (Janowski, B. A.; Grogan, M. J.; Jones, S. A.; Wisely, G. B.; Kliewer, S. A.; Corey, E. J.; Mangelsdorf, 1999; Janowsky, Bethany A.; Willy, P. J.; Rama Devi, T.; Falck, J. R.; Mangelsdorf, 1996). Another characteristic of 26-HC is its ability to modify cell membrane dynamics (Bielska *et al.*, 2014). When incorporated in the plasma membrane, side-chain oxysterols, including 26-HC, increase the lipid disorder, especially in the presence of unsaturated fatty phospholipids, and expand the membrane. The oxysterol-induced membrane disorder increases membrane cholesterol accessibility by lowering the basal threshold for cholesterol activation. In this way, the membrane environment becomes more sensitive to little changes of cholesterol intracellular levels (Bielska *et al.*, 2014). More recently, 26-HC has also been found to be a potent selective oestrogen receptor (ER) modulator (SERM) (Dusell *et al.*, 2008; Umetani *et al.*, 2007). 26-HC activity towards the ER is cell specific. Hence, the sterol act as a competitive antagonist in the cardiovascular tissue (Umetani *et al.*, 2007), while as a partial agonist in the positive breast cancer cells (Umetani *et al.*, 2007). Interestingly, in ER negative cancer, 26-HC shows a completely different activity: if in ER+ enhances tumour growth and metastasis process, in the ER- it slower the cancer development (W. Liu *et al.*, n.d.). Therefore, 26-HC activity not only varies in a cell specific manner but also depends on the different subset of stimuli, in which modifications of receptor expressions might be probably involved. *et al.* All the activities reported above for 26-HC are referred to the free and active form of the oxysterols. Recently, 26-HC activity has also been tested against the new virus SARS-CoV-2 (Marcello *et al.*, 2020). The study demonstrates an inhibitory effect of 26-HC on SARS-CoV-2 infection without significant cells cytotoxicity (Marcello *et al.*, 2020). The same work shows a reduction as well in 26-HC

plasma levels of COVID-19 patients (Marcello *et al.*, 2020). The 26-HC anti-viral molecular mechanism has not been identified yet, however enhanced in membrane accessible cholesterol caused by incorporation of 26-HC has been proposed as a possible mechanism implicate in this activity. Seeing the many physiological roles held by 26-HC, there is strict control of its activity by its esterification or its further metabolised to 3ß-hydroxycholest-5-en-(25R)26-oic acid (3ß-HCA) or to 7α,26-diH), catalysed by CYP27A1 and CYP7B1, respectively. 7α,26-diHC is a dihydroxy sterol poorly represented in human plasma, where it accounts for few nanograms per mL (Dzeletovic *et al.*, 1995; Karuna *et al.*, 2015; Yutuc *et al.*, 2021). 7α,26-diHC is an Epstein Barr Virus-Induced gene G protein coupled-receptor (GPR-183) agonist. GPR-183 is a G coupled receptor belonging to the subfamily of rhodopsin A transmembrane protein (Daugvilaite *et al.*, 2014). The receptor is mostly expressed on the lymphoid cell surface, mostly by lymphocyte B and T, but also dendritic cells, monocytes, and astrocytes (Duc *et al.*, 2019) . It is believed that GPR-183 might be involved in the modulation of inflammatory response. GPR-183 exercises control on the adaptive immune response upon a chemoattractant activity controlled by a 7α,26-diHC and 7α,25-diHC gradient (C. Liu *et al.*, 2011a). The dihydroxy oxysterols direct GPR-183 expressing cells towards inflammation sites, which stimulates the migration of antigen-presenting cells to T and B lymphocytes and culminates into T and B cells specialisation.(Daugvilaite *et al.*, 2014).

Continuing with CYP-derived monohydroxy sterols, important to mention is the sterol (24S)-hydroxycholesterol (24S)-HC, which is the principal cholesterol metabolite in human brain (Lütjohann *et al.*, 1996a). (24S)-HC is another side-chain oxysterol possessing a second

OH functional group at C24 position. In humans, (24S)-HC is almost exclusively synthesised in the brain, but it can diffuse through the blood brain barrier and be redistributed in the blood stream and cerebrospinal fluid. The oxysterol formation involves the C24 hydroxylation of cholesterol, catalysed by the enzyme CYP46A1 which is almost exclusively expressed in neuronees (E. G. Lund *et al.*, 1999a) . The main function of (24S)-HC is to remove the excess of cholesterol from brain acting as its transport form. When brain cholesterol exceeds the healthy physiological levels, its catabolism to (24S)-HC is induced in neuronees. *et al.et al.*neuroneneurone. The oxysterol diffuses across neuronee plasma membrane into the extracellular compartment, where it can be further excreted into the blood passing the BBB or taken-up by astrocytes (Abildayeva *et al.*, 2006). In astrocytes, it can bind to LXR-RXR obligate heterodimer in the nucleus, inducing LXR activation, translocation to subnuclear compartments, and the expression of LXR target genes ABCA1 and ABCG1, the cholesterol transporters, and the apolipoprotein APOE for more details see section 1.2.1 (Abildayeva *et al.*, 2006). The increased expression of cholesterol transporters in the astrocytes triggers the cholesterol mobilisation to the neuronees and its metabolism. In addition to the LXR pathway, recent studies support an involvement of (24S)-HC in the control of SREBP-2 mediated cholesterol synthesis, suggesting a suppression of SREBP-2 via INSIG binding (Cartagena *et al.*, 2010; Y. Wang *et al.*, 2008). If not take-up by astrocytes, (24S)-HC is constantly excreted into the blood, with a daily efflux of about 6-7 mg/day (Gliozzi *et al.*, 2021). This process is also fundamental to maintain physiological cholesterol levels in brain cells as the sterol cannot freely pass the blood-brain-barrier (BBB). In plasma, (24S)-HC can be present as either free or esterified form in LDL or HDL. Free or LDL/HDL (24S)-HC reaches

the liver where it can be converted to bile acids through 24-hydroxycholesterol-7α-hydroxylase, CYP39A1, hydroxylation and 7α,(24S)-dihydroxy cholesterol, 7α(24S)-diHC, formed (Li-Hawkins *et al.*, 2000). In the liver, (24S)-HC can be also conjugated with glucoronate and sulphate groups for final elimination (Björkhem *et al.*, 2001). For a long time, it has been believed that the main function of (24S)-HC was the regulation of brain cholesterol metabolism, however, the oxysterol has also other important biological implications. (24S)-HC is a potent positive allosteric modulator of the N-methyl-D-aspartate (NMDA) receptor. NMDA is a heterotetrametric ligand-gated ion channel which regulate neuronees excitatory synapses through the formation of a net flux of calcium (Husi, 2004). Upon glutamate and glycine binding, NMDA endogenous ligands, the flux of calcium ions forms an inward current that depolarise postsynaptic neuronees, the location of NMDA (Hansen *et al.*, 2018). With respect to the other glutamate receptors, NMDA provides a slow but constant flow of current, inducing the so-called long-term potentiation (LTP) (Hansen *et al.*, 2018). LTP is involved in the learning and memory process thanks to its ability to form new synapses while strengthening the new and the old ones (Hansen *et al.*, 2018; Husi, 2004). (24S)-HC binds the NMDA channel in an allosteric binding site causing a conformational change which reduces the subthreshold stimuli necessary to induce LTP (S. M. Paul *et al.*, 2013). On top of that, it has been demonstrated that (24S)-HC is also able to act in a both autocrine and paracrine way in the synaptic space (S. M. Paul *et al.*, 2013). Furthermore, (24S)-HC showed to be a ligand for the Smoothened (SMO) protein (Qi *et al.*, 2019). SMO is a transmembrane GPCR protein involved in the activation of the hedgehog (Hh) pathway. Hh pathway induction is essential for embryonic cell differentiation and development (Rohatgi

et al., 2007). Upon (24S)-HC binding, SMO is activated and can translocate into the primary cilium to activate the glioma-associated-oncogene protein or Gli transcription factor, which will then induce the synthesis of Hh associated genes (Qi *et al.*, n.d.; Raleigh *et al.*, 2018; Rohatgi *et al.*, 2007).*et al.et al.et al.et al.et al.et al.*

All the sterols reported thereby constitutes the main mono-oxygenated, CYP-derived side-chain oxysterols, found in human plasma. However, other enzymes can be involved in the production of monohydroxy sterols. A clear example is represented the 25-hydroxysterol (25-HC). 25-HC is formed through a cholesterol C25 side chain carbon hydroxylation, catalysed by the enzyme cholesterol-25-hydrolase (CH25H). CH25H is an oxidoreductase which favours the reduction of molecular O_2 and the simultaneous oxidation of cholesterol (Fox *et al.*, 1994). *et al.et al. Even* if CH25H represents the preferrable way for 25-HC production, it should be mentioned that also CYP3A4, CYP27A1 and CYP46A1 can produce the oxysterol, however as a side product of oxidations (W. J. Griffiths & Wang, 2020; Honda *et al.*, 2011; E. G. Lund *et al.*, 1999b). With respect to the other CYP-derived oxysterols, 25-HC plasma and tissue levels are normally quite low but stable, in the range of few nanograms per mL of plasma (Stiles *et al.*, 2014a). However, it can rapidly change in non-physiological conditions, mostly during pathogen-derived inflammation (Zhao *et al.*, 2020). During inflammatory events, 25-HC concentration can rise-up to 200 ng/mL (total, free plus esterified, 25-HC plasma content), indicating a clear role for this molecule in the inflammatory process (Bauman *et al.*, 2009) . There are still concerns about whether 25-HC can play a pro- or anti-inflammatory role during viral and bacterial infections. However, the growing amount of evidence indicates a double role for

the sterol which are stimuli and extracellular environment dependent but also immunity cell type specific, innate, or adaptive (Zhao *et al.*, 2020). *et al.et al.et al.et al.* Some studies suggested 25-HC to have a pro-inflammatory effect through the induction of the nuclear factor kappa-B (Nf-KB) signalling, and consequent production of interleukin IL-6, tumour necrosis factor (TNF) (Pokharel *et al.*, 2019) or through extracellular signal-regulated kinase 1/2 (ERK1/2) pathway, and consequent production of interleukin 8 (IL-8) (Lemaire-Ewing *et al.*, 2009). On the contrary, other recent findings associate increased 25-HC levels to anti-inflammatory activity upon Nf-KB pathway inhibition (Reboldi *et al.*, 2014). *et al.* Furthermore, macrophages derived- 25-HC is also believed to regulate innate immunity in an LXR-dependent fashion (A-Gonzalez *et al.*, 2009; Joseph *et al.*, 2004; Korf *et al.*, 2009). It becomes clear that 25-HC is an important signalling molecule rather than a solely cholesterol metabolism regulator, but deeper understanding is needed to clarify its contribution during infections. *et al.et al.et al.et al.*

The broad varieties of pathways in which 25-HC is or seems to be involved along with the concentration-dependent activity reflects the contrasting findings upon immunity regulation brought by this sterol. To complicate even more the scenario, the main metabolite of the monohydroxy sterol, 7α,25-dyhydroxycholesterol or 7α,25-diHC, has been proven to be the most potent chemoattractant sterol for B and T-cells expressing GPR183 receptors (Hannedouche *et al.*, 2011; C. Liu *et al.*, 2011b). 7α,25-diHC is synthesised through C-7 hydroxylation of 25-HC by CYP7B1, introducing a second hydroxyl group into the sterol body. With respect to the parent sterol, 7α,25-diHC shows only a chemoattractant activity and not anti-

inflammatory ones (Hannedouche *et al.*, 2011; C. Liu *et al.*, 2011) and no effects on SREBP-2 cleavage nor on LXRs activation. The dihydroxy sterol is also an intermediate metabolite in bile acid formation and a substrate for HSD3B7 which catalysed an oxidative reaction at the 3ß-OH position, forming 7α,25-dihydroxycholest-4-en-3-one (7α,25-diHCO). 7α,25-diHCO plasma levels are very low (Karuna *et al.*, 2015) however, it is a SMO agonist, possibly playing an important role in cell differentiation (Abdel-Khalik *et al.*, 2021).

Alongside 7α,25-diHC, 7ß,25-dyhydroxycholesterol (7ß,25-diHC) is also present in human plasma. With respect to its epimer, 7ß,25-diHC biosynthesis is still uncertain but it is believed to be originated through C-25 hydroxylation of 7ß-hydroxycholesterol (7ß-HC) by CH25H. 7ß,25-diHC, like its isomer, is a ligand and an agonist of SMO (Abdel-Khalik *et al.*, 2021) as well as an activator of GPR183, exerting the same chemoattractant activity towards immune cells (Hannedouche *et al.*, 2011; C. Liu *et al.*, 2011b). In addition, 7β,25-diHC can be further oxidised by HSD11B, which converts the 7-hydroxy function into a 7-keto one, forming 3ß,25-dihydroxycholest-4-en-7-one, 25H,7O-C. Interestingly, 25H,7O-C can be also interconverted to 7ß,25-diHC by HSD11B. This reaction might be involved in the switching off the pro-inflammatory activity of 7ß,25-diHC, as 25H,7O-C is not a ligand of GPR183 (Abdel-Khalik *et al.*, 2021).

7ß,25-diHC belongs to the class of sterols which derived from the lipid peroxidation of cholesterol, the autoxidation derived-oxysterols (Zielinski & Pratt, 2016). Along with 7ß,25-diHC and 7ß-HC, the most abundant plasma autoxidation sterols are 7-oxocholesterol, 7-OC, and 6ß-dihydroxy cholesterol, 6ß-HC. The autoxidation of cholesterol is a quite common event, being the sterol molecule vulnerable to free

radical oxidative attack, particularly in its reactive points in A and B rings. Therefore, it is legitimate to questioning on the origin of autoxidation derived oxysterols when analysing biological matrixes, whether it is a solely artefact of peroxide oxidation ex-vivo or endogenous formation. Even though some lines of evidence link peroxidation oxysterols to disease development, e.g., Griffiths *et al.* found elevated 7β-HC plasma levels in patients affected by Niemann Pick type C disorder (Griffiths, Yutuc, *et al.*, 2019), there are too many uncontrollable factors which can contribute to spontaneous and unmanageable autoxidation. Hence, without knowing the exact impact of peroxidation to the oxysterol levels, data should be interpreted with care and the use of antioxidant should be preferred when the analysis focus on this class of sterols. In this thesis the main research focus is on the enzymatic derived cholesterol metabolites, as such autoxidation oxysterols remains only a marginal aspect of this study. For a deep explanation of cholesterol autoxidation and relative products the reader is invited to see the Iuliano and Zerbinati paper where the argument is extensively explained (Zerbinati & Iuliano, 2017) .

Among the oxysterols found in human plasma, there is one which does not directly derive from cholesterol oxidation but rather from its precursors: (24S,25)-epoxycholesterol, (24S,25)-EC. There are two possible ways which bring to the formation of (24S,25)-EC: one is represented by a shunt of the classical cholesterol synthetic pathway, the Bloch pathway (see the section 1.1.1.2) (J. A. Nelson *et al.*, 1981) while the second involves the hydroxylation of desmosterol by CYP46A1, figure 1.11 (Goyal *et al.*, 2014). The first pathway involves a double epoxidation of squalene involving C2 and C3 carbons as C22 and C23, catalysed by the enzyme squalene monooxygenase SQLE to

give 2,3S-22S,23-dioxosqualene. 2,3S-22S,23-dioxosqualene then follows the same set of reactions its parent 2,3S-oxosqualene undergoes (see section 1.1.1.2 and figure 1.11) to give (24S,25)-EC and cholesterol, respectively. (24S,25)-EC is very underrepresented in biological samples because of the high reactivity towards hydrolytic reactions and nucleophilic attack of the epoxide and consequent ring opening(W. J. Griffiths *et al.*, 2013; Stiles *et al.*, 2014b). Nonetheless (24S)25-EC is on the most potent LXR agonist (Janowski, B. A.; Grogan, M. J.; Jones, S. A.; Wisely, G. B.; Kliewer, S. A.; Corey, E. J.; Mangelsdorf, 1999; Janowsky, Bethany A.; Willy, P. J.; Rama Devi, T.; Falck, J. R.; Mangelsdorf, 1996; Peet, Janowski, *et al.*, 1998) and the most potent endogenous oxysterol to activate the Hh pathway upon SMO binding (Raleigh *et al.*, 2018). (24S,25)-EC also shares the capacity to block cholesterol synthesis and be a master regulator of cholesterol homeostasis though INSIG binding and inhibiting of the SREBP-2 mediated cholesterol biosynthesis (Radhakrishnan *et al.*, 2007).

In this section we reported the main mono- and dihydroxy sterols found in human body, which derived from cholesterol, or its precursors, oxidation. However, other, less represented, oxysterols can be found in mammalian and human organisms, most of which have been identified only in relations to pathological conditions where cholesterol homeostasis disruption would have brought to an accumulation (Brzeska et al., 2016; Marelli et al., 2018; Zmysłowski & Szterk, 2019) . The next section will be dedicated to the metabolites of mono and dihydroxy sterols, which are usually the most represented sterols in human body fluids: the cholestenoic acids.

1.1.2.2 Cholestenoic acid

Cholestenoic acids are C_{27} cholestane sterols formed as intermediates of both classical and acidic bile acid biosynthetic pathways (Meaney *et al.*, 2003; Yutuc *et al.*, 2021). Cholestenoic acids are characterised by the presence of a carboxylic group at C-26 of the sterol side chain, which confers a more hydrophilic nature respect to the precursor oxysterols and cholesterol. The acids have been considered for many years only as a form of extrahepatic cholesterol transport, metabolism, and excretion, however, they are themselves important bioactive molecules (Schöls *et al.*, 2017; Theofilopoulos *et al.*, 2014; Yutuc *et al.*, 2021) as well as nuclear receptors ligands (Ogundare *et al.*, 2010a; Song & Liao, 2000; Theofilopoulos *et al.*, 2014). The major cholestenoic acids found in human plasma are CA, 3ß,7α-dihydroxy-5-cholestenoic acid (3ß,7α-diHCA), and 7α-hydroxy-3-oxo-4-cholestenoic acid (7α-H-3O-CA), with a concentration of hundreds of ng per mL of plasma (Meaney *et al.*, 2003). Researcher have deeply investigated the origin of these molecules, as emerging evidence associates them with putative biological functions. The studies have evidenced that they are mainly synthesised from extrahepatic tissues and subsequently taken up by liver cells for further metabolism to bile acids (Meaney *et al.*, 2003). Specifically, Meaney *et al.* demonstrate that the cholestenoic acid CA found in human plasma comes from mainly extrahepatic CYP27A1-mediated- 26-HC hydroxylation and that there is a net daily uptake of CA in the liver (Meaney *et al.*, 2003). Moreover, 3ß,7α-diHCA plasma levels strongly correlates with CA ones but there is no correlation with 7αH,3O-CA, indicating not only the plausible formation of 3ß,7α-diHCA from CA, but also its extrahepatic origin (Meaney *et al.*, 2003). 3ß,7α-diHCA is

formed through the C-7 hydroxylation of CA by CYP7B (Meaney *et al.*, 2003). In the same study it has been demonstrated that 7α-H-3O-CA positively correlates with 7α-HC and 7-OC plasma levels, which are considered biomarker of liver activity (Axelson *et al.*, 1988, 1991; Meaney *et al.*, 2003). However, Bjorkhem lab demonstrated that there is also a net daily uptake of 7α-H-3O-CA in the liver, suggesting an extrahepatic metabolism of 7α-HC and/or 7-OC to the cholestenoic acid (Axelson *et al.*, 1988). Interestingly, the cholestenoic acids are not exclusively present in human liver, even if synthesised elsewhere, but also in CSF and brain, suggesting an additional pathway involved in the maintenance of brain cholesterol metabolism (Meaney *et al.*, 2007; Ogundare *et al.*, 2010a; Theofilopoulos *et al.*, 2014). Furthermore, recent studies report the ability of 3β,7α-diHCA to promote motor neuronees survival through an LXR-mediated fashion and of its oxidised form, 7α-H-3O-CA, to promote their maturation to adult motor neuronees, but not in an LXR-dependent manner (Theofilopoulos *et al.*, 2014). On the other side, CA has demonstrated to have a cytotoxic effect on the same cells (Theofilopoulos *et al.*, 2014). It becomes clear how cholestenoic acid are not synthesised to be only cholesterol regulators, but they also seem to be involved in developmental process in the brain. In a 2021 paper, Abdel-Khalik *et al.* show the ability of 7α-H-3O-CA to activate the Hh signalling through SMO binding (Abdel-Khalik *et al.*, 2021). The contribution of bile acid precursors to human cells development makes them a new potential druggable target for a broad window of diseases, nevertheless there is still need for clarifications and more studies are being carrying out.

1.2 Oxysterols bioactivity

Classically, oxysterols have been considered only as a metabolic step to favour the elimination of the endogenous lipid cholesterol, although following evidence showed their contribution to the regulation of many essential biochemical pathway (Mutemberezi *et al.*, 2016a). The next paragraphs will give the reader a deeper look through oxysterols bioactivities, concentrating on the general molecular mechanism in which they exert their function and, whether possible, on the structural-activity relationship.

1.2.1 Oxysterols as regulators of cholesterol homeostasis

The importance of cholesterol for eucaryotic cell development, survival and signalling is nowadays well established. It depends on the sterol structural properties and modulation of plasma membrane functions (Das *et al.*, 2014; Lange *et al.*, 1999; Yeagle, 1991), and on the modulation of several metabolically active pathways, as it constitutes the starting material for the synthesis of the bile acids, adrenal and mineral and cortico-steroid hormones (Chiang, 1998; J. Hu *et al.*, 2010; Miller & Auchus, 2011; Sanderson, 2006). As a result, evolution built a complex and intricated machinery through which cholesterol homeostasis can be maintained, preventing cholesterol accumulation, which it has been demonstrated to be cytotoxic (M. S. Brown & Goldstein, 1997).

One of the main ways through which cholesterol physiological intracellular levels are maintained is its biosynthesis regulation (Duan *et al.*, 2022; Gliozzi *et al.*, 2021). Initially, it was believed that cholesterol alone could act as a negative feedback regulator of its own synthesis but Kandutsch, Chen, and Heinige proposed the Oxysterol Hypothesis of Cholesterol Homeostasis (Kandutsch *et al.*, 1978). Nowadays it has been proved that both oxysterols and cholesterol act in a concert manner towards the regulation of the sterol physiological levels. The diverse mechanism, including the negative feedback regulation of cholesterol ER synthesis, promoted by intracellular cholesterol overload is widely described in section 1.1.1 of this thesis. Here we described the different contribution of the oxysterols to the control of cholesterol levels, see figure 1.12.

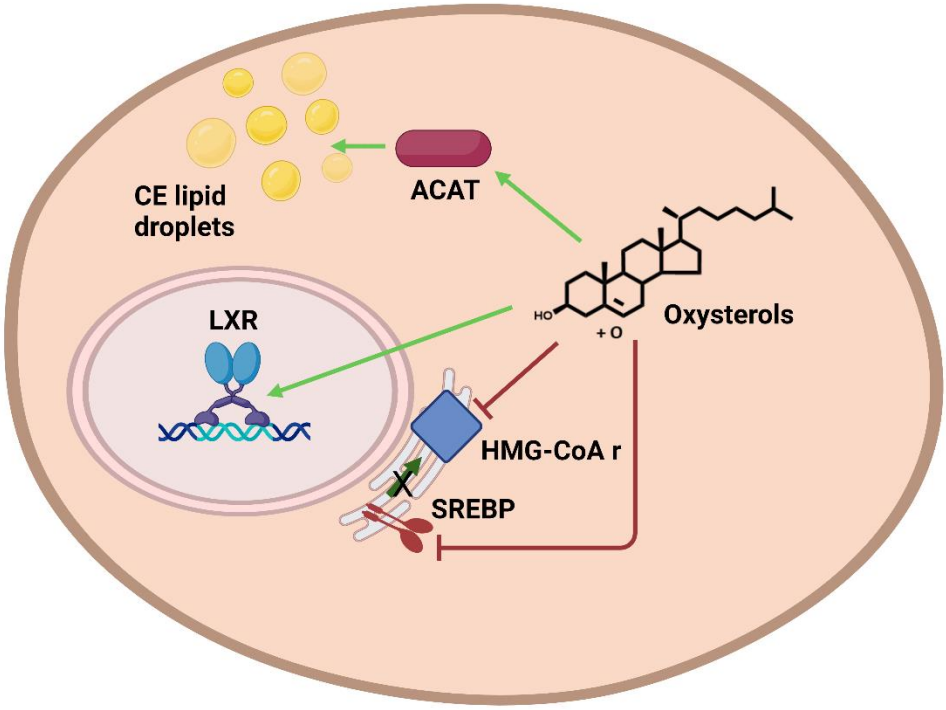

Figure 1.12 Oxysterols transcriptional and non-transcriptional mechanisms for controlling cholesterol homeostasis.
The trancritpional pathway to control cholesterol homeostasis involved both an oxysterols inhibition of the SREBP induced production of HMG-CoA r and an induction of the LXR mediated

reverse cholesterol transport. On the other side, the non-transcriptional mechanism consists of a direct induction of the ACAT driven cholesterol esterification and accumulation in cytosilic lipid droplets as well as degradation of the HMG-CoA r.

A noticeable property of oxysterols is their ability to induce very rapid changes in cellular cholesterol levels, which can be manifested with a timescale of minutes to hours. It is proposed that the first line of action of oxysterol in response to cholesterol level modification is an acute response exerted at a-non transcriptional level. This fast reaction involves the induction of cholesterol esterification and accumulation in lipid droplets (Cheng *et al.*, 1995; Lange & Steck, 1997; Okwu *et al.*, 1994; Pannu *et al.*, 2013; Weingärtner *et al.*, 2010), promotion of 3-hydroxymethylglutaril-CoA reductase, HMG-CoA r, degradation (Jo & DeBose-Boyd, 2010) and the modification of cholesterol membrane pools, which leads mobilisation of active cholesterol from plasma membrane to the ER, where inhibits its synthesis (Bielska *et al.*, 2014; W. J. Griffiths & Wang, 2021; Schroepfer, 2000a). The time-consuming effect is to be ascribed to transcriptional regulation of cholesterol synthesis and a modification of its uptake and efflux though nuclear and transmembrane receptors binding (Beyea *et al.*, 2007; Forman *et al.*, 1997; Nohturfft *et al.*, 1998; Peet, Janowski, *et al.*, 1998; Radhakrishnan *et al.*, 2007)(Pannu *et al.*, 2013; Weingärtner *et al.*, 2010).

Oxysterols' ability to reduce cholesterol synthesis was firstly identified by Kandutsch and colleagues in 1978 when they showed a direct inhibitory effect of HMG-CoArby oxysterols when directly added cultured cells (Kandutsch *et al.*, 1978). Soon after other studies demonstrated that side chain oxidised oxysterols, but not ring-oxidised ones, were able induce the degradation of HMG-CoAr

through the INSIG protein binding (Jo & DeBose-Boyd, 2010). When cholesterol levels exceed the physiological 5% mol in the ER, the sterol is immediately converted into its more soluble form, oxysterols, which accumulate in the ER and bind to the INSIG protein (Jo & DeBose-Boyd, 2010). The oxysterols-INSIG binding induce the recruitment of the ubiquitin ligase gp78 which in turn, induces the ubiquitination of HMG-CoA r and its consequent proteasomal degradation(Jo & DeBose-Boyd, 2010).

Side chain oxysterols, in particular 25-HC, are also potent positive allosteric modulator of the Acyl-coenzyme A: cholesterol acyltransferases ACAT enzyme . When intracellular cholesterol levels rise above the physiological, the sterol metabolism rise and the resulting oxysterols boost ACAT activity, dictating an increase of cholesterol esterification and accumulation in lipid droplets (Cheng *et al.*, 1995; Du *et al.*, 2004).

The transcriptional regulatory activity of oxysterols is classically reconducted to the inhibition of the SREBP-2 transcription factor (Eberlé *et al.*, 2004; Nohturfft *et al.*, 1998; Radhakrishnan *et al.*, 2007). Similarly, to cholesterol, oxysterols can block SREBP-2 transport to the Golgi and consequent cleavage to its active form (M. S. Brown & Goldstein, 1997; Horton *et al.*, 2002a; Nohturfft *et al.*, 1998; Radhakrishnan *et al.*, 2007). Respect to the parent sterol which exercises its inhibitory activity through SCAP binding, oxysterols bind to INSIG protein instead (Radhakrishnan *et al.*, 2007). Radhakrishnan *et al* demonstrated in a structure-activity relationship (SAR) study that the tetrahydro cyclopentane phenanthrene nucleus and the isooctyl side chain are fundamental structural requirements for binding, shared with SCAP protein (Radhakrishnan *et al.*, 2007). However, an oxygenated, polar, group

on the C22, 24, 25, or 26, is fundamental for INSIG activity and binding but not for SCAP (Radhakrishnan *et al.*, 2007). Regardless of what protein is bonded first, cholesterol and oxysterols block the transcriptional activity of SREBP-2 through the formation of an INSIG-SCAP-SREBP-2 complex, which keep the protein anchored to the ER membrane. Through the blockage of SREBP-2 function and consequent suppression of cholesterol synthesis, the cholesterol metabolites effectively reduce the lipid intracellular concentration, largely contributing to the homeostasis maintenance.

Oxysterols are also able to keep cholesterol physiological levels through the modulation of its uptake, intracellular transport, and excretion.(Beyea *et al.*, 2007; Duval *et al.*, 2006; Forman *et al.*, 1997; Janowski, B. A.; Grogan, M. J.; Jones, S. A.; Wisely, G. B.; Kliewer, S. A.; Corey, E. J.; Mangelsdorf, 1999; Janowsky, Bethany A.; Willy, P. J.; Rama Devi, T.; Falck, J. R.; Mangelsdorf, 1996; Mutemberezi *et al.*, 2016a; Peet, Janowski, *et al.*, 1998; Schroepfer, 2000a; Venkateswaran *et al.*, 2000; N. Wang *et al.*, 2006). Notably, LXR activation through oxysterols binding is required for the abovementioned activities (Janowski, B. A.; Grogan, M. J.; Jones, S. A.; Wisely, G. B.; Kliewer, S. A.; Corey, E. J.; Mangelsdorf, 1999; Janowsky, Bethany A.; Willy, P. J.; Rama Devi, T.; Falck, J. R.; Mangelsdorf, 1996; Peet, Janowski, *et al.*, 1998; Peet, Turley, *et al.*, 1998). Liver X receptors or LXRs are transcriptional factors belongings to the nuclear receptors' superfamily. Firstly identified in the 90's (Apfel *et al.*, 1994; Seol *et al.*, 1995; Shinar *et al.*, 1994; Song *et al.*, 1994; Teboul *et al.*, 1995; Willy *et al.*, 1995), the LXR family is composed of two distinct isoforms, LXRα and LXRß. LXRα is manly expressed in steroidogenic systems and tissues, also involved in the general lipid metabolism, like liver, spleen, brain, kidney, adipose

tissue, pituitary and adrenal gland (Auboeuf *et al.*, 1997; Song *et al.*, 1994; Teboul *et al.*, 1995) while LXRß is ubiquitously expressed in all extra-hepatic tissues (Kainu *et al.*, 1996; Song *et al.*, 1995). However, the two isoforms have a quite conserved DNA and amino acid sequences, sharing a 77%*)* amino acid identity. The LXR protein is composed of four different domains:

a. The **ligand independent transactivation domain**, involved in the transcriptional activation of the LXRs in the absence of a ligand.
b. The **two zinc-fingers DNA binding domain**, required for anchoring the transcription factor to the LXR responsive elements (LXRE)on the DNA
c. The **ligand binding domain**, represented by a hydrophobic pocket which can accommodate the ligand and cause a conformational change in the LXR structure fundamental for dimerization and transactivation.
d. The ligand dependent **C-terminal** which serve to stimulate transcription upon ligand binding.

In the steady-state form, LXRs form an obligate heterodimer with the transcription factor Retinoid X receptor (RXR) in the nucleus of the cell and bind to LXREs in the promoter region of the target gene (Wójcicka *et al.*, 2007). LXREs are a repeated sequence of 5'-AGGTCA-3', separated by four nucleotides (Wójcicka *et al.*, 2007), usually known to have an invariant nucleotide on the consensus sequence. However, the four nucleotide spacers might vary a lot, and these differences can modify the affinity each of the two isoforms of LXRs have for them, and so on their different transcriptional activities (Edwards *et al.*, 2002; Joseph *et al.*, 2002).

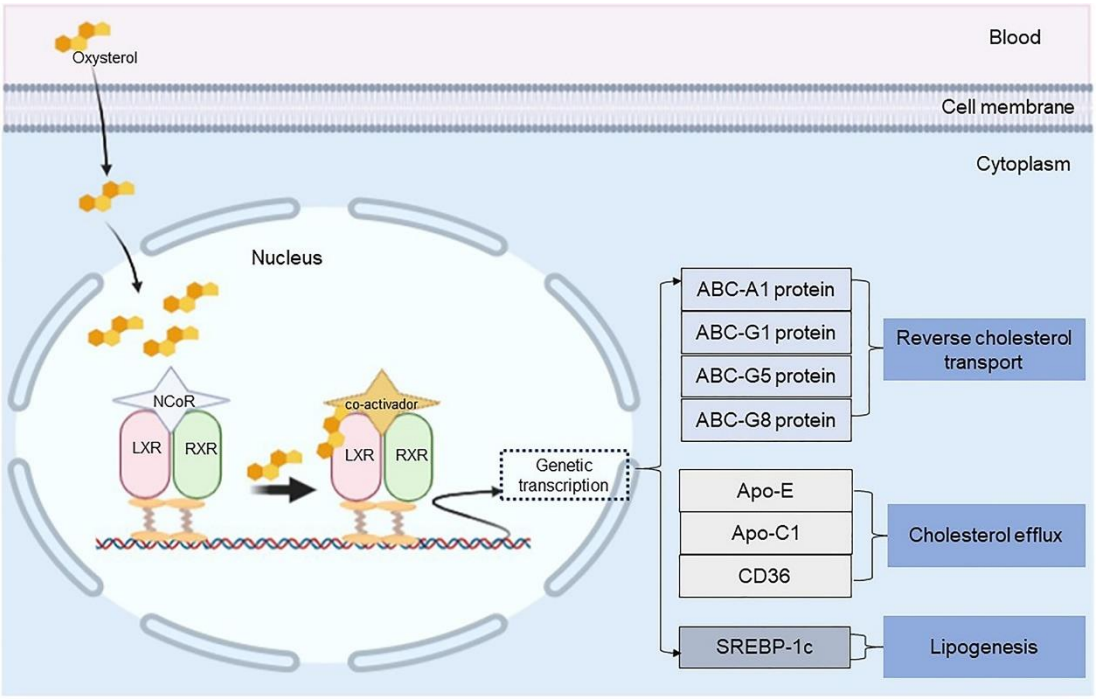

Figure 1.13 Oxysterols are endogenous ligand to the nuclear receptors LXRs.
Oxysterols binding to LXRs determines the release of the co-repressors complex and the transcriptional activation of the nuclear receptors, which results in the induction of reverse cholesterol transport, efflux, and lipogenesis. Figure taken from (Reichert *et al.*, 2021)

The oxysterols 25-HC, (24S)-HC, and (24S,25)-EC are endogenous the ligands of LXRs, able to effectively activate the nuclear receptors at micro/nano molar concentration, which resembles the physiological intracellular levels of the free, un-esterified oxysterols (Janowski, B. A.; Grogan, M. J.; Jones, S. A.; Wisely, G. B.; Kliewer, S. A.; Corey, E. J.; Mangelsdorf, 1999; Janowsky, Bethany A.; Willy, P. J.; Rama Devi, T.; Falck, J. R.; Mangelsdorf, 1996). Depending on the phenotypic expression and tissue distribution of the LXRs, endogenous oxysterols keep cholesterol homeostasis upon LXR binding through, see figure 1.13:

i. Induction of the reverse cholesterol transport RCT
ii. Inhibition of cholesterol intestinal absorption

The RCT process has been extensively described in the section 1.1.1.2 and here will be reported only the contribution of the oxysterols to it. Upon elevated intracellular cholesterol levels, oxysterols bind to LXRs determining the recruitment of co-activator complexes and inducing the expression of cholesterol transporters ABCA1 and G1, main LXR target genes, in liver, small intestine, adipocytes, brain, steroidogenic tissues, and macrophages (lo Sasso *et al.*, 2010; Ouimet *et al.*, 2019; Pannu *et al.*, 2013; Weingärtner *et al.*, 2010; X. Xu *et al.*, 2022; Yasuda *et al.*, 2010). Oxysterols can increase up to 1000-fold the expression of ABCA1/G1 via LXRs binding and consequently induce the creation of a cholesterol-loaded HDL, which pushes RCT and effectively diminishes cholesterol intracellular levels (X. Xu *et al.*, 2022). (Beyea *et al.*, 2007; Jun *et al.*, 2013; N. Wang *et al.*, 2006). Moreover, another LXR target gene is APOE which is also involved in the RCT, but mainly in the Central Nervous System (CNS) (Courtney & Landreth, 2016). APOE and ABCA1 over expression is selectively induced in case of excessive intracellular cholesterol upon oxysterols LXRs activation in astrocytes and neuroneal cells, determining the formation of a cholesterol-loaded HDL and restoring cholesterol physiological levels (Chang *et al.*, 2017; Courtney & Landreth, 2016; Gliozzi *et al.*, 2021).

Oxysterols LXR activation can potently inhibit cholesterol intestinal absorption through the overexpression of the nuclear receptor target genes for ABCG5 & ABCG8, cholesterol transporters located on the enterocyte's plasma membrane and involved in the execration of free cholesterol form the enterocyte to the lumen for faecal elimination (Zein *et al.*, 2019). The LXR-induced expression of the transporter stimulates the elimination of free cholesterol (Repa *et al.*, 2000, 2002).

*et al.et al.*Since the identification of LXRs endogenous ligands in early 90's and the discovery of contributions to the maintenance of cholesterol homeostasis, oxysterols biological functions have grown more and more attention around the scientific community. The last two decades have been dedicated to study and interpretation of oxysterols biological effects, shedding lights on the molecular pathways initiated or modified by the sterol molecules (W. J. Griffiths & Wang, 2018, 2019b, 2022; M.-W. Kim *et al.*, 2020; Y. Wang, Yutuc, *et al.*, n.d.; Yutuc *et al.*, 2021)

1.2.2 Oxysterols and immunity

In the previous paragraphs we understood the importance of oxysterols in the regulation of cholesterol intracellular physiological levels and how little changes in oxysterols levels can profoundly affect cholesterol levels. Seen the plethora of different cellular pathways in which oxysterols have been proved to have a role or participation to the maintenance of healthy sterol concentration, further investigations have shown how these mechanisms can contribute to the regulation of different cell functions (W. J. Griffiths & Wang, 2018, 2019b; Y. Wang, Yutuc, *et al.*, 2021.). As an example, over the last twenty years, evidence showed how some oxysterols can influence the outcome of a microbial infection through the regulation of inflammatory response(W. J. Griffiths & Wang, 2021, 2022).

Among all the endogenous sterols, 25-HC is the one which seems to be most involved in the modulation of the immune response. It has been demonstrated that bacterial lipopolysaccharide (LPS) is able to tremendously increase the levels of 25-HC upon activation of toll-like receptors 3 and 4 (TLR-3 and -4), in both several immune cell lines (Dennis *et al.*, 2010) (Bauman *et al.*, 2009) and in human (Diczfalusy *et al.*, 2009). The increase in 25-HC in response to bacterial infection is believed to be one of the possible mechanisms involved in the anti-inflammatory response exerts by immune cells. Hence Baumann *et al.* demonstrated the ability of 25-HC to modulate the adaptive immune cells response by blocking the lymphocytes B class-switch recombination and consequent immunoglobulin A production. (Bauman *et al.*, 2009). Another way the oxysterols have been shown to contribute to the immune response regulation is through the modification of plasma membrane properties (Abrams *et al.*, 2020;

Dang *et al.*, 2020; Zhou *et al.*, 2020). In a recent study of 2020, Zhou *et al.* demonstrate the ability of 25-HC to prevent bacterial infection upon modification of membrane accessible cholesterol content upon porin-toxins stimulation (Zhou *et al.*, 2020).

25-HC, and other oxysterols like 26-HC and (24S,25)-EC, have been shown to also have anti-inflammatory and anti-viral properties which are exerts upon similar pathways, including SRBEP-2 pathway modulation, remodelling of plasma membrane through reduction of free accessible cholesterol and consequent inhibition of viral replication (W. J. Griffiths & Wang, 2021). All the above mechanism are extensively and well described in a recent review form Griffiths *et al.* (W. J. Griffiths & Wang, 2022).

1.2.3 Oxysterols and Hedgehog pathway

Oxysterols cannot be considered as solely guardians of cholesterol homeostasis but proper signalling molecule, able to regulate a series of different fundamental biological pathways and exerting autocrine and paracrine effects. One good example of their signalling-like activity is the modulation of the Hedgehog pathway (Hh). Hh pathway is a well conserved mechanism through which vertebrates' cells coordinate cell-cell communication and regeneration, especially during organogenesis (Jacob & Lum, 2007). Defective Hh signalling can bring to cancer development or birth defects (Cochrane *et al.*, 2015; Gupta *et al.*, 2010; Jacob & Lum, 2007; Katoh & Katoh, 2009; T. L. Lin & Matsui, 2012). Side chain oxysterols have been identified as new potential endogenous ligands of the Hh pathway, as they are able to activate Hh signalling in the absence of the Sonic Hedgehog glycoprotein, SHH, the Hh's endogenous activator.(Nachtergaele, S.; Mydock, L.; Krishnan, K.; Rammohan, J.; Schlesinger, P. H.; Covey, D. F.; Rohatgi, 2012; Nedelcu *et al.*, 2013; Raleigh *et al.*, 2018). (24S,25)-EC has been identified as Hh signalling activator, able to bind the G-coupled transmembrane protein Smoothened (SMO) which is responsible for the initialization of the Hh cascade, (Carballo *et al.*, 2018). However, there is still a lack of knowledge about the specific effects of an oxysterol's activation of Hh. For example, it has been noted that synthetic, non-steroidal, LXRs agonist are able to block SMO activation, probably through the LXR-mediated reduction of cholesterol (W.-K. Kim *et al.*, 2009). Oxysterols are the endogenous ligands of LXRs so a similar effect would probably be expected in a cellular context. More studies are needed to shed lights on the effective oxysterols' contribution to the Hh signalling.

1.3 Sterols in the brain

Cholesterol is the most abundant lipid in human brain, where it accounts for almost 25% of whole-body cholesterol (Dietschy & Turley, 2004a). In adult human brain, the sterol is mainly found as free-unesterified form while in developing brain cholesteryl esters are quite well represented. 70 to 80% of the brain cholesterol is concentrated between the myelin sheets, the insulating lipid layer which cover neuroneal axons, and neuroneal cells plasma membrane (Dietschy & Turley, 2004a). The sterol is fundamental for the transmission of the action potential, and for the synapsis, between different neuronees as well as for the maintenance of the cell morphology, and ultimately, for its survival (Dietschy & Turley, 2004a; Gliozzi *et al.*, 2021). The sterol is an essential structural component of myelin and plasma membrane (Dietschy & Turley, 2004a; Gliozzi *et al.*, 2021) and it is also required for dendrite formation (Fester *et al.*, 2009; Goritz *et al.*, 2005a) and axonal guidance (de Chaves *et al.*, 1997a). Moreover, cholesterol metabolism products, specifically the oxysterols, have been shown to act as proper signalling molecules, modulating cellular function, and contributing to the neuroneal cell survival (Björkhem, 2006; Courtney & Landreth, 2016; Lütjohann *et al.*, 1996a; S. M. Paul *et al.*, 2013; Pingale & Gupta, 2021a; Sodero, 2021a; Yutuc *et al.*, 2020). Therefore, the cholesterol levels are tightly regulated to maintain a constant, threshold, level of cholesterol in the membrane and myelin (Gliozzi *et al.*, 2021). Cholesterol depletion results impaired synaptic vesicles exocytosis and, consequently, neuroneal transmission and activity which can ultimately bring to dendritic spine and synapses degradation and cell death (Linetti *et al.*, 2010a; Q. Liu *et al.*, 2007,

2010). Furthermore, growing evidence raised from the last twenty years of research indicates a link between disrupted brain cholesterol metabolism and the development of several neurological diseases, in particular the ones with a neurodegenerative component like Parkinson's and Alzheimer's diseases (PD & AD) (Chang *et al.*, 2017; W. J. Griffiths *et al.*, 2021a; X. Huang *et al.*, 2019; Jin *et al.*, 2019a; Pingale & Gupta, 2021b; Puglielli *et al.*, 2003; Ramanan & Saykin, 2013; Singh *et al.*, 2021; Varma *et al.*, 2021; Whitfield, 2006; Xicoy *et al.*, 2019). Hence, cholesterol turnover in brain has been pointed out as new possible drug target as it represents a pivotal event in the maintenance of cholesterol homeostasis. However, several different pathways and small molecules contribute to cholesterol homeostasis, complicating the development of effective medical treatments. In the next sections a deeper look to human brain cholesterol homeostasis and its relationship with neurodegenerative diseases aimed to shed a light on the contributions of the cholesterol oxygenated metabolites to the above-mentioned pathological conditions and to the reason why these molecules should be elected as a preferential biomarker.

1.3.1 Brain cholesterol biosynthesis and homeostasis

Human brain is the most cholesterol enriched organ of whole body, with a sterol concentration reaching 15 to 20 mg of cholesterol per gram of wet brain (Dietschy & Turley, 2004a). Seen the importance of this molecule for neuroneal physiology, cholesterol homeostasis is maintained through the activation of several different mechanisms (Lutjohann *et al.*, 1996). However, respect to other metabolically

active organs, steady concentration of brain cholesterol remains quite stable, with a daily turnover of only 0.03% (Dietschy & Turley, 2004a). Most of the cholesterol in the brain, almost 70% represent a specific pool called bulk cholesterol. This specific pool is not metabolically active and constitute myelin membranes and white matter. Half -life of bulky-cholesterol in membranes and myelin is between 6 months and 5 years in human brain (Lütjohann *et al.*, 1996a), reflecting the low replacement rate. However, a little pool of cholesterol is replaced everyday by brain cells to keep constant steady state of cholesterol (Russell *et al.*, 2009) This pool is the metabolically active and is found in the plasma membrane and subcellular compartments of neuronees and glial cells of grey matter (Russell *et al.*, 2009). The blood brain barrier (BBB) is a semipermeable physical barrier made of an intricated central nervous system ,CNS, microvasculature and several cells and enzymes (Daneman & Prat, 2015). Under physiological conditions, an intact and functional BBB prevents the passage of cholesterol carrying lipoproteins. For this reason, brain cells cholesterol needs are met through its *de novo* synthesis and recycling, mainly in astrocytes and neuronees (Dietschy & Turley, 2004a).

Astrocytes are the main cholesterol producing cells in adult human brain (Abildayeva *et al.*, 2006; Ferris *et al.*, 2017a; Nieweg *et al.*, 2009a). Cholesterol *de novo* synthesis takes place in the ER of astrocytes where it starts with the mevalonate pathway and proceed with classical Bloch pathway (Woodward R. B. & Konrad Bloch, 1953), for a detailed description of the Bloch pathway please see the section 1.1.1.2. Free *de novo* cholesterol is then transported to the plasma membrane or redistributed in a vesicular- or protein-mediated fashion to other subcellular compartment see figure 1.14

(F. Arenas *et al.*, 2017; DeGrella & Simoni, 1982; J. Hu *et al.*, 2010; Shi *et al.*, 2022; Soccio & Breslow, 2004), for a detailed description of intracellular cholesterol trafficking see the section 1.1.1.2. As astrocytes are the main cholesterol producing cells of the adult brain, they supply neuroneal cells cholesterol needs through its secretion in APOE containing lipoproteins (Linetti *et al.*, 2010b; Madra & Sturley, 2010; Nieweg *et al.*, 2009b). APOE is the predominant transporter of cholesterol and phospholipids in the human brain, primarily synthesized by astrocytes, with subsequent production by oligodendrocytes and glial cells (Madra & Sturley, 2010). Once synthesised, APOE is in a delipidated form and it is secreted in the extracellular space only upon cholesterol binding (Ferris *et al.*, 2017b; Liao *et al.*, 2017a; Nieweg *et al.*, 2009b). The ABCA1 membrane transporter expressed on the astrocyte's plasma membrane is fundamental for the APOE-cholesterol loading: once the sterol reaches the plasma membrane, it binds to ABCA1, which also binds APOE and aids the free cholesterol loading of the lipoprotein, leading to the formation of a pre-HDL (de Chaves *et al.*, 1997b; Ferris *et al.*, 2017a; Liao *et al.*, 2017a). Pre HDL is released into the extracellular space and up taken by neuronees through the LDL receptor related protein 1LRP1, the most expressed in neuronees. LRP1 is among the lipoprotein receptors the one with the highest transport capacity for APOE, characterised by a very high endocytic rate(Li *et al.*, 2001). Upon LRP1 binding, the pre-HDL is internalised by endocytosis and an endosome is thus formed. Acidification of the endosome transforms it in a lysosome, bringing to HDL disassembly, and hydrolysis mediated release of free cholesterol (Gliozzi *et al.*, 2021; Liao *et al.*, 2017a). Once internalised into neuronees, astrocytes derived cholesterol is redistributed to different subcellular compartment, organelles, or ER through NPC1 and 2 transport (F.

Arenas *et al.*, 2017), for a schematic representation of cholesterol brain homeostasis refer to figure 1.14.

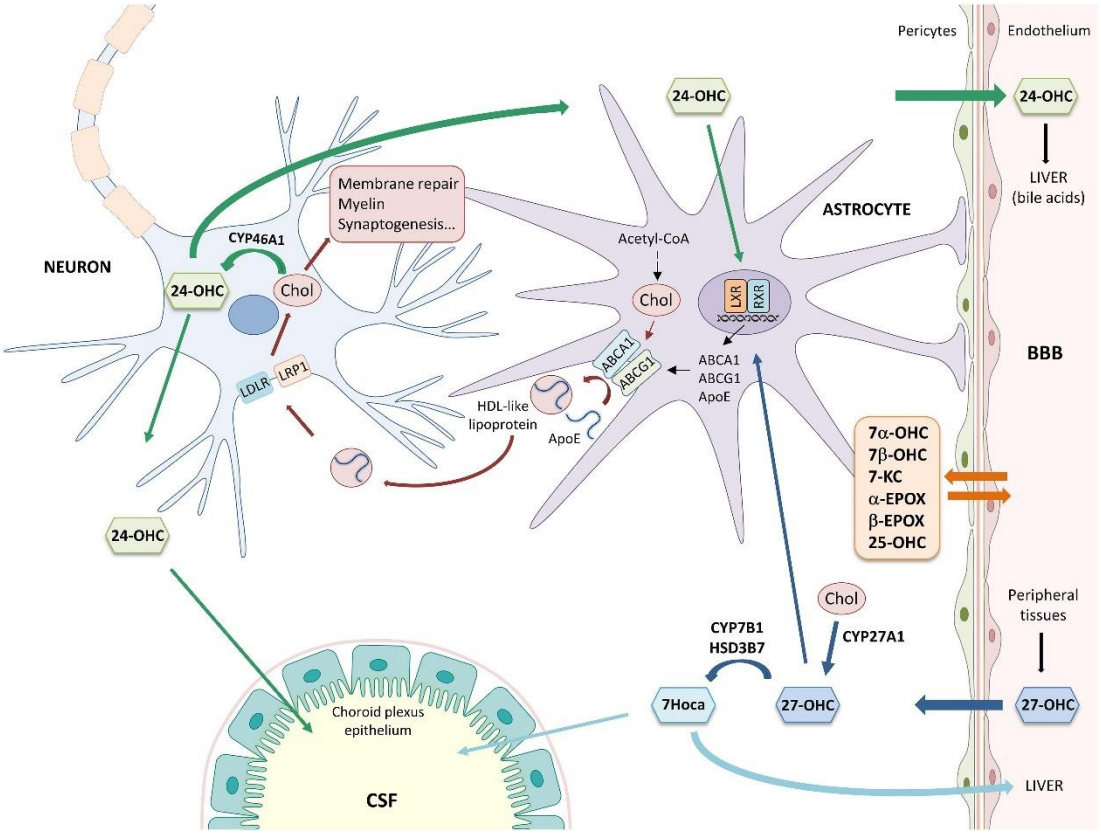

Figure 1.14 Brain cholesterol homeostasis: a balance between astrocytes biosynthesis, extracellular transport, and metabolism in the neuroneal cells.
Figure taken from (Gamba *et al.*, 2019)

Cholesterol represents a fundamental building block of neuroneal plasma membrane and myelin (Adibhatla & Hatcher, 2007; Courtney & Landreth, 2016; Dietschy & Turley, 2004a; Gliozzi *et al.*, 2021; Jin *et al.*, 2019a; Lütjohann *et al.*, 1996a; Martin *et al.*, 2014). Its absence or excess it is detrimental not just for neuronees but for all brain cells, leading to the development of a series of different pathological conditions (Ayciriex *et al.*, 2017; Browne *et al.*, 2006; Kreilaus *et al.*, 2016; Liao *et al.*, 2017a; Schöls *et al.*, 2017). The importance of

cholesterol for cell survival has brought to the development of a complete and integrated mechanism for the maintenance of cholesterol homeostasis. The brain control of cellular cholesterol levels shares many similarities with the one of extra cerebral tissues and organs, however the presence of the BBB restricts the possibility for brain cells to benefit of some pathways, like RCT. Despite of that, specific brain mechanism for cholesterol level modulation have been adopted by cerebral cells, thanks to which cholesterol essential pool is constantly maintained in its physiological range of concentration.

One of the shared mechanisms brain cells use to control cholesterol *de novo* synthesis is a simple negative-feedback loop involving SREBP-2 protein inactivation, as it has been already described in section 1.1.1.2 (F. Arenas *et al.*, 2017).

Respect to all the various mechanism above cited, which contribute to the maintenance of a physiological cholesterol level in human brain, cholesterol oxidation to (24S)-HC by CYP46A1 represents the major excretion pathway induced by neuroneal cells in regards of cholesterol excess (Björkhem, 2006a; Lütjohann *et al.*, 1996a). Almost 50 to 60% of the entire cholesterol turnover is accomplished by CYP46A1 in neuronees, making 24-HC the major contributor to brain cholesterol homeostasis (Björkhem *et al.*, 2018). CYP46A1 is postulated to be a constitutive expressed enzyme in neuroneal cells, with its gene *CYP46A1* covering a housekeeping function (Ohyama *et al.*, 2006). Indeed, it was demonstrated that is expression was not cholesterol dependant, reinforcing the hypothesis of substrate independent production (Ohyama *et al.*, 2006). The enzyme is mainly expressed in neuronees which accounts most of the (24S)-HC production (Lütjohann *et al.*, 1996a). However, CYP46A1 expression has been reported in other tissues, for example the glands of the

adrenal, but their contribution to the (24S)-HC levels is not known, but considered minimal (CYP46A1 Human Protein Atlas , 2023; Lutjohann *et al.*, 1996) . The subcellular location of enzyme is the ER membrane, but it is also found in the plasma membrane (Russell *et al.*, 2009; Sodero, 2021a). Constitutive expression of CYP46A1 results in a baseline (24S)-HC production, which balanced the turnover of metabolically active cholesterol (Lütjohann *et al.*, 1996b). Once formed, (24S)-HC can passively diffuse across the ER's membrane with a very high rate and rapidly leave the neuronees ER. In the cytosol of the neuronee, both passive diffusion and protein aided transport let the oxysterol to be first excreted to the extracellular space and secondly diffused across the BBB (Lütjohann *et al.*, 1996a; Meaney *et al.*, 2002). It is estimated for (24S)-HC a net efflux across the BBB of 6-7 mg-oxysterol per day (Lütjohann *et al.*, 1996a; Meaney *et al.*, 2002). With respect to the parent sterol, (24S)-HC, possesses one extra oxygenated function which confers a lesser hydrophobic character and a better ability to pass the phospholipid bilayers (Meaney *et al.*, 2002). In particular, the presence of a second hydroxyl-function on the side chain, but not on the body, seems to extremely enhance the coefficient of diffusion of the molecule across the membranes and so, the flow rate across it (Meaney *et al.*, 2002). Being that CYP46A1 is almost exclusively expressed in neuronees, in addition to the fact that (24S)-HC concentration in the brain is 30-to-1500-fold higher with respect to any other organ of the human body, most of the circulating (24S)-HC has a brain origin. Plasma (24S)-HC can be found as a free or esterified form: the enzyme LCAT, present on HDL surface, catalyses the esterification of the oxysterol in plasma (Szedlacsek *et al.*, 1995b). Esterified (24S)-HC can associate to LDL, HDL or albumin and ultimately reach the liver, where it is further metabolised to bile acids, or the kidneys for urine elimination

(E. Lund *et al.*, 1996; Lütjohann *et al.*, 1996a). Less than 1% of brain (24S)-HC pass into the cerebrospinal fluid (CSF) (Lütjohann *et al.*, 1996a). (24S)-HC does not only represent a major catabolic elimination product of cholesterol for neuronees but a proper cholesterol synthesis modifier. Produced in the ER, the oxysterol can bind to the INSIG protein, block the SREBP-2-SCAP translocation to the Golgi and SREBP-2 pathway activation (Radhakrishnan *et al.*, 2007). Furthermore, ER (24S)-HC can translocate into the nucleus where it binds to the ligand binding domain of LXR-RXR heterodimer and activate the transcription of LXRs target genes, specifically ABCA1/G1 and APOE, in neuronees and astrocytes (Janowski *et al.*, 1996; Peet, Janowski, *et al.*, 1998; Spencer *et al.*, 2001). (24S)-HC does not only represent a cholesterol level modulator but also a proper signalling molecule, able, for example, to modify the learning and memory process in brain upon NMDA receptor binding (Hansen *et al.*, 2018).

Respect to the other steroidogenic and non-steroidogenic cells, neuronees and brain cells seems to manly rely on cholesterol conversion to (24S)-HC as the principal cholesterol catabolic pathway (W. J. Griffiths & Wang, 2020; Mutemberezi *et al.*, 2016b; Schroepfer, 2000a). However, recently other oxysterols have been identified in CSF, revealing other metabolic fate of cholesterol. . For instance, Griffits *et al.* detected certain cholestenoic acids, cholesterol metabolites, and bile acids intermediates in human cerebrospinal fluid (CSF). This suggests that the acidic pathway to bile acids synthesis may represent a novel route for preserving brain cholesterol homeostasis. (Y. Wang, Yutuc, & Griffiths, 2021)(Y. Wang, Yutuc, & Griffiths, 2021).

1.4 Sterols and Neurodegeneration

The maintenance of plasma membrane fluidity and permeability as well as myelin sheet integrity and isolation properties are imperative for normal brain function. As we have previously seen, cholesterol is the principal structural component of plasma membrane and myelin, able to modulate their characteristic depending on its distribution and concentration (Das *et al.*, 2014; Infante & Radhakrishnan, 2017b; Lange *et al.*, 1989b). Alteration of its intracellular and membrane levels can cause several brain cell dysfunctions (Dai *et al.*, 2021; X. Huang *et al.*, 2019; Pfrieger & Ungerer, 2011). Modification of the lipid rafts composition caused by cholesterol alteration, generally of accessible cholesterol, result in a loss of transmembrane protein function and, consequently, of signalling pathways (Pommier *et al.*, 2010; Sezgin *et al.*, 2017). Cholesterol incorporation in pre- and post-synaptic vesicle seems to be fundamental for the reduction of membrane fluidity and vesicle formation (Simons & Ehehalt, 2002). Alteration of cholesterol content might avoid the formation of synaptic engagements between neuronees (Simons & Ehehalt, 2002). Moreover, loss of cholesterol from the myelin sheets will contribute to a degenerative process called demyelination (Prunet *et al.*, 2006).

Because of its central role in the development and survival of neuronees, astrocytes and glial cells, disruption of cholesterol metabolism has been pointed out as one of the possible mechanisms contributing to neurodegenerative diseases. The term neurodegenerative diseases (ND) indicate a series of disorders characterised by an uncontrollable loss of neuroneal cells. Neurodegeneration, the process which ultimately leads to neuroneal

cell death, is characterised by synaptic dysfunction, neuroneal network malfunctioning, often deposition of misfolded proteins, oxidative stress, neuroinflammation and mitochondrial dysfunctions (BEAL, 2006; Blesa *et al.*, 2015; Burbulla *et al.*, 2017; Hoover *et al.*, 2010; Kovacs, 2019; Lei *et al.*, 2021; Mattson *et al.*, 2005; Milnerwood & Raymond, 2010; Scott *et al.*, 2010; Q. Wang *et al.*, 2015). The most common ND include Alzheimer's disease (AD), Parkinson's diseases (PD) , amyotrophic lateral sclerosis (ALS), multiple sclerosis (MUS) and Huntington's disease (HG) (Abdel-Khalik *et al.*, 2017; Goritz *et al.*, 2005b; Grimm *et al.*, 2005; X. Huang *et al.*, 2019; Karasinska & Hayden, 2011; Lei *et al.*, 2021; Leslie *et al.*, 2003; Masters *et al.*, 2015a; Tysnes & Storstein, 2017; Vonsattel *et al.*, 2011). Over the last fifty years the incidence and the risk associated with the development of ND has grown massively due to a rapid population ageing, affecting millions of people worldwide. Despite the several efforts in understanding the clinical and physio pathological hallmarks of ND there is still a lack of knowledge, which results in an absence of effective medical treatments and, in most of the cases, of a specific diagnose. ND, severely affect patients' life, limiting their ability to perform easy daily life tasks but also their cognitive functions. For all this reasons, ND represent a substantial public health problem for which there is a strong need for clear diagnose and reliable biomarker, in addition to specific and effective disease treating drugs.

However, recent findings have linked an alteration of brain cholesterol metabolism with the development of the main ND, like AD and PD (Chang *et al.*, 2017; X. Huang *et al.*, 2019; Jin *et al.*, 2019a; Mata *et al.*, 2006; Pingale & Gupta, 2021a; Puglielli *et al.*, 2003; Varma *et al.*, 2021). An engagement of the sterol molecule in the molecular mechanism of ND has been proposed by different

researchers in distinct experimental conditions, however, it still not clear at which level cholesterol contributes to the pathologies. Contrasting results associate higher or lower plasma or CSF levels with AD or PD (Agarwal & Khan, 2020; Chelliah *et al.*, 2022; Fu *et al.*, 2020; W. J. Griffiths *et al.*, 2021a; P. Wang *et al.*, 2020; Wong *et al.*, 2017). Moreover, most of the data collected on potential cholesterol contribution to the hallmark of ND like oxidative stress (Blesa *et al.*, 2015; Browne *et al.*, 2006; Sayre *et al.*, 2008) or misfolded protein polymerisation (Björkhem *et al.*, 2018; Chang *et al.*, 2017; Jin *et al.*, 2019b; Pingale & Gupta, 2021a; Puglielli *et al.*, 2003) come from cell or animal model of the diseases, which may vary a lot with respect to the actual human being. The complexity brought by these multifactorial pathologies makes the interpretation of the results even more complicated. A better understanding of the data should consider that ND are compartmentalised diseases, which affect specific areas of the brain, specific neuroneal populations, and related subcellular compartments. As we have seen in other paragraphs of this thesis, cholesterol distribution varies a lot between different cell organelles and microstructures (Cerqueira *et al.*, 2016; Das *et al.*, 2014; Ikonen & Parton, 2000; McNamara, 2013; Mouritsen & Zuckermann, 2004; Shi *et al.*, 2022; Simons & Ikonen, 2000; Soccio & Breslow, 2004). Ultimately, we must remember that cholesterol is not the only sterol present in the human CNS. The cholesterol metabolite oxysterols, in particular (24S)-HC, effectively contribute to neuroneal cell health, as above described (Cartagena *et al.*, 2010; Sodero, 2021b). Not surprisingly, recent studies have shown a correlation between altered oxysterol levels in the brain and ND development (Agarwal & Khan, 2020; Bjorkhem *et al.*, 2006; Björkhem *et al.*, 2013; Doria *et al.*, 2016; W. J. Griffiths *et al.*, 2021b; Testa *et al.*, 2016a, 2016b; P. Wang *et al.*, 2020).

In this thesis we will focus on the cholesterol and oxysterol contribution to AD and PD.

1.4.1 Alzheimer's Disease

Alzheimer's disease, AD, is a progressive and debilitating neurodegenerative disorder, characterised by the loss of neuronees in the parietal and temporal lobe and frontal cortex (Masters *et al.*, 2015b; A. D. Smith, 2022.; Wenk, 2003). AD is the most common form of dementia, affecting more than 50 million people worldwide. The incidence of AD has been estimated to be 1-3% of worldwide population, with prevalence of 10 to 30% of people aged more than 65 y/o (Bachman *et al.*, 1993; Evans *et al.*, 2003; Kawas *et al.*, 2000; Masters *et al.*, 2015b). AD present a peak of incidence on the age group between 70 and 90, like many NDs, which sharply increases with age after 90 (Kawas *et al.*, 2000; P. T. Nelson *et al.*, 2011). Accurate determination of AD incidence is, however, biased by the lack of information on confounding factors and co-morbidities, for example cerebrovascular diseases, which can affect the diagnosis. Classical symptoms of AD are loss of memory, cognitive dysfunction, and behavioural changes that severely affect everyday life, and which can ultimately bring to patient death.

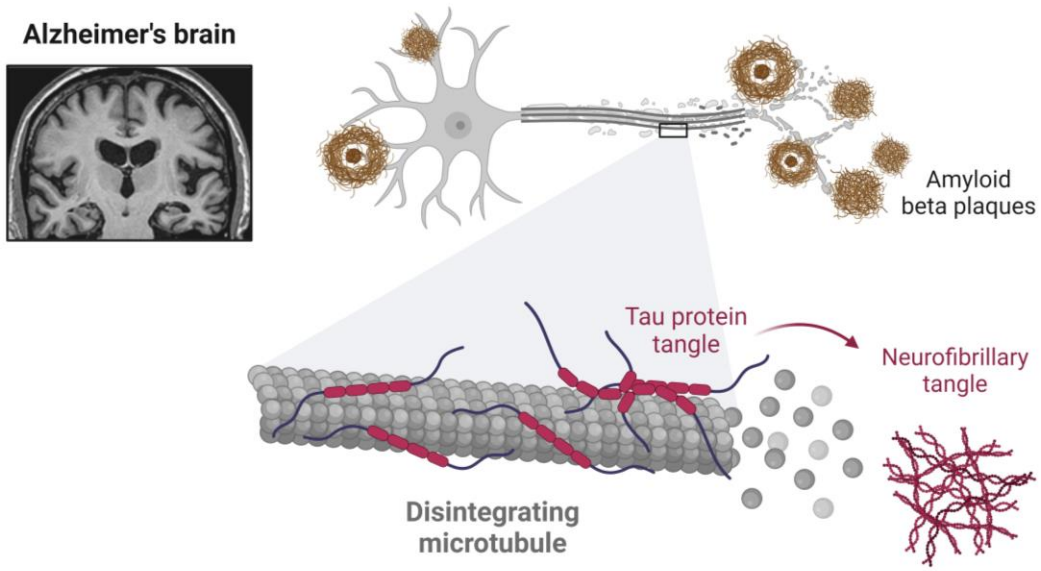

Figure 1.15 Typical AD pathological alterations.
Toxic Aß extracellular aggregates, phosphorylated τ-tangles and NFT constitute the main pathological changes associated with AD.

Typical biochemical alteration associated with AD are extracellular deposition of insoluble amyloid beta (Aß) aggregates, also called senile plaques or Aß plaques, and hyperphosphorylated microtubule protein tau τ intracellular inclusions, called the neurofibrillary tangles or NFT, see figure 1.15 (Alzheimer's Disease Facts and Figures. 2020a; Masters *et al.*, 2015b; A. D. Smith, 2022.; Wenk, 2003). Usually, Aß deposition and plaque formation starts in specific areas of the frontal and temporal lobe and further expand to hippocampus and limbic system, even if to a lesser extent to the latter, in classical AD (Alzheimer's Disease Facts and Figures. 2020b; Masters *et al.*, 2015b). The Aß oligomer formation is believed to precede the NFT creation and deposition which starts in the medial temporal lobe and hippocampus to expand then into the neocortex. (Alzheimer's Disease Facts and Figures. 2020b; Masters *et al.*, 2015b).

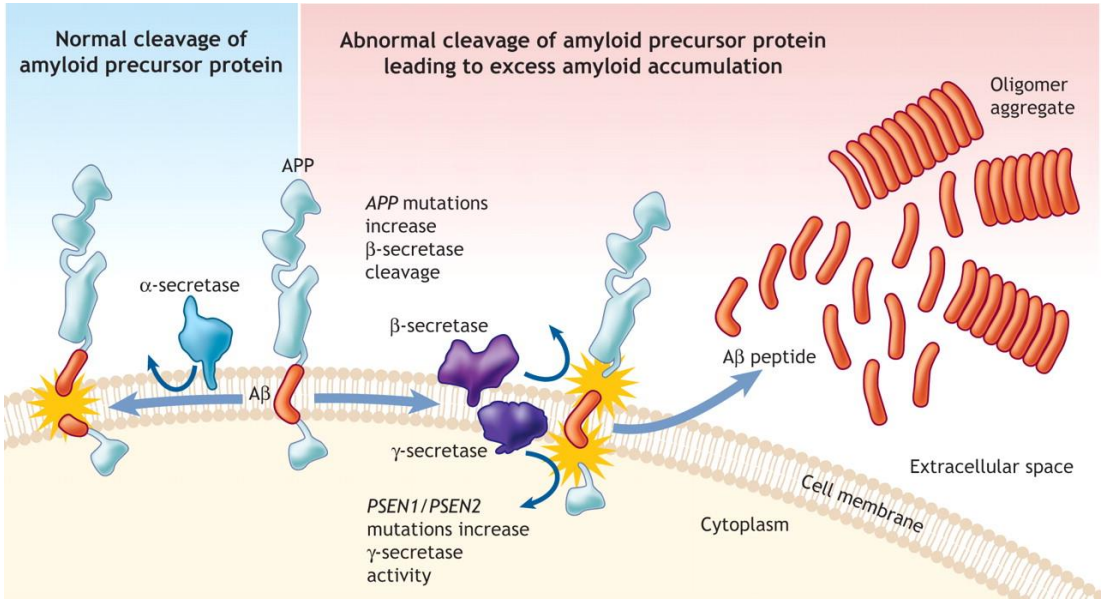

Figure 1.16 Physiological and pathological cleavage of the APP protein.
Depending on the type of secretase expressed by the neuroneal cell, APP can be cleaved into soluble/non-toxic or pro-aggregating toxic Aß peptides. Figure taken form (Patterson *et al.*, 2008)

The Aß peptide is physiologically produced in neuronees through the proteolytic cleavage of the amyloid protein precursor (APP) (Haass *et al.*, 1992), see figure 1.16. APP is a transmembrane protein produced in the ER, matured in the Golgi, and transported to the plasma membrane where it has an important function for the CNS. (Dawkins & Small, 2014; Kim, 2000; Masliah *et al.*, 1992). Human APP is cleaved by a family of enzymes called secretase and based on the isoform, α-, ß- or γ-secretase involved in the hydrolysis process, different fragments of APP can be formed (Nunan & Small, 2000). When α-secretase first and secondly γ-secretase are involved in the double proteolytic cleavage of APP, a soluble, small, peptide of 3 kDa, P3, is produced and released in the extracellular space (Iwatsubo, 2004; Nunan & Small, 2000). P3 does not lead to protein aggregates and can easily be eliminated by neuroneal cells, hence this pathway is called the non-amyloidogenic pathway. When ß- and γ-secretase

are involved a 4 kDa peptide the Aß, is produced at the extracellular surface but subsequently internalised to be further hydrolysed by γ-secretase into smaller fragments of 40 and 42 amino acids, the Aß40 and Aß42 (Haass *et al.*, 1995; Nunan & Small, 2000; Olsson *et al.*, 2014). The proteolytic cleavage of APP to Aß40 and Aß42 defines the amyloidogenic pathway, which is a physiological event during normal neuronees' cell life. In fact, Aß peptides exert several important functions for neuronees (Brothers *et al.*, 2018; Morley *et al.*, 2010; Puzzo *et al.*, 2008).*et al.et al.et al.et al.*. However, the effect of the peptide is dose and time dependent and accumulation of the Aß exacerbates its functions and results in a cytotoxic effect for neuronees. neuroneDuring AD pathology, the amyloidogenic pathway prevails, resulting in Aß overproduction (Brothers *et al.*, 2018; Masters *et al.*, 2015b). In normal conditions, Aß is cleared from the extracellular space in an APOE-HDL manner. Soluble monomer of Aß binds to APOE-HDL and can be either flushed away from the brain upon LDL-r binding on the inner surface of BBB and be excreted into the blood or internalised in an LDL-r endocytosis manner into micro glial cells, particularly astrocytes, for endosomal degradation (G. Chen *et al.*, 2017; Masters *et al.*, 2015b). During AD pathology both over production and defective elimination system result in Aß monomer accumulation which leads to oligomerisation and, ultimately, plaque formation (Masters *et al.*, 2015b).. Aß senile plaque and fibrils can modify phosphatase/kinase activity through overactivation of astrocytes and microglia causing aberrant inflammatory response (Selkoe & Hardy, 2016).. The modification of phosphatase/kinase activity results in τ protein hyperphosphorylation, leading to NFT formation and exacerbating the degenerative process (Selkoe & Hardy, 2016). The amyloid hypothesis is the combination of the events above described, which

sees Aß and NFT as the main protagonists of the neurodegeneration process in AD. The amyloid hypothesis has been formulated George Glenner in 1984 and it has been accredited as the main leading cause of AD since then (Beyreuther & Masters, 1991; Glenner & Wong, 1984; Selkoe, 2011; Selkoe & Hardy, 2016). However, contrasting results on mice model and failing clinical trials have let the scientific audience to question the validity of the theory. Major step forwards in the comprehension of AD pathology are represented by the identification of genetic risk factors, which can even be causative in some specific cases (Bachman *et al.*, 1993; Masters *et al.*, 2015b).*% (v/v)% (v/v)et al.et al.et al.et al.et al.et al.% (v/v)et al.*, Mutation on the gene encoding for the lipid transporter APOE has been associated with increased risk of developing late onset AD , with the allele ε4 being linked with AD and the allele ε2 being neuroprotective (Liao *et al.*, 2017b; Nathan *et al.*, 1994; Van Giau *et al.*, 2015). *et al.* APOE is a an apolipoprotein cholesterol and lipid transporter present in three isoforms in humans: APOE2, APOE3 and APOE4. These isoforms differ for only one or two amino acids, but this substitution can deeply affect the protein charge and 3D structure, resulting in altered binding properties for receptors and lipoprotein. APOE is highly expressed in the brain, mainly by astrocytes (Liao *et al.*, 2017b; Van Giau *et al.*, 2015). The main cellular effect of the APOE in the brain is to facilitate the mobilisation of cholesterol between astrocytes and neuronees, as the latter relays on astrocytes derived cholesterol for survival. In addition to its main role as lipid transporter, APOE is also implicated in regulating Aß clearance (Van Giau *et al.*, 2015). APOE containing lipoprotein reduces Aß deposition by sequestering Aß monomers from the interstitial space (Liao *et al.*, 2017b; Van Giau *et al.*, 2015).*et al.et al.*. Studies on cell culture and animal models clearly show that the isoform APOE4, respect to the others, possesses

a lowered clearance capacity of Aß40 and 42 monomers and oligomers, reconducted to a diminished Aß loading capacity and elimination (Bales *et al.*, 1999; DeMattos *et al.*, 2004; Holtzman, 2001; Holtzman *et al.*, 1999, 2000; Y. Huang *et al.*, 2001; Nathan *et al.*, 1994, 1995; Shibata *et al.*, 2000; Strittmatter *et al.*, 1993). The reduced Aß elimination through APOE4-binding causes the peptide accumulation which triggers Aß plaque formation and engulfment of the clearing apparatus, ultimately leading to AD.

1.4.2 Parkinson's Disease

Parkinson disease (PD) is the second most widespread neurodegenerative disorder after AD. PD is characterised by the loss of dopaminergic neuronees in the Substantia Nigra Pars Compacta, a part of the basal ganglia which helps to control the movement, and the presence of intracellular protein inclusions called Lewy body, see figure 1.17 (Poewe *et al.*, 2017a). More than 10 million people worldwide suffer from PD, with an incidence of 5 to 35 cases per 10,000 people, depending on the world area (Pringsheim *et al.*, 2014; Twelves *et al.*, 2003; Tysnes & Storstein, 2017). The overall incidence of PD is 1% for people over 60 but it markedly increases above 3% in population over 80 (Tysnes & Storstein, 2017). However, the incidence varies between subgroups based on age, sex, ethnicity, and environment. As for AD, PD mostly affects people aged over 60, with a peak in between 65 and 75, defining this age group as the classical onset for PD but in 5 to 10% of the cases PD is diagnosed before 50, the so-called juvenile onset.

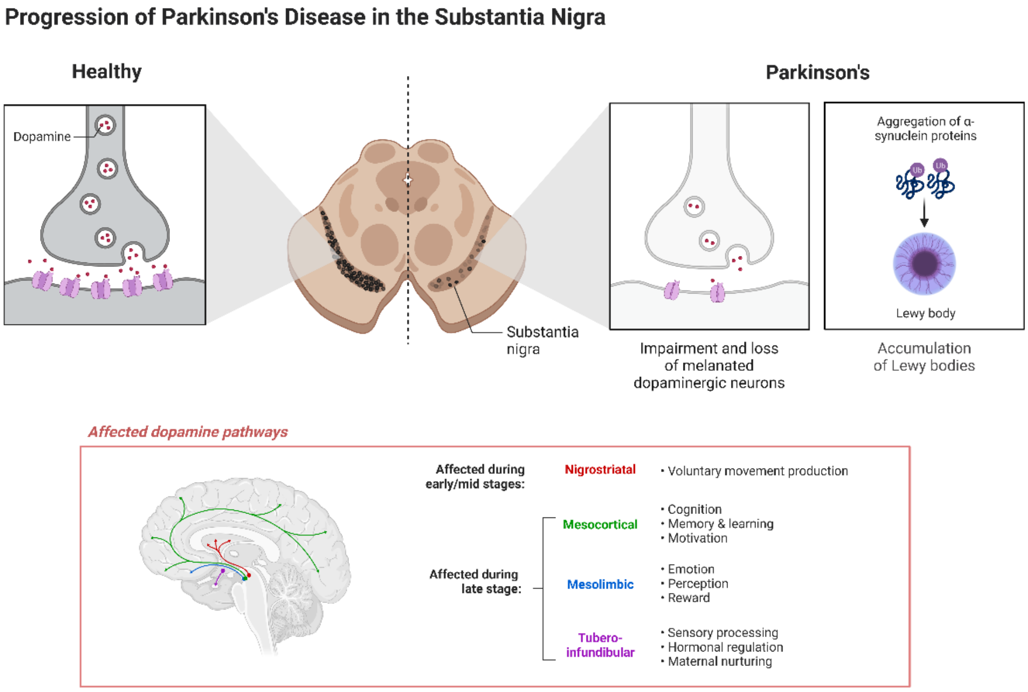

Figure 1.17 Pathological changes in PD and relative symptomatology.

PD was firstly described in 1817 by James Parkinson as a "shaking palsy", in fact classical symptoms associated with PD are bradykinesia, slowness of the movement, tremor and rigidity. The dopaminergic neuronees in Substantia Nigra are part of the thalamus-cortico-basal ganglia motor circuit which has important function in movement control and goal-directed behaviour. The circuit stars in the Substantia Nigra pars compacta, which controls the direct and indirect pathway in the striatum upon dopamine release.
neuroneneuroneneuroneneuroneneuroneneuroneneuroneneuronene uroneneuroneDuring PD, the loss of dopaminergic neuronees causes a decreased dopamine release, resulting in reduced dopaminergic transmission from Substantia Nigra to the striatum, and,

consequently, in a disproportionate motor circuit activity. The classical motor symptoms of PD are, therefore, a reflection of motor cortex inhibition, caused by an unbalanced thalamus-cortico-basal ganglia motor circuit activity (Poewe *et al.*, 2017a). Alongside motor symptoms, PD pathology is also accompanied by the development of non-motor symptoms (Chaudhuri & Schapira, 2009) like sleep disorders, insomnia, cognitive impairment, dementia, hallucinosis, mood disturbances, including behaviour changes, autonomic dysfunctions, mainly constipation, hypotension, and urogenital dysfunction, hyposmia and pain (Chaudhuri & Schapira, 2009). New findings suggest that these symptoms might be still the consequences of dopaminergic neuronees loss (Chaudhuri & Schapira, 2009; Politis *et al.*, 2008).neurone

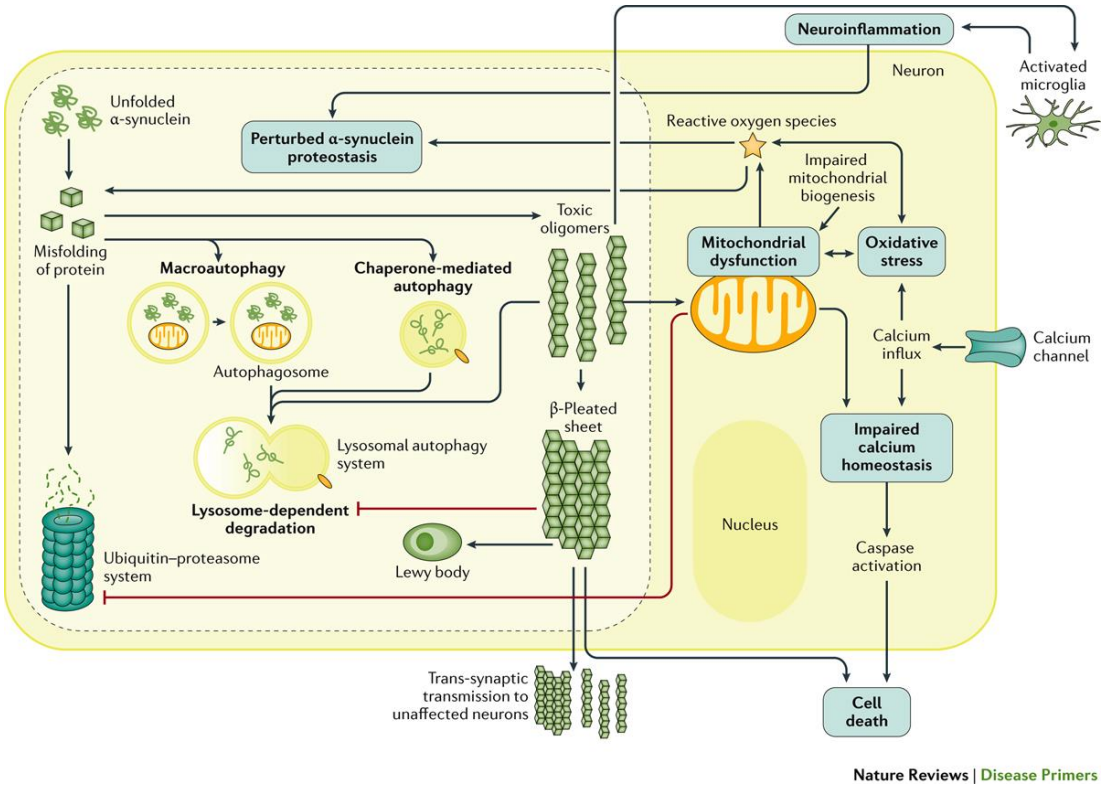

Figure 1.18 Pathological mechanisms involved in PD.
Neuroinflammation, mitochondrial dysfunctions, oxidative stress, impaired calcium homeostasis and altered α-syn proteostasis have

been identified as the principal molecular pathways contributing to the neuropathology and consequent DA neuroneneuronees degeneration in PD. Figure taken from (Poewe *et al.*, 2017b)

The two major neuropathology that characterised PD includes dopaminergic neuronees death and the intracellular accumulation of abnormal α-synuclein (α-syn), which results in toxic aggregates formation, normally called Lewy body, refer to figure 1.18 for a representation of the main PD molecular mechanisms contributing to the neuropathology. Interestingly, none of these two macroscopic brain alterations is typical of the PD, but their concomitant presence is imperative and specific for the definitive diagnose of idiopathic PD (Dickson *et al.*, 2009). In the last decades big step forward have been moved to the comprehension of PD aetiology and, consequently, to the causes of its associate neuropathology, underlying the main molecular mechanisms that seems to be involved in the disease's development. Dysregulation of α-syn proteostasis strongly contributes to the PD development. α-syn is a protein made of 140 amino acids that localise at neuroneal terminal. Its physiological functions are still unclear, but strong evidence suggests an important role in synaptic vesicle formation and neurotransmitter release (Burré, 2015). *et al.et al.*α-syn is, therefore, a constitutive protein in neuronees but it shows neurotoxic properties when soluble monomers start to aggregate in oligomers. Oligomers can also combine in protofibrils and form large insoluble aggregates of α-syn called Lewy body (C. Kim & Lee, 2008; Melki, 2015). The aggregation process seems to be a consequence of different pathological mechanism *et al.et al.et al.et al.et al.et al.et al.et al.*including defective α-syn degradation and elimination system. α-syn homeostasis is mainly maintained through a balance between protein synthesis and

degradation. The principal elimination systems are lysosomal autophagy system (LAS) and ubiquitin-proteasome system (UPS) (Vekrellis *et al.*, 2004). Even if the specific contribution of UPS and to Lewy body formation and PD development is still a matter of debate, LAS seems to be more involved. LAS, chaperone-mediated autophagy, and macro autophagy are suggested to mediate the clearance of both misfolded α-syn monomers and oligomers (Chu & Kordower, 2007; Sarkar *et al.*, 2007; Steele *et al.*, 2013; Xilouri *et al.*, 2009a). Decreased content of lysosomal enzymes has been found in substantia nigra of PD patients, as well as in experimental models, reinforcing the hypothesis of a reduced LAS degradation leading to α-syn accumulation (Chu *et al.*, 2009). This decrease was more pronounced in PD patients respect to healthy individuals of same age group, eliminating ageing as possible confounding factor for diminished LAS functions and reinforcing the hypothesis of a α-syn clearance disruption during PD (Chu & Kordower, 2007). Malfunctioning LAS and UPS brings to accumulation of α-syn which, in turn, drives the aggregation process to oligomers and Lewy body. *et al.et al.et al.et al.et al.et al.et al.et al.et al.et al.et al.et al.et al.et al.et al.et al.*In summary, disrupted proteostasis of α-syn leads to the accumulation of the protein, which exacerbates the malfunctioning of the degradation system, increasing intracellular protein build-up and exponentially worsening the cytotoxic effect on dopaminergic neuronees. Engulfment of the α-syn degradation system has also been associated Leucine rich repeat kinase 2 (LRRK2) mutations a, specifically with disruption of the autophagic pathway involved in LAS (Anand & Braithwaite, 2009; Rideout & Stefanis, 2014). LRRK2 autosomal dominant mutation is the most common genetic cause for both familial and sporadic PD. LRRK2 is a well conserved large multidomain protein whose physiological function has not yet been

clarified. However, it has a clear kinase and hydrolytic activity (Anand & Braithwaite, 2009; Skibinski *et al.*, 2014), and seems to be involved, in the regulation of the autophagy lysosomal protein degradation system via Mitogen-activated protein kinase kinase/ Extracellular signal-regulated kinases (MEK/ERK) and 5' AMP-activated protein kinase (AMPK) pathways. (Rideout & Stefanis, 2014). LRRK2 bringing the G2019S mutation cause alteration of MEK/ERK and AMPK pathways resulting in impaired LAS system (Bravo-San Pedro *et al.*, 2013). LRRK2 driven disruption of LAS system causes a consequent α-syn accumulation in dopaminergic neuronees (Volpicelli-Daley *et al.*, 2016). Other mutations are involved in the disruption of the α-syn elimination system, however none of them provided to be causative for PD (Fernandes *et al.*, 2016; Sidransky *et al.*, 2009) (Dehay *et al.*, 2012; Ramirez *et al.*, 2006; Vilariño-Güell *et al.*, 2011; Zimprich *et al.*, 2011).

*et al.et al.et al.et al.et al.et al.et al.et al.et al.et al.et al.*neurone*et al.*The α-syn protein accumulation and aggregates formation hypothesis alone as the leading cause of dopaminergic neuronees death in PD, however, is not sufficient to entirely explain the pathology. Firstly, the presence of Lewy bodies and α-syn aggregates do not constitute alone a discriminating factor to diagnose PD. Many other neurological diseases share this characteristic like dementia with Lewy body, multiple system atrophy and sometimes also AD (Dehay *et al.*, 2012). Secondly, even if α-syn might represent a feasible and reliable druggable target, no new treatments aiming to reduce or eliminate the over accumulation of the protein have been approved yet (Menon *et al.*, 2022). A consistent involvement of α-syn to the development of PD is

undeniable but a cross talk between misfolded protein aggregation and other mechanisms might be the key to fully explain the pathology. Nowadays neurodegenerative diseases are considered complex multifactorial disorders, in which disruption of several different pathways contributes to the degeneration of the neuronees. This idea has contributed to shed light on the ethology of PD, individuating three more mechanism deeply involved in the pathogenesis: mitochondrial dysfunction, oxidative stress and neuroinflammation.

Several lines of evidence showed a strong engagement of mitochondrial dysfunction to the development of PD (Bose & Beal, 2016; Schapira, 2007). This theory is supported by the fact that isolated mitochondrial complex I, fundamental component of the electron transport chain, from PD patients' tissues is much less active than the healthy one (Devi *et al.*, 2008). *et al.et al.et al.et al.* From the sum of these information the resulting picture sees the formation of a vicious cycle where aberrant mitochondrial activity results in a toxic effect for dopaminergic neuronees which also worsen the α-syn accumulation, triggering the cytotoxicity. In support to this postulation, animal models injections of different toxins with mitochondria as target result in PD like neuropathology (Bose & Beal, 2016; Schapira, 2007). To note, energy deficit induced by mitochondrial dysfunction might be one of the possible explanations of terminal axonal degeneration (Sossi *et al.*, 2004, 2010). Human brain imaging evidenced how axonal degeneration happens years before the one of substantia nigra dopaminergic neuronees' nucleus (Sossi *et al.*, 2004). The last evidence of a mitochondrial engagement in PD development is the fact that the proteins encoded by mutated genes in PD contribute to the dysregulation of mitochondrial

functions. For example, LRRK2 mutations are associated with mitochondrial impairments (Bose & Beal, 2016).In summary, the dysregulation of mitochondrial system cause a strong metabolic stress in the dopaminergic neuronees of substantia nigra, resulting in impaired energy metabolism, exacerbation of the α-syn aggregation and elevated oxidative stress, all mechanisms involved in the development of PD. *et al.et al.*neurone*et al.* The nigral dopaminergic neuronees are the most susceptible to oxidative and metabolic stress among the neuroneal cells (Bolam & Pissadaki, 2012). The reasons for this enhanced vulnerability are numerous:

- Their morphology. Made of long un-myelinated axons, dopaminergic neuronees can form a huge number of synapses, involving a considerable amount of energy (Bolam & Pissadaki, 2012; Pissadaki & Bolam, 2013)
- Autonomous peace-making activity. Nigrostriatal dopaminergic neuronees alone are able of pace making activity which is required to sustain the release of dopamine necessary for proper motor activity (Guzman *et al.*, 2010; Pissadaki & Bolam, 2013). This activity is guaranteed upon the maintenance of a calcium gradient, which involves calcium level oscillation and extrusion, hence energy (Mosharov *et al.*, 2009; Surmeier *et al.*, 2011, 2017).
- Overproduction of dopamine and its metabolites. Dopamine and its metabolites have been proved to induce oxidative stress when in excess (Lotharius & Brundin, 2002; Mosharov *et al.*, 2009)

Whether oxidative stress represent a cause or a consequence in PD pathogenesis is still not clear and there is a need for more clarification. What can be said is that multiple pathological pathways

are intimately interlinked, and all together contribute to the development of PD.

One last mechanism involved in the PD pathogenesis is neuroinflammation. Both post-mortem brain tissues and plasma and/or CSF from PD patients show moderate levels of inflammatory mediators. Moreover, activated glial cells and astrocytes have been found in different type of ND, including PD. As for oxidative stress and mitochondrial dysfunction, neuroinflammation is interconnected with PD hallmarks. For example, LRRK2 is a protein also expressed in immune cells and fundamental for immune cell mediated autophagy. Its mutations result in LAS deficits and reduced microglial cells activation which, in turn, reduces α-syn clearance and triggers its aggregation. Furthermore, α-syn oligomers promotes innate and adaptive immunity response in both patients and animal models while neuroinflammation boost its aggregation, creating a vicious cycle.

Since its discovery, tremendous steps forward have been made in the comprehension of PD, highlighting the multifactorial nature of the disease and the interplay between the different pathological pathways involved. However, it is not yet clear what insult might or can trigger the start of the degeneration process and why it is not propagating to other brain cells or dopaminergic neuronees in different brain regions respect to the substantia nigra. The contribution of the single mechanisms to the PD united to the weight confounding factors like environment, sex, age, ethnicity, pollution, diet have on the disease development is another aspect to be determined.

1.4.3 Sterols as a fluid biomarker for neurodegenerative diseases

In the first paragraphs of the 1.4 sections, we saw the importance of cholesterol for CNS and brain development and brain cells maturation and survival. Not only cholesterol but also its metabolites, the oxysterols, possess important regulatory activity rather than be solely controllers of cholesterol. In the paragraph 1.2 we have seen how oxysterols can influence the main biochemical pathways involved in cell development, signalling, differentiation, inflammation, and lipid metabolism in several type of human cells (A. J. Brown *et al.*, 2021; Brzeska *et al.*, 2016; Mutemberezi *et al.*, 2016a; Schroepfer, 2000a).Excess or depletion of brain cholesterol results in detrimental effect for neuronees and brain cells, ultimately leading to cell death. This is the reason why in brain, more than in any other organ of human body, cholesterol homeostasis is finely regulated across several different mechanism, which contains multiple checkpoints to assure a constant and physiological intracellular cholesterol level. For detailed description of the main mechanism involved in the brain cholesterol homeostasis see the paragraph 1.2.1.

As we saw in the section brain cholesterol biosynthesis and homeostasis, one of the principal mechanisms involved in cholesterol turnover and homeostasis regulation is the conversion of the sterol into (24S)-hydroxy cholesterol, (24S)-HC, the main brain oxysterols. Almost 60% of the entire brain cholesterol content which undergoes to active turnover, is metabolised to (24S)-HC principally in the neuronees, making the neuroneal cells particularly sensitive to

cholesterol variations (Björkhem *et al.*, 2018). Once produced, (24S)-HC is easily and quickly eliminated through passive diffusion across the BBB (Lütjohann *et al.*, 1996a; Y. Wang *et al.*, 2008), refer to figure 1.19 for (24S)-HC efflux. 99% of the brain derived (24S)-HC is excreted into the circulation while only 1% is eliminated via CSF (Lütjohann *et al.*, 1996b). To note, (24S)-HC is almost exclusively produced in the brain as the enzyme CYP46A1, the (24S) sterol hydrolase, is mainly expressed in the neuronees (CYP46A1 Expression , n.d.; Lütjohann *et al.*, 1996b; Sodero, 2021b; Y. Wang *et al.*, 2008). Consequently, the majority of plasma (24S)-HC content possesses a brain origin. Moreover, considering the high conversion rate of active cholesterol in neuronees, plasma levels of (24S)-HC might be elected as novel biomarker for brain cholesterol turnover.

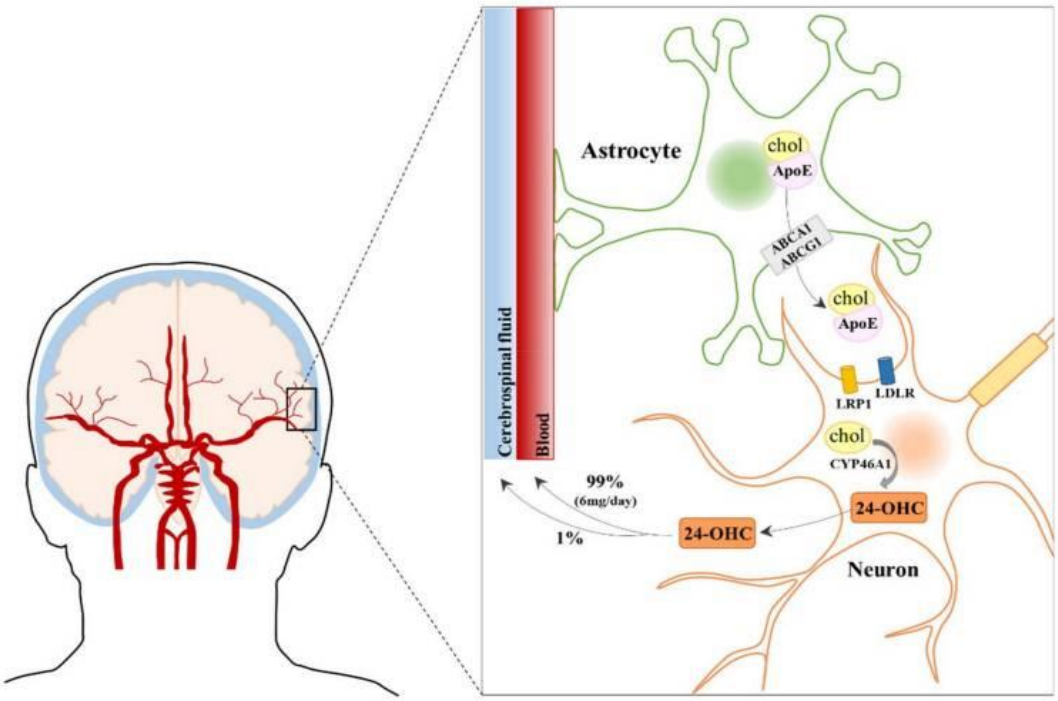

Figure 1.19 Efflux of (24S)-HC from the brain to CSF and circulation. Figure taken from (Gamba *et al.*, 2021)

Seen the implications of cholesterol and oxysterols in neuroneal function, in the last twenty years the research on ND have shifted

the attention towards the study of possible implications of disrupted brain cholesterol homeostasis and ND development. Not surprisingly, several lines of evidence indicate a cholesterol and oxysterol involvement in many different pathological mechanisms seen in ND (Björkhem, 2006a; Bjorkhem *et al.*, 2006; Björkhem *et al.*, 2013; Crick *et al.*, 2019; Doria *et al.*, 2016; Lordan *et al.*, 2009; Testa *et al.*, 2016b; Vejux & Lizard, 2009; Zmysłowski & Szterk, 2019). Cholesterol can modulate γ- and ß-secretase activity, acting as a positive allosteric modulator and increasing their activity (Grimm *et al.*, 2008; Grösgen *et al.*, 2010). Elevated active cholesterol membrane levels can, therefore, stimulate the secretase activity and enhance toxic Aß production. Moreover, cholesterol possesses a binding site on Aß which can stimulate its aggregation to toxic oligomers and fibrils, ultimately leading to Aß plaques formation (Grösgen *et al.*, 2010). All this evidence suggest that cholesterol might possess a physiological role in regulating APP metabolism. Depending on the sterol intracellular concentration, the amyloidogenic or the non-amyloidogenic pathway is favoured against the other. On the contrary, (24S)-HC shows a very effective inhibitory activity on Aß synthesis, balancing, under physiological conditions, the cholesterol activity (J. Brown *et al.*, 2004). However, reduced levels of (24S)-HC have been found in AD post-mortem brains, reflecting neuroneal death but a probable alteration of the oxysterol synthesis rate cannot be excluded. Cholesterol accumulation and reduced (24S)-HC levels in specific compartments of neuronees could, therefore, contribute to toxic protein aggregation in AD (Testa *et al.*, 2016c). A possible explanation for such selective cholesterol accumulation might be related to the expression of the APOE ε4 isoform. altered releasing and binding capacity for cholesterol as well as LDL-r binding affinity, respect to the alleles ε2 and ε3mightcause a congestion of the

cholesterol intracellular and external trafficking, leading to a sterol accumulation (Gong *et al.*, 2002; Husain *et al.*, 2021; Kang *et al.*, 2018; Yajima *et al.*, 2015).. Increased cholesterol levels stimulate Aß aggregation, aggravating the APOE ε4 induced amyloid plaque formation process (Fassbender *et al.*, 2001). Moreover, the reduced cholesterol mobility can affect neuroneal synaptic plasticity and myelin remodelling, resulting in altered neurotransmission and possible cognitive impairment (Arendt *et al.*, 1997; Grösgen *et al.*, 2010; Mauch *et al.*, 2001). As for AD, also in PD numerous evidence reveal an altered cholesterol metabolism involved in the disease development (X. Huang *et al.*, 2019; Jin *et al.*, 2019a). Even in PD, elevated cholesterol brain levels seem to aggravate the PD phenotype (Dietschy & Turley, 2004b) and cholesterol treated human neuroblastoma cells worsen the neuronees survivability, increasing the depolarisation of mitochondrial membrane potential (Raju *et al.*, 2017). Like APOE in AD, α-syn seems to be strongly corelated to the brain cholesterol metabolism (Bosco *et al.*, 2006; Emamzadeh *et al.*, 2016; Fantini *et al.*, 2011; Hsiao *et al.*, 2017a; Kruger *et al.*, 1999; van Maarschalkerweerd *et al.*, 2015). α-syn possesses two cholesterol binding sites allowing the binding to both plasma membrane cholesterol and free intracellular cholesterol to form a carrier structure like lipoproteins and stimulating cholesterol efflux from the cells (Fantini *et al.*, 2011; Hsiao *et al.*, 2017b). In pathological conditions as in PD, α-syn aggregates lose the capacity to export cholesterol outside of the cells but still possess the ability to bind to the lipid. α-syn extracellular oligomers bind to cholesterol and the plasma membrane where they aggregate to form Lewy body, which leads to membrane dysfunction and ultimately cell death (Bosco *et al.*, 2006). Genetic components of PD, as in AD, seem to be also corelated to alter brain cholesterol metabolism (Bae *et al.*, 2018; Cha

et al., 2015; J.-M. Kim *et al.*, 2016; K. S. Kim *et al.*, 2013; K.-Y. Kim *et al.*, 2011a; Yamaguchi *et al.*, 2012). *et al.et al.et al.et al.et al.*

Despite the numerous implications of a dysregulated brain cholesterol metabolism to the wellness of neuroneal cells and all the findings linking an altered cholesterol homeostasis to ND development, there is a debate around the contribution of cholesterol and oxysterols to ND. However, the tireless efforts of the scientific community have underlined a strong relationship between cholesterol brain levels and ND. Hence, cholesterol metabolism might be the perfect candidate to monitor neurodegeneration. Since brain cholesterol is not exchanged between the periphery and the brain, the characterisation of its turnover should proceed through the quantification of its metabolites, the oxysterols. As described on the section 1.4.2, (24S)-HC could represent an ideal marker to monitor brain cholesterol turnover, as it can freely cross the BBB and be mainly excreted in the circulation. (24S)-HC plasma levels might so reflect neuroneal degeneration based on brain cholesterol conversion. Comparative studies between ND patient and healthy individuals focusing on the cholesterol and (24S)-HC plasma/CSF levels show relevant differences between the disease and the control groups, highlighting specific medical-condition related alterations but also sex related ones. (Agarwal & Khan, 2020; W. J. Griffiths *et al.*, 2013, 2021c, 2021a; Leoni *et al.*, 2013; Leoni & Caccia, 2011; Pizarro *et al.*, 2013; P. Wang *et al.*, 2020; Yutuc *et al.*, 2021; J. Zhang *et al.*, 2017). Even tough promising results are arising from the cholesterol and (24S)-HC profile of human fluid matrixes, multiple contrasting results are also emerging. The reasons for the apparent contradicting information are multiples and fall in part in systematic errors. Sterol lipid are vulnerable molecules, sensible to spontaneous autoxidation.

During matrixes extraction, standard operating procedures aimed to minimise oxidative processes must be adopted. Moreover, the different extraction techniques introduce different pitfalls that can in turn modify the outcome of the extraction and modify the composition of the extracted sterol lipids. Standardisation of the extraction protocols and their application might represent a good compromise to obtain reproducible and comparable results between different laboratories and research groups. The same concept is also applicable to the analytical technique used for quantification purposes. Even in this case, a single standard procedure applicable to a single analytical technique must be implemented, optimised, and generally adopted between labs. Attention should also be put to the presence of confounding factors. All the confounding factors must be considered, like patients age, sex, disease progression, comorbidities, presence of a damaged BBB as well as careful disease stratification The controversy around the quantification of the sterol lipids and their relationship with NDs can be therefore tackled upon standardisation of the laboratory procedures, of patients' inclusion criteria and correct disease characterisation. Fine and precise sterolomic profile of human body fluids might represent a new source of easy quantifiably and reliable diagnostic and prognostic biomarker ND.

1.5 Sterolomics

Sterol lipids (ST) are hydrophobic and/or amphipathic small molecules built on a cyclopentanoperhydrophenanthrene skeleton that derives from the carbocation condensation of isoprene units. ST represents one of the eight classes in which lipids have been classified by the web portal Lipid Maps, based on their chemical properties (Fahy *et al.*, 2005; LIPID MAPS® Structure Database (LMSD), n.d.). Sterols, steroids, secosteroids, bile acids and their derivatives, and steroid conjugates are the five subclasses in which ST are divided and comprise all the eukaryote and prokaryote ST identified so far. The vast chemical diversity that characterises this class of lipids reflect the broad range of metabolic and functional pathways in which these molecules take part. For example, cholesterol and its derivatives, whose belong to the sterols subclass, play several important functions for the mammalian and eukaryotic cell, see section 1.1.1.2. Seeing the numerous implications of ST for human health, in the last 50 years various studies have been dedicated to the comprehension of ST biological functions, biosynthetic pathways, metabolisms and the molecular mechanism in which these molecules are involved. However, the characterisation of ST biological activities requires first a fine and precise identification of the different ST in an organism. The need for reliable and reproducible methods for the qualitative and quantitative analysis of ST opened the window to the development of a new branch of science: sterolomics. With the term sterolomics we refer to the quantitative or semi-quantitative profile of all the ST molecules in a specific cell type, tissue, organ, body fluid or system. The vastity of different ST and the presence of isomers make the identification process even more challenging.

The characterisation of ST in a biological matrix is multi stages process made of three to four different steps starting with ST extraction, extract purification and sterols separation, chemical derivatisation, if required, and qualitative-quantitative analysis of the extract. A detailed step-by-step description of the techniques utilised in this thesis for the sterolomic profile is reported in the following sections of this paragraph. In this thesis we will mainly focus on the profiling of cholesterol and its metabolites oxysterols in AD and PD, so all the next sections concentrate on this subcategory of the ST.

1.5.1 Sterols extraction from human biological matrixes

The first step in the characterisation of biological samples for cholesterol and oxysterols content, which will be referred as oxystereolome, is their extraction and separation from all the other unwanted biomolecules. Extraction represents a crucial moment in the sample processing, therefore care and precaution must be taken to avoid contaminations, losses, sterols degradation. Several methods can be applied for the extraction of the sterols, from the classical liquid-liquid extraction to single liquid extraction followed by solid phase extraction (SPE) separation/purification or a newly developed technique implying supercritical fluids. The nature of the matrix as well as the type of the analytical techniques employed for the qualitative and quantitative sterol analysis are the main factors that must be taken into consideration when selecting an extraction procedure. In presence of a fluid sample like plasma, serum, CSF, urine, cell medium etc., it might be preferrable to use a solvent for extraction, mainly represented by liquid-liquid or single solvent - solid phase extractions techniques. This type of matrix is usually rich in polar solutes like salts, ions and proteins which are insoluble in many of the organic solvents employed for the sterol extraction. Depending on their concentration in the biological fluid, the addition of an organic and poorly polar solvents leads, generally, to protein precipitation which can cause formation of unwanted inclusion complexes and reduce the extraction yield. For low abundant sterols like oxysterols (n.b plasma concentration in human goes from dozen of picograms to hundreds on nanograms per mL of fluid) inclusion complexes should be avoided. The unwanted polar material in human

fluids can easily distribute into aqueous layer and be quickly separated from the lipidic/sterols content therefore liquid-liquid extraction with organic solvents and the addition of water buffers can represent a feasible option.

A lot of heterogeneous material is formed during this first part of the protocol which can hugely interfere during the liquid-liquid extractions. In fact, it is often preferred to follow a single solvent extraction followed by centrifugation, recovery of the supernatant and solid phase extraction (SPE) as extraction method for solid-bulky human/biological samples. The techniques here described represents the gold standards for lipid and sterols extraction, but the use of non-green, non-recyclable, pollutants and toxic organic solvents pushed the researchers to develop novel green, less environmental nasty extraction technique. As sterols are basically amphipathic but very hydrophobic molecules, the use of safe solvents like water or acetone is prohibitive. However, the advent of supercritical fluids like supercritical CO_2 opened the doors to a new extraction technique called supercritical fluid extraction (SCFE).

Each extraction technique will be briefly described in the next sections.

1.5.1.1 Liquid-Liquid extraction

The first method to have been developed for sterol enrichment is liquid-liquid extraction. Widley use in the synthetic chemistry world as it represents a quick and efficient way to separate or purify compounds from heterogenous reaction mixtures, this technique has been largely used for the biological sample lipid extraction. The procedure involves the use of an extraction solvent that is added first

to the biological sample followed by the addition of an immiscible second solvent which forms a two-phase separation system, see figure 1.20. Vigorous shaking of the biphasic mixture lets the repartition of the molecules present in the sample between the two solvents, based on their solubility. The extraction solvent is then collected and washed to remove any possible trace of the immiscible solvents. The desired compounds are so extracted from the biological sample. The simplicity of the procedure however requires a careful and accurate design of experiment to not occur in unfortunate contaminations or target molecule degradation. Moreover, while liquid-liquid extraction represents a fast and efficacious method for untargeted analysis, single lipid class extraction, for example STs cholesterol and oxysterols, has some drawbacks which depends on the chemical and physical properties of the target molecules. When ST lipids need to be extracted, accurate extraction solvent selection is required, which needs to be non-polar to slightly polar organic solvents, generally chlorinated (Bligh & Dyer, 1959; Folch *et al.*, 1956), which however, increases the chance of water/salt contamination. For ST lipids liquid-liquid extraction, a water buffer solution is employed as immiscible solvents. The buffer can determine salts and ions contamination of the organic layer, resulting in charge suppression effects or adducts formations of the analyte molecules, which can massively interfere with the mass spectrometry analysis of the sterols extract. Furthermore, if a chromatographic separation of cholesterol and same polarity sterols from more polar oxysterols and cholestenoic acids does not follow the liquid-liquid extraction, the extraction solvent must be added of antioxidants to avoid spontaneous cholesterol autoxidation and artefact enrichment of the extraction mixture of cholesterol peroxidation derived oxysterols.

Again, the use of antioxidants might interfere with the selected analytical technique for ST identification/quantification.

Once recovered, the extraction solvent in generally washed once or twice and the sterol fraction dried down. At this step the dried fraction is reconstituted in a pure organic solvent, generally the same used for the extraction, and either stored between -20°C and -80°C for later usage or immediately analysed.

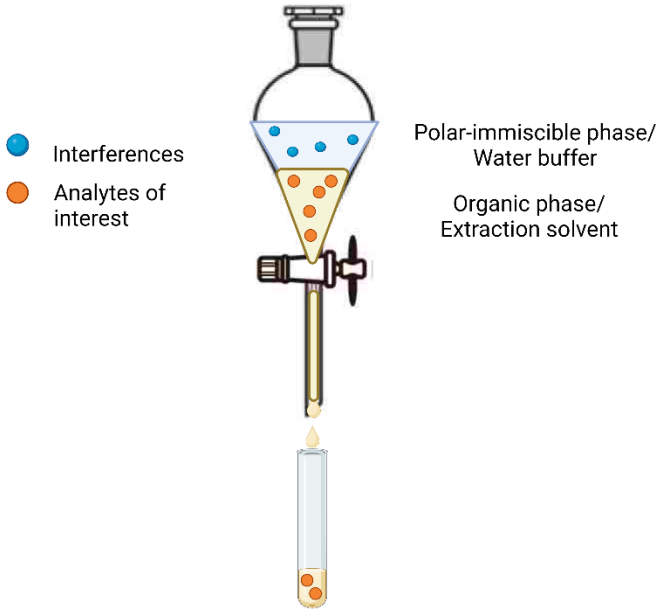

Figure 1.20 General liquid-liquid extraction procedure.

1.5.1.2 Single solvent extraction and Solid Phase Extraction (SPE)

The simplicity, and the relative high speed and the good recovery of the liquid-liquid extraction has made it a widely used technique, however because of its drawbacks in targeted analysis, other extraction techniques have been developed. Single phase solvent extraction uses one or a combination of organic miscible solvents to extract target molecules from a biological matrix. In the initial step the organic solvent or solvent mixture is added to the sample. If the biological matrix is fluid, like plasma, or dispersed, like cell pellet or homogenised tissue, the solvent is generally added under sonication. In this way, the target molecules are efficiently extracted. Care must be taken when choosing the correct extraction solvent. Also in this case, the selection must consider the target molecules chemical properties and solubility with a particular attention to the penetration enhancer properties of the solvents. It becomes particularly true in the presence of bulky samples that needs to be homogenised to let the solvent extracts all the lipids. For cholesterol and oxysterols extractions, short chain alcohols like MeOH or ethanol (EtOH) are often preferred. During sonication, protein precipitation occurs. A following centrifugation step is thus required to separate the protein and any other insoluble molecule from the lipid extract. The lipid extract is recovered and based on the application, targeted or untargeted analysis, can be subjected to an additional SPE step. The SPE method is generally favoured for targeted analysis as it allows a feasible and relatively quick separation of the different lipid classes but also of different subclasses belonging to the same family,

see figure 1.21. Moreover, SPE helps to enrich the extracted fraction of the molecule of interest. The separation behind SPE is quite straightforward and follows the general chromatographic principle of molecule repartition between the stationary and the mobile phase. Before loading the sample, the SPE column needs to be washed with the solvent used for target molecule elution and conditioned with the solvent used for sample loading. The lipidic extract is then loaded to the column and let pass through the column bed. During this phase, the retained molecules make new bonds with the stationary phase. The flow through can be collected if it contains target analytes or discarded at this point. A washing step before elution might be necessary to wash out undesired non retained molecules present in the extract. Elution solvent is now applied and flow-through collected. The targeted molecules elute in this step. The eluate is then dried down and the extracted compounds resuspended in organic solvents for long term storage between -20°C and -80°C or immediately analysed. Crucial point when building a SPE protocol is the selection of the right stationary phase. The analyte must be retained by the column during the loading phase but released when the elution solvent is applied. The type and the number of the interactions between the analyte and the stationary phase determines how strong it is retained. Neutral and hydrophobic compounds like oxysterols and cholesterols tend to form more hydrophobic interactions compared to ionic or hydrogen bonds. Generally, sterols make several Van der Waals and electrostatic interactions via their side chain and ring structure while only few hydrogens bonds with their additional hydroxyl or carbonyl groups. For this reason, an octadecyl (C-18) Reversed Phase(RP) silica SPE column is often preferred for their extraction and separation, but also hydrophilic lipophilic balance (HLB) polystyrene is widely used. Both

C18 RP and HLB can form strong hydrophobic bonds with hydrophobic compounds, in fact they both possess a high carbon loading capacity, however HLB possesses a higher loading capacity than C18 RP. Moreover, HLB can work in a wide pH range than C18 RP, 0 to 14 compared to 2.5 to 8, resulting in a more stable column. The selection of the elution solvent is another important step as it must guarantee the highest analyte recovery but also separation from the other analytes. The elution solvent characteristic might than be so summarised:

- The analytes must be soluble in it.
- The analytes must have more affinity to the mobile phase than to the stationary phase to be elute. However, depending on the application scope of the SPE, target molecules separation or cleaning from undesirable interferents, the elution solvents and stationary phase binding properties towards analyte molecules can vary, ex. part the analyte might not be retained by the column, and this can be used for separation from other analytes.
- No matrix effects.
- No degradation of the analytes.
- Correct pH range to elute the analyte without affecting the stationary phase.
- Adequate viscosity to not cause any back pressure to the column and expand elution time.

Generally, a mixture of EtOH and water or MeOH and water but also acetonitrile (ACN) constitutes the most used elution mixtures as these solvents resemble all the characteristic just cited while exploiting the best separation efficiencies. When single solvent extraction is applied for a targeted cholesterol and oxysterols

extraction, a further SPE step is usually required for two main reasons: purification of the ST fraction from lipids and other molecules with similar polarity and separation of the highly abundant cholesterol from the low abundant oxysterols. In human derived samples cholesterol can be up to 1000-fold higher compared to oxysterols, depending on the origin. If a mass spectrometry analysis follows the single solvent extraction, an SPE intermediate step can be used to avoid any ion suppression effect from highly abundant cholesterol. To note, SPE increases the total time needed to complete the sample preparation and lipid extraction, enhancing the risk for molecules degradation. Longer protocols also increase the risk of contamination and possible sample losses over multiple steps. However, for specific class of lipids, like ST and in particular cholesterol and its metabolites, an additional SPE step is generally needed. Specific and tailored single solvent extraction-SPE protocols overcome the time related issue. Targeted and easy to follow procedures for sterols single solvent-SPE extraction have now been developed with good sterol recovery minimising lipid degradation (W. J. Griffiths *et al.*, 2013, 2021b, 2021c; Y. Wang, Sousa, *et al.*, 2009.; Yutuc *et al.*, 2021)

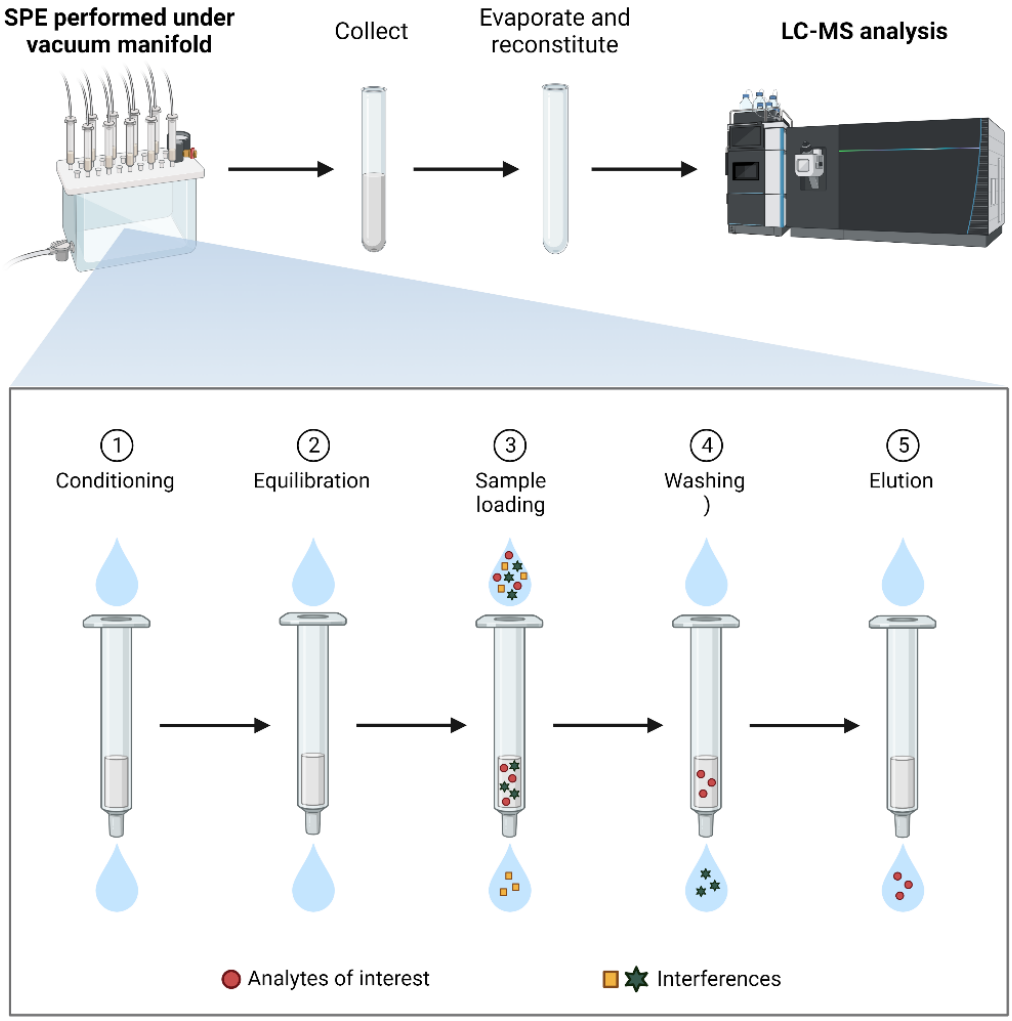

Figure 1.21 General procedure for SPE chromatography extraction/separation of analytes of interest.

1.5.1.3 Supercritical fluid extraction (SCFE)

The word supercritical fluid defines a specific physical status of a substance when it reaches, or go above, its critical point, defined by a critical temperature and a critical pressure. A super critical fluid (SFC) is a homogeneous fluid which has a density and diffusivity in between the one of a gas and a liquid. Usually, SFCs possess the high

density of a liquid but the diffusion and viscosity of a gas (Fjeldsted & Lee, 1984; Scholsky, 1989). This characteristic allows the SCF to solubilising substances like a liquid solvent but also to diffuse like a gas. One of the most well-known applications of SCF is their use as as extraction solvents (Grigonis *et al.*, 2005). In the SCFE apparatus, gaseous CO_2, or other gasses, is pumped to the extraction vessel. Before entering the vessel, the temperature is risen and pressure lowered down, causing the CO_2 to reach the supercritical values and be in the supercritical status. Supercritical CO_2 now enters the extractor where the sample is present. Here, it solubilises and extracts the target molecules form the sample. Once extracted, SC CO2 extract is let to pass into the separator. Here, CO2 is brought back again into its gaseous state upon the release of the pressure valve causing the separation of the extracted molecules. Gas CO2 is then directed to a condensation vessel where, lowering the temperature, is stored as a liquid, ready for a new cycle. In the separator, the extracted molecules are captured in a collection vessel and further purified or analysed if the system is directly coupled with chromatographic apparatus. Lipid extraction using SCF has the tremendous advantage of being very selective upon easy manipulation of its density (Grigonis *et al.*, 2005). SCFE is fast, reducing the total extraction time from 10 to 60 minutes per extraction. In addition to that, SCFE requires only a minimal amount of solvent. Most of the SCFs are inexpensive, nontoxic, inert, and pure, like CO_2, contributing to make it a very advantageous technique. Opposed to the many advantages represented by SCFE, the technique also possesses some limitations. First, the apparatus is quite expensive compared, for example, to the liquid-liquid extractions and requires constant maintenance, further increasing the coasts (Khosravi-Darani, 2010). Secondly, CO_2 has the capacity

to dissolve very polar molecules, contaminating the extract. Recently, SCFE has been applied also for cholesterol extraction from natural products, in particular form food sources (Sahena *et al.*, 2009). The method enables efficient, fast, and high purity cholesterol extraction from a broad variety of foodstuff without a preliminary lipid extraction. A recovery of almost 60% of the whole cholesterol content with a purity of 98% entitles SCFE to be the new quickest and most efficient method for food cholesterol extraction (Sahena *et al.*, 2009). However, for clinical and research purposes SCFE might not be the ideal technique to use, mostly because of its high costs and tedious maintenance procedures.

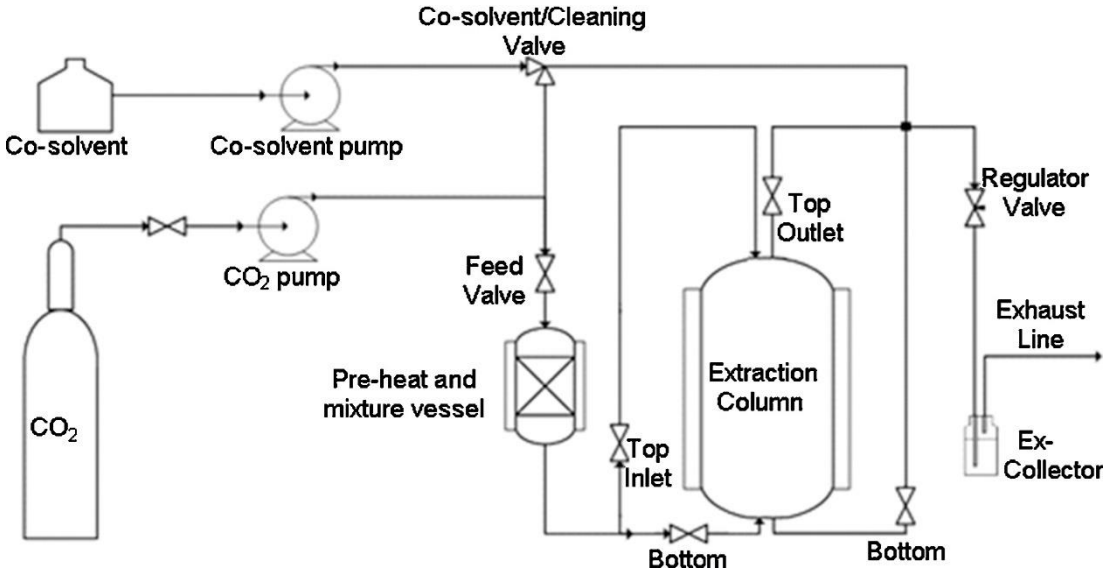

Figure 1.22 Schematic representation of the SCFE.
Figure taken from (P. F. Martins *et al.*, 2016)

1.5.2 Extract purification and derivatisation techniques

The second step that characterise a sterolomic analysis is usually represented by a purification step. Careful sample handling and storge must have always been carried out to avoid the introduction of unwanted molecules. For example, plasticware should be avoided when strong organic solvent is used, to eliminate the risk of contaminating the sample with plasticizers. Moreover, the use of antioxidant is encouraged to avoid sample degradation through oxidation, if a chromatography separation is not carried out. ROS can be already present in the sample to extract but they can also be formed upon sample preparation and extraction, causing easy oxidation of liable lipids. This is particularly true for sterol lipids, in particular cholesterol, that can be easily oxidised and form oxysterols. As previously mentioned, some endogenous oxysterols derive from the cholesterol autoxidation, but they are indistinguishable from the ones made during sample prep. Therefore, there is a high chance of introducing errors in the estimation of the oxysterols content if specific antioxidant procedures or separative SPE are not followed. Purification procedure also helps in stabilising the pH of the extraction, particularly when a chromatography step is involved. With this being said, careful extraction solvent selection is always carried out but sometimes the use of a basic or acidic compounds cannot be avoided (W. J. Griffiths *et al.*, 2013; Yutuc *et al.*, 2021). As an example, when total sterols amounts are to be determined a basic hydrolytic step must be performed during the extraction to hydrolyse sterol esters to the free molecules which are analysed. Low pH can cause dehydration of oxysterols containing 7-

hydroxy-3-oxo-4-ene moieties. To minimise oxysterols degradation a neutralising agent is added after hydrolysis, followed by a SPE purification/separation step.

Most of the extraction methods above cited yields but additional purification might be required for different purposes:

- Targeted qualitative analysis, where more pure extracts are needed.
- Quantitative analysis, where the presence of contaminants should be avoided for fine and precise quantification.
- Clean up of the extract if a mass spectrometry or chromatographic analysis follows. Contaminants might affect not only the analysis itself but also the instrumentation. For e.g., contaminants can saturate the chromatographic column, and results in a dramatical reduction of its separation capacity.
- Avoid target molecule degradation. Sometimes the contaminants might induce ST, or lipids in general, oxidation.

The most common, but also quick and feasible, purification/separation technique is the chromatographic separation. Generally, for sterol analysis, a silica normal phase or reversed phase is employed and atmospheric or pressure chromatography is carried out (Aldana *et al.*, 2020; W. J. Griffiths *et al.*, 2013; Saini *et al.*, 2021). The principles are the same as the ones described above for the SPE. Lipid/ST extracts are loaded into the silica column and analyte molecules eluted based on their polarity. In a normal phase silica column, polar sterols are retained more and elute later while more hydrophobic elute first. The reverse is true for reversed phase silica columns. The advantage of using silica chromatography is the reliability of the technique, constant yield over time, and the reproducibility, which makes it suitable for scale-ups. The

chromatography is also relatively quick and not expensive. The downside of an intermediate chromatography step is not only the extended time, and so on costs, but also the possibility of sterol losses or degradation. Degradation can be avoided with the use of antioxidants, work-up in anhydrous or modified atmosphere and low temperature and optimal chromatography set-up to ensure high recovery yield. Less "time consuming" techniques might involve sterol solvent crystallisation and separation. However, this technique is mainly implied in phytosterols extraction from plants and does not give good yields, but very high purity of about 92-96% (Savinova *et al.*, 2012; H. Yang *et al.*, 2010; H. Zhang *et al.*, 2017).

Pure ST extracts can now be directly qualitative and quantitative analysed or be subjected to a chemical derivatisation. Chemical derivatisation is the process where an analyte is chemically functionalised to improve certain physiochemical properties. In sterolomics, but also lipidomics, chemical derivatisation is a well-adopted approach used for different purposes, based on the analytical technique used for identification. The most widely used analytical techniques are GC, LC, GC-MS and LC-MS. Derivatisation can be useful to:

a. Improve chromatography separation.
b. Lowering the boiling point and so increase the volatility, in the case of GC.
c. Improve analyte stability, for example reducing the thermolability, but also protecting target molecule liable functional groups.
d. Enables chiral compound separation.
e. Increase mass spectrometry sensitivity (detection)

f. Cause specific fragment formation and giving fingerprint-informative structural information (mass spectrometry)

Core principle of the derivatisation is that the chemical reaction must happen only between the reagent and the target molecule, but not with the matrix. However, some unexpected reaction might happen. In that case a sample clean up or additional chromatographic separation might be introduced to get rid of these side products, if they affect target molecule analysis. Chemical derivatisation is usually applied before chromatographic analysis, during or after sample extraction. . Over the years a broad range of different chemical reactions have been developed to improve target molecules analysis, based on the characteristic above cited. The variety of chemical reactions used in derivatisation usually modify more than one chemical property of the target molecule (a-f), bringing a lot of advantages.

Acylation reactions, which consist in a nucleophilic substitution between an active hydrogen of the target molecule, the nucleophile, and an acyl derivative, the electrophile, are commonly use in sterol analysis Picolinic ester formation on the alcohol moieties of sterol lipids, see figure 1.23 C (Honda *et al.*, 2008, 2009a; Ikegami *et al.*, 2012). *m/zet al.et al.*and N,N-dimethylglycine esters formation with sterols alcohol, see figure 1.23 E (Jiang *et al.*, 2007, 2011) are the most used acylation reaction for ST analysis Both derivatisations strongly improve sterol ionisation and MS detection, allowing the detection of the esters in the order of nanograms per mL of plasma*et al.*. Respect to piconylic esters, the dimethylglycine ones also improve chromatographic separation enabling the development of sensitive, reliable, and reproducible LC-MS-MS techniques for sterol plasma analysis (Jiang *et al.*, 2011).

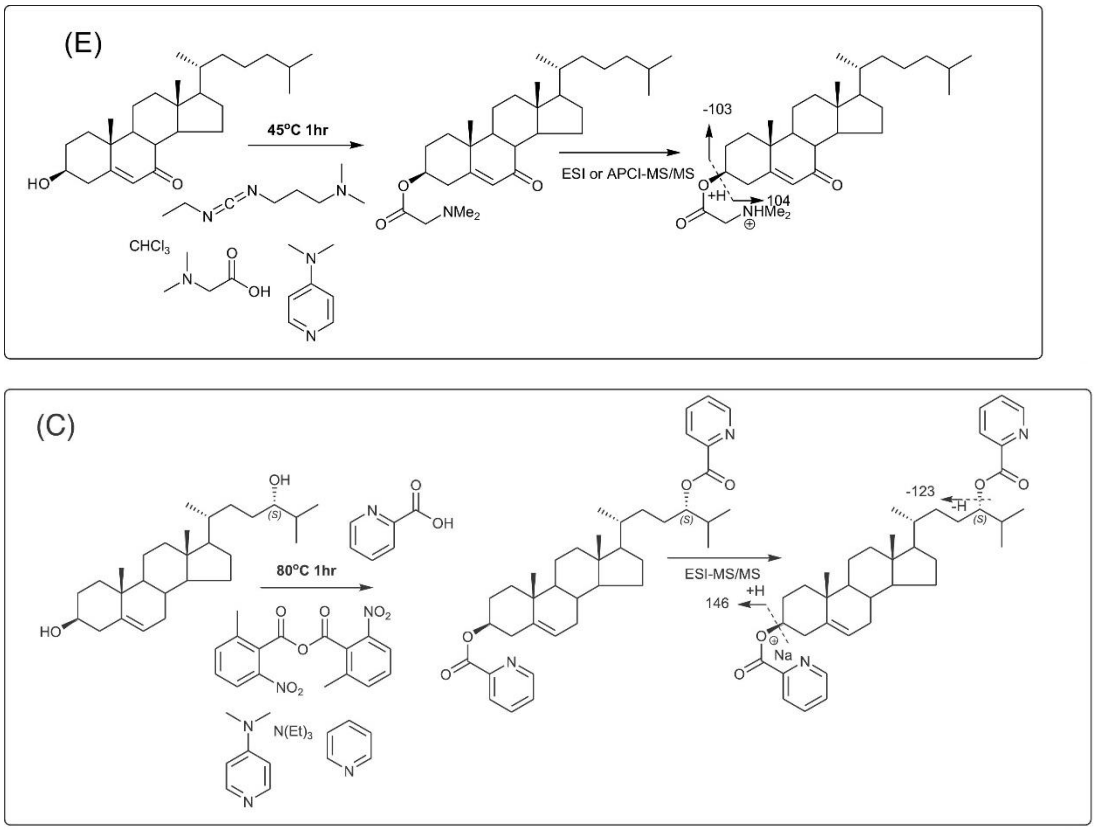

Figure 1.23 Example of steroid acylation.
(E) Steroid acylation with dimethylglycine, 4-dimethylaminopyridine in chloroform and 1-ethyl-3-(3-dimethylaminopropyl) carbodiimide in chloroform to form dimethylglycine esters. (C) Steroid acylation with 2-methyl-6-nitrobenzoic anhydride, 4-dimethylaminopyridine, picolinic acid, pyridine and triethylamine to form picolinic esters. Figure taken from (W. J. Griffiths *et al.*, 2016)

However, mammalian and eukaryotic ST present different isomers, including epimers and positional isomers, which complicate their correct identification. Acylation represents a valuable derivatisation technique, which enables also the characterisation of positional isomers.. Besides these chemical reactions, other derivatisation techniques have been developed to specifically improve sterols properties towards LC-MS analysis. One of the major breakthroughs in the development of targeted chemical reactions has been the possibility to not only improve the ionisation profile of the sterol, while permitting good isomers separation upon LC, but also to

increase the solubility of these hydrophobic molecules in organic-water mixtures. The enhanced solubility in polar solvents avoids sterol precipitation in polar environment and allows the use of a new broad range of solvents to set-up an optimum chromatography, and to guarantee isomers separation. Hydrazones formation employing Girard hydrazine reagents are generally used for the above purposes. Girard reagents were developed in the first half of 1900 by Girard and Sandulesco. Girards are quaternary ammonium acetyl hydrazines which react with carbonyl groups of aldehydes and ketones to give hydrazones. This improved method allows easy separation of ketones and aldehydes out of complex mixture, without requiring extreme hydrolytic conditions during workup to re-obtain the pure carbonyl groups (A. , and S. G. Girard, 1934; A. Girard & Sandulesco, 1936). After the introduction of the first Girard reagents, trimethylammonium acetyl hydrazide chloride and pyridinium acetyl hydrazide chloride, several other hydrazines with improved chemical reactivity followed (Owen H. Wheeler, 1968). The use of Girards for sterol separation was initially used to separate estrone from urine, see figure 1.24 (A. Girard & Sandulesco, 1936). Estrone is the endogenous inactive from of oestradiol and possess a ketone group at C17. The ketone at C17 reacts with the hydrazine group of Girard to give a C17 hydrazone, which can be easily separated from the mixture of the other sterols. Following their introduction, Girards have been amply used for the recovery of steroids naturally possessing a ketone group (Owen H. Wheeler, 1968). Moreover, with the introduction of LC-MS analytical tools, Girard reagents have been leveraged to improve the ionisation profile of steroids (Shackleton *et al.*, 1997). Sterol scientists have extensively explored the chemistry of hydrazone formation, using different types of Girard reagents to develop a new, reproducible, and reliable method for

oxysterols analysis (W. J. Griffiths *et al.*, 2013; Karu *et al.*, 2007, 2011; Meljon *et al.*, 2012; Ogundare *et al.*, 2010; Theofilopoulos *et al.*, 2014; Y. Wang *et al.*, 2008, 2009; Yutuc *et al.*, 2020). On of the best example employing Girards as derivatising agents for sterols LC-MS analysis is a procedure called Enzyme Assisted Derivatisation for Sterol Analysis or EADSA, which it composed of two step, see figure 1.25:

1. Specific enzymatic oxidation of the sterol 3ß-OH group, which is converted in a 3-ketone group (3-CO)
2. Derivatisation of the 3-CO with the use of [$^2H_5$]Girard P (GP D_5) or [$^2H_0$]GP reagent (GP D_0).

A detailed description of the analytical method can be found in the Methods section, chapter 2, section 2.6. As previously mentioned, the introduction of a quaternary nitrogen moiety, in this case a quaternary nitrogen on the pyridine group, greatly improves the sterol sensitivity towards MS technique. An EADSA-LC-ESI-MS-MS-MS or EADSA-LC-ESI-MS^3, where ESI stands for electrospray ionisation technique, has been developed for the detection of more than 60 different sterols in only one mass spectrometry run (W. J. Griffiths *et al.*, 2013). The use of EADSA and GPs has allowed the sterolomic profile of several biological matrixes, from human plasma to human organs and tissues or cultured cells but also mice plasma to brain, making it a very reproducible, reliable, adaptable, and chameleonic approach for sterolomic profile of a broad range of biological samples.

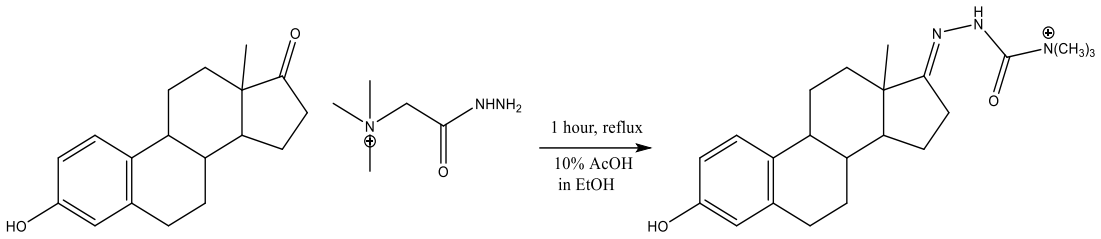

Figure 1.24 Girard P derivatisation of estrone.
The Girard T, trimethylammonium acetyl hydrazide, reacts with the estrone's C-17 ketone in 10% AcOH ethanolic solution under reflux to give the desired positively charge tagged estrone hydrazone.

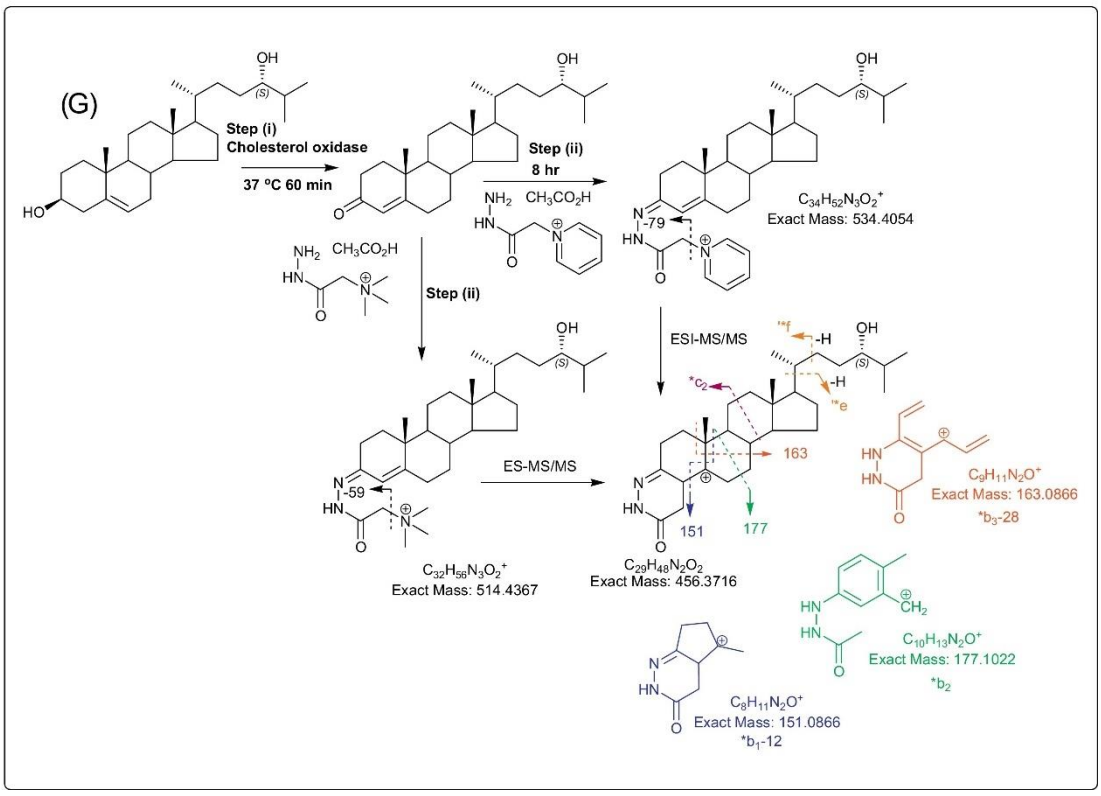

Figure 1.25 Sterol derivatisation with the Girard hydrazine.

Sterol derivatisation with Girard hydrazine requires an initial enzymatic oxidative step which converts the 3-OH into a 3-keto, forming a 3-ketone-4-en structures. The following step see the formation of the sterol hydrazone through the nucleophilic addition of the Girard reagent. Positively charged hydrazones are able to form specific fingerprint fragments upon neutral loss of the pyridine ring in multistage fragmentation MS. Figure taken from (W. J. Griffiths *et al.*, 2016)

1.5.3 Chromatographic separation

The last, but not least, step for a complete sterolomic profile is the identification and quantification of ST present in the extracts. The main techniques implied for sterols identification are nuclear magnetic resonance (NMR), GC, LC, and MS. Whether NMR is broadly used in organic synthesis for the fine and precise identification of synthesised sterol molecules, it is not the preferred technique when sterolomic analysis must be carried out.

With respect to the selectivity, isomer separation, and easy sample preparation, NMR has been rapidly substituted by chromatographic techniques for two main reasons: lack of sensitivity, and difficult spectra interpretation due to the magnetic field drift. The first chromatography technique to have been employed in sterols separation and identification is thin layer chromatography or TLC (Schroepfer, 2000b). The TLC method is quite rapid and doesn't require long and tedious sample preparations. The sterol mix is dissolved in the minimal amount of organic solvent and loaded into the thin silica layer which cover an aluminium foil and let develop in a chamber saturated with the vapours of the mobile phase. (Schroepfer, 2000b). TLC is a very fast, unexpensive and easy technique, broadly used to monitor sterols organic synthesis fate. However, it is not suitable for the resolution of complex sterols mixtures from biological sample.

With the advent of GC and LC techniques, TLC has been readily substituted with the new and improved chromatographic procedures,

which have become the new gold standards for metabolomics approaches, particularly for lipidomic and sterolomics analysis.

1.5.3.1 Liquid Chromatography

The liquid chromatography, LC, has been one of the first chromatographic technique to have been invented in 1906 by the Russian botanist Mikhail Tswett (Tswett, 1905). He used liquid-adsorption column chromatography with calcium carbonate as stationary phase and petrol ether/ethanol mixtures as mobile phase to separate chlorophylls and carotenoids. Since then, LC has seen a huge improvement and optimisation over the years, partially because of its easy adaptability and ability to separate a broad range of different molecule simply modulating the elution solvents and/or changing the stationary phase. Briefly, LC is a technique where compounds are separated based on the type and number of interactions they have between the stationary phase and the mobile phases. Historically, LC apparatus was made of an analytical column packed with the stationary phase through which the mobile phase, or elution solvents, were let to pass by, at atmospheric pressure. The sample, containing the molecules to separate, was loaded into a pre-conditioned stationary phase, and subsequently eluted with the eluent mixture. Nowadays atmospheric pressure LC has been almost completely substituted with the newest high performance liquid chromatography (HPLC), also called high pressure liquid chromatography. To avoid any misunderstanding, in this thesis the term LC refers to the analytical technique High Performance Liquid Chromatography. The LC apparatus is made of 3 different modules

which consist of an autosampler, a column oven and a binary pump module, which also include a degasser, figure 1.26. The LC workflow is made of 6 easy steps, figure 1.26: column equilibration, sample loading, separation, elution, final column wash and column re-equilibration. Before the start of the chromatographic run, the stationary phase is equilibrated, pre-conditioned, which serves to first eliminate any possible residue form previous run and secondly to prepare the column for sample loading. The preconditioning step accounts for five to ten column washes or a couple of minutes. Sample are then loaded into the autosampler trays, and an injection needle will be responsible for the pick-up of the sample and loading into the sample loop (loading phase). A six-port valve in the autosampler is responsible for the load of sample into the sample loop as well as for column loading. The switch to the injection position allows the sample to be introduced into the mobile phases flow and pumped into the analytical column. Analytes molecule now interact with the stationary phase and are separated and then eluted. Once all the target molecules have been eluted from the column a column wash usually follows, to clean the stationary phase, and the re equilibration phase can now start. The second equilibration step serves to bring back the column to the original conditions, which have been set up to permit an optimal sample loading.

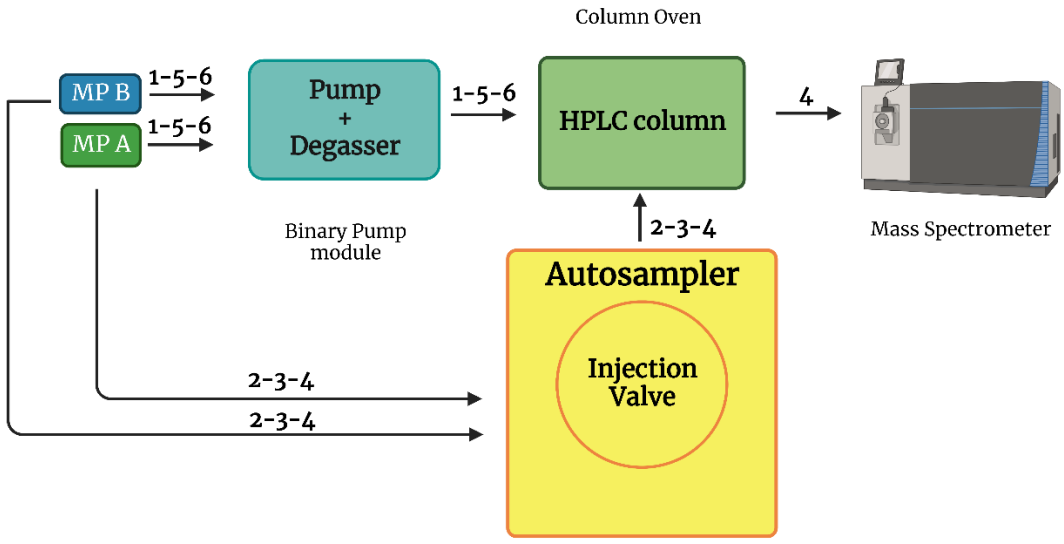

Figure 1.26 HPLC workflow.
In the figure 1.26 a general HPLC workflow is represented. Step **1** sees a column equilibration where the solvents are only flushed through the pump module to prepare the column for the run. Step **2,3 and 4** involves sample loading through the injection valve in the autosampler, sample pumping into the analytical column thanks to mobile phases flow, separation of the analytes upon analytical column binding and analytes elution on a polarity based. After elution, step **5** and **6** are used to wash the column and re-equilibrate it for the next run. To note that in steps 2,3 and 4 mobile phases passes through all the 3 modules while for steps 1-5 and 6 only between the pump and column oven module. MP, mobile phase.

The chromatographic column is packed with the stationary phase, which can be made of different materials and particle sizes, based on the characteristic of the molecules to separate. The column is in a centimetre-scale, usually 1 to 30 cm long, with an internal diameter (id) in our studies in the order of millimetres, usually 1 to 4.6 mm. A degasser is used to avoid the generation of air bubbles in the mobile phase. The choice of the stationary phase depends on the chemical structure of the molecule to separate, and so on the type of interactions that are established between it and the analytes. Three are the main and classical physical interactions on which a column is developed:

1. **Polarity-based separation.** Most of the columns now available are developed based on physical interactions: functionalised stationary phase can make hydrogen bonds, dipole-dipoles interactions, London and wan Deer Walls force or complex formation. The type and the number of interactions between the analyte molecule and the stationary phase determines the separation efficiency and the analyte retention time (RT,) time needed for the compound to be completely eluted form the column). The more interaction, the longer the RT. Normal Phase(NP) and Reversed Phase (RP) silica columns as well as hydrophilic interaction liquid chromatography (HILIC) are the most employed polarity-based columns.
2. **Ion exchange separation.** This method is solely based on the electrostatic interaction and coulomb force between cations and anions, analytes, and the stationary phase. The stationary phase can be composed of positively or negatively charged functional groups. If the stationary phase contains positively charged groups, a negative counter ion will be bound to it. When a negative analyte encounters the stationary phase, it will replace the counter ion. The charge of the stationary phase and analytes can be modulated by adjusting the pH or composition of the mobile phase, extending the range of possible modifiable parameters, and helping in the resolution of complex-polar mixtures of compounds. This type of chromatography is applied to small molecules (ions) (Amran *et al.*, 2020) and macromolecules (R. Zhang *et al.*, 2014)
3. **Size exclusion chromatography.** This method allows compound separation based on dimensions: the molecule is trapped into stationary phase particle pores, meaning that the smaller the molecule, the better should fit into the pores and so the more

will be retained by the column. This technique is widely used for proteins (Sathitnaitham *et al.*, 2021), carbohydrates (Perez-Moral *et al.*, 2018), polymers (Janco *et al.*, 2013) and surfactants (Kothencz *et al.*, 2018)

Over the last 20 years, different stationary phases have been developed and implemented, in most of the cases combining the 3 principles above to obtain a better separation and giving birth to the so called mixed-mode chromatography (Aral *et al.*, 2015; Hosseini & Heydar, 2021; Shen *et al.*, 2013; J. Wei *et al.*, 2012; Xiong *et al.*, 2018). For sterol analysis, the preferred stationary phase is usually a RP, however also NP has been used. RP is a more stable and easier to modify stationary phase and is preferred for ST analysis. RP columns are often made of a hydrophobic alkylated silica stationary phase. The C8 or C18 stationary phases, are generally the most utilised for sterol separation and give good results in terms of peak resolution, when a gradient elution is implied (Griffiths *et al.*, 2021b; Honda *et al.*, 2009b; Karu *et al.*, 2007, 2011; McDonald *et al.*, 2012a). The RP is characterised by a polarity-based chromatographic separation which implies the formation of London and wan Deer Waals interactions between the stationary phase, the analyte molecules. Sterols, ST, elute order depends onto their Log P, with bile acids and cholestenoic acids in general eluting before side chain oxysterols and lastly ring oxysterols, cholesterol, and precursors (Careri *et al.*, 1998; Poole & Lenca, 2017). Different derivatising agents, like piconyl esters or Girard reagents, do not seem to interfere with the retention order as much as the column type or the mobile phases. To note, derivatisation can still bring to the formation of diastereomers and as such helping in the chromatographic resolution of isomers, but not at the same extent as mobile or stationary phase change. Chaining

mobile phase composition can dramatically affect the separation and peak resolution, as shown by Shan *et al* (Shan *et al.*, 2003). Shan and co-workers compared oxysterol separations when two solvent systems, acetonitrile: water and methanol: water, were applied on C8 and C18 columns. They showed that even with same solvent system, the chromatographic mobility and selectivity between C8 and C18 columns were considerably different. While C8 column was able to resolve several oxysterol pairs, including 7α- and 7β-HC, when MeOH:H_2O were used, C18 showed no separation using the same mobile phase. However, when ACN:H_2O was applied to C18 column, improved resolution of oxysterol pairs 27-HC/(24R)-HC/20α-hydroxycholesterol and 7α-HC/7β-HC was seen. Moreover, several different methods have been optimised to obtain base-line separation of several oxysterols like (24S)-HC and 25-HC, which are very difficult to separate. Debarber *et al* (DeBarber *et al.*, 2008a) and Burkard *et al* (Burkard *et al.*, 2004) are only some examples of how, even using the same solvent mixtures but in different composition and experimental condition (e.g. column oven temperature), chromatographic resolution can be improved, and with it the time of analysis. Separation of epimers is one of the major challenges in LC, and stationary phase modifications can also improve the chromatographic efficiency. The reduction of the particle size from 5 µm to 3 (HPLC) or sub 2 µm (UHPLC) has greatly extended the surface area of the stationary phase, improving the chromatography. One example of this type of RP is the Thermo Fisher Hypersil GOLD™ column, an end-capped silica-based RP. This column has been extensively used in ESI-LC-MS or ESI-LC-MS^n of oxysterols mixtures, derivatised with Girard P or picolinyc esters, obtaining very good isomers resolution and peak separation (W. J. Griffiths, Abdel-Khalik, *et al.*, 2019; Honda *et al.*, 2009c, 2010; Karu *et al.*,

2007, 2011; Ogundare *et al.*, 2010; Y. Wang *et al.*, 2008, 2009, 2021; Y. Xu *et al.*, 2013; Yutuc *et al.*, 2021). *et al.et al.et al.et al.*

Another important factor which affects the separation efficiency is the dimension of the analytical columns implied for the sterols analysis. The most used column has an internal diameter of 2.1 mm and a LOD of low ng/mL. Among the ST, oxysterols are particularly low abundant, usually they reach a concentration in human plasma of few ng/mL to hundreds of ng/mL (Pataj *et al.*, 2016; Yutuc *et al.*, 2021). The minimal plasma concentration of these lipids usually requires the extraction of at least 50 µL of fluid to be detected and separated by the analytical column of 2.1 mm. If the sample size to be analysed is smaller than that a narrower column could be employed to enhance the sensitivity, usually in the µm scale for the internal diameter (nano and capillary LC) (I. H. K. Dias *et al.*, 2018; Roberg-Larsen *et al.*, 2017; Vehus *et al.*, 2016).

1.6 Mass spectrometry (MS) based sterolomic approaches

In recent years, an increasing number of studies have elucidated the role of sterols and oxysterols in the control of several and essential biological pathways, underlighting also possible engagements in various diseases (A. J. Brown *et al.*, 2021; Duc *et al.*, 2019; W. J. Griffiths & Wang, 2019a, 2020; Janowsky, Bethany A.; Willy, P. J.; Rama Devi, T.; Falck, J. R.; Mangelsdorf, 1996; Leoni & Caccia, 2011; Mutemberezi *et al.*, 2016b; Vesa M. Olkkonen; Olivier Béaslas; Eija Nissilä, 2012; Zmysłowski & Szterk, 2019). While information about ST biochemical function were collected, great efforts have been dedicated to the development of reliable, fast, and reproducible

analytical techniques for the identification and quantification of sterols, and as such the sterolomic field of science was born. As we saw in the previous paragraphs, sterolomics is a multiple step process which starts with sterols extraction and culminates with their identification and measurement. This last step, the qualitative/quantitative profile has probably represented the hardest part of the entire procedure due to the chemical diversity of ST category.

Mass Spectrometry(MS) is the preferred analytical method that identifies molecules through the study of their mass to charge (*m/z*) ratio by the means of a mass spectrometer apparatus. The physical and chemical principles on which MS is based were discovered by the German physicist Wilhelm Wien and the British chemist J.J. Thomson between 1886 and 1912 (J. Griffiths, 2008). Wien discovered that the trajectory of a charge molecule, an ion, in the gaseous phase could have been deflected through the application of a magnetic field. Thomson, after the discovery of the electron and the possibility to deflect its trajectory through the application of an electrical field, reported in the seminal nature paper of 1914 that a beam of positively charged ions could also be deflected by the application of a combined electrostatic and magnetic field (J.J. Thomson, 1914). Thomson was also able to detect and measure the entity of the deflection as the ions could produce a series of parabolic curve on a lithographic plate. Soon after the lithographic plate was substitute by a metal sheet with a parabolic slit, like a microchannel plate detector. When the positive ions were hitting the electrically charged metal sheet, by photoelectric effect many electrons would have been emitted from the plate, generating a cascade of electrons and so a discharge in the plate. Measuring the charge and discharge

effect of the metal plate through the coupling with the high voltage applied to the plate, Thomson was able to quantify the electrical signal produced by the ion, and so on its *m/z*. With the advent of the parabola spectrograph, the very first mass spectrometer, a new era of molecule identification based on their mass, charge and chemical properties characterisation started, the MS.

A mass spectrometer is an instrument composed of an inlet, an ion source, a mass analyser, a detector, and a data processing system, see figure 1.27. The mass spectrometer can also be coupled to a LC or GC instrument, increasing the specificity and selectivity of the analysis. The analyte molecule is introduced into the mass spectrometer through the inlet as solute or gas. The analyte molecules need to be first ionised to be detected by the mass detector. The ion source represents the first part of the mass spectrometer and is responsible for the generation of charged molecules in the gaseous phase. Once ions are formed, they are directed towards the mass analyser where they are separated according to their mass to charge ratio and measured by the detector. In the following sections we will have a look at the part of the MS instrumentations, and we will have an in-depth look of the most employed in the sterolomic field.

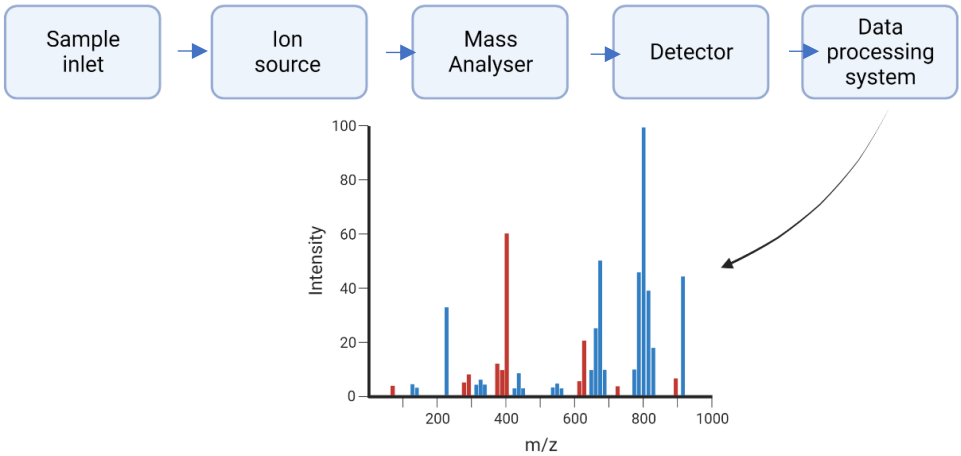

Figure 1.27 General Mass Spectrometer diagram.

1.6.1 Ion sources

The ion source is the first component of the mass spectrometer instrument and is the site for analyte molecules ionisation. Several ionisation techniques have been developed over the years to cover the huge chemical diversity of several different organic and inorganic molecules. However, independently from the type of ionisation, the most important point to consider when applying or developing an ionisation technique is the internal energy transfer and the physio chemical properties of the molecule to be analysed. For this reason, very energetic and mild ionisation sources exist. The most powerful ones are suitable for hardly ionisable-neutral molecules ionisation, although they are prone to in source fragmentation and fragment ion formation, with consequently loss of structural information. On the contrary, soft techniques tend to form only ions of the molecular species, with no or minimal in source fragmentation. An example of hard ionisation technique is the electron ionisation (EI), where electrons emitted from a high heated filament collide into the analyte molecule in the gaseous phase (Famiglini *et al.*, 2021). A milder ionisation technique is represented by chemical ionisation where gaseous phase analyte molecules collide whit the ones of an ionised collision gas plasma (Munson, 2000). The collision results in energy transfer from the plasma to the analyte molecule and an ion is thus formed. The techniques here described are only suitable for thermostable and volatile analytes that can be easily turned into the gas phase. For thermally label and/or involatile compounds (low vapour pression) other ionisation methods have been implemented. These methods are distinguished by the operational mode in which the analyte molecules are employed: liquid-phase or solid-state ion

sources (Sleeman R. & Carter J. F., 2005). Among the liquid phase ion sources, electrospray ionisation (ESI), atmospheric pressure chemical ionisation (APCI), atmospheric pressure photoionization (APPI) are the most represented while for the solid state are matrix-assisted-laser-desorption (MALDI), plasma desorption, fast atom bombardment and field desorption. In the liquid state, analyte solution is nebulised as a fine aerosol into the ion source where ions are produced in the gaseous phase at atmospheric pressure. Ions are thus directed towards the mass analyser thanks to a vacuum pumping stage. In the solid state, involatile analytes are sprayed as a thin layer alongside a matrix to cover a target and form a deposit. The deposit is subsequently irradiated with a laser beam or photons that desorb ions from the target surface. The ions can be extracted through the application of an electrical field and be directed to the mass analyser. Whatever ion source is utilised, most of them produce ions from the neutral analyte molecule in the gas phase. The reactions involved in the ionisation process are different and based on the ionisation technique used, one can prevail on the others. An ion can be obtained upon electron ejection, electron capture, protonation, deprotonation, adduct formation or by charge transfer.

The *electron ejection* is the event that characterise EI and is caused by the kinetic energy transfer that occurs when electrons emitted by the heated capillary of EI pass by analyte molecules. The electron repels and distort the electron cloud surrounding the analyte, causing energy transfer, which results in the knocking out of a valence electron and the formation of radical cation (Famiglini *et al.*, 2021).:

$$M + e^- \rightarrow M^+ + 2e^-$$

The *electron capture* ionisation mode can also be a complete separate ionisation source rather than a type of ionisation which can occur in chemical ionisation sources (Cappiello *et al.*, 2022). It consists of two probable events:

1. A resonance electron capture, in which the analyte molecule captures an electron and forms a negative radical ion:

$$M + e^- \rightarrow M^{-\cdot}$$

2. Dissociative electron capture, in which the analyte is split into two fragments where one is a negative ion and the other a radical:

$$M + e^- \rightarrow [M^-A^+ + 2e^-] + A^\cdot$$

Protonation is one of the most frequent ionisation events and characterised most of the soft ionisation techniques that allows collisions like ESI, APCI, APPI, MALDI (Böhme, 2016). In proton transfer, a neutral molecule can act Bronsted-Lowry base and accept a proton form a protonated molecule:

$$M + AH^{n+}_{n} \rightarrow [M+H]^+ + + AH^{(n-1)+}_{(n-1)}$$

In some cases, when the proton transfer reaction is particularly energetic, the residual internal energy of the newly formed cation might result in bonds breakage and fragments formation.

Deprotonation follows protonation but is less frequent then then latter. During deprotonation, a Bronsted-Lowry acid, a negatively charged conjugated base of an acid, accepts a proton from the analyte resulting in analyte negative ion and a neutral molecule formation(Böhme, 2016).

$$MH + A^- \rightarrow [M]^- + AH$$

Adduct formation is often seen in all types of ionisation techniques and involves the combination of the analyte neutral molecule and a positive or negative ion, also called ionising ion. This reaction is possible when the analyte molecule possesses several electron pairs, allowing the formation of covalent dative bonds or transient covalent bonds. Adduct formation generally happens between electronegative heteroatoms in organic compounds and metal mono cations like Na^+, K^+, NH_4^+ or conjugate bases of moderate acid compounds like Cl^-, Br^-, $HCOO^-$ (Böhme, 2016; Harvey, 2005; Kruve *et al.*, 2013) . An example for positive and negative ion formation follows:

$$M + Na^+ \rightarrow [M+Na]^+$$

$$M + Cl^- \rightarrow [M+Cl]^-$$

Protonation and adduct formation compete to produce positive ions from the same analyte molecule. However, to let the protonation happen a basic site in the molecule must be present. If a solution is not well desalted, metal or adduct formation might prevails on the protonation products.

Charge transfer ionisation is the process generally involved in MALDI, or in solid state ionisations in general. Gas-phase charge transfer requires the presence of a matrix radical ion produced upon laser or photoionization in the gaseous phase which react with the desorbed neutral analyte molecule:

$$M + R^{+\cdot} \rightarrow [M]^{+\cdot} + R$$

$$R^{+\cdot} = \text{matrix radical ion}$$

This reaction can happen when the energy of the matrix radical ion exceeds the ionisation energy necessary to ionise M, the analyte (Macha *et al.*, 1999).

Almost all the ionisation techniques above describe have been used for the lipidomics but also sterol analysis, however ESI is the most widely used for sterolomics and the most well characterised and implemented and will be described in deeper details in the next section.

1.6.1.1 ESI

Electrospray ionisation or ESI is an atmospheric pressure mild ionisation technique which allows the formation of charged and multiple charged ions from analyte molecules dissolved in solution. ESI is based on two principles of fluid mechanics:

I. The Rayleigh limit, discovered by Lord Rayleigh in 1882. It describes the maximum amount of charge that a droplet can carry before exploding into a fine jet of fluid (Rayleigh L, 1882).
II. The formation of a Taylor cone, formulated by Sir Geoffrey Ingram Taylor in 1964 (Geoffrey Ingram Taylor, 1964). The Taylor cone is the physical event which happens when charged liquid is let to pass through a strong voltage. Under the application of an electrical voltage, the fluid droplets start to deform, as the electrical field-force overcome the surface tension. The droplets start to deform and convert into a cone shape with a whole angle of 98.6°. If the voltage overcomes the solution surface tension force, which depends on the total charge and composition of the fluid, a conical liquid meniscus is formed with a tiny jet end, which enables the formation of a fine aerosol.

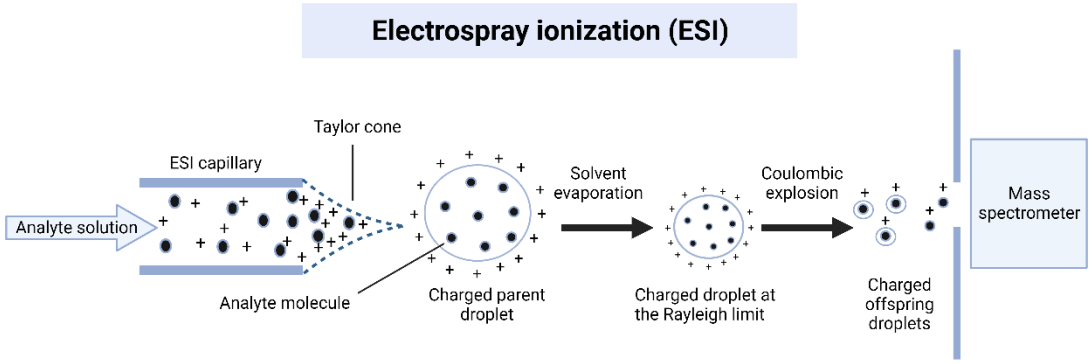

Figure 1.28 General principle of electrospray ionisation of solute analytes.

In the ESI, the solution of analytes of interest is let pass through a heated capillary inlet to enter the ion source, see figure 1.28. A Taylor cone at the narrow end of the inlet capillary is formed as the result of the voltage applied to the capillary and the mechanical forces imparted to the fluid. The Taylor cone passes into a fine jet cone followed by nebulisation of a fine aerosol into the ion source chamber. The high voltage can cause oxidative/reduction event to the solvent molecules. Therefore, upon the above-described reactions, solvent and solute molecules can be ionised. The resulting aerosol possess a net charge. The type of ions formed depend on the operational mode selected for the ionisation: in positive mode, a positive electric potential is applied at the spray tip and the resultant droplets possess a net positive charge. The opposite is true for the negative operational mode. Once the droplets are in their aerosol form, they are subjected to extensive solvent evaporation, often encouraged by a heated gas, the pressure gradient. The more the solvent evaporates, the smaller the droplet size until it reaches the Rayleigh limit. Upon Rayleigh limit, the repulsion forces between like charges overcomes the surface tension ones and Coulomb fission happen. The Coulomb

fission is the event where a charged droplet disintegrates into smaller, charged, droplets. The smaller droplets follow the same destiny of the parent one until the desolvation is completed and ions released in the gaseous phase. How gas phase analytes ions are exactly emitted during the Coulomb fission is not completely clear, however three theories seem to be the most accredited:

1. *The ion evaporation model.* In this model, the desolvation process let the droplet to reach a certain dimension with the formation of a strong surface field force. This force aids the ion desorption and the consequent formation of gas phase ions. In this model, a proton transfer or charge transfer from the solvent could contribute to the analyte ion formation.
2. *The charge residue model.* The theory of the charge residue model hypothesises that over continuous cycle of evaporation and fission explosion, the remaining droplets could carry only one analyte ion. The analyte ion will be released upon solvent evaporation and will possess the charge of the droplet. Charge transfer is the main ionisation event contributing to the formation of analyte ions.
3. *Charge residue-field emission model*. In this model, the analyte ions formed are mainly as proton or sodium adducts, which can be formed upon a combination of theory 1 and 2.

Depending on the analyte molecule, one theory can prevail upon the other. For example, low mass molecules generally form ions upon theory one (Nguyen & Fenn, 2007) while heavier ones upon theory two (Fernandez de la Mora, 2000).

With ESI a large range of different molecules can be easily ionised, especially if they intrinsically possess a charge or even if they are neutral but possess dipoles or ionisable groups. In this optic, sterol

lipids are mostly neutral, non-polar, low ionisable compounds, especially the subclass of cholesterol, its cyclic precursors, and the mono- and di-hydroxy sterols. Cholesterol and derivatives form protonated $[M+H]^+$, or protonated less a water molecule $[M-H_2O+H]^+$ ions or positively charge adducts. The type of adduct depends on the experimental conditions but generally ammonium adducts are detected $[M+NH_4]^+$ (DeBarber *et al.*, 2008b). Although the intensity of these types of ions is generally low, due to the poor ionisable nature of the sterol molecules. Multiple reaction monitoring (MRM) or single reaction monitoring (SRM) are usually employed for the precise identification of ESI ionised oxysterols (DeBarber *et al.*, 2008b; McDonald *et al.*, 2012a). Derivatisation can enhance the ionisation efficiency of up to 1000-fold and is another widely used strategy for low abundant sterol identification upon ESI ionisation (Böhme, 2016; W. J. Griffiths *et al.*, 2021b; Honda *et al.*, 2009c, 2010; Karu *et al.*, 2007; Kruve *et al.*, 2013; Y. Xu *et al.*, 2013) .

The advantage of using an ESI source for lipid and sterol analysis are multiple and can be summarised as follow:

I. ESI is a soft ionisation technique with minimal in-source fragmentation and formation of intense charged molecules.
II. Minimal in-source fragmentation permits correct structure attribution and precise quantification, especially when tandem mass spectrometry analysis is involved for the molecule characterisation.
III. ESI is a very mild ionisation technique. Solvent, metals, dimers adduct are not frequently seen and are considered more as side products of ionisation due to non-covalent binding with analyte molecules. This characteristic could represent an advantage when sterol or lipid aggregation study is to be carried out.

However, it is a quite new area and only few studies have been published on it (Han & Gross, 1994; Thomas *et al.*, 2005)

IV. ESI sources can be coupled with LC. This ionisation technique can easily be used with a broad range of mobile phases, flow rates, solvent types and mobile phases modifiers like acid, basis, or salts. In fact, the addition of these kinds of modifiers often improves chromatographic resolution of sterol mixtures while allowing the formation of transient adducts, which helps in the structure elucidation through MS analysis.

V. Through the adjustment of the voltage in the ESI chamber, the ionisation can be extended to almost any lipid molecule, including the sterol lipids, ST. Moreover, ESI can also work as a selective separation device as, by modifying the voltage, it can ionise only a specific class of lipids in a complex mixture and helps in the target MS characterisation of biological samples.

VI. When coupled to MS, ESI-MS represents one of the most sensitive analytical techniques for lipid and ST analysis, reaching a limit of detection (LOD) of fmol/µL to amol/µL.

VII. Linear dynamic relationship between peak intensity and concentration is very broad and allows quantification of individual analytes through direct comparison of peak intensities with the one of an internal standard of the same class or the same molecule (when the latter is deuterated).

VIII. Lastly, the technique is highly reproducible, higher than 95% reproducibility.

Considering all the advantages of ESI technique applied to MS of ST, it has been implemented for the study of sterolme variation in healthy and pathological conditions (Björkhem, 2009; de Medina *et al.*, 2022; Honda *et al.*, 2009c, 2009a; Jiang *et al.*, 2007; Karu *et al.*,

2007; Leoni & Caccia, 2011; Lordan *et al.*, 2009; Meljon *et al.*, 2012; Spann, N. J.; Glass, 2013; Y. Wang *et al.*, 2009; Yutuc *et al.*, 2021; Zmysłowski & Szterk, 2019)

1.6.2 Mass analysers

Once the analyte compounds have been ionised in the ion source, they are directed towards the mass analyser. Mass analysers are the mass spectrometer components able to discriminate the different ions based on their mass, m, and their net charge, z. The charged molecules entering the mass analyser are separated based on their *m/z* ratio and subsequently sent to the detector. Mass analysers utilise a static or dynamic electrical and/or magnetic field to separate the ions, which can be modulated in different manners. These devices can be classified in different ways, for example on the type of electrical or magnetic field used for separation, how they can be modulated, or the resolution, or on the detection limits. A common way to classify them is generally based on the scanning mode, how many and which ions are separated at the time. *Continuous* or *Scanning* instruments can transmit only ions of a specific *m/z* at a time. An advantage of this type of analyser is the elevation of the signal to noise ratio, S/N, with a consequent increase in sensitivity and specificity, for a small *m/z* scan range. The continuous type of instruments arevalid machine for quantification purpose due to the type of scans but when qualitative analysis is required the *Simultaneous* or *Pulsed* analysers are often preferred. Simultaneous analyser allows the detection of all the ions sent from the ion source to the mass analyser per scan event. In contrast to continuous instruments where ions of a given *m/z* are constantly transmitted to the analyser, in pulsed instruments only a packed of different *m/z* ions are sent at a time to the detector. The advantage of a pulsed mass analyser is clearly the extended mass range of ions that can be analysed simultaneously compared to the continuous instruments,

however the latter allows faster analysis. Both categories can possess good resolution, however pulsed instruments are generally more accurate in terms of mass accuracy determination. Examples of continuous instruments are the quadrupole and triple quadrupole, which use electrical field, or magnetic sector instruments, which use a magnetic field instead. Time of flight (TOF) ion traps, and orbitraps, all utilising electrical filed, and are some examples of pulsed mass analysers. Most of the mass analyser listed here, of both categories, have been employed and implemented in the sterolomic profile of several different samples, adapting the scan mode and the sample preparation to overcome specific disadvantages (Cardenia *et al.*, 2012; Carvalho *et al.*, 2011; W. J. Griffiths *et al.*, 2013; Hailat & Helleur, 2014; Karu *et al.*, 2007, 2011; Leoni *et al.*, 2005) .

Analyser performance can be established over five essential parameters which are:

1. *Mass accuracy*, the value representing the difference between the theoretical *m/z* ($m_{theoretical}$) and the measured *m/z* ($m_{easured}$):

   $$m_{theoretical} - m_{measured}$$

   The unit is usually millimass unit or mmu but it is often reported as part per million, ppm.

   $$(m_{theoretical} - m_{measured}) / m_{theoretical} X10^6$$

   Accurate mass largely depends on the stability and resolution of the mass analyser and as such, high resolution instruments like the orbitrap can provide high mass precision while low resolution ones like triple quadrupole are less suitable for accurate mass determination. High mass resolution mass spectrometer also allows the ion's elemental composition characterisation.

2. *Mass range*, the range of *m/z* the mass analyser can discriminate.
3. *Transmission*, which represent the ratio between the ions reaching the detector and the ion present in the mass analyser. This parameter represents the efficiency of the mass analyser in sending the scanned ions towards the detector. Quadrupole instruments are the analyser with the best transmission and are often incorporated in hybrid mass spectrometer to function as filters and focusing elements for charged particles. To note, the reader should not confound the transmission, which in this case is a characteristic of the mass analyser alone, with the term duty cycle. The duty cycle is the proportion of ions produced in the ion source of a certain *m/z* which effectively reach the detector. It is a characteristic of whole the mass spectrometer as it depends on the ion source efficiency, on the solvent matrix where analyte molecules are dissolved, on the operational mode and on the transmission.
4. *Analysis speed* is the time a mass analyser takes to record a scan.
5. *Resolution*, is the ability of the mass analyser to discriminate between two isobaric ions of very similar *m/z.* It has been defined by Marshall as follow: "two peaks can be considered well resolved if the valley between them is equal to 50% of the weakest peak intensity when a quadrupole, ion trap, TOF, orbitrap and so on are used". The equation defining the peak resolution is:

$$R = \frac{m}{\Delta m}$$

Where R is the resolving power, Δm is the smallest difference between two peaks of mass m and m+ Δm. Resolution can also

be determined for single peaks as the full width at the half maximum of the peak or FWHM. Mass analyser with FWHM>10,000 are considered high resolution instruments, like orbitrap, magnetic sector, ion cyclotron resonance and some TOFs.

Nowadays many different mass analysers exist and can be used for a complete and reliable sterolomic profile of different matrixes. For instance, in this thesis will be reported only a brief description of the two-mass analyser which have been used for the sample analysis, the linear trap and the orbitrap.

1.6.2.1 Linear Ion Trap

An ion trap is a mass analyser which trap the ions by means of an oscillating electrical field. A quadrupolar resonance frequency field is applied to store the ions into two, 2D or linear trap, or three, 3D traps, dimensions, see Figure 1.29. The first description of an instrument able to confine plasma, not ions, upon the formation of a 3D electrical field utilising a circular quadrupole was reported by Paul and Drees in 1964 (Drees & Paul, 1964). Not much later, Church built up the first linear trap bending a linear quadrupole unto a circle to store helium and hydrogen ions for several minutes (Church, 1969). Soon after, the ion trap technology was implemented through the work of Stafford over the 80's which brought to the formation and commercialisation of the first 3D ion trap (Stafford *et al.*, 1984).

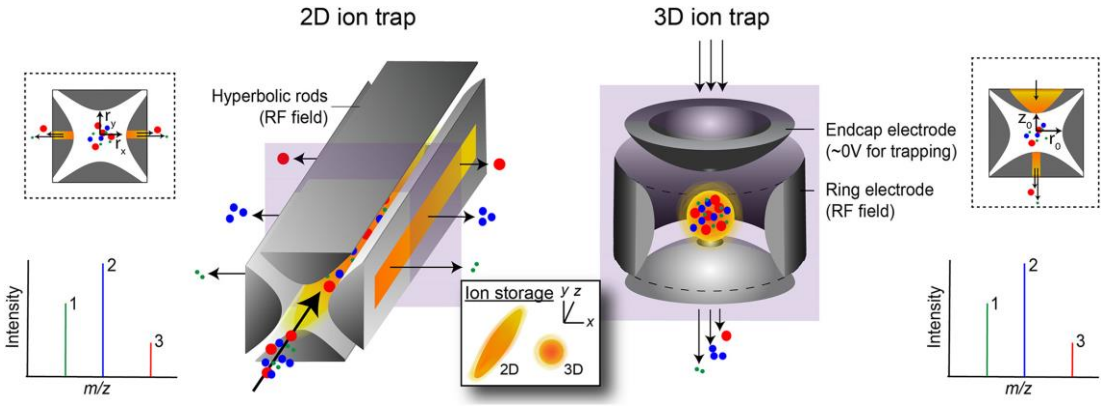

Figure 1.29 Schematic representation of 2D/linear and 3D ion traps. Ions entering the ion traps are separated by means of their *m/z* ratios through the application of an electrical field at a specific voltage. figure taken from (Arevalo *et al.*, 2020).

The 3D ion trap is made of a circular electrode and two ellipsoids electrode caps at the top and bottom of the trap cell. An oscillating alternative potential is applied to the circular electrode such that it can produce a fixed frequency quadruple electrical field. The 3D electrical field created by the circular shaped electrode is saddle shaped and with a minimal potential energy in the middle of the ion trap cell. Ions entering the ion trap are therefore trapped by the means of the 3D electrical field and tend to be stored at the centre of the chamber, where the difference of potential has its minimal energy. The 3D trap permits the separation of the different ions, based on their *m/z*, through their expulsion from the trap. The ion's motion in the trap is a function of their *m/z* and of the voltage of the electrical field applied. As specified above, the electrical field has a fixed frequency, that normally is the resonance frequency, but the amplitude can be changed through the application of a voltage at the electrode caps. The modification of the voltage intensity affects the ion motion, de-stabilising their trajectory. The voltage can be increased up until it causes the ejection of a specific ion *m/z* from the trap. An advantage if the 3D ion trap is the possibility to store all *m/z* ions simultaneously while they can be expelled sequentially based on their *m/z*, without losing the other ions. A disadvantage of the 3D trap is the so-called space charge effect. When many ions are stored in the trap, the outer charges at the centre of the chamber will form a kind of a shield for the inner ions, the space charge effect. The shield partially masks the electrical field sensed by the inner ions, for which a higher voltage would be needed for their ejection. A higher voltage may lead to an error in determination of the correct *m/z* value.

The 3D ion trap has represented a substantial development in the mass analyser history. However, the space charge effect was limiting the amount of sample to be analysed, reducing the information on low abundance molecule analysis. For this reason, and almost concurrently, a 2D ion trap was built. As described above, Church designed the first 2D linear trap in 1969 (Church, 1969). With respect to the 3D trap, the 2D trap, also known as the linear trap (LIT), is composed of four hyperbolic rods and two end caps. An resonance frequency (RF) voltage is applied to the rods while a direct current voltage (DC voltage) is applied to the end caps. The four rods generate a quadrupolar field, which trap the ions in the radial dimension, the x and y axes, while the DC voltage of end caps traps the ions in the z axis. Ions entering the LIT start to oscillate by means of the RF voltage in the x-y direction and back and forward in the z axis because of the DC voltage. Whenever they become closer to the rods or end caps they are promptly repelled back to the centre of the LIT, as the repelling voltage possess the same charge of the ions. Moreover, in the LIT ions are also cooled and retarded by collision with an inert gas particle. In summary, the application of an alternate current (AC) and a direct current (DC) voltage constrict charge particles to be stored at the centre of the LIT. One big advantage of the LIT with respect to the 3D trap, is the higher storage capacity combined with the ability to limit the space charge effect. The LIT has a higher volume capacity and the characteristic to focus the ion not just in a point at the centre of a chamber, as in the 3D trap, but over a central line, avoiding space charge effect. Furthermore, the LIT possesses a much higher trapping efficiency, where >50% of ions ejected from the ion source can be trapped, while only 5% for the 3D trap. LIT instruments possess therefore superior sensitivity and dynamic range. As for the 3D trap, the 2D trap can

eject ions through the variation of the AC voltage. Depending on the mode of variation, ions can be ejected axially, when the voltage is modified between the rods and at the exit lenses, or perpendicularly to the axis, radial ejection, when the voltage is applied only to two opposite rods. The radial ejection has never been marketed so only axial ejection instruments are currently in use.

The LIT is a very powerful and adaptable instrument, broadly used as a scanning mass analyser and as an ion trap alone, especially in hybrid instruments. Interesting is the application of the LIT in tandem mass spectrometry. Tandem mass spectrometry, frequently called MS/MS or MS^n, is a technique used in MS to gain more structural information from selected ions, allowing almost complete structural elucidation and compound identification. In MS^n, after ionisation, specific ions selected by the mass analyser are sent to a collision cell where they are fragmented and mass-analysed again to give a fingerprint of charged fragments, whose nature depends on the chemical structure of the precursor/parent ion. In LIT and 3D trap analyser MS^n experiments can be carried out by trapping, fragmenting, and scanning the ions formed. The first necessary event in the MS/MS fragmentation is the selection of the *m/z* to fragment. In the ion-trap RF voltage is tuned to expel all the ions with different *m/z* from the selected one. The RF voltage must be weak enough not to excite or expel the selected ions while ejecting all the others, and so under the stability limit. The second event is the ion fragmentation. Fragmentation in ion traps is a consequence of internal energy increase in the selected ions through collision with the inert gas atoms. Helium is generally the inert gas used in ion traps. By adjusting the voltage (amplitude) of the RF quadrupolar field it is possible to superimpose the RF field frequency with the ion's

frequency, called secular frequency. This action causes an increase of the ions kinetic energy which start to collide with the He atoms. During the collision, part of the kinetic energy is transformed to internal energy that results in bond breakage, and so fragment formation. A specific fragment can be retained and excited again before mass analysis to give a MS^3 spectrum. Further selection and fragmentation can occur up to MS^{10}. In LIT instruments it is also possible to carry out broadband excitation and fragmentation. This type of MS^n fragmentation utilises a range of different frequencies, instead of only the secular frequency, enabling the excitation and fragmentation of several different ions and fragments in the ion trap.

To summarise, LIT and 3D ion traps possess good sensitivity, scan speed (milli seconds), good transmission efficiency, especially for LIT, high versatility and ability to be coupled with a broad range of ion sources. Furthermore, the ion trap can simultaneously act as mass analysers, mass filters, ions storages and run MS^n experiments. Lastly, it is relatively in-expensive. For all these reasons, ion traps have been widely used for lipidomics and sterolomics purposes (Agatonovic-Kustrin *et al.*, 2019; Balazy, 2004; Brügger, 2014; W. J. Griffiths, Crick, & Wang, 2013; Honda *et al.*, 2009c; Karu *et al.*, 2007; Meljon *et al.*, 2012; Y. Wang *et al.*, 2009; Yutuc *et al.*, 2021). However, ion traps suffer from poor mass resolution, low mass accuracy (≅100 ppm), low dynamic range and space charge effect for the 3D one.

1.6.2.2 Orbitrap

The orbitrap is relatively new type of ion trap which utilises an electrostatic field to trap ion. The principles of electrostatic trapping

can be track backed to the first half of the 1920, when the first orbital trap was invented by Kingdon in 1923 (Kingdon, 1923). Kingdon demonstrated that ions could be trapped in a cylindrical metal vessel if a charged wire was put inside of the vessel. Because of the electrical field generated by the wire, the ions start to orbit back and forward. The Kingdon trap was the very first rudimental example of orbitrap but with no mass analysis application. In the following decades a lot of work have been done on the Kingdon trap until the early 2000s, when Makarov present for the first time the orbitrap (Makarov, 2000; Makarov *et al.*, 2006a). The Makarov orbitrap is made of an external electrode with a barrel shape cut into two equal pieces and works as a receiver plate for image current, see figure 1.30. A small gap is present to the two external electrodes to allow the tangentially, orthogonally injection of ions. The internal electrode has a spindle like shape. A DC voltage of several kilovolts (kV) is applied to the central electrode to create an electrostatic field, which can be positive or negative. On the other side, the outer electrode is at ground voltage. This setting, along with the shape of the electrodes, allows the formation of an electrostatic field with a quadro-logaritmic potential distribution. This type of distribution can be imagined as a saddle with no minimum. When ions are injected into the orbitrap, they possess a kinetic energy of some kiloelectronvolts and so a linear momentum. The ions linear momentum adds a contribute to the electrostatic field which changes slightly the quadro-logaritmic distribution of the field, forming now a minimum. Therefore, ions entering the orbitrap can be trapped into the minimum and, at the same time, be moved back and forward along the z axis, because of the DC voltage applied to the inner spindle. As a resultant, the ions start to rotate in circular orbit around the spindle by means of electrostatic attraction, which is balanced by their linear momentum

and inertia momentum. Meanwhile, the ion is accelerated back and forward in the z direction because of the force induced by the quadro-logaritmic potential. The resultant force applied to the charged molecule in the orbitrap results therefore in a harmonic oscillation, which describe an intricate helical trajectory. The harmonic motion of the ions in the electrostatic trap causes the production of an image current, which is independent of the ion's initial kinetic energy, but is directly linked to their *m/z*. The image current created by the oscillating ions is measured by the outer electrode: the difference of image current between the two parts of the outer electrode is detected and signal amplified by the amplifier, creating a broad band current signal. The sensitivity in detecting the image current depends on the amplifier electrical components, internal and thermal noise. For the current version of orbitraps, the limit of detection is set to be 2-5 elementary charges per second acquisition. The signal output is therefore in a frequency domain, but it needs to be transformed into a time domain to be interpreted. A Fourier Transform operation is applied to convert the frequency domain in time domain and a mass spectrum is thus created.

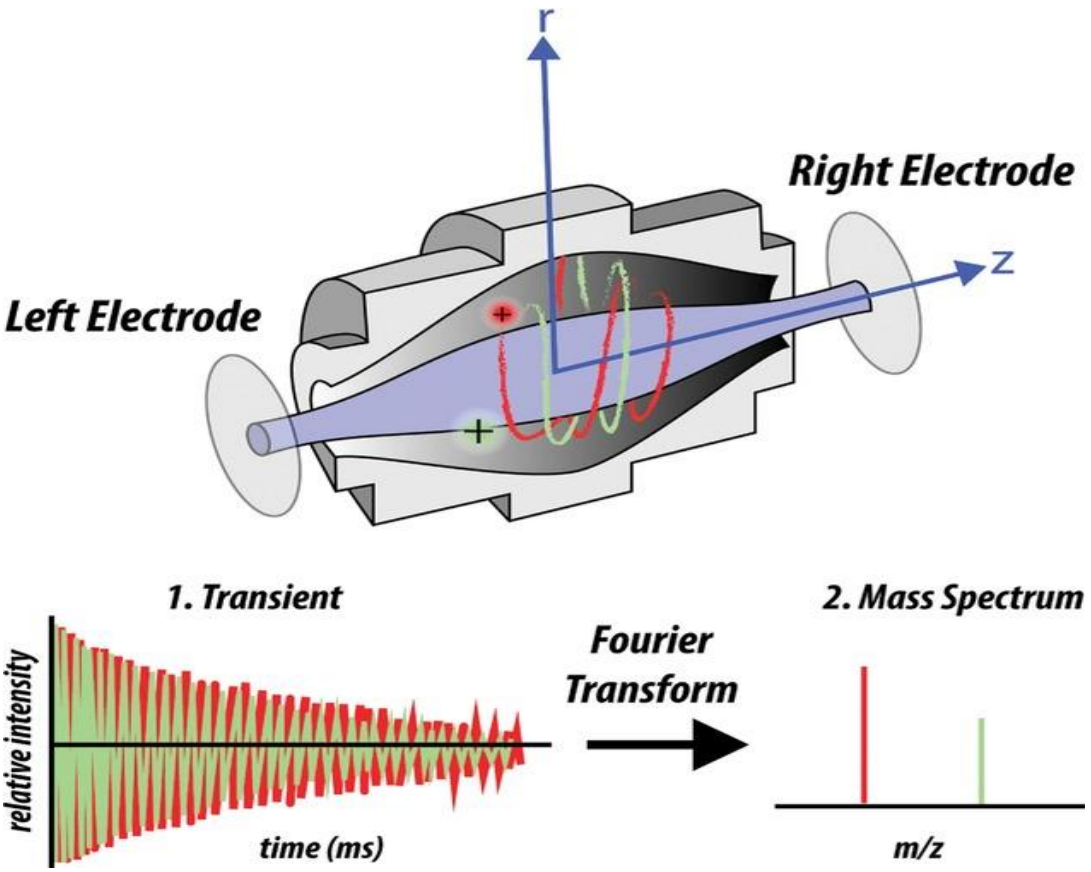

Figure 1.30 The Fourier transform Orbitrap mass analyser.
Ions injected into the Orbitrap starts to oscillate along the central spindle-like electrode r axis while moving along the central spindle-like electrode, the z axis, by means of electrical field. The frequency of the moving ions (transient) is detected and converted into a mass spectrum through a Fourier Transform. Figure taken from (Janulyte *et al.*, 2011)

Orbitrap instruments are often coupled with an external ion storage device, that serves as a concentrator of ions. The function of the ion accumulator is to store ions in significant packet to enhance the signal intensity, and as such the sensitivity of the mass analyser. Essential prerequisite of the storage ion trap is the ability to form ion packets whose dimension is significantly smaller than the amplitude of the harmonic oscillation. To do it, ions are excited off axis during injection into the orbitrap in a process called *excitation by injection*. In the excitation by injection process, ions are trapped into the

external device, which can be a LIT or a curved linear ion trap, the C-trap, made of a set of rods cat RF only potential. Ions are stored by means of the RF voltage. Expulsion of the ions happens when a pulsed voltage is applied to both the end electrodes of the C-trap or LIT and, also, to the RF electrodes. The intra cell collisions are minimised by a fine tuning of the pulsed RF voltage, to avoid ions overexcitation, and by storing the ions toward the exit of the ion trap. While the pulsed voltage is applied to the external accumulation device, the orbitrap internal spindle voltage is ramped down, for positive ion mode, or up, in negative ion mode, to avoid electrostatic repulsion of the ions. Packets of ions are ejected from the external ion trap by means of the pulsed voltage and focused towards the orbitrap entrance orifice by means of charged focus lenses. The energy of the ion packet is smaller than their oscillation amplitude, to let a smooth entrance in the electrostatic trap and avoid internal collisions. When the ions are ejected off axis and enter the orbitrap, the voltage is increased back, causing the start of coherent oscillation around the inner spindle without any need for additional excitation.

In ideal conditions, ions entering the orbitrap could be stored forever, however decay of coherent ion motion occurs, and signal intensity is lost over time. This phenomenon happens for two main reasons:

1. Collision with residual storage gas, which cause a loss in ion momentum and the coherent ion pack to diffuse.
2. Fragmentation due to collisions, and consequent loss of coherence

The loss of coherent ion cloud impedes the ion generation of an image current.

Another issue common to all the trapping devices, and so also the orbitrap, is the space charge effect. The space charge effect can cause inaccurate mass detection, due to many reasons:

- Outer ion shielding the inner ions.
- Coalescence of ion packet of similar *m/z*.
- Diffusion within time, which is the increase of ions packet size.
- Non-linear resonance of excited ions.

All those issues have been addressed in the orbitrap, which shows the lowest space charge effect among all the ion traps, with a little distortion of the inner spindle shape.

The orbitrap is a very efficient and sensitive mass analyser, showing one of the best performances in high resolution mass spectrometry experiments, and accurate mass detection (Makarov, 2000; Makarov *et al.*, 2006a; Zubarev & Makarov, 2013). However, it possesses some limitations in tandem mass-spectrometry assays.

Orbitrap performance mostly depends on the manufacturing technologies and electronics. For example, internal and thermal noise of electronic components affect the image current detection, and so the sensitivity of the instrument. However, limit of detection LOD for current orbitrap analysers is of several elementary charges in 1-second acquisition. The mass error is another good example of the dependence of the mass analyser from the manufacturer components: the drift of the power supply limits the mass accuracy, which is <3 ppm when external calibration is used or <1 ppm if internal calibration is operated. As specified above, the instrument resolution and mass accuracy depend on the stability of electronic components as well as form the space charge effect. Modern orbitraps can reach sub-ppm levels and a resolution of 500,000 to 1,000,000 FWHM at

200 *m/z*, with an isotopic fidelity up to 240,000 FWHM (Orbitrap IQ-X Tribrid Mass Spectrometer, n.d.). On the new instruments, the dynamic range can be higher than 5000 with a scan speed of 0.1 seconds. Another advantage in using an orbitrap instruments is the efficient ion transmission, which allows the detection of 30 to 50% of all the ions produced. Being so efficient, sample analysis using the orbitrap requires less ions and so less sample, which represents an advantage when the sample size is limited.

The LTQ Orbitrap© (Makarov *et al.*, 2006) combines a linear ion trap with radial ejection (C-trap aided) to an orbitrap mass analyser. The instrument is characterised by high sensitivity, excellent control of ion population, short cycle time and MS^n capabilities. Another advantage brought by the LTQ is the possibility to operate with the two-mass analyser alone, one at a time, or in concert. Since the advent of the LTQ, many improvements followed, giving birth to the tri-hybrid series of orbitrap mass spectrometers, which extend the performance of orbitrap coupling three different mass analysers in one instrument. In these types of instruments parallel but independent experiments can be done, extending the number of precise information on the sample under characterisation, decreasing the analysis time (Brunner *et al.*, 2015; Hecht *et al.*, 2019; C. P. B. Martins *et al.*, 2016; McAlister *et al.*, 2014; Senko *et al.*, 2013).

The high resolution, and mass accuracy (<3ppm), and the possibility of running multiple MS^n experiments at the same time while performing full scan MS, make the orbitrap mass analysers and mass spectrometers the ideal instruments to run metabolomics analysis. The unique challenge represented by the vast chemical diversity of the lipid's family along with the difficulties in ionising the different lipid classes, the variety of isomers present, and the challenging

chromatography separation has been addressed with the utilisation of trihybrid orbitrap instruments. Thank to this type of mass spectrometers, which can also be easily coupled with HPLCs-UHPLCs, accurate mass analysis and tandem MS experiments can now be done in only one MS run, reducing the time of analysis, inter and intra batches variation, allowing true lipid characterisation. For all of these reasons, LC-MS^n analysis involving an orbitrap instrument have been implemented in the sterolomic analysis of several different biological matrixes, pointing out the potential of this technique in sterol identification and the possibility of a clinical application in the biomarker research (Dabrowski *et al.*, 2020; DeBarber *et al.*, 2011; I. H. Dias *et al.*, 2019; Gallego *et al.*, 2018; W. J. Griffiths, Crick, & Wang, 2013; W. J. Griffiths, Abdel-Khalik, *et al.*, 2019; W. J. Griffiths & Wang, 2018, 2019a; Karu *et al.*, 2007, 2011; Meljon *et al.*, 2012; Ogundare *et al.*, 2010; Y. Wang *et al.*, 2009; Yutuc *et al.*, 2021)

1.6.3 Detectors

The detector represents the last section of the mass spectrometer and is responsible of ion detection. Generally, the ions are detected by means of an electrical current produced upon the ion hitting a metal surface or by means of their motion. Several different types of detectors exist, and their use depends on the MS application and upon specific mass analysers characteristics (David W. Koppenaal *et al.*, 2005). Whether detector is used, their performance depends on the charge, mass, and velocity of the ion (David W. Koppenaal *et al.*, 2005). In this section, only electron multiplayer and orbitrap mass

detectors will be discussed, as they are the only detectors used within the work described in this thesis.

Electron multiplier is a kinetic energy transfer-based detector (David W. Koppenaal *et al.*, 2005). This type of device is built over the photoelectrical principle. Ions entering the detector hit a metal surface and induce the generation of electrons from the surface. This event occurs several times, which depends on ions kinetic energy and metal surface area, and result in a huge production of electrons, and consequently in an amplified and detectable electrical current signal. Electron multipliers are nowadays used also as signal amplifier for all that type of mass analysers which requires to gain meaningful electron signal to be detected (Dubois *et al.*, 1999). A microchannel plate is one of the most employed electron multipliers: by means of multiple little channels and photoelectric effect, the current generated by ions emits several electrons that are then further amplified (Ladislas Wiza, 1979). The several channels can also increase MS resolution (Ladislas Wiza, 1979).

Orbitrap is not only a mass analyser but also a detector, specifically an image current detector. As we have just seen in the previous paragraph, the orbitrap excites the ions by means of a DC voltage applied to the spindle internal electrode. The image current produced by the harmonic oscillation of the excited ions produced a circuit in the two metal plates close to the ion trajectories, which are the external electrode. This current is therefore detected by the outer metal plates. The Orbitrap is also an array collector because is able to count multiple masses, hence different ions, at the same time.

1.6.4 Tandem mass spectrometry techniques

Mass spectrometry analysis represent a powerful method for a complete sterolomic characterisation, from single cell analysis to complete organs. The versatility of MS instruments has guaranteed the structural elucidation of several hundred of sterol compounds. However, the broad chemical space designed by this class of lipid molecules requires a high grade of accuracy for precise compound identification. Additional chromatographic steps have been introduced prior to the MS analysis to aid the isomeric separation and identification.

Tandem Mass Spectrometry or MS/MS or MS^n is a mass spectrometry method involving at least two or more stages of mass analysis. In this type of analysis, the first mass analyser scans all the ions in the sample to select a specific ion of a certain *m/z*, called precursor ion. The second step involved fragmentation of the precursor ion that can be spontaneous or induced through excitation. Upon fragmentation, both charged and neutral fragments can be produced:

$$M_p^+ = M_f^+ + M_n$$

Where M_p^+ is the precursor ion, M_f^+ is the charged fragment/s and M_n the neutral fragment/s. The charged fragments are therefore analysed, and a second mass spectrum is produced. This second step is called MS^2. The MS/MS methods generate a series of fragments spectra which are ideally specific of the precursor ion alone. Isomeric compounds cannot be distinguished using only high mass accuracy experiments. Depending on the configuration and the conformation of substituent in different isomeric chemical compounds, bonds energy will be different and so the fragmentation patterns. Therefore,

fragmentation can be specific to a chemical entity and constitute a fingerprint for compound identification.

MS/MS methods can be classified as follow:

a. MS^n in space, which requires multiple mass analyser.
b. MS^n in time, which requires a storage device like ion traps.

A typical MS^2 in space device is represented by the triple quadrupole mass analyser, frequently called QqQ (Kaufmann, 2020). This type of instrument uses the first and third quadrupoles, represented by the two uppercases Q, as mass analysers and the middle quadrupole, the lowercase q, as a collision region for fragmentation. No more than two MS experiments are carried out with this configuration.

In time MS^n instruments, ion traps, can select the precursor ions, excite them to fragmentation, and analyse the fragments produced, as described in the linear ion trap and orbitrap paragraphs. The maximum number of MS^n experiments that can be carried out is about 10 because of the decrease in fragments' mass at each single steps and on the number of ions transmitted.

Tandem MS/MS analysis can be run in four different modes, with both in time and in space instruments:

1. *Product ion scan.* The product ion scan is a MS/MS mode where the first analyser is set to select a specific precursor ion with a certain *m/z* (m_x). which is then fragmented in the collision cells, and all the fragment ions (p_1, p_2, p_3, etc) are detected in the second mass analyser, set to be in the scan mode.

   Selected *m/z* (m_x) → CID→ scanning mode on (p_1, p_2, p_3, etc)

This MS/MS mode is often used to obtain structural information on the precursor ion when its chemical structure is unknown (Y.-Z. Chen *et al.*, 2015a; Hailat & Helleur, 2014).

2. *Precursor ion scan (PIS).* In the precursor ion scan mode, the first mass analyser is scanning the ions with different *m/z* (m_1, m_2, $m_{3...}$) while the second mass analyser is fixed. The m ions are sent to the collision cell where they collide with an inert gas to produce fragment ions by means of energy transfer during the collision induced dissociation. The fragments are then sent to the second mass analyser which is fixed (focused on selection mode) at a particular *m/z*, which is/are a specific product fragment ion/s p_x.

   Scanning mode on (m_1, m_2, $m_{3...}$) → CID→ Selected *m/z* (p_x)

   Whitin this mode, all the precursor ions, m_1, m_2 etc, which produce the set product ion p_x are detected, but not any other. This MS/MS mode is utilised when the precursor ion's structure is unknown but one of the functional groups is known. It is broadly utilised to identify a specific class or family of compounds which are all characterised by that specific product ions. (Y.-Z. Chen *et al.*, 2015b; Crick *et al.*, 2019; W. J. Griffiths, Crick, & Wang, 2013; W. J. Griffiths *et al.*, 2021a; Karu *et al.*, 2007, 2011; Meljon *et al.*, 2012; Sandhoff *et al.*, 1999; Yutuc *et al.*, 2021). Of note, this method is not available for in time scan instruments.

3. *Neutral loss scan (NLS).* The neutral loss scan is very similar to a precursor ion scan but with the difference. In this mode,

both the mass analysers are set in scanning mode but offset by a mass corresponding to a "neutral loss" (a). In other words, a mass spectrum will be provided only upon loss of a neutral a mass equivalent to the offset.

Scanning mode on (m_1, m_2, $m_{3...}$) → CID→ Scanning mode on *m/z* offset (m_1 - a, m_2 - a, m_3 – a...)

This scan mode has been extensively used in shotgun lipidomics to identify a class or group of lipids which loses an identical neutral fragment, which generally is a polar head group (Brügger *et al.*, 1997; Han *et al.*, 2004; Lydic *et al.*, 2009; Schwudke *et al.*, 2006; K. Yang *et al.*, 2009). Not only limited to lipidomics, neutral loss scan has been also frequently implied in sterols identification (Johnson *et al.*, 2001; Karu *et al.*, 2007, 2011; Meljon *et al.*, 2012; Y. Wang *et al.*, 2009)

4. *Selected reaction monitoring (SRM).* In this scan mode both the first and second analysers are put in the selection mode, so no scan is performed. With this mode, every precursor/product ion pair forms a transition, and the mass spectrometer will only focus on that specific transition. This technique has been also used for quantification porpoise in sterolomics, especially when a mass spectrometer is coupled with an LC (Baila-Rueda *et al.*, 2013; Borah *et al.*, 2020; Broughton & Beaudoin, 2021; W. J. Griffiths, Crick, & Wang, 2013; W. J. Griffiths *et al.*, 2016; Honda *et al.*, 2009b; Skubic *et al.*, 2020)

1.7 Aim of the thesis

Cholesterol is an essential component of the CNS, involved in several crucial physiological pathways for neuroneal cell development and survival. Alterations of brain cholesterol metabolism are believed to be involved in developing ND, AD and PD. Despite the evidence revealing cholesterol's contribution to the main AD and PD hallmarks, the degree of cholesterol engagement in these diseases remains largely unknown.

This thesis has been designed to study cholesterol alteration over AD and PD. Therefore, the aims of this study are:

- Fully characterise the cholesterol metabolites in AD and PD patients' body fluids (CSF and plasma) and compare them with neurologically healthy controls.
- Identify any statistically significant and biologically relevant difference in the sterols level and test the ability of the newly identified discriminant sterol molecules as a putative diagnostic biomarker for the disease.
- Study sterols level variations over disease progression (longitudinal studies) to study the impact of cholesterol alteration in progressive patients.
- Characterise the sterolome asset of human neuroepithelial stem cells, progenitors of neurones, and neuroepithelial stem cells carrying PD causative mutations to deep dive into cholesterol contribution to neuroneal development and early.

Chapter 2 - Material and methods

In this chapter a general description of the main techniques, protocols, analytical methods, and instrumentations used during this work of thesis is reported.

2.1 Reference internal standard

The identification of novel biomarkers sets the minimal requirements for the quantification methods towards a very high standard. For this reason, all the experiments reported in this work of thesis use isotope-dilution (ID) method for quantification purposes. ID represents nowadays the most reliable strategy for the sterols, and lipid molecules in general, quantification (Breuer & Björkhem, 1990; Dzeletovic *et al.*, 1995). To further minimise inter and intra-batches variation, which may occur during samples handling and processing, high quality isotope labelled quantitative standards (iSTDs) have been employed and added to the biological samples during the very first step of extraction. The different iSTDs are supplied by Avanti Polar Lipids Inc as high pure isotope solutions at specific concentration or in powder. Powder iSTDs have been reconstituted in high pure-HPLC grade organic solvents like MeOH (Fisher Scientific, M/4056/17), EtOH (Fisher Scientific, E/0650DF/17) or isopropanol (iPrOH, Fisher Scientific, P/7507/17). Actual concentration of the iSTDs solution from reconstituted standard powders have been certified against commercial Avanti Polar Lipids Inc high purity isotope standard solutions. For each biological fluid

and pellet a specific mixture of iSTDs, called iSTDs master mix, has been prepared and tested before application. The master mix tests consist in a simulation of the actual experiment, sterol extraction and quantification, of a standard reference material (SRM) of the same biological matrix for which it would have been applied for. The SRM used are:

- For plasma: SRM 1950, metabolites in frozen human plasma, (National Institute of Standards and Technology)
- For CSF: pooled CSF generated by combining individual CSF samples from multiple donors obtained from University Hospital of Umeå, Sweden. Details of the ethical permissions can be found in (Yutuc *et al.*, 2021)

2.1.1 Human neuroepithelial stem cells derived from induced pluripotent stem cells (iPSCs) carrying the LRRK2 mutation

Human Neuroepithelial stem cells (NES) derived from induced pluripotent stem cells (iPSCs) and iPSCs derived NES carrying the LRRK2 mutation were provided by Prof. Ernest Arenas, Karolinska Institutet, MBB, Laboratory of Molecular Neurobiology, Solnavägen 9, Biomedicum 6C, Stockholm 17177, Sweden. The iSTDs master mix for iPSCs derived NES was freshly made in house and tested just before the start of the experiments. The master mix was composed of [$^2H_7$] (22R)-hydroxycholesterol (Avanti Polar Lipids Inc, 700052P) , [$^2H_6$](24R/S)-hydroxycholesterol Avanti Polar Lipids Inc, LM-4110),

and [$^{2}H_{7}$]cholesterol (Avanti Polar Lipids Inc, 700041P). Details about NES iSTDs master mix composition is reported in the table 2.1

able 2.1. Characteristics and chemical composition of iSTDs master mix for NES cells.

Sterol		Commercially available form	Solvent of reconstitution	Concentration of the stock solution (ng/µL)	Concentration of the iSTDs master mix (ng/µL)	Required per sample (ng)
Common name	Systematic name					
[$^2H_6$] (24R/S)-hydroxycholesterol	[$^2H_6$] cholest-5- en-3β, (24R/S)-diol	MeOH solution	N.A.	51.95	1	2
[$^2H_7$] (22S)-hydroxycholesterol	[$^2H_7$] cholest-5- en-3ß,(22S)-diol	powder	EtOH	5	1	2
[$^2H_7$]-cholesterol	[$^2H_7$] cholest-5-en-3ß-ol	powder	iPrOH	1000	200	400

2.1.2 Human plasma

Different types of human plasma were worked out in this work of thesis but all from PD patients and age matched healthy individuals (comorbidities are specified where applicable).

2.1.2.1 NYPUM Parkinson disease baseline plasma

Human plasma from base line PD patients and age matched-neurologically healthy/non-neurodegenerative individuals, was provided by Umea University hospital, belonging to the NYPUM BIOBANK. Michael J Fox Foundation is acknowledged for supporting the Griffiths-Wang lab during the determination of PD plasma sterolome. All the plasma was collected form 2004 within the Umea catchment area. The iSTDs master mix for PD plasma project was freshly made in house and tested just before the start of the experiments The master mix was composed of [$^2H_7$](22S)-hydroxycholesterol (Avanti Polar Lipids Inc, 700051P) , [$^2H_6$](24R/S)-hydroxycholesterol (Avanti Polar Lipids Inc, LM-4110), [$^2H_7$](7α)-hydroxycholesterol (Avanti Polar Lipids Inc, LM-4103), [$^2H_7$]7-ketocholesterol (Avanti Polar Lipids Inc, LM-4107), [$^2H_6$](7α,25)-dihydroxy cholesterol (Avanti Polar Lipids Inc, 111117P), [$^2H_5$]cholestenoic acid (Avanti Polar Lipids Inc, 700151P), [$^2H_3$] 7α-hydroxy-3-oxocholest-4-enoic acid (Avanti Polar Lipids Inc, 700194P) and [$^2H_7$]cholesterol (Avanti Polar Lipids Inc, 700041P). Details

about NYPUM PD plasma master mix composition are reported in the table 2.2.

Table 2.2. Characteristics and chemical composition of iSTDs master mix for NYPUM PD plasma

Sterol		Commercially available form	Solvent of reconstitution	Concentration of the stock solution (ng/µL)	Concentration of the iSTDs master mix (ng/µL)	Required per sample (ng)
Common name	Systematic name					
[$^2H_6$] (24R/S)-hydroxycholesterol	[$^2H_6$] cholest-5-en-3β, (24R/S)-diol	MeOH solution	N.A.	51.95	0.40	20
[$^2H_7$] (22S)-hydroxycholesterol	[$^2H_7$] cholest-5-en-3ß, (22S)-diol	powder	EtOH	5	0.20	10
[$^2H_7$] (7α)-hydroxycholesterol	[$^2H_7$] cholest-5-en-3ß,7α-diol	MeOH solution	N.A.	48.74	0.40	20
[$^2H_7$]7-ketocholesterol	[$^2H_7$]7-oxo-cholest-5-en-3ß-ol	MeOH solution	N.A.	51.42	0.40	20
[$^2H_6$] (7α,25)-dihydroxy cholesterol	[$^2H_6$] cholest-5-en-3β,7α,25-triol	powder	iPrOH	10	0.04	2
[$^2H_5$] cholestenoic acid	[$^2H_5$]3ß-hydroxy-cholest-5-enoinc acid	powder	EtOH	491.14	0.40	20
[$^2H_3$]7α-hydroxy-3-oxocholestenoic acid	[$^2H_3$]7 α -hydroxy-3-oxo-cholest-4-enoic acid	powder	EtOH	239.64	0.40	20
[$^2H_7$]-cholesterol	[$^2H_7$]cholest-5- ene-3ß-ol	powder	iPrOH	1000	400.00	20,000

2.1.2.2 ICICLE Parkinson disease longitudinal plasma

Human plasma from progressive PD patients belongs to the Incidence of Cognitive Impairment in Cohorts with Longitudinal Evaluation-PD (ICICLE PD, https://portal.dementiasplatform.uk/CohortDirectory/Item?fingerPrintID=ICICLE-PD), an observational cohort study aiming to identify the biomarker for PD evolution. All the plasma was collected from 2009 within the Newcastle and Cambridgeshire catchment area. The ICICLE PD plasma was provided by Marta Caramacho, PhD, Department of Clinical Neurosciences, Cambridge centre for brain repair. The iSTDs master mix for ICICLE PD plasma project was freshly made in house and tested just before the start of the experiments The master mix was composed of [$^2H_7$](22S)-hydroxycholesterol (Avanti Polar Lipids Inc, 700051P) , [$^2H_6$](24R/S)-hydroxycholesterol (Avanti Polar Lipids Inc, LM-4110), [$^2H_7$](7α)-hydroxycholesterol (Avanti Polar Lipids Inc, LM-4103), [$^2H_7$]7-ketocholesterol (Avanti Polar Lipids Inc, LM-4107), [$^2H_6$](7α,25)-dihydroxy cholesterol (Avanti Polar Lipids Inc, 111117P), [$^2H_5$]cholestenoic acid (Avanti Polar Lipids Inc, 700151P), [$^2H_3$] 7α-hydroxy-3-oxocholest-4-enoic acid (Avanti Polar Lipids Inc, 700194P), and [$^2H_7$]cholesterol (Avanti Polar Lipids Inc, 700041P). Details about ICICLE PD plasma master mix composition are reported in the table 2.3.

Table 2.3 Characteristics and chemical composition of iSTDs master mix for ICICLE PD plasma.

Sterol		Commercially available form	Solvent of reconstitution	Concentration of the stock solution (ng/µL)	Concentration of the iSTDs mix (ng/µL)	Required per sample (ng)
Common name	Systematic name					
[$^2H_6$](24R/S)-hydroxycholesterol	[$^2H_6$]cholest-5-en-3β,(24R/S)-diol	MeOH solution	N.A.	51.95	0.40	20
[$^2H_7$](22S)-hydroxycholesterol	[$^2H_7$]cholest-5-en-3ß,(22S)-diol	powder	EtOH	5	0.20	10
[$^2H_7$](7α)-hydroxycholesterol	[$^2H_7$]cholest-5-en-3ß,7α-diol	MeOH solution	N.A.	48.74	0.40	20
[$^2H_7$]7-ketocholesterol	[$^2H_7$]7-oxo-cholest-5-en-3ß-ol	MeOH solution	N.A.	51.42	0.40	20
[$^2H_6$](7α,25)-dihydroxy cholesterol	[$^2H_6$]colest-5-en-3β,7α,25-triol	powder	iPrOH	100	0.02	2
[$^2H_5$]cholestenoic acid	[$^2H_5$]3ß-hydroxy-cholest-5-enoinc acid	powder	EtOH	273.91	0.40	20
[$^2H_3$]7α-hydroxy-3-oxocholestenoic acid	[$^2H_3$]7α-hydroxy-3-oxo-cholest-4-enoic acid	powder	EtOH	239.64	0.40	20
[$^2H_7$]-cholesterol	[$^2H_7$]cholest-5- ene-3ß-ol	powder	iPrOH	1000	800.00	20,000

2.1.2.3 BioFIND Parkinson disease base line plasma

Human plasma from base line PD patients belongs to Fox Investigation for New Discovery of Biomarkers (BioFIND) observational clinical study, (https://www.michaeljfox.org/news/biofind), an observational cohort study aiming to identify the biomarker for PD diagnosis, progression, and the differentiation among the clinical PD subtypes. All the plasma was collected from 2012 to 2015 within the United States of America enrolment area. The BioFIND PD observational study was sponsored by Michael J. Fox Foundation for Parkinson's Research (MJFF) and supported from the National Institute of Neurological Disorders and Stroke. The iSTDs master mix for BioFIND PD plasma project was freshly made in house and tested just before the start of the experiments The master mix was composed of [$^2H_7$](22S)-hydroxycholesterol (Avanti Polar Lipids Inc, 700051P) , [$^2H_6$](24R/S)-hydroxycholesterol (Avanti Polar Lipids Inc, LM-4110), [$^2H_7$](7α)-hydroxycholesterol (Avanti Polar Lipids Inc, LM-4103), [$^2H_7$]7-ketocholesterol (Avanti Polar Lipids Inc, LM-4107), [$^2H_6$](7α,25)-dihydroxycholesterol (Avanti Polar Lipids Inc, 111117P), [$^2H_5$]cholestenoic acid (Avanti Polar Lipids Inc, 700151P), [$^2H_3$] 7α-hydroxy-3-oxocholest-4-enoic acid (Avanti Polar Lipids Inc, 700194P), [$^2H_6$]desmosterol (Avanti Polar Lipids Inc, LM-4108) and [$^2H_7$]cholesterol (Avanti Polar Lipids Inc, 700041P). Details about BioFIND PD plasma master mix composition are reported in the table 2.4

Table 2.4. Characteristics and chemical composition of iSTDs master mix for BioFIND PD plas

Sterol		Commercially available form	Solvent of reconstitution	Concentration of the stock solution (ng/µL)	Concentration of the iSTDs mix (ng/µL)	Required per sample (ng)
Common name	Systematic name					
[$^2H_6$](24R/S)-hydroxycholesterol	[$^2H_6$]cholest-5-en-3β,(24R/S)-diol	MeOH solution	N.A.	51.95	0.40	20
[$^2H_7$](22S)-hydroxycholesterol	[$^2H_7$]cholest-5-en-3ß,(22S)-diol	powder	EtOH	5	0.20	10
[$^2H_7$](7α)-hydroxycholesterol	[$^2H_7$]cholest-5-en-3ß,7α-diol	MeOH solution	N.A.	48.74	0.40	20
[$^2H_7$]7-ketocholesterol	[$^2H_7$]7-oxo-cholest-5-en-3ß-ol	MeOH solution	N.A.	51.42	0.40	20
[$^2H_6$](7α,25)-dihydroxycholesterol	[$^2H_6$]colest-5-en-3β,7α,25-triol	powder	iPrOH	100	0.02	2
[$^2H_5$]cholestenoic acid	[$^2H_5$]3ß-hydroxy-cholest-5-enoinc acid	powder	EtOH	273.91	0.40	20
[$^2H_3$]7α-hydroxy-3-oxocholestenoic acid	[$^2H_3$]7α-hydroxy-3-oxo-cholest-4-enoic acid	powder	EtOH	239.64	0.40	20
[$^2H_6$]-desmosterol	[$^2H_6$]cholesta-5,24-dien-3ß-ol	powder	iPrOH	100	2.40	60
[$^2H_7$]-cholesterol	[$^2H_7$]cholest-5- ene-3ß-ol	powder	iPrOH	1000	800.00	20,000

2.1.3 Human CSF

Different types of human CSF have been worked out in this work of thesis but all from AD and PD patients.

2.1.3.1 Clinical database (GEDOC) Subjective cognitive impairment, Mild cognitive impairment, and AD CSF

CSF from subjective cognitive impairment (SCI), mild cognitive impairment (MCI) and Alzheimer's AD patients was provided by Prof Ingemar Björkhem, PhD, and Anna Sandebring Matton, PhD, Karolinska Institutet, Department of Neurobiology Care Sciences and Society, Division of Neurogeriatrics, Centre for Alzheimer Research, Stockholm, Sweden. The CSF belongs to the GEDOC memory clinic, collected by the Karolinska University Hospital memory clinic in Huddinge, Sweden. The iSTDs master mix for GEODC SCI, MCI and AD CSF project was freshly made in house and tested just before the start of the experiments The master mix was composed of [$^2H_7$](22S)-hydroxycholesterol (Avanti Polar Lipids Inc, 700051P) , [$^2H_6$](24R/S)-hydroxycholesterol (Avanti Polar Lipids Inc, LM-4110), [$^2H_7$](7α)-hydroxycholesterol (Avanti Polar Lipids Inc, LM-4103), and [$^2H_7$]cholesterol (Avanti Polar Lipids Inc, 700041P). Details about GEODC SCI, MCI and AD CSF plasma master mix composition are reported in the table 2.5.

Table 2.5 Characteristics and chemical composition of iSTDs master mix for GEDOC SCI, MCI and AD CSF.

Sterol		Commercially available form	Solvent of reconstitution	Concentration of the stock solution (ng/µL)	Concentration of the iSTDs mix (ng/µL)	Required per sample (ng)
Common name	Systematic name					
[$^2H_6$](24R/S)-hydroxycholesterol	[$^2H_6$]cholest-5-en-3β,(24R/S)-diol	MeOH solution	N.A.	51.95	0.0699	2
[$^2H_7$](22S)-hydroxycholesterol	[$^2H_7$]cholest-5-en-3ß,(22S)-diol	powder	EtOH	5	0.0003	1
[$^2H_7$](7α)-hydroxycholesterol	[$^2H_7$]cholest-5-en-3ß,7α-diol	MeOH solution	N.A.	48.74	0.0699	2
[$^2H_7$]-cholesterol	[$^2H_7$]cholest-5- ene-3ß-ol	powder	iPrOH	1000	0.0538	200

2.1.3.2 NYPUM Longitudinal PD CSF

Human CSF from progressive PD patients was provided by Umea University hospital, belonging to the NYPUM BIOBANK. Michael J Fox Foundation is acknowledged for supporting the Griffiths-Wang lab during the determination of PD CSF sterolome. All the CSF was collected form 2004 within the Umea catchment area. The iSTDs master mix for NYPUM PD CSF project was freshly made in house and tested just before the start of the experiments The master mix was composed of [$^2H_7$](22S)-hydroxycholesterol (Avanti Polar Lipids Inc, 700051P) , [$^2H_6$](24R/S)-hydroxycholesterol (Avanti Polar Lipids Inc, LM-4110), [$^2H_7$](7α)-hydroxycholesterol (Avanti Polar Lipids Inc, LM-4103), [$^2H_7$]7-ketocholesterol (Avanti Polar Lipids Inc, LM-4107), [$^2H_6$](7α,25)-dihydroxycholesterol (Avanti Polar Lipids Inc, 111117P), [$^2H_5$]cholestenoic acid (Avanti Polar Lipids Inc, 700151P), [$^2H_3$] 7α-hydroxy-3-oxocholest-4-enoic acid (Avanti Polar Lipids Inc, 700194P) [$^2H_6$]desmosterol (Avanti Polar Lipids Inc, LM-4108) and [$^2H_7$]cholesterol (Avanti Polar Lipids Inc, 700041P). Details about NYPUM PD plasma master mix composition are reported in the table 2.6.

Table 2.6 Characteristics and chemical composition of iSTDs master mix for NYPUM PD CSF

Sterol		Commercially available form	Solvent of reconstitution	Concentration of the stock solution (ng/µL)	Concentration of the iSTDs mix (ng/µL)	Required per sample (ng)
Common name	Systematic name					
[$^2H_6$](24R/S)-hydroxycholesterol	[$^2H_6$]cholest-5-en-3β,(24R/S)-diol	MeOH solution	N.A.	51.95	0.10	2
[$^2H_7$](22S)-hydroxycholesterol	[$^2H_7$]cholest-5-en-3ß,(22S)-diol	powder	EtOH	5	0.05	1
[$^2H_7$](7α)-hydroxycholesterol	[$^2H_7$]cholest-5-en-3ß,7α-diol	MeOH solution	N.A.	48.74	0.05	1
[$^2H_7$]7-ketocholesterol	[$^2H_7$]7-oxo-cholest-5-en-3ß-ol	MeOH solution	N.A.	51.42	0.05	1
[$^2H_6$](7α,25)-dihydroxycholesterol	[$^2H_6$]colest-5-en-3β,7α,25-triol	powder	iPrOH	10	0.01	0.1
[$^2H_5$]cholestenoic acid	[$^2H_5$]3ß-hydroxy-cholest-5-enoinc acid	powder	EtOH	136.95	0.05	1
[$^2H_3$]7α-hydroxy-3-oxocholestenoic acid	[$^2H_3$]7α-hydroxy-3-oxo-cholest-4-enoic acid	powder	EtOH	119.8	0.10	2
[$^2H_6$]-desmosterol	[$^2H_6$]cholesta-5,24-dien-3ß-ol	MeOH solution	N.A.	144	0.15	3
[$^2H_7$]-cholesterol	[$^2H_7$]cholest-5- ene-3ß-ol	powder	iPrOH	1000	10.00	200

2.2 Sterol extraction from NES cells derived from iPSCs

The sterolomic profile of all the cell medium and pellet from NES cells derived from iPSCs analysed in this work of thesis includes only the free-non esterified sterols fraction.

2.2.1 Cell pellet of NES cells derived from iPSCs

The protocol (figure 2.1) which follows is an adaptation of the one described in Blanc *et al.* paper (Blanc *et al.*, 2013b).

Frozen cell pellet from NES cells derived from iPSCs is let to thaw at 4˚C in ice. To avoid autoxidation of the sterols, the cell pellet is defrosted just before processing, minimising the frozen/thaw cycles to one. In a 1.5 mL Eppendorf tube containing 1 mL of absolute EtOH, 2 µL of the iSTDs master mix for NES from iPSCs are added, forming the ethanolic working solution of the iSTDs. Once completely defrost, the cell pellet is vortexed for 30 seconds and 1.002 mL of the ethanolic working solution are added while sonicating. Additional 50 µL of absolute EtOH are dropwise added while sonicating for further 5 minutes. After sonication, the extraction tubes are centrifuged at 4˚C, 13,300rpm, for 30mins in a Sorvall Legend RT Plus centrifuge, 75002431, to separate the debris from the ethanolic sterol extract. The sterol extract is collected and 400 µL of HPLC H_2O are added to dilute the ethanol concentration down to 70*% (v/v)* EtOH. This last step in the sterol extraction procedure will allow the separation of the

polar sterols, mainly the oxysterols and cholestenoic acids, from the non-polar ones like cholesterol and its precursor, see section 2.5 for details. Furthermore, sterols separation will prevent the enrichment of the Fr1 cholesterol autoxidation products, endogenous metabolites present in the biological matrixes, with the ex vivo cholesterol autoxidation products, which are undistinguishable from the formers.

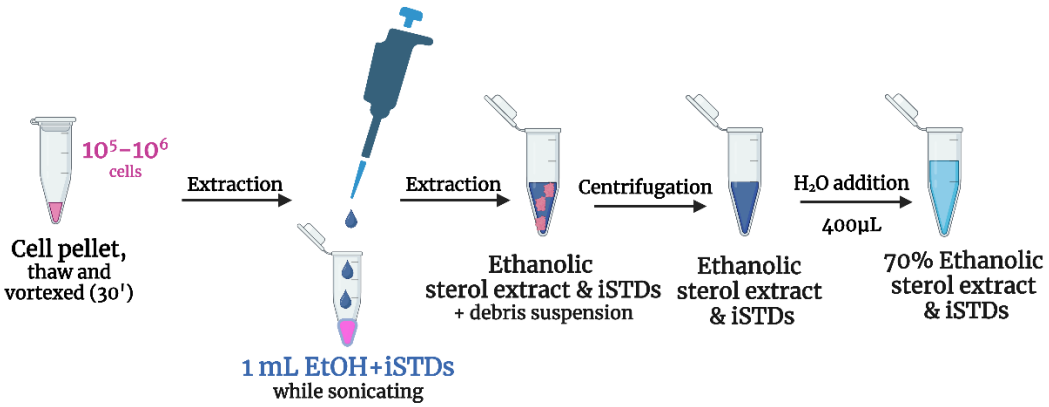

Figure 2.1 Schematic representation of cell pellet free sterol extraction.

2.2.2 Cell medium of NES cells derived from iPSCs.

The protocol (figure 2.2) which follows is an adaptation of the one described in Blanc *et al.* paper (Blanc *et al.*, 2013b) for the free sterol analysis.

1 mL of frozen medium from NES cells derived from iPSCs is let to thaw at 4˚C in ice. To avoid autoxidation of the sterols, the cell pellet is defrosted just before processing, minimising the frozen/thaw cycles to one. Once completely defrost, the medium is vortexed for 30

seconds and spin down. In a 1.5 mL Eppendorf tube containing 1 mL of absolute EtOH, 2 µL of the iSTDs master mix for NES from iPSCs are added, forming an ethanolic working solution of the iSTDs. In a 15 mL Falcon tube 1 mL of medium is dropwise added while sonicating to 1.33 mL of absolute EtOH. The 1.002 mL of iSTDs working solution is now dropwise added to the extraction solution to reach the final concentration of 70 *% (v/v)* EtOH. The sterol extract is let sonicating for further 5 minutes. This step in the sterol extraction procedure will allow the separation of the polar sterols, mainly the oxysterols and cholestenoic acids, from the hydrophobic ones like cholesterol and its precursor, see section 2.5 for details. After sonication, the medium sterol extracts are centrifuged at 4˚C, 4000rpm, for 1 hour in a Sorvall Legend RT Plus centrifuge, 75004373.

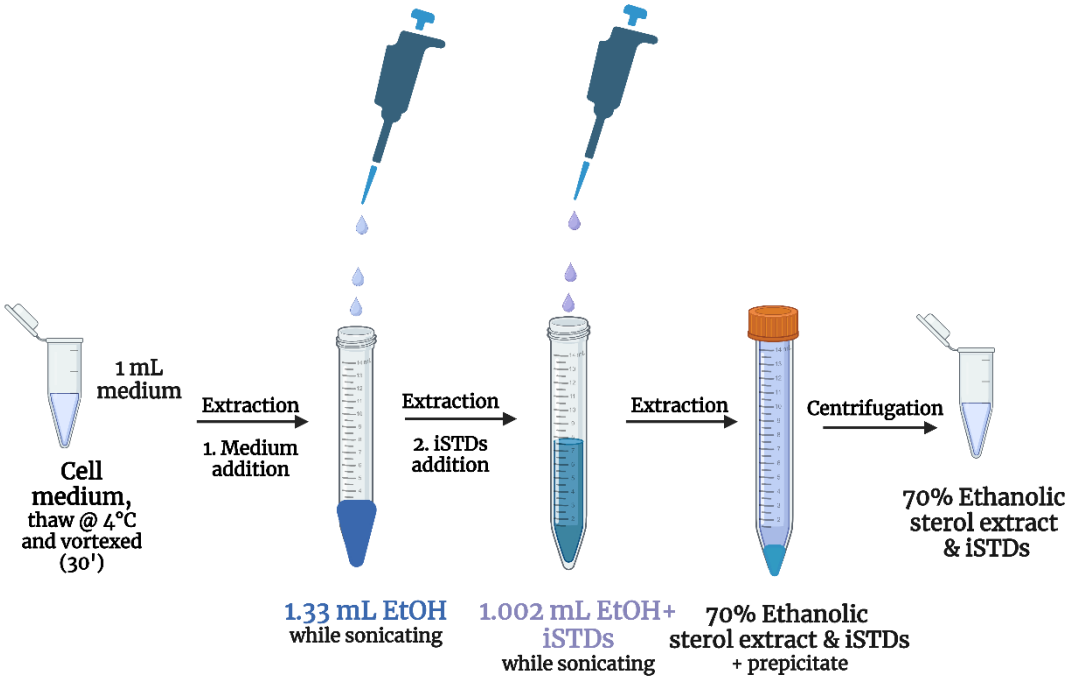

Figure 2.2 Schematic representation of cell medium free sterols extraction.

2.3 Sterol extraction from human plasma

The sterolomic profile of all the plasma analysed in this work of thesis includes only the free-non esterified sterols fraction. Therefore, no hydrolytic steps have been added to the plasma extraction protocol (figure 2.3). Human plasma is normally received in aliquots of 100 µl each, however when the available volume is higher than that, the plasma is immediately fractioned in 100 µl aliquots and stored at -80 °C to avoid autoxidation of the sterols. 100 µl of frozen human plasma is let to thaw at 4˚C in ice. Plasma is defrosted just before processing, minimising the frozen/thaw cycles to one, where applicable. In a 2 mL Eppendorf tube containing 1 mL of absolute EtOH, a specific amount of iSTDs master mix is added, forming an ethanolic working solution of the iSTDs, see table 2.7. Once completely defrost, the plasma is vortexed for 30 seconds, spin down, and dropwise added to the 1.5 mL tube containing the iSTDs master mix. The sterol extract is let sonicating for 5 minutes. After 5 minutes, 350 µL of HPLC H_2O are dropwise added to reach the final concentration of 70*% (v/v)* EtOH. This step in the sterol extraction procedure will allow the separation of the polar sterols, mainly the oxysterols and cholestenoic acids, from the unipolar ones like cholesterol and its precursor, see section 2.5 for details. After sonication, the extraction tubes are centrifuged at 4˚C, 13,300rpm, for 30mins in a Sorvall Legend RT Plus centrifuge, 75002431.

iSTDs mix used for plasma sterol extraction.

Plasma type	Amount of iSTDs master mix (µL)
NYPUM PD plasma	50
ICICLE PD plasma	25
BIOFIND PD plasma	25

Table 2.7 Amount of

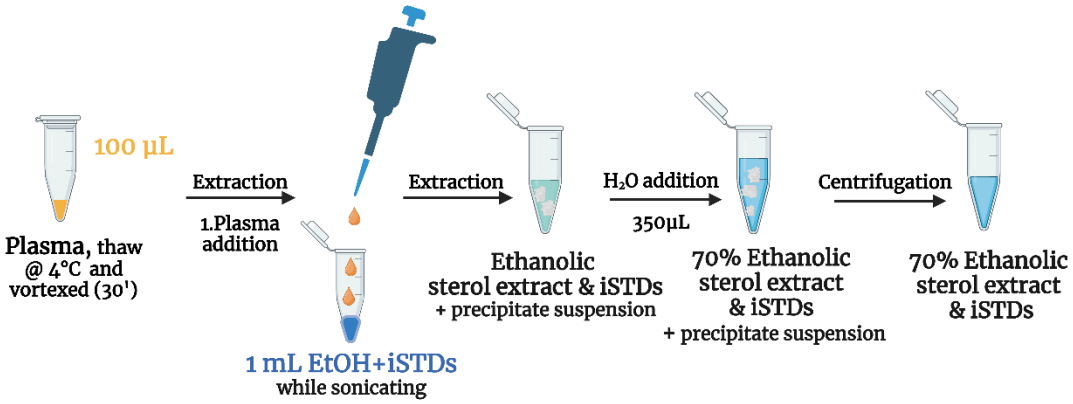

Figure 2.3 Schematic representation of free sterol plasma extraction.

2.4 Sterol extraction from human cerebrospinal fluid (CSF)

The sterolomic profile of the CSF analysed in this work of thesis includes both the free/non-esterified and the total sterols fraction. Therefore, a hydrolytic step has been added to the CSF extraction protocol. To note, to identify and quantify total and free sterols, two extraction protocols must be carried out separately. Therefore, the double of minimum CSF extraction volume is needed.

Human CSF is normally received in aliquots of 100 µl each, however when the available volume is higher than that, the CSF is immediately fractioned in 100 µl aliquots and stored at -80°C to avoid autoxidation of the sterols. 100 µl of frozen human CSF is let to thaw at 4˚C in ice. CSF is defrosted just before processing, minimising the frozen/thaw cycles to one, where applicable.

2.4.1 No Hydrolysis protocol, free sterols content

In a 2 mL Eppendorf tube containing 1 mL of absolute EtOH, a specific amount of iSTDs master mix is added, forming an ethanolic working solution of the iSTDs, see table 2.8. Once completely defrost, the CSF is vortexed for 30 seconds, spin down, and dropwise added to the 2 mL tube containing the iSTDs master mix (figure 2.4). The sterol extract is let sonicating for 5 minutes. After 5 minutes, 350 µL of HPLC H_2O are dropwise added to reach the final concentration of 70*% (v/v)* EtOH. This step in the sterol extraction procedure will allow the separation of the polar sterols, mainly the oxysterols and cholestenoic acids, from the unipolar ones like cholesterol and its precursor, see section 2.5 for details. After sonication, the extraction tubes are centrifuged at 4˚C, 13,300rpm, for 30mins in a Sorvall Legend RT Plus centrifuge, 75002431.

Table 2.8 Amount of iSTDs mix and protocol used for CSF sterol extraction.

CSF type	Amount of iSTDs master mix (µL)	No-hydrolysis protocol	Hydrolysis protocol
GEDOC SCI, MCI & AD CSF	30	N.A.	yes
NYPUM PD CSF	20	yes	N.A.

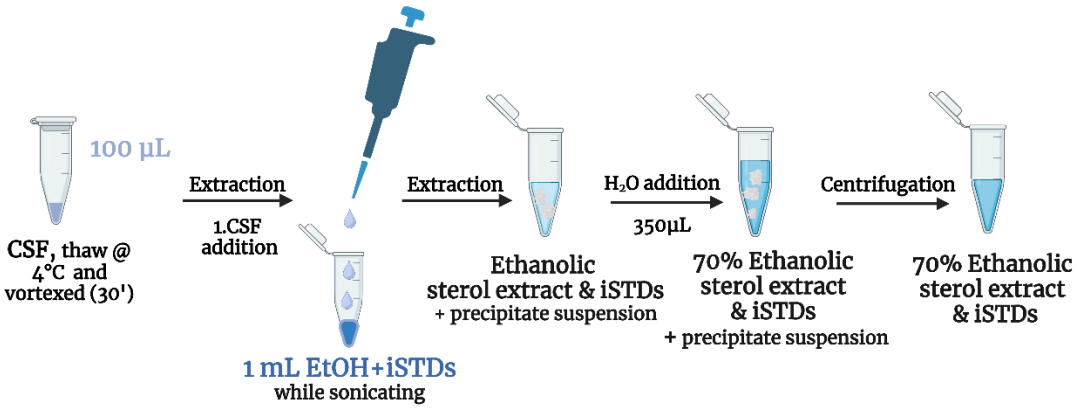

Figure 2.4 Schematic representation of CSF free sterols extraction.

2.4.2 Hydrolysis protocol, total sterols content

In a 25 mL volumetric flask 49.1 mg of KOH pellet (Sigma-Aldrich, 221473) are added and the flask is made up to volume with absolute EtOH. A basic 0.35 M ethanolic KOH solution is therefore made (pH= 13.55). In 15 mL Falcon tube containing 2.030 mL of 0.35 M ethanolic KOH, a specific amount of iSTDs master mix is added, forming an ethanolic working solution of the iSTDs, see table 2.8. Once completely defrost, the CSF is vortexed for 30 seconds, spin down, and dropwise added to the 15 mL tube containing the iSTDs master mix (figure 2.5). The KOH ethanolic solution is let sonicating for 5 minutes. After 5 minutes, the KOH ethanolic solution is incubated at room temperature in the dark for two hours. After two hours, the basic extraction solution is neutralised by adding 800 µL of a 0.9 M aqueous glacial acetic acid (Fisher Scientific, 11475160) solution while sonicating. The final extraction solution concentration is at 70*% (v/v)* EtOH. The system is let to sonicate for further 5 minutes. This step in the sterol extraction procedure will allow the separation of the polar sterols, mainly the oxysterols and cholestenoic acids,

from the unipolar ones like cholesterol and its precursor, see section 2.6 for details. After sonication, the CSF sterol extracts are centrifuged at 4˚C, 4000rpm, for 1 hour in a Sorvall Legend RT Plus centrifuge, 75004373.

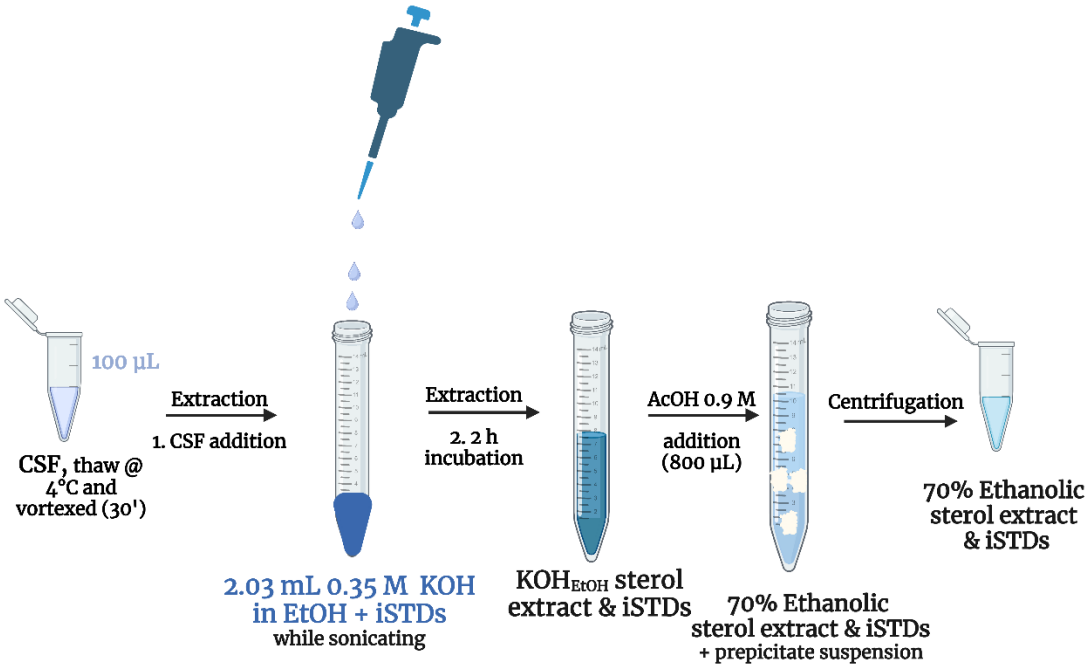

Figure 2.5 Schematic representation of CSF total sterols extraction.

2.5 Separation of cholesterol and oxysterols through SepPak RP columns (SPE-1)

After the extraction step, which slightly changes with the biological matrix type, the sterol molecules in the sterol's extracts are separated through a solid phase extraction chromatography, see Figure 2.6. The sterol lipids ,ST, separation is based on compounds polarity and affinity for a silica based, RP, C18, SPE column. More polar sterols will be separated from the very hydrophobic ones. Furthermore, the separation prevents the enrichment of the

endogenous cholesterol autoxidation products, with the ex vivo cholesterol autoxidation products, which are undistinguishable from the formers. For further details on the SPE principles refers to the paragraph 1.5.1.2.

The SPE step is equal for all the extracts and essentially follows the method described in Abdel-Khalik *et al.* (Abdel-Khalik *et al.*, 2017)

Sep-Pak®, RP C18, vacuum cartridge (Waters, 200mg, 37-55 µm,186004618) is firstly pre-conditioned with 4 mL of absolute EtOH. Vacuum is applied until a stable flow of 0.25 mL/min is reached and ethanol is let to pass through the column bed. A further rinse with 6 mL of 70*% (v/v)* EtOH follows. The sterol extract, whose volume varies depending on the biological sample (see table 2.9) is applied to the preconditioned column with a flow of 0.25 mL/min. The flow-through is collected and combined with an additional wash of 5.5 mL of 70*% (v/v)* EtOH. This is the first fraction collected, called Fr1, where oxysterols and cholestenoic acids elute. A washing step between the collection of polar and the non-polar sterols is necessary to avoid any contamination of the hydrophobic fraction with late-eluting polar molecules. 4 mL of 70*% (v/v)* EtOH are applied as a washing step and collected, second fraction or Fr 2. 2 mL of absolute EtOH are now applied and collected. This eluate constitutes the hydrophobic sterols fraction, mainly composed of cholesterol and precursors, fraction 3 or Fr3. A final 2 mL of absolute EtOH wash step followed and eluate collected, fraction 4 or Fr4.

Fr1 and Fr3 are divided into two equal volume fractions, FR1A & Fr1B plus Fr3A & Fr3B, respectively. The Fr1s and Fr3s are evaporated to dryness for 16 hours, 1500 rpm, 1mBar in a ScanVac ScanSpeed MaxiVac vacuum concentrator (Labogene, 7.008.500.003) coupled with CoolSafe cold trap set at -110°C.

Table 2.9 Sterol extracts amount depends on the biological matrix

Matrix	Sterol extract volume (in 70% *(v/v)* EtOH, mL)
Cell medium	3.3
Cell pellet	1.45
Plasma	1.5
CSF (no-hydrolysis protocol)	1.5
CSF (hydrolysis protocol)	3

.

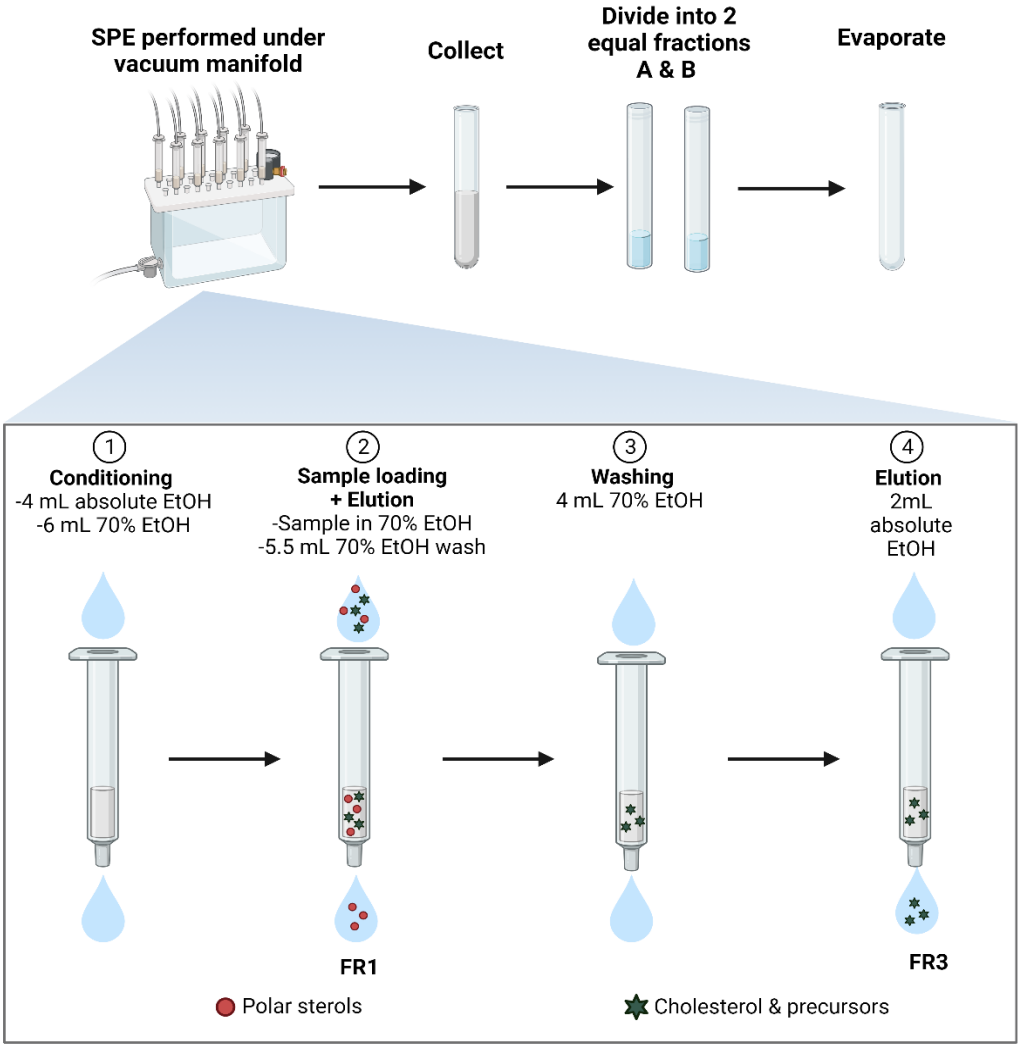

Figure 2.6 Schematic representation of the ethanolic extracts sterol molecules separation through SPE.

2.6 Enzyme-assisted derivatisation for sterol analysis (EADSA)

Sterol molecules are neutral, amphipathic, and hydrophobic lipids, which make their ionisation challenging, especially through a soft ionisation technique like electrospray ,ESI. However, increasing the ionisation potential with a hard ionisation turns out in in-source fragmentation and massive production of general fragments ions. These kinds of ions complicate the spectrum interpretation as they don't give any fundamental structural information. Hard ionisation also decreases the abundance of the sterol molecular peaks, which, on the contrary, provide several information for structural elucidation. For these reasons, in this work of thesis a derivatisation reaction is employed to introduce a positive charge in the sterol lipids and, consequently, enhance their ionizability and sensitivity towards MS analysis using ESI. The enzyme assisted derivatisation for sterol analysis, the EADSA, developed by the Griffiths-Wang group in the early 2000 (W. J. Griffiths, Crick, Wang, *et al.*, 2013) has been adopted, figure 1.24. Briefly, the 3ß-hydroxy-5-ene group of the cholestane body is selectively oxidised first, to a 3-oxo-4-ene with a bacterial (streptomyces) cholesterol oxidase. The formation of 3-ketone moiety alone allows the Wolff-Kishner nucleophilic addition of the positively charged hydrazine Girard P, GP D5 or D0, to the C3 position only. The introduction of a positive charge, belonging to the quaternary ammonium of the Girard P pyridine group, increase the sterol molecule signal intensity in the mass spectrometer by a factor of 10^2 to 10^3. Moreover, the polar nature of the GP reagent deeply improves the solubility profile of sterols in organic polar solvents, avoiding precipitation and allowing the efficient build-up of a solid

HPLC method for sterol epimers separation on a RP column. Lastly, when MS^n experiments are performed, a characteristic neutral loss from GP D0 and D5 derivatised sterols is seen, of 79 and 84 Da, respectively. This event permits to operate in neutral loss and precursors ion scan mode and to acquire structural information from specific and characteristic fragmentation patterns. To summarise, EADSA derivatisation procedure improves the ionisation profile of sterol lipids through ESI while boosting the production of characteristic finger-prints fragments when MS^n is employed.

The lyophilised fractions, Fr1A & Fr1B and Fr3A & Fr3B, are re-dissolved in 100 µL of iPrOH and vortex mixed for 1 minute. To the reconstituted fractions 1 mL of 50 mM phosphate buffer (Sigma-Aldrich Ltd, P9791-500g), pH 7, is added and solution vortexed for mixing (2 minutes). To FrAs, 3 µL of a cholesterol oxidase from *Streptomyces sp.* solution (2 mg/ml in H_2O, 44 units/mg protein, Sigma-Aldrich Ltd, C8649) are added, and vortex mixed (1 minute). The reaction mixture is let to react at 37 °C in a water bath for an hour. No cholesterol oxidase is added to FrBs, but they are treated as FrAs. After 1 hour, the oxidation of cholesterol oxidase is quenched with 2 mL of MeOH, and vortex mixed for 30 seconds. The sterols fractions are now at 70*% (v/v)* MeOH. To Fr1s and Fr3s 150 µL of glacial acetic acid are added followed by the addition of 190 mg of in-house synthesised GP D5 to FRAs only and 150 mg of commercially available GP D0 to FrBs only. After vortexing for 1 minute the solution is let to react overnight (16 hours) in the dark at room temperature (20-23 °C). In FrAs, by means of cholesterol oxidase oxidation, all the sterols should possess a 3-ketone group and, therefore, react with the GP d5 reagent. On the other side, in FrBs only the ST naturally possessing the 3-oxo group form a hydrazone

with the GP D0. Hence, sterols possessing 3ß-hydroxy-5-ene can be deducted over the subtraction of FRAs sterols with the FrBs ones, see Figure 2.7. The use of two different GP reagents, characterised by a 5 Da mass difference, allows the differentiation of FrAs ST from the FrBs when a MS analysis is used for identification and quantification, which would be otherwise undistinguishable with the use of LC/HPLC chromatography alone.

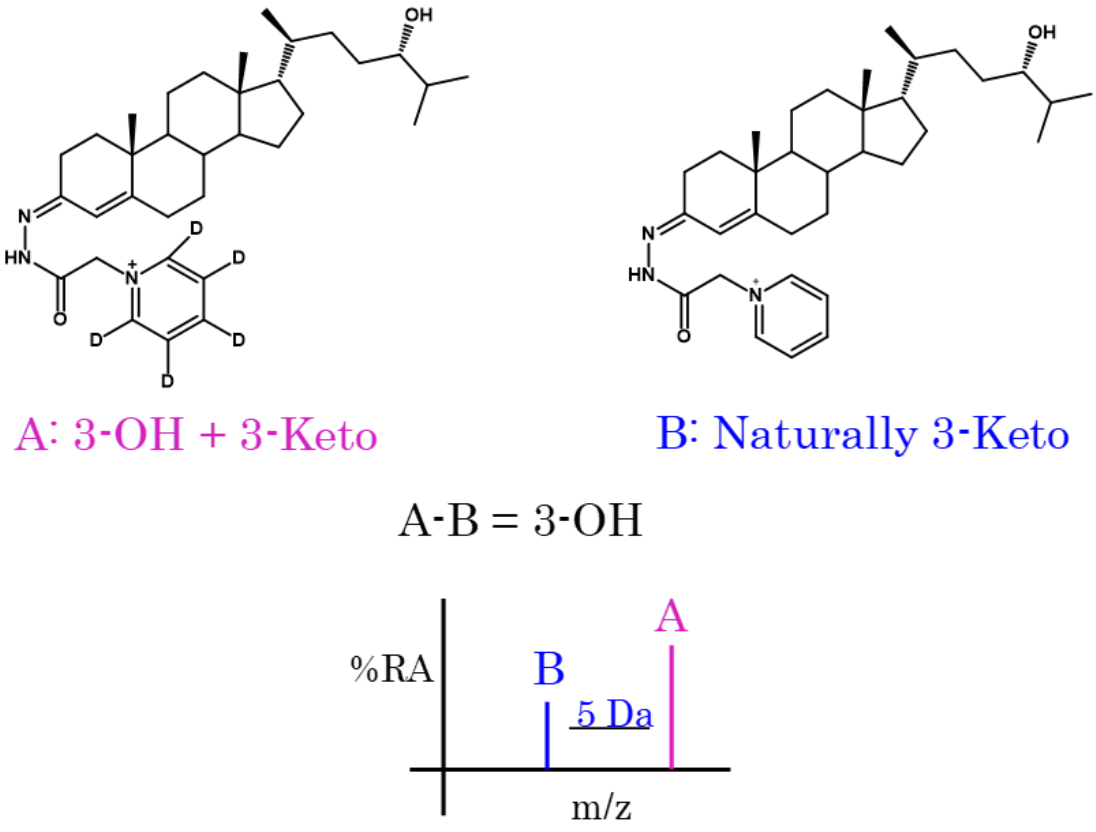

Figure 2.7 The EADSA method for the concomitant determination of 3-hydroxyl and 3-ketone sterols.
The oxidation of only one sterol fraction (A) and the use of two different charged mass tags, GP D5 (A) and D0 (B), allows the differentiation of 3-ketones from 3-hydroxyl sterols by MS analysis

.

2.6.1 [$^2H_5$] Girard P synthesis

The deuterated hydrazine GP D5 is synthesised in house as it is not commercially available in bulky amounts. Large biomarker discovery projects, as the ones described in this work of thesis, requires large, pure, and reliable amounts of reagents constantly.

The GP D5 synthesis here described represents an optimisation and scale-up of the Girard *et al.* synthesis (A. Girard & Sandulesco, 1936). In a 500 mL round bottom flask 20 mL, 232.8 mmol, of [$^2H_5$] Pyridine (Goss Scientific, DLM-39-5) are dropwise added to 250 mL of absolute EtOH under magnetic stirring, followed by the dropwise addition of 25.8 mL, 232.8 mmol, of ethyl bromoacetate (Merck, 133973-100G). The system is then brought to reflux with an oil bath and let to react for 3.5 hours. After 3.5 hours, the reaction mixture is let to cool down to room temperature and then to 0°C in an ice-water bath. When the reaction mixture reaches 0°C, 14.7 mL, 232.8 mmol, of hydrazine 80 *% (v/v)* in aqueous solution (Merck, 8046040250) are dropwise added under magnetic stirring and a white solid precipitate is thus formed. The amorphous white solid is filtered under vacuum and washed with cold EtOH. The precipitate is let to dry under vacuum for 3 days. GP D5 precipitate weight after drying 55 ± 0.50 g, overall yield 99%*)*.

2.7 Oxysterols fraction purification using HLB Oasis column (SPE-2)

The amount of the reagent GP D0/5 employed for sterols derivatization is in large excess and needs to be removed before MS

analysis of the sterols extract. Otherwise, heavy ion suppression effect will compromise the identification of the ST. To this purpose, a SPE chromatography is employed to eliminate the unreacted GP from the ST extract, see Figure 2.8. A recycling elution method is used for sterols recovery and GP elimination. Even if the derivatization with GP enhances the sterols solubility in organic polar solvents, when these solvents are mixed with a high percentage of water, derivatized sterols might not be sufficiently soluble and form a suspension rather than a solution. Moreover, when applied to a RP SPE, sterols might be over retained by the column when highly aqueous mixture of organic solvents are used as eluents. The use of recycling elution methods helps to overcome these issues. Furthermore, the re application of the flow through, while increasing the water content, avoids losses of more polar sterols, which might be initially less retained by the column bed, and assure excellent recovery.

A 60 mg Oasis hydrophilic-lipophilic balanced (HLB) column (Waters, WAT094226) is preconditioned with 6 mL of 100*% (v/v)* MeOH followed by 6 mL of 10*% (v/v)* MeOH and 4 mL of 70*% (v/v)* MeOH (set the manifold pressure to let a flow from the column of ≅ 0.25 mL/min). At this point, the derivatized sterols fraction, either Fr1s A and B or Fr3s A and B, (≅ 3 mL in 70*% (v/v)* MeOH, 5*% (v/v)* acetic acid) is applied. 1 mL of fresh 70*% (v/v)* MeOH is used to wash the tubes containing sterols fraction and then applied to the SPE column, to assure a complete load of the sterols and avoid any losses. Then, 1 mL 70*% (v/v)* MeOH wash is combined to the ≅ 3 mL sterols eluate. A 1 mL of 35*% (v/v)* MeOH column wash follows. The combined flow-though (≅ 5 mL) is mixed in a 12 mL falcon tube with 4 mL of HPLC H_2O to make 9 mL of a 35*% (v/v)* MeOH solution. The

9 mL are re-applied to the column, followed by a 1 mL 17*% (v/v)* MeOH column wash. The 10 mL eluate is combined with 9 mL of HPLC H_2O in a 50 mL Falcon tube to make 19 mL of 17*% (v/v)* MeOH solution. The 19 mL are re-applied to the column and the flow-through discarded. 6 mL of 10*% (v/v)* MeOH are now applied to the column to extract the excess of GP from the stationary HLB phase and eliminate it. 3 mL of 100*% (v/v)* MeOH are now applied and collected in single 1 mL aliquots, A1-A2-A3 and B1-B2-B3, see the figure. The 3 x 1mL 100*% (v/v)* MeOH aliquots contain the pure sterols extracted from the biological matrixes, which are mainly present in the first two fractions, A1-A2 and B1-B2. One extra mL of absolute ethanol is applied to the column to extract any remaining sterols and collected (A4 and B4). Finally, each sample resulted in 16 Eppendorf's tubes containing the pure extracted sterols in either methanolic (Fr1 A1-3, Fr1 B1-3, Fr3 A1-3 and Fr3 B1-3) or ethanolic solution (Fr1 A4, Fr1 B4, Fr3 A4 and Fr3 B4) (figure 2.8). The sterols in methanolic and ethanolic solutions are stable at low temperature and can be stored at -20°C for several months or at -80°C for long term storage.

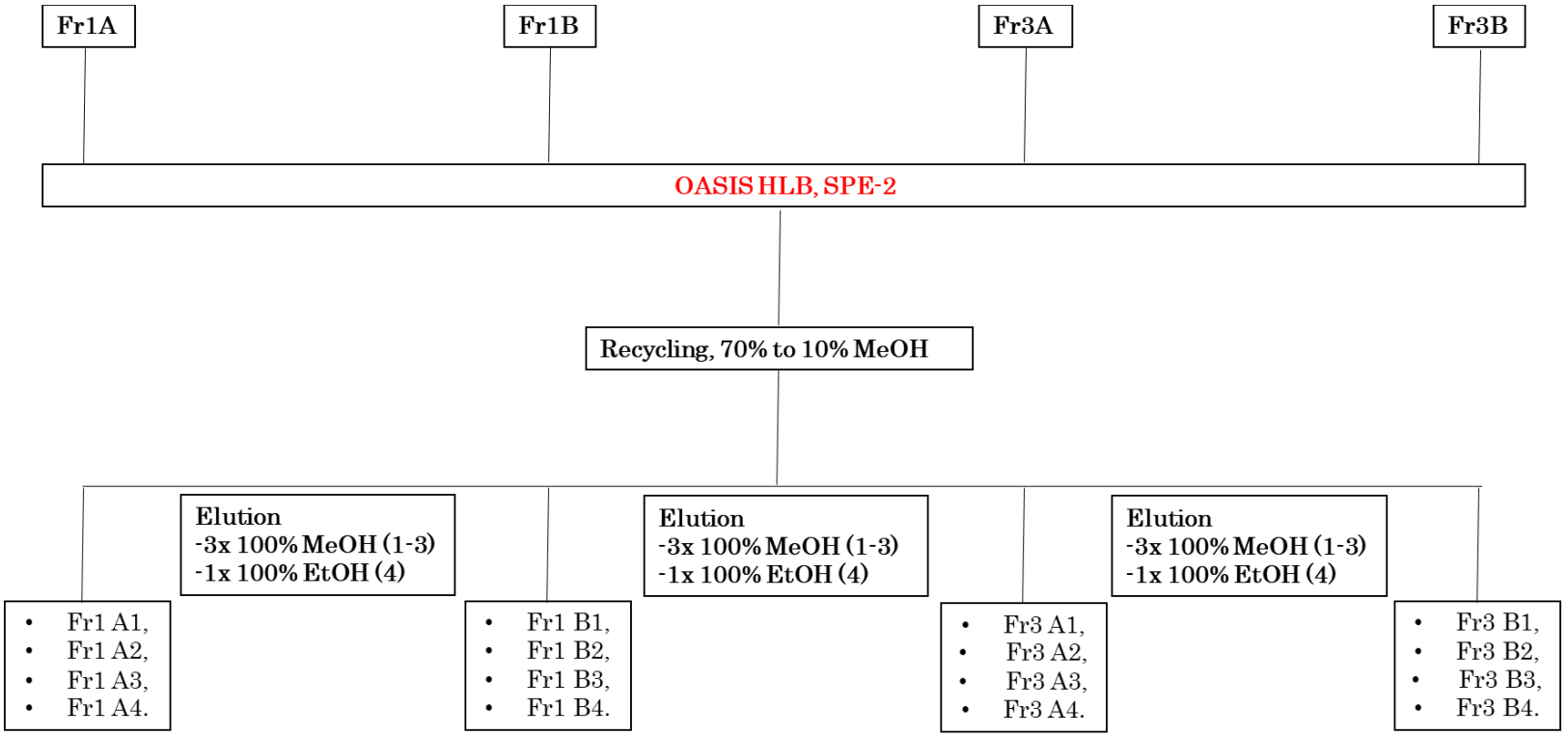

Figure 2.8 Workflow of the SPE-2 HLB purification step.

2.8 Sterol extracts analysis using a coupled LC-ESI-MS^n technique.

The analysis of the sterols extract is performed through a coupled LC-ESI-MS^n technique.

Chromatographic separation of the derivatised sterol lipids in the methanolic extract is performed using an Ultimate 3000 UHPLC (Dionex, now Thermo Fisher Scientific) composed of a WPS 3000 TPL RS autosampler and a NCS 3500 RS Nano pro flow pump module. The column used is a RP Hypersil Gold C18 (502.1 mm, 1.9mm, Thermo Fisher Scientific). Two mobile phases, A and B, have been freshly made before each run, see table 2.10 for composition.

Table 2.10 Mobile phase composition for the sterol analysis of the sample methanolic extract.

	MeOH (% (v/v))	ACN (% (v/v))	H_2O (% (v/v))	HCO_2H
A	33.3	16.7	50	0.1
B	63.3	31.7	5	0.1

17- and 37-minutes gradient elution methods have been employed for the separation and resolution of derivatised sterol isomers/epimers, as previously described (Agatonovic-Kustrin *et al.*, 2019; W. J. Griffiths *et al.*, 2018). Briefly, for the 17 minutes method an initial equilibration phase with a 20% B and 80% A mobile phase composition is maintained for 1 minute. From minute 1 a gradual enrichment of the mobile phase B starts up until minute 8, where it reaches 80% B and 20% A and remains at this concentration for further 4 minutes (plateau phase) before returning to 20% B in 0.1 minutes (minute 12.1). A reconditioning phase starts at 12.1 minutes,

at 20% B and 80% A, and is maintained for 4.9 minutes. With this method, column employed and mobile phase composition, the elution of the sterols follows polarity decrease. In the first minutes of the chromatographic separation, more polar ST like cholestenoic acids and di-hydroxy sterols, elute, followed by mono-hydroxy sterols. In the last third of the time (around 11 minutes in the 17 minutes method) the least polar compounds, cholesterol, and precursors, elute.

The 37 minutes method is an extension of the 17 one but allows a better base-line separation of first eluting polar sterols, especially oxysterols and cholestenoic acids. Shortly, the initial equilibration phase at 20% B is maintained for 10 minutes followed by a ramped increase in mobile phase B composition to 50% over 10 minutes (minute 20). The 50/50 A/B composition of the eluent is maintained for further 6 minutes (minute 26). From minute 26 the mobile phase B enrichment starts again to reach 80% B composition over 3 minutes (minute 29). The plateau phase is then maintained at 80% B for further 3 min before returning to 20% B in 0.1 minutes (minute 32.1). The reconditioning phase at 20% B is maintained for 4.9 minutes. The flow rate is maintained at 200µL/min for all the time of analysis.

The eluting sterols from the UHPLC are subsequently analysed on the Orbitrap IDX Trihybrid (Thermo Fisher Scientific) mass spectrometer, equipped with an ESI probe. After ambient ionisation in the ESI source, see table 2.11 for ESI parameters, the ions are subjected to three to six scan events, in positive ion mode:

1. A first high-resolution FT-MS scan (120000 FWHM, at 400 *m/z*) in the Orbitrap mass analyser for accurate mass identification of the molecular ions of interest. Mass range 400-610 *m/z*.

2. In parallel, three to six data dependent-precursor ion scans events in the linear trap ,LIT, are performed, each one followed by two fragmentation stages (MS^3), with the first *m/z* selection (MS isolation mode) operated by the triple quadrupole mass filter.

Table 2.11 Electrospray configuration for the LC-ESI-MS^3 method used.

ESI parameters	
Ion source type	H-ESI
Spray voltage	Static
Positive ion mode (V)	3800
Gas mode	Static
Sheath Gas (Arb)	35
Aux gas (Arb)	7
Ion transfer tube temperature (°C)	300
Vaporiser temperature (°C)	300

For the MS^n experiments, an inclusion list of the precursor ion masses is used for data dependent acquisition. The use of an inclusion list based on the molecular ion $[M^+]$ *m/z* of the target sterols allows the quadrupole selection of these ions alone and their analysis in the LIT, if their intensity exceed a certain threshold. Thanks to this event the number of specific charged species increase in the detector, and so the sensitivity of the multistage fragmentation. When desired $[M^+]$ ions rich the LIT, a first fragmentation experiment (MS^2) happens (MS activation type is collision induced dissociation (CID) with a collision energy of 30 % and activation time of 30 milli seconds). The inclusion list also contains the *m/z* of the molecular ion's fragments produced over the specific neutral loss of 79 or 84 Da (pyridine ring from GP D0 or D5, respectively). If a $[M\text{-}79/84^+]$ fragment is observed in a MS^2 event, a MS^3 fragmentation event happens (CID energy 35% with an activation time of 30 milli seconds).

For the detection, identification, and quantification of sterols in Fr1s, the more polar sterols, a total of 9 methods have been employed, 7 of 17 minutes and 2 of 37 minutes, to screen a total of 25 *m/z* values while 4 per 17 minutes method have been used for Fr3s sterols screening, for a total of 11 *m/z* values. For methods specification see table 2.12 while for details of each mass inclusion list refer to tables 7.1 to 7.13 in appendix.

Table 2.12 LC-MS3 methods specification for Fr1 and Fr3 sterols screening: duration and mass inclusion list.

Method name	Sterols fraction	Minutes	Inclusion mass list (*m/z*)
1	Fr1	17	522-527-532-537
2	Fr1	17	550-555-561
3	Fr1	17	564-569-567-572
4	Fr1	17	548-553-506-511
5	Fr1	17	534-539-545-541-546
6	Fr1	17	550-555-561-553-548
7	Fr1	17	522-527-585-580
8	Fr1	37	545-539-541-546-534-569
9	Fr1	37	545-539-555-561-596-572
10	Fr3	17	518-523-520-525-530
11	Fr3	17	514-519-516-521-530
12	Fr3	17	514-519-516-521-527
13	Fr3	17	522-527-516-521-530

Only the methanolic extracts of each sample, (Fr1 A1-3, Fr1 B1-3, Fr3 A1-3 and Fr3 B1-3) are used for the sterol analysis through the LC-ESI-MS^3. The above-mentioned method requires a dilution to 60*% (v/v)* MeOH of the methanolic sterol fractions before injection into the LC. Specifically, for Fr1 equal volumes of Fr 1 A1 and A2 plus Fr 1 B1 and B2 are mixed and diluted to 60*% (v/v)* MeOH before injection. For all the biological matrixes analysed in this work of

thesis, Fr1 have been injected at neat after dilution to 60*% (v/v)* MeOH, due to the low sterol levels (pg to ng per mL of sample or millions of cells). Respect to Fr 1s, Fr 3s require the use of all the 3 methanolic extracts, Fr 3 A1 to A3 and Fr 3 B1 to B3, that are mixed in equal volumes. Depending on the biological sample, Fr 3s are diluted to 60*% (v/v)* MeOH first and further diluted as 1 in 1000, 1 in 100 or 1 in 10. Precisely, human plasma sample and cell pellet Fr 3s are diluted 1000 times. Free cholesterol concentration reaches hundreds of µg/mL in human plasma (Yutuc *et al.*, 2021). In human cells, free cholesterol concentration varies on the cell type, especially when cell pellet is extracted. To avoid RP column saturation, carry-over, and consequent ion suppression plus charge space effect in the mass analyser, 1 in 1000 dilution is always preferred. Fr3s' from non-hydrolysed CSF and from cell medium have been diluted with a 1 in 100 dilution as free cholesterol levels are lower in human CSF only reach hundreds of ng per mL (Yutuc *et al.*, 2021), while Fr3s from hydrolysed CSF were diluted 1 in 10. Even if a 1 in 100 dilution for Fr3s hydrolysed CSF would have allowed the identification of total cholesterol, accounting for few µg/mL in human CSF, the lower dilution had allowed the identification of cholesterol precursors like desmosterol or Δ7-dehydro-cholesterol.

2.8.1 MS-instrumentation: Orbitrap ID-X

All the mass spectrometry analysis reported in this work of thesis have been carried out with the use of an Orbitrap ID-X Trihybrid mass spectrometer (Thermo Fisher Scientific). This new type of Orbitrap instruments couple a series of different mass analyzers for

high precision accurate mass determination and better resolution over tandem MS experiments. As we can see from the ID-X ion path figure 2.9, the sample in solution is sprayed in an OptaMax NG ion source, with improved sprayer alignment and stability. The new ESI source is composed of an exhaust port which can efficiently reduce the chemical noise by removing the excess of solvent vapor without interfering with analysis time and performance. Once formed, ions are focused through optic S-Lenses, which are spaced stacked ring ion guides able to create a tight ion beam while avoiding in-source fragmentation. The ion beam passes then into an active beam guide which serves as initial screening for cluster ions. The beam guide eliminates cluster ions before they can enter the mass filter through neutralization on charged curved rods while an axial field is applied along all the length of the rods to improve ion transfer to the quadrupole mass filter. Ions entering the quadrupole mass filter undergo MS isolation mode with a first MS/MS precursor ion selection at high transmission efficiency between 400 and 610 *m/z* (as described above). Ions of selected masses are then sent to the ion-routing multipole which provides efficient trapping (storage), and ions transfer to either Orbitrap or linear trap. A first high accuracy full mass scan (400-610 *m/z*) is performed in the high field Orbitrap mass analyser, which possesses a resolving power of 500,000 FWHM, full-width-at-half-maximum, at 200*m/z* and isotopic fidelity up to 240,000 FWHM. Contemporary, ions are sent to the dual-pressure linear ion trap, a dual-dynode detector with high dynamic range. The two cells of the linear trap possess different pressure values which serve for different scopes. The low-pressure cell is used for improved scan speed and better resolving power, along with mass accuracy. The higher-pressure cell is suitable for collision induced dissociation experiments and the consequent generation of the fragment ions. The

entire mass spectrometer relies on a new vacuum system composed of a split-flow turbomolecular pump able to easily control the vacuum in multiple regions, with a low mTorr pressure in the ion-routing multipole. The pressure can reach less than 2 x 10^{-4} Torr in the linear trap and 2 x 10^{-10} Torr in the Orbitrap. For general ID-X specifications see table 2.13 below. The Thermo Fisher's software Thermo Scientific™ Xcalibur™ is used for data processing and acquisition. The integrated Xcalibur™ Qual browser is used for raw data visualization, interpretation, and identification.

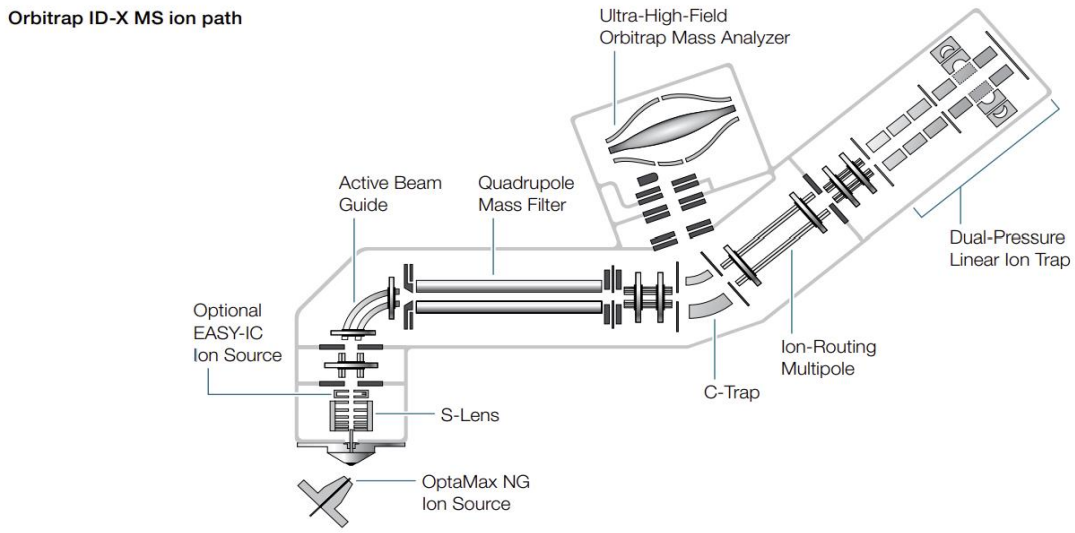

Figure 2.9 Schematic representation of the Thermo Fisher™ Orbitrap iDX™ ion path.

Table 2.13 ID-X performance characteristics.ID-X performance parameters	
Mass range	50-2000 *m/z*
Resolution (Orbitrap)	7,500-500,00 FWHM at 200 *m/z*
Orbitrap scan rate	up to 30 Hz
Ion trap scan rate	up to 40 Hz

Mass accuracy	<3 ppm with external calibration <1 ppm with internal calibration
MS/MS ESI ion trap sensitivity	femtograms of reserpine solution, as per producer instruction
Dynamic range	> 5,000(single scan
MS scan power	MS^n, with 1<n<10
Multiples of ion-routing multipole	up to 10 precursors per scan in a MS^2 or SIM experiment
Polarity switching	one full cycle, from positive to negative, in 1.1 seconds

2.9 Quantification methods

Sterols identification and quantification have been performed using the Thermo Fisher™ software Trace Finder™, where raw files were directly loaded. Briefly, the sterols present in the sample extracts, both Fr1s and Fr3s, are first identified by accurate mass and retention time match (full scan Fourier Transform FT-MS spectrum). Additional direct comparison of the ion trap IT-MS fragmentation spectra with the in-house spectra library can also be performed for an accurate and precise molecule identification. The in-house sterol spectral library has been built over the course of the years by our lab, based on our established method for sterols identification through LC-ESI-MS^3 (W. J. Griffiths *et al.*, 2006). Full scan FT-MS is the result of Fourier transform transformation of the ion frequencies acquired in the Orbitrap mass analyser into a spectrum, with mass

range domain. IT-MS spectrum originates from the MS^3 fragmentation experiments in the LIT and detection of the positive ion's fragments. Each IT-MS spectrum represent a fingerprint fragmentation pattern of each sterol, which complete the structure attribution. After identification, quantification is performed through the Trace Finder software by means of the deuterated isotope dilution method used during sample preparation. Specifically, sample's endogenous sterols and externally added deuterated internal standards, iSTDs, peak area integration is initially performed on a FT-MS chromatogram. A relative quantification then follows, where a sterol is quantified against a deuterated standard with identical structure, for example (24S)-HC has been quantified against [$^2H_6$] (24R/S)-hydroxycholesterol in Fr1s or cholesterol against [$^2H_7$] cholesterol in Fr3s. Semi-quantification is also performed because identical deuterated standards are not always available and a surrogate with similar structure has been used, for example, in Fr1s (7β)-HC has been quantified against [$^2H_7$] (7α)-hydroxycholesterol or desmosterol against [$^2H_7$]-cholesterol in Fr3s. In this work of thesis, different iSTDs master mixes have been used for each biological matrixes, therefore absolute and semi-quantification differs among sample types. For specific details about sterols quantification mode refer to tables 7.14 to 7.19 in the appendix section.

2.10 Statistical analysis

All the statistical analysis has been performed using Graph Pad Prism software (GraphPad by Docmatics). All the data sets obtained over Trace Finder quantification have been tested for normality utilising Anderson-Darling test, D'Agostino & Pearson test, Shapiro-Wilk test, Kolmogorov-Smirnov test and log normality through Anderson-Darling test, D'Agostino & Pearson test, Shapiro-Wilk test, and Kolmogorov-Smirnov test. Classical descriptive statistics have also been calculated for all the data sets like 25% percentile, median, 75% percentile, mean, standard deviation, standard error of mean, lower 95% confidential interval of mean and upper 95% confidential interval of mean.

2.10.1 Parkinson

All the plasma data sets belonging to patient affected by PD (Nypum, ICICLE) and CSF (Nypum) were tested for normal distribution as first. None of them resulted as normal distributed so non-parametrical tests were performed to check data sets differences. Mann Whitney and Kolmogorov Smirnov test (non-parametric T-test) have been used to compare the medians and the cumulative frequency distributions between PD and non-PD samples, respectively. When sex was introduced as confounding variable, Kruskal-Wallis test was used to compare the medians between the groups, followed by correction through Benjamini and Hochberg post-hoc test. ROC analysis has also been performed to check whether the plasma sterols could have differentiated between the pathological

and the healthy case, speculating on their diagnostic biomarker nature. For the longitudinal cohorts of plasma and CSF PD patients, two-stage multiple comparison method of Benjamini, Krieger and Yekutieli has been used to look for statistical variation in the plasma sterols among two different time points. This type of test will assess if a variation in two data sets is a real discovery or not by calculating the false discovery rate. For the longitudinal CSF data, a mixed effect analysis method has been used to test the sterol variation among three time points. This statistical method is very similar to a repeated measure ANOVA but can handle null or not entered values. As in the longitudinal CSF data set the number of entries (patient samples) is different in each time point, the mixed model had to be used to correct for the missing values.

2.10.2 Alzheimer

The GEDOC CSF was tested for normal distribution as first. Data resulted as no-normal distributed so non-parametrical tests were performed to check data sets differences. Kruskal-Wallis test was used to compare the medians between the groups, followed by Dunn's multiple comparison test, which compares in the sum of ranks between two data sets and the expected average difference, which is based on the number of groups under analysis and the size. Correlation test, Pearson test, was also made to check the interdependence of the principal CSF sterols.

Chapter 3 - Sterolomic profile of human CSF in Alzheimer's disease (AD)

3.1 Introduction

Alzheimer's disease (AD) is a neurodegenerative disorder leading to irreversible cognitive impairment. AD is widely recognised as the most common form of dementia, affecting 3-4% of adult population worldwide aged over 65 years old (Tahami Monfared *et al.*, 2022). The progressive cognitive decline characterising AD is the result of an irreversible and incessant neuroneal cells loss in the hippocampal and entorhinal cortex regions of the brain. Pathologically, AD is defined by the abnormal accumulation of extracellular insoluble amyloid ß (Aß) plaques and intracellular phosphorylated τ aggregates called neurofibrillary tangles (NFTs), which, however, are not sufficient to fully explain the death of the brain cells. Hence, the mechanistic cause of the neurodegenerative disease is still uncertain, and no curative medical therapy or specific set of clinical biomarkers are nowadays available, placing the disease as the top priority for elder people health.

However, hypercholesterolemia, highly prevalent in old population, and dysregulated cholesterol metabolism have been linked to the development of AD (Feringa & van der Kant, 2021). The contribution of cholesterol to the disorder has been debated for several years as controversial findings emerged from numerous studies on associations between cholesterol plasma levels and AD (Agarwal & Khan, 2020; Puglielli *et al.*, 2003; Selkoe, 2011; P. Wang *et al.*, 2020;

Whitfield, 2006; Wong *et al.*, 2017). Since the identification of the disorder by Dr Alois Alzheimer at the beginning of the 20th century, accumulation of intracellular lipid overloaded droplets has been reported in post-mortem brain of AD patients (Stelzmann *et al.*, 1995). Nevertheless, the fat accumulation started to gain attention only after the detection of elevated cholesterol blood levels during AD. Investigations of brain cholesterol alterations, rather then is peripheral/extracerebral counterpart, has highlighted the participation of the sterol lipid to more than one pathological event connected to AD (J. Brown *et al.*, 2004; Chang *et al.*, 2017; Fassbender *et al.*, 2001; Feringa & van der Kant, 2021; Gamba *et al.*, 2015, 2019; Heverin *et al.*, 2004; Puglielli *et al.*, 2003; Testa *et al.*, 2016c; Varma *et al.*, 2021; Wong *et al.*, 2017; Zelcer *et al.*, 2007). Studies on mice and cellular models of the disease and on the post-mortem AD brain have highlighted the ability of the endoplasmic reticulum, ER, cholesterol to contribute to the amyloid precursor protein APP processing. Elevated ER cholesterol levels can block the dimerization of the APP monomers and induce the migration of the transmembrane protein to the plasma membrane. At the plasma membrane level, high cholesterol levels cause the colocalization of the BACE1 enzyme, γ-secretase, and APP in lipid rafts, which determines APP cleavage to toxic Aß oligomers (Bodovitz & Klein, 1996; Cordy *et al.*, 2003; Cossec *et al.*, 2010; Fassbender *et al.*, 2001; Götz *et al.*, 2004; Grimm *et al.*, 2008; Langness *et al.*, 2021; Shibata *et al.*, 2000; Wahrle *et al.*, 2002). The combination of elevated ER and plasma membrane cholesterol results, therefore, in the promotion of the amyloidogenic pathway. Interesting to note, the effect on APP is specific, as cholesterol accumulation does not affect any other transmembrane protein localisation. In addition to APP, cholesterol, in particular cholesteryl esters (CEs), have been found to stimulate

the phosphorylation of τ protein, inducing the formation of NFTs (Feringa & van der Kant, 2021). This effect seems to rely on CE modulation of the proteasomal activity towards phosphorylated τ, which is, however, not seen in regards of Aβ clearance (Feringa & van der Kant, 2021). Respect to Aβ, the relationship between phosphorylated τ and brain cholesterol is still under debate and needs to be further clarified. Despite the effective contribution of cholesterol to AD pathology, the exact role of the lipid is still not completely clear. However, all the current literature on the topic agrees on the presence of an altered brain cholesterol homeostasis over the neurodegeneration (Bjorkhem *et al.*, 2006; Chang *et al.*, 2017; Gamba *et al.*, 2015; Perez Ortiz & Swerdlow, 2019; Puglielli *et al.*, 2003; Varma *et al.*, 2021; Zelcer *et al.*, 2007)(Bjorkhem *et al.*, 2006; Chang *et al.*, 2017; Gamba *et al.*, 2015; Perez Ortiz & Swerdlow, 2019; Puglielli *et al.*, 2003; Varma *et al.*, 2021; Zelcer *et al.*, 2007). Abnormal brain cholesterol levels have been linked to a dysregulation of the APOE-mediated lipid transportation, which represents the main brain cholesterol mobilisation mode (Gamba *et al.*, 2015; Gong *et al.*, 2002; Husain *et al.*, 2021). The presence of the human isoform ε4 (APOE4) represents one of the major risk factors for AD, especially for the ones who's carrying the homozygous variant. Astrocytes expressing APOE4 present the highest concentration of cholesterol biosynthetic enzymes compared to the ones expressing the other isoforms (Tcw *et al.*, 2019). Moreover, APOE4-astrocytes display cholesterol accumulation in lysosomes (Tcw *et al.*, 2019). Studies on cholesterol distribution and APOE variants in AD post-mortem brain confirm the astrocytes findings (Y. T. Lin *et al.*, 2018; Tcw *et al.*, 2019). The accumulation of intracellular cholesterol upon APOE4 expression might be linked to the altered binding capacity of apolipoprotein to the LDL-r receptors and lesser

capacity to form HDL particles. Although there is a strong association between altered cholesterol levels in AD brain and the expression of the APOE4, there is still a lack of knowledge upon the exact mechanism triggering the cholesterol dysregulation via the apolipoprotein.

Dysregulation of cholesterol homeostasis over AD pathology also affects one of the major pathways involved in the control of the sterol physiological level, its metabolism to oxysterols, to (24S)-hydroxy cholesterol, (24S)-HC. Several studies have reported altered (24S)-HC level in AD post-mortem brain (Gamba *et al.*, 2015; Testa *et al.*, 2016b), CSF and plasma (Bjorkhem *et al.*, 2006; Gamba *et al.*, 2015; Leoni & Caccia, 2011; Testa *et al.*, 2016a). Changes in the brain (24S)-HC levels may influence several brain cells health, especially neuronees where it is mainly produced. It has been demonstrated that higher (24S)-HC promotes neuroneal cellular damage, which can result in neurodegeneration (Gamba *et al.*, 2015). Moreover, elevated cellular (24S)-HC seems to be also involved in the amyloidogenic pathway and to contribute to the neuroinflammation characterising AD pathology (Gamba *et al.*, 2015, 2019; Sodero, 2021b). However, the exact role of the oxysterol in the development of the AD is still not clear and needs further investigation. Nevertheless, (24S)-HC is not solely considered an intermediate in the cholesterol homeostasis maintenance but also its major brain transport form. Indeed, cholesterol cannot cross the BBB and it needs to be converted into its more soluble form to exit the brain and pass into the bloodstream. Almost all the (24S)-HC in the circulation originates from brain cholesterol, in human (Bjoandŕkhem *et al.*, 2006a). Alteration of its plasma and CSF levels might reflect modification of cholesterol brain turnover and, therefore, of the metabolic state of neuronees.

Confirming disrupted brain cholesterol metabolism as one of the hallmarks of AD pathology and the degree of the alteration over the progression of disease can open the door to the development of new series of diagnostic and prognostic biomarker. Despite the recognised proteinopathies associated with AD and the consequent development of sensitive and reproducible analytical techniques for the detection of soluble Aβ40 and Aβ42 and phosphorylated τ 217 in blood and CSF, the cut-off for the differentiation of the disease state and for the diagnose are still not established (Hansson *et al.*, 2022). One of the main reasons for the delay in cut-off definitions lies in the minimal fold change of brain derived proteins between the AD patient and control subjects. Being the Aβ40 and Aβ42 produced also elsewhere outside the CNS, it becomes harder to distinguish the peripheral and brain forms in the plasma, and the rigor required to detect the brain isoform and maintain the results reproducible might not meet the clinical standard (Hansson *et al.*, 2022). Moreover, even if phosphorylated τ proteins levels might differentiate AD cases from healthy subject, τ proteins alone cannot discriminate between AD and other neurodegenerative pathologies or dementias presenting τ pathology (Hansson *et al.*, 2022) . Individuating novel blood-based biomarkers, whose differences in fold change can be clinically appreciated, is imperative for AD diagnosis.

3.2 Aims

Over the last thirty years several studies have indicated in dysregulated brain cholesterol metabolism a potential novel pathway contributing to the development of Alzheimer disease. Nonetheless, it is still not clear if disrupted cholesterol brain homeostasis represents a cause or consequence of neuroneal loss. Qualitative and quantitative profile of brain cholesterol, precursors and metabolites are therefore needed for a better understanding of its metabolic changes over the AD pathology.

During this work of thesis, CSF samples from a memory clinic cohort composed of subjective cognitive impairment, SCI, mild cognitive impairment, MCI, and AD patients have been characterised from a sterols point of view. The first objective of this investigation is to assess the mono hydroxy sterols profile of patients at different stages of cognitive impairment, from a qualitative and quantitative perspective. Internal quality control CSF samples have been used to check the reproducibility of the protocol and the analytical method, a LC-MS^3 approach. The second aim is to highlight any statistical and biological valuable variation between the different pathological groups to evaluate sterols variation over the disease progression. The work described in this chapter seeks to identify new, reliable, and easy-to-detect biomarkers for AD progression while providing a reproducible and clinically translatable protocol for CSF sterolome determination. The present investigation is part of a larger study on a memory clinic cohort called GEDOC (Makrina Daniilidou *et al.*, 2022) who's aim is to investigate the contribution of some CSF biomarkers, to the cognitive impairment displayed at different stages of AD.

3.3 Material and methods

3.3.1 AD, MCI and SCI CSF cohort

90 CSF samples from SCI (n=30), MCI (n=30) and AD (n=30) patients were provided by Prof Ingemar Björkhem, PhD, and Anna Sandebring Matton, PhD, Karolinska Institutet, Department of Neurobiology Care Sciences and Society, Division of Neurogeriatrics, Centre for Alzheimer Research, Stockholm, Sweden. The CSF belongs to the GEDOC memory clinic, whose participants were diagnosed at the Karolinska University Hospital memory clinic in Huddinge, Sweden, during 2008 and 2014. The diagnosis process was based on clinical assessments made of neurological examination, review of the patients' medical history, Mini-Mental State Examination (MMSE), comprehensive neuropsychological testing, routine blood test, brain imaging, including magnetic resonance imaging, MRI, or computed tomography, TC, and measurements of AD CSF biomarkers levels (soluble $A\beta_{42}$, phosphorylated-τ and total-τ). Diagnoses were made approximately 2 months after the start of the clinical assessment by consensus agreement between a multidisciplinary clinical staff, in an unblinded manner. MCI was diagnosed when the criteria for mild cognitive impairment were verified, thus both objective and subjective cognitive impairment were present and were involving one or more cognitive domains without affecting the patient daily life activities and no presence of dementia (Winblad *et al.*, 2004). Dementia was diagnosed according to the Diagnostic and Statistical Manual of Mental Disorders, 4th edition (DSM-IV) (Guze, 1995) while Alzheimer's Disease was

diagnosed using the National Institute of Neurological and Communicative Disorders and Stroke- Alzheimer's Disease and Related Disorders Association (NINCDS-ADRDA) (McKhann *et al.*, 1984) . Patient not meeting the criteria for either MCI or AD were diagnosed of SCI. The exclusion criteria were stroke, other neurodegenerative disorders, hypertension, hypercholesterolemia, and diabetes. Ethical approval was obtained through the Ethical Review Board in Sweden (ethical permits 2019-06056 and 2011/1987-31/4) and is in concordance with the 1964 Helsinki declaration. All the participant's provided the written informed consent. Patients' chronic co-morbidities compatible with the selection criteria are listed in the appendix table 21. Due to the lack of the Institutional Review Board approval and Material Transfer Agreement, anonymized data were not available for the sterolome study. Therefore, no information on gender, age, MRI scans, amyloid ß and APOE status of SCI, MCI and AD groups have been made available. CSF samples were collected by lumbar puncture between L3/L4 or L4/L5 intervertebral space using a 25-gauge needle. Samples were collected in propylene tubes, aliquoted and stored at -80°C until use.

3.3.2 CSF sample preparation and sterols extraction

The GEDOC memory clinic cohort CSF has been characterised for its total sterol content, details of the extraction procedure in the section 2.4 to 2.7. The extraction, recovery and analysis of the total CSF sterols content require an initial saponification step which enables the release of the sterol alcohols and fatty acids form their ester

forms. The hydrolytic step is described in detail in section 2.4.2. Briefly, 100 µL of CSF are extracted in a 0.35 M KOH ethanolic solution containing the designated iSTDs mixture, details of the standard mixture can be found in section 2.1.3.1. The reaction mixture is left to react in the dark for 2 hours prior acidic neutralisation with a 0.9 M solution of glacial acetic acid. The ethanolic extracts are centrifuged and sterols polarity based separated through a SPE chromatography (section 2.5). Polar (Fr1s) and un-polar (Fr3s) fractions are charge tagged with the hydrazine Girard P D5 and D0, following cholesterol oxidase oxidation (, EADSA protocol, section 2.6). Girard P excess is removed through a second SPE and pure methanolic extracts are therefore obtained (section 2.8). The methanolic sterols extracts are then diluted to 60*% (v/v)* MeOH prior analysis. For the sterol analysis, 70 µL of the polar sterol fractions, Fr1s, are injected at 60*% (v/v)* MeOH into an Ultimate 3000 UHPLC coupled with the Orbitrap Trihybrid I-DX® mass spectrometer. The hydrophobic fraction, Fr3s, are first diluted 1 in 10 in 60*% (v/v)* MeOH to overcome instrument overload. 35 µL of the 1 in 10, 60*% (v/v)* MeOH Fr3 extract are then injected into the system. An LC-ESI-MS^3 analysis is employed for qualitative/quantitative profile of total CSF sterols content.

3.3.3 Oxysterols analysis

The strategy adopted for the sterol profile of the AD human CSF implies a combined gradient elution chromatography and tandem Mass Spectrometry, including precursor ion and neutral loss scans. A detailed description of the technique and methods applied to the

LC-ESI-MS^3 methods can be found in the section 2.8. Sterols quantification has been performed upon peaks identification and integration utilising the Thermo Fisher™ software Trace Finder™, see section 2.9 for details. Briefly, after peaks identification, conduct upon accurate mass and retention time match, always integrated to a manual screening of the MS^3 fragmentation pattern and comparison with the internal library, the sterols are quantified against same structure or surrogate deuterated standard. Details of deuterated standard used for quantification purposes are reported in table 18 of the appendices for GEDOC memory clinic cohort CSF. Relative quantification has been performed.

3.4 Results

Human CSF samples from SCI (n=30), MCI (n=30), and AD (n=30) patients, GEDOC cohort, have been screened for the total, free plus esterified, polar sterols, mainly mono hydroxy sterols, cholesterol, and relative precursors. Following the 3 days protocol described in sections 3.3.2 to 3.3.3, 9 different sterols have been totally or partially identified in human CSF, including include 5 mono-hydroxy sterols of which seven mono-hydroxy cholesterols (24S)-HC, 25-HC, 26-HC, 3ß-H-7-OC & 6ß-HC, one mono-hydroxy cholestenones, 7-OC, 2 cholesterol precursors, desmosterol and Δ7-dehydro-cholesterol and cholesterol itself, see figures 3.4 to 3.7. Six cholestenoic acids, including (25S)3ß,7α-diHCA ,(25S)7α-H-3O-CA, (25R)3ß,7α-diHCA, (25R)7α-H-3O-CA, 3ß,7α-diHCA, and 7α-H-3O-CA, have been recognised but not identified and quantified due to the absence of the specific identical or surrogate deuterated internal standard and MS^3

fragmentation, see figure 3.6. However, the main porpoise of this project was the screening of brain cholesterol and its direct metabolites, therefore full identification and quantification have been optimised only for ions belonging to mass of 534 and 539 *m/z*, which correspond to mono hydroxy sterols mass to charge ratio when derivatised with hydrazine Girard P D0 and D5, respectively, and of 523 and 521 *m/z*, which represent cholesterol and its direct precursors. The analysis resulted in the quantification of 9 sterols, ranging in concentration from 0.07 ± 0.03 to 3800.03 ± 1845.80ng/mL, see table 3.1.

Table 3.1 CSF levels of the main total sterols in GEDOC SCI, MCI and AD patients.
Results expressed as means in ng/mL ± standard deviation. SD: standard deviation; 3ß-H-7-OC: 3ß-hydroxy-cholsten-7-one, the 3-hydroxyl form of the 7-OC, cholestene-3,7-dienone.

Sterols	SCI (ng/mL ±SD)	MCI (ng/mL ±SD)	AD (ng/mL ±SD)
(24S)-HC	1.85 ± 0.69	2.10 ± 1	2.53 ± 0.67
25-HC	0.07 ± 0.03	0.08 ± 0.06	0.09 ± 0.04
26-HC	1.18 ± 0.55	1.28 ± 0.60	1.47 ± 0.60
7-OC	0.9 ± 0.64	0.72 ± 0.65	0.98 ± 0.52
7-OC + 3ß-H-7-OC	1.61 ±1.38	1.65 ± 1.95	1.28 ± 1.84
6ß-HC	1.89 ± 3.29	1.83 ± 2.14	1.33 ± 0.95
Desmosterol	2.53 ± 1.71	3.69 ± 1.99	3.14 ± 2.82
Δ7-dehydro-cholesterol	0.37 ± 0.4	1.12 ± 2.28	0.66 ± 0.86
Cholesterol	2987.56 ± 806.37	3062.08 ± 1662.77	3800.03 ± 1845.80

An internal quality control human CSF has been used to test protocol reproducibility and added to every batch analysed. An inter-batches

variation lower than 20 % has been obtain for all the main enzymatic-derived sterols, see table 3.2. Cholesterol autoxidation product resulted in higher CVs, which is expected and mainly due to freeze and thaw cycles, sample handling and preparation. Wherever possible, freeze and thaw cycles were restricted to just one round, however, the QC CSF have been provided in 200 µL aliquots, which are enough for two batches. Cholesterol precursors, desmosterol, and Δ7-dehydro-cholesterol, turns out to be high in CV as well. This fact might be explained by the low abundance of the sterol compared to cholesterol, which might also interfere in the analysis with a space charge effect, partially suppressing the other sterols signal. Good chromatographic separation is obtained when the 17-minutes gradient elution mode is employed, resulting in base line peak separation for most of the Girard P-derivatised plasma sterols, see figures below. To note the separation of the epimers (24S)- and (24R)-HC belonging to the internal standard [$^{2}H_{6}$] (24R/S)-HC (figure 3.1), which is usually hard to obtain without a high selective chromatographic system. The specificity and selectivity of the elution methods employed bring the disadvantage of separating the two conformers, *E* and *Z*, deriving from the Girard P derivatisation, complicating the chromatogram, see figure 3.1.

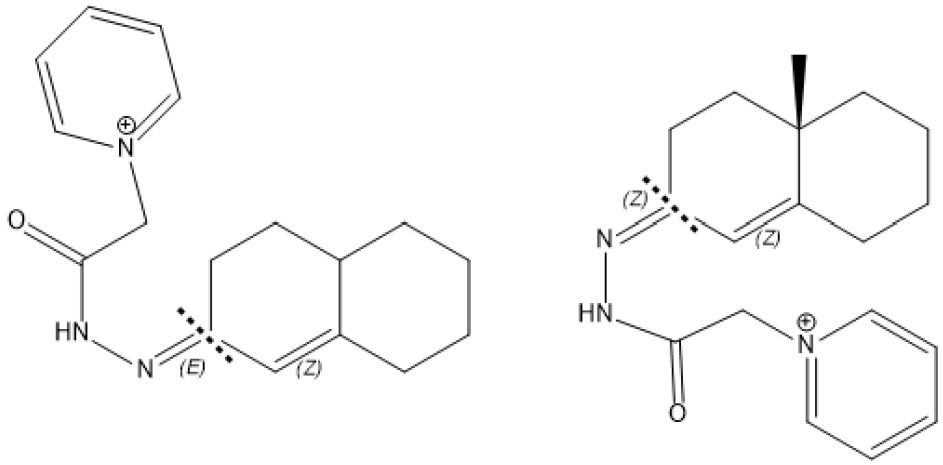

Figure 3.1 Geometrical isomers, E and Z, resulting from the GP derivatisation. $^2H_0$ GP derivatisation displayed.

However, thanks to the multistage fragmentation experiments, structure identification results quite straightforward. Structure attribution of the chromatogram peaks with mass to charge ratio of 521, 523, 534, and 539 is done through chromatogram and mass spectrum analysis. This assessment consists in concomitant retention time match of the chromatogram peaks with the one in the sterols' internal library and of the spectrum informative/fingerprint fragments obtained through precursor and neutral ion scans in MS^3 experiments, refer to the tables 7.5, 7.10 and 7.11 in the appendix for details. Relative quantification is performed against the designated deuterated internal standard, refer to table 7.18 in the appendix for details. Details of internal standard mix used can be found in section 2.1.3.1.

Table 3.2 Main QC CSF total sterol levels. Results expressed as means in ng/mL ± standard deviation. SD: standard deviation; 3ß-H-7-OC: 3ß-hydroxy-cholsten-7-one, the 3-hydroxyl form of the 7-OC, cholestene-3,7-dienone. N/D, not detected, sterol below the Orbitrap limit of detection.

	QC BATCH #1	QC BATCH #2	QC BATCH #3	QC BATCH #4	QC BATCH #5	QC BATCH #6	QC BATCH #7	QC BATCH #8	QC BATCH #9	QC BATCH #10	QC BATCH #11	QC BATCH #12	Mean	SD	CV
(24S)-HC	1.98	1.57	1.43	1.95	1.75	1.74	1.38	1.83	1.77	1.82	1.41	1.70	1.69	0.20	0.12
25-HC	0.04	0.07	0.06	0.08	0.08	0.07	0.08	0.07	0.07	0.04	0.08	0.05	0.07	0.01	0.20
26-HC	1.40	1.20	1.03	1.49	1.26	1.26	1.08	1.16	1.11	1.19	0.90	1.13	1.18	0.15	0.13

7-OC	0.88	0.39	0.55	0.65	0.99	1.83	2.40	1.71	2.65	2.20	0.67	1.97	1.41	0.77	0.55
7-OC + 3ß-H-7-OC	1.53	0.97	0.95	0.49	1.18	1.84	2.41	0.41	0.38	2.20	2.20	0.69	1.27	0.71	0.56
6ß-HC	0.79	0.25	0.36	0.47	0.54	0.45	0.67	1.06	1.94	1.79	1.79	1.07	0.93	0.58	0.62
Δ7-dehydro-cholesterol	N/D	0.35	0.54	0.50	0.46	0.60	0.40	N/F	2.47	0.14	0.92	0.83	0.72	0.62	0.86
Desmosterol	2.26	2.29	1.92	2.27	2.00	1.39	1.64	3.27	5.05	2.83	2.08	2.24	2.44	0.92	0.38
Cholesterol	3937.25	3988.73	3005.44	3832.55	3536.53	3030.60	2934.22	3902.82	3832.14	3071.38	3846.11	3843.96	3563.48	405.49	0.11

Sterols data from the three pathological groups resulted to be non-normally distributed, therefore nonparametric statistical tests have been used for their comparison. Out of the 9 different sterols identified in the human hydrolysed CSF, none statistically differs between the three groups, see example figure 3.2 of (24S)-HC and 26-HC, the main research focus. To correct for any contribution of not disease-related cholesterol variation, sterol values have been normalised to cholesterol levels but, also in this case, no relevant difference has been reported. Ratios between 26-HC and (24S)-HC levels have also been investigated in the three pathological groups as it has been demonstrated to change over certain neurological conditions like meningitis (Leoni *et al.*, 2003). As for the individual sterols' levels, no significant variation appears form this analysis. However, correlation analysis demonstrated quite strong positive interdependence between the levels of the monohydroxy sterols (24S)-HC and 26-HC, as shown in figure 3.3 panel A for all the three pathological groups SCI (Spearman r=0.78), MCI (Spearman r=0.82) and AD (Spearman r=0.86). A similar scenario can also be observed between the 26-HC and the cholesterol levels in SCI (Spearman r=0.73), MCI (Spearman r=0.70) but not in AD (Spearman r=0.59), figure 3.3 panel B. Remarkably, an opposite scenario is detected when correlation analysis is applied to (24S)-HC and cholesterol CSF levels, with SCI (Spearman r=0.62) and MCI (Spearman r=0.55) barely corelating while AD (Spearman r=0.78) is, figure 3.3 panel C.

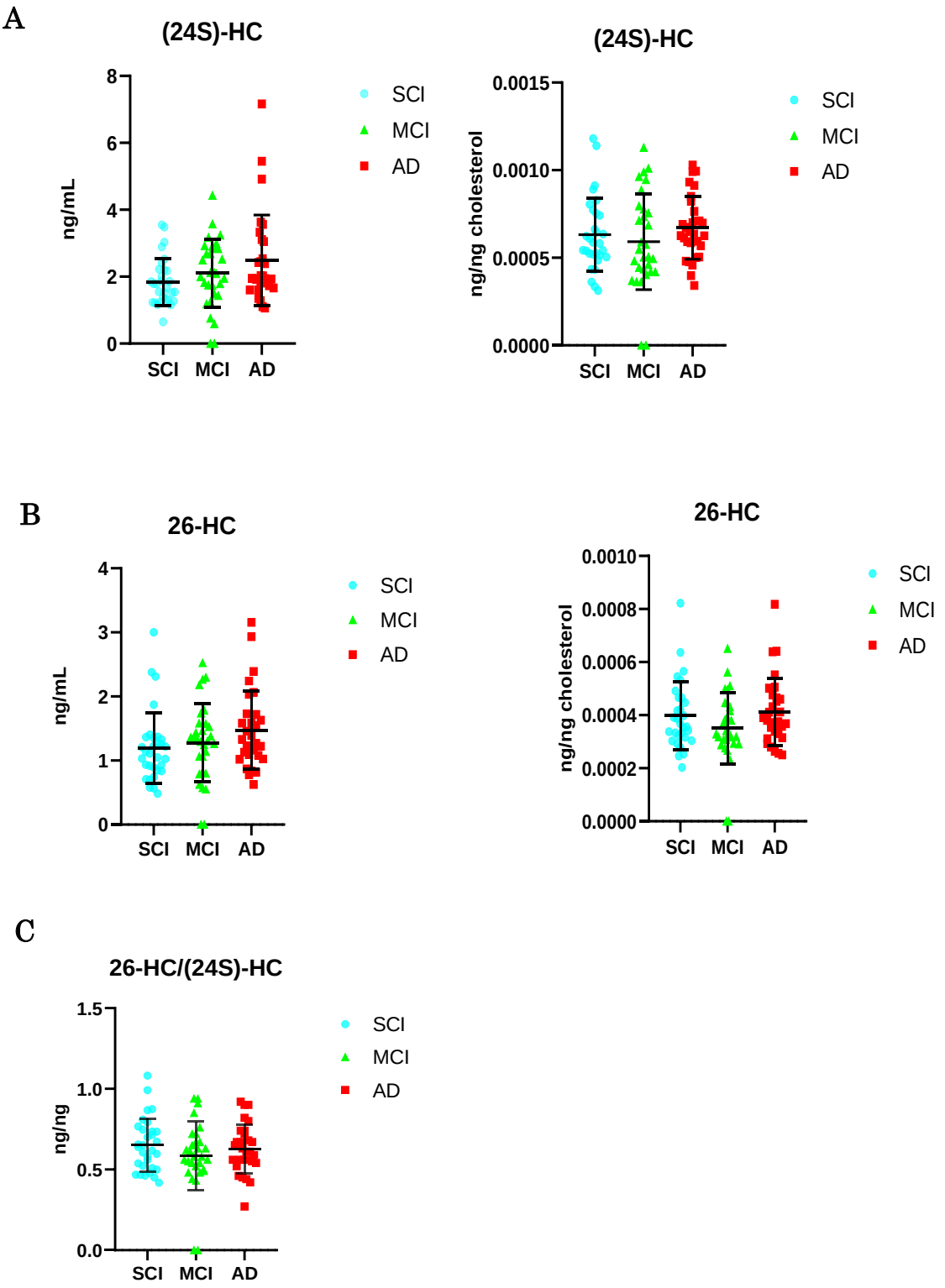

Figure 3.2 CSF levels of SCI. MCI and AD (24S)-HC and 26-HC.

(A). Absolute and cholesterol normalised (24S)-HC CSF levels result to be not different among the three pathological groups. **(B)** Absolute and cholesterol normalised 26-HC CSF levels result to be not

different among the three pathological groups. (C) 26-HC/(24S)-HC ratio does not differ between the pathological groups.

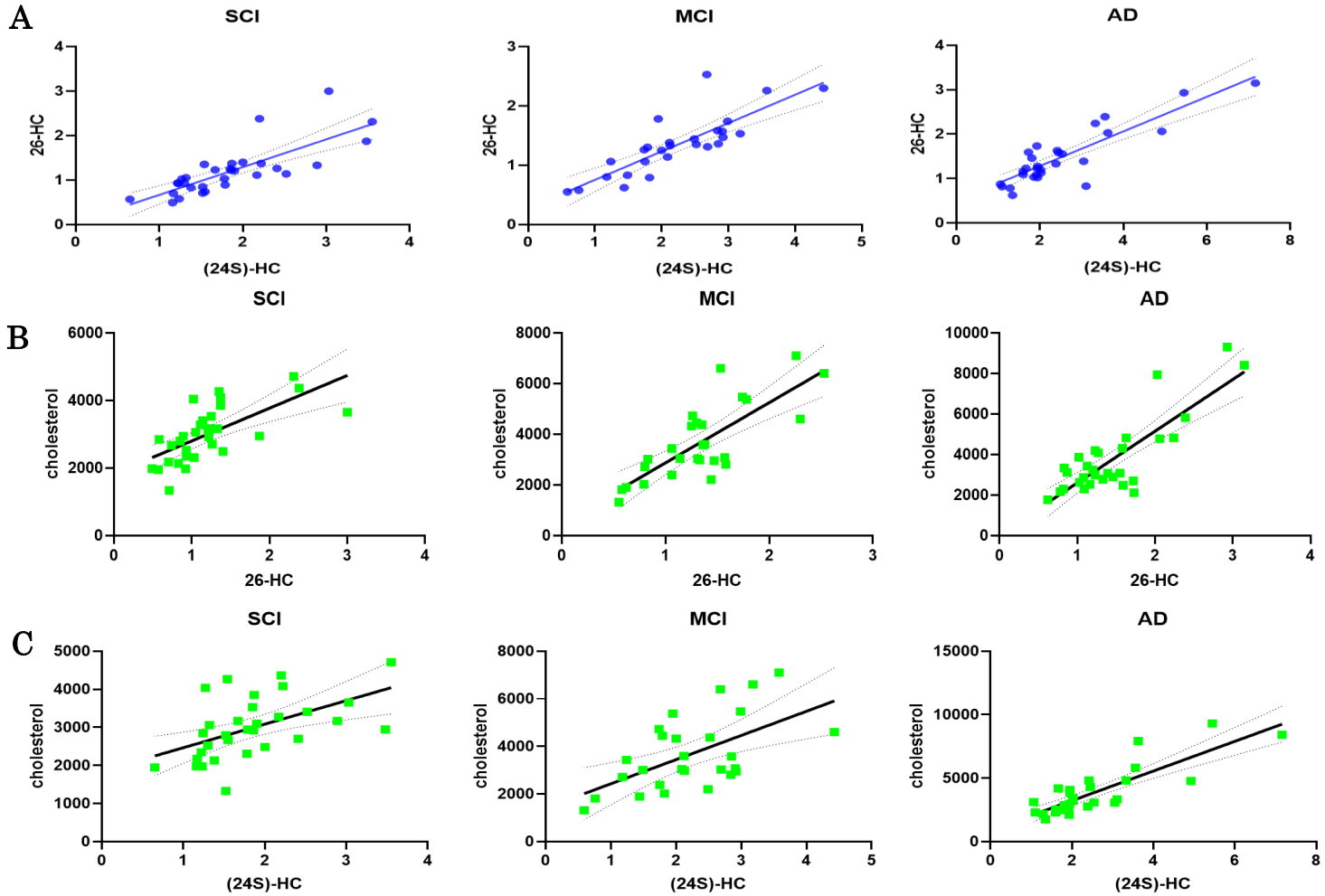

Figure 3.3 Correlation analysis on the CSF sterols (24S)-HC, 26-HC, and cholesterol.
(A) Correlation is verified between (24S)-HC and 26-HC in all the pathological groups. **(B).** Corelation between (24S)-HC and cholesterol is only verified in Alzheimer's patients. **(C).** 26-HC and cholesterol CSF levels correlates only in the SCI and MCI group.

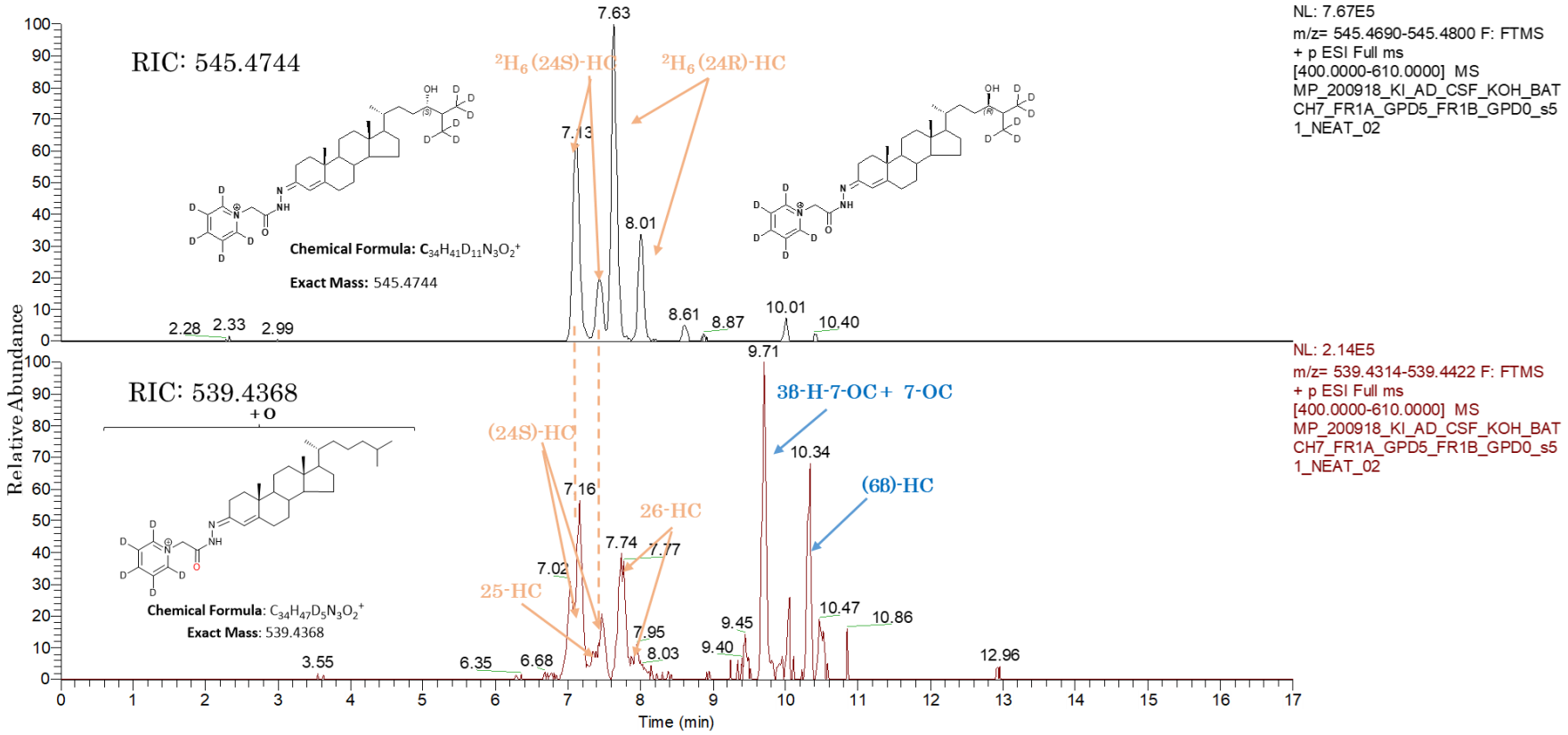

Figure 3.4 Chromatogram of GEDOC CSF showing the internal standard $^2H_6$(24R/S)-HC and the main CSF monohydroxy sterols.

The peaks showed in the upper panel of figure 3.4 represent the molecular ions with exact mass of 545.4744 *m/z*, result of $^2H_6$(24R/S)-HC derivatisation with the hydrazine GP D5. The peaks showed in the lower panel of figure 3.4 represent the molecular ions with exact mass of 539.4368 *m/z*, result of basic hydrolysis of the main monohydroxy sterols esters in human CSF after derivatisation with the hydrazine GP D5. RIC, reconstructed ion chromatogram.

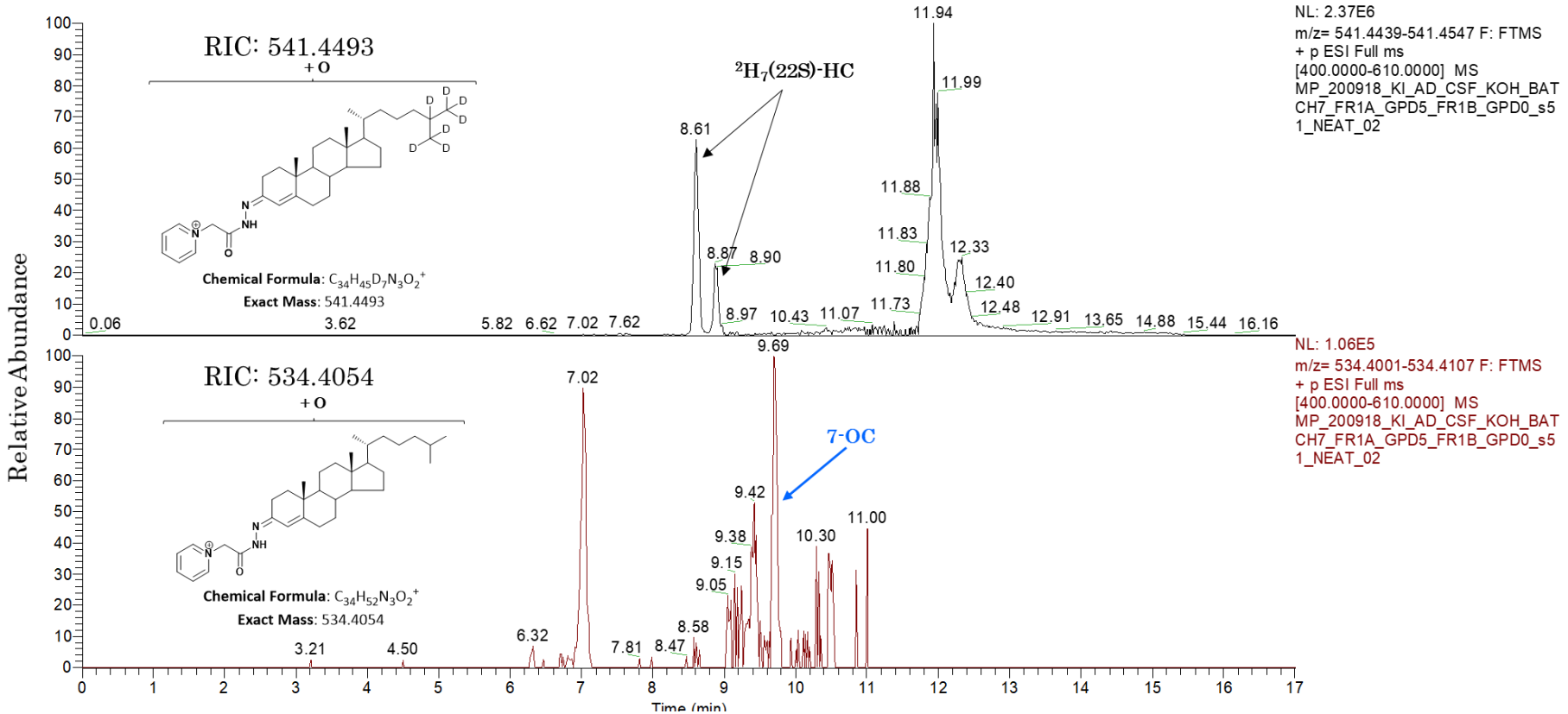

Figure 3.5 Chromatogram of GEDOC CSF showing the internal standard $^2H_7$(22S)-HC and the main CSF main.

The peaks showed in the upper panel of figure 3.5 represent the molecular ions with exact mass of 541.4493 *m/z*, result of $^2H_7$(22S)-HC derivatisation with the hydrazine GP D5. The peaks showed in the lower panel of figure 3.5 represent the molecular ions with exact mass of 534.4054 *m/z*, result of basic hydrolysis of the main monohydroxy sterols esters in human CSF after derivatisation with the hydrazine GP D5. RIC, reconstructed ion chromatogram.

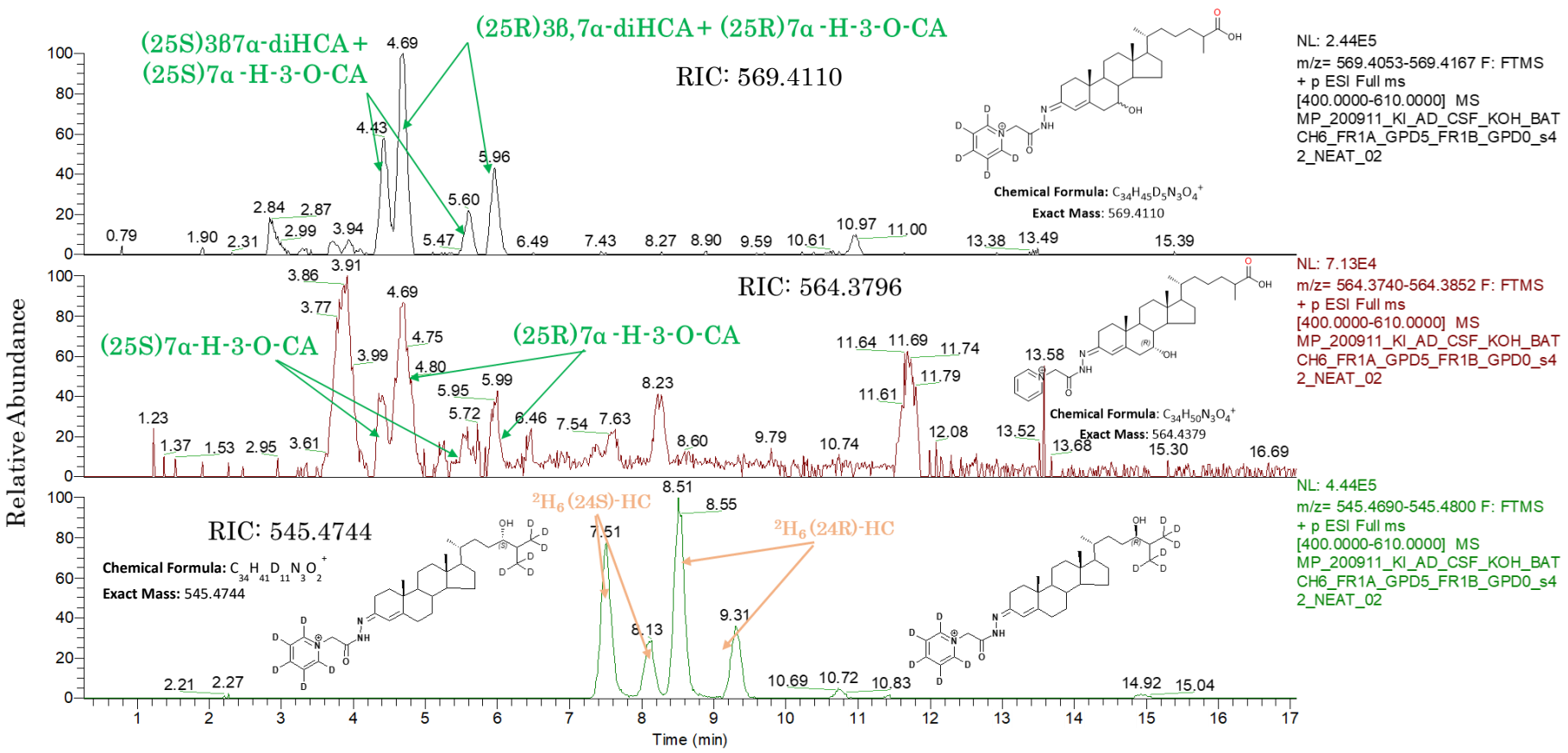

Figure 3.6 Chromatogram of GEDOC CSF showing the internal standard $^2H_6$(24R/S)-HC and the main plasma cholestenoic acids.

The peaks showed in the upper panel of figure 3.6 represent the molecular ions with exact mass of 569.4110 *m/z*, result of the basic hydrolysis of the 3ß,7α(25S)-diHCA and 3ß,7α(25R)-diHCA esters and subsequent derivatisation with the hydrazine GP D5. The peaks showed in the middle panel of figure 3.6 represent the molecular ions with exact

mass of 564.3796 *m/z*, result of the basic hydrolysis of (25S)7α-H-3O-CA and (25R)7α-H-3O-CA esters and subsequent derivatisation with the hydrazine GP D5. RIC, reconstructed ion chromatogram.

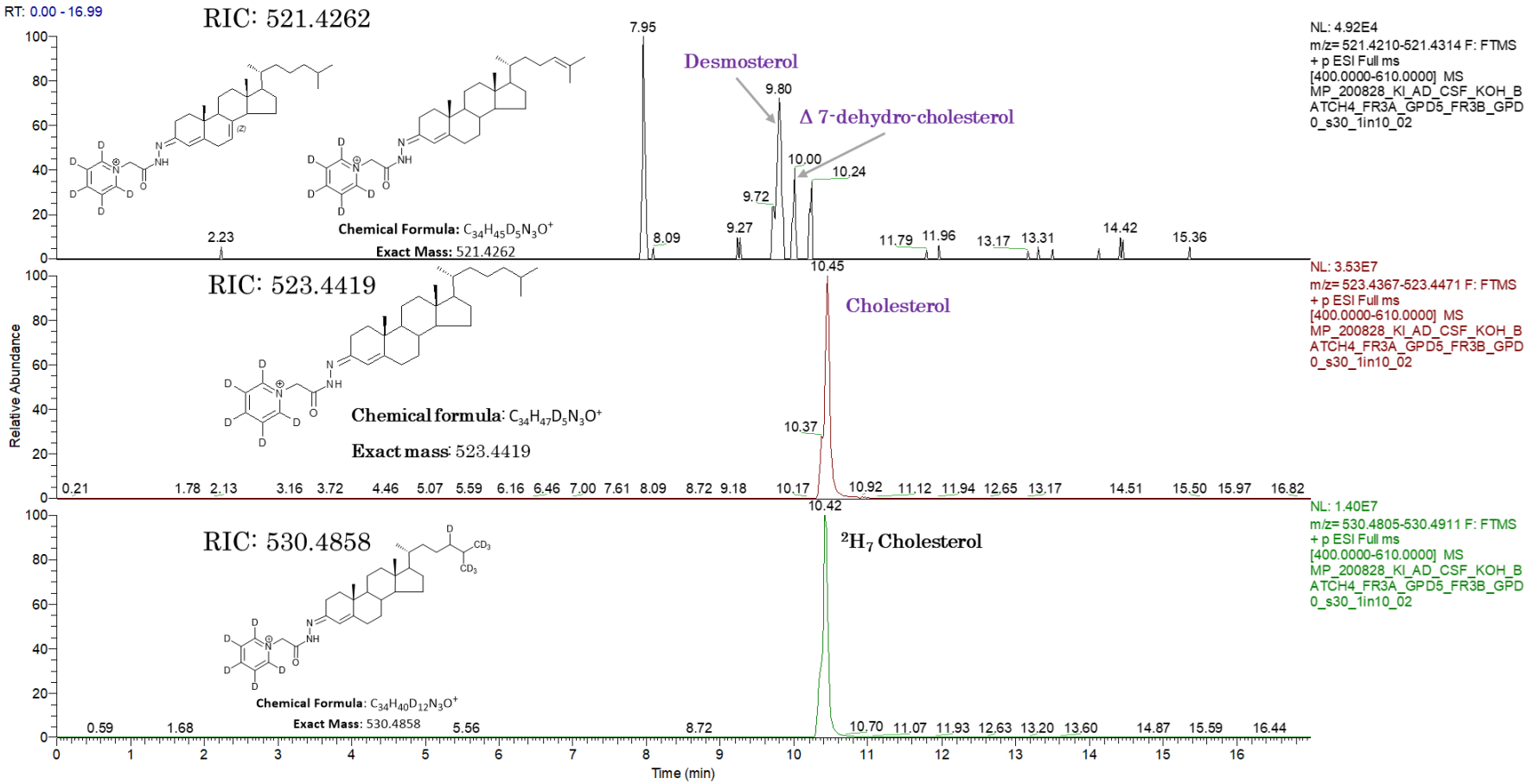

Figure 3.7 Chromatogram of CSF plasma showing endogenous cholesterol, its precursors Desmosterol, Δ7-dehydrocholesterol and $^{2}H_{7}$Cholesterol.

The peak showed in the upper panel of figure 3.7 represent the molecular ions with exact mass of 521.4262, result of basic hydrolysis of the cholesterol precursor Δ7-dehydrocholesterol and desmosterol esters and subsequent derivatisation with the hydrazine GP D5. The peak showed in the middle panel represent the molecular ions with exact mass of 523.4419 *m/z*, result of basic hydrolysis of cholesterol esters and subsequent derivatisation with the hydrazine GP D5. The peak showed in the lower panel represent the molecular ions with exact mass of 530.4858 *m/z*, result of the internal standard $^{2}H_{7}$Cholesterol derivatisation with the hydrazine GP D5. RIC, reconstructed ion chromatogram.

3.5 Discussion

In this work of thesis, the cholesterol metabolites and precursors have been investigated as potential discriminating biomarkers for Alzheimer's disease. CSF samples from a memory clinic cohort composed of patients with different degrees of cognitive impairment, subjective cognitive impairment, mild cognitive impairment and Alzheimer, SCI, MCI, and AD, have been screened for their total sterol content. To note, patients with chronic comorbidities like diabetes type 2, hypertension and hypercholesterolemia have been excluded to eliminate potential interferents with cholesterol homeostasis.

The designed protocol described in the section 3.3 has served for the human CSF characterisation of the total sterol content. 18 different sterols can be identified in the CSF from SCI, MCI, and AD patients, however only 7 sterols, mainly mono hydroxy sterols, have been confidently structure attributed and quantified. The current state of art in terms of sterolome characterisation of AD reports altered CSF levels of the monohydroxy sterols (24S)-HC and 26-HC. Generally, the two monohydroxy sterols have been found to be elevated in the CSF from AD or MCI patients respect to healthy controls (Bjorkhem *et al.*, 2006; H. L. Wang *et al.*, 2016). Therefore, the main research focus of this project aimed to picture the levels of total cholesterol mono oxygenated metabolites in the memory clinic cohort. Hence, the analytical methodology selected for this screening has priories the identification of monohydroxy sterols like (24S)-HC and 26-HC and of cholesterol and its precursors. Consequently, the selected internal standard mixture was mainly composed of deuterated identical or surrogates mono hydroxy sterols and cholesterol for quantification.

In this study no significant differences emerged between the pathological groups respect to absolute or cholesterol normalised total sterol values. Ratio between 26-HC and (24S)-HC CSF levels has also been included into the sterols analysis as its alteration has been associated with certain neurological conditions. As for the lipid's levels, no variation has been observed. Need to note that 26-HC/(24S)-HC alteration reported for the brain diseases has been linked to damaged blood brain barrier, BBB, rather than the illnesses themselves (Leoni *et al.*, 2003). Due to the lack of the Institutional Review Board approval and Material Transfer Agreement, no clinical data of SCI, MCI and AD patient brain status like MRI scans were available, thus no speculations on BBB integrity can be made. The absence of significant differences between SCI, MCI and AD groups is, therefore, partially in contrast with the elevation in 26-HC and (24S)-HC CSF levels elsewhere reported. The lack of significance may be explained as the sum of three main facts:

1. All the data sets reported in this work are from subjects at different stages of cognitive impairment. All the data available into the literature regarding abnormal CSF levels of 26-HC or (24S)-HC resulted from a comparison of a pathological group, for example AD or MCI, with neurologically healthy controls, but no data are reported when diseased groups are compared, like in this work. If the cholesterol disruption occurs in the very beginning of the disease, even before the development of the first symptoms, the biggest differences in sterol levels might be appreciated when a neurologically healthy subject is compared with a SCI, MCI, or AD patient. With the disease progression and the death of several neuronees, the enzymes involved in cholesterol metabolism and homeostasis should

decrease and a less pronounced effect on sterol level might be appreciated.

2. The data set is relatively small (90 samples in total, equally distributed among the pathological groups, n=30 CSF samples each). Probably, expanding the data sets would help in highlighting differences in the sterol levels, particularly for the ones which are very low abundant.

3. CSF oxysterols levels are lower respect to any other human body fluid and most of the lipids are mainly present in the form of esters. Moreover, free monohydroxy sterols in CSF are almost absent or under the limit of detection of sensitive instruments like Orbitrap mass spectrometer. Hence, a hydrolytic step becomes essential for the identification of the low abundant sterols, especially the mono hydroxy ones. As the research focus of this project was this class of molecules, a saponification step has been introduced. However, the presence, even if minimal, of free monohydroxy sterols cannot be excluded. Therefore, if the disruption of cholesterol metabolism is reflected by alteration of its direct metabolites' levels in their active form, which is the free one, the necessary hydrolytic step might have masked this difference. Ideally, a double extraction allowing the identification of both free and total sterols would compensate for the disadvantages of both extractions. However, the CSF availability for this project would have only allowed one of the two extractions. Thus, seen the aims of the work, hydrolysis has been carried over.

Although the CSF levels of (24S)-HC and 26-HC do not differ in this cohort, correlation studies highlight a positive relationship between the two sterols in all the groups (SCI (Spearman r=0.78), MCI (Spearman r=0.82) and AD (Spearman r=0.86)). While they have two different origins, cerebral for (24S)-HC and extra-cerebral/peripheric for 26-HC, both can diffuse through the BBB, establishing a net daily efflux and influx from and into the brain, respectively. Therefore, it is hypothesised that peripheral 26-HC might influence the brain cholesterol metabolism, which reflects into the (24S)-HC brain levels. Physiologically, 26-HC is produced in most of the human cells and is subsequently secreted into the circulation. In the blood stream it reaches the BBB and diffuse into the brain. In the brain it is converted into 3ß,7α-diHCA, a cholestenoic acid which is secreted into the blood passing by the BBB. 26-HC has many physiological roles, including the modulation of cholesterol homeostasis upon the induction of its metabolism to bile acids and by inhibiting SREBP-2 *de novo* cholesterol synthesis in an INSIG-mediated manner (Radhakrishnan *et al.*, 2007). However, the role of the sterol in different types of brain cells has not been clarified yet, not in healthy or pathological conditions like AD (Loera-Valencia *et al.*, 2019). Hence, contradictory findings on the role of 26-HC during AD have been reported (Bjorkhem *et al.*, 2006; Loera-Valencia *et al.*, 2019; Testa *et al.*, 2016c). However, it might represent the connecting element between peripheral cholesterol and brain cholesterol. Hypercholesterolemia has been identified as one of the main risk factors for AD development and increased plasma cholesterol levels results in extensive metabolism of the sterol lipid into 26-HC. Elevated plasma 26-HC can be the driving force to push the diffusion of the monohydroxy sterol into the brain across the BBB. Non-physiological, elevated, 26-HC brain levels might display a toxic

effect on brain cells. Several studies have shown the ability of 26-HC to stimulate an inflammatory response and promote radical oxygen species production in a concentration dependent manner. Moreover, excess of 26-HC is rapidly converted into 3ß,7α-diHCA. The positive corelation between the two-sterol highlighted in this work supports the idea of a 26-HC and (24S)-HC interplay in the brain cholesterol homeostasis management. In conclusion, this work has not spot out any differences on terms of mono oxygenated CSF sterol levels between three different stages of dementia, however the findings suggest an influence of the extracerebral sterol 26-HC onto brain cholesterol metabolism.

Chapter 4 - Sterolomic profile of human plasma and CSF in Parkinson's disease

4.1 Introduction

Parkinson's disease, PD, is a neurodegenerative disorder characterised by a progressive loss of dopaminergic neuronees in a brain region called Substantia Nigra Pars Compacta. This loss results in striatal dopamine deficiency (Poewe *et al.*, 2017a), which causes classical symptoms associated with PD like bradykinesia, tremor, and rigidity. These symptoms typically worsen with disease progression. In addition to motor symptoms, PD is also characterised by non-motor symptoms such as hyposmia, urinary retention, sleep and behaviour disorders, and cognitive impairment which severely impact patient quality of life. PD affects more than 10 million people worldwide aged over 65 years old and is the second most widespread neurodegenerative disease, second only to AD. Currently, only symptomatic treatments are available for PD, and no curative and/or preventive drugs exist. PD is identified based on neurological and mobility evaluation of the patient, MRI brain scans, and the restoration of the motor symptoms upon L-dopa treatment (Poewe *et al.*, 2017a). The lack of curative medical treatments as well as of a specific diagnosis makes PD a substantial public health problem.

However, the pathological manifestation of PD, which includes dopaminergic neuroneal loss and cytoplasmatic accumulation of misfolded α-syn protein, have been associated with mitochondrial dysfunction (Ekstrand *et al.*, 2007; Schapira, 2007), oxidative stress

(Blesa *et al.*, 2015; V. Dias *et al.*, 2013), neuroinflammation (Q. Wang *et al.*, 2015) and engulfment of protein elimination system (Burbulla *et al.*, 2017; Dehay *et al.*, 2012; Winslow *et al.*, 2010), in particular of misfolded α-syn. Although these pathological pathways provide some understanding of PD's aetiology, they still cannot fully explain the onset of the neurodegeneration process. A combination of factors triggering the cascade of PD hallmarks, rather than one mechanism alone, seems to be the most plausible explanation to determine the disease's onset. Unfortunately, research is still far from uncovering the multifactorial cause of PD, or neurodegeneration in general.

However, over the last few decades, several lines of evidence have suggested a connection between altered brain cholesterol metabolism and the development of PD (Doria *et al.*, 2016; Jin *et al.*, 2019b, 2019a). Since cholesterol is the second most abundant lipid in the human brain, accounting 30% of the total brain lipid composition and more than 20% of total body cholesterol (Hyuk Yoon *et al.*, 2022), alterations of its homeostasis would likely to be pathologically implicated in the disturbances of neuroneal cells viability and functionality. A decrease in cholesterol synthesis has been reported in fibroblast from PD patients (Musanti *et al.*, 1993). In agreement with these findings, some observational and case-control studies report reduced total cholesterol serum levels in PD patients (Guo *et al.*, 2015; Ikeda *et al.*, 2011; Rozani *et al.*, 2018). Moreover, higher LDL-cholesterol levels have been associated with better motor performances in progressive PD patients, compared to normal level low density lipoprotein LDL PD ones (Sterling *et al.*, 2016a). However, contrasting findings have shown either no association with PD (Sterling *et al.*, 2016b; Q. Wei *et al.*, 2013) or higher total serum and HDL cholesterol levels in baseline PD patients, compared to

healthy controls (Bakeberg *et al.*, 2021; G. Hu *et al.*, 2008). Furthermore, increased consumption of cholesterol, and consequent enhanced LDL levels, seems to be associated with higher risk of developing PD (Miyake *et al.*, 2010). Although several clinical and non-clinical studies provide a complex interpretation about the relationship between blood cholesterol, lipoprotein-associated cholesterol and PD, the peripheral level of this lipid might not fully reflect its brain alterations over PD. Indeed, cholesterol cannot pass the blood brain barrier and brain needs are covered upon astrocytes synthesis and release in the extracellular space and its recycling (Gliozzi *et al.*, 2021; Lütjohann *et al.*, 1996a). To better understand brain cholesterol alterations during PD, animal and cell models have been used. From the disease models, a general agreement has merged regarding the toxic effect of higher brain cholesterol levels on brain cells, aggravating the PD phenotype (Ayciriex *et al.*, 2017; García-Sanz *et al.*, 2021). High brain cholesterol levels worsen motor functions, and the dopaminergic neuronees decline in 1-methyl-4-phenyl-1,2,3,6-tetrahydropyridine (MPTP) treated mice (R. Paul *et al.*, 2017a). Moreover, genetic mutation associated with an elevated risk of developing familial PD are involved in the alteration brain cholesterol metabolism regulation (Cha *et al.*, 2015b). Mutation on the Parkin gene is the most common form of early onset PD and has been linked to higher total cellular cholesterol content. Parkin acts a lipid-responsive regulator of fat uptake, so function altering mutations may result in cholesterol overload in neuroneal cells, leading to neurotoxicity (K.-Y. Kim *et al.*, 2011b). Moreover, the second genetic cause predisposing for familial and sporadic PD is the mutation affecting the glucocerebrosidase (GBA) gene (Fernandes *et al.*, 2016; Sidransky *et al.*, 2009). GBA mutation cause lysosomal malfunctioning and engulfment of the protein elimination system,

aggravating the proteinopathy associated with the neurodegenerative disease. Interestingly, GBA knock-out SH-SY5Y cells, a model of dopaminergic neuronees, and mouse embryonic fibroblast (MEF) exhibit disruption of lysosome generation, probably due to an alteration in the cellular cholesterol and lipid content (Magalhaes *et al.*, 2016). The GBA gene encodes for a protein called ß-glucocerebrosidase or GCase, which is a lysosomal hydrolase. One of the possible explanations for the mutated GBA-dependent autophagic protein degradation system's engulfment may be the reduced activity and expression of the Gcase. Defective Gcase leads to autophagy lysosomal reformation dysfunction, triggering oxidative stress and alteration of the cholesterol homeostasis, resulting in cytotoxic effects for the cells. Additionally, accumulation of cholesterol in the lysosome is observed in the N370S GBA mutated cells, one of the principal mutations associated with higher risk of developing PD (García-Sanz *et al.*, 2017).

Cholesterol has also been found to be a ligand of the α-syn protein, facilitating its interactions with membranes. In pathological conditions, cholesterol enrichment may lead to enhanced formation of α-syn oligomers upon stimulation of α-syn aggregation (R. Paul *et al.*, 2017b; van Maarschalkerweerd *et al.*, 2015). Moreover, α -syn-APOE binding may alter brain cholesterol trafficking (Emamzadeh *et al.*, 2016b).

The implications of an altered brain cholesterol homeostasis Are, therefore, generally detrimental for neuroneal cells survival, resulting in cell malfunctioning or death (Dietschy & Turley, 2004b). Many neurodegenerative diseases have been associated with disrupted brain cholesterol metabolism (F. Arenas *et al.*, 2017; Dai *et al.*, 2021; Mariani *et al.*, 2005; Mouzat *et al.*, 2016; Pfrieger, 2021;

Valenza, Carroll, *et al.*, 2007; Valenza, Leoni, *et al.*, 2007). However, it is still uncertain whether this event is a consequence or a cause of the disorder. Nonetheless, studies on cholesterol metabolites, such as oxysterols and cholestenoic acids, might help to shed a light on cholesterol contribution on PD. As bioactive molecules, alterations of their levels, especially in a cell specific or cell-compartment way, would result in cellular pathway misfunctioning (Bjoandŕkhem *et al.*, 2006; Leoni & Caccia, 2011; Mutemberezi *et al.*, 2016b; Schroepfer, 2000b; Vesa M. Olkkonen; Olivier Béaslas; Eija Nissilä, 2012; Zmysłowski & Szterk, 2019). Changes in brain sterols levels are strongly corelated to variations in brain cholesterol levels, being its metabolites or precursors. The primary mechanism involved in regulating brain cholesterol homeostasis is its oxidation to (24S)-HC, which is the most abundant oxysterol in human brain. The efflux of (24S)-HC across the BBB eliminates approximately 6-8 mg of cholesterol per day, which is converted and exported as (24S)-HC (Lütjohann *et al.*, 1996b). After being secreted into the circulation, (24S)-HC travels to the liver, where it is catabolised for elimination. (24S)-HC is primarily produced by CYP46A1 oxidation of the C24 position of cholesterol sidechain in neuronees, in human body. Therefore, nearly 80% of this oxysterol plasma levels have a brain origin, making it an ideal candidate to monitor brain cholesterol levels, especially over pathological conditions like PD.

4.2 Aims

Altered brain cholesterol metabolism compromises neuroneal cells wellness and survival and has been linked with PD development.

Nonetheless, it is still not clear if disrupted cholesterol brain homeostasis represents a cause or consequence of dopaminergic neuronees loss. Therefore, a sterolome characterisation of PD patients' plasma and CSF might help to shed a light on the contribution of cholesterol and its metabolites to the development of PD.

During this work of thesis, plasma samples from base line PD patients and age/sex matched neurologically healthy donors have been characterised from a sterols point of view. The first objective of this investigation is to assess the sterol profile of baseline PD patients form a qualitative and quantitative perspective. The second aim is to highlight any statistical and biological valuable variation between the disease and control group. I non-diseased counterpart would serve also to assess physiological sterols biological variation in aged population. Longitudinal CSF and plasma from PD patients have also been analysed to evaluate sterols variation over the disease progression. The third aim of this chapter is, therefore, to determine whether the sterols levels fluctuations, if any, corelates with PD advancement/severity. The work described in this chapter seeks to identify new, reliable, and easy-to-detect biomarkers for PD while providing a reproducible and clinically translatable protocol for sterolome determination in human body fluids. An ongoing validation study on sterolome profile of plasma form North America PD patients is in progress to assess the nature of the findings of the first work on European baseline PD patient described in this thesis, however only preliminary data are reported.

4.3 Material and methods

4.3.1 PD cohorts

Plasma from 2 different cohort of PD patients has been analysed, one from base line PD patients and the other from longitudinal PD ones. Plasma from age/sex matched healthy individuals (comorbidities are specified where applicable) have also been provided for the comparison with the baseline patients. CSF from longitudinal PD patients has also been analysed.

4.3.1.2 NYPUM Parkinson disease baseline plasma

100 human plasma samples from base line PD patients and 100 from age matched non-neurodegenerative individuals, were provided by Umea University hospital, belonging to the NYPUM BIOBANK. Michael J Fox Foundation is acknowledged for supporting the Griffiths-Wang lab during the determination of PD plasma sterolome. All the plasma was collected form 2004 within the Umea catchment area, Sweden, Europe. All participants provided informed consent and the studies were performed with institutional review board approval and adhered to the principles of the Declaration of Helsinki(Linder *et al.*, 2010). Specific comorbidities of the neurologically healthy donors are reported in table 7.20 in supplementary section. The usage of medical treatments with a

direct or indirect effect on the cholesterol synthesis and/or metabolism was not an exclusion criterion for patient and control selection. However, no data has been made available regarding patients or control group drug therapies in place. PD patients' and controls' demographics are depicted in the table 4.1. The total 200 plasma samples have been analysed in batches composed of 8 samples each, one internal quality control (QC) plasma and one water blank. The extraction and sterolome profile for the entire 200 plasma samples data set has taken a total of 25 batches to complete. The QC plasma is obtained from a healthy 61-year-old female under informed consent, collected at Swansea University Clinical Research Facility (CRF).

Table 4.1 Age and sex details of the PD patients and control individuals at sampling.

	Control	PD
Total number of samples	100	100
Age (mean ± SD)	67. 58 ± 4.54	70.39 ± 9.11
Number of female samples	50	42
Female Age (mean ± SD)	66.92 ± 4.32	70.26 ± 9.07
Number of male samples	50	58
Male Age (mean ± SD)	68.28 ± 4.66	70.48 ± 9.13

4.3.1.3 ICICLE Parkinson disease longitudinal plasma

36 human plasmas from progressive PD patients were provided by Marta Caramacho PhD, Department of Clinical Neurosciences, Cambridge centre for brain repair as part of the Incidence of Cognitive Impairment in Cohorts with Longitudinal Evaluation-PD study (ICICLE PD,

https://portal.dementiasplatform.uk/CohortDirectory/Item?fingerPrintID=ICICLE-PD. All the plasma was collected from 2009 within the Newcastle and Cambridgeshire catchment area. All participants provided informed consent during their first visit and the study was performed with institutional review board approval and adhered to the principles of the Declaration of Helsinki. The sample set is made of 16 different patients, all affected by PD, divided in 12 males and 4 females. Blood, and consequently plasma, has been collected over 5 different time points, called visits see table 4.2 for details. All the patients completed visit 1, 12 completed visit 2, 3 presented at visit 3 as well as for visit 4 while 2 patients entered visit 5. For details, refers to table 4.3.

Table 4.2 ICICLE longitudinal PD plasma months of blood collection.

	Visit 1	Visit 2	Visit 3	Visit 4	Visit 5
Months	0 (baseline)	36	54	72	90

Table 4.3 ICICLE longitudinal cohort plasma collection points and patients gender specification.

ICICLE	Sex	Visit 1	Visit 2	Visit 3	Visit 4	Visit 5
IC007	Female	X	X			
IC008	Male	X	X			
IC015	Male	X			X	
IC017	Male	X	X			
IC018	Male	X	X			
IC023	Male	X	X			
IC024	Male	X	X			
IC026	Female	X	X			
IC027	Female	X	X		X	
IC031	Male	X	X		X	
IC036	Male	X	X			
IC037	Male	X		X		
IC038	Male	X		X		X
IC041	Female	X	X			
IC042	Male	X		X		X
IC049	Male	X	X			

4.3.1.5 NYPUM Longitudinal PD CSF

143 human CSF samples from progressive PD patients were provided by Umea University hospital, belonging to the NYPUM BIOBANK. Michael J Fox Foundation is acknowledged for supporting the Griffiths-Wang lab during the determination of PD longitudinal CSF. All the CSF was collected form 2004 within the Umea catchment area. All participants provided informed consent during their first visit and the studies were performed with institutional review board approval and adhered to the principles of the Declaration of Helsinki. The data set is made of from 80 different PD patients, sampled at 4 different time points (months 12, 36, 60 and 96). The tables 4.4 and 4.5 below resume demographics and CSF availability for the 80 PD patients.

Table 4.4 NYPUM longitudinal PD CSF patients' demographics, at baseline.

Total number patients	80
Age (mean ± SD)	70.85 ± 7.38
Number of female samples	23
Female Age at baseline (mean ± SD)	72.22 ± 5.06
Number of male samples	57
Male Age at baseline (mean ± SD)	70.29 ± 8.07

Table 4.5NYPUM longitudinal cohort collection points and gender specifications.

Patient ID	Sex	12 months	36 months	60 months	96 months
19	f	x	x	x	x
20	m	x	x	x	x
21	m	x	x		
23	f	x	x	x	x
33	m	x	x	x	
34	m	x	x	x	x
37	m	x	x	x	
57	m	x			
58	m	x			
61	f	x			
62	f	x	x	x	
64	f	x			
65	m	x			
74	m	x	x		
75	m	x	x		
76	f	x			
78	m	x	x	x	
82	m	x			
88	f	x	x		
89	m	x	x		
96	m		x	x	
101	f		x		
106	m		x		
141	f	x	x	x	
146	m	x			
150	m	x	x	x	
154	m		x		
157	m	x	x	x	
175	m			x	
177	f		x	x	
180	m		x	x	
187	f	x	x	x	
188	m	x			
195	m	x	x	x	
198	m	x	x	x	
201	m	x			
208	m	x			
218	f	x			
233	f		x		

239	m	x	x	x	
240	m	x			
245	m	x	x		
257	f	x			
278	f	x			
284	f	x	x	x	
290	m	x			
291	m	x			
301	m	x		x	
302	m	x			
309	m	x	x	x	
311	m	x	x	x	
315	m	x	x	x	
323	f	x			
324	m	x	x	x	
328	f	x	x		
335	m	x	x		
336	m	x	x	x	
344	m	x			
355	m	x			
356	f	x			
358	m	x			
367	m	x	x		
371	m		x	x	
375	m	x			
383	m	x			
389	m	x			
402	m	x			
405	f		x		
406	m	x			
408	f	x			
414	m	x	x		
416	f	x			
426	m	x			
446	m	x			
454	m	x			
464	m	x			
467	m		x		
473	m	x	x		
492	m	x	x		
493	m	x			

4.3.1.4 BioFIND Parkinson disease base line plasma

240 samples from base line PD patients and age/sex matched control individuals were provided as part of the Fox Investigation for New Discovery of Biomarkers (BioFIND) observational clinical study, (https://www.michaeljfox.org/news/biofind). All the plasma was collected from 2012 to 2015 within the United States of America enrolment area. The BioFIND PD observational study was sponsored by Michael J. Fox Foundation for Parkinson's Research (MJFF) and supported from the National Institute of Neurological Disorders and Stroke. All participants provided written informed consent and the study, BioFIND, has been conducted in accordance with Good Clinical Practice (GCP), International Conference on Harmonization (ICH), and the Food and Drug Administration (FDA), and any applicable national and local regulations including FDA regulations under 21 CFR Parts 11, 50, 54, 56, 312 and 314.

4.3.2 Plasma sample preparation and sterols extraction

All the human plasma reported in this work of thesis has been processed in the same manner for the extraction of the free, non-esterified, sterols, see section 2.3. Briefly, 100 µL of human PD, healthy control and QC plasma are extracted in 1.05 mL of an ethanol solution containing the designated iSTDs mixture to be then diluted to 70*% (v/v)* EtOH. For each PD plasma sample set, a specific iSTDs master mix has been used. Details of deuterated standard mixes are reported in chapter 2.1.2. The ethanolic extracts are centrifuged and sterols separated on polarity based through a SPE chromatography, obtaining polar (Fr1s) and un-polar (Fr3s) sterols extract which are divided into two equal fractions, A and B, and then dried under vacuum (section 2.5). Fr1's As and Fr3's As are firstly reconstituted in a phosphate buffer solution containing 10*% (v/v)* iPrOH to be then then oxidised through EADSA methodology. Oxidated fractions are consequently charge tagged with the hydrazine Girard P D5 completing the EADSA methodology (section 2.6). Reconstituted FrBs, both Fr1s and 3, are treated as FrAs apart from enzymatic oxidation and derivatised with the hydrazine Girard P D0. Girard P excess is removed through a second SPE and pure methanolic extracts are therefore obtained (section 2.8). The methanolic extracts containing the polar sterols, FR1s A and B, are diluted to 60*% (v/v)* methanol prior LC-ESI-MS^3 analysis. 35 µL of the 60*% (v/v)* MeOH Fr1s are injected into an Ultimate 3000 UHPLC coupled with the Orbitrap Trihybrid I-DX® mass spectrometer. The cholesterol containing fractions, Fr3s A and B, are firstly dilute 1 in 1000 in 60*% (v/v)* MeOH prior to inject 35 µL of this solution into the HPLC-MS system cited above. An LC-ESI-MS^3 analysis has been employed for the qualitative-quantitative sterol profile.

4.3.3 CSF sample preparation and sterols extraction

The NYPUM longitudinal PD CSF has been characterised for its free sterol content, details of the extraction procedure in the section 2.4.1. Even though most of the human CSF sterols are present in their esterified form, Griffiths-Wang lab previous findings have highlighted an alteration of the free dihydroxy cholestenonic acids in neurodegenerative diseases like Spastic paraplegia type 5 and Cerebro tendinous xanthomatosis(Abdel-Khalik *et al.*, 2018). These alterations were so significant to be considered diagnostic biomarkers. Moreover, free sterols screening of baseline PD CSF form the same group has shown an alternation of the monohydroxy cholestenoic acids 3ß,7α-diHCA and 7α-H-3O-CA levels respect to the healthy controls (data not published yet). Thus, the focus of this work is on the unesterified and active form of the CSF sterols, with a particular emphasis on the cholestenoic acid content.

The protocol for sterol extraction resembles the one for PD plasma. Briefly, 100 µL of CSF are extracted in 1.05 mL ethanolic solution containing the designated iSTDs mixture, to be then diluted to 70*% (v/v)* EtOH. The ethanolic extracts are centrifuged and sterols separated on polarity based through a SPE chromatography to obtain polar (FR1s) and un-polar (Fr3s) (section 2.5). Polar (Fr1s) and un-polar (Fr3s) fractions are both divided into two fractions, A and B, and only FrAs treated with cholesterol. After enzymatic oxidation, FrAs and Bs are charge tagged with the hydrazine Girard P D5 and D0, respectively (section 2.6). Girard P excess is removed through a second SPE and pure methanolic extracts are therefore obtained (section 2.8). The pure methanolic sterols extracts are then diluted to 60*% (v/v)* MeOH prior analysis. For the sterol analysis, 70 µL of the polar sterol fractions, Fr1s, are injected at 60*% (v/v)* MeOH into an Ultimate 3000 UHPLC coupled with the Orbitrap Trihybrid I-DX® mass spectrometer. The

hydrophobic fraction, Fr3s, are first diluted 1 in 100 in 60% *(v/v)* MeOH to overcome instrument overload. 35 µL of the 1 in 100, 60% *(v/v)* MeOH Fr3 extract are then injected into the system. An LC-ESI-MS^3 analysis is employed for qualitative/quantitative profile of CSF free sterols content.

4.3.4 Sterols analysis

The strategy adopted for the sterol profile of the PD human biofluids implies a combined gradient elution chromatography and tandem Mass Spectrometry, including precursor ion and neutral loss scans. A detailed description of the technique and methods applied to the LC-ESI-MS^3 methods can be found in the section 2.8. Sterols quantification has been performed upon peaks identification and integration utilising the Thermo Fisher™ software Trace Finder™, see section 2.9 for details. Briefly, after peaks identification, conduct upon accurate mass and retention time match, accompanied with manual comparison of the MS^3 fragmentation pattern with the internal spectra library, the sterols are quantified against same structure or surrogate deuterated standard. Details of deuterated standard used for quantification purposes are reported in tables 7.15, 7.16, 7.17 and 7.19 of the appendices for NYPUM PD baseline plasma, ICICLE longitudinal PD plasma, BioFIND PD baseline plasma, and NYPUM longitudinal CSF, respectively. Relative quantification has been performed against the designated internal standard.

4.4 Results

4.4.1 Sterolome profile of base line PD patients: the discovery phase

Human plasma samples from base line PD patients (n=100) and age matched non-neurodegenerative individuals (n=100), NYPUM cohort, have been screened for the free/non-esterified polar sterols, cholesterol, and relative precursors content. Following the 3 days protocol described in sections 4.3.2 to 4.3.4, 21 different sterols have been identified in human plasma, ranging in concentration from 0.07 to 1,220,000 ng/mL, see table 4.6. The sterol lipids include 8 mono-hydroxy sterols of which six mono-hydroxycholesterols (24S)-HC, 25-HC, 26-HC, 7β-HC, 7α-HC & 6β-HC and two mono-hydroxy cholestenones, 7-OC and 7α-HCO, 4 di-hydroxy sterols of which two di-hydroxycholesterols (7a,25-diHC & 7α,26-diHC) and two di-hydroxy cholestenones, 7α,25-diHCO & 7α,26-diHCO, 7 cholestenoic acids, of which three mono-hydroxy cholestenoic acids (3β,7α-diHCA, (25S)3β,7α-diHCA & (25R)3β,7α-diHCA), three mono-hydroxy cholestenonic acids (7α-H-3O-CA, (25S)7α-H-3O-CA & (25R)7α-H-3O-CA), and cholestenoic acid (CA), the cholesterol precursors desmosterol, and cholesterol, see figures 4.1 to 4.9. Good chromatographic separation is obtained when the 17-, for cholesterol and precursors, and 37-, for cholesterol metabolites, minutes gradient elution modes are employed, resulting in base line peak separation for most of the Girard P-derivatised plasma sterols, see chromatograms below. To note the separation of the epimers (24S)- and (24R)-HC belonging to the internal standard $^{2}H_{6}$(24R/S)-HC (figure 4.1), which is usually hard to obtain without a high selective chromatographic system. Moreover, base-line peak separation is also seen for the two epimers of the cholestenoic acid

(7α)-HCA, the (25S) and the (25R), figure 4.6. Structure attribution of the chromatogram peaks with mass to charge ratio of 521, 523, 534, 539, 553, 548, 550, 555, 564 and 569, corresponding to cholesterol precursors, cholesterol, monohydroxy sterols, cholestenoic acid, di hydroxy sterols and mono hydroxy cholestenoic acids, is done through retention time match with sterols internal library and direct comparison of the fragmentation pattern obtained through precursor and neutral loss ion scans in MS^3 experiments, refer to the tables 7.1 to 7.13 in the appendix for details. Relative quantification is performed against the designated deuterated internal standard, refer to table 7.15 in the appendix for details. Details of internal standard mix used can be found in section 2.1.2.1. Note that all the sterols present in human plasma as both 3ß-OH and 3-oxo are generally more abundant in the latter form.

Our methodology enables the identification of the sterols naturally possessing the 3-keto group by direct detection and quantification of fractions B and indirectly of the 3-hydroxyl forms by subtracting fraction B from fractions A, where both 3-oxo and 3-hydroxy structures are present. However, this difference cannot be applied when sterols in fractions A and B are quantified or corrected against different standards. In this project, dihydroxy-cholesterols 7α,25-diHC & 7α,26-diHC cannot be calculated for absence of identical standard in fraction B, which would have been $^2H_6$ 7α,25-diHCO, which is also not commercially available. In fact, the fraction A, containing 7α,25-diHC & 7α,26-diHC plus their relative 3-one forms, 7α,25-diHCO & 7α,26-diHCO, have been quantified against the identical and surrogate internal standard $^2H_6$ 7α,25-diHC. On the other side, the cholestenone forms in fraction B, 7α,25-diHCO & 7α,26-diHCO, have been calculated against the most similar standard available, in terms of chemical similarity, retention time and polarity, that is $^2H_6$ (7α,25)-diHC, and corrected for the faction A/B response factor of the cholestenoic acids

standards $^{2}H_3$ (7α)-HCA. $^{2}H_3$ (7α)-HCA has been chosen among the 3-one standards as correction factor for the best match in terms of chemical similarity and supposed behaviour in the orbitrap mass spectrometer. Therefore, no values are reported for the di-hydroxy cholesterols 7α,25-diHC & 7α,26-diHC.

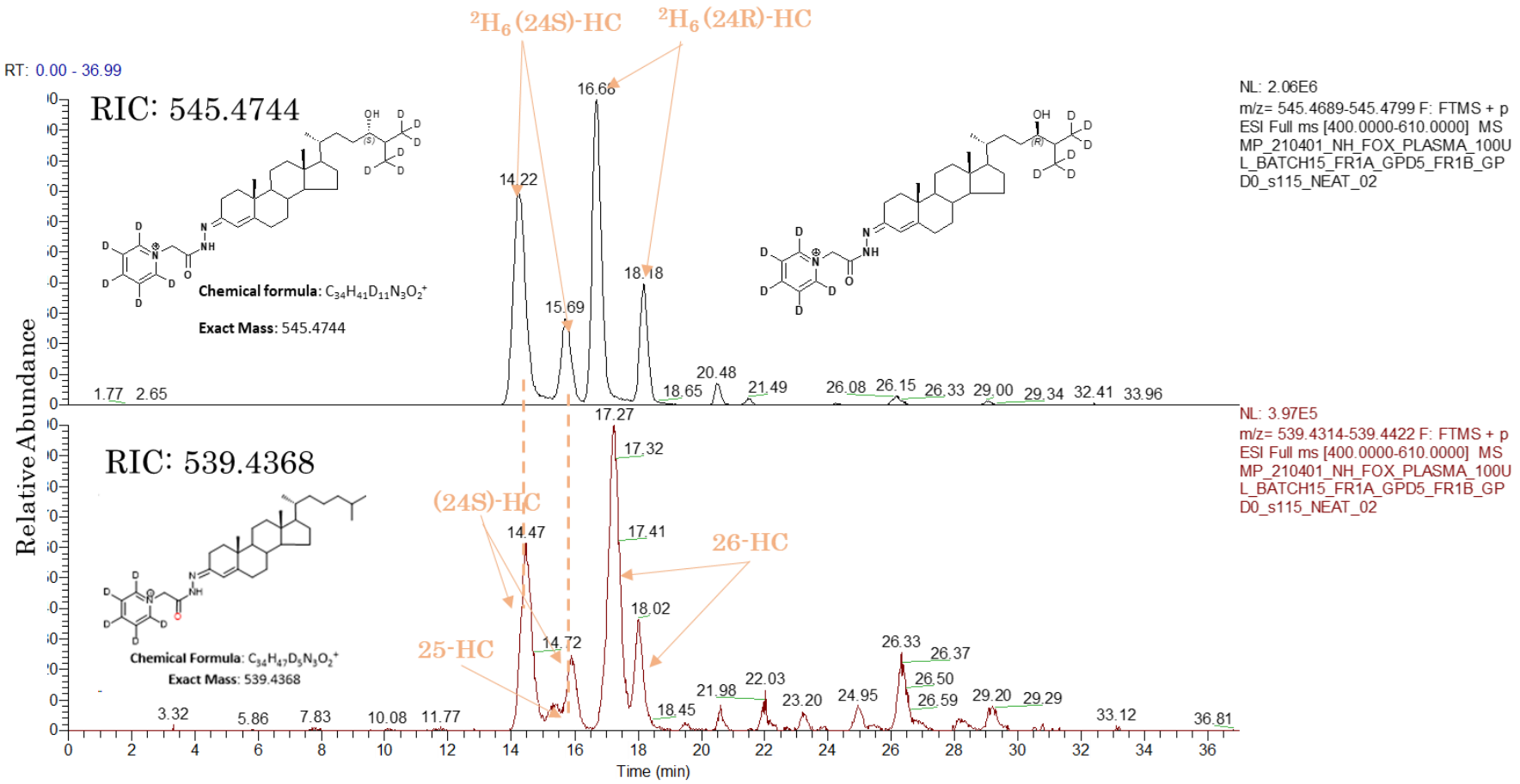

Figure 4.1 Chromatogram of NYPUM plasma showing the internal standard $^2H_6$(24R/S)-HC and the main plasma sterols.

The peaks showed in the upper panel of figure 4.1 represent the molecular ions with exact mass of 545.4744 *m/z*, result of $^2H_6$(24R/S)-HC derivatisation with the hydrazine GP D5.The peaks showed in the lower panel of figure 4.1

represent the molecular ions with exact mass of 539.4368 *m/z*, result of (24S)-HC, 25-HC and 26-HC derivatisation with the hydrazine GP D5. RIC, reconstructed ion chromatogram.

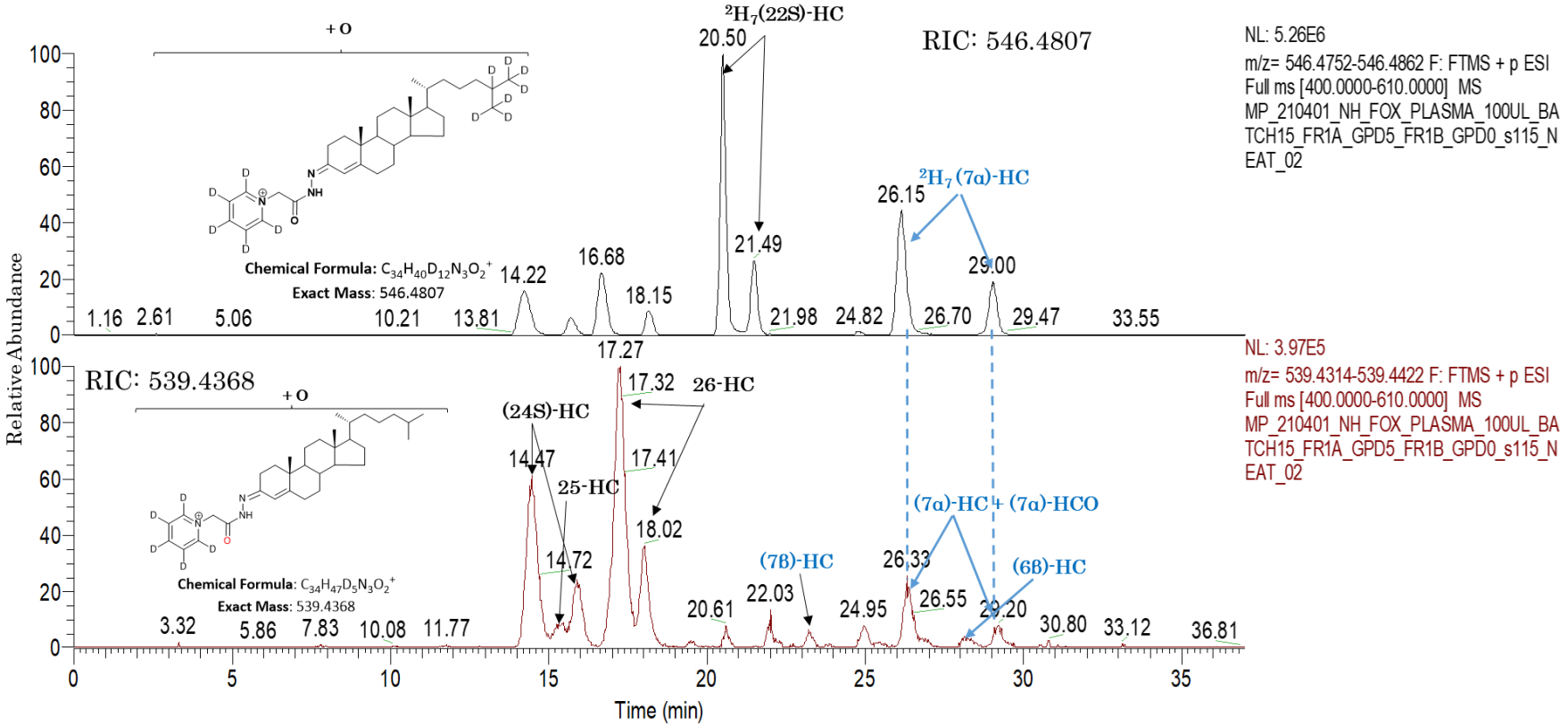

Figure 4.2 Chromatogram of NYPUM plasma showing the internal standard $^2H_7$ (22S)-HC, $^2H_7$ (7α)-HC and the main plasma sterols.

The peaks showed in the upper panel of figure 4.2 represent the molecular ions with exact mass of 546.4807 *m/z*, result of $^2H_7$(22S)-HC, $^2H_7$ (7α)-HC derivatisation with the hydrazine GP D5. The peaks showed in the lower panel of figure 4.2 represent the molecular ions with exact mass of 539.4368 *m/z*, result of 7β-HC, 7α-HCO + 7α-HC and 6β-HC derivatisation with the hydrazine GP D5. RIC, reconstructed ion chromatogram.

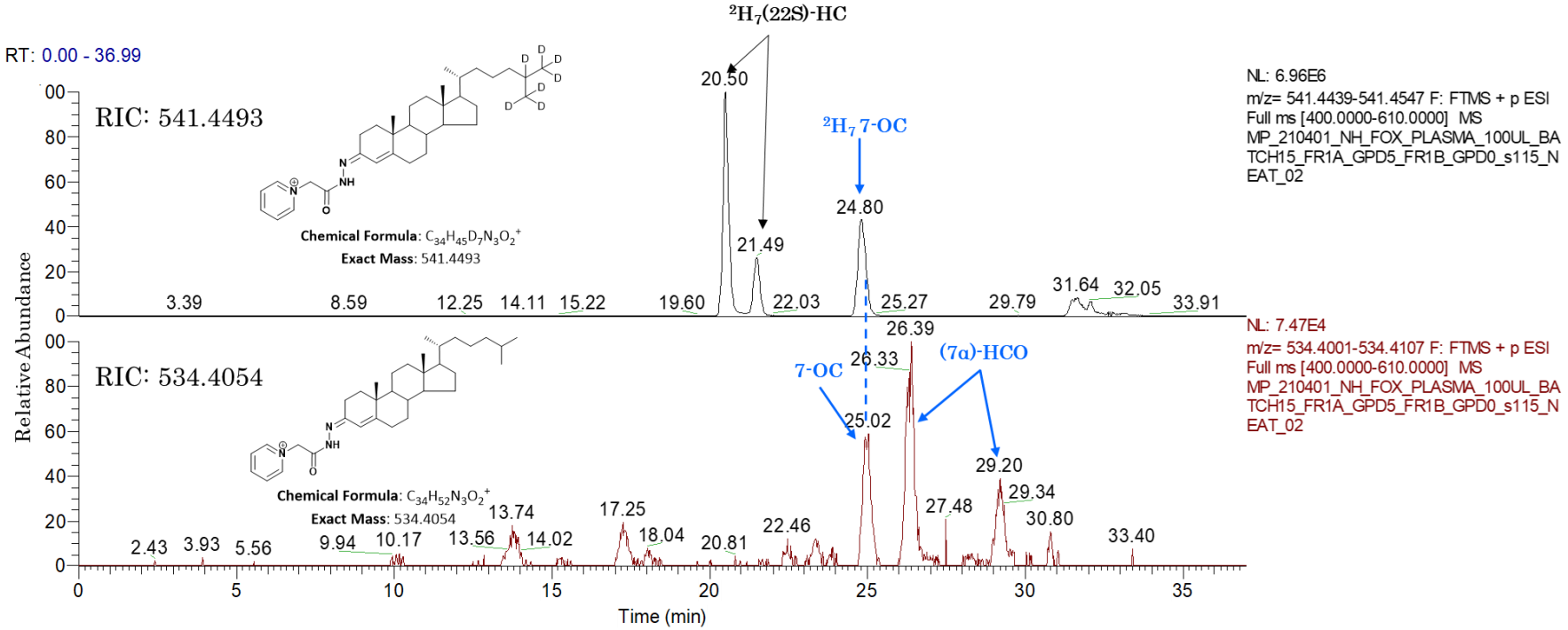

Figure 4.3 Chromatogram of NYPUM plasma showing the internal standard $^2H_7$ (22S)-HC, $^2H_7$ 7-OC, and the main plasma sterols.

The peaks showed in the upper panel of figure 4.3 represent the molecular ions with exact mass of 541.4493 *m/z*, result of $^2H_7$(22S)-HC, $^2H_7$ 7-OC derivatisation with the hydrazine GP D0. The peaks showed in the lower panel of figure 4.3 represent the molecular ions with exact mass of 534.4054 *m/z*, result of main 3-ketone mono-hydroxy sterols present in human plasma derivatisation with the hydrazine GP D0. RIC, reconstructed ion chromatogram.

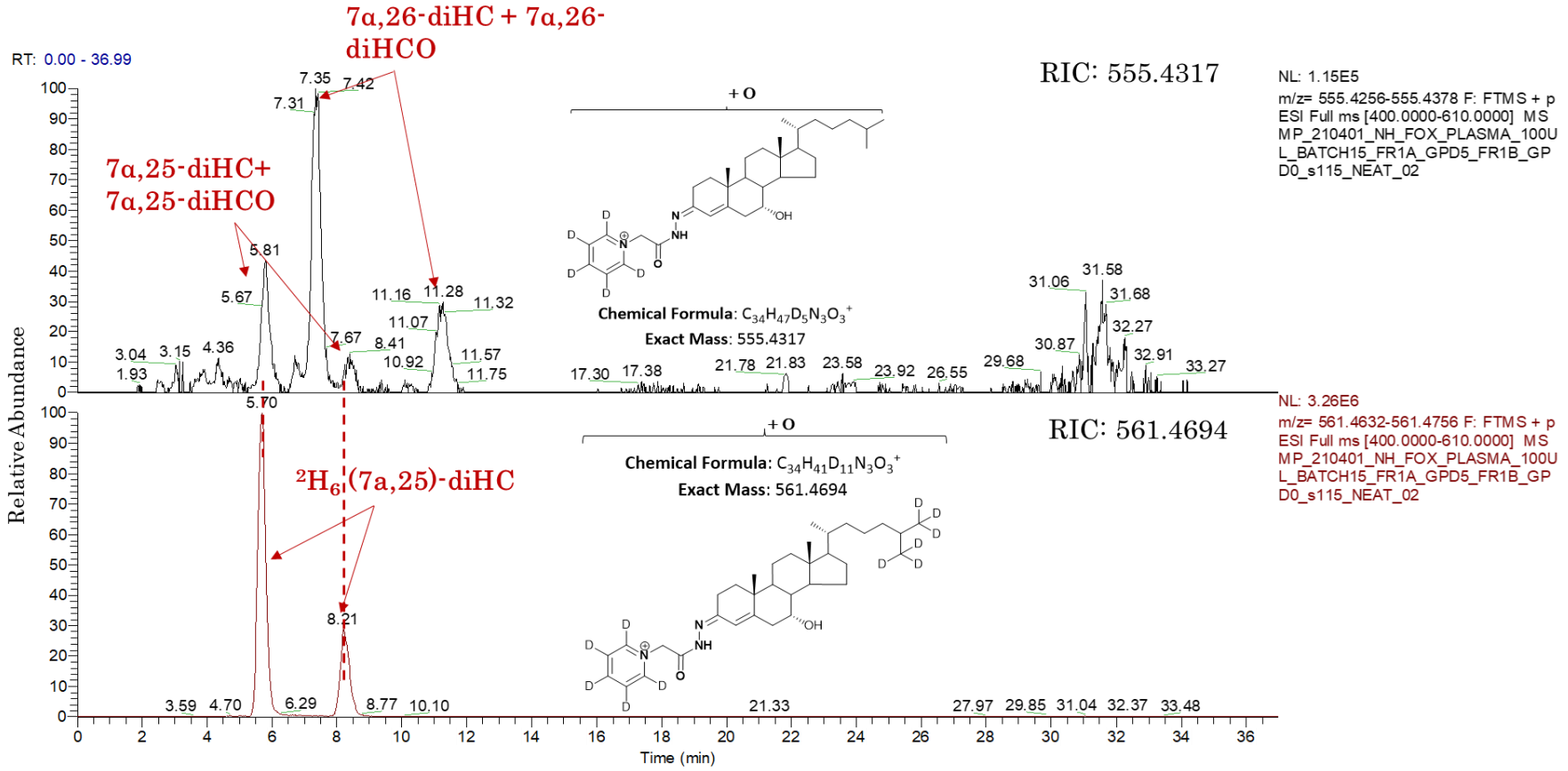

Figure 4.4 Chromatogram of NYPUM plasma showing the internal standard $^{2}H_6$ (7a,25)-diHC and the main plasma sterols.

The peaks showed in the upper panel of figure 4.4 represent the molecular ions with exact mass of 555.4317 *m/z*, result of main di-hydroxy sterols present in human plasma derivatisation with the hydrazine GP D5. The peaks showed in the lower panel of figure 4.4 represent the molecular ions with exact mass of 561.4694 *m/z*, result of $^{2}H_6$ (7a,25)-diHC derivatisation with the hydrazine GP D5. RIC, reconstructed ion chromatogram.

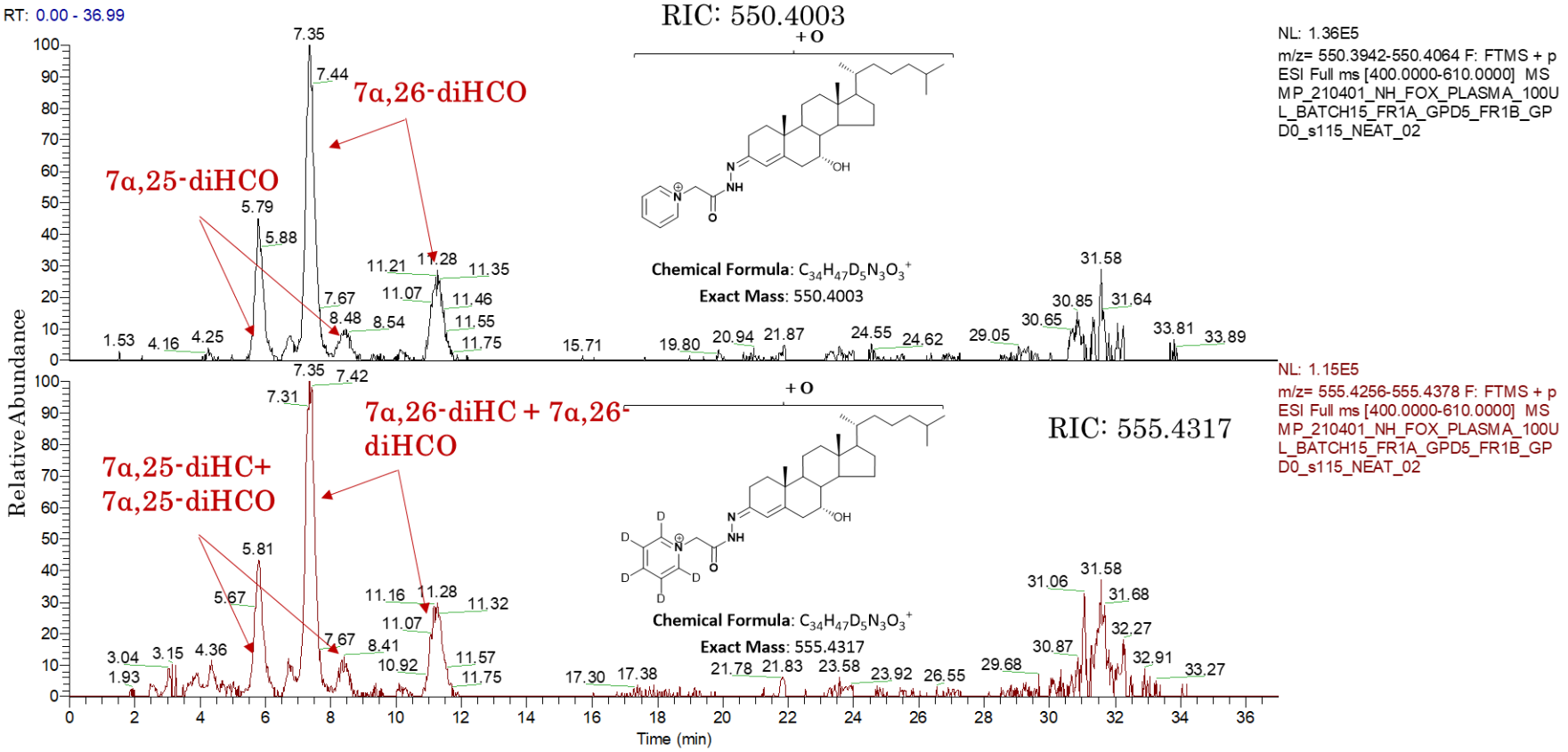

Figure 4.5 Chromatogram of NYPUM plasma showing the main plasma dihydroxy sterols.
The peaks showed in the upper panel of figure 4.5 represent the molecular ions with exact mass of 550.4003 *m/z*, result of 7α,25-diHCO and 7α,26-diHCO derivatisation with the hydrazine GP D0.The peaks showed in the lower panel of figure 4.5 represent the molecular ions with exact mass of 555.4317 *m/z*, result of 7α,25-diHC+7α,25-diHCO and 7α, 26-diHC+7α,26-diHCO derivatisation with the hydrazine GP D5. RIC, reconstructed ion chromatogram.

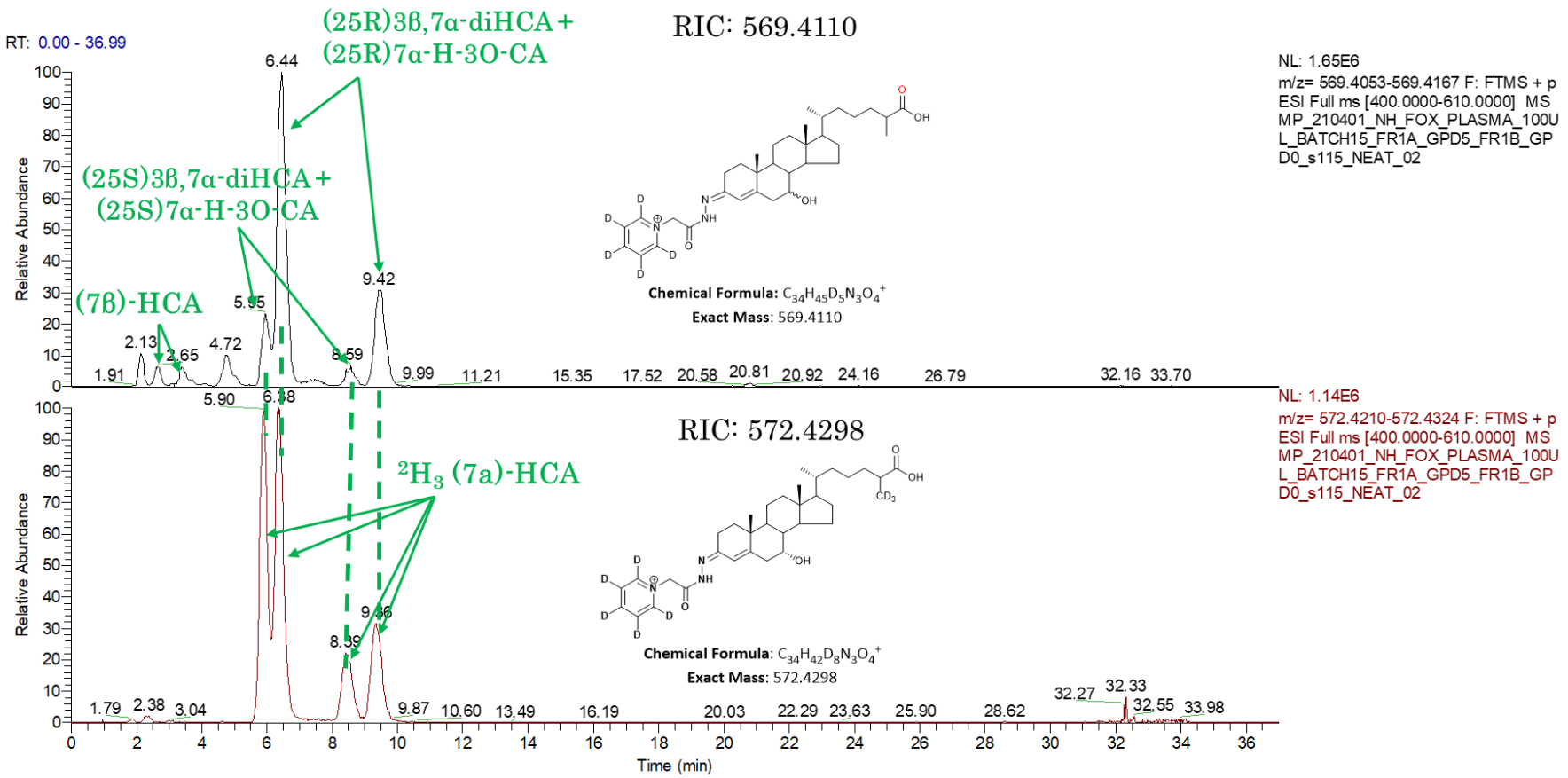

Figure 4.6 Chromatogram of NYPUM plasma showing the main plasma cholestenoic acids.
The peaks showed in the upper panel of figure 4.6 represent the molecular ions with exact mass of 569.4110 *m/z*, result of 3ß,7ß-diHCA, (25S)3ß,7α-diHCA + (25S)7α-H-3O-CA and (25R)3ß,7α-diHCA + (25R)7α-H-3O-CA derivatisation with the hydrazine GP D5.The peaks showed in the lower panel of figure 4.6 represent the molecular ions with exact mass of 572.4298 *m/z*, result of the internal standard $^{2}H_{3}$ (7a)-HCA derivatisation with the hydrazine GP D5. RIC, reconstructed ion chromatogram,

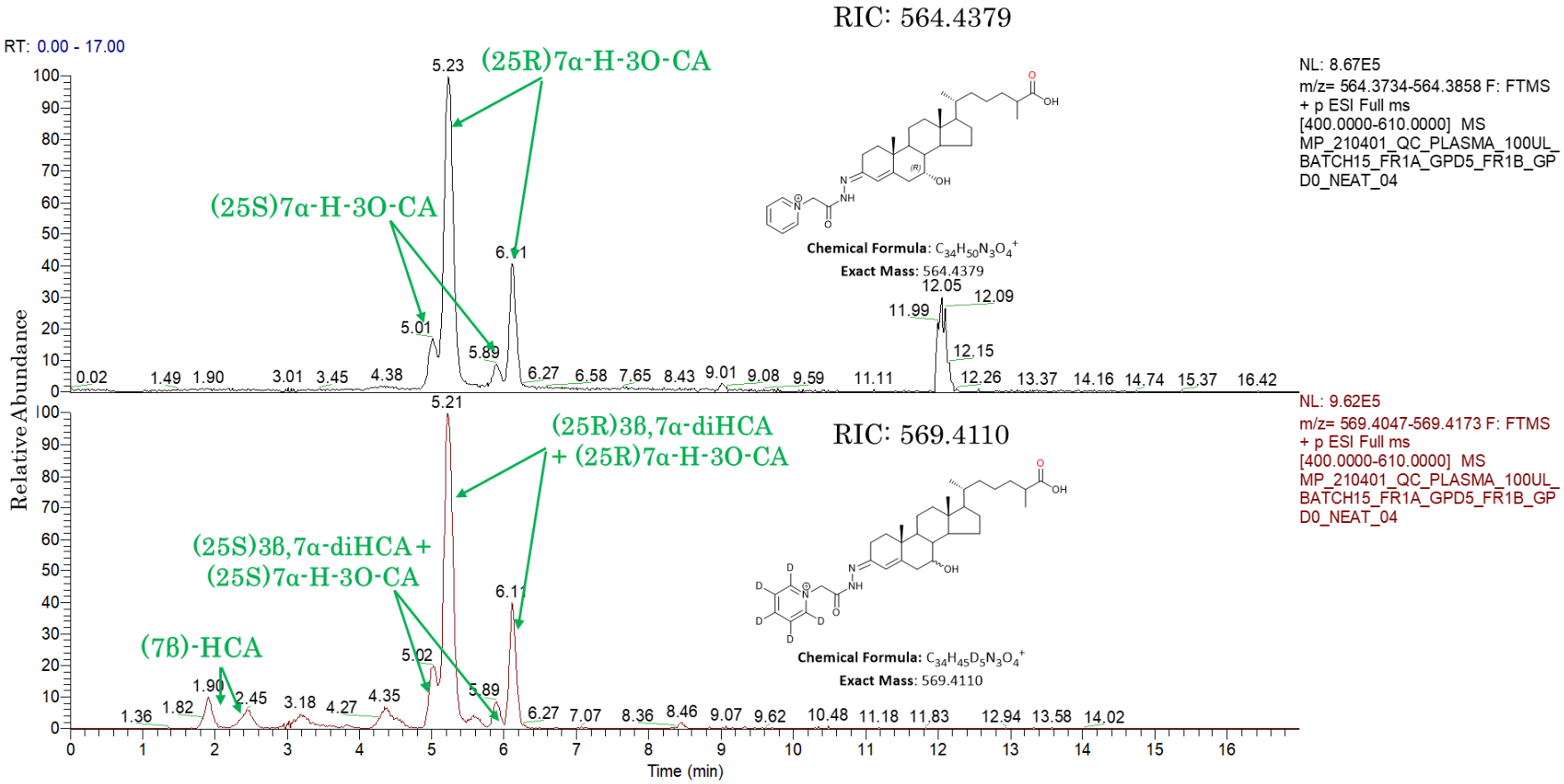

Figure 4.7 Chromatogram of NYPUM plasma showing the main plasma cholestenoic acids.
The peaks showed in the upper panel of figure 4.7 represent the molecular ions with exact mass of 564.4379 *m/z*, result of (25S)7α-H-3O-CA and (25R)7α-H-3O-CA derivatisation with the hydrazine GP D0. The peaks showed in the lower panel of figure 4.7 represent the molecular ions with exact mass of 569.4110 *m/z*, result of the 3β,7β-diHCA, (25S)-3β,7α-diHCA + (25S)7α-H-3O-CA and (25R)3β,7α-diHCA + (25R)7α-H-3O-CA derivatisation with the hydrazine GP D5. RIC, reconstructed ion chromatogram.

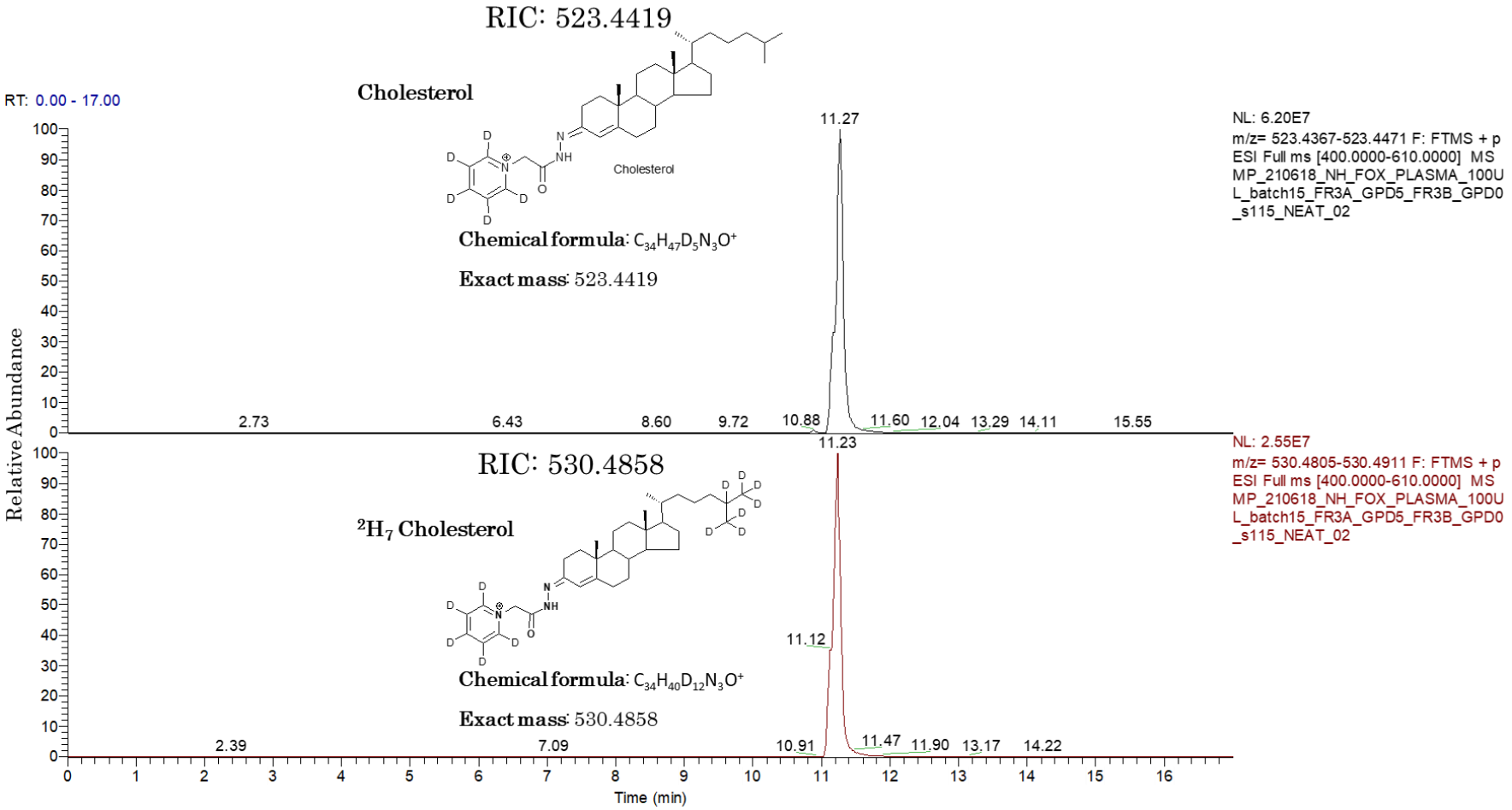

Figure 4.8 Chromatogram of NYPUM plasma showing endogenous cholesterol and $^{2}H_{7}$ Cholesterol.
The peak showed in the upper panel of figure 4.8 represent the molecular ions with exact mass of 523.4419 *m/z*, result of cholesterol derivatisation with the hydrazine GP D5. The peak showed in the lower panel of figure 4.8 represent the molecular ions with exact mass of 530.4858 *m/z*, result of the internal standard $^{2}H_{7}$ Cholesterol derivatisation with the hydrazine GP D5. RIC, reconstructed ion chromatogram.

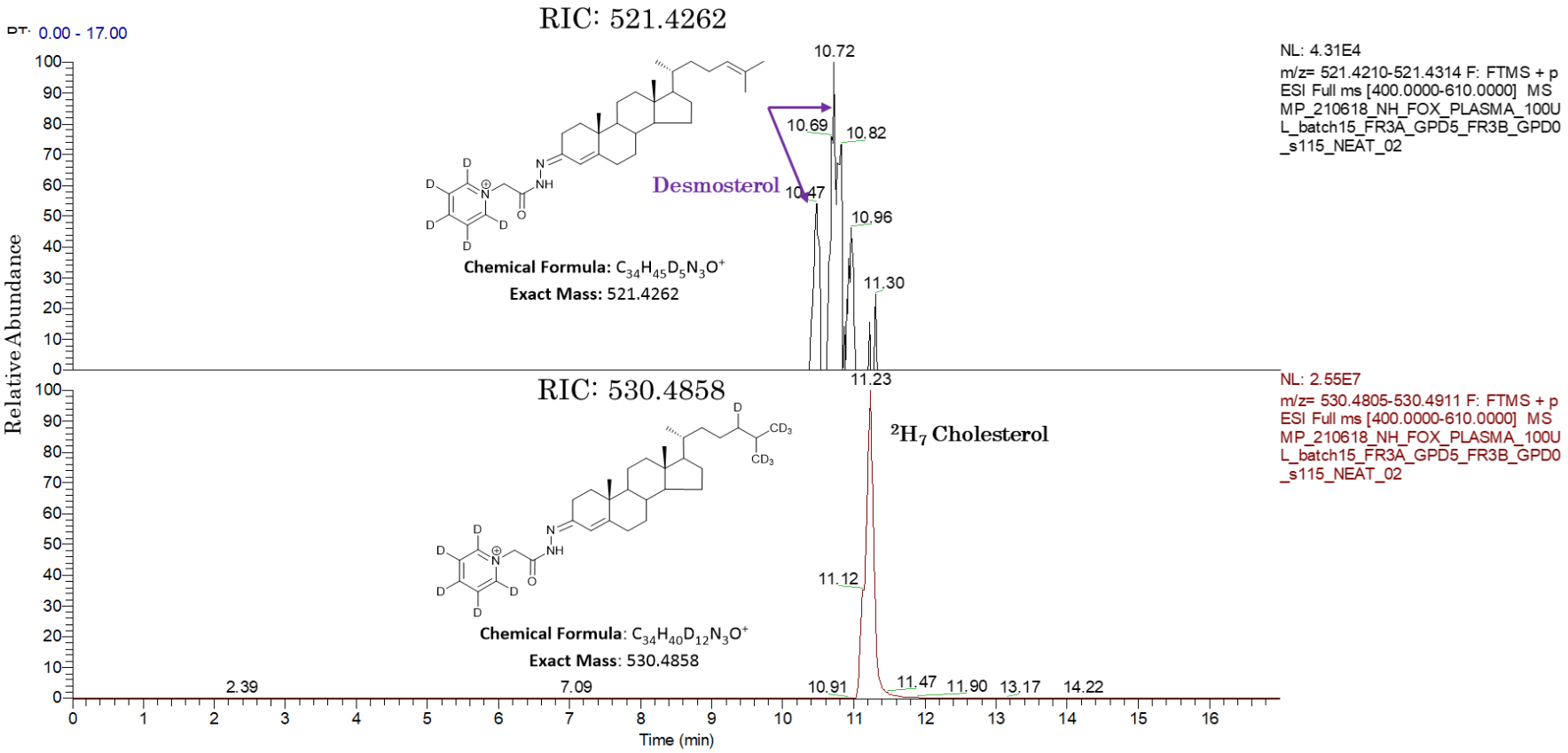

Figure 4.9 Chromatogram of NYPUM plasma showing endogenous desmosterol and $^{2}H_{7}$Cholesterol.
The peak showed in the upper panel of figure 4.9 represent the molecular ions with exact mass of 521.4262 *m/z*, result of desmosterol derivatisation with the hydrazine GP D5. The peak showed in the lower panel of figure 4.9 represent the molecular ions with exact mass of 530.4858 *m/z*, result of the internal standard $^{2}H_{7}$ Cholesterol derivatisation with the hydrazine GP D5. RIC, reconstructed ion chromatogram.

Table 4.6 Plasma levels of the main sterols in NYPUM PD patients and healthy controls. Results expressed as means in ng/mL of plasma. SD: standard deviation

	PD				Control			
	Male	SD	Female	SD	Male	SD	Female	SD
7α,25-diHC + 7α,25-diHCO	0.94	0.07	1.06	0.07	0.89	0.07	1.08	0.09
7α,25-diHCO	0.90	0.12	1.08	0.22	0.88	0.12	0.91	0.19
7α,26-diHC + 7α,26-diHCO	2.86	0.24	2.89	0.22	2.83	0.31	2.84	0.23
7α,26-diHCO	2.75	0.41	3.08	0.69	2.71	0.35	3.24	0.60
(25S)3ß,7α-diHCA + (25S)7α-H-3O-CA	38.85	13.16	33.21	7.18	34.75	11.28	32.36	8.47
(25S)7α-H-3O-CA	21.15	8.21	19.52	5.54	18.57	5.54	18.14	6.46
3ß,7α-diHCA + 7α-H-3O-CA	247.40	67.88	210.46	41.01	219.02	54.69	203.26	52.16
7α-H-3O-CA	162.62	46.41	147.49	33.67	142.80	30.50	139.91	40.34
(25R)3ß-7α-HCA + (25R)7α-H-3O-CA	208.55	56.87	177.25	36.05	184.28	45.57	170.90	44.57
(25R)7α-H-3O-CA	141.47	39.67	127.98	30.49	124.63	27.20	121.77	35.14
(25S)3ß,7α-diHCA	17.70	9.25	13.69	6.57	16.18	10.25	14.22	5.65
3ß,7α-diHCA	84.79	31.98	62.96	17.17	75.83	40.34	63.35	25.54
(25R)3ß-7α-HCA	67.08	26.00	49.27	12.86	59.64	32.09	49.13	21.82
(24S)-HC	14.92	3.23	16.89	3.53	13.25	3.21	16.24	4.51
25-HC	1.66	0.34	1.67	0.33	1.57	0.43	1.71	0.45
26-HC	27.52	5.52	24.49	5.08	26.73	6.62	25.48	6.42

7β-HC	1.80	1.55	2.25	1.18	2.10	1.32	2.10	0.93
7-OC	5.34	3.84	6.37	3.07	5.44	3.48	6.73	7.46
7α-HC +7α-HCO	21.26	16.93	21.80	19.08	22.01	15.69	21.17	15.82
7α-HCO	17.92	18.90	17.31	14.78	21.01	22.89	18.46	16.80
7α-HC	3.34	11.92	4.49	8.68	1.00	13.65	2.71	10.56
6β-HC	2.52	1.85	2.59	1.12	3.21	4.28	3.21	1.78
cholestenoic acid (3β-HCA)	136.84	36.75	120.12	25.87	129.97	53.41	118.71	38.13
Desmosterol	247.91	143.49	222.54	116.69	264.06	106.71	244.82	143.02
Cholesterol	622822.76	117640.48	713577.72	124908.83	690555.31	145126.71	763333.83	165594.16

Among the 21 different sterols identified in human plasma, the cholestenoic acids (25S)7α-H-3O-CA and (25R)-7α-H-3O-CA, the mono hydroxy cholesterol (24S)-HC, and cholesterol levels result to be statistically different between the disease group, PD, and the healthy controls, despite the spread of values around the mean in both groups, see figure 4.10a, 4.11a, 4.12a and 4.13a. The spreading in human samples is mainly to reconduct to the biological variation, calculated as the between-subjects coefficient of variation or CV_G, table 4.7. The bona fide of the results is further proven through the low analytical variation, less than 6%, in all sterols except for (25S)-7α-H-3O-CA where it reaches 11.3%, which is still widely acceptable. Analytical variation is calculated as the coefficient of variation of the quality control (QC) samples, or CV_A.

Table 4.7 . Biological (CVG) and analytical (CVA) variation in human PD and healthy control and QC plasma samples for the oxysterol (24S)-HC, the cholestenoic acids (25S)7α-H-3O-CA and (25R)-7α-H-3O-CA and cholesterol.

	PD			Control			QC		
	Mean (ng/mL)	SD	CV_G (%)	Mean (ng/mL)	SD	CV_G (%)	Mean (ng/mL)	SD	CV_A (%)
(25S)7α-H-3O-CA	20.46	7.28	35.58	18.32	6.03	32.91	15.22	1.72	11.30
(25R)7α-H-3O-CA	135.70	36.86	27.16	123.00	31.57	25.67	145.09	8.42	5.80
(24S)-HC	15.60	3.51	22.50	14.66	4.13	28.17	20.16	1.18	5.85
Cholesterol	662061.00	136050.00	20.55	729543.00	155925.00	21.37	923599.36	53385.17	5.78

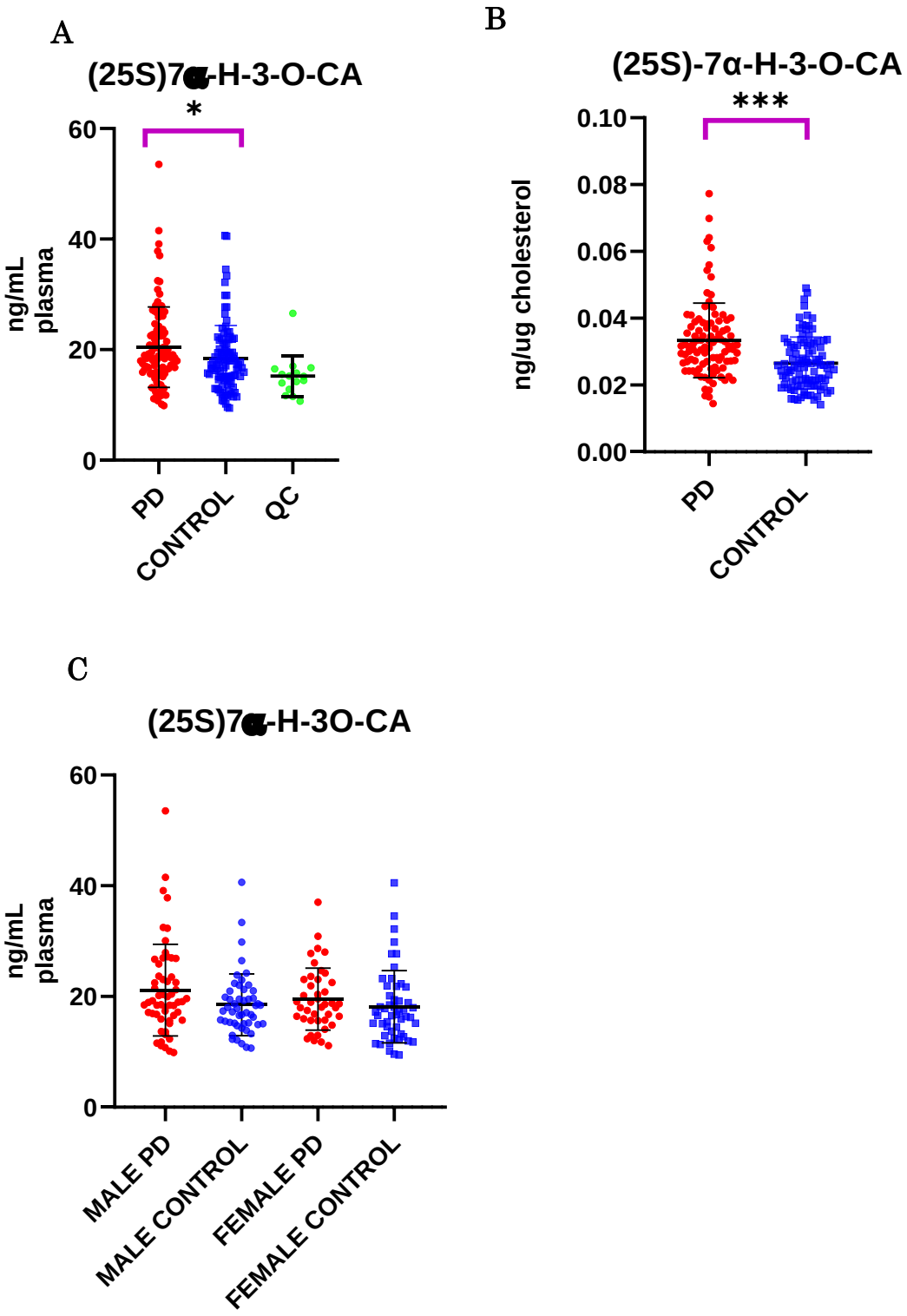

Figure 4.10 Plasma levels of (25S)7α-H-3O-CA.
(A) (25S)7α-H-3O-CA is elevated in PD patients (in red), n=100, respect to the healthy controls (in blue), n=100. Quality control plasma (in green), n=26. **(B)** (25S)7α-H-3O-CA plasma levels normalised to cholesterol: the (25S)7α-H-3O-CA/cholesterol ratio is lower in PD patients respect to controls. **(C)** PD and control males

and females (25S)7α-H-3O-CA plasma levels: gender does not discriminate between diseased and healthy groups. *= $p<0.05$, ***=$p<0.001$

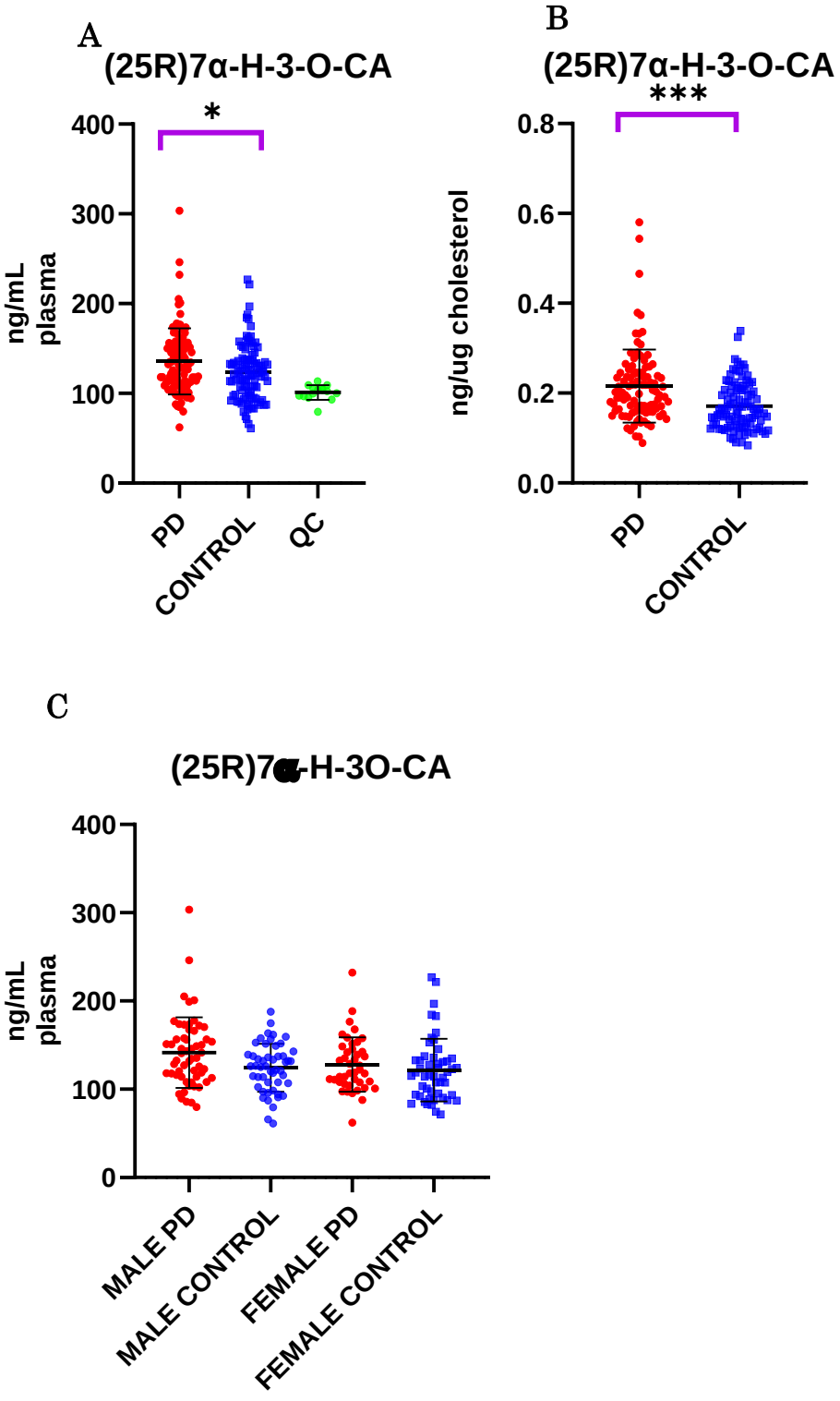

Figure 4.11 Plasma levels of (25R)7α-H-3O-CA.
(A) (25R)7α-H-3O-CA is elevated in PD patients (in red), n=100, respect to the healthy controls (in blue), n=100. Quality control plasma (in green), n=26. **(B)** (25R)7α-H-3O-CA plasma levels

normalised to cholesterol: the (25R)7α-H-3O-CA/cholesterol ratio is higher in PD patients respect to controls. (C) PD and control males and females (25R)7α-H-3O-CA plasma levels: gender does not discriminate between diseased and healthy groups. *= $p<0.05$, ***=$p<0.001$.

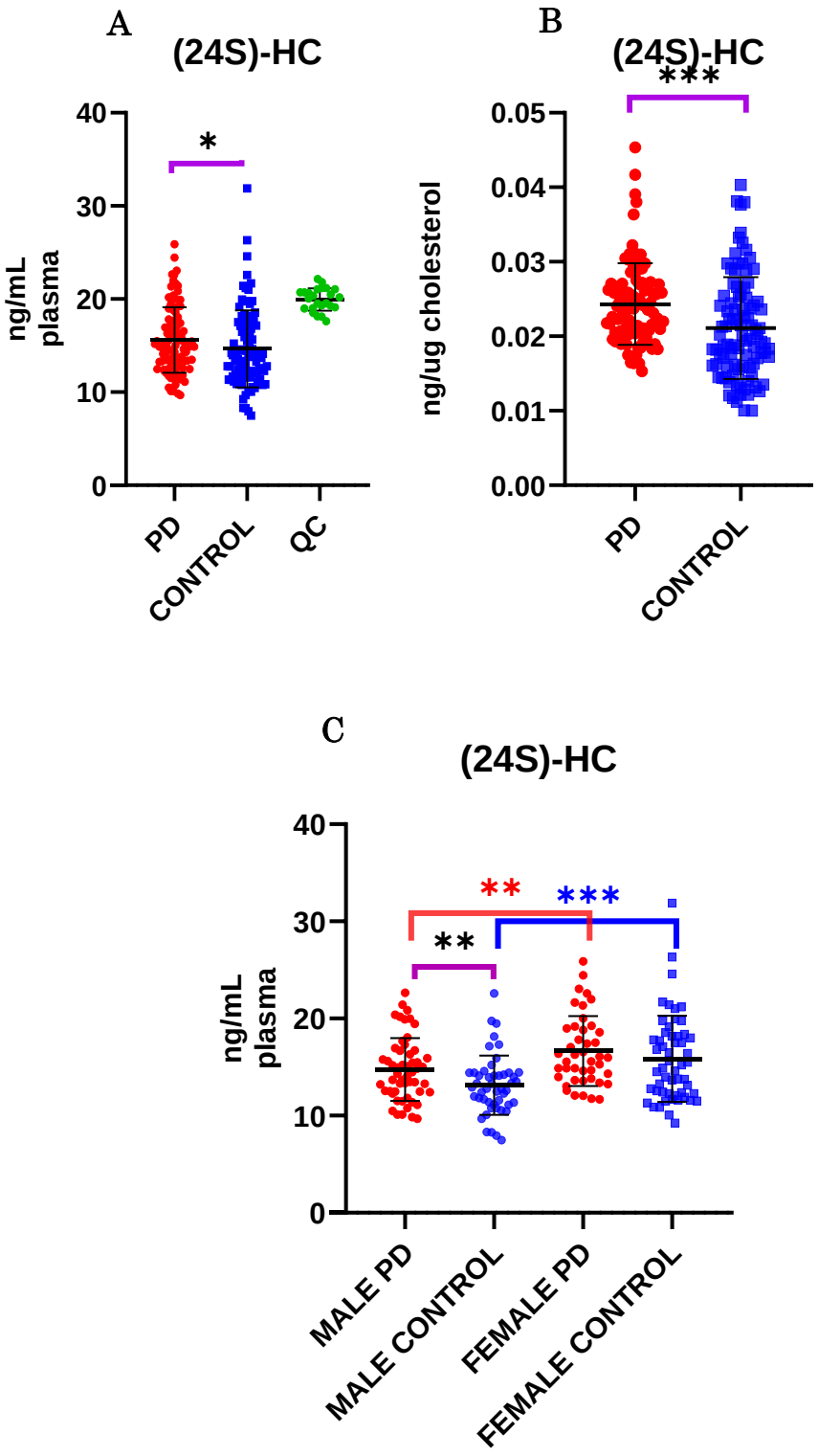

Figure 4.12 Plasma levels of (24S)-HC.
(A) (24S)-HC is elevated in PD patients (in red), n=100, respect to the healthy controls (in blue), n=100. Quality control plasma (in green), n=26. **(B)** (24S)-HC plasma levels normalised to cholesterol: the

(24S)-HC/cholesterol ratio is higher in PD patients respect to controls. (C) PD and control males and females (24S)-HC plasma levels: gender does discriminate between males and females, in both PD and healthy groups, being always higher in the PD counterpart. *= $p<0.05$, **=$p<0.01$, ***=$p<0.001$

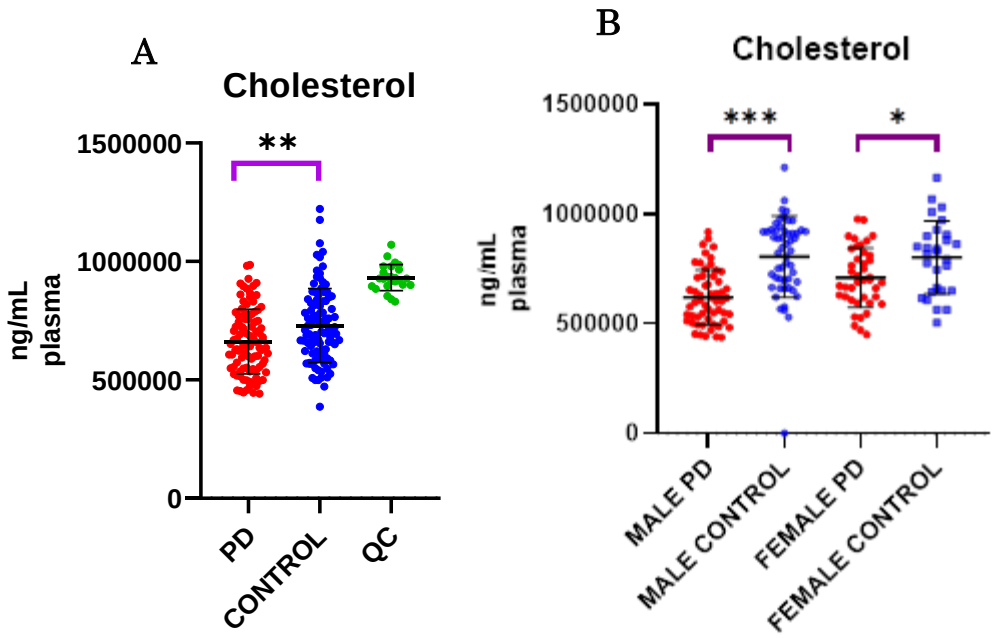

Figure 4.13 Plasma levels of cholesterol.
(A). The cholesterol plasma levels result to be lower in the diseased group, PD, respect to healthy controls. **(B)** Gender discriminates between males and females affected by PD. *= $p<0.05$, **=$p<0.01$, ***=$p<0.001$

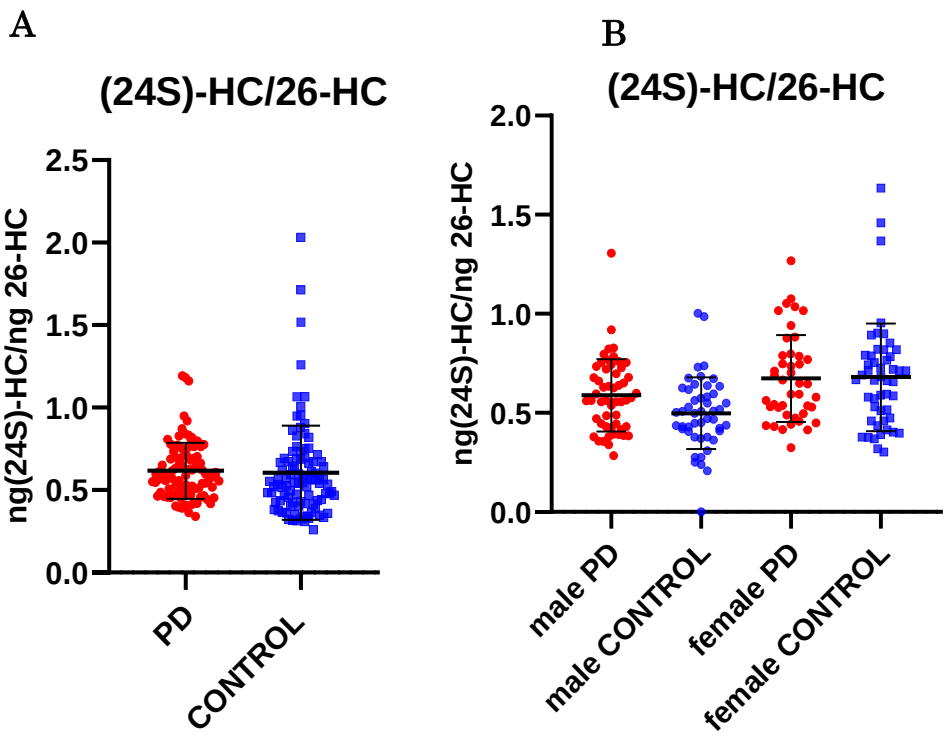

Figure 4.14 Ratio of (24S)-HC and 26-HC plasma levels.
(A). No significant variation of (24S)-HC/26-HC ratio between the PD and control group is observed, **(B)** even when gender is introduced as a confounding variable.

With a closer look at the sterols' levels, (25S)7α-H-3O-CA resulted in being 12%higher in PD (20.46 ± 7.28 ng/mL) respect to the healthy controls (18.32 ± 6.03 ng/mL), p=0.012, Mann-Whitney. The same trend is observed for the epimer (25R)-7α-H-3O-CA, being 10% higher in PD (135.7 ± 36.86 ng/mL) respect to the controls (123.0 ± 31.57 ng/mL), p=0.013, Mann-Whitney. Interestingly, the brain-derived mono-hydroxy sterol (24S)-HC is also higher in the disease group, accounting for an 8% increase in the PD patients' group (15.60 ± 3.51) respect to the control group (14.66 ± 4.13), p=0.024, Mann-Whitney. On the other side, cholesterol plasma levels turned out to be 10% lower in PD (662061 ± 136050 ng/mL) respect to the healthy individuals (729543 ± 155925 ng/mL), p=0.002, Mann-Whitney. All the results are expressed as means plus/minus the standard deviation. To further validate the findings and correct for any PD-unrelated cholesterol/sterol plasma variations, e.g., due to hypercholesterolemia or subjects not being in fasting during plasma collection, the sterol values have been normalised to the cholesterol plasma levels, see table 4.8.

Table 4.8 Normalisation of the significant sterols to free cholesterol plasma levels.

ng/µg		(24S)-HC / cholesterol	(25S)7α-H-3O-CA / cholesterol	(25R)7α-H-3O-CA / cholesterol
PD	mean	0.024	0.033	0.216
	sd	0.005	0.011	0.081
Control	mean	0.021	0.027	0.171
	sd	0.005	0.008	0.052

Cholesterol normalisation strongly reinforces the differences between the Parkinson group and the healthy control group, which resulted in being even more statistically significantly different, figures 4.10, 4.11, 4.12 Bs. Additional investigation of the sterolome profile sees the introduction of gender as a potential confounding variable. Interestingly, (24S)-HC plasma levels seem to be gender discriminating factor. Hence, the sterol is always lower in males respect to females, in both PD (males= 14.92 ± 3.23 & females= 16.89 ± 3.53, Kruskal-Wallis p=0.008) and controls (males=13.25 ± 3.21 & females= 16.24 ± 4.51, Kruskal-Wallis, p=0.0009), figure 4.12 C Moreover, the (24S)-HC data seems to help in differentiating males affected by PD (14.92 ± 3.23), and healthy male controls (13.25 ± 3.21), Kruskal-Wallis p=0.009. However, this difference is not seen for the females (PD= 16.89 ± 3.53 & control= 16.24 ± 4.51, Kruskal-Wallis p>0.05) figure 4.12 C. No such discrimination is seen for all the other relevant sterols, apart from cholesterol, where both PD male and female sterol levels are sensibly lower than the control counterpart, figure 4.10 and 4.12 Cs. To further investigate the nature of the (24S)-HC variation in PD, the ratio between the levels of (24S)-HC and 26-HC have been calculated, as it has been reported to be altered in some neurological diseases (Leoni *et al.*, 2003). Moreover, (24S)-HC/26-HC ratio is also considered be a measure of BBB integrity, which can be affected over PD. In this cohort of PD patients, no difference in the ratios (24S)-HC/26-HC can be appreciated between controls and PD patients, see figure 4.14. Two separate correlation matrixes analyses have been performed to finalise the data analysis and to screen for any correlation among the sterols in PD and non-PD groups. As depicted in the figure 4.15, the sterols behave similarly in the two groups, with comparable Spearman coefficient for non-parametric data. Interestingly, the analysis highlights a significant corelations (Sperman > 0.6, p value

<0.05) between the main plasma cholestenoic acids 3β,7α-diHCA and 7α-H-3O-CA, which represent back-to-back intermediates in the bile acids biosynthesis. However, no corelation has been reported between the sterols which differs in the PD group respect to the non-PD, (24S)-HC, (25S)7α-H-3O-CA, (25R)7α-H-3O-CA and cholesterol.

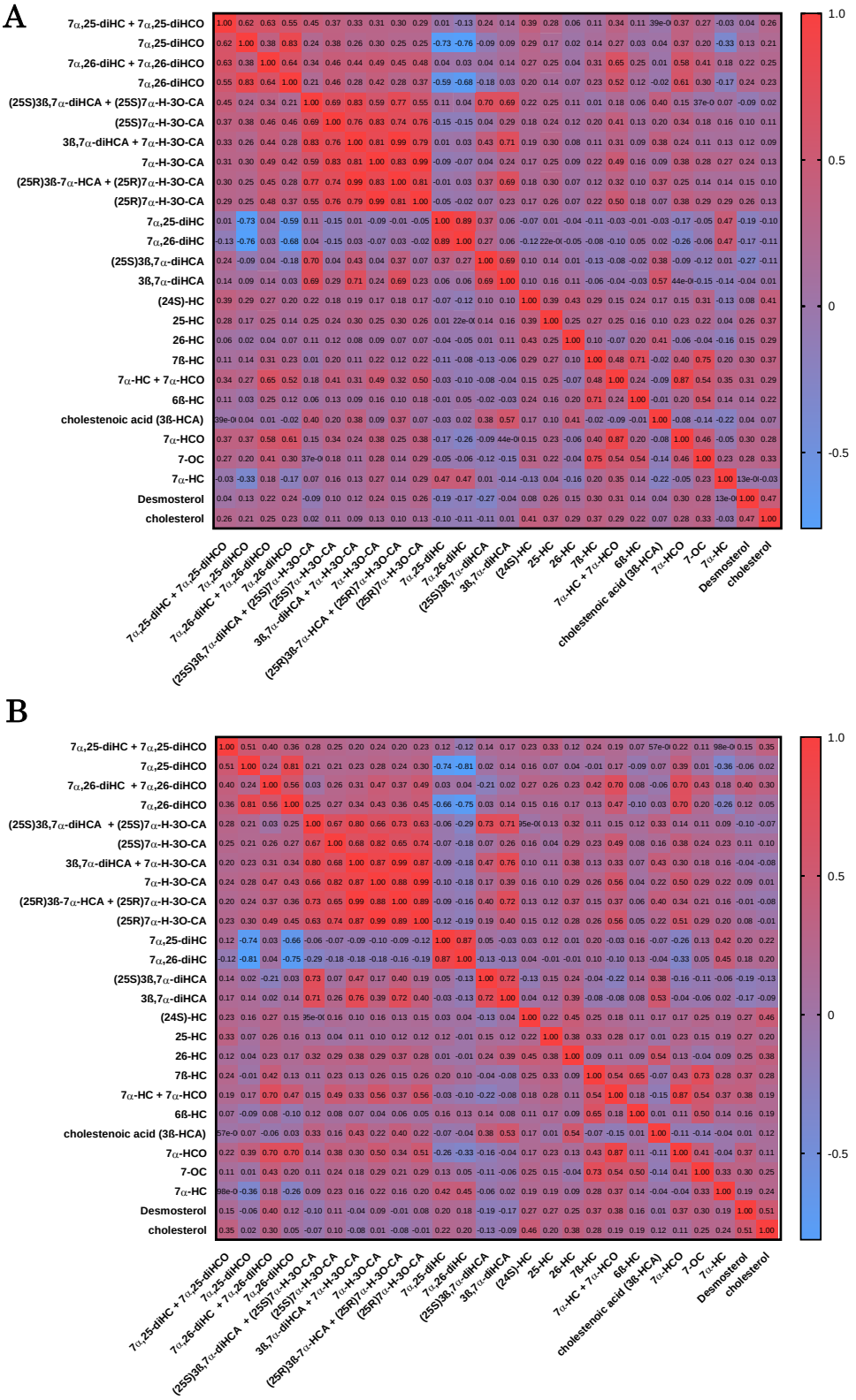

Figure 4.15 Corelation matrixes for PD (A) and non-PD (B).
In the heat map, Sperman coefficient values are expressed for each sterol match as both colour gradient (scale bar on the right, -1<Sperman<1) as with its original value in the cell. PD, graph A, and

controls, graph B, shows the same corelation, and no variation, among the plasma sterols.

From the data reported above, (24S)-HC seems to be the most plausible candidate biomarker for PD, therefore an ROC analysis has been carried out. The diagnostic ability of (24S)-HC plasma levels to predict PD is of almost 60% when referring to absolute (24S)-HC plasma levels (AUC=0.59) and roughly 70% when its levels are normalised to the cholesterol one (AUC=0.66), figure 4.16.

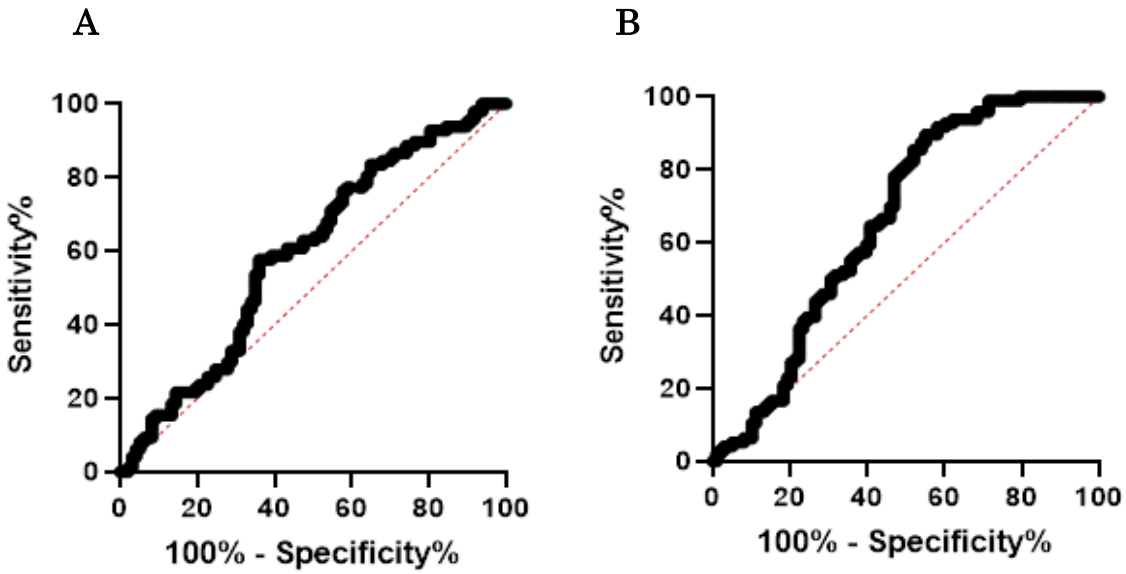

Figure 4.16 ROC analysis on (24S)-HC plasma levels.
(A). When referred to absolute (24S)-HC plasma levels, PD is predicted in 6 out of 10 cases (AUC=0.59). **(B)** When referred to cholesterol normalised (24S)-HC plasma levels, PD is predicted in almost 7 out of 10 cases (AUC=0.66).

4.4.2 Sterolome profile of longitudinal plasma from progressive PD patients: in search for disease progression predictor biomarkers

Several plasma samples belonging to the ICICLE cohort of progressive PD patients present haemolysis, see picture 4.17.

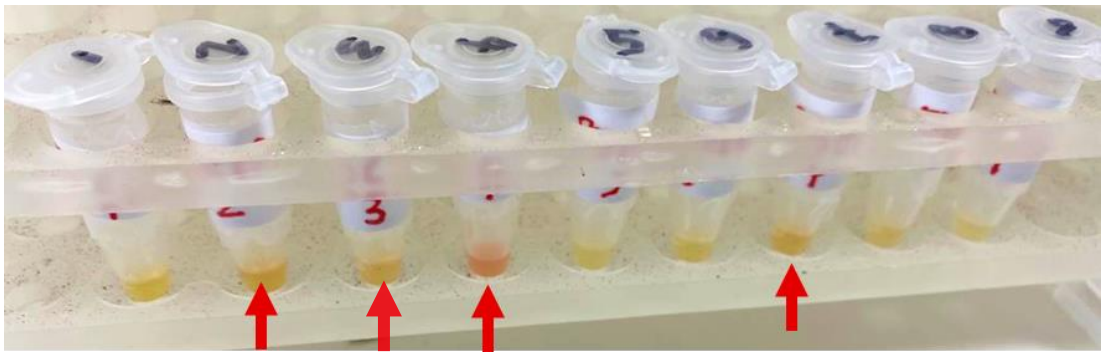

Figure 4.17 Representative picture of the haemolytic plasma sample from ICICLE cohort.

The haemolytic process involves the rupture of erythrocytes membranes and the consequent release of their contents into blood stream. Plasma enrichment in haemoglobin, potassium, cytosolic proteins, and several different lipids, including cholesterol, is expected when haemolysis occurs, causing several challenges for analytical determination of specific plasma analytes. Additionally, most of the ICICLE plasma samples, both the ones presenting haemolysis and the ones with an apparent normal appearance, have been particularly hard to pipette-out form the sample vials due to clotting and formation of gelatine-like suspension after the thawing process. Hence, even though the sterol extraction procedure has been

followed with care, the uptake of the 100 uL plasma required for the sterolome analysis was particularly difficult, requiring several attempts, which have increased the extraction time. Cholesterol is a quite susceptible to oxidation, and the extended sample preparation and extraction procedure might have affected the content of its autoxidation products. Alterations of non-enzymatic oxidation products cannot be excluded. Moreover, plasma suspensions might have partially trapped some of the sterols present in plasma. Therefore, it cannot be guaranteed a total plasma sterol extraction. Another concern is related to the release of cholesterol from blood cells during haemolysis, which can alter its quantification. However, an attempt to sterol identification and quantification has been done.

36 different plasma samples, belonging to 16 different patients collected over period covering 90 months after diagnosis, have been analysed. For the extraction, identification, and quantification of free plasma sterols has been followed the same protocol used for the Nypum cohort of base line PD patients, described in sections 4.3.2 and 4.3.4, which has allowed the identification of the same set of 21 sterols found in the baseline group, example chromatograms can be found in figures 4.18 and 4.19. Structure attribution made by retention time and accurate mass match with trace finder plus fingerprint fragmentation match with internal library, see the tables 7.1 to 7.13 in the appendix for details. The sterol lipids include 6 mono-hydroxy sterols of which seven mono-hydroxycholesterols (24S)-HC, 25-HC, 26-HC, 7β-HC, 7α-HC & 6β-HC and two mono-hydroxy cholestenones, 7-OC and 7α-HCO, 4 di-hydroxy sterols of which two di-hydroxycholesterols (7a,25-diHC & 7α,26-diHC) and two di-hydroxy cholestenones, (7α,25-diHCO& 7α,26-diHCO), 7 cholestenoic acids, of which three mono-hydroxy cholestenoic acids

(3ß,7α-diHCA, (25S)3ß,7α-diHCA & (25R)3ß,7α-diHCA), three mono-hydroxy cholestenonic acids (7α-H-3O-CA, (25S)7α-H-3O-CA & (25R)7α-H-3O-CA), and cholestenoic acid (CA), and cholesterol itself. Relative quantification has been done against same structure or surrogate deuterated internal standard, refer to table 7.16 in the appendix for details.

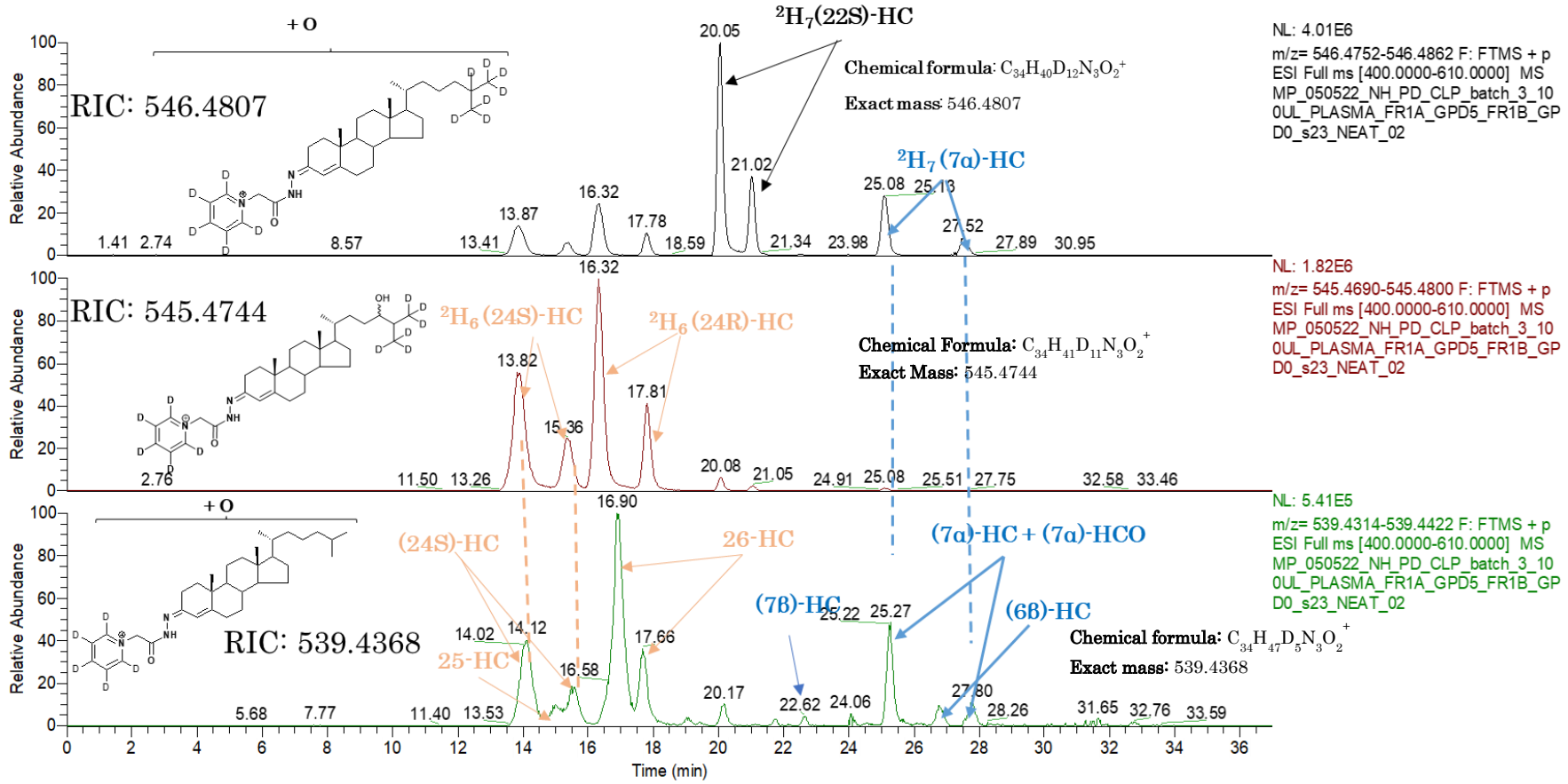

Figure 4.18 Chromatogram of ICICLE plasma showing the internal standard $^2H_7$ (22S)-HC, $^2H_7$ (7α)-HC, $^2H_6$ (24R/S)-HC and the main plasma sterols.

The peaks showed in the upper panel of figure 4.18 represent the molecular ions with exact mass of 546.4807 *m/z*, result of $^2H_7$(22S)-HC, $^2H_7$ (7α)-HC derivatisation with the hydrazine GP D5. The peaks showed in the lower panel of

figure 4.18 represent the molecular ions with exact mass of 545.4744 *m/z*, result of $^{2}H_{6}$(24R/S)-HC derivatisation with the hydrazine GP D5. The peaks showed in the middle panel of figure 4.18 represent the molecular ions with exact mass of 539.4368 *m/z*, result of (24S)-HC, 25-HC, 26-HC, 7ß-HC, 7α-HCO + 7α-HC and 6ß-HC derivatisation with the hydrazine GP D5. RIC, reconstructed ion chromatogram.

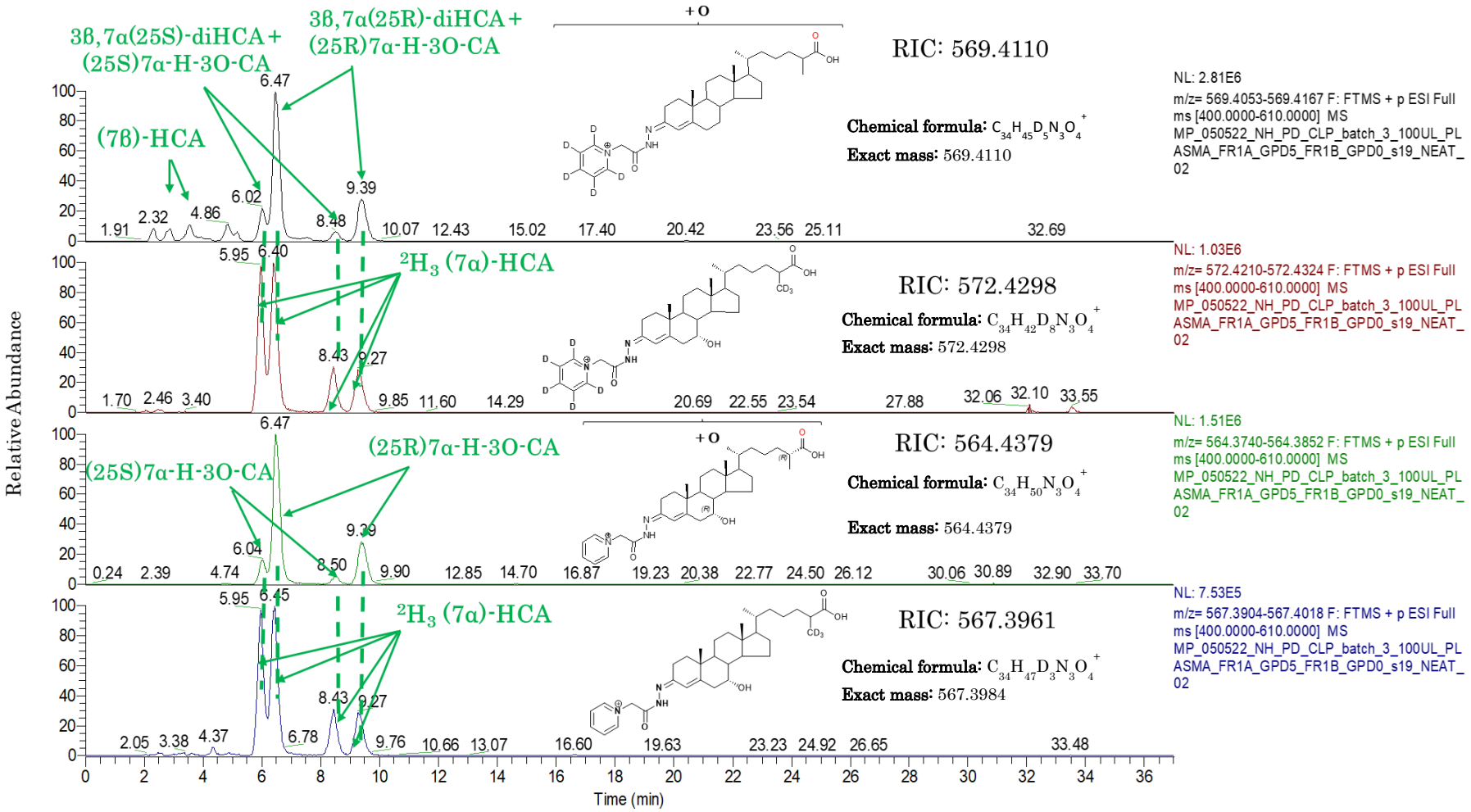

Figure 4.19 Chromatogram of ICICLE plasma showing the main plasma cholestenoic acids.
The peaks showed in the upper panel of figure 4.19 represent the molecular ions with exact mass of 569.4110 *m/z*, result of 3ß,7ß-diHCA, (25S)3ß,7α-diHCA + (25S)7α-H-3O-CA and (25R)3ß,7α-diHCA + (25R)7α-H-3O-CA derivatisation with the hydrazine GP D5. The peaks showed in the second panel of figure 4.19 represent the molecular

ions with exact mass of 572.4298 *m/z*, result of the internal standard $^{2}H_{3}$ (7a)-HCA derivatisation with the hydrazine GP D5. The peaks showed in the third panel of figure 4.19 represent the molecular ions with exact mass of 564.4379 *m/z*, result of (25S)7α-H-3O-CA and (25R)7α-H-3O-CA derivatisation with the hydrazine GP D0. The peaks showed in the lower panel of figure 4.19 represent the molecular ions with exact mass of 567.3961 *m/z*, result of the internal standard $^{2}H_{3}$ (7a)-HCA derivatisation with the hydrazine GP D0. RIC, reconstructed ion chromatogram.

Most of the plasma samples belonging to this longitudinal cohort of PD patients has been collected among the first visit, base line, and the second visit, month 36, with 16 and 13 samples respectively. The remaining 7 samples were almost equally distributed into the other 3 time points. Due to the high variation in the patient distribution among the different time points at visit 3, 4 and 5 no statistical analysis could be carried out. However, to assess any variation between baseline and 36 months, a two-stage multiple comparison method of Benjamini, Krieger and Yekutieli was performed.

With regards to sterols variation over time, depicted in the graphs 4.20, 4.21, 4.22, 4.23, and 4.24, a decreasing trend seems to characterise the plasma concentration of this class of lipid molecules after 36 months. With closer look to the single sterol subclasses over this first 3 years of time, low abundant dihydroxy sterols, cholestenoic acids and monohydroxy sterols, it can be appreciated a large standard deviation in the sterol's concentrations, graphs 4.25, 4.26, 4.27 and 4.28. In fact, no statistical variation has been found in any of the sterols identified (two-stage multiple comparison method of Benjamini, Krieger and Yekutieli).

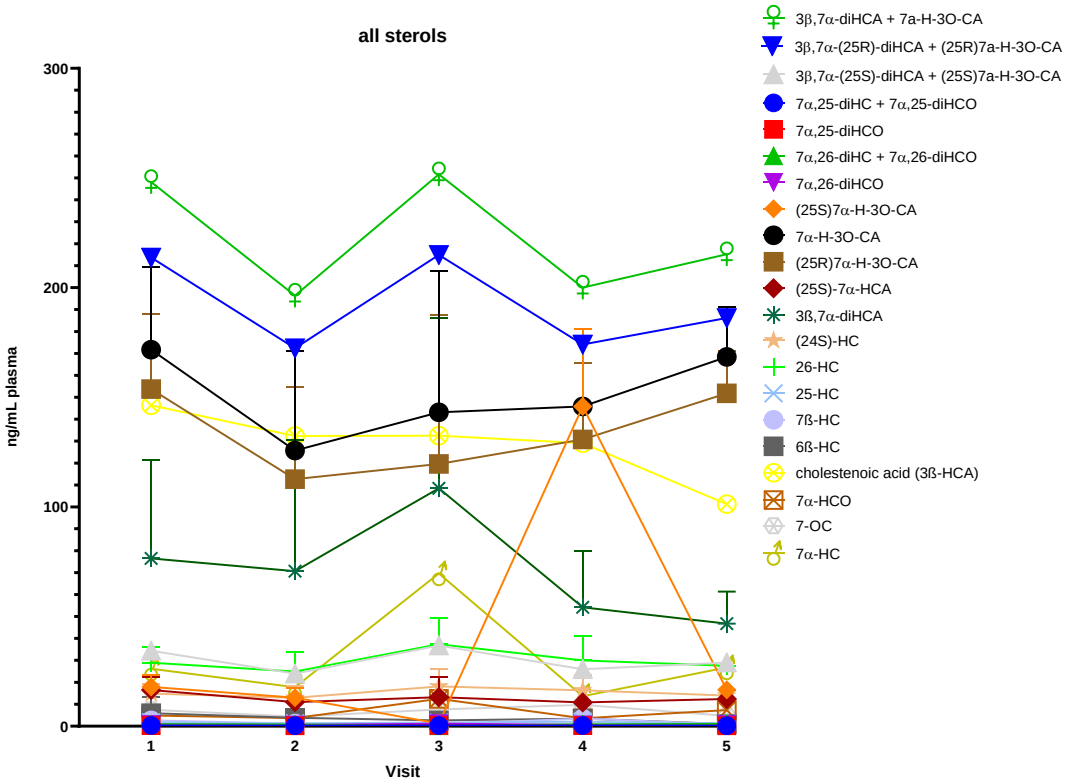

Figure 4.20 Sterol plasma variation in PD patients over 90 months. Visit 1, 0 months; visit 2, 36 months: visit 3. 54 months; visit 4, 72 months; visit 5, 90 months.

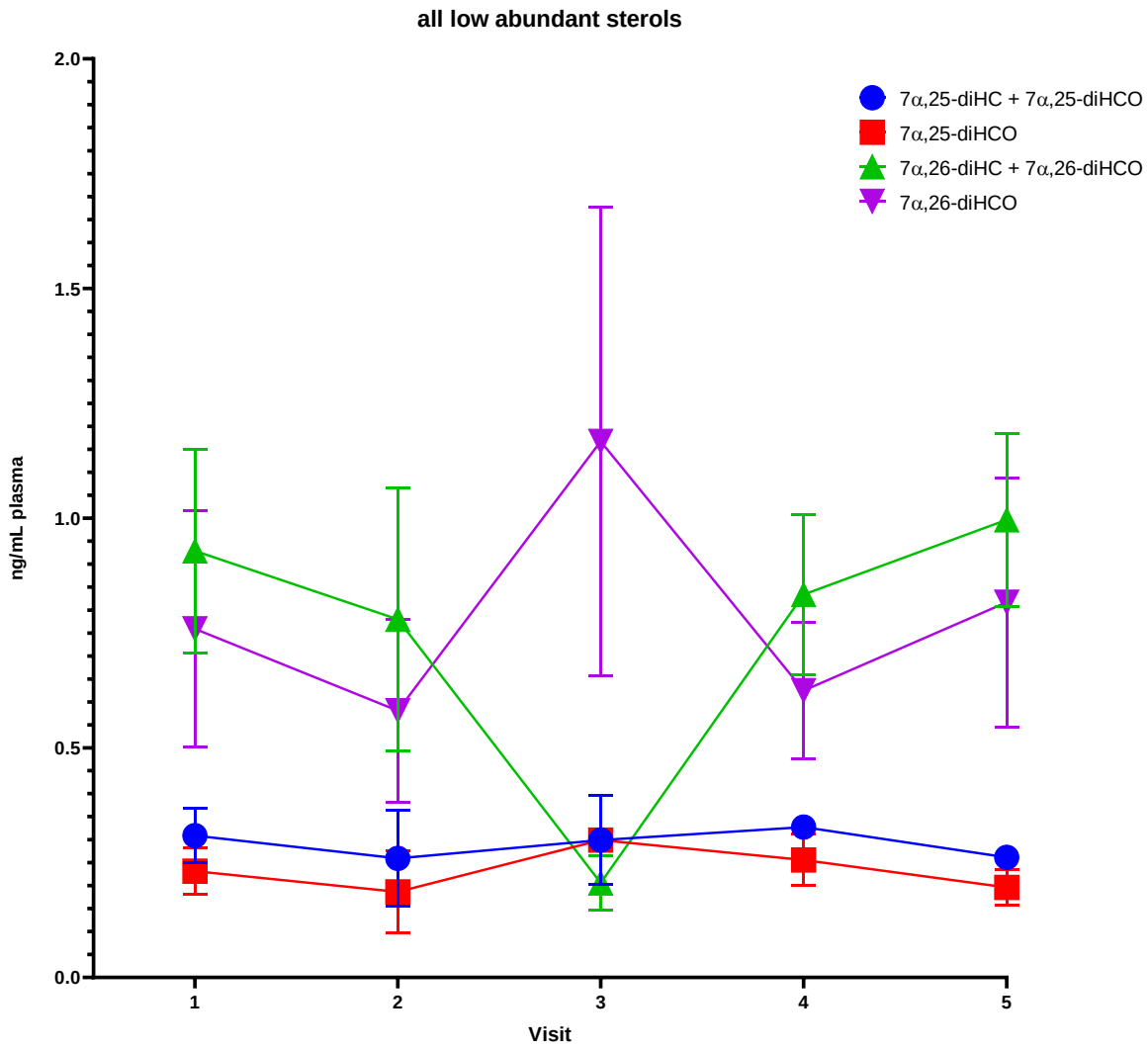

Figure 4.21 . Low abundant sterol plasma variation in PD patients over 90 months.
Visit 1, 0 months; visit 2, 36 months: visit 3. 54 months; visit 4, 72 months; visit 5, 90 months.

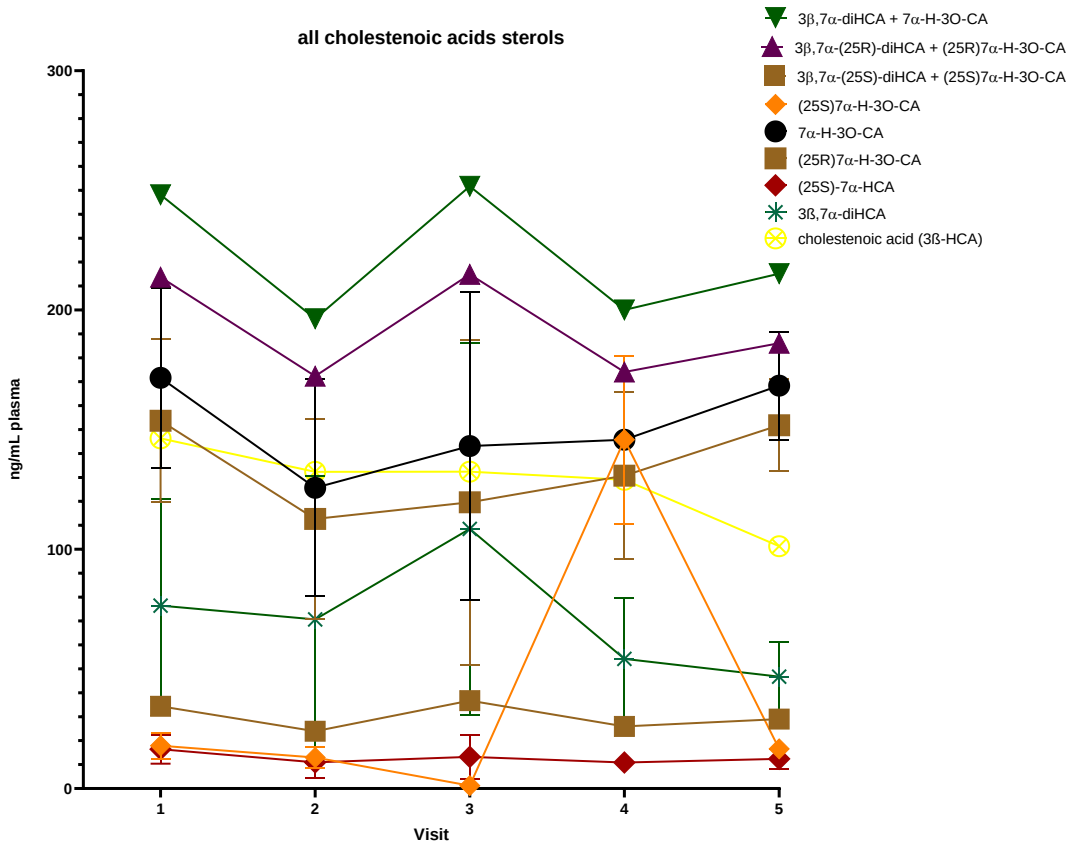

Figure 4.22 Cholestenoic acids plasma variation in PD patients over 90 months.

Visit 1, 0 months; visit 2, 36 months: visit 3. 54 months; visit 4, 72 months; visit 5, 90 months.

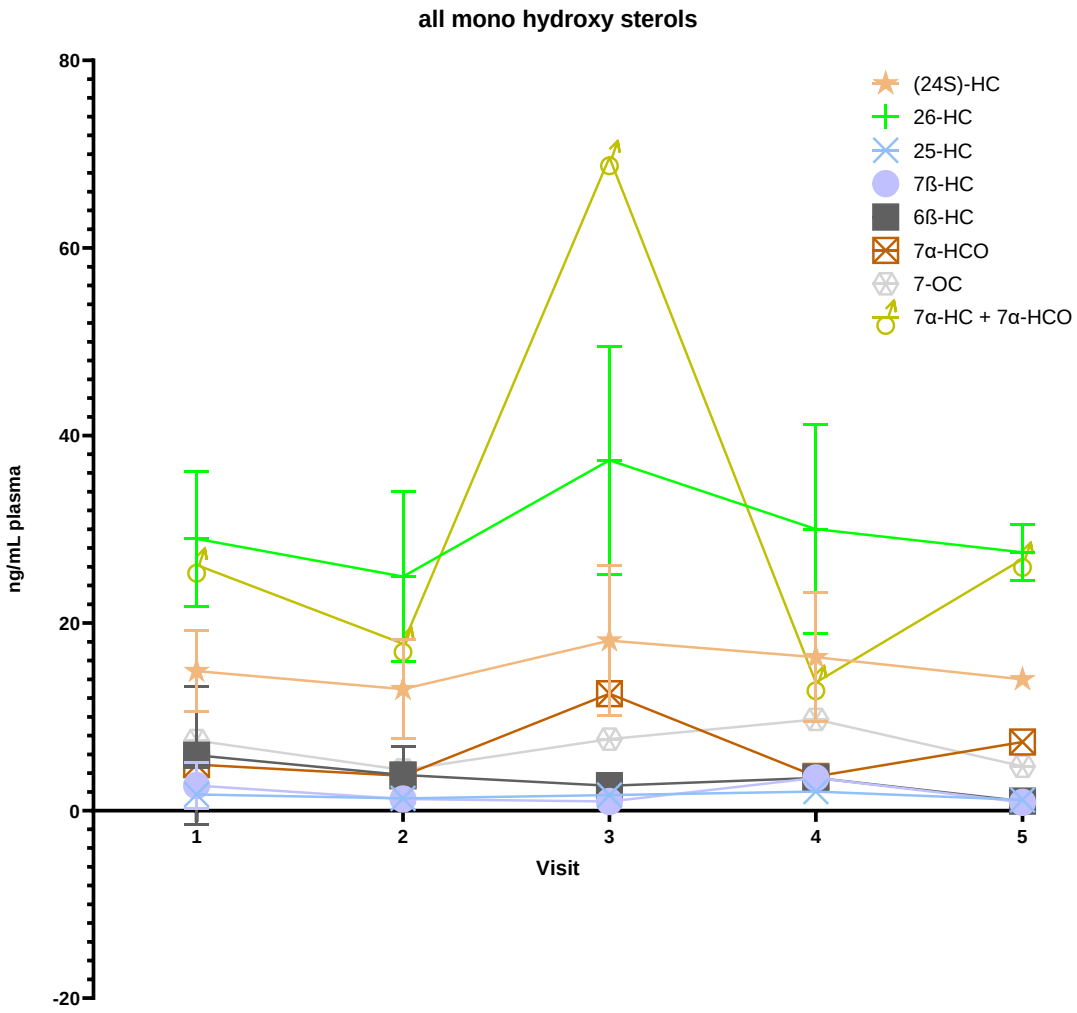

Figure 4.23 Mono hydroxy sterols plasma variation in PD patients over 90 months.
Visit 1, 0 months; visit 2, 36 months: visit 3. 54 months; visit 4, 72 months; visit 5, 90 months.

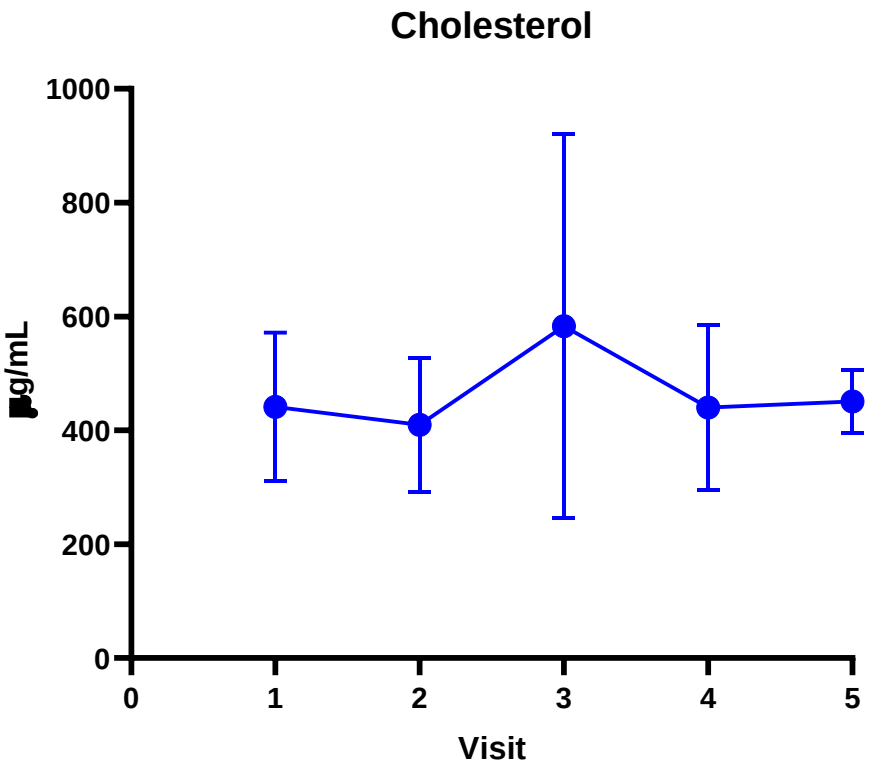

Figure 4.24 Cholesterol plasma variation in PD patients over 90 months.
Visit 1, 0 months; visit 2, 36 months: visit 3. 54 months; visit 4, 72 months; visit 5, 90 months.

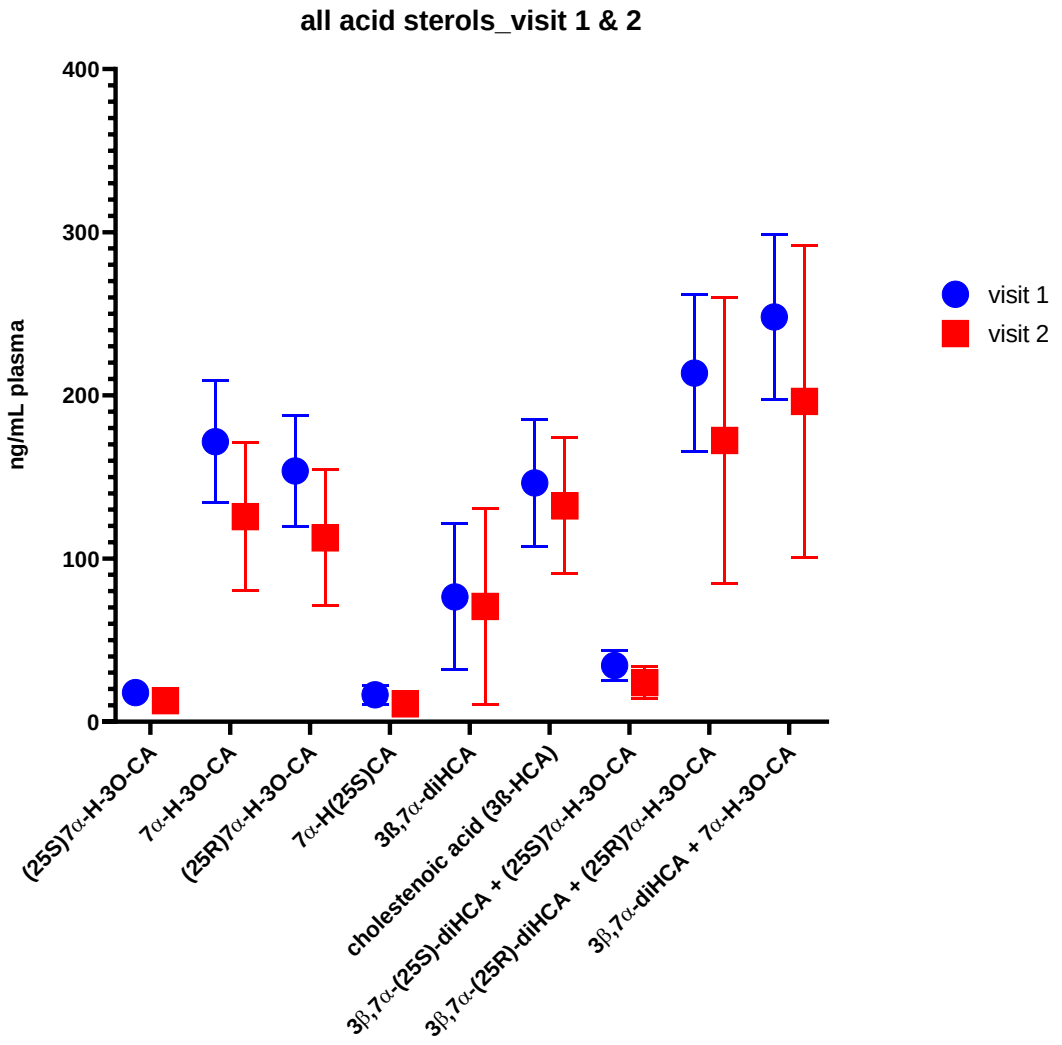

Figure 4.25 Comparison of the cholestenoic acids plasma values between Visit 1 (baseline) and Visit 2 (36 months).
The large spread among the mean value for each set of sterols between visit 1 and 2 nullify the apparent tendency to a diminished plasma concentration in 36 months' time.

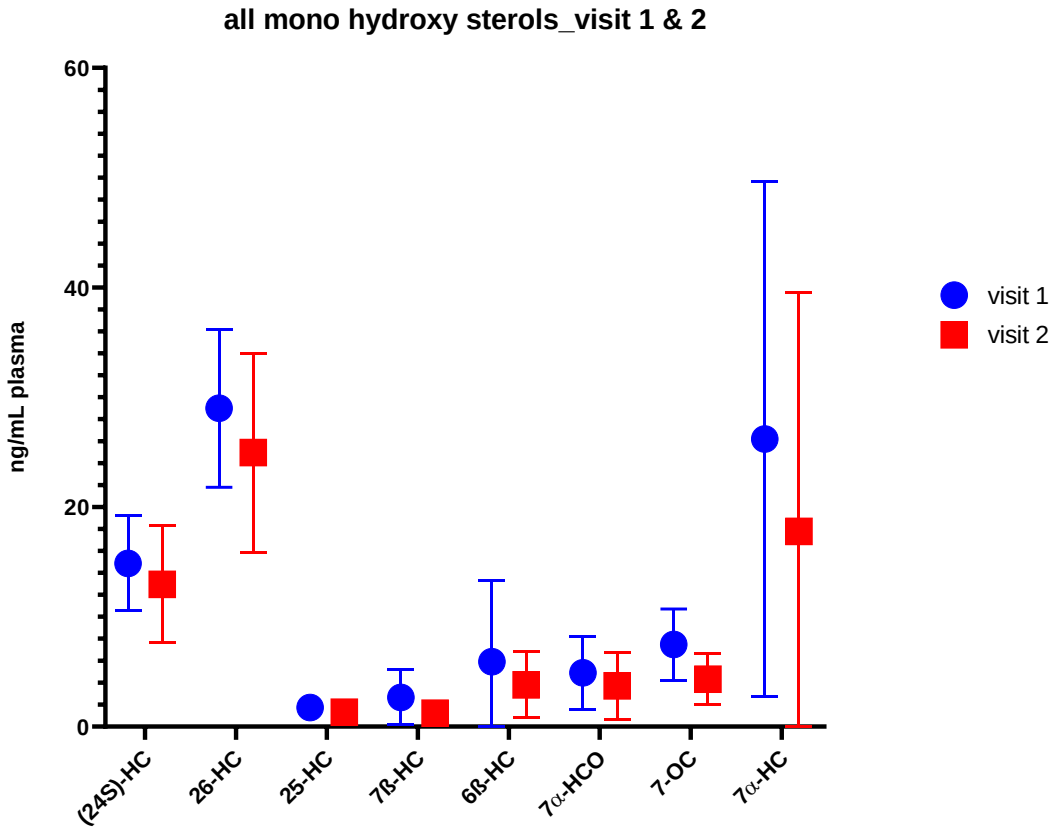

Figure 4.26 Comparison of the mono hydroxy sterols plasma values between Visit 1 (baseline) and Visit 2 (36 months).

The large spread among the mean value for each set of sterols between visits 1 and 2 nullify the apparent tendency to a diminished plasma concentration in 36 months' time.

.

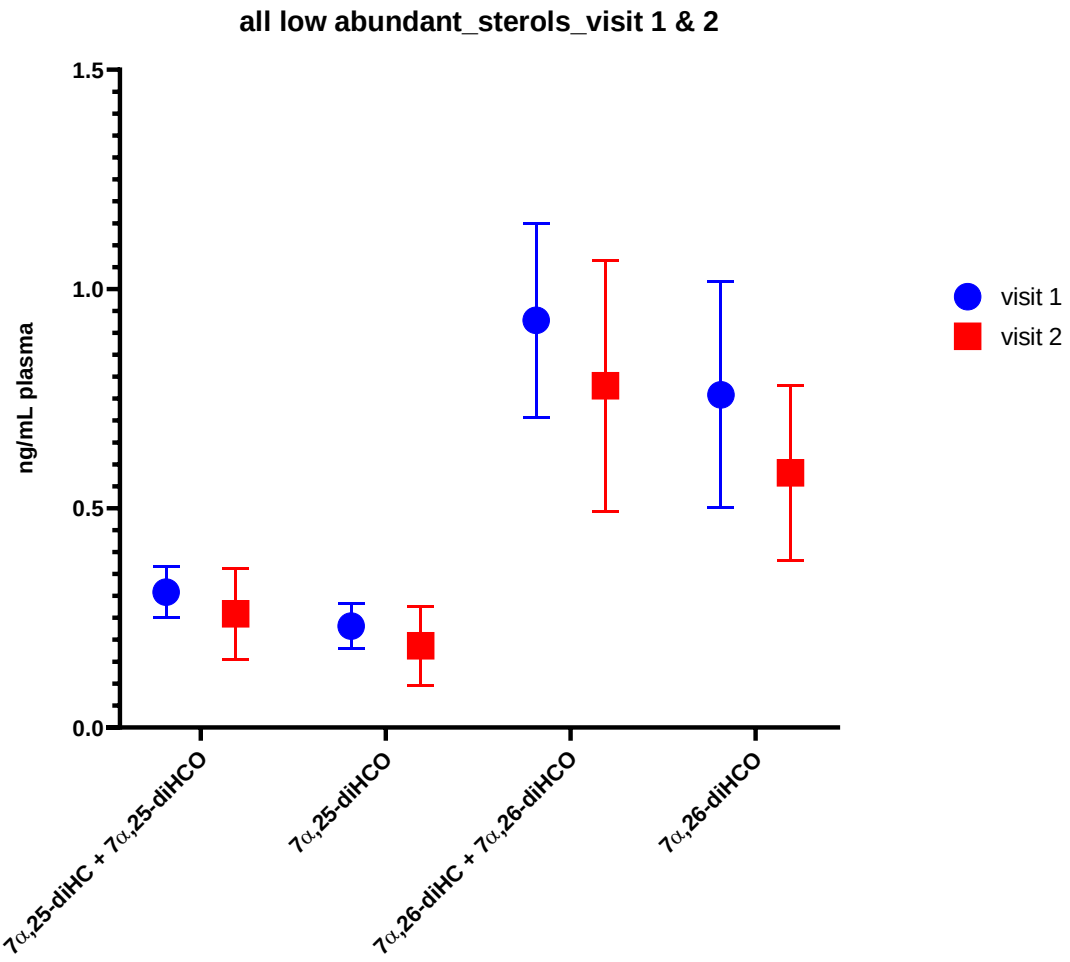

Figure 4.27 Comparison of the di hydroxy-low abundant sterols plasma values between Visit 1 (baseline) and Visit 2 (36 months). The large spread among the mean value for each set of sterols between visits 1 and 2 nullify the apparent tendency to a diminished plasma concentration in 36 months' time.

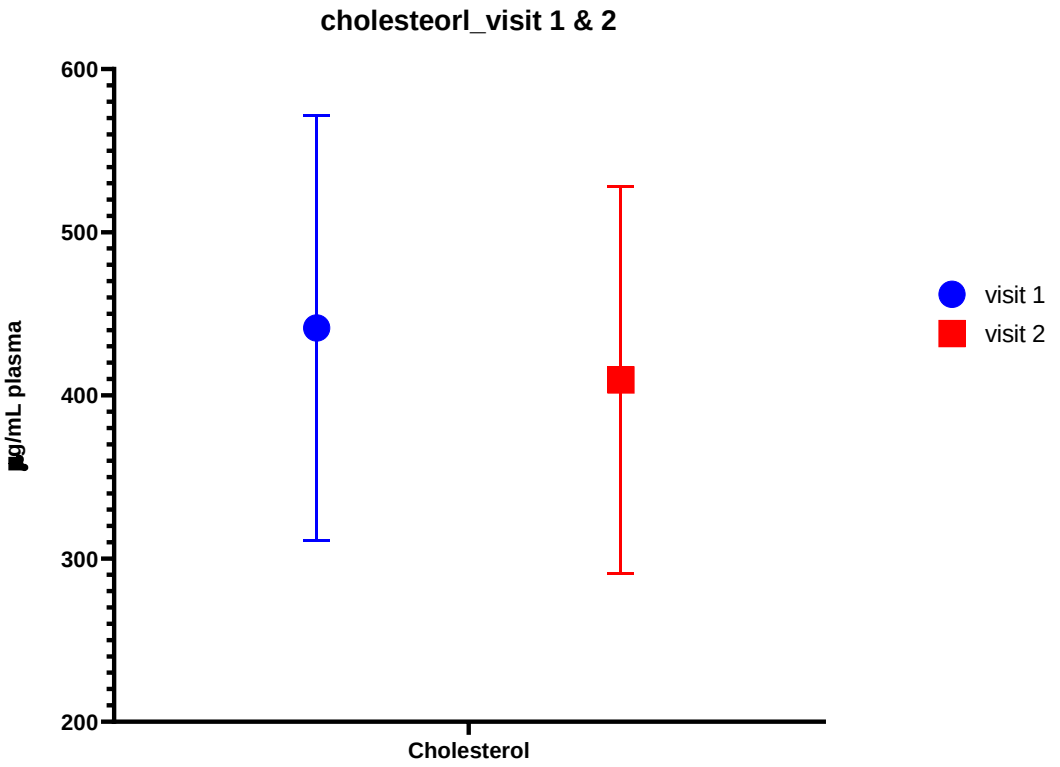

Figure 4.28 Comparison of the cholesterol plasma values between Visit 1 (baseline) and Visit 2 (36 months).
The large spread among the mean value for cholesterol between visits 1 and 2 nullify the apparent tendency to a diminished plasma concentration in 36 months' time.

The lack of statistical variance in the 36 months progression of the disease has led us to consider the possibility that it might be attributable to patients' specific personal variation. Therefore, single patients' sterol values have been plotted over the 36 months period to evaluate the contribution of the biological variation, figure 4.29 panels A, B and C. The graphs of figure 4.29 endorsed our speculation on the masking effect of intrinsic human plasma sterol biological variation on the overall trend of either decline or relative stability over time in PD patients.

A

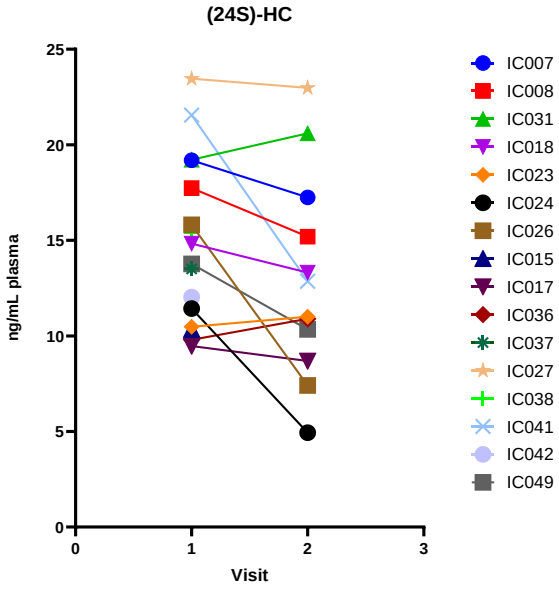
(24S)-HC
ng/mL plasma
Visit
IC007
IC008
IC031
IC018
IC023
IC024
IC026
IC015
IC017
IC036
IC037
IC027
IC038
IC041
IC042
IC049

B

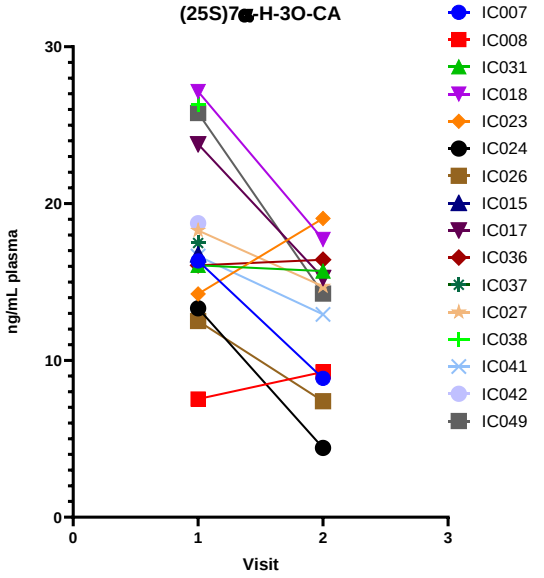
(25S)7α-H-3O-CA
ng/mL plasma
Visit
IC007
IC008
IC031
IC018
IC023
IC024
IC026
IC015
IC017
IC036
IC037
IC027
IC038
IC041
IC042
IC049

C

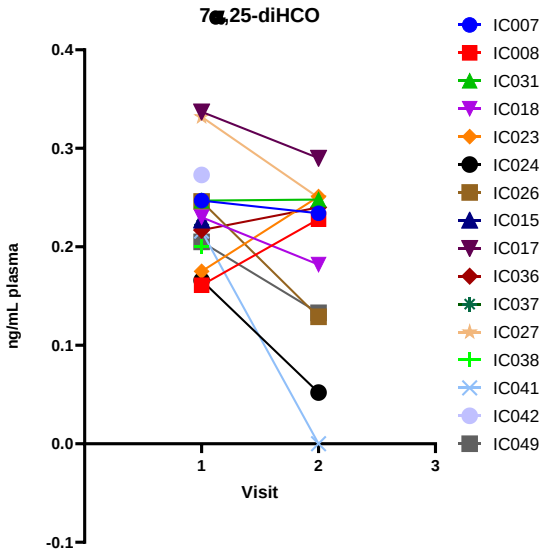
7α,25-diHCO
ng/mL plasma
Visit
IC007
IC008
IC031
IC018
IC023
IC024
IC026
IC015
IC017
IC036
IC037
IC027
IC038
IC041
IC042
IC049

Figure 4.29 (24S)-HC, (25S)7α-H-3O-CA and 7α,25-diHC single patients levels variations.
(A) (24S)-HC plasma levels in longitudinal PD patient over 36 months period. Values reported as absolute ng/mL per patients. (B) (25S)7α-H-3O-CA plasma levels in longitudinal PD patient over 36 months period. Values reported as absolute ng/mL per patients. (C) 7α,25-diHCO plasma levels in longitudinal PD patient over 36 months period. Values reported as ng/mL per patients.

4.4.3 Sterolome profile of longitudinal CSF from progressive PD patients: in search for disease progression predictor biomarkers

143 CSF samples from 80 different PD patients, sampled over a period of 96 months after the onset of the disease, have been screened for the free/non-esterified polar sterols content. Following the 3 days protocol described in sections 4.3.2 to 4.3.4, 10 different sterols have been identified in human CSF, all belonging to the subclass of cholestenoic acids, of which 3 mono-hydroxy cholestenoic acids (3ß,7α-diHCA, (25S)3ß,7α-diHCA & (25R)3ß,7α-diHCA), three mono-hydroxy cholestenonic acids (7α-H-3O-CA, (25S)7α-H-3O-CA & (25R)7α-H-3O-CA), cholestenoic acid (CA), and three di-hydroxy cholestene-3-noic acids (7α,24S)-diH-3O-CA, 7α,X-diH-3O-CA and 7α,25-diH-3O-CA. Good chromatographic separation is obtained when the 37-minutes gradient elution modes is employed, resulting in base line peak separation for most of the Girard P-derivatised CSF sterols, see figure 4.30 and 4.31. Structure attribution of the chromatogram peaks with mass to charge ratio of 580, 585, 564, which correspond to di-hydroxy and mono-hydroxy cholestenoic acids *m/z* when derivatised with GP D5/0, and 569 is done through retention time and accurate mass match with the software trace finder plus additional comparison of the fragmentation pattern MS^3 with internal library, refer to the tables 7.5, 7.7, 7.8, 7.10 & 7.11 in the appendix for details. Relative quantification is done against the designated deuterated internal standard, refer to table 7.19 in the appendix for details. Details of internal standard mix used can be found in section 2.1.3.1.

The cholestenonic acids (7α,24S)-diH-3O-CA, 7α,X-diH-3O-CA and 7α,25-diH-3O-CA are low abundant cholesterol metabolites and intermediates in the bile acids biosynthetic pathway. Even though most of the human sterols can be present as both 3-hydroxyl and 3-oxo forms, the 3-OH form of these three di-hydroxy cholestenoic acids is mainly present in human urine and plasma (W. J. Griffiths, Abdel-Khalik, *et al.*, 2019; W. J. Griffiths & Wang, 2020; Ogundare *et al.*, 2010b; Yutuc *et al.*, 2021). Indeed, more than 90% of the human CSF di-hydroxy cholestenoic acids is present as their 3-oxo form. Being (7α,24S)-diH-3O-CA, 7α,X-diH-3O-CA and 7α,25-diH-3O-CA low abundant sterols in CSF (average concentration is between less than 1 to few ng/mL) their 3-hydroxyl counterpart, which represent less than 10%*)* of the di-hydroxy CA content, may not be detected as it could fell under the limit of detection of the analytical technique employed (Abdel-Khalik *et al.*, 2018). The analytical methodology employed in this thesis is quite sensitive (LOD estimated to be 10 pg/mL for sterols) but the di-hydroxy CA values might fell under the limit of quantification, which is estimated to be 100 pg/mL(Yutuc *et al.*, 2021). Moreover, the protocol used for sterol identification cannot directly identify the naturally possessing 3β-OH sterols, if not indirectly, either by differences between FrAs (accounting for both 3-hydroxyls and 3-oxo) and Bs (only 3-oxo) or by no sterol detection in FrBs. Hence, it is assumed that (7α,24S)-diH-3O-CA, 7α,X-diH-3O-CA and 7α,25-diH-3O-CA represent the main and exclusive CSF form and that their values equals between FrAs and Bs. As such only FrBs data are reported.

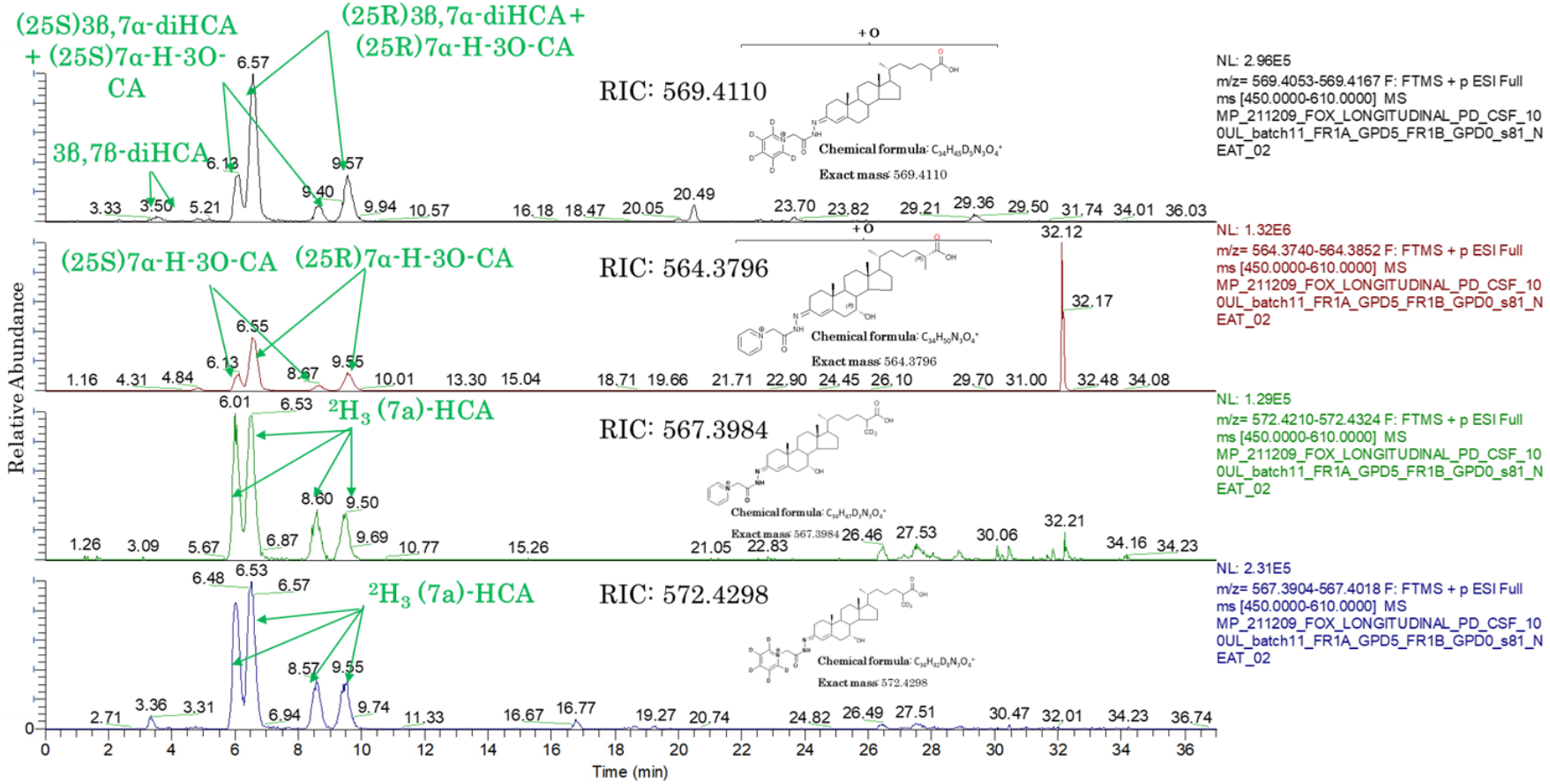

Figure 4.30 Chromatogram of NYPUM longitudinal CSF showing the main CSF cholestenoic acids.

The peaks showed in the upper panel of figure 4.30 represent the molecular ions with exact mass of 569.4110 *m/z*, result of 3β,7β-diHCA, (25S)3β,7α-diHCA + (25S)7α-H-3O-CA and (25R)3β,7α-diHCA + (25R)7α-H-3O-CA derivatisation with the hydrazine GP D5.The peaks showed in the second panel of figure 4.30 represent the molecular ions with exact mass of 564.3796 *m/z*, result of (25S)7α-H-3O-CA and (25R)7α-H-3O-CA derivatisation with the

hydrazine GP D0. The peaks showed in the third panel of figure 4.30 represent the molecular ions with exact mass of 567.3961 *m/z*, result of the internal standard $^{2}H_{3}$ (7a)-HCA derivatisation with the hydrazine GP D0. The peaks showed in the lower panel of figure 4.30 represent the molecular ions with exact mass of 572.4298 *m/z*, result of the internal standard $^{2}H_{3}$ (7a)-HCA derivatisation with the hydrazine GP D5. Peak at 32.17 minutes in 564.3796 *m/z* is a contaminant coming from the mobile phases and not interfering with the analysis and relative quantification of the designated sterol molecules. RIC, reconstructed ion chromatogram.

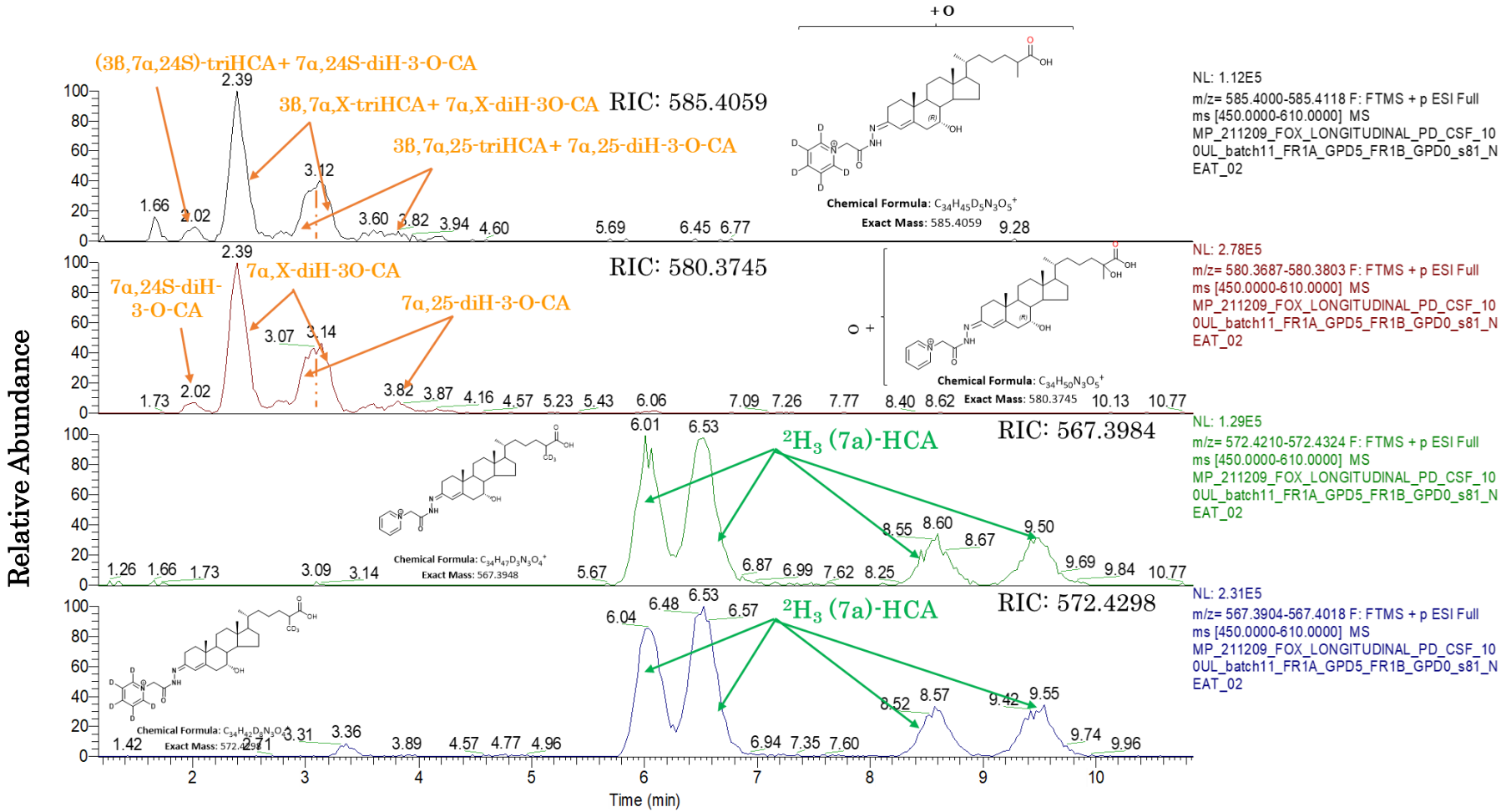

Figure 4.31 Chromatogram of NYPUM longitudinal CSF showing main CSF cholestenoic acids.
The peaks showed in the upper panel of figure 4.31 represent the molecular ions with exact mass of 585.4059 *m/z*, result of the (3β,7α,24S)-triHCA + 7α,24S-diH-3-O-CA, 3β,7α,25-triHCA + 7α,25-diH-3-O-CA and 3β,7α,X-triHCA+ 7α,X-diH-3-O-CA derivatised with the hydrazine GP D5. The peaks showed in the second panel of figure 4.31 represent

the molecular ions with exact mass of 580.3745 *m/z*, result of (7α,24S)-diH-3-O-CA 7α,25-diH-3O-CA and 7α, X-diH-3O-CA derivatisation with the hydrazine GP D0. The peaks showed in the third panel of figure 4.31 represent the molecular ions with exact mass of 567.3961 *m/z*, result of the internal standard $^{2}H_{3}$ (7a)-HCA derivatisation with the hydrazine GP D0. The peaks showed in the lower panel of figure 4.31 represent the molecular ions with exact mass of 572.4298 *m/z*, result of the internal standard $^{2}H_{3}$ (7a)-HCA derivatisation with the hydrazine GP D5. RIC, reconstructed ion chromatogram.

With regards to sterols variation over time, depicted in the graphs 4.32, 4.33, and 4.34 the cholestenoic acid values seems to remain quite stable during the disease progression.

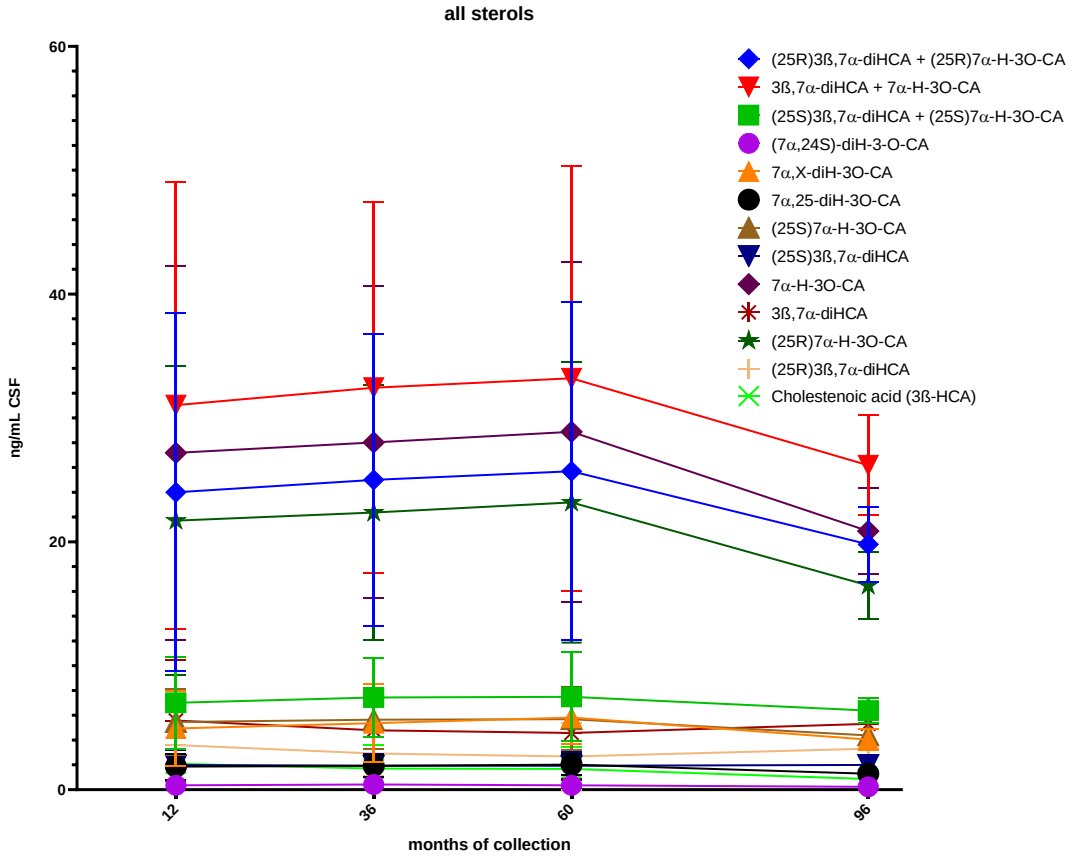

Figure 4.32 CSF sterols variation over 96 months after PD diagnosis. All the values are expressed in ng per mL of CSF. No major variations are appreciated in this cohort of PD patients.

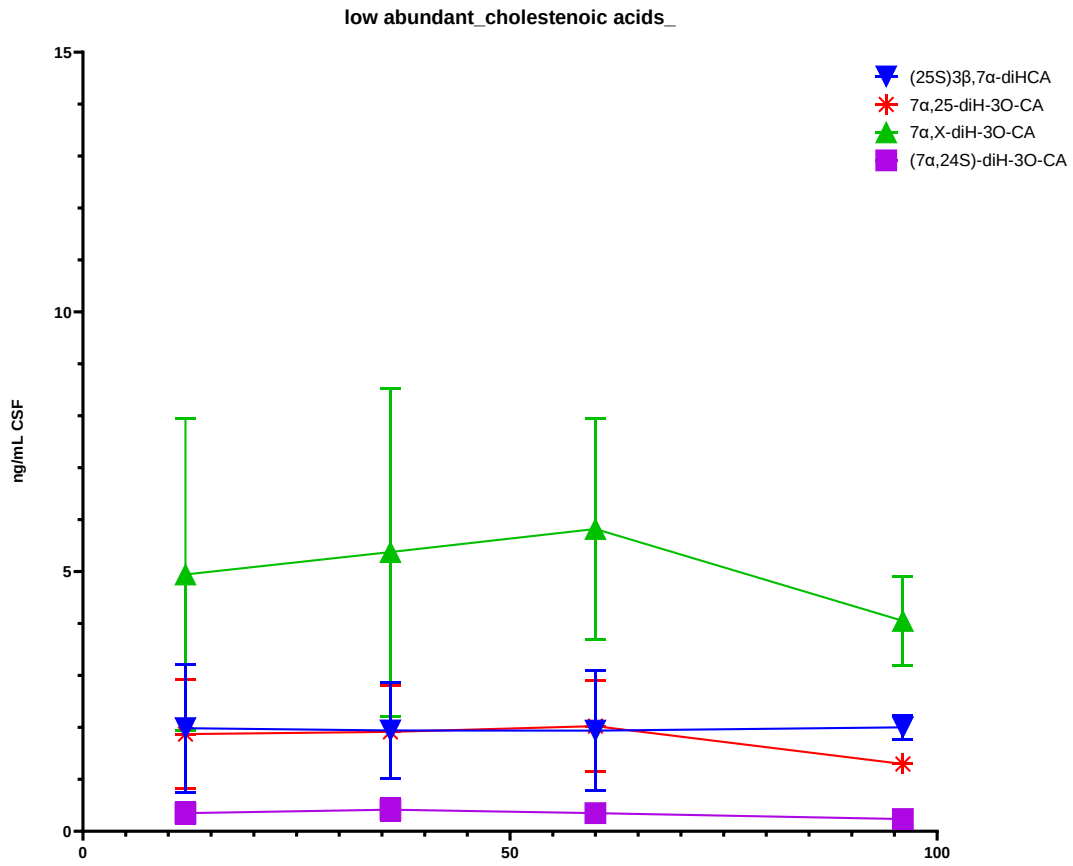

Figure 4.33 CSF low abundant cholestenoic acid variation over 96 months after PD diagnosis.
All the values are expressed in ng per mL of CSF. No major variations are appreciated in this cohort of PD patients.

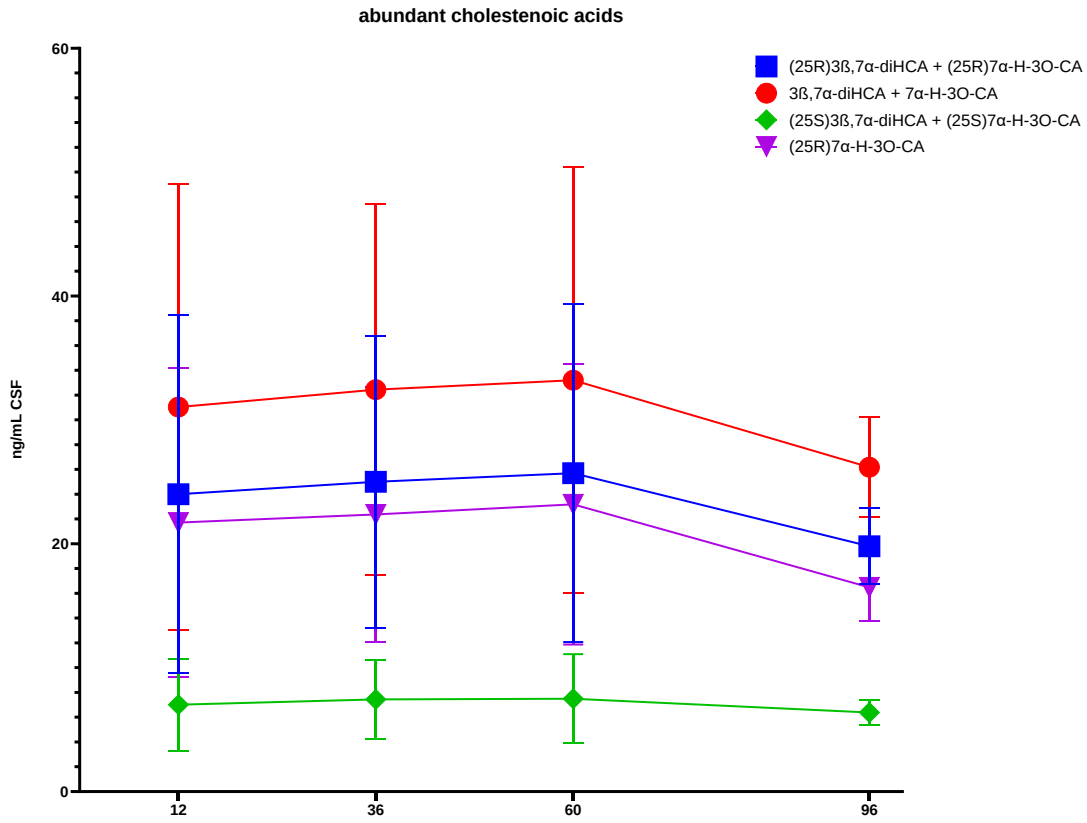

Figure 4.34 CSF most abundant cholestenoic acid variation over 96 months after PD diagnosis.
All the values are expressed in ng per mL of CSF. No major variations are appreciated in this cohort of PD patients.

Most of the CSF samples from this longitudinal cohort of PD patients have been collected between 12, 36 and 60 months, with 69, 43 and 27 samples, respectively. The remaining four samples belong to the 96 months' time point. Due to the high variation in the patient distribution of the first three collection points with the last one, statistical analysis was carried out only between 12, 36 and 60 months. A mixed effect model for repeated measures analysis has been used to test sterol variation over 60 months. However, no variation for any CSF sterols over time is reported, graphs 4.35, 4.36 and 4.37.

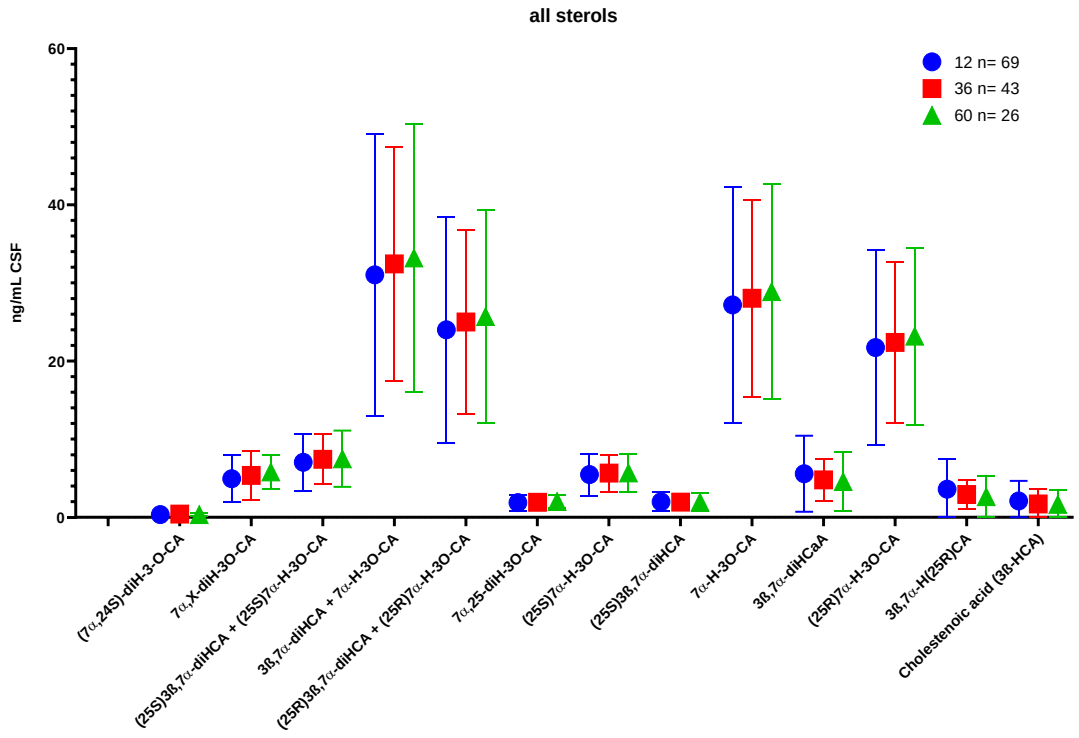

Figure 4.35 Comparison of the CSF sterol values between 12, 36 and 60 months.

The mean value for each cholestenoic acid among the three points of collection seem to be quite constant over time. The absence of statistical variation, tested with mixed effect model for repeated measures analysis, might be consequence of a large spread among the mean value for each set of sterols. The biological variation is, however, maintained constant over 5 years, from 12 to 60 months.

.

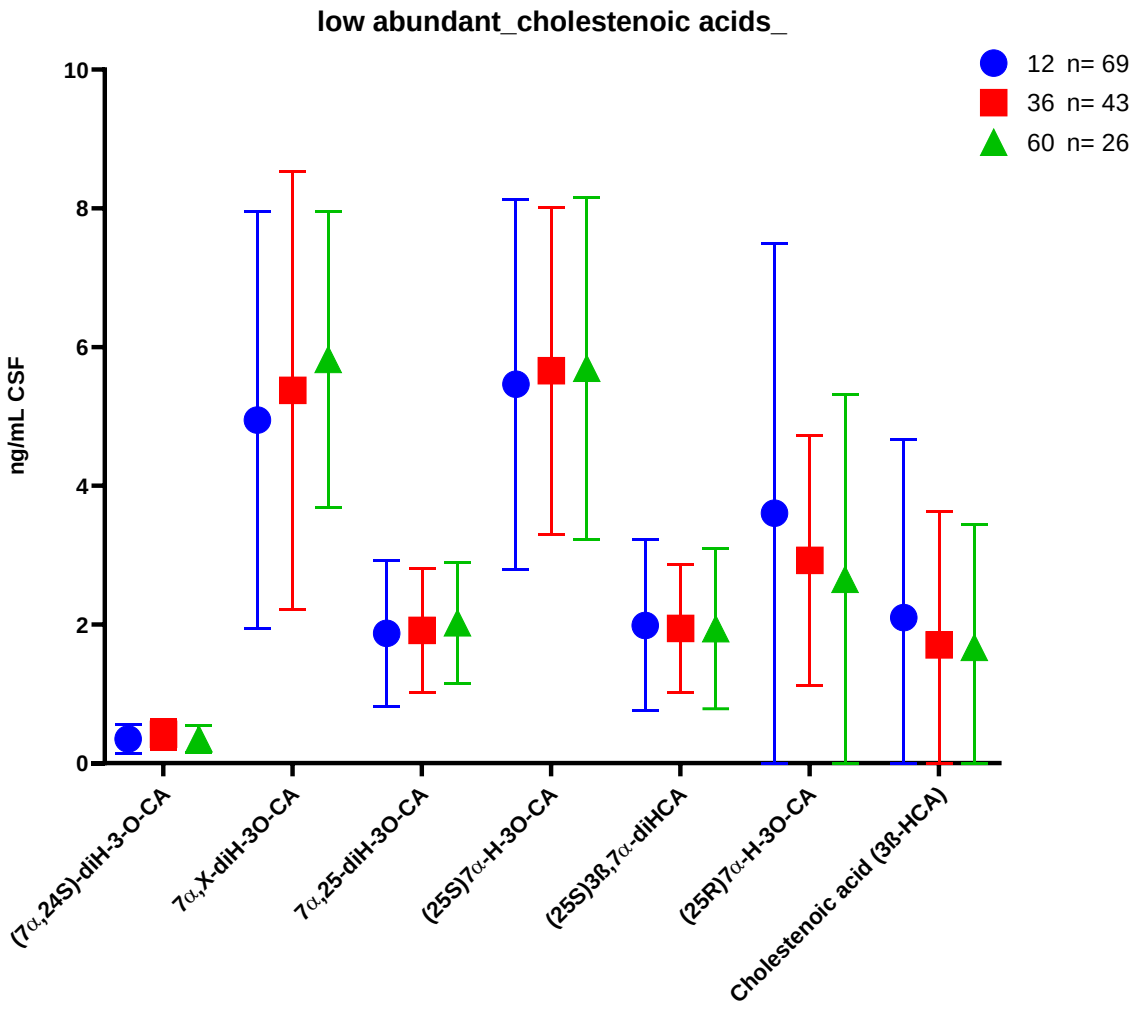

Figure 4.36 Comparison of the CSF low abundant cholestenoic acids values between 12, 36 and 60 months.

The mean value for each cholestenoic acid among the three points of collection seem to be quite constant over time. The absence of statistical variation, tested with mixed effect model for repeated measures analysis, might be consequence of a large spread among the mean value for each set of sterols. The biological variation is, however, maintained constant over 5 years, from 12 to 60 months.

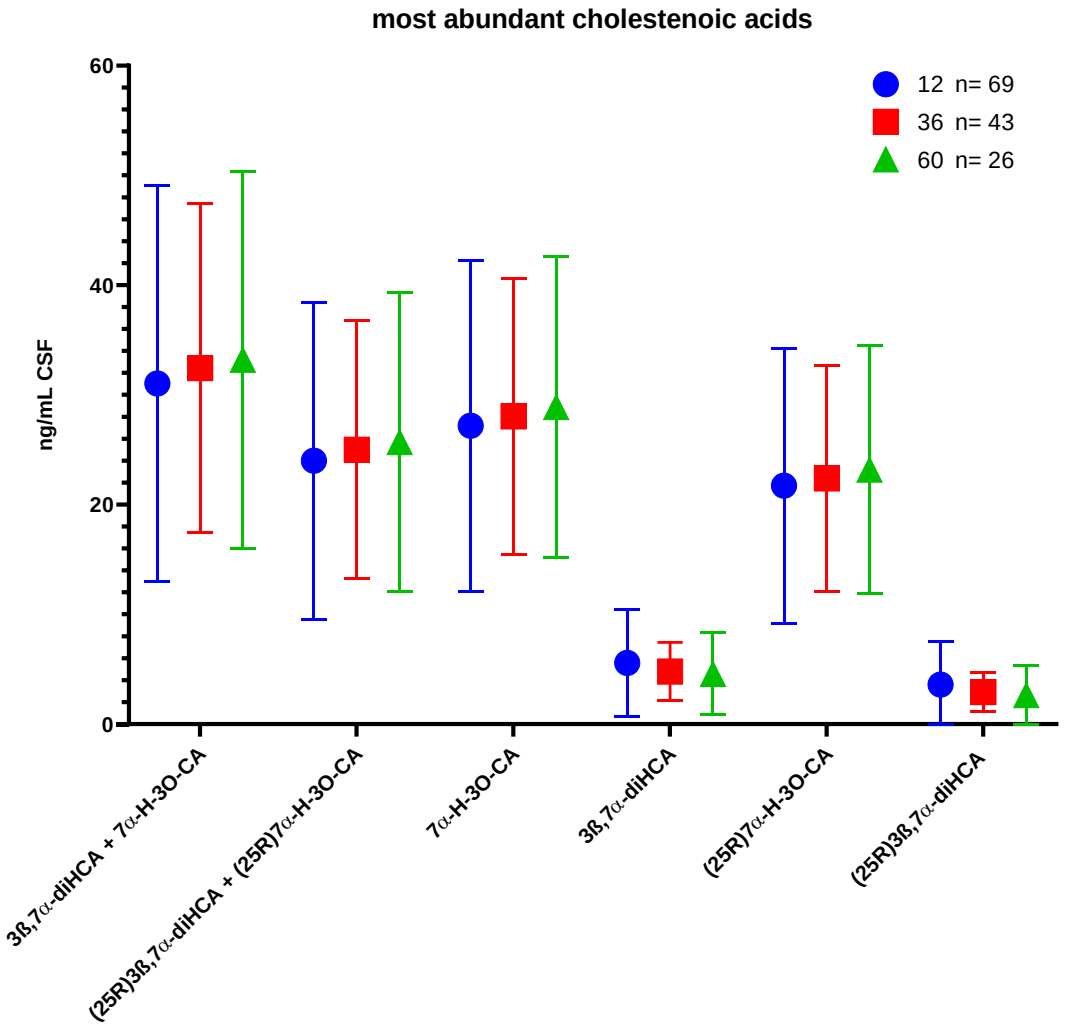

Figure 4.37 Comparison of the most abundant CSF cholestenoic acids between 12, 36 and 60 months.
The mean value for each cholestenoic acid among the three points of collection seem to be quite constant over time. The absence of statistical variation, tested with mixed effect model for repeated measures analysis, might be consequence of a large spread among the mean value for each set of sterols. The biological variation is, however, maintained constant over 5 years, from 12 to 60 months.

From Figures 4.35, 4.36 and 4.37, it is possible to notice a quite large biological variation within all the sterols, which might have affected the statistical test result. However, the spread of the values around the mean is maintained quite constant over time. Indeed, when the individual sterol values are plotted per single patient, figure 4.38,

most of the sterol levels remains in the +/- one SD range, particularly between months 12 and 36, figure 4.38 panel A. However, some major fluctuations are seen between months 36 and 60, which however affect a minimal part of the patients, figure 4.38 panel B. The huge biological variation complicates data interpretation, but we could affirm that the majority of the sterol values tend to remain stable over time with minimal variation.

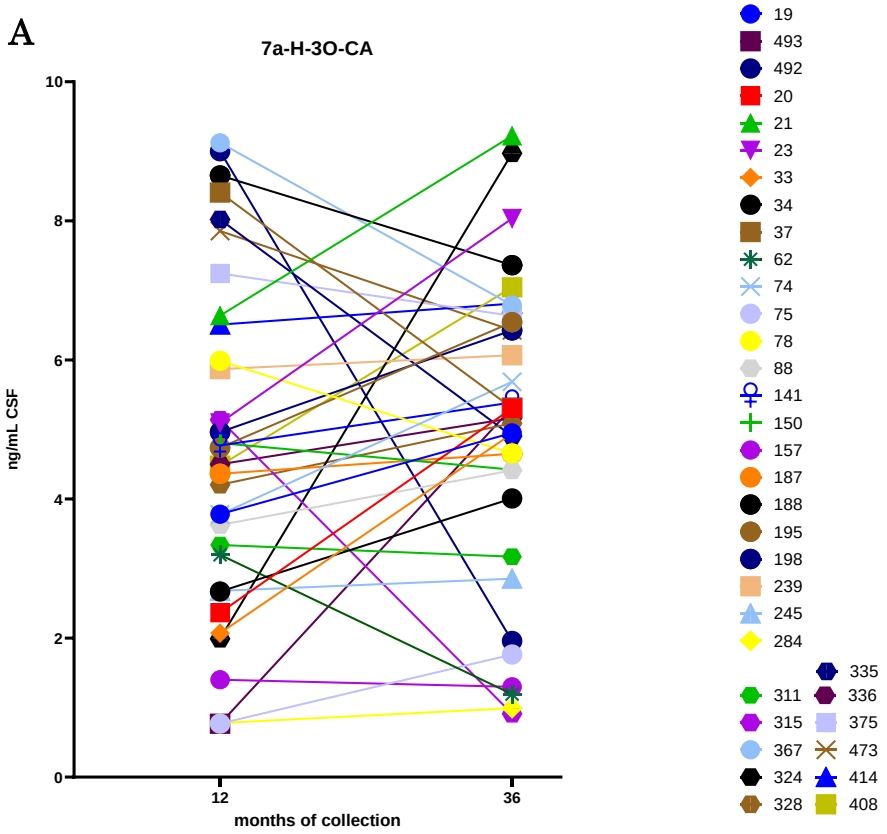
A
7a-H-3O-CA
ng/mL CSF
months of collection
0
2
4
6
8
10
12
36
19
493
492
20
21
23
33
34
37
62
74
75
78
88
141
150
157
187
188
195
198
239
245
284
311
315
367
324
328
335
336
375
473
414
408

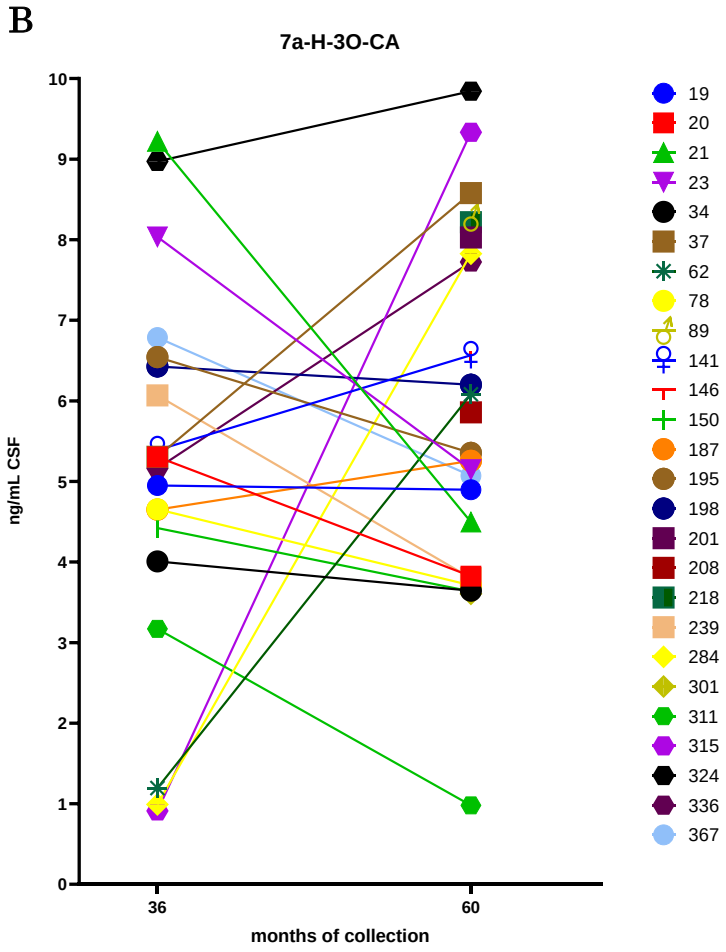
B
7a-H-3O-CA
ng/mL CSF
months of collection
0
1
2
3
4
5
6
7
8
9
10
36
60
19
20
21
23
34
37
62
78
89
141
146
150
187
195
198
201
208
218
239
284
301
311
315
324
336
367

Figure 4.38 Single patients CSF values for 7α-H-3O-CA over 60 months after diagnosis of PD.
Over 60 months period, the single patients CSF values for 7α-H-3O-CA tend to almost unchanged, with minor fluctuations that tend to balance out over time. Although some significant variation can be identified, they represent the minority in the group. Evident is the huge spread of values around the mean, due to biological variation. Need to note that for some patients 36- and 60-months collection point were not available. (A) variations between 12 and 36 months. (B) variations between 36 and 60months.

The gender contribution to sterol levels has also been investigated, see Figure 4.39. The mixed effect model for repeated measures analysis has also been used to test for any variation in males' and females' CSF sterol values. However, the outcome did not change. No statistical variation has been reported in males' and females' sterols values among 60 months, except for the sterols 7α-H-3O-CA and (25R)7α-H-3O-CA ($p=0.043$ and $p=0.041$, respectively) between the 36 and 60 months in females. However, among the 23 females recruited in this study, only six have both data points at 36 and 60 months, which makes the findings most likely not representative of the actual sterol fluctuations.

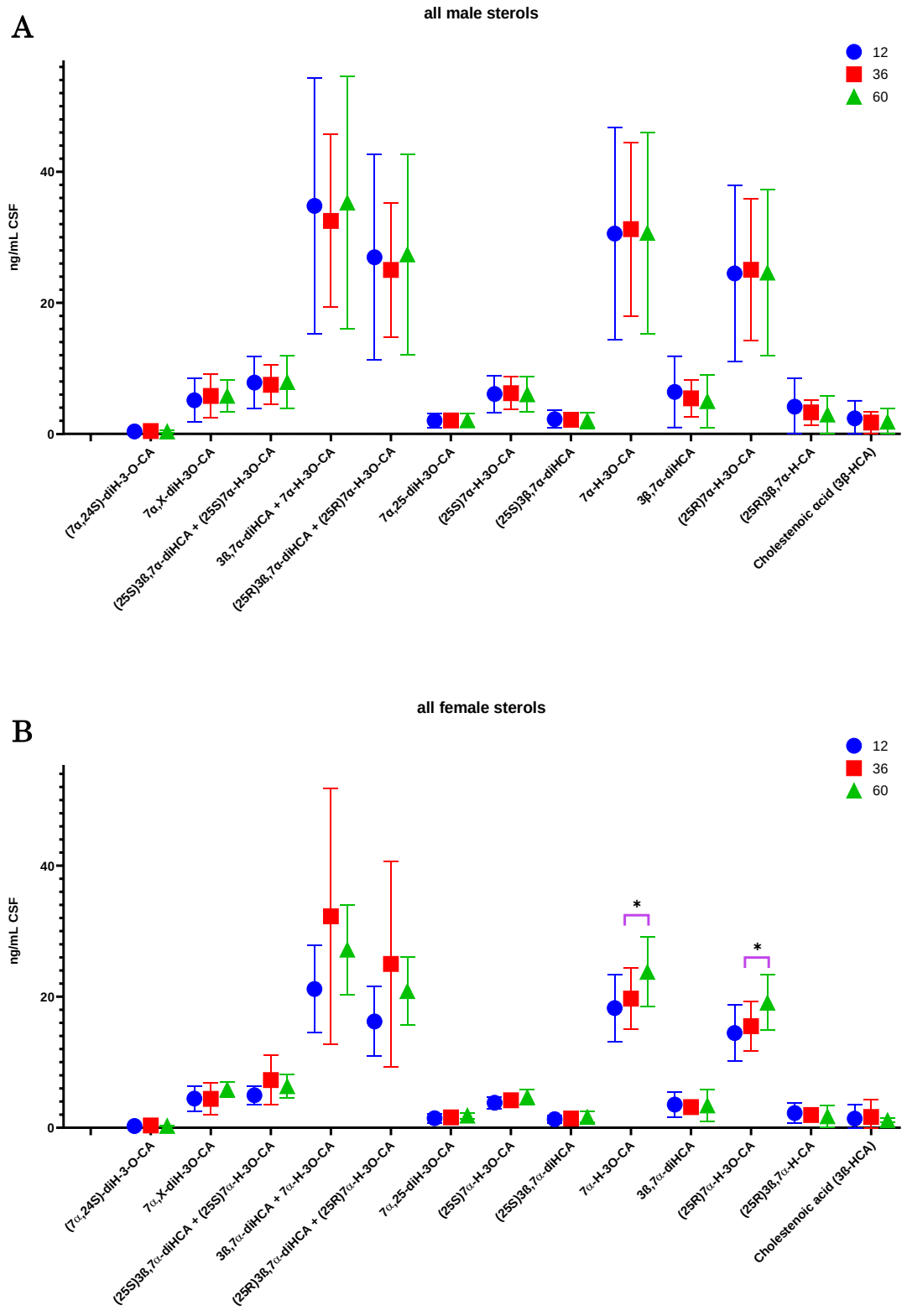

Figure 4.39 Males and females' distribution of the most abundant CSF cholestenoic acids values between 12, 36 and 60 months.
The mean value for each cholestenoic acid collection among the three points of collection seem to be quite constant in males, panel A. The absence of statistical variation, tested with mixed effect model for

repeated measures analysis, might be consequence of a large spread among the mean value for each set of sterols. The biological variation is, however, maintained constant over 5 years, from 12 to 60 months. Panel B reveals a similar situation for PD females over time, with the exception of 7α-H-3O-CA and (25R)7α-H-3O-CA, which is, however, a result obtained from only 6 females PD patients.

4.4.4 Sterolome profile of a second cohort of base line PD patients: the validation phase

243 human plasma samples from base line PD patients and from age/sex matched neurologically healthy individuals, BioFIND cohort, have been screened for the free/non-esterified polar sterols, cholesterol, and relative precursors. Following the 3 days protocol described in sections 4.3.2 to 4.3.4, the same set of 21 sterols found in the NYPUM PD baseline group have been identified, example chromatograms can be found in figures 4.40 (for individual values refer to table 7.24 in the appendix). Structure attribution has been made by retention time and accurate mass match with trace finder plus fingerprint fragmentation match with internal library, see the tables 7.1 to 7.13 in the appendix for details. The sterol lipids include 6 mono-hydroxy sterols of which seven mono-hydroxycholesterols (24S)-HC, 25-HC, 26-HC, 7β-HC, 7α-HC & 6β-HC and two mono-hydroxy cholestenones, 7-OC and 7α-HCO, 4 di-hydroxy sterols of which two di-hydroxycholesterols (7a,25-diHC & 7α,26-diHC) and two di-hydroxy cholestenones, (7α,25-diHCO & 7α,26-diHCO), 7 cholestenoic acids, of which three mono-hydroxy cholestenoic acids (3β,7α-diHCA, (25S)3β,7α-diHCA & (25R)3β,7α-diHCA), three mono-hydroxy cholestenonic acids (7α-H-3O-CA, (25S)7α-H-3O-CA & (25R)7α-H-3O-CA), and cholestenoic acid (CA), and cholesterol itself.

Good chromatographic separation is obtained when the 17- and 37-minutes gradient elution modes are employed, resulting in base line peak separation for most of the Girard P-derivatised plasma sterols. Relative quantification is against the designated deuterated internal standard, refer to table 7.17 in the appendix for details. Details of internal standard mix used can be found in section 2.1.2.

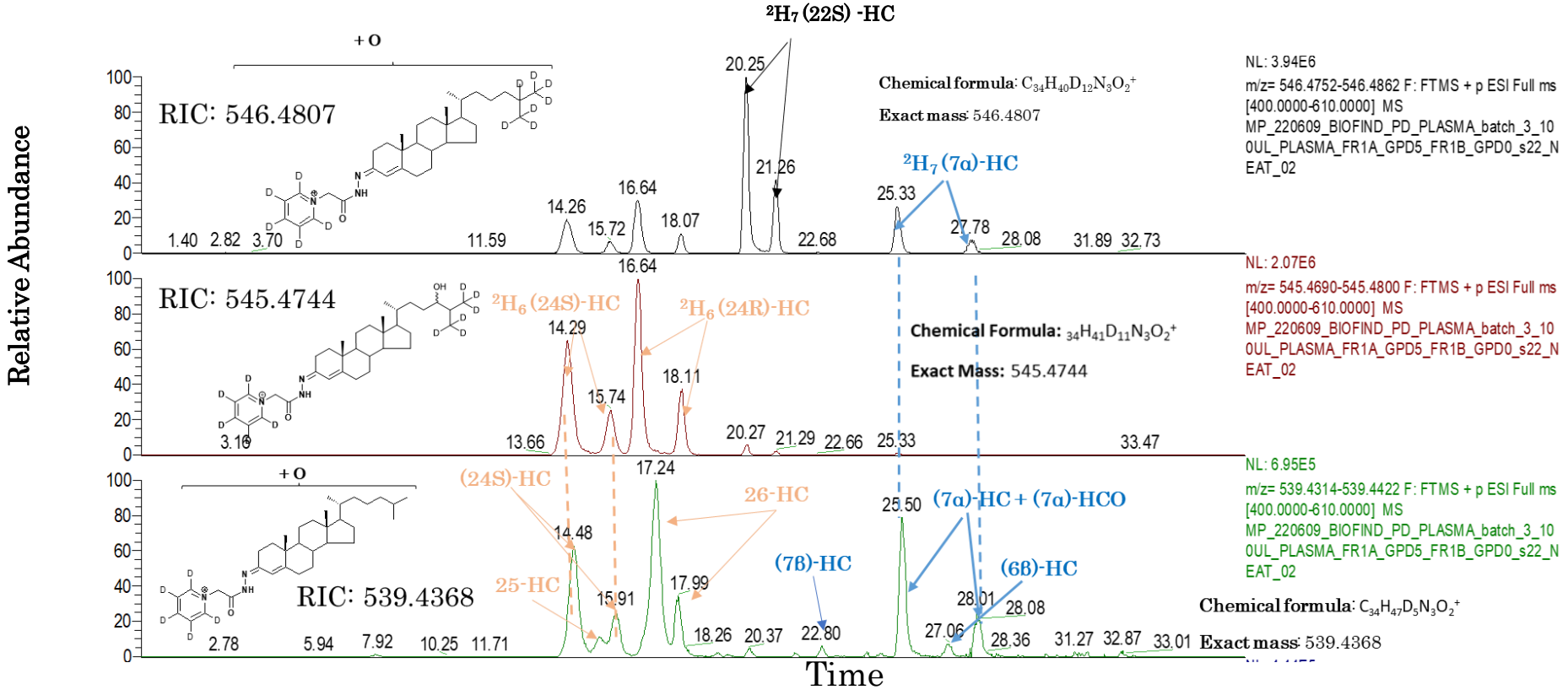

Figure 4.40 Chromatogram of BioFIND PD plasma showing the internal standard $^2H_7$(22S)-HC, $^2H_7$((7α)-HC, $^2H_6$ (24R/S)-HC and the main plasma sterols.

The peaks showed in the upper panel of figure 4.40 represent the molecular ions with exact mass of 546.4807 *m/z*, result of $^2H_7$(22S)-HC, $^2H_7$(7α)-HC derivatisation with the hydrazine GP D5. The peaks showed in the lower panel of figure 4.40 represent the molecular ions with exact mass of 545.4744 *m/z*, result of $^2H_6$(24R/S)-HC derivatisation with

the hydrazine GP D5. The peaks showed in the middle panel of figure 4.40 represent the molecular ions with exact mass of 539.4368 *m/z*, result of (24S)-HC, 25-HC, 26-HC, 7ß-HC, 7α-HCO + 7α-HC and 6ß-HC derivatisation with the hydrazine GP D5. RIC, reconstructed ion chromatogram.

Every sterol screening reported in this working thesis has been conducted unbiasedly, which requires being completely blind towards sample identities during the identification and quantification process. Therefore, information about the sample identities is available once the sterols profile of the entire sample set is completed. The BioFIND PD plasma project is still ongoing; as such, no information on PD and controls identities is yet accessible. However, preliminary data showing the main plasma mono-hydroxy cholesterols values are below the reported table 4.9. With regards to 24(S)-HC, 25-HC, 26-HC, 7β-HC, 7α-HC + 7a-HCO and 6β-HC plasma levels, both mean, and SD values are similar to the data reported for the NYPUM cohort of baseline PD patients. However, the minimal but significant difference in (24S)-HC between the PD and non-PD identified in the NYPUM cohort might not be appreciated in this group if the biological variation suppresses the variation in sterol levels.

Regarding values distribution, none of the sterols resulted normally distributed (negative for D'Agostino & Pearson test, Shapiro-Wilk test and Kolmogorov-Smirnov test). Moreover, it can be noted that most of the samples fall into the range +/- SD, even though some exceptions are present, figure 4.41. Future work will elucidate if any of the sterols identified would cluster or differ between PD and non-PD groups.

Table 4.9 Mean values, standard deviations, and coefficient of variation for the main plasma monohydroxy sterols of the BioFIND cohort.

Values expressed in ng/mL.

	24(S)-HC	25-HC	26-HC	7β-HC	7α-HC + 7a-HCO	6β-HC
Mean	15.03	1.42	25.24	2.16	33.08	3.98
Standard Deviation	4.37	0.37	6.31	1.66	31.26	3.48
CV	0.29	0.26	0.25	0.77	0.94	0.23

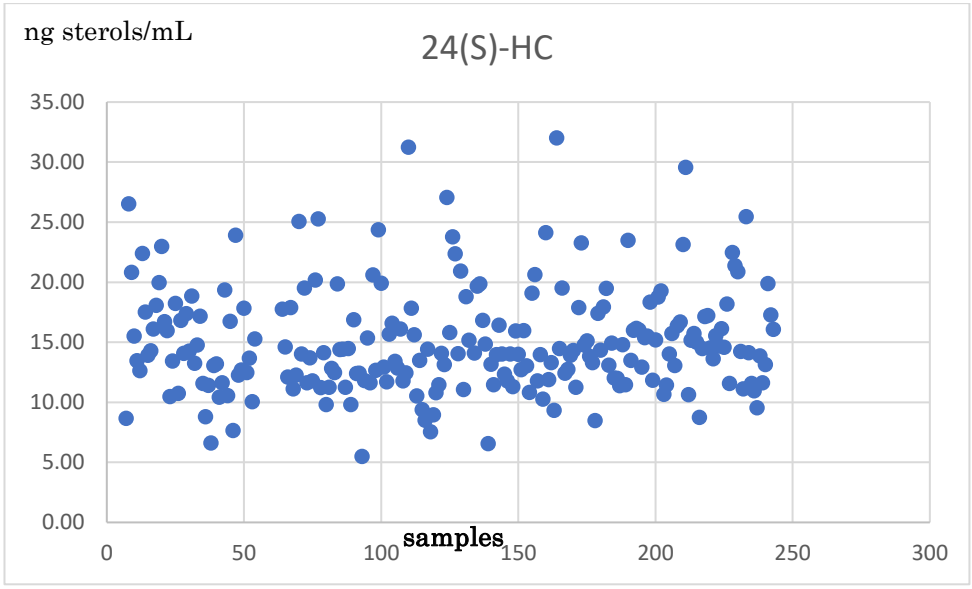
ng sterols/mL
24(S)-HC
35.00
30.00
25.00
20.00
15.00
10.00
5.00
0.00
0
50
100
150
200
250
300
samples

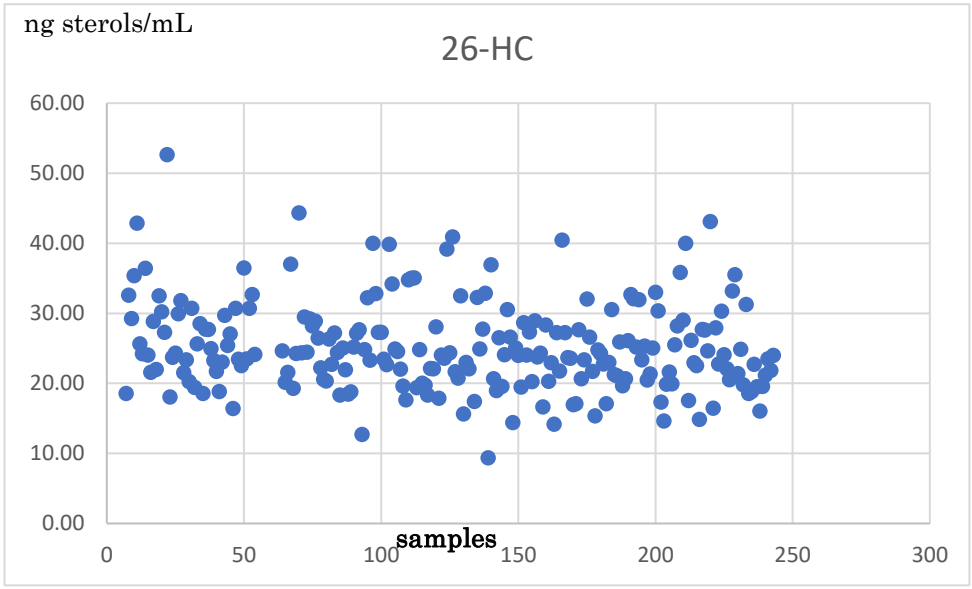
ng sterols/mL
26-HC
60.00
50.00
40.00
30.00
20.00
10.00
0.00
0
50
100
150
200
250
300
samples

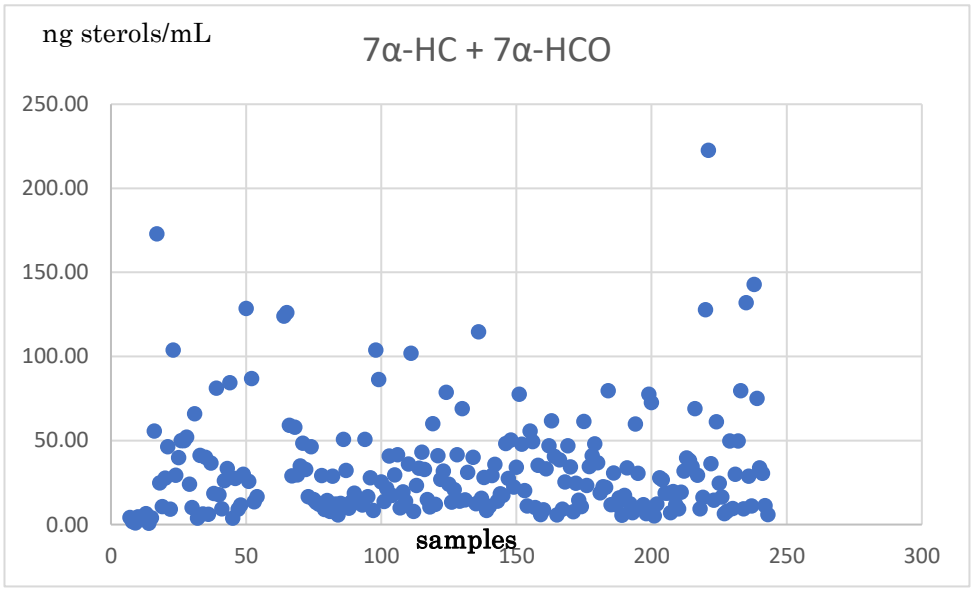
ng sterols/mL
7α-HC + 7α-HCO
250.00
200.00
150.00
100.00
50.00
0.00
0
50
100
150
200
250
300
samples

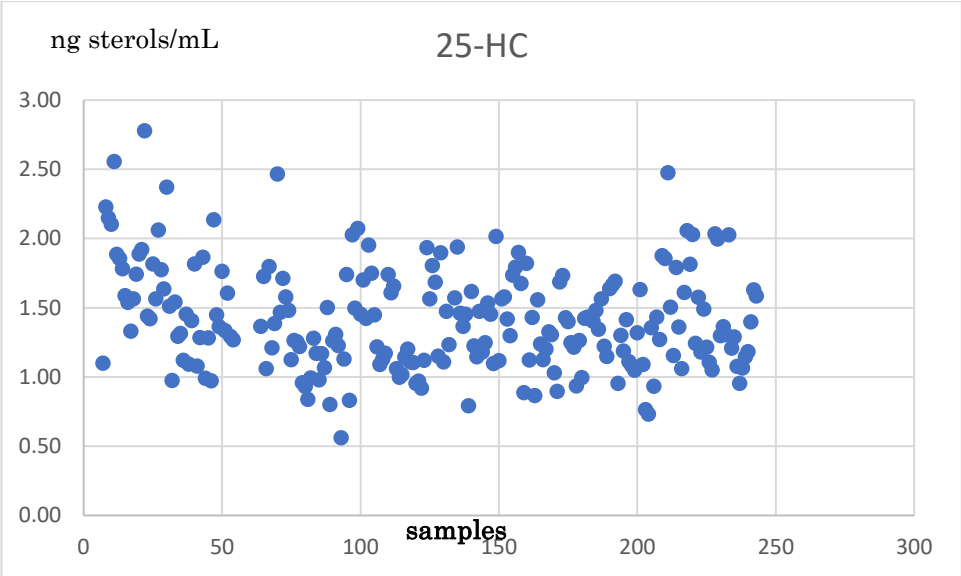

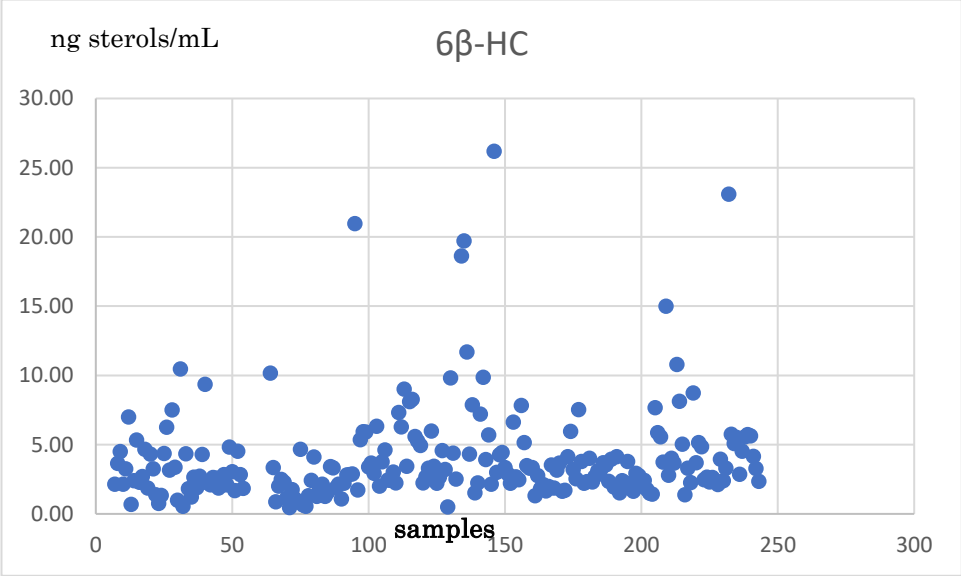

Figure 4.41 Plasma level of the main mono-hydroxy cholesterols found in human plasma from the BioFIND cohort of PD samples and healthy controls.

The distribution of the main plasma mono-hydroxy oxysterols values seems to be quite constant, even though some samples seem to clusters outside of the main mean values. Data reported as ng/mL

4.5 Discussion

Parkinson's Disease (PD) is a neurological disorder characterised by progressive loss of dopaminergic neuronees and intracellular accumulation of misfolded α-syn aggregates. Recent findings have reported that PD also involves the death of some monoaminergic neuronees (Obeso *et al.*, 2017). The disease's typical motor symptoms, including tremors, bradykinesia, and rigidity, result from an unbalanced thalamus-cortico-basal ganglia motor circuit's control due to dopamine. In addition to these symptoms, PD patients may experience urinary retention, constipation, depression, dementia, cognitive impairment, and other symptoms that can severely impact their everyday lives. Unfortunately, no effective medical treatment for PD is currently available, and the disease's multifactorial nature makes it a substantial public health problem. While the aetiology of PD remains uncertain, a growing body of evidence suggests that alterations in brain lipids, particularly cholesterol, might play a central role in disease development. (Poewe *et al.*, 2017a)(Xicoy *et al.*, 2019). Interestingly, both idiopathic and familial/genetic forms of PD seem to be related to lipid profiles alterations (Fais *et al.*, 2021; Xicoy *et al.*, 2019). Cholesterol is believed to be one of the most involved lipids in PD pathological manifestations (Fu *et al.*, 2020; R. Paul *et al.*, 2017b)(Doria *et al.*, 2016; X. Huang *et al.*, 2019; Jin *et al.*, 2019a). Alterations of cholesterol homeostasis in dopaminergic neuronees, and, consequently, of its metabolism, are the most accredited hypothesis on the sterol contribution to PD. However, it is not clear whether cholesterol dysregulation precedes or follows neurodegeneration. Numerous studies on animals and cellular PD models have produced contradictory information on cholesterol

contribution to PD, possibly due to the exacerbation of the disease conditions (Calvano *et al.*, 2019; Doria *et al.*, 2016; García-Sanz *et al.*, 2021; X. Huang *et al.*, 2019; Ji *et al.*, 2019; Jin *et al.*, 2019a; Musanti *et al.*, 1993; R. Paul *et al.*, 2017a; Xicoy *et al.*, 2019). The administration of the heavy treatments needed to develop the PD phenotype might impact too strongly on the brain's physiological pathways affected during the disease. The result is a model which does not represent the real human brain conditions over the neurodegenerative process, which may cause over or under-estimation of the cholesterol impact on the PD hallmarks. Furthermore, most studies on brain cholesterol in humans with PD are conducted on post-mortem brain tissues, which only picture a late stage of the disease, where cholesterol variation might be minimal due to the death of most dopaminergic ,DA, neuroneal cells. Observational studies on PD cohorts at different stages of the disease have highlighted the need for a real-time, in -vivo analytical technique to study the brain's cholesterol fluctuations during disease progression. An accurate profile of the cholesterol and its metabolites during PD would not only shed light on the lipid's actual contribution to the disease but also serve a diagnostic purpose.

In this thesis, the plasma from baseline and progressive PD patients have been analysed from a qualitative and quantitative sterol point of view, producing one of the most comprehensive free sterolome profiles of human plasma during PD. The protocol reported in the 2.3 to 2.9 sections ensures not only a complete extraction of different subclasses of human plasma sterols, from oxysterols to cholestenoic acid to cholesterol precursors, but also the detection of low abundant sterols (order of picograms/mL plasma) in only one LC-MS^3 run, thanks to the derivatisation step united to the LC-ESI-MS^3 technique

employed, see chromatograms reported in figures of paragraph 4.4.1 to 4.4.4. A similar procedure has been employed for the CSF sterols characterisation, guaranteeing the same result obtained for the plasma. The study on the cohort of baseline PD patients, NYPUM baseline paragraph 4.4.1, revealed that the oxysterol (24S)-HC may be a potential biomarker for the disease, demonstrating the ability to predict the disorder in almost 70 % of the cases (ROC analysis, AUC = 0.66), and of discriminating between males and females affected by PD. Hence, the mono-hydroxy sterol is 12 % higher in PD males than in control males (p=0.009 Kruskal-Wallis). However, this does not apply to females. The plasma levels of the brain-derived sterol (24S)-HC are considered good indicators of the neuroneal cells' cholesterol metabolic activity. By identifying a variation between individuals with PD and controls, we do speculate whether this distinction is due to actual change in the brain cholesterol homeostasis or to other influencing factors. One potential aspect affecting the oxysterol plasma level is the integrity of blood-brain barrier (BBB), which could be compromised over PD (Al-Bachari *et al.*, 2020) . Notably, alterations of (24S)-HC plasma levels and of the extracerebral sterol 26-HC can occur when BBB permeability is compromised (Leoni *et al.*, 2003). Both sterols diffuse through the microvascular system daily, leading to a net influx and efflux upon the membrane. To assess BBB integrity, we compared the (24S)-HC/26-HC ratio between the diseased and healthy groups, but no significant variations were found in the data sets. Although there are no statistical differences in the ratios of the two mono-hydroxy sterols and no distinction in plasma levels of 26-HC between the PD and non-PD groups emerges from the plasma analysis, the possibility of a disruption does not completely rule out. There may still be other contributing factors to consider.

However, with the data in our hands, (24S)-HC is the most appealing biomarker in this cohort of PD patients.

Hypothesising the plasma levels of the cerebrosterol (24S)-HC as a discriminating factor for PD, its variation over disease progression has been investigated. The plasma sterolome profile of a longitudinal cohort of PD patients, spanning 90 months after the time of diagnosis, has revealed no significant variations in the 21-plasma sterol identified in the baseline cohort, including (24S)-HC. However, the sterol plasma screening has indicated a general decreasing trend from baseline to 36 months of diagnosis. The absence of significant variation may be imputed to the large, yet quite consistent, dispersion of the sterol values around the mean. It is important to note that this cohort of patients consist of only 16 individuals, which might not be sufficiently representative to detect the same level of sterol variation observed in the baseline cohort, characterised by minimal yet statistically significant differences. Furthermore, haemolysis and coagulation might have affected the sterol extraction and, therefore, the calculated plasma concentration.

To continue the sterol screening over PD, CSF from a longitudinal PD cohort has been analysed. Our laboratory has previously reported variation in the cerebrospinal fluid-free sterols levels in PD patients (W. J. Griffiths *et al.*, 2021b). However, differences were minimal and only related to a restricted cohort of patients. A bigger cohort of PD baseline patients has been recently screened for the CSF-free sterol profile, highlighting small but significant differences (data not published yet). Therefore, in this work of thesis, the longitudinal CSF from 80 PD patients has been screened from a sterol point of view to look for any variation of the sterol lipid molecule levels over 96 months after diagnosis. As for the longitudinal PD plasma, no

statistical nor significant differences have been identified in the 18 cholestenoic acids found in the human CSF. The CSF sterol acids levels seem to remain quite univariate over time, with also a constant spread of values (SD). Indeed, when sterol levels were singularly plotted case by case (patient by patient), the levels remained constant over time. No gender influence is reported, as the sterols do not cluster nor change when sex is considered.

In conclusion, based on data availability, the oxysterols (24S)-HC might be considered a candidate diagnostic but not a prognostic biomarker for PD. However, it should be noted that there was a minimal, albeit significant, change in the sterol levels between the patients and the controls, which may not be suitable for clinical diagnostic purposes. Nevertheless, the sterol plasma level could help to differentiate on a gender basis. From the longitudinal studies on plasma and CSF, none of the sterols seems to correlate with disease progression/severity.

It must be noted that sterol body fluids levels are affected by several different factors like gender, age, and disease severity, which must be taken into consideration when sterolome profile analyses are carried out. In this thesis, sterol values have been corrected based on patients' demographics, when available, and disease progression, longitudinal studies. However, many other aspects, including lifestyle, environment, diet, protein phenotype distribution and ethnicity, can modify and influence cholesterol and sterol levels. Therefore, the outcomes of the NYPUM PD study need to be validated on a broader range of populations with different ethnicity and provenience, which is the purpose of the BioFIND baseline cohort of PD patients (data in progress).

Chapter 5 - Sterolomic profile of Human neuroepithelial stem cells derived from induced pluripotent stem cells (iPSCs) carrying the LRRK2 mutation

5.1 Introduction

Cellular and animal models of human diseases represent an invaluable resource to deep dive into illnesses' pathological pathways and to uncover key features of their molecular mechanisms. While they provide novel insights into diseases' aetiology, they also represent suitable platform for the discovery of new diagnostic biomarkers or druggable targets and, therefore, for development of new medical treatments. Indeed, animal, and cellular models are of particular importance for the study of molecular mechanisms of complex and multifactorial illnesses like neurodegenerative diseases.

Even if studies on animal and cellular models and on human cohort of patients have associated brain cholesterol homeostasis imbalances with PD, it is still not clear at which stage cholesterol dyshomeostasis starts and how much affects PD. Elucidating the role cholesterol and sterol lipid in PD is also challenged by the fact that brain cholesterol biosynthesis and metabolism differs respect to all the peripheral sites of the lipid production and it is cell specific (Gliozzi *et al.*, 2021; X. Huang *et al.*, 2019; Lütjohann *et al.*, 1996a). For instance, different brain cells are responsible for the sterol production and catabolism in human, with a steroidogenic capacity that changes with the

development state of the brain, ageing or disease condition (Berghoff *et al.*, 2021; Genaro-Mattos *et al.*, 2019; Korade *et al.*, 2022). It is widely accepted that developing neuronees and astrocytes are the major producers of cholesterol during brain development while the formers lose this ability once become mature and brain fully developed (J. Zhang & Liu, 2015). However, most of the studies reported in literature focus on cholesterol precursors and its biosynthesis only, not on the metabolism. Moreover, all the studies on developing neuroneneuronees and the majority of the ones on PD cell models have been developed on mouse brain cells, no human.

Technological development has aided the growth of human induced pluripotent stem cells(iPSCs) upon reprogramming of differentiated cells. iPSCs can be differentiated in any cell type, including neuronees, and therefore be used to characterise cholesterol homeostasis in developing and mature human neuroneal cells, bridging the gap between mice and humans. Moreover, iPSCs neuroneneuronees carrying PD phenotypes can be informative for sterol lipid characterisation upon neurodegeneration over the disease. Specifically, research should be addressed on dopaminergic (DA) neuronees, the most involved cell population over sporadic PD, the most common form of the disease. Reprogramming pluripotent stem cells or somatic, fibroblast like, cells from PD patients can represent the perfect scaffold for the study of biological alteration over the disease. Moreover, throughout the newly developed genome editing techniques different types of mutated neuroneal cells can be created to resemble the most common form of genetic PD. For example, leucine-rich repeat kinase 2, LRRK2, mutated DA neuroneneuronees can be created to study, and clarify, the contribution of cholesterol the most common genetic cause for both

familial and sporadic PD. LRRK2 bringing the G2019S mutation is an autosomal dominant mutation widely recognised to cause PD. This mutation causes a structural modification in LRRK2 which impairs its controlling function towards MEK/ERK and AMPK pathways, resulting in a disrupted autophagy lysosomal protein degradation system (Rideout & Stefanis, 2014). Malfunction protein elimination machinery is believed to aid the accumulation of toxic α-syn, ultimately turning or contributing to PD (Anand & Braithwaite, 2009; Rideout & Stefanis, 2014).

Nowadays, a very limited number of studies have characterised cholesterol variation in human PD and iPSCs-PD cell models. Recent papers on iPSCs neuroneneuronees from healthy human donors or different neurodegenerative disease have shown physiological changes of the lipid's metabolism upon differentiation but also odd changes in the lipid profile during degeneration (E. Arenas, 2022; Carsana *et al.*, 2022; Gopalan *et al.*, n.d.; Mou *et al.*, 2023; Tomasello *et al.*, 2022). Currently, no data on iPSCs expressing PD phenotype sterolome are available.

5.2 Aims

Brain cholesterol dyshomeostasis is nowadays believed to be as a contributing factor to the PD development. However, the cholesterol's degree of engagement in the PD pathology is still unclear, mainly due to the high disease heterogeneity and animal models studies. A feasible way to address the lack of knowledge on cholesterol contribution to human normal neuroneal development and overcome the aggravation of the pathological mechanisms in the PD animal

models could be the use of iPSCsFor this study, iPSCs and LRRK2 gene edited iPSCs cell line have been differentiated into neuroepithelial stem cells (NES) and employed for the characterisation of their sterolome. NES cells are the progenitors of neuroneneuronees and represent the best cell lines to differentiate, under specific stimuli, into mature neuronees and glial cells, including midbrain dopaminergic neuronees (Calvo-Garrido *et al.*, 2021; Falk *et al.*, 2012).

This is a pilot study whose aim is to give for the first time a fingerprint of the cholesterol and cholesterol-metabolites levels of the neuroneal cells' progenitors differentiated from human iPSCs. The sterolome profiling of NES cells will firstly clarify if they are oxysterols/sterols producing cells, and secondly, based on the type of sterol molecules identified, it could be hypothesised which cholesterol metabolic way is induced in this type of cells. Hence, this work can contribute to clarify the cholesterol metabolic activity before the differentiation to DA neurones. Moreover, the sterolome profile of iPSCs-derived NES carrying LRRK2 mutation would highlight if cholesterol metabolism were affected in a cell line which is supposed to develop PD phenotype once differentiated to DA neurones, respect to normal NES.

5.3 Material and methods

5.3.1 iPSCs NES cells

iPSCs derived NES cells carrying the LRRK2 mutation and healthy iPSCs derived NES cells pellets and media were provided by Prof. Ernest Arenas, Karolinska Institutet, MBB, Laboratory of Molecular

Neurobiology, Solnavägen 9, Biomedicum 6C, Stockholm 17177, Sweden. iPSCs cells were grown and differentiated into active NES. NES cells have been then split and seeded into 3 separate wells and grown for few hours in proliferation medium. The three wells of the belonging to LRRK2 NES and control NES have been merged and cell pellet collected into one single tube for sterol extraction, details in table 5.1. Medium from the three wells was collected and combined in one single 15 mL Falcon tube. Cell pellets and media have been subsequently frozen at -80°C until further processing.

Table *5.1* NES cell characteristic.

Name of sample	Cell line	Day of proliferation	Treatment	Number of cells at the time of collection
A1	control	0	Proliferation medium	$2{,}52*10^6$
A2	PD-LRRK2	0	Proliferation medium	$1{,}56*10^6$

5.3.2 Sterols extraction

Free/ not-esterified sterols have been extracted from cell pellets and media belonging to NES cell samples A1 and A2 as described in the sections 2.2, which represents a modification protocol for sterol extraction from cell pellets described in (Blanc *et al.*, 2013b). Briefly, sterol lipids have been extracted from the cell pellet using 1 mL absolute ethanol containing the iSTDs mix for NES cell. On the other side, cell medium sterols have been extracted adding 1 mL of defrosted medium to 2.35 mL of absolute ethanol containing the

iSTDs mix for NES cell. Following the extraction, cell medium and pellet sterol extracts have been centrifuged first, and supernatant recovered from the pellet. The supernatant has been further diluted down to 70*% (v/v)* EtOH while the medium one was already at that desired concentration after the centrifugation step. Polar sterols (Fr1) are separated from cholesterol and hydrophobic precursors (Fr3) through a C18-RP SPE chromatography and fractions dried down overnight. The EADSA methodology has been employed for the sterols derivatisation with the charge tagged hydrazine Girard P d5 or D0 and excess of derivatising agent eliminated through a second HLB SPE chromatography step.

5.3.3 Oxysterols analysis

The strategy adopted for the determination of the NES cell pellet and media's sterols implies a combined gradient elution chromatography and tandem Mass Spectrometry, including precursor ion and neutral loss scans. A detailed description of the technique and methods applied to the LC-ESI-MS^3 analysis can be found in the section 2.8. Sterols quantification has been performed upon peaks identification and integration utilising the Thermo Fisher™ software Trace Finder™, see section 2.9 for details. Briefly, after peaks identification, conducted upon accurate mass and retention time match, the sterols have been quantified against same structure or surrogate deuterated standard. Details of deuterated standard used for quantification purposes are reported in section 2.1.1 and table 7.14 of the appendices for NES cell derived from iPSCs. Relative quantification has been performed.

5.4 Results

The application and adaptation of cell pellet sterols extraction protocol described in Blanc *et al.* paper (Blanc *et al.*, 2013b) followed by LC-MS^3 analysis results in the identification of 9 different sterol in the NES iPSCs, see figures 5.1, 5.2, 5.3, 5.4 and 5.5. Good chromatographic separation is obtained when the 17-minutes gradient elution mode is employed, resulting in base line peak separation for most of the Girard P-derivatised sterols, see figures 5.1, 5.2, 5.3, 5.4 and 5.5. This pilot study has been designed to investigate, from a qualitative point of view, the ability of NES cells to metabolise cholesterol. Therefore, only direct metabolites of cholesterol, which are mono and di hydroxy sterols, have been properly identified. Structure attribution has been made through comparison of the fingerprint MS^3 fragmentation pattern of precursor ions with mass 539 and 534 *m/z*, which represent mono hydroxy sterols derivatised with hydrazine GP D5 and D0, and 555 & 550 *m/z*, di hydroxy sterols derivatised with GP D5/D0, with internal library, for details of fragmentation methods see tables 2,5,10 &11 in the appendix. However, some peaks with mass 537 and 569 *m/z*, GP D5 derivatised, & 564 *m/z*, GP D0 derivatised, can be seen in figure 5.3 and 5.4. They have been recognised as (24S,25)-epoxycholesterol and 24-ketocholesterol, (24S,25)-EC and 24-HCO, 537 *m/z*, and cholestenoic acids 3ß,7α-diHCA + 7α-H-3O-CA, 564/9 *m/z*. However, they couldn't have been properly identified just from accurate mass match. Therefore, they have not been quantified. Relative

quantification is performed against the designated deuterated internal standard with trace finder software, refer to table 7.14 in the appendix for details.

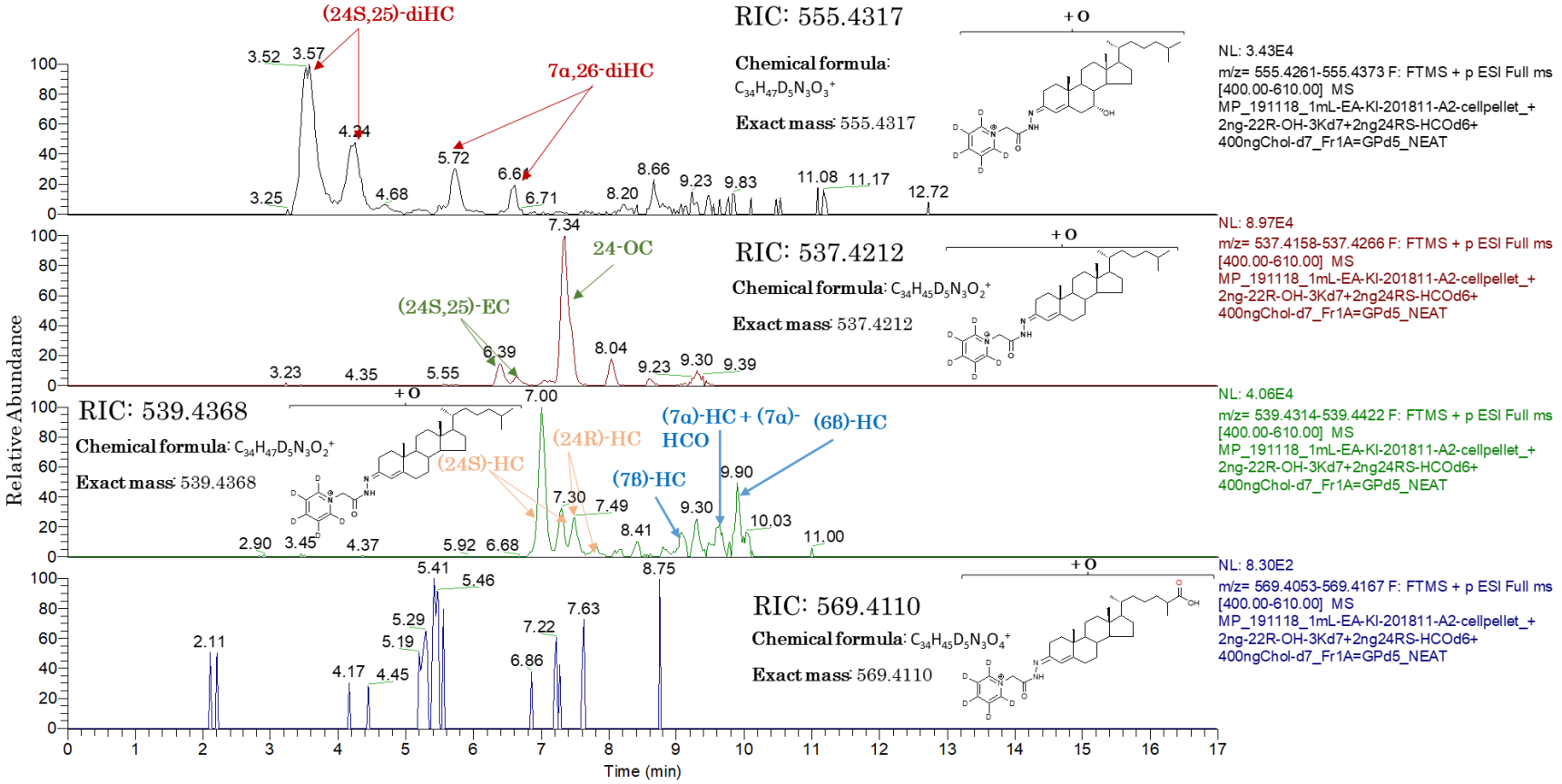

Figure 5.1 Chromatogram of iPSCs derived NES cell pellet extracts showing the main monohydroxy, dihydroxy, epoxy, keto and cholestenoic sterols found.

The peaks showed in the first three upper panels of figure 5.1 represent the molecular ions with exact mass of 555.4317, 537.4212 and 539.4368 *m/z*, result of sterol derivatisation with the hydrazine GP D5. No molecular ions with 569.4110 *m/z* have been identified in the cell pellet. RIC, reconstructed ion chromatogram.

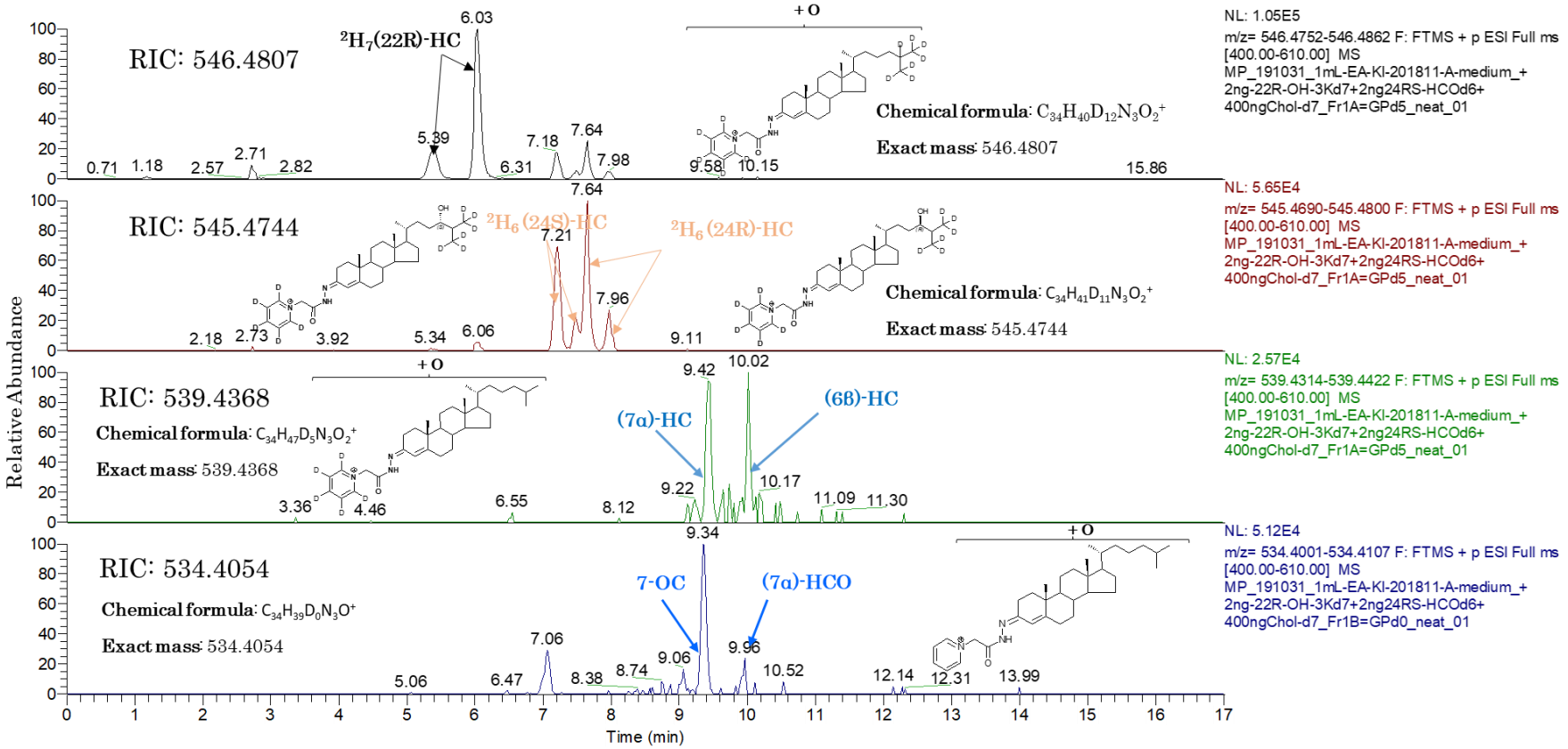

Figure 5.2 Chromatogram of iPSCs derived NES medium extracts showing the internal standards 2H6(24R/S)-HC, 2H7(22R)-HC and the main monohydroxy sterols.

The peaks showed in the two upper panels of figure 5.2 represent the molecular ions with exact mass of 546.4807 and 545.4744 *m/z*, result of $^2H_7$(22R)-HC and $^2H_6$(24R/S)-HC derivatisation with the hydrazine GP D5. The peaks showed in the lower panel of figure 5.2 represent the molecular ions with exact mass of 534.4054*m/z*, result of the monohydroxy sterols derivatisation with the hydrazine GP D5 and GP D0, respectively. RIC, reconstructed ion chromatogram.

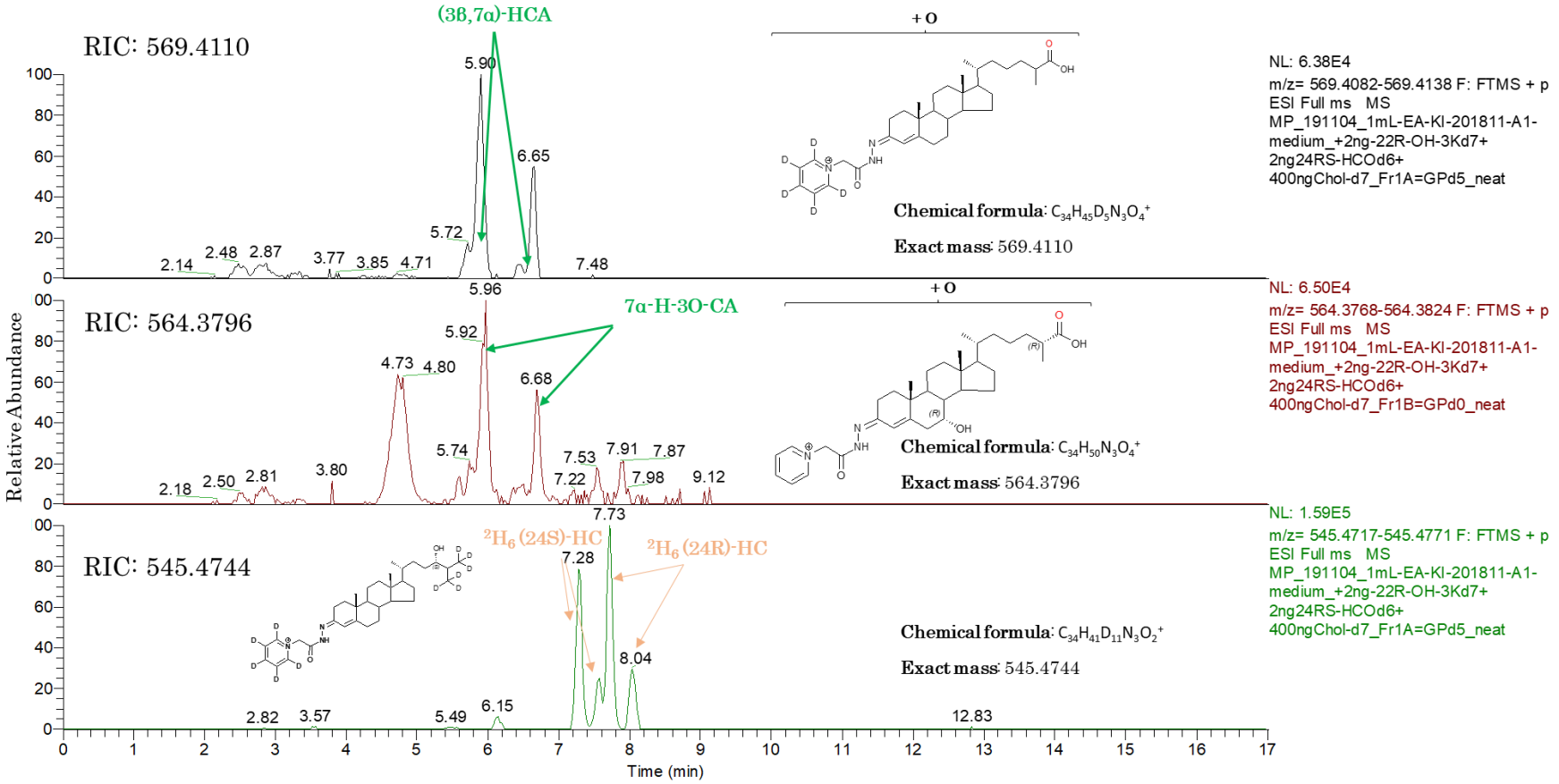

Figure 5.3 Chromatogram of iPSCs derived NES cell medium extracts showing the internal standard $^2H_6$(24R/S)-HC, and the main dihydroxy, ketone and epoxy sterols.

The peaks showed in the upper panel of figure 5.3 represent the molecular ions with exact mass of 545.4744 *m/z*, result of $^2H_6$(24R/S)-HC derivatisation with the hydrazine GP D5. The peaks showed in the middle and third panels of figure 5.3 represent the molecular ions with exact mass of 555.4317 and 537.4212 *m/z*, result of sterol derivatisation with the hydrazine GP D5. RIC, reconstructed ion chromatogram.

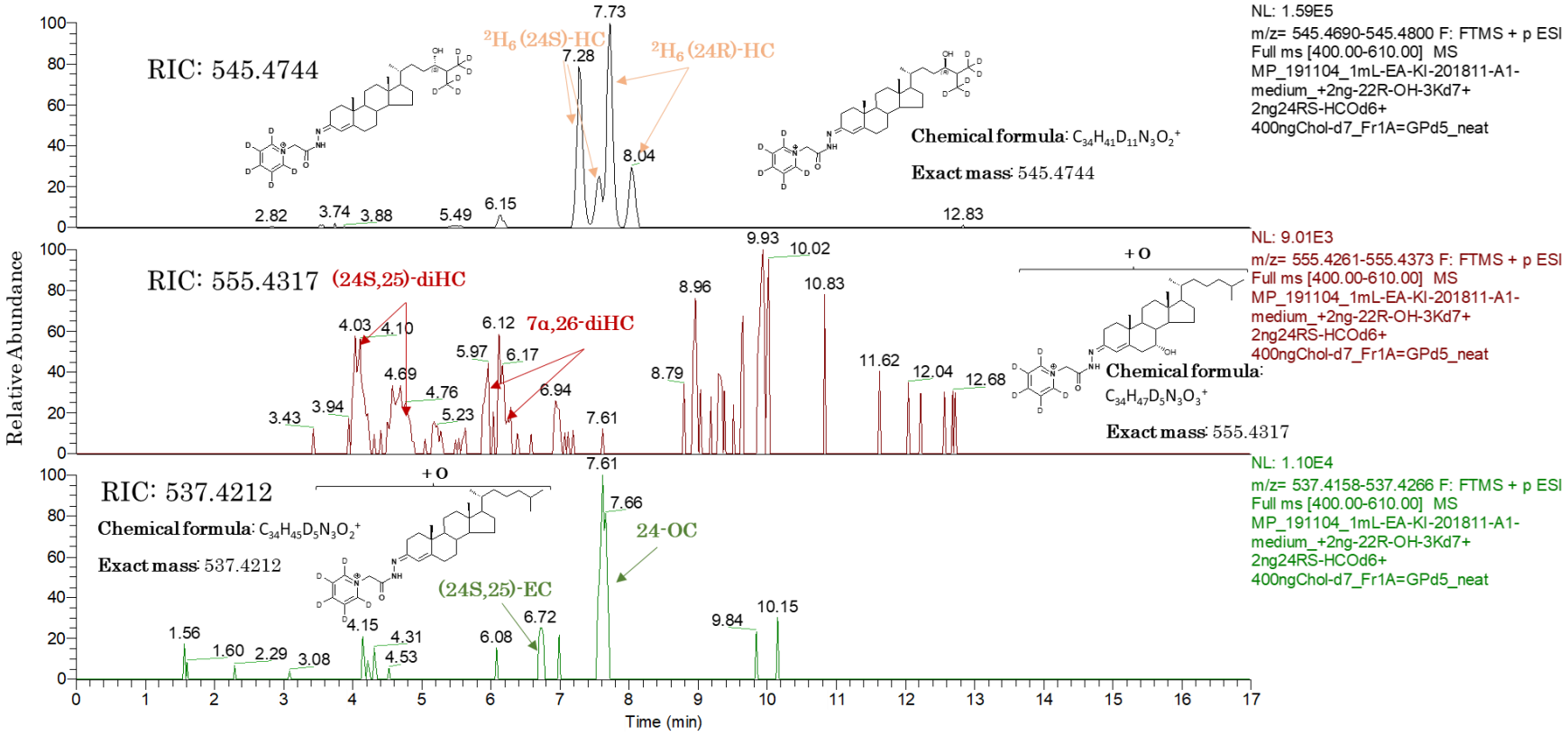

Figure 5.4 Chromatogram of iPSCs derived NES cell medium extracts showing the internal standard $^2H_6$(24R/S)-HC, and the main dihydroxy, ketone and epoxy sterols.

The peaks showed in the upper panel of figure 5.4 represent the molecular ions with exact mass of 545.4744 *m/z*, result of $^2H_6$(24R/S)-HC derivatisation with the hydrazine GP D5. The peaks showed in the middle and third panels of figure 5.4 represent the molecular ions with exact mass of 555.4317 and 537.4212 *m/z*, result of sterol derivatisation with the hydrazine GP D5. RIC, reconstructed ion chromatogram.

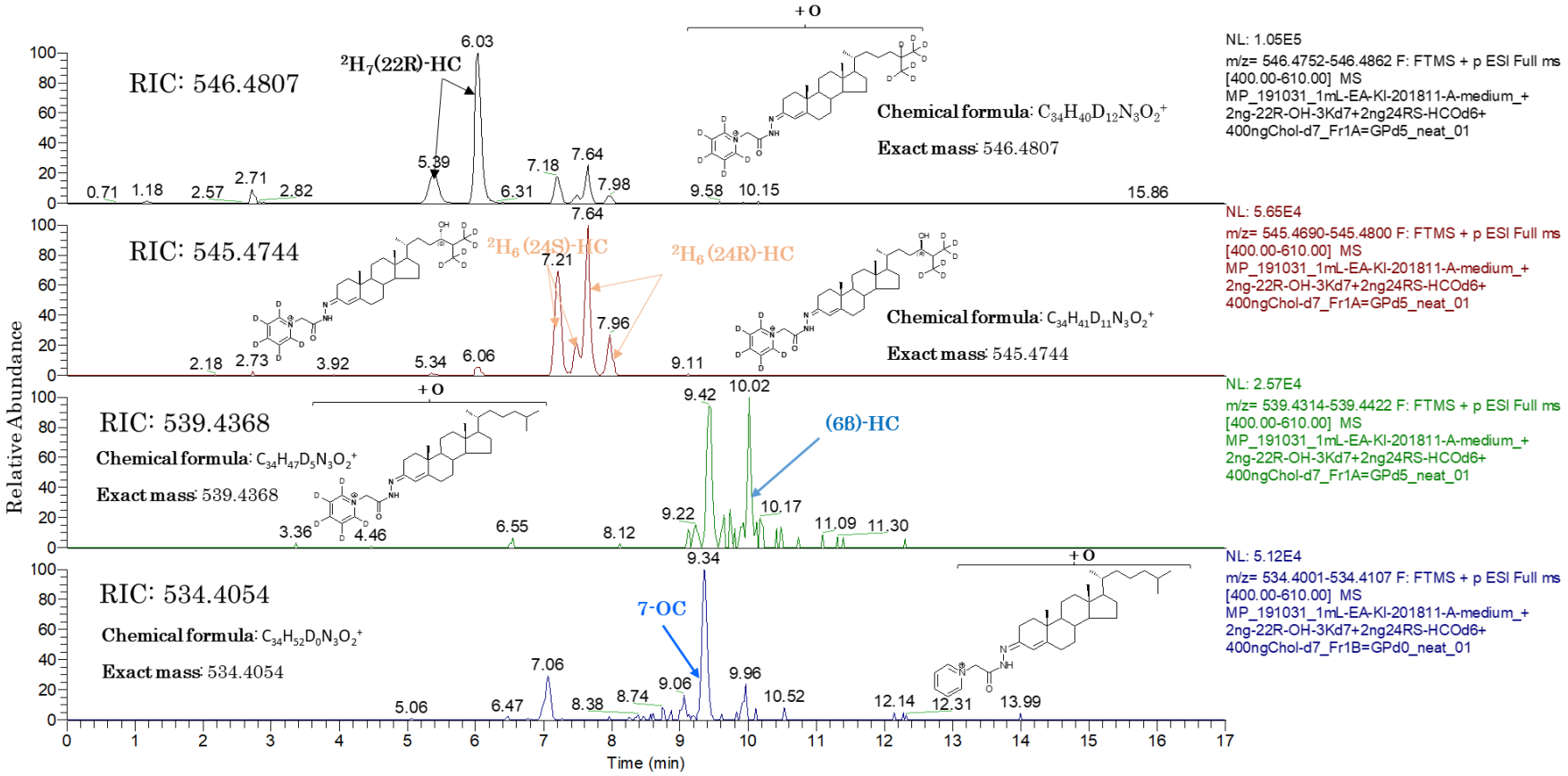

Figure 5.5 Chromatogram of iPSCs derived NES proliferation medium extract showing the internal standards $^2H_6$ (24R/S)-HC, $^2H_7$(22R)-HC and the main monohydroxy sterols.

The peaks showed in the two upper panels of figure 5.5 represent the molecular ions with exact mass of 546.4807 and 545.4744 *m/z*, result of [$^2H_6$](24R/S)-HC and $^2H_7$(22R)-HC derivatisation with the hydrazine GP D5.The peaks showed in the lower panel of figure 5.5 represent the molecular ions with exact mass of 539.4368 and 534.4054 *m/z*, result of the main monohydroxy sterols in proliferation medium after derivatisation with the hydrazine GP D5 and D0, respectively. RIC, reconstructed ion chromatogram.

The nine sterols correctly identified comprise two dihydroxy sterols, 7α,26-diHC + (24S,25)-di-HC, one ketone 7-OC, FIVE monohydroxy sterols, (24S)-HC + (24R)-HC + 7α-HC + 7ß-HC + 6ß-HC and cholesterol have been identified between cell pellet and medium. The cell pellet sterols levels range in concentration from 0.02 to 2698.80 ng/million cells, see table 5.2. Cell medium sterol lipids levels range in concentration from 0.02 to 0.92 ng/mL of medium, table 5.3. Proliferation medium has also been included in the analysis to investigate on the presence of background sterols, which have been therefore subtracted to the media sterol samples, see table 5.3.

Table 5.2 . Sterols levels in iPSCs derived NES and LRRK2 NES cell pellet.

Sterols have been quantified against the designated standard $^{2}H_{6}$ (24R/S)-hydroxycholesterol or $^{2}H_{7}$ cholesterol, value expressed an ng/millions of cells. **A1,** iPSCs derived NES control; **A2,** iPSCs derived NES LRRK2

Endogenous sterol in ng/million cells	A1	A2	A1/A2
(24S,25)-di-HC	1.49	1.24	1.20
7α,26-diHC	0.15	0.19	0.78
(24S)-HC	0.62	0.59	1.05
(24R)-HC	0.20	0.16	1.26
7ß-HC	0.02	0.07	0.34
7α-HC +7α-HCO	0.15	0.14	1.08
6b-HC	0.11	0.22	0.51
7-OC	0.29	0.38	0.76
Cholesterol	2698.80	2663.04	1.01

Table 5.3 Sterols levels in iPSCs derived NES and LRRK2 NES medium.
Sterol have been quantified against the designated standard $^{2}H_{6}$ (24R/S)-hydroxycholesterol or $^{2}H_{7}$cholesterol. Results adjusted by medium background sterols (A1-A0 and A2-A0). **A1**, iPSCs derived NES control; **A2**, iPSCs derived NES LRRK2; **N/D**, not detected; **N/A**, not applicable.

Endogenous sterol in ng/mL	A	A1	A2	A1-A0	A2-A0	A1/A2
(24S,25)-di-HCO	N/D	0.09	0.11	N/D	N/D	0.80
7α,26-diHC	N/D	0.06	0.13	N/D	N/D	0.45
(24S)-HC	N/D	0.02	0.04	N/D	N/D	0.52
7β-HC	0.07	0.07	N/F	0.00	N/A	N/A
7α-HC +7α-HCO	0.24	0.31	0.92	0.07	0.68	0.33
6b-HC	0.24	0.31	0.92	0.07	0.68	0.33
7-OC	0.44	0.26	0.36	-0.18	-0.08	0.73
Cholesterol	N/D	N/D	N/D	N/A	N/A	N/A

From the sterolome analysis of NES cell pellet and media we did identify both cholesterol metabolites formed enzymatically, (24S)-HC, (24R)-HC, 7α-HC, 7α,26-diHC & (24S,25)-HC, and cholesterol autoxidation products 7β-HC & 6β-HC. We can therefore conclude that this type of cells does produce oxysterols. The most abundant sterol in the found in the cell pellet seems to be the (24S,25)-diHC, which however can be also formed during sample preparation for spontaneous hydrolysis of the epoxide (24S,25)-EC. As we did recognise a peak which match in retention time and accurate mass with (24S,25)-EC, we assume that part of the (24S,25)-diHC should

come from it. Hence, we cannot affirm the di hydroxy sterol is the most abundant. The second most abundant is the monohydroxy (24S)-HC, which can only be formed through CYP46A1 enzymatic oxidation of cholesterol. Thus, we assume it as the most abundant sterol produced by NES cells. Interestingly, we did also identify the di hydroxy sterol 7α,26-diHC but no 26-HC. With our method, (24R)-HC and 26-HC coelutes as one chromatographic peak with 539.4368 *m/z* but they can be distinguished because of their different MS^3 fragmentation pattern, see figure 5.6. In this work, the MS^3 spectra of the peak assigned as (24R)-HC doesn't seem to be contaminated of 26-HC, which is therefore not reported, see figure 5.6. However, the 26-HC presence cannot be excluded as its levels can be under the mass spec limit of detection. 7α,26-diHC can be form in two ways in human cells, either through cholesterol C-26 hydroxylation first and a following C-7α oxidation (acidic pathway to bile acid formation, see section 1.1.1.2) or upon C-7α oxidation first followed by C-26 hydroxylation (neutral pathway to bile acid formation, see section 1.1.1.2). Further studies will clarify which pathway is induced in this type of cell.

A

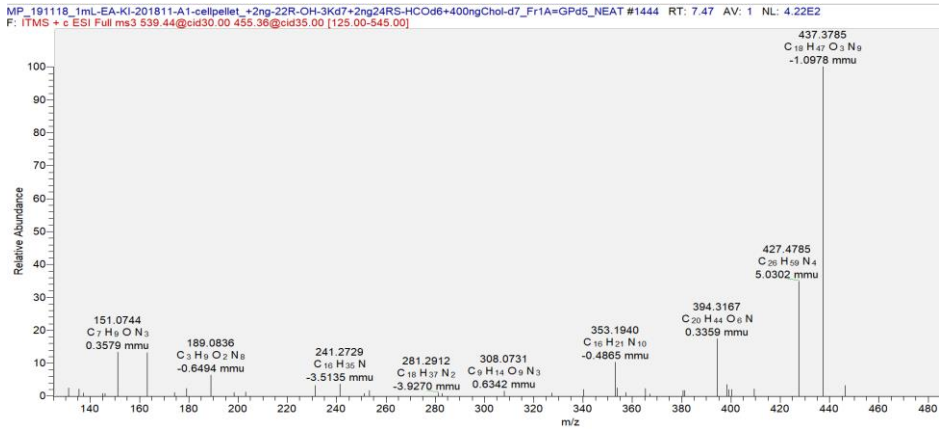

B

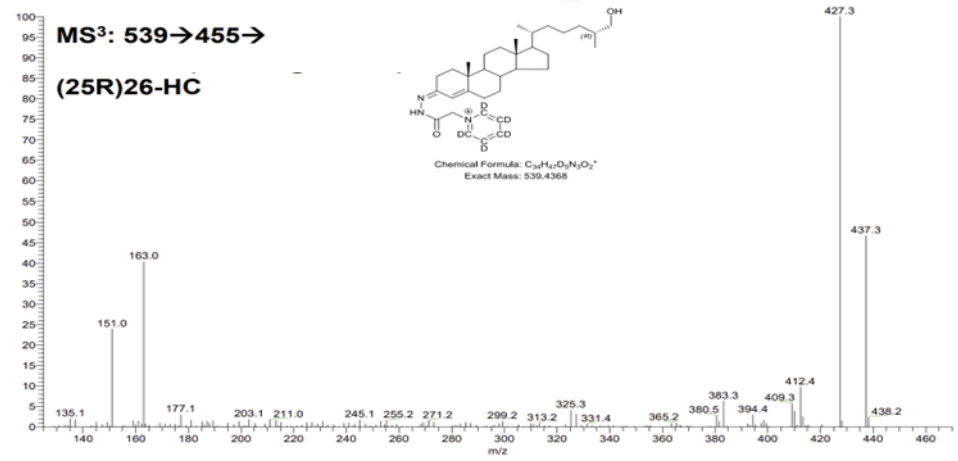

C

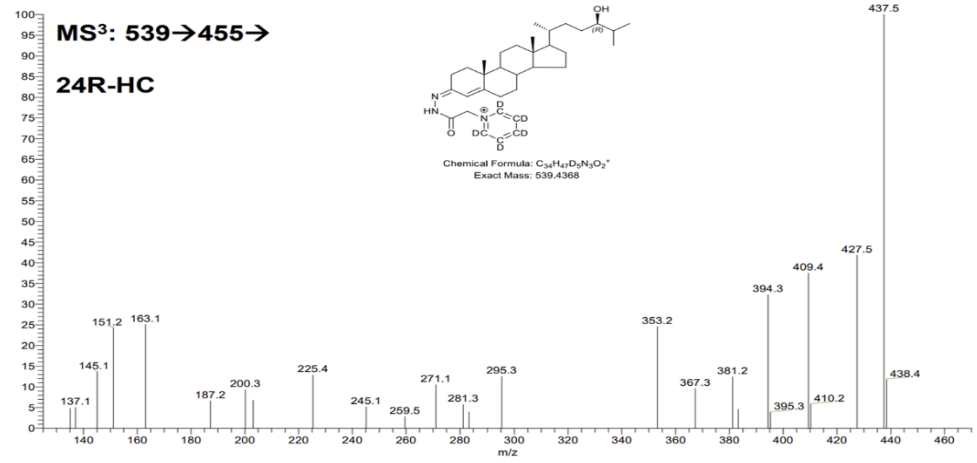

Figure 5.6 MS³ fragmentation pattern of (24R)-HC and 26-HC.
(A) MS³ fragmentation pattern of the NES cell pellet peak with Rt=7.47 minutes, identified as (24R)-HC. **(B)** MS³ fragmentation pattern of 26-HC, taken from Yutuc, E., Dickson, A. L., Pacciarini, M., *et al.* 2021 **(C)** MS³ fragmentation pattern of (24R)-HC, taken from Yutuc, E., Dickson, A. L., Pacciarini, M., *et al.* 2021

5.5 Discussion

The absence of effective medical treatments for neurodegeneration associated diseases is genuinely linked to a lack of knowledge around the main pathological pathways causing the above cited illnesses. The study of the neurodegenerative diseases, NDs, molecular mechanisms will open the door to a new era of drug discovery, unravelling new draggable targets, and new reliable biomarkers.

Over the last decades, brain cholesterol dysregulation emerged as one of the potential protagonists of the neurodegeneration process involved in several NDs (F. Arenas *et al.*, 2017; Dai *et al.*, 2021; Jin *et al.*, 2019a; Karasinska & Hayden, 2011; Kreilaus *et al.*, 2016; Pfrieger, 2021; Puglielli *et al.*, 2003; Sodero *et al.*, 2011; Y. Wang *et al.*, 2008). Hence, the lipid seems to take part in numerous, if not all, hallmarks of the neurodegenerative disorders, resembles a common thread for disease development. Therefore, characterising brain cholesterol metabolism, including a complete profile if its metabolites, and homeostasis may represent a valuable resource to deep dive into ND aetiology.

Technology advances, in parallel with increasing understating of the main biological mechanisms of cell development, survival and death, have enabled the generation of cell disease models which closely reproduce the pathological alteration happening over the illness progression. Thanks to study of these models, fundamental insights have been discovered for a plethora of sicknesses, allowing the development of medical treatments and discovery of new biomarkers. Therefore, a cell model of different NDs can represent the ideal

platform for the study of cholesterol alteration over disease progression.

Parkinson's Disease, PD, is the second most widespread NDs nowadays, affecting millions of people worldwide. The paucity in information regarding PD's aetiology is reflected by the absence of effective disease modifying drugs and of specific PD biomarkers. Even though the scientific community efforts have uncovered the main pathological pathways involved in PD development and progression, there are still some missing key elements which delayed the appearance of new drugs. As described above, brain cholesterol might represent one these missing elements, thus its characterisation can provide novel insights into the comprehension of heterogeneous disorder.

To understand the sterol modification over disease progression, a complete determination of its variation during physiological brain development must precede the characterisation of the pathological case. Specifically, attention should be addressed over the lipid alterations during neuroneal cells development, the main cells affected in PD and in neurodegenerative processes. Hence, iPSCs or embryonic stem cells can be used to this purpose when appropriately stimulated to differentiate as a mature neurone. Up to date, little is known about cholesterol changes during neuroneal development of human mid-brain dopaminergic neuronees, the main cell type affected in PD.

In this work of thesis neuroepithelial stem cells (NES) derived from human iPSCs and iPSCs derived NES carrying LRRK2 mutation have been characterised from a sterol point of view. Preliminary data (n=1) indicates the ability of iPSCs derived NES, both normal and mutated, to produce a different panel of sterols, including the main

cerebral metabolite of cholesterol, (24S)-HC, which seems to be the most abundant sterols. (24S)-HC is mainly produced in human neuroneal cells and astrocytes in the brain through CYP46A1 oxidative activity (CYP46A1 Human Protein Atlas , 2023). To note is, therefore, the capacity of this type of cells, the NES, to produce the sterol (24S)-HC from a very early stage, day 0 of differentiation. We do speculate if the cholesterol 24S hydroxylation pathway is therefore induced in NES cells. In addition, the identification of the di hydroxy sterols (7α,26)-HC, the presence of the enzymatic derived 7α-HC with the absence of 26-HC, let us venture whether the neutral pathway to bile acids has been induced in this cell type to maintain cholesterol homeostasis. Moreover, we recognised, but not identified, some sterols which might be 7α-HCAs, supporting the bile acids hypothesis Recently, cholestenoic acids, the main bile acids precursors, have been identified in both human CSF and mouse brain(Abdel-Khalik *et al.*, 2018; Crick *et al.*, 2019; W. J. Griffiths, Abdel-Khalik, *et al.*, 2019; Yutuc *et al.*, 2020) but little is known about their effective production in human brain. Certainly, they do have an impact on brain cells, as demonstrated in the paper of (Ogundare *et al.*, 2010a). Further experiments are needed to clarify whether bile acids metabolism is effectively indicted in NES cells.

Some of the identified sterols have been found exclusively or principally in the cell pellet, mainly enzymatically derived monohydroxy sterols like (24S)-HC and (24R)-HC and dihydroxy sterols, like (24S,25)-HC and (7α,26)-diHC, while the hypothesised cholestenoic acids (3ß,7α)-diHCA and 7α-H-3O-CA seemed to be only present in the cell medium. This finding letting us speculate whether this type of cells should require an external mechanism of transport to excrete more hydrophobic cholesterol metabolites while the more

polar ones can diffuse through the plasma membrane. It is widely recognised that cholesterol trafficking among organelles and plasma membranes requires a system of carriers, represented by lipoproteins or vesicles (F. Arenas *et al.*, 2017; Ikonen & Parton, 2000; Mukherjee & Maxfield, 2004). Less is known about its metabolites transport in the brain, however more hydrophilic cholesterol-derived sterols like (24S)-HC and 26-HC can generally diffuse among plasma membranes (Lütjohann *et al.*, 1996a). Nevertheless, diffusion does not only depend on the chemical features of the sterol lipid, especially hydrophilicity and dimension, but also on membrane thickness and cholesterol concentration, which might be quite high in fast growing cells like NES. Different and various parameters can affect sterols diffusion or passage through membranes which is worth to take into consideration for further experiments. In terms of sterol content, no assumption can be made from one single experiment between NES and LRRK2 NES, however both cell types produce the same panel of molecules. More replicates are needed to shed lights on differences, if any, in terms of concentration. However, a reliable, efficient, and reproducible protocol for sterol extraction, identification and quantification from both cell pellets and medium have been provided.

Chapter 6 - General Discussion and conclusions

6.1 Discussion

Cholesterol is human beings' most abundant sterol lipid and an essential structural component of cell membranes (McNamara, 2013). Depending on its concentration, cholesterol can modify the membrane's lipids and proteins organisation which can determine the rearrangement of transmembrane protein folding and/or changes in membrane permeability (Lange *et al.*, 1999; McNamara, 2013; Yeagle, 1991). The role of cholesterol in the human body is not only relegated to a merely structural function but it has been demonstrated to be a proper signalling molecule. For example, it is involved in the modulation of inflammation and immune response (Holst *et al.*, 2004; J. Hu *et al.*, 2010; Jp, 2006; Schade *et al.*, 2020b; Staels & Fonseca, 2009; Tall, A. R.; Yvan-Charvet, 2015). Moreover, cholesterol is the scaffold for several other important bioactive molecules, including bile acids, mineral and glucocorticoids and steroid hormones (Arman Qamar & Deepak L. Bhatt, 2015; Holst *et al.*, 2004; J. Hu *et al.*, 2010; Jp, 2006; Staels & Fonseca, 2009; Voisin *et al.*, 2017). While the research is still elucidating the various role of cholesterol in physiological functions, several shreds of evidence linked alteration of the cholesterol metabolism/homeostasis with numerous diseases, from atherosclerosis to dyslipidaemia, from cardiovascular diseases to cancer (Courtney & Landreth, 2016; de Boussac *et al.*, 2013; Kuzu *et al.*, 2016; Z. Ma *et al.*, 2017; Maxfield & Tabas, 2005; Poirot & Silvente-Poirot, 2013b) (Y. Chen *et al.*, 2017;

W. Liu *et al.*, n.d.; Pedro-Botet & Pintó, 2019). Most interestingly, a plethora of evidence over the last 20 years is linking the alteration of brain cholesterol homeostasis with the development of neurodegenerative diseases (Chang *et al.*, 2017; X. Huang *et al.*, 2019; Jin *et al.*, 2019a; Mata *et al.*, 2006; Pingale & Gupta, 2021a; Puglielli *et al.*, 2003; Varma *et al.*, 2021).

Neurodegenerative diseases are heterogeneous age-related disorders characterised by an uncontrollable loss of neuroneal cells in different brain areas specific to the disease, leading to several life-treating symptoms like cognitive decline, dementia, tremor, bradykinesia, and others (chapter 1). The neurodegeneration process is irreversible, and no cure is available nowadays, condemning the patient to death. The two major forms of neurodegeneration are AD, the most common dementia, and PD, the "shaking palsy". Together, the two diseases account for millions of people worldwide for which only symptomatic treatments are available. Moreover, specific, and selective biomarkers for AD and PD have not been identified yet, relegating the diagnosis process to a long clinical assessment which delays the start of the medical treatment, possibly worsening the patient's conditions. Therefore, AD and PD constitute a major healthcare system economic burden in developed countries. Several efforts have been made to investigate the pathological mechanisms causing AD and PD, which identified shared hallmarks associated with disease progression like misfolded protein accumulation, neuroinflammation, oxidative stress and mitochondrial dysfunction (chapter 1.4.1 and 1.4.2). However, none of the treatments developed for the specific pathways cited above proved to be effective or beneficial for AD or PD.

The hypothesis of cholesterol engagement in the development of neurodegenerative diseases is supported by several findings which see the sterol contributing to the main AD and PD hallmarks ((Jin *et al.*, 2019a). This is unsurprising as cholesterol is the most abundant sterol lipid in the brain, the major myelin component and a key player in neuroneal development and survival (chapter 1.3). However, if a cholesterol contribution to AD and PD is almost certain, the degree of participation in the neurodegeneration is unclear. Contrasting and confounding findings link alteration of the brain, plasma and CSF cholesterol levels to the disorders without clarifying if the sterol positively or negatively influences disease progression. The confusion mainly arises from the fact that the extracerebral levels of cholesterol do not always match the supposed alteration of brain cholesterol metabolism (Chang *et al.*, 2017; X. Huang *et al.*, 2019; Jin *et al.*, 2019a; Puglielli *et al.*, 2003). The brain is called a "drug sanctuary", with the BBB shielding for all the undesired molecules. Furthermore, brain cholesterol biosynthesis and homeostasis are unique and mostly independent of the external cholesterol supplies. While the whole body relies on dietary and newly synthesised liver cholesterol, with a high-rate turnover, the minimal brain cholesterol needs are satisfied by both recycling of the existing lipid or by low-rate astrocytes synthesis (chapter 1.3). Therefore, extracerebral cholesterol levels might not reflect the actual brain cholesterol modification. To monitor brain cholesterol alteration minimally invasively, attention should be addressed to the cholesterol metabolites levels, particularly the oxysterol (24S)-HC. (24S)-HC is the main brain cholesterol metabolite, produced in the neuroneal cells and able to cross the BBB (Lütjohann *et al.*, 1996a). Neuroneal cells are the principal producers of the sterol (24S)-HC in the human body, and it is calculated that more than 80% of the plasma (24S)-HC

has a brain origin, making this oxysterol an ideal candidate to monitor brain cholesterol alteration. Furthermore, it is believed that extracerebral cholesterol can still influence brain cholesterol but in an indirect way. The main extracerebral mono-oxygenated cholesterol metabolite is 26-HC, representing the first intermediate in converting cholesterol to bile acids (chapter 1,1). It has been shown that 26-HC is the other oxysterol to pass the BBB, like (24S)-HC, and be up-taken by the brain (Björkhem, 2006b). In the brain, 26-HC can act as a bioactive molecule blocking cholesterol synthesis in an insulin-induced gene 1 protein (INSIG)-mediated manner, consequently diminishing the (24S)-HC synthesis. 26-HC can also be converted into cholestenoic acids, which have been demonstrated to have a positive or negative effect on dopaminergic neuroneal survival (Chelliah *et al.*, 2022; Ogundare *et al.*, 2010b; Radhakrishnan *et al.*, 2007). Therefore, changes in cholesterol peripheral level can be reflected by alteration of 26-HC, which can diffuse into the brain and modify brain cholesterol homeostasis. It is, therefore, clear that prioritising the profile of body fluids cholesterol oxygenated metabolites can be much more informative regarding brain cholesterol alteration and help to define a clearer picture of brain cholesterol engagement in AD & PD.

This thesis has been designed to study the alterations of the main cholesterol plasma and CSF metabolites in AD and PD and try to bridge the gap between the contradictory information on cholesterol plasma and CSF levels reported in the literature for the cited neurodegenerative illnesses. Therefore, we have profiled the CSF and plasma from different cohorts of AD and PD patients, including baseline and longitudinal cases. Moreover, human neuroepithelial stem cells, NES, have also been included in the sterolome profile

characterisation to picture the cholesterol metabolism at a very early stage of neuroneal development. The cell sterol profile would help to shed light on cholesterol contribution to normal brain cell development. LRRK2 mutated NES have been also screened as a model of PD. LRRK2 NES will serve to deeply investigate cholesterol role in the development of the PD phenotype.

In this thesis, a coupled liquid chromatography-mass spectrometry analytical technique has allowed the identification of up to 21 different sterols in a single mass spectrometry run, reaching a limit of detection of picograms to mL of human blood, CSF, medium from cells or ng per million of cells (chapters 3, 4 and 5).

6.1.1 Alzheimer Disease

With regards to the AD cohort (chapter 3), the profile of total CSF main mono hydroxy sterols has evidenced no variation in terms of concentration among the three subsets of patients, SCI, MCI and AD, The current state of the art of AD CSF sterolomics sees an increase in total (24S)-HC and 26-HC CSF levels respect to healthy controls (Bjoandrkhem *et al.*, 2006b; Schönknecht *et al.*, 2002) . Our finding does not contrast with the data reported in the literature because, in this project, the level of (24S)-HC and 26-HC have been screened in a memory clinic cohort, meaning that the groups under the study, SCI, MCI & AD were all already patients with symptoms. In contrast, the literature compares AD and neurologically healthy controls. Indeed, in a similar study involving the detection of total CSF (24S)-HC alone in SCI, MCI, AD and control patients, the only difference found was between the diseased groups and the controls, but not

between the neurodegenerative patients (Leoni, Solomon, *et al.*, 2013). Moreover, data reported in terms of (24S)-HC were comparable to our findings. It is, therefore, hypothesised that the disease state and, most of all, the severity of the neurodegeneration might have already affected neurone viability and their capacity to produce (24S)-HC in our cohort of patients. Neuroneal cell death at the very early stages of AD or any other ND, determines a massive release of cholesterol in the brain. The fastest way to bring back cholesterol to normal physiological level is its conversion to (24S)-HC and excretion through the BBB. Consequently, elevation of the oxysterol level during the first stages of the disease is expected while compensation generally characterised following stages of the disease. In our case, data on the disease stage were not available for any of the groups, however, a certain degree of severity is expected as all the groups were showing dementia symptoms. Furthermore, only 1% of the brain (24S)-HC pass into the CSF that along with the disease-severity related (24S)-HC compensating mechanism challenge the identification of sterol variations. Additionally, BBB permeability changes can cause variation in the CSF, plasma, and brain concentration of the sterols because their principal mechanism to pass the brain membrane is a simple concentration-dependent diffusion. A more permeable BBB induce a major uptake of 26-HC form the blood stream, where it is more concentrated, which might induce (24S)-HC displacing from the brain into plasma and CSF. Thus, the (24S)-HC BBB leakage might cause a raise in the sterol CSF level and alteration of the 26-HC/(24S)-HC ratio, which have been proven to be a marker of BBB integrity. Whether BBB damage cannot be excluded, it can be hypothesised that no major variation affected the BBB composition among the three groups. Lastly, when correlation analysis between the levels of the sterol (24S)-HC and 26-

HC are performed, a positive and quite strong correlation emerged in all the three groups under study (SCI (Spearman r=0.78), MCI (Spearman r=0.82) and AD (Spearman r=0.86)). A positive correlation is also observed between cholesterol and 26-HC and between cholesterol and (24S)-HC in all the pathological groups. The correlation supports the hypothesis of an indirect effect of peripheral cholesterol on brain cholesterol homeostasis and (24S)-HC biosynthesis via 26-HC.

6.1.2 Parkinson Disease

The sterolome profile of PD patients' body fluids has started with what we have called the discovery phase, which consists of a free plasma sterol screening of a baseline cohort of PD patients and a gender/age-matched group of neurologically healthy individuals. Although several papers have already reported PD body fluids sterol profiles, much disagreement and consistent variation are reported, making the data of difficult interpretation (Bakeberg *et al.*, 2021; Björkhem *et al.*, 2013; Doria *et al.*, 2016; Fu *et al.*, 2020; W. J. Griffiths *et al.*, 2021b; G. Hu *et al.*, 2008; X. Huang *et al.*, 2019; Pingale & Gupta, 2021a; Rozani *et al.*, 2018). From a careful literature review screening, the apparent variation seems to depend on the analytical method employed for sterol characterisation, and consequently on the form, free or esterified or both, of sterols under the analysis, but also on the disease severity. Sterolomics is a quite new branch of the omics sciences which has seen its development over the last 20-30 years, along with the evolution of the mass spectrometry, elected as a gold standard for sterol analysis.

Therefore, the sterols characterisation during PD has seen many analytical challenges associated with the sterol chemical nature and the low amount of this class of small molecules in the human body fluids. In many papers, to overcome the difficulties associated with the MS identification of poorly ionisable-low abundant sterols chemical derivatisation techniques have been widely used (chapter 1). Unfortunately, the increase in sensitivity brought by the derivatisation techniques generally determines a loss of information on sterolome under analysis, from impossibility to separate/distinguish sterol isomers to the determination of only one form of plasma sterols. Moreover, depending on sensitivity and specificity the chosen mass spectrometry (MS) analytical technique, besides derivatisation, an additional hydrolytic step might become necessary, forcing the analysis to the determination of the total sterol content alone. Analysing only the total sterol plasma content, little variations of its singular components, free and esterified sterols, can be masked. Moreover, in most PD papers, the type of sterols analysed, free or total, is not reported and can be only presumed by the extraction method and the analytical technique employed (W. J. Griffiths *et al.*, 2016). Hence, comparing sterolome data becomes challenging when multiple factors contribute to the quantification of this class of molecules, not only in PD but also in any other disease. Secondly, it has been demonstrated that a better clustering of the PD patients based on disease severity can reveal variations in sterol levels which tend to be masked when all the data are taken together (Björkhem *et al.*, 2013; W. J. Griffiths *et al.*, 2021b; X. Huang *et al.*, 2019; Jin *et al.*, 2019a). In PD, brain cholesterol homeostatic disruption should be reflected by variations in its metabolite's level, particularly in plasma and CSF. However, it cannot be predicted whether the disturbance would affect the esterified or the free

plasma sterols forms, or both. Therefore, to shed lights on the variation of the plasma sterol lipids during PD, instead of characterising the total sterol content, the studies should be addressed to the determination of both free and esterified forms.

To the best of my knowledge, in chapter 4, we show for the first time the most comprehensive sterolome profile of the free plasma sterols in PD and compare it with the one from the neurologically healthy aged population. From the sterolome screening, 21 different sterols have been confidently identified and quantified in human plasma as their free-not esterified form, including mono hydroxy sterols, dihydroxy sterols, cholestenoic acids, the cholesterol precursor desmosterol and cholesterol. Among the panel of sterols identified, (25S)7α-H-3O-CA resulted in being 12% higher in PD (20.46 ± 7.28 ng/mL) as well as its epimer (25R)-7α-H-3O-CA, 10% higher in PD (135.7 ± 36.86 ng/mL) and (24S)-HC, accounting for an 8% increase in the PD patients' group (15.60 ± 3.51 ng/mL).

Conversely, plasma cholesterol levels were 10% lower in PD (662061 ± 136050 ng/mL). Interestingly, one sterol that differs between PD and non-PD is (24S)-HC. Among the cholestenoic acids, (24S)-HC and cholesterol, the monohydroxy sterol is the only one with an almost exclusive brain origin, considered to be a good surrogate biomarker to monitor brain cholesterol alteration and neuroneal metabolic activity. Indeed, (25R)-7α-H-3O-CA and (25S)-7α-H-3O-CA plasma levels are heavily influenced by the liver function, being mainly produced by hepatocytes, but also by the rate of bile excretion and faecal & renal elimination (Jp, 2006; Ogundare *et al.*, 2010b; Staels & Fonseca, 2009). Likewise, cholesterol plasma level depends on even more mechanisms, from hepatic biosynthesis and diet absorption to steroid hormones and bile acids metabolism, from HDL-driven

reverse cholesterol transport to LDL-cholesterol accumulation (chapter 1). Therefore, even if discriminating among PD and non-PD individuals, these three sterols can be excluded from the nominee to PD biomarker, electing (24S)-HC as a preferable soluble biomarker. Even though the majority of (24S)-HC is derived from the brain, the sterol plasma level results from the combination of three main events:

1. Diffusion from the brain through the BBB into the blood stream, with an estimated net daily efflux, roughly 5 to 7 mg in 24 hours (Björkhem, 2006b) (Lutjohann *et al.*, 1996)
2. Equilibrium between its free and esterified-lipoprotein plasmatic form.
3. Hepatic uptake for the sterol metabolism, which is about 7 mg/24 hours (Björkhem, 2006a; Lütjohann *et al.*, 1996b)

Therefore, correlation analysis has been carried out first to check for any influence between the (24S)-HC and the other sterol level. No correlation with any sterols identified in human plasma can be appreciated in PD and controls. Moreover, to investigate the contribution of the BBB integrity to the sterol plasma level, the (24S)-HC/26-HC ratio have been calculated in PD and non-PD group, reporting no differences between the two groups. Since a damaged BBB cannot be excluded from just this simple analysis and without information on the patients and controls clinical conditions, the absence of relevant variation in the level of 26-HC, along with the reduction in plasma cholesterol levels, pushed through a deeper investigation on the (24S)-HC variation. Gender has, therefore, been considered a confounding variable. When (24S)-HC levels have been clustered for sex and disease, the sterol variation could discriminate between males and females in both PD and control groups (chapter

4.4.1). Surprisingly, (24S)-HC is always significantly higher in females with respect to males. However, disease-related variations are only seen in the male counterpart, with (24S)-HC continuing to be significantly higher in PD males with respect to controls (12% higher in PD males with respect to non-PD males). The gender differences are difficult to interpret without any other clinical data and being aware of no age differences between the subgroups of our study (male PD vs female PD, male controls vs female controls). However, it is widely recognised that PD affects more male than females, and recent papers from Parrado-Fernández *et al.* has just shown gender differences in the BBB permeability in both controls and neurological diseases (Parrado-Fernández *et al.*, 2018; Parrado-Fernandez *et al.*, 2021). Moreover, it can be noted that the male values for (24S)-HC show a better clustering or diminished spread of the values respect to the female. Thus, the variation in (24S)-HC plasma levels between males and females can be imputed to intrinsic gender-related BBB permeability characteristics. It can also be hypothesised that the variation in the PD group is mainly to be reconducted to the male PD counterpart, and that might be related to dopaminergic neurones or brain-specific alteration occurring during PD and heavily affecting males, with respect to females. Lastly, we tested the power of (24S)-HC as a putative diagnostic biomarker for PD, and we showed that, when referring to the sterol plasma level, the chance to predict PD is almost 70% (ROC with AUC=0.66)

Assessed the bona fide of our findings from the baseline cohort of PD patients, we passed on the free sterols screening of a longitudinal cohort of PD patients, where the plasma was collected over 90 months (7.5 years) after diagnosis (chapter 4.4.2). To the best of my

knowledge, there are no data in the literature regarding the free sterolome profile of plasma in a longitudinal cohort of PD patients, except from a total plasma cholesterol study on longitudinal PD (K. Wang *et al.*, 2021). Therefore, this work represents the first study of plasma sterols variation throughout PD. The same panel of 20 sterols found in the baseline PD plasma has also been identified in this cohort. However, instead of 100 PD patients, only 16 belong to this cohort. Concerning the sterols level variation over time, no statistical and sensible difference in any of the sterols identified so far is reported, accompanied by a large value dispersion. However, a general decreasing trend can be appreciated between the first two time points, corresponding to baseline and 36 months. Curiously, the high SD is constant over the 36 months in almost all the sterols. This fact lets us speculate whether the intrinsic and patient-related biological variation might mask the little sterol variations over time. However, no assumption can be made without additional information on the clinical state, PD progression, medical treatments, and patient demographics, which can contribute to altering the sterol value. Moreover, the haemolysis, the plasma quality and the restricted number of patients might also have biased the sterol's quantification. We need to note that gender has not been tested as a confounding variable for the high discrepancy between the number of males patient (12) with respect to the females (4).

To complete the sterolome profile assessment for PD, longitudinal CSF from 80 PD patients was screened for its free sterol content over 96 months. This study's peculiarity is identifying the free, not total, CSF sterols in humans. Most of the literature is focused on the quantification of the total CSF sterols content for two main reasons:

1. Most of the CSF sterols are in their esterified form.

2. The analytical technique used for the screening was not sensitive enough to detect the low abundant free CSF sterols, or they would require an intrinsic saponification step (ex. GC-MS) (Björkhem *et al.*, 2013, 2018; Lütjohann *et al.*, 1996a).

Recently, our lab demonstrated for the first time that free CSF sterols, which are mainly cholestenoic acids, are not only able to discriminate between PD and non-PD but also to correlate with disease severity (W. J. Griffiths *et al.*, 2021c). Additionally, in another study on a bigger cohort of PD patients, our group confirmed the ability of the CSF-free cholestenoic acids to discriminate between PD and controls (data not published yet). Therefore, profiling the free CSF sterols in the longitudinal PD cohort has been considered the best option to evaluate PD-related sterols variation over time. All the following conclusions are made based on comparing values from the 12, 36 and 60 months, as, except for four samples, all the CSF belongs to these collection points.

Ten different free cholestenoic acids have been identified and quantified in PD CSF over 60 months. No significant variation has been observed in the CSF levels of the cholestenoic acids, with almost no changes in the mean values. Similarly, to the longitudinal plasma cohort, the SD in this cohort was marked but constant over time. Therefore, single-patient values have been evaluated over 60 months, and almost no changes are seen for all 80 patients. However, from this analysis, it can be appreciated how much the sterols values vary among the patients. The gender contribution has been evaluated as we did prove it to be a confounding variable in the PD baseline plasma cohort, but no differences have been reported.

Concluding, the sterolome profile of PD body fluids throughout the disease has identified in the (24S)-HC free plasma levels a potential

biomarker for the diagnosis, but not the prognosis of Parkinson's. None of the several sterols proved to be suitable for the evaluation of the disease state. However, the diagnostic outcome results from a single cohort of PD patients. Therefore, this finding needs to be validated by screening another cohort of PD patients, preferably of different ethnicity and provenience.

The validation phase is an ongoing study where the plasma sterolome profile of another cohort of American PD baseline patients will be used to verify the observations made on the NYPUM baseline cohort reported in this thesis. Preliminary data on the free mono hydroxy sterols' plasma levels show a similar distribution to the NYPUM cohort, with also a similar mean value. Future work will reveal whether the American PD patients' sterols behave like the Sweden ones.

6.1.3 NES cells

The sterolome profile of the iPSC-derived NES and iPSCs NES with LRRK2 mutation was born to complement the work on sterols body fluids screening over PD and characterise cholesterol/sterols variation during neuroneal development.

Nowadays, the participation of cholesterol in the main pathological mechanisms contributing to neurodegeneration is considered certain. However, the degree of sterol impact on neurodegenerative disorders is still unknown. To shed light on the role of cholesterol alteration over the neurodegenerative process, the sterol function during neurogenesis and neuroneal development should be investigated and clarified first. Little is known about cholesterol level modification

during the development of neuroneal cells, and a complete sterolome characterisation is needed.

This thesis represents the first sterolome profile of human NES cells. From NES and LRRK2 NES cell pellet and medium analysis cholestenoic acids, two dihydroxy sterols, 7α,26-diHC + (24S,25)-di-HC, one ketone 7-OC, six monohydroxy sterols, (24S)-HC + (24R)-HC + 7α-HC +7α-HCO + 7β-HC + 6β-HC and cholesterol have been identified. Moreover, two cholestenoic acids, 3β,7α-diHCA + 7α-H-3O-CA, 1 epoxy sterol, (24S,25)-EC, and one ketone, 24-OC have been recognised but identified. From this analysis, we can affirm that oxysterols, including (24S)-HC, are already produced in NES cells, precursors of neuroneal and glial cells. Interestingly, we have also identified (24R)-HC, the epimer of (24S)-HC. CYP46A1, the enzyme responsible for (24S)-HC production, is epimer specific and the only one responsible for 24-OH sterols production in the human body(CYP46A1 Human Protein Atlas, 2023). Indeed, from the screening of several human body fluids and tissue homogenates, the R epimer has never been identified in human beings but only in mice, representing around 10% (Saeed *et al.*, 2014). A certain degree of isomerisation might occur when the sterol concentration is high. However, the process is generally slow without the presence of a catalyser. We speculate if other proteins might contribute to the 24-HCs synthesis at this stage or if epimerisation occurs. More experiments are needed for clarification. Furthermore, the identification of 7α,26-HC along with 7α-HC and the probably 7α-cholestenoic acids raises the possibility of an active cholesterol classical catabolic pathway towards bile acids. Future studies will shed lights on all the cholesterol catabolic and anabolic pathways involved in the maintenance of its homeostasis in the NES cells.

From the comparison of medium and cell pellet, it can be appreciated a qualitative difference: the more polar cholestenoic acids are exclusively present in the medium of the cells, while the less polar mono and di-hydroxy sterols are principally present in the cell pellet. This finding is quite interesting as mono-hydroxy sterols are widely recognised to cross plasma barriers through simple diffusion, while no precise data are available for cholestenoic acids. More experiments are needed to clarify this behaviour, including the contribution of medium components or detergent/washing solutions to the NES cell membrane permeability.

Having in hands a single replicate, no assumption can be made from a quantitative point of view between NES and LRRK2 NES. However, an efficient and reliable protocol for the complete screening of both cell pellets and medium sterols is provided within this thesis. Future experiments will shed light on qualitative and quantitative differences between the two cell types.

6.2 Concluding findings

In this thesis we aimed to study the cholesterol and cholesterol metabolite variations in AD and PD. For the first time we report a complete free sterolome profile for PD plasma/CSF and total sterolome for AD CSF, identifying up to 24 different sterols.

In PD patients, free plasma levels of (24S)-HC and of 7α-hydroxy-3-oxo- cholestenoic acid have been reported to be increased compared to healthy controls while the plasma cholesterol was lower. Notably, (24S)-HC levels were also able to discriminate between males and females and exhibit diagnostic power in predicting the disease.

However, CSF and plasma sterols were found to be unsuitable prognostic biomarkers for PD as they fail to show any significant variation.

In the CSF from AD patients, the levels of extracerebral 26-hydroxycholesterol and (24S)-HC displayed a positive correlation with the disease severity but the difference between them didn't reach a significant variation.

Finally, as in ND neuronees are the most affected cells, we analysed for the first time the sterolome of human NES cells to complement the work in AD and PD. The sterols screening of NES and LRRK2 NES revealed that cholesterol metabolites are synthesised form a very early stage of neuroneal differentiation.

In conclusion, the work on this thesis focuses on finding suitable cholesterol metabolites that could be used as biomarker for ND.

6.3 Limitations of the work

The work presented within this thesis provides one of the most comprehensive human AD and PD body fluids sterol screenings. However, there are some criticisms which can be classified into three categories:

1. Protocol-method dependent
2. Sample dependent
3. Information dependent

Concerning point 1, the weaknesses lie mainly in the analytical technique employed. Even if the LC-MS technique is sensitive enough to detect very low abundant sterol lipids, it consents the direct detection of only sterols which possess a 3-ketone function due to GP derivatisation. In most cases, it is possible to obtain the portion of sterol possessing the 3β-hydroxyl moiety indirectly, mainly by subtraction between the sterols extract oxidised and derivatised (containing, therefore, 3-OH and 3-ketone sterols) and the non-oxidised one (only containing 3-ketone). However, this step is not always possible, largely when the proportion of the 3-OH sterols is less than 10% of the 3-ketones, which might also fall under the limit of detection, and when the standard used for quantification of the 3-ketone differs with respect to the one used for the 3-OH+3-ketone. The lack of an identical or surrogate deuterated standard constitutes the second methodology downside, which we compensate for by introducing at least one standard for each subclass of sterol lipid. Ionised sterols' properties depend on their chemical nature and the spatial distribution of their functionalised groups. Therefore, quantifying a sterol against a not identical standard might cause

under or overestimation of their quantity, which reflects in the impossibility of obtaining 3-hydroxyl values by the difference when the 3-ketone-only sterol extracts are quantified using a different internal standard with respect to their 3-OH+3-one-counterpart. However, we tried to create the most comprehensive deuterated standard mixes, but some standards were missing for market unavailability reasons.

In this thesis, a good number of patient samples have been provided; however, we have identified some issues.

One of the biggest concerns when analysing the body fluids sterols is the sample size. We did identify a quite large biological variation as a characteristic of this class of sterol. Therefore, restricted sample sizes might mask small differences among patients and controls. This could have been the case of the AD cohort, (n=30 per group) but also of the longitudinal PD plasma, composed of only 16 patients for 36 samples. Furthermore, in this cohort, haemolysis, coagulation, and suspension formation were present in almost all the plasma samples, interfering with sterol extraction. Therefore, longitudinal plasma sterol data might have been biased by plasma quality.

This thesis report for the first time one of the most comprehensive sterolome profiles of human plasma free sterols in PD and NES cells and of total in AD CSF. However, a complete sterol screening would have also required the analysis of the free and total forms in AD and PD/NES, respectively, which could also have contributed to the determination of the esterified part alone. Due to sample availability, we decided to analyse one class of sterols or the other based on the high sensitivity of our analytical technique and literature findings, to complement and/or add new insights into ND sterolome characterisation.

The last concern, predominantly identified within the AD cohort, is the lack of patient demographics (age, gender, BMI) and disease-related clinical features like MRI scans, APOE status or Aß CSF levels. We did demonstrate with the baseline PD cohort that sex might be a confounding variable and critical determinant for the definition of a sterol biomarker. Moreover, it is well recognised how several parameters like age, lifestyle, and diet habits can influence plasma, CSF, and sterol levels. It has been demonstrated before that cholesterol brain metabolism is affected by toxic aggregates of Aß or APOE variant ε4 (Bodovitz & Klein, 1996; Grösgen *et al.*, 2010; Q. Liu *et al.*, 2007). Therefore, our findings on AD sterolome might be incomplete.

Co-morbidities, especially chronic metabolic pathologies like diabetes or dyslipidaemia, might alter cholesterol metabolism and sterol levels, especially when cholesterol synthesis modifying or interfering drugs are administered. For all the PD cohorts, metabolic co-morbidities and cholesterol-modifying medical treatments were not included in the exclusion criteria for patient recruitment. Therefore, we are not aware if these conditions might have effectively contributed to our findings.

6.4 Future developments

The work reported in this thesis has highlighted the importance of characterising the sterol variation over different NDs, which can turn in the identification of putative biomarkers for the diseases and, secondly, shed light on the contribution of cholesterol to the neurodegenerative processes.

(24S)-HC has been identified as a candidate diagnostic biomarker for PD. However, this finding must be validated in a broader range of PD patients and gender/age-matched controls. The ongoing work on the US PD samples and controls will therefore assess this sterol as a PD biomarker. Confirmation studies are therefore needed also for the longitudinal cohorts.

Healthy control CSF sterols will be analysed and compared with the respective SCI, MCI and AD groups to complement the findings of this thesis. If a difference in sterol levels is spotted, AD cholesterol metabolites variations over AD progression will be characterised.

The preliminary work on NES cells assessed the feasibility of sterolome characterisation in this cell type. Therefore, future studies will clarify the cholesterol metabolites variation over normal neuroneal development and in LRRK2 mutated cells.

The sterol extraction protocol, sample preparation and the LC-ESI-MS^3 technique used in this thesis have allowed the precise and accurate determination of the sterol content in several biological matrixes, both fluid and solid. If future works confirm the ability of one or more sterols to be used as diagnostic biomarkers, the methodology will be scaled-up for high-throughput screening. Attempts to automation of the entire procedure are planned for the foreseeable future.

Chapter 7 Appendix

Precursor ion [M+] *m/z*	z	MS² *m/z*	MS² z	Start time (minutes)	End time (minutes)
522.3326	1	443.2904	1	0	17
527.364	1	443.2904	1	0	17
532.3898	1	443.3476	1	0	17
537.4212	1	443.3476	1	0	17

Table 7.1 LC-MS method 1, for Fr1, inclusion list specifications.

Precursor ion [M+] *m/z*	z	MS² *m/z*	MS² z	Start time (minutes)	End time (minutes)
550.4003	1	471.3581	1	0	17
555.4317	1	471.3581	1	0	17
561.4694	1	477.3958	1	0	17

Table 7.2 LC-MS method 2, for Fr1, inclusion list specifications.

Precursor ion [M+] *m/z*	z	MS² *m/z*	MS² z	Start time (minutes)	End time (minutes)
569.411	1	485.3374	1	0	17
564.3796	1	485.3374	1	0	17
567.3984	1	458.36	1	0	17
572.4298	1	458.36	1	0	17

Table 7.3 LC-MS method 3, for Fr1, inclusion list specifications.

Precursor ion [M+] *m/z*	z	MS^2 *m/z*	MS^2 z	Start time (minutes)	End time (minutes)
548.3847	1	469.3425	1	0	17
553.4161	1	469.3425	1	0	17
506.3377	1	427.2955	1	0	17
511.3691	1	427.2955	1	0	17

Table 7.4 LC-MS method 4, for Fr1, inclusion list specifications.

Precursor ion [M+] *m/z*	z	MS^2 *m/z*	MS^2 z	Start time (minutes)	End time (minutes)
541.4493	1	462.4071	1	0	17
545.4745	1	461.4009	1	0	17
546.4807	1	462.4071	1	0	17
539.4368	1	455.4071	1	0	17
534.4054	1	455.4071	1	0	17

Table 7.5 LC-MS method 5, for Fr1, inclusion list specifications.

Precursor ion [M+] *m/z*	z	MS^2 *m/z*	MS^2 z	Start time (minutes)	End time (minutes)
548.3847	1	469.3425	1	0	17
553.4161	1	469.3425	1	0	17
550.4003	1	471.3581	1	0	17
555.4317	1	471.3581	1	0	17
561.4694	1	477.3958	1	0	17

Table 7.6 LC-MS method 6, for Fr1, inclusion list specifications.

Precursor ion [M+] *m/z*	z	MS^2 *m/z*	MS^2 z	Start time (minutes)	End time (minutes)
522.3326	1	443.2904	1	0	17
527.364	1	443.2904	1	0	17
580.3744	1	501.3321	1	0	17
585.4959	1	501.3321	1	0	17

Table 7.7 LC-MS method 7, for Fr1, inclusion list specifications.

Precursor ion [M+] *m/z*	z	MS^2 *m/z*	MS^2 z	Start time (minutes)	End time (minutes)
569.411	1	485.3374	1	0	37
541.4493	1	462.4071	1	0	37
545.4745	1	461.4009	1	0	37
546.4807	1	462.4071	1	0	37
539.4368	1	455.4071	1	0	37
534.4054	1	455.4071	1	0	37

Table 7.8 LC-MS method 8, for Fr1, inclusion list specifications.

Precursor ion [M+] *m/z*	z	MS^2 *m/z*	MS^2 z	Start time (minutes)	End time (minutes)
569.411	1	485.3374	1	0	37
545.4745	1	461.4009	1	0	37
555.4317	1	471.3581	1	0	37
561.4694	1	477.3958	1	0	37
539.4368	1	455.4071	1	0	37

572.4298	1	458.36	1	0	37

Table 7.9 LC-MS method 9, for Fr1, inclusion list specifications.

Precursor ion [M+] *m/z*	z	MS² *m/z*	MS² z	Start time (minutes)	End time (minutes)
518.4105	1	439.3683	1	0	17
523.4419	1	439.3683	1	0	17
520.4261	1	441.3839	1	0	17
525.4575	1	441.3839	1	0	17
530.485	1	446.4122	1	0	17

Table 7.10 LC-MS method 10, for Fr3, inclusion list specifications.

Precursor ion [M+] *m/z*	z	MS² *m/z*	MS² z	Start time (minutes)	End time (minutes)
514.3729	1	435.337	1	0	17
519.4106	1	435.337	1	0	17
516.3948	1	437.3526	1	0	17
521.4262	1	437.3526	1	0	17
530.485	1	446.4122	1	0	17

Table 7.11 LC-MS method 11, for Fr3, inclusion list specifications.

Precursor ion [M+] *m/z*	z	MS² *m/z*	MS² z	Start time (minutes)	End time (minutes)
514.3729	1	435.337	1	0	17
519.4106	1	435.337	1	0	17

516.3948	1	437.3526	1	0	17
521.4262	1	437.3526	1	0	17
527.4539	1	443.3903	1	0	17

Table 7.12 LC-MS method 12, for Fr3, inclusion list specifications.

Precursor ion [M+] *m/z*	z	MS² *m/z*	MS² z	Start time (minutes)	End time (minutes)
522.4325	1	443.3903	1	0	17
530.485	1	446.4122	1	0	17
516.3948	1	437.3526	1	0	17
521.4262	1	437.3526	1	0	17
527.4539	1	443.3903	1	0	17

Table 7.13 LC-MS method 13, for Fr3, inclusion list specifications.

Endogenous sterols	Quantified against	ng /mL	Corrections
(24S,25)-di-HC	[$^2H_6$](24R/S)-hydroxycholesterol	2	
7α,26-diHC	[$^2H_6$](24R/S)-hydroxycholesterol	2	
(24S)-HC	[$^2H_6$](24R/S)-hydroxycholesterol	2	
(24R)-HC	[$^2H_6$](24R/S)-hydroxycholesterol	2	
7β-HC	[$^2H_6$](24R/S)-hydroxycholesterol	2	
7α-HC +7α-HCO	[$^2H_6$](24R/S)-hydroxycholesterol	2	

6b-HC	[$^2H_6$](24R/S)-hydroxycholesterol	2	
7-OC	[$^2H_6$](24R/S)-hydroxycholesterol	2	correct to[$^2H_7$](22S)-hydroxycholesterol A/B
Cholesterol	[$^2H_7$]-cholesterol	400	

Table 7.14 NES cells derived from iPSCs quantification table.

Endogenous sterols	Quantified against	ng/mL	Corrections
(24S)-HC	[$^2H_6$](24R/S)-hydroxycholesterol	200	
26-HC	[$^2H_6$](24R/S)-hydroxycholesterol	200	
25-HC	[$^2H_6$](24R/S)-hydroxycholesterol	200	
7β-HC	[$^2H_7$](7α)-hydroxycholesterol	200	
7α-HC +7α-HCO	[$^2H_7$](7α)-hydroxycholesterol	200	
6β-HC	[$^2H_7$](7α)-hydroxycholesterol	200	correct to[$^2H_7$](22S)-hydroxycholesterol A/B
cholestenoic acid (3β-HCA)	[$^2H_5$]cholestenoic acid	200	
7-OC	[$^2H_7$]7-ketocholesterol	200	
7α-HCO	[$^2H_7$](7α)-hydroxycholesterol	200	correct to[$^2H_7$](22S)-hydroxycholesterol A/B
7a-HC	calculated as: (7α)-HC (7α)-HCO - (7α)-HCO		
7α,25-diHC + 7α,25-diHCO	[$^2H_6$](7α,25)-dihydroxycholesterol	20	

7α,25-diHCO	[$^2H_6$](7α,25)-dihydroxycholesterol	20	correct to 7αH,3O-HCA-D3 A/B
7α,25-diHC	calculated as: 7α,25-diHC + 7α,25-diHCO - 7α,25-diHCO		
7α,26-diHC + 7α,26-diHCO	[$^2H_6$](7α,25)-dihydroxycholesterol	20	
7α,26-diHCO	[$^2H_6$](7α,25)-dihydroxycholesterol	20	correct to 7αH,3O-HCA-D3 A/B
7α,26-diHC	calculated as: 7α,26-diHC + 7α,26-diHCO - 7α,26-diHCO		
(25S)3β,7α-diHCA + (25S)7α-H-3-OCA	[$^2H_3$]7α-hydroxy-3-oxocholestenoic acid	200	
(25S)7α-H-3O-CA	[$^2H_3$]7α-hydroxy-3-oxocholestenoic acid	200	
(25S)3β,7α-diHCA	calculated as: (25S)3β,7α-diHCA + (25S)7α-H-3-OCA - (25S)7α-H-3O-CA		
3β,7α-diHCA + 7α-H-3-OCA	[$^2H_3$]7α-hydroxy-3-oxocholestenoic acid	200	
7α-H-3O-CA	[$^2H_3$]7α-hydroxy-3-oxocholestenoic acid	200	
3β,7α-diHCA	calculated as: 3β,7α-diHCA + 7α-H-3-OCA - 7α-H-3O-CA		
(25R)3β-7α-diHCA +(25R)7α-H-3O-CA	calculated as: 3β,7α-diHCA + 7α-H-3-OCA -(25S)3β,7α-HCA +(25S)7α-H-3O-CA		
(25R)7α-H-3O-CA	calculated as: 7αH,3O-CA - (25S)7α-H-3O-CA		
(25R)3β,7α-diHCA	calculated as: (25R)3β,7α-diHCA + (25R)7α-H-3-OCA - (25R)7α-H-3O-CA		
Desmosterol	[$^2H_7$]-cholesterol	200 000	

Cholesterol	[$^2H_7$]-cholesterol	200 000	

Table 7.15 NYPUM PD plasma quantification table.

Endogenous sterols	Quantified against	ng/ mL	Corrections
(24S)-HC	[$^2H_6$](24R/S)-hydroxycholesterol	200	
26-HC	[$^2H_6$](24R/S)-hydroxycholesterol	200	
25-HC	[$^2H_6$](24R/S)-hydroxycholesterol	200	
7ß-HC	[$^2H_7$](7α)-hydroxycholesterol	200	
7α-HC +7α-HCO	[$^2H_7$](7α)-hydroxycholesterol	200	
6ß-HC	[$^2H_7$](7α)-hydroxycholesterol	200	correct to[$^2H_7$](22 S)-hydroxycholesterol A/B
cholestenoic acid (3ß-HCA)	[$^2H_5$]cholestenoic acid	200	
7-OC	[$^2H_7$]7-ketocholesterol	200	
7α-HCO	[$^2H_7$](7α)-hydroxycholesterol	200	correct to[$^2H_7$](22 S)-hydroxycholesterol A/B
7a-HC	calculated as: (7α)-HC (7α)-HCO - (7α)-HCO		
7α,25-diHC + 7α,25-diHCO	[$^2H_6$](7α,25)-dihydroxycholesterol	20	
7α,25-diHCO	[$^2H_6$](7α,25)-dihydroxycholesterol	20	correct to 7αH,3O-HCA-D3 A/B

7α,25-diHC	calculated as: 7α,25-diHC + 7α,25-diHCO - 7α,25-diHCO		
7α,26-diHC + 7α,26-diHCO	[$^2H_6$](7α,25)-dihydroxycholesterol	20	
7α,26-diHCO	[$^2H_6$](7α,25)-dihydroxycholesterol	20	correct to 7αH,3O-HCA-D3 A/B
7α,26-diHC	calculated as: 7α,26-diHC + 7α,26-diHCO - 7α,26-diHCO		
(25S)3β,7α-diHCA + (25S)7α-H-3-OCA	[$^2H_3$]7α-hydroxy-3-oxocholestenoic acid	200	
(25S)7α-H-3O-CA	[$^2H_3$]7α-hydroxy-3-oxocholestenoic acid	200	
(25S)3β,7α-diHCA	calculated as: (25S)3β,7α-diHCA + (25S)7α-H-3-OCA - (25S)7α-H-3O-CA		
3β,7α-diHCA + 7α-H-3-OCA	[$^2H_3$]7α-hydroxy-3-oxocholestenoic acid	200	
7α-H-3O-CA	[$^2H_3$]7α-hydroxy-3-oxocholestenoic acid	200	
3β,7α-diHCA	calculated as: 3β,7α-diHCA + 7α-H-3-OCA - 7α-H-3O-CA		
(25R)3β-7α-diHCA +(25R)7α-H-3O-CA	calculated as: 3β,7α-diHCA + 7α-H-3-OCA -(25S)3β,7α-HCA +(25S)7α-H-3O-CA		
(25R)7α-H-3O-CA	calculated as: 7αH,3O-CA - (25S)7α-H-3O-CA		
(25R)3β,7α-diHCA	calculated as: (25R)3β,7α-diHCA + (25R)7α-H-3-OCA - (25R)7α-H-3O-CA		
Cholesterol	[$^2H_7$]-cholesterol	200 000	

Table 7.16 ICICLE PD plasma quantification table.

Endogenous sterols in human plasma	Quantified against	ng/mL	Corrections
(24S)-HC	[$^2H_6$](24R/S)-hydroxycholesterol	200	
26-HC	[$^2H_6$](24R/S)-hydroxycholesterol	200	
25-HC	[$^2H_6$](24R/S)-hydroxycholesterol	200	
7β-HC	[$^2H_7$](7α)-hydroxycholesterol	200	
7α-HC +7α-HCO	[$^2H_7$](7α)-hydroxycholesterol	200	
6β-HC	[$^2H_7$](7α)-hydroxycholesterol	200	correct to[$^2H_7$](22S)-hydroxycholesterol A/B
cholestenoic acid (3β-HCA)	[$^2H_5$]cholestenoic acid	200	
7-OC	[$^2H_7$]7-ketocholesterol	200	
7α-HCO	[$^2H_7$](7α)-hydroxycholesterol	200	correct to[$^2H_7$](22S)-hydroxycholesterol A/B
7a-HC	calculated as: (7α)-HC (7α)-HCO - (7α)-HCO		
7α,25-diHC + 7α,25-diHCO	[$^2H_6$](7α,25)-dihydroxycholesterol	20	
7α,25-diHCO	[$^2H_6$](7α,25)-dihydroxycholesterol	20	correct to 7αH,3O-HCA-D3 A/B
7α,25-diHC	calculated as: 7α,25-diHC + 7α,25-diHCO - 7α,25-diHCO		
7α,26-diHC + 7α,26-diHCO	[$^2H_6$](7α,25)-dihydroxycholesterol	20	
7α,26-diHCO	[$^2H_6$](7α,25)-dihydroxycholesterol	20	correct to 7αH,3O-

			HCA-D3 A/B
7α,26-diHC	calculated as: 7α,26-diHC + 7α,26-diHCO - 7α,26-diHCO		
(25S)3ß,7α-diHCA + (25S)7α-H-3-OCA	[$^2H_3$]7α-hydroxy-3-oxocholestenoic acid	200	
(25S)7α-H-3O-CA	[$^2H_3$]7α-hydroxy-3-oxocholestenoic acid	200	
(25S)3ß,7α-diHCA	calculated as: (25S)3ß,7α-diHCA + (25S)7α-H-3-OCA - (25S)7α-H-3O-CA		
3ß,7α-diHCA + 7α-H-3-OCA	[$^2H_3$]7α-hydroxy-3-oxocholestenoic acid	200	
7α-H-3O-CA	[$^2H_3$]7α-hydroxy-3-oxocholestenoic acid	200	
3ß,7α-diHCA	calculated as: 3ß,7α-diHCA + 7α-H-3-OCA - 7α-H-3O-CA		
(25R)3ß-7α-diHCA +(25R)7α-H-3O-CA	calculated as: 3ß,7α-diHCA + 7α-H-3-OCA -(25S)3ß,7α-HCA +(25S)7α-H-3O-CA		
(25R)7α-H-3O-CA	calculated as: 7αH,3O-CA - (25S)7α-H-3O-CA		
(25R)3ß,7α-diHCA	calculated as: (25R)3ß,7α-diHCA + (25R)7α-H-3-OCA - (25R)7α-H-3O-CA		
Desmosterol	[$^2H_6$]-desmosterol	600	
Cholesterol	[$^2H_7$]-cholesterol	200 000	

Table 7.17 BioFIND PD plasma quantification table.

Endogenous sterols	Quantified against	ng/mL iSTD	Corrections
(24S)-HC	[$^2H_6$](24R/S)-hydroxycholesterol	20	

26-HC	[$^2H_6$](24R/S)-hydroxycholesterol	20	
25-HC	[$^2H_6$](24R/S)-hydroxycholesterol	20	
6ß-HC	[$^2H_7$](7α)-hydroxycholesterol	20	
3ß-H-7-OC + 7-OC	[$^2H_7$](7α)-hydroxycholesterol	20	
7-OC	[$^2H_7$](7α)-hydroxycholesterol	20	correct to[$^2H_7$](22S)-hydroxycholesterol A/B
Δ7-dehydro-cholesterol	[$^2H_7$]-cholesterol	2000	
Desmosterol	[$^2H_7$]-cholesterol	2000	
Cholesterol	[$^2H_7$]-cholesterol	2000	

Table 7.18 GEDOC SCI, MCI, AD CSF quantification table.

Endogenous sterols	Quantified against	ng/mL iSTD
Cholestenoic acid (3ß-HCA)	[$^2H_5$]cholestenoic acid	10
(25S)3ß,7α-diHCA + (25S)7α-H-3-OCA	[$^2H_3$]7α-hydroxy-3-oxocholestenoic acid	20
(25S)7α-H-3O-CA	[$^2H_3$]7α-hydroxy-3-oxocholestenoic acid	20
(25S)3ß,7α-diHCA	calculated as: (25S)3ß,7α-diHCA + (25S)7α-H-3-OCA - (25S)7α-H-3O-CA	

3ß,7α-diHCA + 7α-H-3-OCA	[$^2H_3$]7α-hydroxy-3-oxocholestenoic acid	20
7α-H-3O-CA	[$^2H_3$]7α-hydroxy-3-oxocholestenoic acid	20
3ß,7α-diHCA	calculated as: 3ß,7α-diHCA + 7α-H-3-OCA - 7α-H-3O-CA	
(25R)3ß-7α-diHCA +(25R)7α-H-3O-CA	calculated as: 3ß,7α-diHCA + 7α-H-3-OCA -(25S)3ß,7α-HCA +(25S)7α-H-3O-CA	
(25R)7α-H-3O-CA	calculated as: 7αH,3O-CA - (25S)7α-H-3O-CA	
(25R)3ß,7α-diHCA	calculated as: (25R)3ß,7α-diHCA + (25R)7α-H-3-OCA - (25R)7α-H-3O-CA	
(3ß,7α,24S)-triHCA	[$^2H_3$]7α-hydroxy-3-oxocholestenoic acid	20
3ß,7α,25-triHCA +7α,25-diH-3O-CA	[$^2H_3$]7α-hydroxy-3-oxocholestenoic acid	20
7α,25-diH-3O-CA	[$^2H_3$]7α-hydroxy-3-oxocholestenoic acid	20
3ß,7α,25-triHCA	calculated as: 3ß,7α,25-triHCA +7α,25-diH-3O-CA - 7α,25-diH-3O-CA	
3ß,7α,X-triHCA +7α,X-diH-3O-CA	[$^2H_3$]7α-hydroxy-3-oxocholestenoic acid	20
7α,X-diH-3O-CA	[$^2H_3$]7α-hydroxy-3-oxocholestenoic acid	20
3ß,7α,X-triHCA	calculated as: 3ß,7α,X-triHCA +7α,X-diH-3O-CA - 7α,X-diH-3O-CA	
Cholesterol	[$^2H_7$]-cholesterol	2000

Table 7.19 Longitudinal NYPUM CSF quantification table.

Control Donors Comorbidities
Suspected disease of the nervous system
Cricopharyngeusalsia
Fainting and collapse
Bilat papilledema
Polyneuropathy
Effect of polio

Essential Hypertension (Bene Paraesthesia)
Fever
Oculopharyngeal muscular dystrophy
Muscle weakness
Motor axonal polyneuropathy
Disturbance of balance
Muscle weakness
Unsteady gait
Paraesthesia
Trigeminal
Cerebellar ataxia
Vogt-Koyanagi-Harada Disease
Multiple cranial nerve involvement
Bell's palsy
Cervical myalgia (Headache)
Optic nerve inflammation
normal pressure hydrocephalus
Gait disturbance
Spinal-Bulbar Muscular Atrophy (SBMA)
Myasthenia gravis
Hyperesthesia
Hyperesthesia
C-fiber polyneuropathy
Carpal tunnel syndrome
Axial spondylarthritis
(Small vessel disease in the CNS)/Dysarthria
Migraine
Ataxia
Paresthesia
Vocal cord palsy/ oropharyngeal dysphagia
Trigeminal neuralgia
Neuralgia UNS
Total ophthalmoplegia external (bilat Abd paresis) Chronic Progressive External Ophthalmoplegia (CPEO)
Spinal stenosis
Adult hydrocephalia
Disturbance of balance
Disturbance of skin sensation
Muscle cramps
Visual disturbance UNS
Dysphagua

Polyneuropathy with ganglioside antibodies
Trigeminal neuralgia
Gait disturbances due to neuropathy
Bell's palsy
Myasthenia gravis
Paresthesia
Unspecific disease of the nerve roots
Confusion
Capillary telangiectasias in the cerebellum
Hypersomnia (fatigue)

Table 7.20 Comorbidities affecting non-PD age/sex matched controls of NYPUM PD base-line plasma screening.

Chronic conditions	SCI	MCI	AD
Cardiovascular	3.30% *(v/v)*	6.70% *(v/v)*	0.00% *(v/v)*
Autoimmune	3.30% *(v/v)*	6.70% *(v/v)*	6.70% *(v/v)*
Osteoarthritis	13.30% *(v/v)*	13.30% *(v/v)*	6.70% *(v/v)*

Table 7.21 Comorbidities affecting SCI, MCI and AD of GEDOC memory clinical cohort.

Disease status	Sample name	(24S)-HC	25-HC	26-HC	7-OC	3β-H-7-OC + 7-OC	6β-HC	Desmosterol	Δ7-dehydro-cholesterol	Cholesterol
1	1	2.20	0.12	2.38	0.73	1.72	0.98	5.95	2.11	4366.30
1	10	0.65	0.05	0.57	1.70	0.54	1.58	0.93	0.00	1948.67
1	12	1.24	0.03	0.58	0.72	0.86	1.49	2.22	0.78	2846.18
1	18	1.54	0.04	1.35	1.11	0.62	0.57	3.81	0.00	4269.75
1	23	1.55	0.07	0.74	0.50	0.58	0.18	2.99	0.40	2668.61
1	28	1.85	0.05	1.25	0.90	0.18	0.52	2.43	0.46	3531.13
1	32	1.22	0.01	0.93	1.48	7.08	1.70	1.31	0.63	2348.83
1	38	2.41	0.14	1.26	1.47	0.58	0.86	2.72	0.54	2701.03
1	43	2.17	0.07	1.11	0.01	0.47	0.05	0.00	0.00	3278.95
1	44	3.48	0.08	1.87	2.15	1.22	1.58	0.00	0.00	2946.53
1	51	1.87	0.12	1.37	0.91	0.76	1.04	1.34	0.67	3853.32
1	59	1.17	0.07	0.70	1.06	2.06	1.61	0.00	0.00	2172.42
1	60	1.52	0.04	0.85	0.96	1.86	1.19	0.00	0.00	2792.44
1	66	3.55	0.09	2.31	1.65	1.70	3.00	6.50	0.37	4712.31
1	73	1.86	0.14	1.22	1.96	4.03	1.83	3.08	0.00	2923.87
1	74	3.03	0.12	3.00	0.00	3.28	18.65	4.74	0.48	3653.30
1	90	2.00	0.05	1.40	0.48	1.88	1.46	3.11	0.84	2486.91
1	2	1.32	0.04	1.05	0.82	1.54	1.75	4.34	0.00	3059.64
1	25	1.27	0.09	1.02	0.77	0.40	0.67	1.71	0.73	4041.04
1	27	2.22	0.07	1.37	0.67	0.56	0.25	4.00	0.34	4085.20
1	40	1.16	0.08	0.49	0.00	2.73	1.49	0.30	0.16	1979.07
1	45	1.38	0.04	0.83	0.00	2.67	0.27	1.71	0.55	2132.67
1	65	1.52	0.07	0.71	2.22	1.13	6.01	2.73	0.16	1330.10
1	72	1.79	0.07	0.89	0.00	2.52	1.59	4.36	0.00	2943.25
1	86	1.78	0.06	1.03	0.60	1.71	0.93	2.64	0.79	2306.97

1	16	1.23	0.03	0.92	0.99	1.09	1.54	1.54	0.00	1972.78
1	17	1.30	0.05	0.93	1.64	0.64	0.74	1.56	0.00	2524.81
1	41	1.67	0.08	1.23	1.27	0.29	1.36	2.17	0.49	3170.76
1	55	2.52	0.11	1.14	0.00	2.04	0.79	4.10	0.56	3404.21
1	80	2.89	0.13	1.33	0.90	1.60	0.99	3.95	0.00	3168.83
2	5	3.18	0.09	1.53	1.70	0.55	1.41	5.08	1.72	6600.44
2	6	2.85	0.08	1.36	2.79	0.88	2.53	5.82	1.38	3578.52
2	15	2.13	0.06	1.33	0.76	8.36	3.26	4.01	1.72	2978.79
2	29	1.95	0.20	1.78	0.00	1.25	0.98	3.64	0.92	5377.73
2	33	2.99	0.19	1.74	0.00	2.74	1.11	5.00	1.34	5472.76
2	35	0.00	0.27	0.00	0.16	0.43	0.25	2.28	0.19	2335.03
2	47	3.58	0.10	2.26	0.61	0.18	0.26	6.67	2.89	7102.01
2	49	0.00	0.00	0.00	1.38	0.38	0.97	0.00	0.00	8.85
2	52	2.52	0.05	1.35	1.23	0.46	0.58	3.66	0.22	4374.88
2	68	1.18	0.07	0.80	0.00	2.61	1.66	2.20	0.00	2719.92
2	75	2.68	0.10	2.53	1.12	0.32	1.60	6.43	1.17	6402.21
2	84	1.75	0.04	1.06	0.55	1.08	1.23	2.55	0.72	2387.25
2	87	2.49	0.07	1.44	0.83	1.05	3.57	2.41	0.29	2206.00
2	11	4.43	0.16	2.30	0.70	1.18	1.85	6.23	1.51	4603.64
2	22	2.09	0.06	1.14	0.56	0.60	0.23	2.99	0.62	3044.46
2	39	1.24	0.04	1.06	0.00	3.40	0.79	3.30	0.71	3428.64
2	53	1.49	0.10	0.83	0.90	0.81	0.62	2.73	0.68	3009.89
2	62	0.76	0.07	0.58	1.15	1.50	1.08	0.00	0.00	1809.26
2	83	0.59	0.03	0.55	0.38	0.62	1.08	0.20	0.00	1316.69
2	21	2.12	0.08	1.38	0.46	0.73	0.60	3.98	1.16	3597.24
2	56	3.24	0.10	2.18	0.60	0.78	0.50	4.08	0.90	6400.17

2	67	2.91	0.09	1.57	1.55	1.34	2.69	4.08	0.00	3079.71
2	76	1.44	0.06	0.62	0.00	1.78	1.76	2.02	0.00	1898.48
2	78	1.82	0.05	0.79	0.00	1.89	3.23	2.31	0.00	2025.26
2	79	2.92	0.09	1.47	1.12	0.78	1.87	2.75	0.00	2953.18
2	81	2.84	0.10	1.58	0.00	2.62	1.85	4.40	0.14	2812.00
2	4	1.79	0.03	1.30	1.46	1.52	2.70	5.21	0.80	4449.89
2	13	2.00	0.12	1.25	1.08	0.92	1.61	3.35	0.45	4327.80
2	30	1.74	0.04	1.26	0.51	0.57	0.68	4.20	1.19	4727.70
2	58	2.69	0.27	1.31	0.00	8.29	12.26	9.18	12.80	3032.03
3	3	1.10	0.06	0.82	0.91	1.11	0.83	2.70	0.00	2290.95
3	9	3.33	0.05	2.24	0.96	0.59	1.35	4.22	1.97	4822.92
3	19	3.56	0.14	2.39	1.00	0.33	0.60	6.49	1.74	5817.61
3	36	5.45	0.10	2.93	0.02	0.31	0.00	11.91	3.41	9306.95
3	42	2.74	0.13	1.21	1.04	1.43	0.85	5.04	0.98	4191.43
3	48	3.11	0.07	0.83	1.37	1.48	0.54	3.02	0.50	3332.67
3	57	1.60	0.12	1.09	1.68	0.26	0.93	0.00	0.00	2293.74
3	63	2.42	0.14	1.63	1.18	0.63	0.86	0.00	0.00	4822.48
3	77	2.54	0.13	1.55	1.67	0.25	2.37	4.76	0.35	3081.53
3	82	1.35	0.06	0.62	1.00	0.78	1.64	1.63	0.10	1762.05
3	85	1.93	0.06	1.73	1.25	0.08	0.85	2.01	0.00	2114.08
3	88	1.92	0.08	1.72	0.85	1.22	1.45	2.26	0.00	2691.97
3	89	1.29	0.05	0.78	0.76	0.99	1.41	1.38	0.00	2166.08
3	34	3.63	0.19	2.03	1.27	0.29	3.62	6.14	1.14	7936.22
3	64	1.86	0.05	1.03	0.66	0.76	0.94	0.00	0.00	2620.35
3	31	2.39	0.08	1.33	0.00	1.41	1.13	1.88	0.00	2767.18
3	69	1.94	0.17	1.23	1.77	10.48	4.50	3.87	0.41	2984.60

3	71	1.92	0.07	1.08	2.19	0.95	2.52	2.06	0.00	2851.37
3	7	2.03	0.05	1.13	1.02	0.73	1.20	0.00	0.00	3423.77
3	14	1.95	0.07	1.02	0.89	0.81	1.30	3.51	1.65	3863.45
3	20	1.73	0.11	1.59	0.41	1.25	1.40	2.50	0.54	2480.85
3	24	4.92	0.11	2.06	0.85	0.90	0.40	7.03	2.26	4781.11
3	46	1.06	0.05	0.87	0.64	0.01	0.42	0.00	0.00	3112.52
3	50	1.81	0.07	1.46	1.08	2.11	1.37	1.64	0.33	2886.88
3	61	2.02	0.13	1.20	1.29	1.41	1.38	0.00	0.00	3231.17
3	70	2.45	0.08	1.58	0.81	2.08	0.86	3.76	1.34	4303.55
3	8	3.05	0.13	1.39	0.00	3.01	2.70	2.97	0.43	3069.33
3	26	1.95	0.09	1.27	0.84	0.42	0.48	3.77	0.89	4076.36
3	37	1.60	0.09	1.16	0.00	2.01	1.29	0.38	0.13	2523.72
3	54	7.16	0.18	3.15	1.16	0.26	0.68	9.27	1.66	8414.16

Table 7.22 Complete sterol profile table for GEDOC memory clinic cohort SCI (n=30), MCI(n=30) and AD (n=30) patients' CSF sample.

Results expressed as ng/mL. Disease status: 1= SCI; 2= MCI; 3= AD.

Gender	group	age	Sample ID	7α,25-diHCA (A)	7α,25-diHCO	7α,26-diHCA (A)	7α,26-diHCO	(25S)3β,7α-diHCA (A)	(25S)7α-H-3O-CA	3β,7α-diHCA (A)	7α-H-3O-CA	(25R)3β-7α-HCA (A)	(25R)7α-H-3O-CA	7α,25-diHC	7α,26-diHC	7α-H(25S)CA	3β,7α-diHCA	(24S)-HC	25-HC	26-HC	7β-HC	7α-HC (A)	6β-HC	cholestenoic acid (3β-HCA)	7α-HCO	7-OC	7α-HC	Desmosterol	cholesterol
m	Control	74	1	0.37	0.42	0.97	1.09	32.33	15.76	191.24	123.57	158.91	107.81	-0.05	-0.12	16.57	67.67	18.56	2.18	25.79	1.63	10.02	2.36	85.58	10.02	3.12	5.10	110.00	730848.00
m	PD	70	2	0.22	0.19	0.87	0.74	42.66	18.52	243.36	136.54	200.70	118.02	0.03	0.12	24.14	106.82	13.69	1.68	35.13	1.04	5.10	1.17	219.56	9.79	2.91	3.40	130.00	503680.00
f	Control	65	3	0.32	0.28	0.97	0.81	31.36	15.06	182.29	102.49	150.93	87.43	0.04	0.15	16.30	79.80	16.49	2.16	24.15	1.21	6.76	1.22	233.37	5.11	3.12	1.65	N/F	746448.00
f	PD	65	4	0.38	0.45	1.47	1.89	28.30	16.43	200.82	143.42	172.52	126.99	-0.08	-0.42	11.86	57.40	16.07	1.56	23.23	2.08	35.43	2.02	177.65	40.48	4.28	-5.05	40.00	527360.00
f	Control	64	5	0.43	0.50	1.24	1.58	30.48	17.83	214.92	150.65	184.44	132.82	-0.07	-0.34	12.66	64.27	17.72	1.92	24.89	1.45	20.48	1.60	164.12	25.05	5.72	-4.57	200.00	804240.00
m	PD	79	6	0.32	0.36	0.77	1.04	35.57	19.22	225.32	146.52	189.75	127.30	-0.04	-0.27	16.35	78.80	15.44	1.73	21.00	0.92	11.83	1.22	184.61	11.51	2.56	0.31	70.00	530608.00
f	PD	78	7	0.27	0.20	0.88	0.75	36.70	16.75	252.93	149.20	216.23	132.44	0.07	0.13	19.95	103.73	13.81	1.80	30.35	1.96	15.04	1.81	267.41	9.52	5.11	5.52	160.00	545024.00
m	Control	62	8	0.21	0.25	0.68	0.85	22.46	14.73	188.71	121.62	166.25	106.90	-0.03	-0.17	7.73	67.08	11.68	1.34	25.84	1.12	6.19	1.62	162.50	13.67	2.65	-7.47	160.00	637264.00
f	PD	70	9	0.35	0.33	0.94	1.05	41.81	18.98	246.16	160.76	204.35	141.77	0.01	-0.11	22.83	85.41	21.34	2.44	30.22	3.91	27.78	3.60	228.42	21.50	12.00	6.28	160.00	687104.00
f	Control	64	10	0.46	0.43	1.40	1.46	46.18	27.74	325.81	224.64	279.63	196.91	0.02	-0.06	18.45	101.17	21.17	2.44	27.16	2.44	39.63	2.88	198.39	37.01	9.25	2.61	300.00	864992.00
m	PD	65	11	0.28	0.25	0.73	0.60	23.44	18.41	177.66	122.28	154.22	103.87	0.03	0.13	5.03	55.38	11.13	1.30	21.24	1.13	21.36	1.80	128.42	25.42	2.51	-4.07	130.00	543008.00
m	Control	73	12	0.27	0.21	1.05	0.92	27.10	22.05	225.75	158.19	198.65	136.13	0.06	0.13	5.05	67.56	12.75	1.37	23.47	2.49	49.70	3.75	168.22	37.22	6.89	12.49	100.00	654496.00

m	Control	70	13	0.30	0.23	1.05	0.91	41.98	18.42	234.01	150.64	192.04	132.23	0.06	0.13	23.56	83.37	13.33	1.52	25.44	1.93	46.13	3.62	185.68	40.79	5.15	5.34	170.00	563184.00
f	PD	73	14	0.48	0.42	1.23	1.10	39.21	15.71	258.63	161.25	219.42	145.54	0.05	0.13	23.50	97.38	16.27	0.80	24.94	1.74	16.34	2.82	225.82	35.73	7.64	-19.39	170.00	623696.00
m	PD	72	15	0.39	0.29	1.24	1.14	49.22	30.08	370.11	235.23	320.89	205.14	0.10	0.10	19.13	134.88	13.34	2.18	28.22	10.95	45.82	9.51	371.93	41.77	27.09	4.04	170.00	601936.00
f	Control	71	16	0.36	0.28	1.02	0.85	40.35	21.91	264.32	154.46	223.97	132.54	0.08	0.17	18.44	109.86	21.40	1.21	38.22	1.22	7.96	2.96	284.13	6.46	3.09	1.50	90.00	773680.00
f	Control	63	17	0.41	0.21	1.04	0.55	28.91	17.23	196.92	144.90	168.01	127.67	0.20	0.49	11.68	52.02	13.76	2.02	20.02	3.06	29.83	2.89	174.31	11.81	7.04	18.03	260.00	832848.00
f	PD	69	18	0.35	0.29	0.83	0.72	27.16	15.62	176.86	127.00	149.70	111.38	0.06	0.11	11.54	49.86	16.39	1.81	25.71	1.18	4.40	1.42	244.76	7.94	2.71	-3.54	220.00	788448.00
m	Control	68	19	0.33	0.18	2.21	1.27	23.33	19.67	163.95	151.38	140.62	131.71	0.15	0.94	3.66	12.57	8.33	0.84	12.65	3.89	100.31	3.49	67.43	82.25	10.47	18.05	230.00	696000.00
m	PD	64	20	0.28	0.18	1.11	0.76	33.01	20.43	223.29	174.40	190.28	153.97	0.10	0.35	12.57	48.88	15.50	2.00	35.04	1.54	22.63	1.23	214.63	24.63	4.89	-2.00	230.00	692304.00
f	Control	63	21	0.37	0.56	1.24	1.89	29.79	22.27	210.93	178.52	181.14	156.25	-0.19	-0.65	7.52	32.41	21.69	2.25	31.76	2.00	33.46	3.12	139.70	74.08	5.32	-40.62	330.00	785872.00
f	PD	76	22	0.41	0.43	0.67	0.75	29.65	16.44	193.01	130.61	163.36	114.17	-0.03	-0.08	13.21	62.40	14.63	1.07	17.68	1.16	6.18	1.44	236.00	5.48	3.48	0.70	40.00	470320.00
m	PD	57	23	0.30	0.38	0.95	1.01	29.07	15.92	187.22	130.25	158.15	114.33	-0.07	-0.06	13.15	56.97	11.81	1.83	28.07	0.71	9.62	1.10	238.61	8.73	1.86	0.90	130.00	495728.00
m	Control	60	24	0.34	0.40	0.88	1.26	30.28	19.27	186.72	145.55	156.45	126.28	-0.06	-0.38	11.01	41.18	10.10	1.74	25.30	9.79	9.99	7.73	177.13	18.96	21.81	-8.98	170.00	606112.00
f	Control	61	25	0.37	0.29	0.98	0.96	38.01	17.75	229.40	130.79	191.39	113.04	0.08	0.02	20.26	98.61	17.52	2.27	29.66	1.73	15.76	2.68	326.10	6.21	3.48	9.55	150.00	615760.00
m	Control	60	26	0.29	0.23	1.08	0.86	51.05	17.23	314.92	148.17	263.87	130.94	0.06	0.22	33.82	166.76	11.33	2.14	37.28	1.50	17.62	4.43	454.91	21.27	3.19	-3.66	170.00	825760.00
m	PD	71	27	0.23	0.21	0.67	0.59	36.95	15.75	252.72	148.14	215.78	132.39	0.03	0.08	21.20	104.59	11.40	1.46	20.12	1.34	8.02	4.70	209.90	3.23	5.32	4.79	10.00	441184.00

f	PD	69	28	0.28	0.31	0.87	1.01	24.79	12.05	181.93	120.22	157.15	108.18	-0.03	-0.15	12.74	61.71	19.19	1.93	24.08	2.61	13.04	5.48	209.63	25.21	6.38	-12.18	277.00	611421.94
m	Control	66	29	0.20	0.27	0.75	1.14	22.88	15.09	148.90	167.89	126.02	152.81	-0.07	-0.39	7.80	-18.99	9.67	1.50	30.57	1.47	11.56	2.24	128.99	4.96	3.10	6.60	170.00	723424.00
m	PD	67	30	0.26	0.19	0.96	0.77	28.11	10.13	229.42	106.73	201.31	96.60	0.08	0.20	17.98	122.69	14.94	2.10	35.60	1.19	20.78	2.67	199.47	28.10	3.71	-7.31	140.00	621040.00
f	PD	79	31	0.31	0.24	0.90	0.74	28.12	12.37	171.18	113.83	143.06	101.46	0.07	0.16	15.75	57.35	13.40	1.70	25.37	1.19	8.14	3.09	178.74	11.49	2.66	-3.35	160.00	765136.00
f	Control	60	32	0.33	0.29	0.90	0.90	25.55	10.16	149.66	98.69	124.11	88.53	0.04	0.00	15.39	50.98	16.43	2.01	27.26	2.11	10.18	4.41	165.30	11.81	5.53	-1.63	200.00	683936.00
f	Control	72	33	0.26	0.22	1.00	0.90	22.34	12.72	164.44	120.20	142.10	107.48	0.04	0.10	9.62	44.25	12.08	1.50	24.53	1.47	26.78	1.20	141.55	13.74	5.76	13.04	220.00	825152.00
m	Control	72	34	0.24	0.18	0.71	0.60	24.82	10.84	184.75	109.18	159.94	98.34	0.06	0.11	13.98	75.58	14.12	1.75	25.77	3.93	13.01	3.19	242.22	10.46	10.22	2.55	230.00	717424.00
m	PD	58	35	0.30	0.22	1.25	1.03	33.64	17.16	263.98	190.97	230.34	173.81	0.08	0.22	16.48	73.01	22.66	2.23	28.10	1.67	54.12	1.18	187.89	36.87	5.59	17.26	230.00	823024.00
f	PD	76	36	0.35	0.30	0.75	0.65	35.58	14.82	248.52	168.23	212.94	153.41	0.05	0.10	20.77	80.30	14.88	1.93	20.95	0.84	10.70	0.54	192.27	7.39	2.63	3.31	60.00	606800.00
m	Control	64	37	0.29	0.24	0.86	0.71	28.11	14.94	211.79	157.69	183.69	142.76	0.05	0.14	13.17	54.10	17.32	2.18	34.69	2.45	16.23	3.96	154.40	12.65	14.24	3.58	N/F	602880.00
f	Control	75	38	0.36	0.30	0.97	0.85	27.48	11.97	196.61	130.87	169.14	118.91	0.06	0.11	15.51	65.74	18.19	2.21	21.07	1.62	20.93	0.79	186.38	23.98	5.39	-3.05	200.00	941664.00
m	PD	67	39	0.33	0.23	1.18	0.96	26.00	11.77	192.25	119.65	166.25	107.88	0.09	0.21	14.24	72.61	13.46	1.99	22.13	1.37	28.79	0.75	220.22	20.52	4.11	8.27	130.00	541264.00
f	PD	43	40	0.28	0.24	1.09	1.00	33.04	20.16	280.79	208.58	247.75	188.42	0.04	0.10	12.88	72.21	15.28	1.86	29.50	1.27	26.41	1.38	248.46	19.53	3.99	6.88	180.00	630416.00
m	PD	66	41	0.33	0.20	1.22	0.87	36.35	19.64	234.51	176.22	198.16	156.58	0.14	0.35	16.71	58.29	11.61	0.86	14.41	2.12	25.63	1.68	128.28	12.12	59.02	13.50	380.00	887520.00
f	Control	63	42	0.32	0.22	0.95	0.62	30.12	18.06	172.46	134.08	142.34	116.02	0.10	0.33	12.06	38.39	11.37	1.26	33.60	1.14	3.27	1.44	241.28	1.85	4.29	1.42	130.00	560288.00

m	Control	65	43	0.25	0.17	0.74	0.48	22.36	12.11	117.41	73.29	95.05	61.19	0.08	0.26	10.25	44.12	10.78	1.67	31.72	2.59	34.80	1.84	206.57	20.21	5.61	14.58	200.00	674720.00
m	PD	71	44	0.35	0.20	1.24	0.91	37.36	18.90	234.24	162.18	196.88	143.28	0.15	0.33	18.46	72.06	11.92	1.69	21.48	1.93	14.51	2.50	215.06	12.57	5.57	1.94	150.00	653968.00
f	Control	65	45	0.31	0.28	0.99	0.94	25.72	12.94	150.86	96.06	125.14	83.11	0.03	0.05	12.78	54.81	10.78	1.24	21.45	1.38	24.91	1.59	189.54	24.44	3.24	0.46	120.00	689952.00
m	Control	75	46	0.31	0.44	0.86	1.29	36.17	19.55	202.68	133.47	166.50	113.92	-0.13	-0.43	16.63	69.21	10.12	1.43	24.19	1.07	10.38	1.04	333.02	9.09	3.35	1.29	90.00	536000.00
m	PD	77	47	0.21	0.22	0.61	0.83	45.42	18.48	229.25	126.58	183.82	108.09	-0.01	-0.22	26.94	102.67	13.00	1.28	21.78	5.53	9.40	3.56	202.73	7.44	13.05	1.96	N/F	438128.00
f	PD	77	48	0.33	0.39	0.75	0.93	32.48	17.45	182.06	126.24	149.58	108.79	-0.06	-0.19	15.03	55.82	12.30	1.53	18.41	1.15	16.70	1.75	215.03	8.34	3.39	8.36	30.00	620064.00
m	Control	64	49	0.23	0.13	0.64	0.39	46.78	21.00	281.27	184.57	234.48	163.57	0.10	0.25	25.78	96.70	13.21	1.37	28.91	1.07	14.29	2.21	227.05	12.60	3.13	1.69	N/F	494640.00
m	PD	79	50	0.25	0.25	0.83	0.92	55.42	32.46	299.56	205.86	244.15	173.40	0.00	-0.09	22.96	93.70	12.09	1.60	22.69	1.95	29.22	1.90	251.06	26.99	5.12	2.22	N/F	511248.00
f	PD	72	51	0.39	0.43	1.15	1.41	44.32	24.22	264.58	181.99	220.26	157.77	-0.04	-0.26	20.10	82.59	11.30	1.55	18.85	2.16	23.94	4.15	167.74	31.01	4.48	-7.07	N/F	589392.00
f	Control	68	52	0.57	0.98	1.04	1.89	32.78	18.89	196.42	143.01	163.63	124.13	-0.41	-0.85	13.90	53.40	11.48	1.63	22.63	1.14	14.15	1.70	166.46	9.83	4.10	4.32	N/F	467632.00
m	PD	63	53	0.22	0.15	0.76	0.56	24.20	10.80	136.20	90.78	112.00	79.98	0.07	0.20	13.40	45.42	7.94	1.27	18.91	1.72	10.83	1.54	218.73	10.00	5.07	0.83	N/F	750224.00
m	Control	62	54	0.34	0.36	0.88	1.02	31.63	12.30	181.71	102.60	150.09	90.30	-0.03	-0.14	19.33	79.12	21.64	1.43	18.62	1.35	5.32	1.87	219.00	6.11	5.61	-0.79	N/F	541712.00
f	PD	76	55	0.39	0.63	0.78	1.37	41.56	18.79	231.03	140.99	189.46	122.19	-0.24	-0.59	22.77	90.04	11.52	1.99	27.55	1.26	9.71	2.13	164.84	5.79	2.80	3.92	N/F	812224.00
f	Control	66	56	0.28	0.20	0.92	0.68	31.37	16.24	164.23	117.05	132.86	100.81	0.09	0.24	15.13	47.18	17.62	1.42	36.26	0.88	10.24	1.82	219.02	12.93	3.00	-2.69	N/F	544304.00
m	PD	62	57	0.29	0.20	0.73	0.56	24.36	11.57	186.94	113.75	162.58	102.18	0.09	0.17	12.79	73.19	12.47	1.22	20.42	1.34	10.12	1.89	218.09	6.85	3.92	3.27	140.00	674224.00

f	PD	56	58	0.33	0.33	0.91	0.99	30.88	15.99	189.85	123.84	158.97	107.85	0.00	-0.08	14.89	66.00	18.99	1.79	34.97	1.61	11.44	2.46	244.33	9.78	4.45	1.65	210.00	901200.00
m	Control	75	59	0.45	0.35	1.28	1.00	47.27	18.38	282.45	170.01	235.18	151.63	0.10	0.28	28.89	112.44	14.43	2.11	37.25	1.73	25.02	2.04	271.18	17.45	4.66	7.57	60.00	688160.00
f	Control	72	60	0.28	0.26	0.70	0.66	29.94	9.44	197.74	91.49	167.80	82.04	0.02	0.04	20.50	106.26	10.05	0.65	19.52	0.70	6.80	1.24	225.42	5.36	2.90	1.43	10.00	505936.00
f	PD	84	61	0.38	0.30	1.13	0.96	34.80	18.05	265.33	169.49	230.53	151.44	0.08	0.18	16.75	95.84	17.41	1.91	37.40	5.24	18.50	4.34	253.87	11.07	10.99	7.43	10.00	888688.00
m	PD	72	62	0.23	0.49	0.71	1.62	26.73	15.60	184.08	128.50	157.35	112.90	-0.26	-0.91	11.13	55.58	18.04	0.82	23.88	1.24	9.95	1.71	196.46	12.18	3.66	-2.23	120.00	584048.00
f	Control	74	63	0.39	0.29	0.76	0.64	33.37	15.15	189.22	113.09	155.85	97.94	0.09	0.12	18.22	76.13	17.51	0.92	18.81	2.55	7.05	2.55	167.02	4.09	6.15	2.95	60.00	682224.00
m	Control	73	64	0.31	0.25	1.15	1.04	24.47	15.50	174.96	141.93	150.50	126.42	0.06	0.11	8.96	33.04	14.12	1.92	23.85	3.22	43.49	3.20	113.62	29.17	8.92	14.32	150.00	895680.00
f	Control	70	65	0.38	0.30	0.93	0.71	36.42	20.14	206.93	152.04	170.50	131.90	0.08	0.22	16.28	54.89	17.82	1.92	25.33	1.79	23.31	3.60	177.93	16.35	4.98	6.96	70.00	752976.00
m	PD	87	66	0.29	0.31	0.72	0.90	52.12	25.86	271.37	191.91	219.25	166.06	-0.02	-0.18	26.26	79.45	15.91	1.68	27.23	2.27	16.32	3.32	208.64	15.04	5.61	1.28	60.00	642224.00
m	Control	71	67	0.26	0.16	0.98	0.65	66.85	22.05	306.37	142.13	239.52	120.08	0.09	0.33	44.81	164.24	10.56	1.22	20.89	1.37	18.62	1.71	405.93	9.88	2.30	8.74	20.00	521296.00
f	PD	59	68	0.20	0.20	0.67	0.66	52.72	28.69	273.39	187.34	220.67	158.65	0.00	0.00	24.03	86.06	12.60	1.57	26.78	1.58	34.54	4.84	278.71	24.71	3.50	9.83	80.00	666992.00
m	PD	79	69	0.25	0.17	0.56	0.37	28.18	13.70	147.11	98.42	118.93	84.72	0.08	0.18	14.48	48.69	10.48	1.16	16.87	0.89	9.71	1.72	179.25	5.07	3.72	4.64	N/F	482912.00
f	Control	71	70	0.33	0.03	0.68	0.07	29.49	14.59	160.94	99.94	131.45	85.35	0.30	0.61	14.90	61.00	13.79	1.89	21.19	1.01	10.65	1.21	214.20	46.49	2.90	-35.84	N/F	741824.00
m	PD	58	71	0.36	0.46	1.36	1.88	39.00	21.22	225.23	162.09	186.23	140.87	-0.11	-0.52	17.78	63.14	16.73	1.87	32.96	1.91	42.47	3.18	227.95	38.18	6.85	4.29	290.00	800832.00
m	Control	72	72	0.18	0.13	0.47	0.36	28.63	13.29	168.12	110.54	139.50	97.26	0.05	0.11	15.34	57.58	19.20	1.79	34.72	1.60	11.57	2.44	136.98	7.62	4.50	3.95	50.00	383728.00

f	PD	79	73	0.32	0.16	0.87	0.43	45.17	23.64	225.55	141.35	180.38	117.71	0.16	0.44	21.54	84.20	14.89	1.59	23.58	1.84	23.78	2.88	233.71	10.65	5.05	13.13	120.00	771520.00
m	PD	76	74	0.34	0.48	0.82	1.12	41.35	17.35	224.28	135.16	182.93	117.81	-0.14	-0.30	24.00	89.12	13.69	1.75	26.85	1.24	8.42	1.85	283.62	8.27	2.71	0.15	170.00	710048.00
f	Control	62	75	0.23	0.24	0.70	0.83	31.60	12.20	171.51	102.65	139.91	90.45	-0.01	-0.13	19.40	68.86	10.87	1.32	21.75	1.44	14.00	3.31	212.13	14.14	3.26	-0.14	140.00	754512.00
m	Control	66	76	0.21	0.24	0.43	0.52	27.06	11.49	135.31	77.49	108.25	66.00	-0.02	-0.09	15.57	57.82	10.79	1.56	21.91	1.55	7.39	1.79	181.09	5.52	3.72	1.87	200.00	579312.00
m	PD	58	77	0.26	0.30	1.68	2.25	50.77	37.82	343.36	283.86	292.59	246.05	-0.04	-0.57	12.96	59.50	9.68	1.21	20.89	1.72	91.81	2.56	169.55	90.39	9.56	1.42	110.00	452624.00
f	PD	70	78	0.39	0.35	1.15	1.09	43.63	30.88	318.31	263.09	274.68	232.21	0.05	0.05	12.75	55.22	14.89	2.00	18.21	2.15	51.77	1.35	133.66	32.31	10.32	19.46	N/F	491152.00
f	Control	64	79	0.42	0.51	1.25	1.67	57.75	25.27	316.11	189.58	258.36	164.31	-0.08	-0.43	32.48	126.53	21.02	2.54	39.09	2.01	29.46	2.58	348.81	29.41	4.30	0.05	390.00	953792.00
m	Control	66	80	0.19	0.13	0.49	0.39	22.01	10.68	132.66	90.19	110.65	79.51	0.06	0.10	11.33	42.47	7.48	1.10	19.26	0.93	10.05	1.06	151.49	7.10	2.22	2.96	N/F	505456.00
f	PD	69	81	0.29	0.13	0.83	0.44	33.66	21.93	208.45	170.54	174.79	148.61	0.16	0.39	11.73	37.91	14.31	1.37	20.76	2.56	29.34	3.03	134.68	13.69	12.32	15.65	30.00	594432.00
m	PD	77	82	0.31	0.18	0.72	0.54	58.31	20.15	282.11	143.11	223.80	122.96	0.13	0.18	38.16	139.00	14.86	1.71	35.92	2.48	15.08	3.38	444.04	8.82	5.93	6.27	170.00	549776.00
f	Control	65	83	0.31	0.21	0.83	0.72	31.92	18.46	181.79	133.55	149.87	115.08	0.10	0.11	13.46	48.24	14.62	1.55	27.59	1.77	22.17	2.55	237.78	15.31	5.57	6.86	120.00	759360.00
m	Control	68	84	0.28	0.20	0.77	0.58	26.92	12.99	150.18	103.66	123.26	90.67	0.08	0.18	13.93	46.52	10.44	1.22	22.31	1.04	17.26	1.85	188.34	12.79	3.14	4.47	100.00	586080.00
m	PD	71	85	0.25	0.29	0.64	0.86	48.37	23.53	278.52	172.31	230.15	148.79	-0.05	-0.22	24.84	106.20	12.49	1.40	27.69	0.85	7.97	1.42	327.96	6.75	3.63	1.22	170.00	568480.00
m	PD	65	86	0.34	0.25	0.84	0.70	36.20	16.58	225.99	142.33	189.79	125.76	0.09	0.14	19.62	83.66	13.50	1.48	26.19	1.31	16.52	1.74	240.48	12.28	3.74	4.24	240.00	679216.00
f	Control	62	87	0.29	0.30	0.67	0.71	29.55	16.40	201.37	152.14	171.82	135.74	0.00	-0.04	13.16	49.23	12.77	1.27	21.89	1.21	10.38	2.23	159.54	7.50	3.75	2.88	50.00	585664.00

m	Control	72	88	0.32	0.30	0.64	0.66	35.90	16.74	223.19	148.88	187.29	132.14	0.02	-0.03	19.16	74.31	12.77	1.91	28.99	1.66	18.77	1.92	282.28	13.50	4.59	5.27	190.00	655120.00
m	PD	64	89	0.36	0.25	0.82	0.67	37.48	18.42	212.84	138.87	175.36	120.45	0.11	0.16	19.07	73.98	19.45	2.09	48.15	1.30	5.74	1.88	285.10	3.67	4.36	2.06	180.00	743264.00
f	PD	78	90	0.37	0.21	0.85	0.54	22.46	11.13	161.59	99.12	139.13	87.99	0.17	0.31	11.33	62.47	15.55	1.52	22.14	1.36	10.90	1.19	181.37	5.10	4.88	5.80	100.00	842240.00
f	Control	67	91	0.44	0.26	1.30	0.99	35.48	23.21	257.50	207.66	222.01	184.44	0.17	0.30	12.27	49.84	19.14	1.96	29.91	1.43	41.63	1.40	203.89	22.95	9.05	18.69	60.00	686784.00
m	Control	63	92	0.36	0.50	0.87	1.29	26.05	15.16	162.60	107.74	136.54	92.58	-0.14	-0.42	10.89	54.86	12.58	1.55	23.64	1.09	30.73	1.22	156.33	37.37	3.39	-6.64	190.00	765696.00
f	PD	54	93	0.42	0.50	1.13	1.64	31.18	23.08	212.08	156.50	180.89	133.42	-0.08	-0.51	8.10	55.57	17.04	1.83	29.01	1.69	41.73	1.88	232.85	35.31	7.70	6.42	210.00	824080.00
m	Control	69	94	0.20	0.15	0.71	0.72	27.14	13.87	155.54	101.18	128.40	87.31	0.05	0.00	13.27	54.36	14.11	1.35	29.86	1.29	11.47	1.18	188.37	6.67	2.69	4.80	90.00	662784.00
f	Control	68	95	0.43	0.45	0.98	1.15	35.39	15.91	227.62	161.46	192.23	145.55	-0.02	-0.17	19.48	66.17	9.91	1.21	20.79	1.71	91.00	3.08	95.20	64.59	9.14	26.40	260.00	1008800.00
m	PD	72	96	0.35	0.16	1.04	0.62	52.15	23.68	278.09	181.63	225.94	157.96	0.19	0.42	28.47	96.46	17.70	1.91	31.37	2.12	29.28	2.59	274.62	13.78	7.24	15.50	260.00	778320.00
m	Control	71	97	0.13	0.17	0.39	0.35	41.70	18.67	221.16	132.60	179.46	113.93	-0.04	0.04	23.03	88.56	19.50	2.31	31.04	3.26	6.77	4.76	299.38	3.42	5.39	3.35	160.00	661072.00
f	Control	71	98	0.22	0.28	0.56	0.63	21.96	11.30	131.18	82.88	109.23	71.58	-0.06	-0.08	10.65	48.31	10.86	1.32	14.59	4.05	11.71	4.80	168.84	8.06	5.38	3.65	110.00	564560.00
m	PD	64	99	0.15	0.16	0.55	0.50	35.45	16.80	184.39	124.92	148.94	108.12	-0.01	0.05	18.66	59.48	10.12	1.89	27.88	2.08	13.93	2.53	249.38	9.34	2.76	4.59	80.00	536192.00
f	PD	74	100	0.24	0.24	0.67	0.70	30.09	18.00	175.37	136.24	145.29	118.24	0.00	-0.03	12.09	39.13	13.59	1.49	26.58	2.23	14.70	2.32	171.71	12.75	3.72	1.96	220.00	530464.00
m	Control	71	101	0.17	0.14	0.69	0.55	28.47	15.21	163.04	109.39	134.58	94.18	0.03	0.14	13.26	53.66	13.99	1.45	30.81	2.68	11.04	30.38	202.30	5.68	4.00	5.35	200.00	652192.00
f	Control	73	102	0.28	0.27	0.84	0.75	41.03	21.84	227.17	150.62	186.14	128.78	0.01	0.09	19.19	76.55	13.69	1.62	25.86	2.78	14.86	3.61	272.05	10.47	3.59	4.39	110.00	616880.00

m	PD	59	103	0.31	0.11	0.74	0.36	43.06	22.71	260.74	168.63	217.68	145.92	0.21	0.38	20.35	92.12	20.84	2.17	31.99	2.14	12.84	4.19	321.60	5.65	3.44	7.18	140.00	646480.00
f	PD	74	104	0.44	0.30	0.84	0.62	42.01	20.36	246.64	162.75	204.62	142.38	0.14	0.22	21.65	83.89	22.57	2.29	27.80	2.96	18.14	3.73	245.55	10.64	5.79	7.50	240.00	878320.00
f	PD	54	105	0.29	0.32	0.92	1.16	30.59	19.09	204.74	156.37	174.15	137.28	-0.03	-0.24	11.50	48.38	19.26	1.81	30.02	3.55	25.89	4.87	215.01	29.58	7.29	-3.68	150.00	711360.00
f	Control	72	106	0.32	0.36	0.67	0.89	25.09	13.25	146.40	100.68	121.30	87.43	-0.05	-0.22	11.85	45.72	15.49	2.16	28.73	1.76	18.45	1.78	192.31	22.52	4.41	-4.06	70.00	664048.00
m	Control	75	107	0.23	0.16	0.83	0.65	42.58	21.27	247.42	158.83	204.85	137.56	0.07	0.19	21.30	88.59	11.59	1.58	24.12	2.59	35.13	3.02	216.00	23.47	5.93	11.66	N/F	#VALUE!
m	PD	82	108	0.28	0.24	0.81	0.66	28.98	12.35	152.15	98.16	123.17	85.82	0.04	0.15	16.64	53.99	21.41	1.72	27.73	1.36	8.74	2.09	175.85	6.83	3.29	1.91	70.00	513520.00
f	PD	71	109	0.33	0.22	1.12	1.04	40.71	19.59	227.21	158.89	186.51	139.31	0.10	0.08	21.12	68.32	23.04	1.93	27.44	5.03	56.30	3.52	201.63	40.30	9.25	16.00	230.00	977312.00
f	Control	71	110	0.32	0.17	1.11	0.68	37.14	18.14	225.89	176.65	188.75	158.51	0.15	0.43	19.00	49.24	18.38	1.55	21.02	5.41	53.66	5.37	131.54	31.60	10.29	22.05	170.00	846192.00
m	PD	79	111	0.54	0.52	0.82	0.81	97.31	39.12	544.83	342.73	447.52	303.61	0.02	0.01	58.19	202.10	15.77	1.74	28.26	2.02	13.10	2.84	238.07	10.35	2.98	2.74	170.00	520128.00
m	Control	73	112	0.19	0.11	0.82	0.54	29.60	16.73	178.45	112.57	148.85	95.84	0.08	0.28	12.87	65.89	11.12	1.84	40.10	2.51	13.02	2.59	235.43	6.99	3.41	6.03	140.00	863488.00
m	PD	84	113	0.32	0.49	1.17	1.99	59.75	53.52	378.13	252.73	318.38	199.21	-0.17	-0.82	6.23	125.40	19.21	1.96	29.83	1.43	40.98	1.45	111.97	28.77	9.01	12.21	80.00	716608.00
m	Control	75	114	0.29	0.49	0.70	1.07	33.40	19.46	212.12	152.83	178.72	133.37	-0.21	-0.36	13.94	59.29	14.57	1.25	19.88	1.51	20.19	1.31	212.58	23.48	3.13	-3.29	120.00	576304.00
f	Control	63	115	0.32	0.48	0.76	0.98	30.53	23.25	189.78	146.38	159.24	123.13	-0.16	-0.22	7.28	43.40	14.69	1.63	23.47	1.31	9.04	1.22	158.83	7.41	2.81	1.63	130.00	764272.00
f	PD	61	116	0.26	0.15	0.85	0.48	27.65	37.01	169.66	137.89	142.01	100.88	0.11	0.37	-9.35	31.77	19.79	1.44	30.02	2.00	17.29	2.84	198.42	9.52	18.28	7.77	200.00	973504.00
f	PD	72	117	0.35	0.49	1.00	1.56	38.33	28.04	240.05	190.24	201.72	162.20	-0.14	-0.56	10.29	49.81	17.53	1.39	25.72	3.08	36.81	2.52	210.60	37.65	8.33	-0.85	230.00	859440.00

m	PD	80	118	0.25	0.23	0.62	0.57	59.32	27.93	324.76	205.85	265.43	177.91	0.02	0.06	31.39	118.91	15.01	1.33	32.83	1.12	13.98	1.50	287.27	6.52	3.64	7.46	60.00	634880.00
m	Control	65	119	0.29	0.37	0.72	0.90	28.46	33.37	195.37	159.50	166.92	126.13	-0.09	-0.19	-4.92	35.87	8.27	0.72	15.18	1.51	13.17	1.16	121.98	7.24	5.40	5.93	60.00	529760.00
f	Control	60	120	0.31	0.55	1.05	1.64	49.44	32.16	288.63	155.05	239.20	122.89	-0.24	-0.59	17.28	133.58	31.90	2.01	32.38	2.45	30.28	2.24	522.95	32.23	5.99	-1.95	120.00	905616.00
m	PD	78	121	0.29	0.25	0.74	0.63	62.36	41.52	325.72	197.83	263.36	156.31	0.04	0.11	20.85	127.89	12.30	1.42	26.63	1.29	11.21	2.07	314.33	8.39	3.51	2.82	120.00	577744.00
f	Control	68	122	0.29	0.34	0.72	0.85	27.60	17.95	162.18	109.98	134.58	92.03	-0.05	-0.12	9.65	52.20	13.97	1.48	25.77	2.34	10.08	2.87	252.10	8.81	5.48	1.27	N/F	927808.00
f	PD	77	123	0.36	0.24	0.89	0.62	31.62	22.52	207.25	157.63	175.64	135.10	0.13	0.27	9.09	49.63	25.89	1.70	28.17	1.94	16.51	2.49	182.58	9.28	4.17	7.23	220.00	899328.00
m	Control	75	124	0.34	0.36	1.07	1.03	38.03	29.82	267.43	217.72	229.40	187.91	-0.01	0.04	8.22	49.70	17.17	1.74	27.11	2.83	41.64	3.22	178.78	35.85	7.35	5.79	180.00	734544.00
f	Control	74	125	0.47	0.64	0.83	1.33	37.55	40.51	244.15	193.54	206.60	153.04	-0.17	-0.50	-2.96	50.61	18.01	1.87	39.08	1.60	13.40	4.09	217.15	5.61	4.41	7.79	240.00	1032208.00
m	Control	69	126	0.35	0.76	1.00	2.18	48.31	40.60	255.13	165.83	206.82	125.23	-0.41	-1.18	7.71	89.30	14.41	1.69	30.07	1.92	26.48	2.05	240.36	32.58	4.73	-6.10	280.00	752336.00
f	PD	57	127	0.38	0.35	0.76	0.74	32.68	27.77	185.22	125.35	152.54	97.58	0.03	0.01	4.91	59.87	18.57	1.48	24.35	1.32	10.65	1.44	238.31	7.28	4.51	3.37	130.00	853728.00
m	PD	76	128	0.28	0.20	0.59	0.44	36.57	32.34	237.31	183.25	200.74	150.91	0.08	0.15	4.23	54.06	12.51	1.21	23.19	0.99	7.96	0.92	190.39	5.02	2.30	2.95	10.00	470400.00
f	PD	69	129	0.32	0.19	0.72	0.46	33.04	20.80	153.93	118.13	120.90	97.32	0.14	0.27	12.24	35.81	15.57	1.66	17.87	2.10	16.65	4.23	123.31	8.53	6.74	8.11	170.00	749552.00
m	PD	59	130	0.31	0.23	0.84	0.75	48.92	27.16	296.40	199.26	247.48	172.10	0.08	0.08	21.76	97.14	16.69	1.93	28.60	1.72	30.40	2.96	295.73	26.23	7.83	4.18	190.00	636832.00
f	Control	66	131	0.27	0.14	0.70	0.40	24.20	9.55	125.54	84.09	101.34	74.54	0.13	0.30	14.65	41.45	16.83	1.97	28.72	1.53	11.66	2.68	157.74	5.81	4.84	5.85	160.00	850080.00
m	Control	66	132	222.78	234.33	400.31	455.78	12.44	15.35	117.88	123.27	105.44	107.93	-11.55	-55.47	-2.90	-5.39	523.45	1.85	14154.74	3.87	1045.76	34.21	14067.23	1329.41	9.64	-283.65	150.00	697200.00

m	Control	71	133	0.37	0.29	0.79	0.60	51.80	19.54	270.81	140.25	219.01	120.72	0.08	0.19	32.26	130.55	14.44	1.91	25.72	1.46	13.71	2.32	301.40	8.80	4.97	4.92	240.00	777872.00
m	PD	71	134	0.32	0.35	0.76	0.83	44.08	26.99	286.26	197.35	242.18	170.36	-0.03	-0.07	17.09	88.91	17.32	1.58	24.94	1.24	12.52	1.67	249.06	10.29	4.60	2.23	10.00	443440.00
f	Control	63	135	0.32	0.28	1.26	1.32	39.13	27.70	258.38	210.66	219.25	182.95	0.04	-0.06	11.43	47.73	14.89	2.04	20.80	2.81	93.69	3.10	186.83	86.97	5.67	6.72	230.00	746304.00
f	PD	57	136	0.24	0.15	0.54	0.37	30.27	16.84	184.97	122.69	154.70	105.85	0.09	0.17	13.43	62.28	17.83	1.48	32.35	0.91	6.23	1.58	318.13	2.97	2.54	3.26	30.00	698016.00
f	Control	60	137	0.37	0.28	1.22	1.08	54.13	29.84	341.80	251.32	287.68	221.48	0.09	0.14	24.29	90.49	12.28	2.32	18.61	2.27	56.39	3.50	259.76	42.86	8.52	13.52	N/F	649296.00
m	Control	73	138	0.32	0.30	0.94	0.92	39.88	23.89	252.94	181.87	213.06	157.98	0.02	0.02	15.99	71.07	16.33	1.85	21.54	1.82	31.66	2.11	203.89	18.77	5.93	12.89	140.00	691104.00
m	PD	60	139	0.37	0.34	0.68	0.67	50.53	18.00	272.03	132.24	221.51	114.24	0.04	0.01	32.53	139.79	18.16	1.74	29.85	2.16	8.73	4.59	309.24	4.87	7.14	3.86	180.00	861344.00
f	PD	76	140	0.22	0.28	0.67	0.96	30.70	17.95	184.92	129.55	154.22	111.60	-0.06	-0.29	12.75	55.37	12.04	2.54	29.46	1.42	25.31	1.48	234.61	27.01	5.41	-1.70	130.00	622992.00
f	Control	72	141	0.37	0.80	1.71	4.01	51.64	34.52	338.24	261.48	286.60	226.96	-0.43	-2.31	17.12	76.77	18.81	1.56	22.59	4.55	72.63	2.99	295.99	106.27	15.90	-33.65	N/F	792896.00
f	Control	75	142	0.41	0.76	0.98	2.17	31.46	14.47	178.18	101.54	146.72	87.07	-0.35	-1.19	16.98	76.64	15.65	1.49	43.62	3.59	19.37	5.74	256.13	25.78	7.60	-6.41	130.00	863120.00
m	PD	63	143	0.31	0.32	0.57	0.67	27.24	16.90	164.52	106.49	137.28	89.59	-0.01	-0.11	10.34	58.03	12.42	1.77	12.95	1.15	11.68	2.58	113.35	11.04	3.39	0.65	N/F	494576.00
f	PD	78	144	0.28	0.25	0.80	0.88	38.14	23.07	210.42	151.98	172.28	128.91	0.03	-0.08	15.07	58.44	13.25	1.41	21.48	1.25	37.17	1.76	147.09	35.90	5.63	1.27	200.00	594320.00
f	Control	62	145	0.38	0.22	0.98	0.56	33.24	15.42	215.95	150.32	182.72	134.90	0.16	0.42	17.81	65.63	19.79	1.78	29.34	2.17	28.94	3.92	243.74	18.75	3.65	10.19	80.00	899264.00
m	Control	61	146	0.40	0.27	1.92	1.49	44.41	22.37	267.04	179.31	222.63	156.94	0.14	0.43	22.04	87.73	13.96	1.84	37.98	2.62	88.77	6.22	286.47	37.26	8.06	51.51	240.00	624176.00
m	PD	61	147	0.31	0.24	0.88	0.79	35.73	20.36	213.64	148.88	177.91	128.52	0.07	0.08	15.37	64.76	14.31	2.09	26.18	1.59	42.22	2.29	211.53	23.94	7.46	18.28	470.00	780672.00

f	Control	67	148	0.32	0.22	0.75	0.56	29.15	19.43	173.75	133.98	144.60	114.55	0.09	0.19	9.72	39.77	19.95	2.05	32.73	2.46	17.60	6.97	200.78	9.15	5.84	8.45	140.00	879440.00
f	PD	81	149	0.39	0.37	1.13	1.13	41.90	24.67	257.57	192.55	215.67	167.88	0.02	0.00	17.23	65.02	13.66	1.94	28.39	2.75	38.74	4.05	188.24	28.14	6.11	10.60	90.00	662384.00
m	Control	73	150	0.36	0.20	0.78	0.49	77.30	21.00	408.35	158.29	331.04	137.29	0.16	0.30	56.31	250.06	14.43	2.82	31.28	1.45	4.44	2.47	674.78	1.86	3.26	2.58	160.00	807440.00
f	Control	63	151	0.44	0.79	0.77	1.42	30.68	16.56	167.41	124.75	136.73	108.19	-0.35	-0.65	14.12	42.66	26.33	1.47	32.00	4.04	19.61	9.95	187.55	24.37	8.80	-4.75	210.00	1165152.00
m	PD	85	152	0.34	0.61	0.88	1.62	37.54	19.08	257.61	169.17	220.06	150.10	-0.26	-0.74	18.46	88.43	9.86	1.88	24.86	1.57	22.22	1.67	267.55	30.73	4.22	-8.51	70.00	601616.00
m	PD	59	153	0.38	0.29	0.96	0.82	29.66	18.98	216.66	160.39	187.00	141.41	0.09	0.15	10.68	56.28	15.61	1.60	25.08	2.49	33.96	2.70	226.97	102.47	5.72	-68.51	240.00	630464.00
m	Control	60	154	0.22	0.27	0.55	0.70	27.79	16.26	183.76	130.94	155.97	114.68	-0.05	-0.16	11.53	52.82	11.82	1.89	26.33	1.45	14.71	1.25	272.94	16.02	2.81	-1.31	170.00	665152.00
f	PD	86	155	0.35	0.30	0.44	0.41	28.11	11.79	131.54	73.82	103.43	62.03	0.05	0.03	16.33	57.73	13.99	2.02	18.90	3.28	4.07	4.14	143.73	2.49	8.79	1.58	80.00	689456.00
f	Control	70	156	0.34	0.29	0.84	0.70	33.84	17.25	174.59	112.51	140.74	95.25	0.05	0.14	16.59	62.08	18.14	0.99	28.18	1.29	5.72	2.12	211.41	3.50	3.95	2.22	70.00	649840.00
m	Control	66	157	0.29	0.26	0.64	0.70	41.65	17.38	211.74	119.92	170.09	102.54	0.03	-0.05	24.27	91.82	11.14	2.19	21.95	1.40	15.85	1.52	223.13	13.89	4.00	1.97	150.00	704144.00
m	PD	78	158	0.35	0.24	0.58	0.45	49.16	22.48	263.12	157.95	213.96	135.48	0.11	0.13	26.68	105.17	14.10	0.69	28.99	1.11	6.57	1.46	257.92	5.59	2.60	0.98	100.00	772128.00
f	PD	78	159	0.38	0.73	0.77	1.46	37.72	18.68	205.14	132.81	167.42	114.13	-0.35	-0.69	19.04	72.33	20.03	0.77	30.06	0.91	4.18	1.13	295.91	10.47	3.31	-6.28	120.00	700224.00
m	Control	68	160	0.30	0.35	0.82	0.95	48.97	24.25	269.42	176.21	220.45	151.96	-0.05	-0.13	24.72	93.21	19.75	2.03	36.49	2.25	22.49	1.36	280.31	19.66	6.29	2.83	130.00	1211504.00
m	PD	78	161	0.37	0.25	1.19	0.56	34.87	26.90	271.54	199.92	236.67	173.03	0.13	0.62	7.97	71.61	13.32	2.14	27.51	3.47	34.88	4.49	209.21	16.37	7.96	18.52	290.00	617648.00
f	Control	68	162	0.33	0.46	1.04	1.07	25.91	16.52	209.99	140.74	184.08	124.23	-0.12	-0.04	9.39	69.25	17.10	1.54	30.80	3.23	21.38	5.64	320.87	20.10	7.11	1.28	220.00	1067904.00

m	Control	69	163	0.22	0.38	0.88	1.11	30.72	19.85	258.16	169.00	227.43	149.15	-0.16	-0.23	10.87	89.15	12.91	2.20	17.42	3.02	43.14	2.94	214.03	44.63	7.45	-1.49	240.00	921952.00
m	PD	62	164	0.29	0.33	1.18	1.11	35.95	26.97	325.91	227.64	289.95	200.67	-0.04	0.06	8.99	98.27	19.90	1.49	33.34	7.71	71.21	11.02	318.20	48.06	18.63	23.15	240.00	918656.00
m	PD	85	165	0.20	0.43	0.67	1.03	43.12	18.37	294.37	169.70	251.25	151.33	-0.23	-0.37	24.75	124.68	16.94	1.37	25.50	0.90	5.55	3.67	279.93	7.93	7.71	-2.38	40.00	547008.00
f	Control	68	166	0.19	0.24	0.62	0.74	23.23	13.70	151.38	97.31	128.16	83.61	-0.05	-0.12	9.52	54.07	14.51	1.50	25.67	4.78	9.65	6.59	204.06	14.67	9.54	-5.02	110.00	776912.00
m	PD	79	167	0.26	0.50	0.97	1.34	36.88	23.08	250.21	179.74	213.33	156.66	-0.24	-0.37	13.80	70.47	15.07	1.01	26.02	1.64	31.85	1.64	226.70	38.92	5.60	-7.07	60.00	658720.00
f	Control	69	168	0.19	0.26	1.01	0.94	29.54	21.74	206.49	159.26	176.96	137.52	-0.07	0.07	7.79	47.23	9.24	2.15	18.10	1.96	37.00	4.32	154.65	28.94	5.65	8.06	70.00	504160.00
m	Control	67	169	0.25	0.34	1.03	1.23	31.58	22.96	239.46	162.02	207.88	139.06	-0.09	-0.21	8.62	77.45	22.59	1.50	40.10	3.95	35.07	5.14	240.02	27.81	11.54	7.26	350.00	1018912.00
m	PD	77	170	0.20	0.28	0.92	1.04	32.55	21.50	258.01	189.03	225.46	167.54	-0.08	-0.11	11.05	68.97	20.39	1.44	21.47	1.19	27.01	1.40	183.74	22.93	6.88	4.08	170.00	449424.00
m	PD	74	171	0.19	0.19	0.48	0.40	44.25	17.14	261.82	133.35	217.58	116.21	-0.01	0.07	27.10	128.47	14.48	1.65	25.43	0.87	3.54	1.56	269.38	1.81	2.58	1.73	100.00	493472.00
f	Control	71	172	0.45	0.44	1.24	0.85	44.35	19.19	284.91	138.65	240.56	119.47	0.01	0.39	25.16	146.26	11.69	1.90	18.93	1.81	8.64	3.78	176.78	4.71	4.26	3.93	70.00	606304.00
m	Control	74	173	0.32	0.44	0.98	1.02	35.00	26.46	286.35	201.35	251.35	174.89	-0.13	-0.04	8.54	85.00	11.97	1.82	23.06	2.01	25.97	2.28	203.98	19.75	3.99	6.22	220.00	725232.00
m	PD	47	174	0.29	0.29	1.26	0.96	29.35	26.74	296.50	203.84	267.15	177.10	-0.01	0.31	2.61	92.66	20.20	0.89	34.04	1.18	20.08	1.92	305.94	13.57	3.31	6.51	190.00	850480.00
f	Control	63	175	0.25	0.27	0.85	0.76	20.92	16.72	175.04	131.29	154.12	114.57	-0.03	0.09	4.19	43.75	18.55	2.37	27.06	2.30	25.06	2.37	185.91	17.32	7.57	7.75	280.00	971360.00
m	PD	55	176	0.23	0.17	0.98	0.53	24.50	22.50	213.21	157.02	188.71	134.52	0.06	0.45	2.00	56.19	19.99	1.45	35.81	1.62	39.70	2.82	216.07	18.22	4.21	21.48	280.00	738096.00
m	Control	64	177	0.22	0.22	0.79	0.61	25.03	18.04	219.35	155.55	194.32	137.51	0.00	0.18	6.99	63.80	14.22	1.59	25.82	1.47	12.69	3.03	220.02	10.98	3.15	1.72	230.00	660448.00

f	PD	70	178	0.21	0.20	0.72	0.50	23.59	15.66	178.72	126.62	155.14	110.95	0.01	0.23	7.92	52.11	21.98	1.91	18.43	2.71	24.95	1.87	182.02	17.63	7.85	7.31	300.00	738256.00
f	PD	77	179	0.32	1.47	1.41	4.65	27.53	26.08	255.44	202.45	227.91	176.37	-1.16	-3.24	1.45	52.99	15.99	1.74	26.79	2.78	49.34	2.59	290.63	115.07	7.06	-65.73	210.00	794256.00
m	Control	66	180	0.24	0.34	1.04	1.08	25.63	16.55	233.14	135.10	207.52	118.54	-0.10	-0.05	9.07	98.05	15.93	1.58	31.97	2.02	19.06	2.15	303.47	18.62	4.30	0.44	240.00	756768.00
m	PD	79	181	0.24	0.20	0.84	0.52	33.71	19.99	286.43	165.92	252.72	145.93	0.04	0.32	13.73	120.51	15.19	1.39	27.41	1.59	7.64	1.67	338.18	3.77	5.02	3.87	30.00	563248.00
f	Control	69	182	0.17	0.13	0.67	0.44	20.06	11.60	154.83	105.19	134.78	93.59	0.04	0.23	8.46	49.65	12.38	1.41	28.64	1.50	4.89	1.87	290.70	1.84	3.69	3.05	230.00	830432.00
f	PD	74	183	0.25	0.11	0.95	0.38	19.78	18.58	182.77	137.47	162.99	118.89	0.13	0.57	1.20	45.29	16.55	1.77	21.31	2.53	20.02	2.75	155.45	8.67	7.27	11.35	170.00	662944.00
m	Control	65	184	0.17	0.23	0.63	0.69	29.17	18.70	239.92	152.75	210.75	134.06	-0.06	-0.06	10.48	87.17	13.52	1.41	35.04	1.51	4.42	3.25	364.25	3.25	3.47	1.16	N/F	562176.00
m	PD	76	185	0.19	0.19	0.63	0.44	22.88	9.87	151.16	113.13	128.27	103.25	0.00	0.19	13.01	38.03	11.51	1.70	24.39	1.38	5.35	6.33	140.85	3.09	6.61	2.26	120.00	606704.00
f	Control	72	186	0.28	0.26	0.84	0.64	28.22	11.49	171.04	118.87	142.82	107.38	0.02	0.21	16.73	52.17	24.57	1.66	20.87	1.71	17.00	3.63	277.50	10.65	7.49	6.34	30.00	644496.00
f	Control	66	187	0.21	0.46	0.82	1.20	23.35	15.19	182.26	146.11	158.92	130.93	-0.25	-0.38	8.16	36.15	13.12	1.36	20.76	1.52	28.82	1.59	242.99	16.86	4.47	11.96	260.00	563488.00
m	Control	60	188	0.26	0.13	0.87	0.40	34.16	14.28	228.60	130.16	194.43	115.88	0.13	0.47	19.89	98.44	12.49	1.27	21.81	1.54	11.71	2.79	251.61	9.59	5.92	2.13	140.00	566640.00
f	PD	66	189	0.25	0.15	0.57	0.30	24.48	12.97	161.57	108.44	137.10	95.47	0.09	0.27	11.50	53.13	11.67	1.39	15.30	1.23	6.27	2.35	191.38	3.03	4.88	3.24	10.00	451120.00
m	PD	80	190	0.25	0.12	1.00	0.35	25.12	13.64	183.90	134.94	158.78	121.30	0.14	0.65	11.48	48.96	15.20	1.46	20.00	2.52	19.57	3.19	154.90	6.83	7.10	12.74	140.00	596288.00
m	PD	64	191	0.18	0.13	0.75	0.43	21.71	11.12	154.91	105.77	133.20	94.65	0.05	0.32	10.59	49.14	12.56	1.58	27.72	1.48	6.02	2.08	287.58	3.75	3.72	2.27	230.00	718256.00
m	Control	67	192	0.23	0.22	0.67	0.55	34.83	17.83	255.61	177.26	220.78	159.43	0.01	0.12	16.99	78.35	13.35	1.49	26.52	1.46	8.94	1.32	256.81	5.98	4.19	2.96	120.00	710816.00

f	Control	61	193	0.18	0.20	0.66	0.47	21.97	12.41	155.46	115.94	133.49	103.53	-0.02	0.19	9.56	39.52	11.57	1.81	24.86	1.50	6.54	6.72	141.27	3.40	6.55	3.13	150.00	817200.00
f	PD	65	194	0.27	0.33	0.87	0.71	25.42	12.94	173.15	116.94	147.73	104.01	-0.06	0.16	12.48	56.20	24.46	1.34	20.69	1.88	17.10	3.38	277.61	11.89	7.30	5.21	80.00	672544.00
m	PD	75	195	0.24	0.12	0.89	0.36	29.69	13.11	232.44	132.00	202.75	118.89	0.13	0.53	16.58	100.44	12.43	1.27	21.78	1.65	11.64	2.92	251.06	8.20	5.79	3.44	120.00	549312.00
f	PD	62	196	0.22	0.15	0.60	0.29	23.27	14.07	159.89	112.44	136.62	98.38	0.07	0.31	9.20	47.45	11.75	0.08	15.11	1.12	6.35	2.61	191.15	3.05	4.42	3.30	180.00	718336.00
m	Control	65	197	0.25	0.11	1.01	0.36	28.76	15.09	186.05	136.88	157.29	121.80	0.13	0.65	13.67	49.17	15.22	1.53	19.73	2.59	19.43	2.65	155.48	6.97	7.10	12.47	210.00	703856.00
f	Control	66	198	0.17	0.13	0.72	0.48	23.54	11.78	155.41	105.60	131.87	93.82	0.04	0.24	11.76	49.81	12.28	1.61	27.69	1.47	4.80	1.46	291.20	1.93	3.64	2.86	220.00	840816.00
m	Control	75	199	0.21	0.18	0.71	0.46	31.85	17.09	256.17	179.05	224.32	161.96	0.02	0.25	14.76	77.12	13.30	1.64	26.77	1.53	9.11	1.25	256.08	5.08	4.07	4.03	220.00	621472.00
m	PD	67	200	0.19	0.62	0.85	1.54	22.82	15.12	184.23	147.06	161.41	131.94	-0.44	-0.68	7.70	37.17	13.28	1.30	20.81	1.63	29.69	1.26	242.67	20.79	4.39	8.90	170.00	487072.00

Table 7.23 Complete sterol profile table for NYPUM cohort of baseline PD and healthy control plasma sample (n=200). Results expressed in ng/mL.

Column1	7α,25-diHC + 7α,25-diHCO	7α,25-diHCO	7α,26-diHC +7α,26-diHCO	7α,26-diHCO	(25S)3β,7α-diHCA + (25S)7α-H-3O-CA	(25S)7α-H-3O-CA	3β,7α-diHCA + 7α-H-3-OCA	7α-H-3O-CA	(25R)3β-7α-HCA + (25R)7α-H-3O-CA	(25R)7α-H-3O-CA	7α,25-diHC	7α,26-diHC	(25S)3β,7α-diHCA	3β,7α-diHCA	(24S)-HC	25-HC	26-HC	7β-HC	7α-HC + 7α-HCO	6β-HC	cholestenoic acid (3β-HCA)	7α-HCO	7-OC	7α-HC	Cholesterol
1	0.20	0.19	0.74	0.67	27.72	16.87	153.98	132.31	126.26	115.45	0.00	0.06	10.85	21.67	8.66	18.57	1.10	3.73	4.29	2.13	98.51	13.75	5.87	9.46	325397.00
2	0.45	0.42	1.11	0.98	37.28	29.06	231.81	224.36	194.53	195.30	0.00	0.13	8.22	7.45	26.52	32.57	2.23	3.14	1.78	3.64	142.55	6.08	5.09	4.29	757121.00
3	0.36	0.35	0.85	0.72	29.78	22.91	161.80	151.70	132.02	128.79	0.02	0.12	6.88	10.11	20.82	29.23	2.15	1.23	0.98	4.49	107.77	2.61	2.30	1.63	471871.00
4	0.35	0.31	1.02	0.84	51.20	19.41	299.15	164.84	247.95	145.43	0.01	0.17	31.79	134.31	15.53	35.37	2.10	1.93	4.59	2.13	144.23	12.20	4.46	7.61	441139.00
5	0.32	0.30	0.94	0.74	36.52	19.82	235.72	175.89	199.21	156.07	0.04	0.20	16.70	59.84	13.45	42.88	2.56	2.20	3.43	3.25	182.72	11.27	5.02	7.84	363009.00
6	0.41	0.40	1.00	0.85	36.42	20.94	249.00	158.26	212.58	137.32	0.03	0.14	15.49	90.74	12.63	25.63	1.89	2.21	4.39	6.99	109.43	14.11	8.10	9.72	337101.00
7	0.34	0.35	0.93	0.81	46.78	23.30	264.23	177.18	217.44	153.88	0.01	0.12	23.49	87.05	22.38	24.23	1.86	1.74	6.44	0.68	102.04	21.02	3.60	14.57	412720.00
8	0.23	0.22	0.71	0.56	34.90	16.26	212.37	130.53	177.47	114.27	0.00	0.15	18.63	81.84	17.51	36.44	1.78	1.49	0.74	2.38	138.40	2.02	4.43	1.28	487573.00

9	0.26	0.24	0.86	0.71	34.07	19.58	210.87	151.04	176.80	131.46	0.02	0.15	14.49	59.83	13.91	24.03	1.59	2.55	4.08	5.32	108.90	12.99	3.64	8.91	420 595.00
10	0.23	0.13	0.88	0.51	17.35	11.37	109.87	88.20	92.52	76.83	0.11	0.37	5.97	21.67	14.29	21.57	1.54	1.64	55.71	2.27	80.29	6.39	6.82	49.33	431 146.00
11	0.33	0.25	1.75	1.66	195.97	60.83	1264.08	458.43	1068.11	397.60	0.08	0.09	135.14	805.65	16.09	28.83	1.33	2.81	172.87	2.69	159.96	7.82	8.99	165.06	452 363.00
12	0.33	0.25	0.69	0.61	29.78	16.81	165.88	122.98	136.10	106.17	0.08	0.07	12.97	42.90	18.07	22.00	1.57	2.20	24.79	4.65	102.08	1.88	8.34	22.92	524 969.00
13	0.29	0.21	0.79	0.68	29.92	15.76	200.71	139.09	170.79	123.32	0.08	0.11	14.16	61.62	19.97	32.48	1.74	2.35	10.67	1.87	157.80	1.00	5.06	9.67	670 253.00
14	0.32	0.19	0.95	0.71	39.40	18.06	237.29	143.84	197.89	125.78	0.12	0.23	21.34	93.45	22.97	30.19	1.89	5.92	27.72	4.31	219.45	1.96	9.79	25.75	565 693.00
15	0.27	0.23	0.77	0.72	40.63	22.95	222.16	177.06	181.53	154.11	0.03	0.05	17.68	45.10	16.71	27.28	1.92	1.73	46.36	3.23	107.70	4.67	5.62	41.70	336 224.00
16	0.19	0.20	0.60	0.53	29.77	21.68	197.29	175.72	167.52	154.03	-0.01	0.07	8.09	21.58	15.98	52.64	2.78	0.32	9.16	1.36	180.18	0.99	0.96	8.17	503 364.00
17	0.18	0.09	0.94	0.52	30.47	21.98	194.66	177.46	164.19	155.47	0.08	0.42	8.49	17.20	10.48	18.07	1.44	3.15	103.84	0.75	88.68	9.84	7.55	94.00	386 713.00
18	0.22	0.09	0.76	0.39	37.46	21.27	228.26	163.05	190.81	141.79	0.12	0.37	16.19	65.21	13.43	23.70	1.42	2.05	29.40	1.32	125.41	2.37	5.86	27.03	416 330.00
19	0.40	0.29	1.08	0.92	37.10	25.81	147.32	122.75	110.22	96.94	0.11	0.16	11.28	24.57	18.24	24.30	1.82	5.12	39.90	4.36	84.61	4.36	25.13	39.90	600 500.00
20	0.25	0.19	1.05	0.89	50.53	39.30	239.56	205.42	189.04	166.12	0.06	0.16	11.23	34.14	10.75	29.91	1.56	1.48	49.84	6.24	135.55	6.24	7.15	49.84	373 830.00

21	0.38	0.22	1.47	0.86	72.78	47.31	281.07	220.09	208.29	172.78	0.16	0.61	25.47	60.98	16.82	31.80	2.06	2.20	49.86	3.16	133.35	3.16	14.64	49.86	490 920 .00
22	0.45	0.35	1.61	1.30	68.36	51.18	251.94	214.20	183.59	163.02	0.10	0.31	17.18	37.75	14.06	21.51	1.78	2.02	52.07	7.49	102.29	7.49	10.61	52.07	319 218 .00
23	0.40	0.24	1.22	0.83	41.67	43.12	161.97	168.63	120.30	125.51	0.16	0.39	-1.45	-6.66	17.39	23.37	1.64	1.05	24.02	3.36	103.68	3.36	5.89	24.02	379 237 .00
24	0.29	0.17	0.61	0.39	43.36	19.65	157.54	87.81	114.18	68.15	0.12	0.22	23.71	69.74	14.25	20.25	2.37	12.55	10.17	0.98	147.14	0.98	39.53	10.17	432 966 .00
25	0.49	0.38	1.71	1.42	38.29	34.76	209.70	200.01	171.41	165.24	0.11	0.29	3.53	9.70	18.85	30.71	1.51	2.01	65.85	10.46	89.08	10.46	5.31	65.85	558 564 .00
26	0.25	0.13	0.69	0.38	20.55	13.43	106.64	80.90	86.09	67.47	0.11	0.31	7.12	25.74	13.25	19.41	0.97	0.92	3.81	0.53	76.22	0.53	3.33	3.81	422 047 .00
27	0.35	0.17	1.12	0.57	40.66	26.34	226.12	168.05	185.46	141.71	0.18	0.55	14.32	58.07	14.76	25.63	1.54	2.49	41.12	4.32	130.80	4.32	8.09	41.12	443 491 .00
28	0.29	0.11	1.02	0.42	28.38	14.94	149.87	99.61	121.49	84.67	0.18	0.59	13.44	50.26	17.16	28.54	1.29	1.28	6.28	1.80	112.81	0.23	4.45	5.01	498 430 .00
29	0.34	0.44	1.10	1.55	37.01	25.67	193.72	157.67	156.71	132.01	-0.09	-0.45	11.34	36.05	11.57	18.56	1.32	0.87	39.95	1.22	107.83	8.17	3.06	31.78	282 700 .00
30	0.21	0.17	0.76	0.65	41.42	22.87	193.65	136.09	152.23	113.22	0.05	0.12	18.55	57.56	8.80	27.76	1.12	0.85	6.03	2.65	149.47	0.84	2.34	5.19	245 550 .00
31	0.41	0.34	1.19	1.04	25.66	19.20	161.99	140.51	136.33	121.31	0.07	0.14	6.46	21.48	11.40	27.67	1.45	1.23	36.51	1.89	96.42	8.48	4.23	28.03	394 610 .00
32	0.26	0.34	0.92	1.18	16.72	14.09	133.36	121.91	116.64	107.82	-0.08	-0.27	2.63	11.45	6.61	24.95	1.09	0.65	18.44	2.71	79.04	4.97	1.77	13.47	225 140 .00

33	0.41	0.36	1.64	1.61	33.29	27.19	233.87	215.40	200.58	188.20	0.05	0.03	6.10	18.47	13.06	23.28	1.41	1.83	81.14	4.30	83.58	23.90	5.36	57.24	418 660 .00
34	0.44	0.34	0.89	0.74	24.47	14.98	141.88	106.15	117.41	91.17	0.10	0.14	9.50	35.73	13.20	21.72	1.82	9.16	17.67	9.36	92.75	3.60	19.34	14.08	527 040 .00
35	0.22	0.21	0.51	0.55	19.21	10.73	112.87	79.30	93.66	68.56	0.02	-0.03	8.48	33.58	10.43	18.82	1.08	1.15	9.42	2.23	111.05	1.87	3.23	7.55	335 850 .00
36	0.28	0.13	0.91	0.47	42.85	25.82	190.27	134.69	147.42	108.87	0.15	0.44	17.03	55.57	11.63	23.05	1.28	1.49	26.10	2.09	104.46	6.11	4.00	19.99	355 810 .00
37	0.47	0.28	1.38	0.88	48.51	34.08	307.07	255.68	258.56	221.60	0.18	0.50	14.43	51.38	19.36	29.72	1.87	1.55	33.39	2.63	180.49	5.80	7.62	27.59	411 600 .00
38	0.25	0.17	1.13	0.89	33.67	26.80	232.22	201.52	198.56	174.72	0.08	0.25	6.87	30.71	10.57	25.39	0.99	1.26	84.44	2.58	120.60	12.52	6.66	71.93	382 350 .00
39	0.30	0.19	0.70	0.44	46.75	26.38	263.86	200.60	217.11	174.22	0.11	0.26	20.37	63.26	16.73	27.04	1.28	0.87	3.84	1.86	119.02	0.64	4.67	3.20	430 800 .00
40	0.26	0.15	0.76	0.50	22.33	11.74	123.55	87.58	101.22	75.84	0.11	0.26	10.59	35.97	7.65	16.40	0.97	1.33	27.36	2.05	80.10	4.28	4.71	23.09	417 180 .00
41	0.37	0.15	0.84	0.32	27.48	15.66	184.01	129.97	156.54	114.30	0.23	0.52	11.81	54.05	23.92	30.73	2.14	1.84	9.20	2.84	147.92	1.18	13.82	8.02	714 950 .00
42	0.41	0.22	1.33	0.71	21.17	13.84	168.59	139.94	147.43	126.10	0.19	0.63	7.33	28.65	12.27	23.44	1.45	1.41	11.71	2.08	81.00	2.04	11.44	9.67	389 110 .00
43	0.33	0.20	1.10	0.68	19.89	12.61	140.59	102.36	120.70	89.75	0.13	0.43	7.28	38.23	12.69	22.52	1.36	2.98	29.92	4.81	164.44	4.70	8.03	25.23	424 550 .00
44	0.45	0.32	2.00	1.56	47.34	35.38	321.00	272.74	273.67	237.36	0.12	0.44	11.96	48.26	17.83	36.47	1.76	2.46	128.61	3.03	216.54	19.75	6.15	108.86	536 950 .00

45	0.26	0.14	0.76	0.46	29.62	16.11	206.04	144.31	176.43	128.20	0.12	0.30	13.50	61.73	12.48	23.50	1.34	1.56	25.77	1.68	111.85	4.15	4.21	21.62	378 010 .00
46	0.30	0.18	1.30	1.02	36.74	24.75	271.57	236.65	234.83	211.89	0.12	0.29	11.99	34.93	13.67	30.69	1.61	2.74	86.94	4.52	125.78	9.28	7.70	77.66	425 520 .00
47	0.29	0.17	1.00	0.67	17.84	17.08	154.43	142.55	136.59	125.47	0.11	0.33	0.75	11.88	10.05	32.68	1.29	0.95	13.59	2.84	148.98	2.87	2.48	10.72	312 290 .00
48	0.35	0.17	0.96	0.48	28.90	14.87	176.77	118.14	147.87	103.27	0.18	0.48	14.03	58.63	15.27	24.14	1.27	1.06	16.65	1.84	155.67	3.07	5.30	13.58	379 950 .00
49	0.49	0.20	1.96	0.82	41.22	35.77	256.80	248.08	215.59	212.32	0.29	1.14	5.45	8.72	17.74	24.61	1.37	5.77	124.01	10.16	100.60	22.40	10.25	101.61	555 560 .00
50	0.46	0.18	1.40	0.62	33.29	27.33	194.22	171.54	160.93	144.21	0.28	0.78	5.96	22.68	14.61	20.15	1.73	2.29	126.01	3.34	89.74	23.92	6.16	102.09	581 490 .00
51	0.30	0.24	1.32	1.14	43.27	35.06	266.29	244.89	223.02	209.83	0.06	0.17	8.21	21.40	12.10	21.59	1.06	2.07	59.10	0.86	101.59	13.86	3.85	45.25	374 330 .00
52	0.25	0.15	0.99	0.68	33.00	22.21	215.81	170.35	182.80	148.14	0.10	0.31	10.80	45.46	17.88	37.01	1.80	1.21	28.95	1.99	148.06	6.78	3.04	22.17	446 640 .00
53	0.28	0.14	1.20	0.73	27.36	18.94	177.37	147.73	150.02	128.79	0.14	0.47	8.42	29.64	11.13	19.29	1.21	2.11	57.88	2.48	84.28	10.60	7.35	47.27	398 770 .00
54	0.30	0.15	1.03	0.56	32.52	19.31	204.06	148.47	171.54	129.17	0.15	0.46	13.21	55.59	12.26	24.26	1.39	1.73	29.61	2.27	113.06	5.79	4.17	23.83	400 140 .00
55	0.22	0.22	0.76	0.71	17.15	9.54	184.63	133.88	167.47	124.34	0.00	0.05	7.61	50.75	9.87	22.29	1.44	3.30	13.17	2.14	114.73	8.77	1.48	4.40	399 370 .00
56	0.26	0.24	0.99	0.81	42.97	21.92	252.31	177.58	209.33	155.66	0.02	0.18	21.05	74.72	13.65	33.06	1.48	2.34	11.08	9.16	158.27	6.80	7.04	4.28	391 450 .00

57	0.25	0.25	0.90	0.80	35.90	19.18	199.09	164.98	163.20	145.80	0.00	0.10	16.72	34.11	14.45	26.35	1.48	4.41	18.50	5.29	148.26	11.75	1.22	6.76	440550.00
58	0.24	0.24	0.94	0.76	31.14	19.80	226.69	171.90	195.56	152.10	0.00	0.18	11.34	54.79	12.15	25.66	1.19	1.62	11.11	2.81	148.21	5.05	0.90	6.07	360090.00
59	0.22	0.22	0.52	0.47	27.76	16.08	149.88	121.73	122.12	105.65	0.00	0.05	11.68	28.15	11.89	20.61	1.28	1.45	3.73	4.11	115.16	2.32	2.38	1.42	344770.00
60	0.25	0.23	0.86	0.74	23.11	18.13	165.05	147.65	141.94	129.53	0.01	0.12	4.98	17.40	12.11	23.14	1.45	3.37	14.96	4.20	97.05	11.34	1.95	3.62	391420.00
61	0.17	0.18	0.57	0.55	15.22	19.26	94.84	124.96	79.62	105.70	-0.01	0.02	-4.05	-30.12	7.73	18.48	1.04	2.17	7.72	3.60	66.51	6.25	1.08	1.47	319410.00
62	0.24	0.21	0.56	0.45	30.47	16.74	180.61	125.44	150.15	108.70	0.02	0.11	13.73	55.18	11.65	30.06	1.85	1.51	1.71	0.81	163.46	1.14	1.21	0.57	416730.00
63	0.24	0.23	0.68	0.64	31.93	23.87	176.14	156.66	144.20	132.79	0.01	0.05	8.06	19.47	12.07	25.88	1.43	1.98	11.97	2.74	109.47	7.49	4.00	4.48	453820.00
64	0.42	0.20	1.08	0.55	56.19	32.09	258.88	187.76	202.69	155.67	0.22	0.53	24.10	71.12	25.06	44.31	2.47	3.14	34.88	1.13	202.30	2.88	8.37	32.00	817540.00
65	0.32	0.20	1.03	0.72	29.53	23.59	171.10	149.33	141.56	125.75	0.12	0.31	5.95	21.76	14.03	24.38	1.47	1.51	48.43	0.44	137.38	5.74	3.74	42.69	389510.00
66	0.33	0.25	1.08	0.84	35.99	20.58	188.02	131.04	152.03	110.46	0.08	0.23	15.41	56.98	19.52	29.48	1.71	1.43	32.87	1.73	183.86	4.14	5.64	28.73	444290.00
67	0.31	0.26	0.77	0.62	40.56	22.45	179.69	128.52	139.14	106.07	0.05	0.15	18.10	51.17	11.62	24.44	1.58	1.09	16.61	1.07	127.17	2.29	4.75	14.32	270700.00
68	0.45	0.20	1.60	0.70	21.82	21.53	175.96	180.54	154.14	159.01	0.26	0.89	0.29	-4.58	13.70	29.19	1.48	2.95	46.35	0.92	113.94	6.43	8.93	39.92	335080.00

69	0.30	0.42	0.89	1.15	44.53	28.58	219.96	162.60	175.43	134.02	-0.11	-0.26	15.95	57.36	11.79	28.18	1.12	2.72	14.94	4.66	150.20	2.13	4.65	12.81	315 760 .00
70	0.32	0.18	0.83	0.50	20.34	18.93	137.04	134.24	116.70	115.32	0.14	0.33	1.41	2.79	20.17	28.88	1.26	1.23	13.12	0.64	116.35	2.06	3.36	11.05	616 580 .00
71	0.34	0.20	0.98	0.66	15.36	10.02	132.72	103.62	117.36	93.60	0.14	0.32	5.34	29.10	25.26	26.48	1.26	1.93	12.08	0.53	134.31	1.29	2.78	10.79	551 040 .00
72	0.29	0.18	0.88	0.60	19.98	17.29	154.89	139.06	134.92	121.78	0.11	0.28	2.69	15.83	11.23	22.20	1.22	1.91	29.10	1.30	107.42	4.32	5.34	24.78	350 260 .00
73	0.34	0.33	0.70	0.67	27.81	15.16	183.61	134.81	155.80	119.66	0.02	0.04	12.65	48.80	14.13	20.58	0.96	1.32	8.93	2.41	109.51	0.88	8.10	8.05	435 450 .00
74	0.31	0.19	0.78	0.52	28.32	17.83	164.86	130.28	136.53	112.46	0.12	0.26	10.50	34.57	9.82	20.36	0.93	1.66	14.30	4.10	106.47	1.41	8.32	12.89	332 030 .00
75	0.33	0.31	0.66	0.65	18.13	14.28	122.40	107.00	104.27	92.72	0.02	0.02	3.85	15.40	11.26	26.34	0.84	1.43	7.76	1.25	133.51	0.93	4.08	6.82	463 210 .00
76	0.28	0.19	0.70	0.55	22.02	13.38	154.56	124.17	132.55	110.79	0.09	0.16	8.63	30.39	12.82	22.70	0.99	2.41	28.75	1.70	98.01	3.38	7.26	25.37	422 750 .00
77	0.33	0.30	0.91	0.86	26.84	23.83	157.27	149.48	130.43	125.65	0.03	0.05	3.01	7.79	12.47	27.20	1.28	2.78	12.23	2.13	93.84	0.82	3.21	11.41	377 470 .00
78	0.28	0.20	0.60	0.46	42.34	24.81	178.84	126.10	136.50	101.29	0.08	0.14	17.53	52.74	19.87	24.40	1.17	1.09	5.66	1.26	157.15	0.82	4.78	4.84	362 850 .00
79	0.30	0.23	0.68	0.52	23.07	14.39	138.24	108.53	115.17	94.13	0.07	0.16	8.68	29.72	14.41	18.33	0.98	1.10	12.64	1.56	121.61	2.26	4.54	10.38	393 730 .00
80	0.36	0.26	1.07	0.81	30.99	19.26	191.36	147.51	160.37	128.25	0.10	0.26	11.73	43.86	14.42	25.03	1.17	1.59	50.70	3.41	139.90	8.01	5.78	42.69	511 210 .00

81	0.29	0.20	0.85	0.64	28.58	19.83	179.95	141.00	151.38	121.17	0.08	0.22	8.75	38.95	11.25	21.94	1.07	1.70	32.17	3.32	110.12	4.64	4.26	27.53	369380.00
82	0.34	0.21	0.63	0.41	20.33	16.57	156.32	115.17	135.98	98.59	0.14	0.23	3.76	41.15	14.47	18.48	1.50	1.70	9.67	1.89	99.64	1.58	4.27	8.10	221470.00
83	0.24	0.16	0.67	0.45	19.34	13.13	118.93	100.46	99.60	87.32	0.08	0.22	6.20	18.48	9.82	18.76	0.80	1.30	13.63	2.14	89.23	2.93	3.63	10.71	455570.00
84	0.45	0.22	0.94	0.51	24.90	17.14	146.47	117.45	121.57	100.31	0.23	0.44	7.76	29.02	16.87	25.18	1.26	2.71	18.65	1.06	117.64	1.98	2.86	16.66	312120.00
85	0.28	0.13	0.82	0.36	18.94	12.59	120.11	91.65	101.17	79.05	0.16	0.46	6.35	28.47	12.40	27.13	1.31	1.98	13.23	2.21	100.13	1.81	3.83	11.43	566900.00
86	0.28	0.19	0.84	0.51	21.73	14.41	121.01	93.48	99.28	79.07	0.09	0.33	7.32	27.53	12.41	27.66	1.23	1.82	13.30	2.79	100.50	2.07	4.51	11.24	488790.00
87	0.14	0.10	0.39	0.28	11.85	8.89	68.01	59.67	56.16	50.78	0.04	0.10	2.96	8.34	5.50	12.71	0.56	0.88	11.65	2.84	58.22	2.43	6.00	9.22	305300.00
88	0.27	0.17	0.82	0.61	37.50	21.92	223.26	168.94	185.76	147.01	0.10	0.21	15.58	54.33	11.82	24.82	1.13	2.54	50.73	2.87	145.74	11.81	4.88	38.92	463080.00
89	0.37	0.21	0.97	0.59	26.78	16.71	156.19	126.45	129.40	109.74	0.15	0.38	10.07	29.74	15.34	32.20	1.74	3.38	16.69	20.95	115.91	2.46	3.36	14.23	647330.00
90	0.28	0.19	0.82	0.62	33.37	20.54	188.25	141.72	154.88	121.19	0.08	0.19	12.83	46.53	11.63	23.30	0.83	1.54	27.81	1.72	111.80	5.82	5.77	22.00	374320.00
91	0.22	0.07	0.46	0.19	32.62	14.44	192.72	111.82	160.10	97.39	0.15	0.27	18.19	80.90	20.60	40.01	2.03	2.08	8.42	5.36	188.77	0.91	5.92	7.51	519500.00
92	0.35	0.07	1.24	0.27	41.34	23.17	228.72	151.72	187.38	128.55	0.28	0.97	18.17	77.00	12.67	32.80	1.50	2.81	103.85	5.92	138.68	18.93	4.69	84.92	490290.00

93	0.50	0.29	1.80	1.15	61.62	42.45	371.22	258.14	309.60	215.69	0.21	0.65	19.16	113.08	24.36	27.30	2.07	4.93	86.27	5.91	114.80	16.48	12.86	69.79	544 230 .00
94	0.32	0.17	0.90	0.50	33.71	20.19	210.16	154.74	176.46	134.55	0.15	0.40	13.51	55.43	19.92	27.28	1.45	1.66	25.43	3.39	93.31	4.93	6.41	20.50	465 750 .00
95	0.22	0.23	0.58	0.68	27.33	14.26	155.69	107.32	128.35	93.06	-0.01	-0.09	13.07	48.37	12.93	23.42	1.70	1.53	13.68	3.66	111.84	2.17	4.90	11.51	460 000 .00
96	0.30	0.08	0.66	0.21	34.18	16.50	178.10	113.99	143.92	97.49	0.22	0.45	17.68	64.11	11.70	22.65	1.42	1.31	21.57	2.92	98.25	3.47	4.27	18.11	338 850 .00
97	0.32	0.26	1.09	1.05	72.07	39.37	311.48	213.63	239.41	174.26	0.05	0.04	32.70	97.85	15.67	39.84	1.95	2.28	40.86	6.32	150.18	7.30	13.60	33.56	497 400 .00
98	0.35	0.25	1.05	0.80	19.41	15.14	145.78	122.42	126.37	107.29	0.10	0.25	4.28	23.36	16.59	34.16	1.75	1.46	17.45	2.00	125.82	3.94	4.49	13.51	506 900 .00
99	0.27	0.19	0.75	0.57	38.66	18.83	224.39	138.71	185.73	119.88	0.09	0.17	19.83	85.67	13.41	24.91	1.45	1.85	29.51	3.76	114.73	4.57	9.61	24.94	394 960 .00
100	0.30	0.21	0.98	0.70	66.15	39.57	264.26	190.01	198.11	150.44	0.09	0.28	26.58	74.25	12.84	24.55	1.22	1.97	41.49	4.62	154.31	4.98	4.76	36.51	397 180 .00
101	0.29	0.12	0.70	0.32	29.68	15.83	144.15	103.13	114.47	87.30	0.17	0.37	13.85	41.02	16.09	22.01	1.09	1.11	10.00	2.44	73.02	1.34	2.57	8.65	363 440 .00
102	0.27	0.18	0.88	0.61	38.43	24.47	170.63	129.48	132.20	105.01	0.09	0.27	13.96	41.16	11.79	19.62	1.13	1.39	19.47	2.42	94.15	2.75	4.38	16.72	371 710 .00
103	0.26	0.19	0.57	0.46	31.82	18.55	142.33	103.60	110.51	85.05	0.07	0.11	13.27	38.73	12.44	17.65	1.17	2.03	13.88	3.02	93.32	1.87	5.74	12.01	394 270 .00
104	0.42	0.19	1.37	0.67	52.17	30.92	332.17	244.16	280.01	213.24	0.23	0.70	21.25	88.02	31.24	34.76	1.74	1.92	36.02	2.22	213.60	5.33	5.45	30.68	468 460 .00

105	0.36	0.28	1.48	1.27	40.98	28.28	229.37	171.67	188.39	143.39	0.08	0.21	12.69	57.70	17.83	34.99	1.61	6.60	101.86	7.32	183.33	23.11	12.79	78.75	594740.00
106	0.34	0.16	0.87	0.45	93.92	47.38	299.80	177.45	205.89	130.07	0.18	0.43	46.53	122.35	15.62	35.04	1.66	1.34	7.88	6.28	235.66	1.05	5.13	6.83	398430.00
107	0.32	0.17	0.86	0.52	30.46	17.76	145.72	98.72	115.25	80.96	0.15	0.34	12.70	47.00	10.54	19.39	1.06	1.74	23.21	9.01	90.45	2.80	2.66	20.41	398370.00
108	0.30	0.15	0.87	0.47	0.30	21.44	171.60	145.12	171.30	123.68	0.15	0.40	-21.14	26.48	13.48	24.83	1.00	1.84	33.48	3.44	121.53	4.70	3.75	28.78	404640.00
109	0.26	0.19	0.87	0.73	34.63	23.20	184.46	124.51	149.83	101.31	0.06	0.15	11.43	59.94	9.38	20.01	1.02	4.00	43.09	8.09	118.18	4.50	8.29	38.59	333840.00
110	0.31	0.26	0.79	0.74	40.41	30.85	190.09	134.71	149.68	103.86	0.05	0.05	9.55	55.38	8.50	19.73	1.14	3.74	32.81	8.25	128.53	3.69	8.72	29.12	459620.00
111	0.28	0.14	0.76	0.42	39.06	28.87	208.03	157.26	168.98	128.40	0.14	0.33	10.19	50.77	14.42	18.32	1.20	1.78	14.82	5.58	101.14	1.44	6.53	13.38	347550.00
112	0.20	0.13	0.54	0.40	41.28	23.14	202.14	115.45	160.86	92.31	0.07	0.13	18.14	86.69	7.53	22.12	1.11	1.41	10.49	5.26	156.94	1.18	5.63	9.31	308940.00
113	0.26	0.14	0.96	0.61	48.45	32.03	269.26	170.26	220.81	138.23	0.12	0.35	16.43	99.00	8.96	22.07	1.11	1.63	60.01	4.94	150.07	5.41	15.22	54.60	220970.00
114	0.18	0.12	0.49	0.38	24.55	16.61	151.10	104.48	126.54	87.87	0.06	0.11	7.94	46.62	10.81	28.08	0.95	1.03	12.10	2.24	117.99	2.15	5.32	9.96	363280.00
115	0.21	0.11	0.71	0.45	30.07	23.09	222.16	168.91	192.09	145.83	0.09	0.26	6.98	53.24	11.46	17.87	0.97	1.37	40.97	2.66	76.81	6.15	3.91	34.83	288900.00
116	0.37	0.26	0.93	0.74	21.21	16.16	158.89	122.59	137.68	106.43	0.10	0.19	5.06	36.31	14.07	24.02	0.92	1.46	26.85	3.28	85.64	3.89	2.36	22.96	371780.00

117	0.25	0.17	0.72	0.52	40.63	24.76	234.58	145.43	193.95	120.67	0.08	0.20	15.86	89.15	13.13	23.60	1.12	2.18	31.79	5.96	118.46	3.10	8.62	28.70	340140.00
118	0.26	0.20	1.06	0.86	48.83	24.81	273.12	188.92	224.28	164.10	0.06	0.19	24.02	84.20	27.06	39.18	1.93	2.43	78.67	3.42	171.51	7.43	N/F	71.24	413520.00
119	0.27	0.10	0.92	0.33	31.45	17.85	176.24	128.87	144.79	111.02	0.17	0.59	13.60	47.37	15.80	24.34	1.56	0.60	23.99	2.20	106.89	2.30	0.33	21.68	414660.00
120	0.41	0.26	1.10	0.73	35.01	18.36	228.30	159.61	193.29	141.26	0.15	0.37	16.65	68.69	23.78	40.91	1.80	1.15	13.30	2.65	172.93	1.02	N/F	12.28	520780.00
121	0.34	0.24	0.87	0.61	30.32	16.30	177.83	116.88	147.51	100.58	0.09	0.26	14.02	60.95	22.37	21.67	1.68	2.32	20.83	4.55	122.77	2.74	N/F	18.09	635080.00
122	0.29	0.12	1.05	0.45	28.44	16.51	162.41	118.50	133.98	102.00	0.17	0.59	11.93	43.91	14.04	20.75	1.15	2.24	41.57	3.20	93.14	5.80	N/F	35.77	441140.00
123	0.28	0.18	0.76	0.49	40.41	16.92	206.76	125.71	166.34	108.79	0.10	0.27	23.50	81.05	20.93	32.47	1.90	0.48	13.89	0.49	134.63	1.94	N/F	11.94	387140.00
124	0.29	0.20	1.10	0.84	41.11	30.43	235.17	165.81	194.06	135.38	0.09	0.26	10.68	69.36	11.06	15.64	1.11	1.34	69.04	9.81	90.34	8.21	1.90	60.84	306740.00
125	0.27	0.21	0.79	0.66	37.54	19.78	190.84	133.08	153.31	113.30	0.06	0.13	17.76	57.77	18.79	22.97	1.47	1.05	14.63	4.39	128.08	1.42	3.73	13.21	348650.00
126	0.28	0.19	0.85	0.60	43.99	19.74	240.90	153.53	196.91	133.80	0.09	0.24	24.25	87.37	15.18	22.07	1.23	1.10	31.02	2.50	123.25	3.12	5.45	27.91	413910.00
127	0.38	0.38	0.25	0.56	28.66	14.74	154.26	112.51	125.60	97.77	-0.01	-0.31	13.92	41.75	14.11	17.41	1.57	6.19	39.93	18.62	94.29	2.81	30.95	37.12	#VALUE!

128	0.35	0.24	0.32	0.72	35.11	19.56	217.24	146.00	182.13	126.44	0.11	-0.40	15.55	71.24	19.67	32.29	1.94	13.15	12.34	19.70	157.46	0.69	25.48	11.65	311540.00
129	0.43	0.17	0.69	0.90	80.40	49.10	429.03	341.54	348.63	292.45	0.26	-0.21	31.30	87.49	19.87	24.90	1.46	5.00	114.72	11.68	99.65	10.92	12.71	103.81	366490.00
130	0.20	0.10	0.23	0.35	32.27	15.64	190.13	127.24	157.86	111.60	0.11	-0.12	16.63	62.89	16.81	27.74	1.37	2.70	15.69	4.30	108.37	1.76	5.81	13.93	345820.00
131	0.32	0.23	0.35	0.78	36.30	19.72	188.44	131.05	152.13	111.33	0.08	-0.43	16.59	57.39	14.84	32.87	1.45	1.88	28.04	7.86	144.24	2.52	6.70	25.52	354650.00
132	0.18	0.25	0.15	0.54	20.67	12.53	127.90	82.15	107.23	69.62	-0.07	-0.39	8.14	45.75	6.56	9.39	0.79	0.81	8.47	1.52	84.64	1.04	2.97	7.43	356050.00
133	0.00	0.00	0.00	0.00	0.00	0.00	0.00	0.00	0.00	0.00	0.00	0.00	0.00	0.00	0.00	0.00	0.00	0.00	0.00	0.00	0.00	0.00	0.00	0.00	353870.00
134	0.23	0.10	0.28	0.35	32.24	14.97	181.95	125.22	149.71	110.25	0.13	-0.07	17.27	56.73	13.17	36.93	1.62	1.28	10.91	2.24	178.69	1.03	4.41	9.88	332850.00
135	0.30	0.26	0.36	0.83	51.29	34.00	188.87	126.78	137.57	92.78	0.04	-0.47	17.29	62.08	11.46	20.68	1.23	1.96	29.15	7.21	97.05	3.18	3.69	25.97	#VALUE!
136	0.24	0.22	0.82	0.89	27.19	15.31	146.59	99.90	119.41	84.59	0.02	-0.07	11.88	46.70	13.97	18.98	1.15	2.32	35.86	9.87	108.36	2.27	7.26	33.58	394080.00
137	0.35	0.26	1.07	0.79	26.84	14.39	164.31	110.76	137.47	96.37	0.09	0.27	12.45	53.56	16.41	26.51	1.47	1.92	13.91	3.92	127.79	1.28	11.92	12.63	513320.00
138	0.46	0.36	1.37	1.03	74.55	27.80	421.08	173.96	346.53	146.16	0.10	0.34	46.75	247.13	14.01	19.55	1.18	2.12	18.33	5.70	240.90	1.81	6.70	16.52	570580.00

139	0.27	0.20	0.77	0.45	43.22	30.78	186.51	131.61	143.29	100.83	0.07	0.32	12.44	54.90	12.34	24.11	1.25	0.86	17.28	2.13	128.94	2.24	1.69	15.05	431 370 .00
140	0.25	0.16	0.91	0.63	20.94	15.39	152.67	122.75	131.73	107.35	0.08	0.27	5.54	29.92	11.77	30.51	1.53	3.15	48.15	26.19	108.74	4.49	24.20	43.67	362 340 .00
141	0.39	0.25	0.89	0.61	27.98	17.83	200.85	140.99	172.87	123.16	0.14	0.28	10.16	59.87	14.03	26.61	1.45	1.46	27.43	2.99	145.65	5.87	4.45	21.56	305 730 .00
142	0.32	0.26	0.99	0.87	32.57	21.65	205.95	158.66	173.38	137.01	0.06	0.12	10.93	47.29	11.31	14.41	1.10	2.80	50.33	4.26	77.69	6.99	6.60	43.35	279 650 .00
143	0.47	0.33	0.84	0.54	28.60	17.43	182.07	139.47	153.47	122.04	0.15	0.29	11.18	42.60	15.95	25.03	2.02	3.66	22.33	4.42	94.99	2.62	8.96	19.71	392 260 .00
144	0.29	0.16	0.90	0.54	49.30	26.42	241.67	158.27	192.37	131.85	0.13	0.36	22.88	83.40	14.00	23.99	1.12	1.74	34.13	3.34	122.67	3.59	4.44	30.54	381 860 .00
145	0.33	0.20	1.18	0.85	66.82	44.98	319.35	253.52	252.53	208.54	0.13	0.33	21.84	65.83	12.71	19.48	1.56		77.50	2.88	127.80	5.51	7.81	71.99	537 739 .00
146	0.27	0.16	1.05	0.69	54.40	34.83	257.40	192.93	203.00	158.11	0.11	0.37	19.58	64.47	15.96	28.64	1.58	5.52	47.73	2.20	120.64	5.52	4.14	42.21	430 468 .00
147	0.30	0.23	0.74	0.63	42.03	24.62	231.81	174.01	189.78	149.38	0.07	0.11	17.41	57.81	13.04	24.03	1.42	2.19	20.19	6.63	125.23	2.19	4.80	18.00	515 143 .00
148	0.20	0.10	0.63	0.37	46.06	25.07	215.97	143.87	169.91	118.80	0.10	0.27	20.99	72.10	10.82	27.33	1.30	1.52	11.07	2.67	129.98	1.52	4.97	9.56	354 998 .00
149	0.32	0.19	1.18	0.77	74.92	46.89	276.84	193.56	201.92	146.67	0.13	0.41	28.03	83.28	19.09	20.22	1.74	6.46	55.66	2.45	123.27	6.46	5.95	49.19	269 002 .00
150	0.38	0.22	1.28	0.95	41.30	21.47	225.18	151.64	183.88	130.17	0.16	0.34	19.84	73.54	20.62	28.92	1.79	2.97	49.40	7.82	131.09	2.97	11.64	46.43	368 068 .00

151	0.21	0.12	0.76	0.46	51.70	29.29	182.14	123.36	130.44	94.06	0.09	0.29	22.41	58.78	11.79	23.75	1.90	1.03	10.03	5.14	118.82	1.03	4.89	9.00	365 939.00
152	0.30	0.19	0.97	0.68	49.57	32.88	218.37	156.22	168.80	123.33	0.11	0.28	16.68	62.15	13.98	24.32	1.68	4.15	35.24	3.48	122.65	4.15	3.94	31.09	424 005.00
153	0.20	0.13	0.69	0.44	28.17	27.66	88.87	85.24	60.70	57.59	0.07	0.25	0.51	3.63	10.26	16.64	0.89	0.70	5.91	3.29	89.05	0.70	8.99	5.20	75.00
154	0.41	0.26	0.91	0.61	27.90	16.12	222.29	158.20	194.38	142.08	0.16	0.30	11.79	64.09	24.11	28.32	1.82	0.84	8.70	3.33	176.99	1.21	3.73	7.48	467 340.00
155	0.36	0.22	0.98	0.66	19.25	11.15	161.20	118.75	141.95	107.60	0.14	0.32	8.11	42.45	11.87	20.30	1.12	1.17	33.09	1.30	81.22	7.07	3.67	26.02	446 149.00
156	0.34	0.19	0.96	0.64	47.70	23.69	274.46	208.01	226.76	184.32	0.15	0.32	24.01	66.45	13.30	22.94	1.43	1.53	46.90	2.75	110.18	5.82	5.85	41.08	433 486.00
157	0.24	0.15	0.92	0.73	32.53	19.99	214.67	162.23	182.14	142.25	0.09	0.19	12.55	52.44	9.32	14.17	0.87	1.74	61.77	1.80	70.81	15.92	6.77	45.85	338 500.00
158	0.39	0.23	1.00	0.67	30.75	20.43	188.48	141.31	157.73	120.88	0.16	0.32	10.32	47.16	32.01	27.26	1.56	2.86	40.67	2.11	131.27	5.08	6.18	35.59	331 091.00
159	0.26	0.18	0.47	0.37	43.77	19.53	218.71	130.55	174.95	111.02	0.07	0.09	24.24	88.17	14.48	21.77	1.24	1.19	5.76	1.65	134.93	0.52	3.00	5.24	595 725.00
160	0.29	0.17	1.16	0.73	36.00	26.03	285.36	237.35	249.36	211.32	0.13	0.42	9.97	48.01	19.51	40.46	1.12	1.33	38.47	1.98	121.60	6.49	4.02	31.98	525 179.00
161	0.21	0.10	0.47	0.26	36.12	16.45	195.80	126.03	159.68	109.58	0.11	0.22	19.68	69.77	12.42	27.26	1.20	1.73	9.18	3.51	132.05	1.10	4.68	8.07	310 299.00
162	0.28	0.16	0.78	0.53	34.55	17.45	227.39	146.26	192.84	128.81	0.11	0.25	17.09	81.13	12.74	23.66	1.33	1.18	25.33	1.85	114.33	3.60	4.37	21.73	371 854.00

163	0.30	0.17	1.02	0.65	40.79	20.91	280.30	190.11	259.39	169.20	0.13	0.38	19.88	90.19	13.91	23.58	1.31	1.49	46.79	3.15	130.85	3.74	N/F	43.05	445619.00
164	0.24	0.17	0.77	0.60	31.14	16.31	198.82	153.68	182.51	137.37	0.07	0.18	14.84	45.14	14.30	16.95	1.03	1.06	34.24	3.65	83.40	5.36	4.66	28.88	321743.00
165	0.28	0.21	0.60	0.47	29.57	15.72	191.37	130.34	175.65	114.62	0.07	0.13	13.85	61.03	11.24	17.10	0.90	0.85	7.60	1.63	91.92	0.97	7.79	6.63	278429.00
166	0.38	0.27	1.13	0.86	23.89	15.17	198.71	144.71	183.54	129.54	0.12	0.27	8.72	54.01	17.90	27.67	1.69	1.00	24.55	1.69	118.09	2.74	17.41	21.80	445624.00
167	0.56	0.37	1.00	0.70	29.04	18.76	195.27	142.26	176.52	123.50	0.19	0.30	10.28	53.02	23.26	20.65	1.73	1.53	14.44	4.12	140.63	1.89	7.17	12.55	439413.00
168	0.28	0.32	0.80	1.01	38.52	20.07	223.43	147.07	203.36	127.00	-0.04	-0.22	18.44	76.36	14.75	23.34	1.43	1.91	10.70	5.96	162.79	0.66	7.70	10.04	433214.00
169	0.30	0.20	1.38	1.03	41.72	27.67	326.46	260.27	298.78	232.60	0.10	0.35	14.05	66.18	15.12	32.05	1.40	1.46	61.35	3.21	148.02	7.91	4.02	53.44	361370.00
170	0.24	0.14	0.98	0.64	23.07	11.01	177.77	111.20	166.76	100.19	0.10	0.34	12.06	66.57	13.83	26.62	1.25	0.80	23.29	2.52	143.93	2.01	N/F	21.29	445891.00
171	0.28	0.21	0.86	0.68	27.71	14.06	229.35	150.53	215.29	136.46	0.07	0.18	13.64	78.82	13.29	21.71	1.21	2.07	34.50	7.53	118.64	2.74	9.64	31.76	393238.00
172	0.26	0.11	0.90	0.46	25.66	15.32	155.64	114.18	140.32	98.86	0.15	0.44	10.34	41.46	8.49	15.34	0.94	2.49	40.88	3.77	105.55	3.77	9.06	37.12	306028.00
173	0.32	0.21	1.08	0.82	51.57	35.87	227.99	181.70	192.12	145.83	0.11	0.26	15.70	46.29	17.39	24.75	1.26	1.29	48.03	2.20	129.66	4.65	1.08	43.38	394765.00
174	0.32	0.13	1.14	0.53	25.55	22.86	187.90	154.66	165.04	131.81	0.19	0.61	2.70	33.24	14.35	24.27	1.00	2.15	36.70	2.33	129.39	4.45	5.30	32.24	442255.00

175	0.41	0.24	1.16	0.68	23.85	12.34	136.20	90.00	123.87	77.67	0.17	0.48	11.52	46.20	17.94	22.74	1.42	1.64	18.83	4.00	138.57	1.94	9.27	16.89	482 570.00
176	0.39	0.19	0.78	0.39	22.00	12.03	124.38	84.16	112.35	72.13	0.20	0.39	9.97	40.22	19.49	17.09	1.43	1.66	22.54	2.31	114.29	3.46	10.67	19.08	346 524.00
177	0.34	0.20	0.83	0.54	25.89	14.89	184.91	131.09	170.02	116.20	0.14	0.29	11.00	53.82	13.10	22.98	1.42	1.75	22.16	2.69	107.36	2.90	6.91	19.26	399 913.00
178	0.28	0.15	1.25	0.87	31.45	21.80	227.40	181.47	205.60	159.68	0.12	0.38	9.66	45.93	14.93	30.53	1.40	2.17	79.53	3.11	138.09	11.27	3.46	68.25	491 948.00
179	0.33	0.21	0.73	0.49	33.11	16.18	189.58	126.67	173.40	110.49	0.13	0.24	16.93	62.91	12.02	21.25	1.48	1.92	11.76	3.13	121.67	1.08	3.44	10.68	384 348.00
180	0.29	0.16	0.89	0.56	27.96	17.46	197.38	139.27	179.92	121.81	0.12	0.33	10.50	58.11	11.99	21.07	1.34	1.70	30.68	3.68	109.65	3.48	7.86	27.20	364 474.00
181	0.23	0.17	0.65	0.53	22.09	9.83	236.81	145.91	226.98	136.08	0.05	0.12	12.27	90.90	11.38	25.91	1.57	1.59	11.58	3.52	169.59	1.70	5.44	9.89	363 099.00
182	0.46	0.37	1.00	0.86	27.33	16.13	183.43	138.37	167.30	122.24	0.08	0.14	11.20	45.06	14.79	19.66	1.22	1.14	15.81	2.35	126.04	2.51	4.93	13.30	356 120.00
183	0.32	0.26	0.71	0.55	26.89	11.03	217.63	128.98	206.60	117.95	0.06	0.15	15.86	88.65	11.47	20.66	1.15	1.80	5.49	3.94	152.28	0.58	6.50	4.91	390 943.00
184	0.36	0.31	0.89	0.80	23.70	14.24	174.60	135.53	160.36	121.29	0.05	0.09	9.46	39.07	23.49	26.11	1.64	2.07	17.44	1.94	117.12	3.20	4.17	14.25	466 507.00
185	0.36	0.28	1.06	0.91	33.99	20.40	202.25	153.72	181.85	133.32	0.09	0.16	13.58	48.53	13.49	32.66	1.67	1.94	33.65	4.13	106.22	4.71	6.20	28.94	413 880.00
186	0.25	0.19	0.85	0.65	31.99	16.66	235.34	146.85	218.68	130.19	0.06	0.20	15.33	88.50	16.01	32.08	1.69	1.39	12.43	1.51	160.43	2.09	4.27	10.34	421 998.00

187	0.30	0.23	0.81	0.71	29.21	14.62	177.99	122.18	163.36	107.56	0.07	0.10	14.58	55.81	16.16	25.17	0.95	0.89	7.09	2.38	113.10	0.84	2.51	6.26	386810.00
188	0.28	0.22	1.27	1.00	19.05	12.15	212.66	166.33	200.52	154.18	0.07	0.27	6.91	46.34	16.02	31.94	1.30	1.56	59.91	2.25	137.17	11.16	5.40	48.75	418506.00
189	0.27	0.22	0.94	0.75	21.57	10.71	221.54	147.66	210.82	136.95	0.04	0.18	10.86	73.88	12.93	23.34	1.19	1.88	30.54	3.78	118.03	4.67	6.32	25.87	153.00
190	0.19	0.15	0.53	0.47	14.23	8.45	141.35	108.32	132.90	99.87	0.04	0.05	5.78	33.03	15.39	25.32	1.41	1.02	9.83	1.94	103.63	1.18	4.24	8.65	393715.00
191	0.27	0.21	0.68	0.58	29.78	15.05	175.13	115.79	160.08	100.75	0.06	0.10	14.73	59.34	15.50	20.48	1.11	1.36	11.82	1.63	99.98	1.84	4.64	9.99	436614.00
192	0.35	0.30	0.86	0.72	20.70	11.15	214.23	145.47	203.09	134.32	0.05	0.13	9.55	68.76	18.34	21.36	1.08	1.12	6.52	2.92	146.41	0.43	4.10	6.09	342589.00
193	0.28	0.22	1.26	1.18	20.53	13.19	243.15	202.71	229.97	189.52	0.05	0.07	7.34	40.45	11.83	25.02	1.05	1.90	77.51	2.76	110.04	11.38	8.41	66.14	424280.00
194	0.24	0.18	1.24	1.04	25.07	14.49	293.93	233.34	279.45	218.85	0.06	0.20	10.59	60.60	15.18	32.99	1.32	2.26	72.62	2.02	145.08	11.33	4.57	61.29	385927.00
195	0.31	0.25	0.82	0.74	23.07	11.58	222.42	150.10	210.84	138.52	0.06	0.08	11.50	72.32	18.77	30.32	1.63	1.36	5.15	2.41	169.99	0.64	3.47	4.51	426634.00
196	0.35	0.32	0.77	0.68	11.54	8.20	112.16	84.93	103.96	76.73	0.03	0.09	3.35	27.23	19.26	17.30	1.09	0.99	12.15	1.77	68.77	1.92	2.79	10.23	411267.00
197	0.26	0.23	0.76	0.70	15.23	9.14	144.93	112.74	135.80	103.60	0.03	0.06	6.09	32.20	10.67	14.62	0.76	1.12	27.76	1.48	41.02	4.03	3.87	23.74	345523.00
198	0.23	0.18	0.74	0.64	16.24	10.79	167.41	122.73	156.62	111.94	0.05	0.10	5.45	44.68	11.43	19.87	0.73	1.51	26.67	1.43	97.75	4.26	3.88	22.41	301652.00

199	0.30	0.23	0.99	0.72	30.73	17.75	182.98	134.77	152.26	117.03	0.07	0.27	12.98	48.21	14.01	21.62	1.36	2.04	18.65	7.65	73.08	2.23	10.55	16.42	203 197.00
200	0.31	0.26	0.75	0.65	27.06	16.61	154.88	118.00	127.81	101.39	0.05	0.10	10.46	36.88	15.74	19.92	0.93	1.55	18.63	5.86	56.85	2.64	4.87	15.99	321 632.00
201	0.37	0.28	1.20	0.90	44.42	25.38	320.92	199.83	276.50	174.45	0.09	0.30	19.04	121.09	13.07	25.51	1.43	1.81	6.98	5.55	223.80	1.04	6.68	5.94	366 891.00
202	0.31	0.24	0.88	0.76	36.70	20.82	221.41	162.90	184.71	142.08	0.07	0.12	15.88	58.50	16.36	28.20	1.27	1.22	19.61	3.73	156.50	3.38	2.79	16.23	304 858.00
203	0.38	0.25	0.89	0.68	42.36	20.33	250.40	158.01	208.04	137.68	0.13	0.21	22.03	92.39	16.69	35.84	1.88	8.95	11.91	14.99	153.20	1.15	14.38	10.76	545 785.00
204	0.36	0.30	0.95	0.76	29.61	12.79	192.58	105.11	162.96	92.32	0.06	0.19	16.82	87.47	23.14	29.00	1.86	1.54	9.44	2.78	116.66	1.18	4.01	8.26	381 601.00
205	0.44	0.35	1.06	0.93	67.26	24.94	364.02	207.52	296.76	182.58	0.09	0.13	42.32	156.51	29.55	40.01	2.48	1.51	19.35	4.01	240.51	2.57	6.24	16.78	585 023.00
206	0.45	0.38	1.07	0.94	22.07	10.65	145.79	105.14	123.72	94.49	0.08	0.13	11.42	40.65	10.64	17.54	1.50	1.45	31.73	3.65	77.68	5.58	7.81	26.15	311 073.00
207	0.32	0.26	1.03	0.87	29.56	25.59	212.93	177.89	183.37	152.30	0.06	0.16	3.97	35.04	15.16	26.16	1.16	2.91	39.62	10.78	131.63	6.08	11.27	33.54	420 618.00
208	0.32	0.26	1.10	0.90	30.25	14.59	182.98	119.72	152.73	105.13	0.06	0.20	15.66	63.26	15.72	22.96	1.79	2.05	38.11	8.11	112.44	4.56	8.75	33.55	475 835.00
209	0.33	0.29	0.97	0.89	15.45	11.47	112.44	95.12	96.99	83.66	0.04	0.08	3.98	17.32	15.02	22.53	1.36	1.94	34.45	5.02	74.88	4.27	6.81	30.18	526 372.00
210	0.26	0.22	1.19	1.17	25.40	19.49	189.10	163.77	163.70	144.29	0.03	0.02	5.91	25.33	8.73	14.86	1.06	1.00	68.92	1.38	52.89	12.19	5.31	56.74	265 650.00

211	0.32	0.28	0.95	0.73	36.07	17.38	216.83	138.52	180.76	121.15	0.04	0.22	18.70	78.31	14.48	27.70	1.61	1.41	29.35	3.29	149.47	2.11	7.67	27.24	512 348 .00
212	0.38	0.31	1.03	0.84	24.39	16.02	174.31	132.61	149.92	116.59	0.07	0.19	8.37	41.70	17.15	27.58	2.06	1.57	9.29	2.25	146.26	1.34	7.39	7.95	470 677 .00
213	0.29	0.23	0.86	0.68	37.53	17.60	231.34	140.59	193.81	122.99	0.06	0.17	19.93	90.75	17.22	24.61	1.81	1.77	16.29	8.73	170.70	2.02	5.06	14.28	331 489 .00
214	0.33	0.25	1.55	1.42	64.99	45.07	412.78	346.43	347.79	301.36	0.07	0.13	19.92	66.35	14.53	43.09	2.03	2.17	127.74	3.69	150.86	21.51	11.77	106.22	503 624 .00
215	0.29	0.25	1.87	1.88	36.97	30.74	295.29	269.19	258.32	238.45	0.04	-0.01	6.23	26.10	13.63	16.47	1.24	7.61	222.53	5.14	58.25	32.36	44.33	190.17	387 281 .00
216	0.33	0.26	1.01	0.89	36.31	18.79	246.89	161.90	210.58	143.11	0.07	0.12	17.52	84.99	15.54	27.94	1.58	2.08	36.27	4.84	131.03	5.99	5.44	30.28	455 950 .00
217	0.29	0.22	0.71	0.56	29.27	15.37	187.11	139.01	157.84	123.63	0.07	0.15	13.90	48.11	14.69	22.74	1.18	1.72	14.59	2.46	75.11	1.97	4.39	12.62	341 008 .00
218	0.38	0.32	1.63	1.36	70.24	48.23	281.68	225.57	211.44	177.35	0.06	0.27	22.01	56.10	16.12	30.29	1.49	2.65	61.15	2.64	112.81	8.36	8.20	52.79	488 713 .00
219	0.26	0.18	0.81	0.72	41.14	22.46	145.38	96.16	104.23	73.69	0.08	0.09	18.68	49.22	14.57	24.09	1.21	2.65	24.51	2.29	122.43	3.05	7.46	21.46	412 947 .00
220	0.31	0.23	0.72	0.62	36.44	21.12	197.25	139.65	160.81	118.53	0.08	0.10	15.32	57.60	18.19	22.08	1.11	2.46	16.40	2.61	117.99	2.85	8.62	13.55	512 046 .00
221	0.23	0.17	0.63	0.47	27.08	16.33	119.26	81.92	92.18	65.59	0.06	0.16	10.75	37.34	11.56	20.53	1.05	1.39	6.58	2.37	113.94	0.76	7.53	5.82	339 591 .00
222	0.40	0.32	1.17	0.96	42.31	20.59	196.71	119.14	154.40	98.55	0.08	0.21	21.72	77.57	22.46	33.20	2.03	1.60	8.04	2.12	145.33	0.78	3.88	7.26	559 167 .00

223	0.47	0.37	1.44	1.16	47.28	23.04	285.62	175.14	238.34	152.10	0.10	0.28	24.24	110.48	21.38	35.49	2.00	1.85	49.66	3.94	203.27	9.37	8.40	40.29	509 916 .00
224	0.43	0.37	0.89	0.80	23.82	12.22	158.00	108.78	134.18	96.56	0.06	0.09	11.60	49.22	20.88	21.39	1.30	1.11	9.57	2.39	78.75	1.47	5.13	8.10	467 961 .00
225	0.24	0.18	0.76	0.60	38.24	17.47	223.88	135.21	185.65	117.74	0.06	0.15	20.77	88.68	14.24	24.86	1.36	1.96	29.95	3.29	111.67	4.19	8.33	25.77	412 288 .00
226	0.31	0.23	0.97	0.85	26.38	15.40	169.93	127.61	143.55	112.21	0.08	0.12	10.98	42.32	11.11	19.77	1.31	7.51	49.81	23.09	110.58	4.04	32.81	45.77	360 871 .00
227	0.27	0.22	1.15	1.00	35.34	22.70	228.38	183.82	193.04	161.13	0.05	0.16	12.64	44.56	25.46	31.26	2.03	1.55	79.66	5.75	83.73	8.83	8.69	70.83	384 900 .00
228	0.33	0.27	0.80	0.66	29.09	16.02	175.91	120.85	146.81	104.83	0.06	0.14	13.07	55.05	14.12	18.57	1.21	1.48	9.35	5.07	107.10	0.87	4.11	8.48	350 575 .00
229	0.36	0.30	2.09	1.90	53.38	36.61	299.91	239.44	246.54	202.83	0.06	0.19	16.77	60.47	11.56	18.81	1.29	3.15	132.01	5.51	98.46	14.30	8.25	117.71	441 930 .00
230	0.32	0.27	0.92	0.78	20.87	13.79	154.38	125.22	133.50	111.43	0.05	0.14	7.08	29.16	10.96	22.70	1.08	1.41	28.82	2.86	88.56	3.61	5.40	25.21	386 211 .00
231	0.28	0.22	0.75	0.59	29.10	13.37	184.87	113.78	155.77	100.41	0.06	0.16	15.72	71.09	9.54	19.51	0.95	0.82	11.09	4.53	96.80	1.33	10.16	9.76	241 713 .00
232	0.39	0.31	2.03	1.80	73.45	52.82	424.11	350.46	350.65	297.64	0.07	0.23	20.63	73.64	13.87	16.03	1.06	2.15	142.83	5.55	93.56	12.40	19.06	130.43	313 393 .00
233	0.31	0.28	1.19	1.06	47.90	26.09	235.60	159.07	187.70	132.98	0.03	0.12	21.81	76.53	11.62	19.57	1.15	2.04	75.10	5.73	149.27	9.15	8.13	65.94	433 098 .00
234	0.30	0.23	0.89	0.76	23.91	15.10	183.97	130.09	160.06	114.99	0.06	0.13	8.81	53.89	13.14	21.18	1.18	1.68	33.68	5.62	106.62	3.84	18.25	29.84	377 580 .00

235	0.32	0.25	0.93	0.76	37.92	21.69	219.35	131.09	181.44	109.40	0.07	0.17	16.22	88.26	19.88	23.51	1.40	3.53	30.51	4.15	152.41	2.88	20.43	27.63	589573.00
236	0.34	0.28	0.76	0.63	38.08	22.73	167.90	103.62	129.83	80.90	0.07	0.13	15.35	64.28	17.26	21.82	1.63	1.62	11.23	3.27	128.14	1.05	9.52	10.18	430893.00
237	0.32	0.25	0.92	0.77	25.65	18.86	133.38	94.41	107.73	75.55	0.07	0.15	6.79	38.97	16.08	24.00	1.59	1.28	5.87	2.35	98.07	0.80	11.11	5.07	412724.00
238	0.31	0.24	1.00	0.81	43.30	24.53	261.34	157.78	218.04	133.25	0.07	0.19	18.77	103.56	16.61	25.48	1.61	2.42	38.40	3.03	132.33	4.15	9.12	34.25	484562.00
239	0.29	0.23	1.08	0.92	32.65	20.92	188.28	126.51	155.62	105.59	0.05	0.16	11.74	61.77	10.81	19.56	1.01	3.81	50.04	3.16	120.56	5.70	8.58	44.34	380215.00
240	0.24	0.18	0.95	0.76	45.42	26.41	270.96	175.76	225.54	149.35	0.06	0.19	19.01	95.20	12.79	27.37	1.83	2.42	54.16	3.60	129.26	7.07	11.10	47.09	392631.00
241	0.36	0.29	1.06	0.92	56.51	31.07	276.16	164.61	219.65	133.54	0.07	0.14	25.44	111.56	19.36	33.58	1.87	2.32	18.87	3.38	213.34	2.44	12.14	16.43	767640.00
242	0.32	0.23	0.96	0.74	45.53	23.45	280.46	146.20	234.93	122.75	0.08	0.21	22.08	134.26	19.76	31.06	1.60	2.34	19.99	7.56	266.53	1.64	10.82	18.35	601173.00
243	0.23	0.16	0.75	0.54	29.86	18.01	156.95	98.59	127.09	80.58	0.07	0.21	11.85	58.36	10.57	22.81	1.28	1.58	17.25	2.80	107.36	1.81	5.80	15.44	328293.00

Table 7.24 Complete sterol profile table for BioFIND cohort of baseline PD and healthy control plasma sample (n=243). Results expressed an ng/mL.

Month of collection	Birthdate	Sample ID	Sample name	(3β,7α,24S)-triHCA	3β,7α,X-triHCA +7α,X-diH-3O-CA	7α,X-diH-3O-CA	3β,7α,X-diHCA	3β,7α,25-triHCA +7α,25-diH-3O-CA	7α,25-diH-3O-CA	3β,7α,25-diHCA	(25S)3β,7α-diHCA + (25S)7α-H-3-OCA	(25S)7α-H-3O-CA	(25S)3β,7α-diHCA	3β,7α-diHCA + 7α-H-3-OCA	7α-H-3O-CA	3β,7α-diHCA	(25R)3β-7α-diHCA +(25R)7α-H-3O-CA	(25R)7α-H-3O-CA	(25R)3β,7α-diHCA	Cholestenoic acid (3β-HCA)
36	10145	324	**1**	0.64	8.45	8.97	-0.52	2.71	2.93	-0.22	11.01	8.45	2.56	50.37	44.62	5.75	39.36	36.17	3.20	1.84
36	12730	198	**2**	0.38	6.08	6.43	-0.35	1.56	2.31	-0.76	8.81	6.82	1.98	40.66	36.23	4.42	31.85	29.41	2.44	1.71
36	15812	180	**3**	0.59	6.61	7.36	-0.75	2.07	2.40	-0.33	9.29	7.10	2.19	40.16	35.36	4.80	30.87	28.26	2.61	1.44
36	17182	96	**4**	0.45	5.78	6.12	-0.34	1.90	1.90	0.00	8.72	7.06	1.65	40.20	36.13	4.07	31.49	29.07	2.42	1.30
36	17795	336	**5**	0.26	4.89	5.16	-0.27	1.24	1.33	-0.09	8.55	6.58	1.97	36.86	32.77	4.09	28.31	26.19	2.12	1.25
60	15061	34	**6**	0.34	3.38	3.64	-0.27	1.00	1.11	-0.11	4.47	3.78	0.69	19.76	17.31	2.45	15.29	13.53	1.76	0.63
36	14739	74	**7**	0.31	5.43	5.69	-0.26	1.53	1.58	-0.05	6.66	4.81	1.86	29.49	25.53	3.96	22.83	20.72	2.11	1.36
12	13218	62	**8**	0.09	2.97	3.20	-0.23	0.70	0.89	-0.20	5.21	4.08	1.13	21.62	18.52	3.09	16.41	14.45	1.96	0.78
36	15061	34	**9**	0.32	3.95	4.01	-0.05	1.18	1.32	-0.14	5.20	4.01	1.19	23.05	19.96	3.09	17.85	15.96	1.89	0.79
12	9747	21	**10**	0.36	6.42	6.64	-0.22	1.74	1.73	0.01	10.06	6.41	3.65	37.55	28.73	8.82	27.49	22.33	5.16	1.74
60	13310	187	**11**	0.17	4.95	5.26	-0.30	1.77	1.77	0.00	5.79	4.62	1.17	27.71	24.59	3.13	21.92	19.96	1.96	1.25
12	13743	218	**12**	0.31	3.75	3.91	-0.16	1.13	1.25	-0.12	4.21	3.18	1.03	17.21	14.52	2.69	13.00	11.34	1.66	0.78

12	12881	311	**13**	0.15	3.11	3.34	-0.23	1.00	1.02	-0.02	4.03	3.12	0.91	17.31	15.25	2.07	13.28	12.13	1.16	0.78
60	17405	78	**14**	0.21	3.71	3.71	0.00	0.99	2.04	-1.05	3.76	2.98	0.78	18.87	16.41	2.46	15.10	13.42	1.68	0.71
36	14027	405	**15**	0.49	6.74	7.04	-0.31	2.30	2.21	0.10	6.45	5.38	1.07	31.11	28.47	2.63	24.66	23.10	1.57	1.20
60	9954	157	**16**	0.57	6.25	6.62	-0.38	2.14	2.36	-0.22	8.84	6.29	2.56	35.32	30.01	5.31	26.47	23.72	2.75	1.51
12	12200	201	**17**	0.28	5.65	5.91	-0.25	1.68	1.91	-0.23	5.58	4.24	1.34	22.40	18.92	3.48	16.81	14.68	2.13	1.60
60	16311	177	**18**	0.38	5.77	5.86	-0.09	1.50	2.01	-0.52	6.71	4.92	1.79	30.07	25.72	4.35	23.36	20.80	2.57	1.16
12	10009	61	**19**	0.27	3.50	3.77	-0.28	0.82	1.22	-0.41	3.70	2.74	0.96	13.66	11.34	2.33	9.96	8.60	1.36	0.81
12	12185	328	**20**	0.24	3.99	4.20	-0.21	1.34	1.27	0.07	3.89	2.75	1.13	14.98	11.99	2.98	11.09	9.24	1.85	0.65
36	17405	78	**21**	0.27	4.40	4.66	-0.26	1.32	1.89	-0.56	4.68	3.71	0.97	20.85	18.90	1.95	16.17	15.19	0.98	0.65
36	11293	367	**22**	0.41	6.56	6.79	-0.23	2.12	2.19	-0.08	7.33	5.02	2.31	29.24	23.96	5.28	21.91	18.94	2.97	1.40
12	12244	464	**23**	0.20	4.74	5.16	-0.42	1.56	2.15	-0.59	4.99	3.47	1.53	20.45	17.88	2.57	15.46	14.42	1.04	0.87
60	17182	96	**24**	0.41	7.65	8.28	-0.63	2.23	2.57	-0.34	9.50	7.47	2.03	44.06	38.90	5.16	34.56	31.43	3.13	1.43
12	18081	239	**25**	0.41	5.66	5.87	-0.21	1.38	1.95	-0.57	6.07	4.83	1.24	26.29	22.43	3.86	20.22	17.60	2.62	1.24
12	14902	290	**26**	0.55	13.01	13.78	-0.77	3.44	3.77	-0.33	15.67	11.97	3.70	73.69	65.95	7.74	58.02	53.98	4.04	2.60
12	13188	416	**27**	0.44	7.20	7.58	-0.38	2.32	2.52	-0.20	5.09	3.78	1.31	19.47	16.66	2.82	14.38	12.87	1.51	0.92
12	14683	37	**28**	0.62	7.92	8.41	-0.49	2.51	2.73	-0.22	10.00	7.10	2.90	43.89	37.04	6.85	33.90	29.95	3.95	1.80
60	10145	324	**29**	0.51	9.30	9.84	-0.54	3.07	3.37	-0.30	8.47	6.71	1.76	35.84	31.22	4.62	27.37	24.51	2.86	1.29
12	10794	473	**30**	0.84	7.17	7.85	-0.68	2.33	2.54	-0.21	7.78	5.74	2.04	33.17	28.12	5.05	25.39	22.38	3.01	1.40

12	8490	383	**31**	0.65	9.15	9.54	-0.39	2.98	3.26	-0.28	8.69	6.93	1.76	42.44	35.40	7.05	33.75	28.47	5.29	2.17
12	11293	367	**32**	0.44	8.25	9.12	-0.88	2.15	3.12	-0.97	6.93	5.05	1.88	28.97	24.61	4.36	22.04	19.56	2.48	2.02
60	17795	336	**33**	0.37	6.59	7.72	-1.14	1.71	1.96	-0.24	9.08	7.49	1.59	41.52	39.06	2.46	32.45	31.57	0.88	1.42
36	13310	187	**34**	0.27	4.18	4.65	-0.47	1.35	1.46	-0.11	4.31	3.39	0.92	18.86	16.91	1.94	14.55	13.52	1.03	0.92
36	11347	467	**35**	0.33	5.78	6.43	-0.65	1.60	1.78	-0.18	6.72	4.78	1.94	27.64	22.88	4.75	20.92	18.11	2.81	0.93
12	15730	315	**36**	0.28	4.70	5.14	-0.44	1.32	1.56	-0.24	6.05	4.90	1.15	26.14	24.59	1.55	20.10	19.69	0.41	1.07
12	10982	89	**37**	0.34	6.42	7.17	-0.76	1.75	1.93	-0.18	9.29	7.35	1.94	38.47	35.27	3.21	29.18	27.92	1.27	1.72
36	12881	311	**38**	0.14	2.84	3.17	-0.33	0.87	0.95	-0.08	4.72	3.66	1.06	18.59	16.42	2.17	13.87	12.76	1.11	0.83
12	13773	257	**39**	0.22	2.92	3.20	-0.28	0.73	0.92	-0.19	3.09	2.46	0.63	13.27	12.06	1.21	10.18	9.60	0.59	0.59
60	14422	301	**40**	0.18	3.15	3.61	-0.46	1.13	1.25	-0.12	4.11	2.91	1.21	16.13	13.88	2.25	12.02	10.97	1.04	0.73
12	9954	157	**41**	0.75	1.30	1.40	-0.10	1.83	1.81	0.02	11.03	7.67	3.36	43.77	35.70	8.07	32.74	28.03	4.72	1.65
12	18173	493	**42**	0.28	0.70	0.77	-0.07	1.04	1.05	-0.01	3.83	2.86	0.97	15.03	12.80	2.23	11.20	9.94	1.26	0.60
12	12239	240	**43**	0.41	1.26	1.34	-0.08	1.91	1.87	0.04	5.88	3.83	2.05	23.04	17.42	5.63	17.16	13.58	3.58	0.94
60	11499	309	**44**	1.05	4.00	4.63	-0.62	5.33	5.30	0.02	20.19	14.17	6.02	97.85	77.66	20.19	77.66	63.49	14.17	3.55
36	10794	473	**45**	0.89	1.81	1.96	-0.15	2.52	2.65	-0.14	8.46	5.85	2.61	36.18	30.00	6.18	27.72	24.15	3.57	1.34
12	10145	324	**46**	0.61	1.82	1.99	-0.18	2.32	2.36	-0.05	9.71	7.20	2.51	41.97	35.78	6.20	32.26	28.58	3.69	1.66
12	12497	20	**47**	0.15	2.63	2.37	0.26	1.00	0.96	0.04	3.46	2.34	1.13	15.25	11.92	3.33	11.79	9.59	2.20	0.63
36	10942	284	**48**	0.38	0.91	0.99	-0.08	1.28	1.34	-0.06	4.47	3.29	1.18	16.44	13.87	2.58	11.97	10.57	1.40	0.60

36	13218	62	**49**	0.21	1.20	1.20	0.00	1.37	1.37	0.00	3.64	5.70	2.07	17.41	21.21	3.80	13.77	15.50	1.73	9.82
12	10942	284	**50**	0.21	0.87	0.78	-0.09	1.10	1.07	-0.03	2.66	4.16	1.50	10.99	14.30	3.31	8.32	10.14	1.81	10.00
12	10108	208	**51**	0.61	1.63	1.77	0.14	2.54	2.68	0.14	7.55	11.66	4.11	36.90	46.98	10.08	29.35	35.32	5.97	9.95
60	12881	311	**52**	0.17	0.91	0.98	0.07	0.88	1.04	0.16	3.10	4.85	1.75	14.61	18.27	3.66	11.51	13.42	1.91	9.96
12	8477	65	**53**	0.29	0.97	0.91	-0.06	1.12	1.22	0.09	3.80	5.20	1.40	17.54	21.01	3.47	13.74	15.81	2.07	9.96
36	15730	315	**54**	0.37	1.27	0.91	-0.36	1.61	1.70	0.09	6.73	8.15	1.41	32.06	36.46	4.40	25.33	28.31	2.98	9.95
12	12283	344	**55**	0.33	1.78	2.06	0.28	2.26	2.55	0.29	6.18	8.55	2.37	31.38	37.69	6.31	25.20	29.14	3.94	9.96
12	14119	146	**56**	0.22	0.61	0.69	0.08	0.90	1.12	0.22	3.28	5.12	1.84	14.90	19.08	4.18	11.63	13.96	2.33	9.94
12	15797	57	**57**	0.24	0.65	0.60	0.05	0.78	0.80	-0.02	4.68	3.35	1.34	19.30	15.82	3.48	14.61	12.47	2.15	9.95
12	12069	302	**58**	0.78	2.84	2.76	0.08	3.12	3.33	-0.21	14.36	9.64	4.72	65.29	50.83	14.45	50.93	41.20	9.73	2.43
12	11499	309	**59**	1.18	3.93	3.39	0.54	5.91	5.90	0.01	21.17	14.80	6.37	106.05	83.99	22.07	84.88	69.19	15.70	4.37
36	9481	233	**60**	0.29	0.77	0.77	-0.01	1.22	1.35	-0.13	4.40	3.02	1.37	15.75	12.80	2.95	11.35	9.77	1.58	0.66
12	10846	291	**61**	0.25	0.70	0.60	0.10	0.87	0.94	-0.07	3.45	2.68	0.77	14.03	12.18	1.86	10.59	9.50	1.09	0.51
36	12173	75	**62**	0.49	1.76	1.76	0.00	1.29	1.47	-0.17	7.00	5.02	1.98	28.45	23.45	5.01	21.46	18.43	3.02	0.93
36	9954	157	**63**	0.81	1.65	1.30	0.35	2.26	2.00	0.26	11.28	8.09	3.19	46.10	37.59	8.51	34.82	29.49	5.33	1.72
36	10982	89	**64**	1.14	2.53	2.44	0.09	3.69	3.81	-0.12	16.89	12.56	4.34	71.62	60.68	10.93	54.72	48.13	6.60	2.52
36	14036	150	**65**	0.24	4.08	4.42	-0.35	1.43	1.29	0.14	5.17	3.83	1.34	21.34	17.68	3.66	16.17	13.85	2.32	0.80
12	13027	278	**66**	0.60	8.65	8.40	0.25	2.50	2.89	-0.39	7.82	4.96	2.86	30.99	23.34	7.66	23.18	18.38	4.80	1.45

60	9365	175	**67**	0.55	8.02	8.03	-0.01	2.58	2.36	0.22	8.81	5.42	3.39	36.08	26.95	9.13	27.27	21.53	5.74	1.51
12	12250	356	**68**	0.21	2.98	3.06	-0.08	0.93	0.91	0.02	4.67	3.86	0.82	23.07	20.55	2.53	18.40	16.69	1.71	0.93
36	10372	154	**69**	0.51	9.11	9.24	-0.13	2.90	2.87	0.03	10.89	7.68	3.21	53.36	43.57	9.78	42.47	35.89	6.57	2.20
60	12497	20	**70**	0.25	3.49	3.83	-0.33	1.41	1.67	-0.26	4.09	2.93	1.16	18.31	15.19	3.12	14.22	12.26	1.97	0.64
12	12154	76	**71**	0.39	5.49	5.60	-0.11	2.03	1.73	0.30	6.23	4.58	1.65	30.62	25.84	4.78	24.39	21.26	3.13	0.97
36	12185	328	**72**	0.37	5.03	5.09	-0.06	1.63	1.55	0.08	4.56	3.20	1.36	19.69	16.10	3.59	15.12	12.90	2.22	0.77
12	16199	406	**73**	0.73	12.33	12.61	-0.28	5.05	5.25	-0.20	14.99	10.36	4.63	75.50	63.24	12.25	60.50	52.88	7.62	2.96
12	16184	389	**74**	0.46	10.75	10.79	-0.05	4.91	4.11	0.80	13.09	9.59	3.50	68.26	57.65	10.61	55.18	48.06	7.11	3.89
12	11299	58	**75**	0.46	5.72	5.94	-0.21	1.52	1.62	-0.10	4.88	3.93	0.95	21.21	18.28	2.93	16.33	14.35	1.98	0.78
12	14772	141	**76**	0.28	4.27	4.77	-0.50	1.42	1.88	-0.46	5.57	4.35	1.22	24.39	20.71	3.68	18.82	16.36	2.47	1.07
12	12173	75	**77**	0.03	0.68	0.77	-0.09		0.27		0.60	0.52	0.08	2.13	1.90	0.23	1.53	1.39	0.15	0.09
36	10005	19	**78**	0.34	4.81	4.95	-0.14	1.87	2.02	-0.16	5.11	3.95	1.17	22.26	18.03	4.23	17.15	14.09	3.06	0.85
36	18081	239	**79**	0.42	5.78	6.07	-0.29	1.84	2.01	-0.17	5.86	4.83	1.03	28.28	23.32	4.96	22.42	18.49	3.94	1.18
12	16552	414	**80**	0.34	6.50	6.51	-0.01	1.30	1.51	-0.20	4.70	3.83	0.86	20.01	17.23	2.78	15.32	13.40	1.92	0.90
12	17026	426	**81**	0.24	3.72	3.58	0.14	1.23	1.59	-0.35	7.73	5.62	2.11	32.86	27.93	4.93	25.13	22.31	2.82	1.54
60	13218	62	**82**	0.41	7.01	6.08	0.92	2.23	2.60	-0.37	9.87	6.55	3.33	38.72	30.43	8.29	28.84	23.88	4.96	1.54
60	16809	371	**83**	0.27	4.99	5.07	-0.09	1.48	1.79	-0.32	5.57	4.43	1.14	23.85	20.79	3.06	18.28	16.36	1.92	1.37
60	14683	37	**84**	0.43	8.23	8.58	-0.35	2.45	2.67	-0.22	9.34	6.71	2.63	44.71	38.20	6.51	35.38	31.49	3.88	1.88

12	10419	64	**85**	0.49	7.81	8.31	-0.50	2.56	2.93	-0.36	7.48	5.66	1.82	33.22	29.07	4.15	25.74	23.41	2.33	1.49
36	10792	106	**86**	0.46	7.74	8.11	-0.37	1.61	1.97	-0.37	7.13	5.45	1.68	32.83	27.97	4.86	25.70	22.52	3.18	1.74
12	13310	187	**87**	0.25	3.78	4.36	-0.58	1.10	1.35	-0.24	3.80	3.12	0.68	17.24	15.60	1.64	13.44	12.48	0.96	0.80
12	13775	375	**88**	0.45	6.66	7.24	-0.58	1.70	3.15	-1.45	6.95	5.37	1.57	30.50	27.49	3.01	23.55	22.11	1.44	1.12
36	12076	101	**89**	0.37	6.34	6.66	-0.32	1.46	1.61	-0.15	6.87	5.64	1.23	28.52	24.83	3.69	21.65	19.20	2.45	1.35
12	17935	355	**90**	0.54	8.37	8.34	0.04	2.07	2.13	-0.07	7.95	6.14	1.81	34.25	29.41	4.84	26.30	23.27	3.04	1.75
36	16809	371	**91**	0.42	5.72	6.64	-0.92	1.54	1.79	-0.25	5.24	4.25	1.00	22.93	21.16	1.77	17.69	16.92	0.77	1.00
60	15730	315	**92**	0.65	8.57	9.33	-0.77	2.06	2.57	-0.51	8.37	6.59	1.78	34.28	30.79	3.49	25.91	24.20	1.71	1.35
60	10942	284	**93**	0.39	6.51	7.83	-1.31	1.66	2.23	-0.57	4.60	3.55	1.06	18.34	17.08	1.26	13.74	13.53	0.21	0.76
36	12110	23	**94**	0.81	7.80	8.04	-0.24	1.69	2.35	-0.66	5.70	4.26	1.44	23.71	20.75	2.96	18.01	16.48	1.52	0.78
36	16552	414	**95**	0.43	6.30	6.81	-0.51	1.19	1.67	-0.48	5.26	4.09	1.16	21.30	18.27	3.03	16.04	14.18	1.86	0.88
36	11499	309	**96**	0.98	18.18	19.37	-1.19	5.84	6.27	-0.43	17.39	13.10	4.29	83.49	71.45	12.04	66.11	58.36	7.75	3.47
12	10640	323	**97**	0.22	3.48	3.99	-0.51	1.05	1.01	0.04	4.90	3.54	1.36	21.31	18.33	2.99	16.42	14.79	1.63	0.89
12	8061	188	**98**	0.38	7.99	8.65	-0.66	2.37	2.36	0.01	10.59	8.14	2.44	48.02	42.62	5.40	37.43	34.48	2.95	2.30
60	12110	23	**99**	0.30	4.49	4.50	-0.01	1.11	1.36	-0.25	5.22	3.97	1.25	22.29	19.92	2.36	17.07	15.95	1.12	0.88
12	12972	335	**100**	0.38	7.58	8.02	-0.44	2.07	2.08	-0.01	11.69	8.49	3.19	56.60	49.70	6.90	44.91	41.21	3.71	2.49
60	14772	141	**101**	0.14	5.37	6.57	-1.19	1.69	1.71	-0.02	6.76	5.73	1.03	31.00	29.92	1.08	24.24	24.19	0.06	1.42
12	12110	23	**102**	0.18	4.53	5.09	-0.57	1.35	1.37	-0.02	4.77	3.67	1.10	20.89	18.70	2.19	16.12	15.03	1.09	0.74

60	12864	195	**103**	0.25	4.96	5.36	-0.40	1.35	1.54	-0.20	8.66	6.59	2.07	39.17	35.16	4.01	30.51	28.57	1.94	2.08
12	14237	492	**104**	0.48	7.12	9.00	-1.88	1.81	3.01	-1.20	8.36	6.50	1.86	37.99	33.87	4.12	29.64	27.38	2.26	1.60
36	17975	33	**105**	0.28	4.19	4.94	-0.76	1.26	1.52	-0.26	6.23	4.78	1.44	25.50	23.06	2.44	19.28	18.28	1.00	1.10
60	12730	198	**106**	0.29	5.44	6.20	-0.76	1.42	1.72	-0.29	7.96	6.14	1.82	38.64	34.92	3.72	30.69	28.79	1.90	1.56
12	15061	34	**107**	0.20	2.59	2.67	-0.08	0.84	1.12	-0.29	5.52	4.47	1.05	25.66	21.56	4.11	20.15	17.09	3.06	0.73
36	12864	195	**108**	0.36	5.83	6.54	-0.71	1.62	1.67	-0.05	8.23	6.02	2.22	37.29	32.21	5.08	29.05	26.19	2.86	1.70
36	12497	20	**109**	0.26	4.48	5.31	-0.82	1.40	1.94	-0.55	3.90	2.69	1.20	16.63	14.41	2.22	12.74	11.72	1.02	0.62
12	14036	150	**110**	0.28	4.39	4.80	-0.41	1.24	1.20	0.05	4.18	3.36	0.82	19.65	18.01	1.64	15.47	14.65	0.82	0.61
60	10005	19	**111**	0.23	4.30	4.90	-0.60	1.42	1.37	0.06	5.41	3.42	1.99	22.29	18.87	3.43	16.88	15.44	1.44	0.88
36	14772	141	**112**	0.28	4.61	5.39	-0.78	1.28	1.42	-0.14	5.26	3.83	1.43	23.08	21.95	1.14	17.82	18.12		1.05
12	17405	78	**113**	0.06	5.22	5.99	-0.77	1.88	2.48	-0.60	11.67	8.01	3.66	34.62	35.72		22.95	27.70		0.00
12	7875	402	**114**	0.49	9.31	10.82	-1.51	2.62	2.77	-0.15	14.95	11.78	3.17	70.18	62.92	26.08	55.22	51.14	22.91	2.47
12	10005	19	**115**	0.16	3.44	3.78	-0.34	1.09	1.06	0.02	5.24	3.83	1.41	21.08	17.89	8.57	15.84	14.06	7.17	0.89
36	14237	492	**116**	0.24	4.75	5.31	-0.56	1.30	1.37	-0.07	9.06	6.10	2.96	36.37	29.43	6.93	27.31	23.33	3.98	1.40
12	11665	446	**117**	0.19	4.15	4.72	-0.57	1.17	1.28	-0.11	6.76	4.66	2.10	26.88	22.18	4.70	20.12	17.53	2.59	1.12
12	16592	245	**118**	0.10	2.38	2.68	-0.30	0.73	0.82	-0.09	5.13	3.75	1.38	21.10	18.16	2.94	15.97	14.41	1.56	0.78
12	12277	82	**119**	0.13	2.54	2.65	-0.11	0.76	0.86	-0.11	5.55	3.85	1.70	21.00	16.43	4.57	15.45	12.58	2.87	1.01
12	14422	301	**120**	0.18	2.94	5.43	-2.49	0.70	1.44	-0.74	5.08	4.77	0.32	20.66	22.56		15.57	17.79		0.76

12	12864	195	**121**	0.25	4.27	4.74	-0.47	0.92	0.96	-0.03	10.09	7.29	2.80	41.94	36.27	5.67	31.85	28.98	2.87	1.82
36	9747	21	**122**	0.43	7.54	9.22	-1.68	1.81	2.36	-0.55	14.69	10.74	3.96	61.48	53.27	8.21	46.79	42.54	4.25	2.72
36	16592	245	**123**	0.14	2.52	2.85	-0.34	0.65	0.65	0.00	5.35	3.73	1.62	21.46	17.99	3.47	16.11	14.26	1.85	0.76
60	14036	150	**124**	0.26	3.35	3.63	-0.29	1.23	1.89	-0.67	5.56	4.09	1.47	23.61	20.05	3.56	18.05	15.95	2.10	0.77
60	15812	180	**125**	0.36	7.51	8.22	-0.71	1.88	2.16	-0.28	15.00	10.97	4.03	66.10	57.38	8.72	51.10	46.41	4.69	2.59
60	17975	33	**126**	0.20	4.16	5.15	-0.99	1.01	1.12	-0.11	7.44	5.59	1.84	31.28	27.79	3.49	23.84	22.19	1.65	1.22
60	18081	239	**127**	0.17	3.34	3.80	-0.46	0.99	1.14	-0.15	5.88	4.85	1.03	26.20	23.60	2.60	20.32	18.75	1.57	1.03
12	10975	454	**128**	0.11	2.12	2.37	-0.25	0.46	0.47	-0.01	3.03	2.46	0.58	12.72	11.39	1.33	9.69	8.94	0.75	0.50
36	12972	335	**129**	0.37	4.85	4.90	-0.05	1.32	1.41	-0.09	9.36	6.81	2.54	45.91	36.71	9.19	36.55	29.90	6.65	2.02
12	11398	88	**130**	0.25	3.36	3.63	-0.26	1.25	1.37	-0.12	6.11	4.43	1.68	26.46	22.45	4.01	20.35	18.02	2.33	0.94
36	14683	37	**131**	0.35	5.51	5.31	0.20	2.45	2.33	0.12	10.90	7.09	3.81	48.72	37.59	11.13	37.82	30.50	7.32	2.00
36	16311	177	**132**	0.23	3.69	3.84	-0.16	1.03	1.10	-0.07	5.43	3.77	1.66	22.54	18.03	4.51	17.11	14.26	2.85	0.85
12	17975	33	**133**	0.27	4.19	2.07	2.13	1.66	0.79	0.87	8.25	3.02	5.23	38.45	15.16	23.29	30.20	12.14	18.06	1.65
12	10356	358	**134**	N/F	1.95	6.93	-4.99	0.73	2.49	-1.76	2.38	6.49		14.73	35.42		12.34	28.94		2.18
12	17652	408	**135**	0.25	4.19	4.48	-0.29	1.47	1.47	0.00	6.64	4.74	1.90	29.21	23.73	5.48	22.56	18.99	3.58	1.06
12	14739	74	**136**	0.21	3.69	3.78	-0.09	1.48	1.36	0.11	6.96	4.90	2.06	33.40	28.00	5.40	26.44	23.10	3.34	1.23
12	17795	336	**137**	0.20	4.32	4.50	-0.18	1.31	1.37	-0.05	9.95	7.01	2.94	42.66	34.57	8.09	32.71	27.56	5.15	1.52
12	12730	198	**138**	0.29	4.79	4.96	-0.17	1.41	1.27	0.14	9.95	6.87	3.08	46.34	37.39	8.96	36.39	30.51	5.88	1.74

36	11398	88	**139**	0.22	3.91	4.41	-0.50	1.34	1.21	0.13	6.95	5.00	1.96	27.60	23.66	3.94	20.65	18.66	1.98	1.03
96	10005	19	**140**	0.15	3.73	4.19	-0.46	1.06	1.29	-0.24	6.14	4.18	1.96	24.88	19.56	5.32	18.74	15.38	3.36	0.92
96	12497	20	**141**	0.15	2.95	3.30	-0.35	1.15	1.11	0.05	5.10	3.41	1.69	21.26	16.76	4.51	16.16	13.34	2.82	0.74
96	12110	23	**142**	0.39	5.01	5.21	-0.20	1.43	1.55	-0.12	7.32	5.09	2.23	30.58	24.73	5.85	23.27	19.64	3.63	1.00
96	15061	34	**143**	0.25	3.44	3.51	-0.07	0.90	1.24	-0.33	6.98	4.85	2.13	28.05	22.45	5.59	21.07	17.60	3.47	0.81

Table 7.25 Complete sterol profile table for NYPUM cohort of progressive PD patients.
143 CSF samples analysed, 80 patients in total. Results expressed an ng/mL.

Sample name	7α, 25-diHC + 7α, 25-diHCO	7α, 25-diHCO	7α, 26-diHC + 7α, 26-diHCO	7α, 26-diHCO	(25S)3β,7α-diHCA + (25S)7α-H-3-OCA	(25S)7α-H-3O-CA	3β, 7α-diHCA + 7α-H-3-OCA	7α-H-3O-CA	(25R)3β-7α-diHCA +(25R)7α-H-3O-CA	(25R)7α-H-3O-CA	7α, 25-diHC	7α, 26-diHC	(25S)3β,7α-diHCA	3β, 7α-diHCA	(24S)-HC	25-HC	26-HC	7β-HC	7α-HCA)	6β-HC	cholestenoic acid (3β-HCA)	7α-HCO	7-OC	7α-HC	Cholesterol

1	0.30	0.25	0.61	0.60	30.47	16.35	279.66	182.72	249.20	166.37	0.05	0.01	14.12	96.95	19.19	22.73	1.20	3.84	13.87	5.18	140.27	2.33	11.56	11.54	490651
2	0.30	0.23	0.70	0.46	15.91	8.85	178.86	92.27	162.94	83.42	0.07	0.24	7.06	86.58	17.25	19.52	0.87	1.77	19.32	6.19	114.26	2.99	8.49	16.33	473613
3	0.35	0.16	0.62	0.28	30.96	7.54	309.59	102.15	278.63	94.62	0.19	0.35	23.42	207.44	17.74	21.73	2.23	11.06	28.27	6.05	79.94	6.37	12.05	21.91	442143
4	0.26	0.23	0.79	0.58	13.56	9.26	185.51	125.43	171.95	116.17	0.04	0.20	4.30	60.08	15.19	19.49	1.02	1.55	50.77	4.75	69.62	8.58	2.27	42.19	345805
5	0.35	0.25	1.07	0.74	26.38	16.06	349.28	209.22	322.89	193.16	0.10	0.33	10.32	140.06	19.22	35.94	2.21	3.96	93.57	10.74	144.35	12.19	6.73	81.37	511609
6	0.41	0.25	1.23	0.70	43.16	15.69	450.75	204.15	407.59	188.46	0.16	0.53	27.47	246.60	20.60	42.96	2.22	2.67	84.47	10.91	192.00	10.08	8.66	74.39	508308
7	0.34	0.32	0.93	0.76	25.14	15.02	261.61	178.41	236.47	163.39	0.02	0.17	10.12	83.19	15.24	29.74	1.55	1.53	34.29	3.25	128.05	4.83	16.37	29.47	425120
8	0.32	0.23	1.31	1.07	51.07	27.15	279.92	214.96	228.86	187.81	0.09	0.24	23.92	64.96	14.83	32.84	1.72	4.36	53.73	2.35	185.69	9.58	3.14	44.15	632154
9	0.24	0.18	0.98	0.84	26.52	17.71	242.32	186.19	215.80	168.47	0.06	0.14	8.81	56.13	13.31	28.95	1.63	1.69	33.19	1.57	154.27	4.95	2.90	28.24	523145
10	0.22	0.18	0.76	0.63	25.72	14.24	220.73	196.18	195.01	181.95	0.04	0.12	11.48	24.54	10.48	26.66	1.41	1.30	14.61	1.11	131.75	2.39	3.21	12.23	186721
11	0.25	0.25	0.63	0.63	32.00	19.05	195.63	148.12	163.64	129.07	0.00	-0.01	12.95	47.52	11.01	26.01	1.30	1.28	6.72	2.34	122.97	1.11	4.19	5.61	314225
12	0.22	0.17	0.68	0.62	27.28	13.32	200.73	144.80	173.45	131.48	0.06	0.06	13.96	55.93	11.43	21.53	1.56	2.52	20.58	5.33	134.78	2.95	6.41	17.63	228405
13	0.08	0.05	0.32	0.21	10.41	4.42	83.69	60.23	73.27	55.81	0.03	0.11	5.99	23.45	4.94	11.03	0.66	0.71	4.72	3.83	66.75	1.09	3.18	3.63	310060
14	0.33	0.25	1.09	0.88	30.97	12.51	219.22	157.19	188.26	144.68	0.08	0.21	18.46	62.03	15.81	32.80	2.03	2.34	23.07	1.11	189.06	3.79	7.62	19.27	581428
15	0.12	0.13	0.38	0.40	13.99	7.40	79.25	53.21	65.26	45.82	-0.01	-0.02	6.59	26.04	7.41	16.21	0.72	0.74	4.28	0.52	91.29	0.93	2.41	3.35	307830
16	0.30	0.23	0.89	0.62	27.87	16.75	169.96	120.31	142.09	103.56	0.07	0.27	11.12	49.65	10.33	24.29	1.97	1.03	38.00	9.78	116.78	4.34	6.56	33.66	453196
17	0.32	0.24	0.63	0.47	28.57	14.43	153.15	108.54	124.59	94.11	0.08	0.16	14.14	44.62	10.10	19.03	1.79	9.32	11.78	4.01	102.04	1.83	6.96	9.95	303462

18	0.40	0.34	1.03	0.91	54.27	23.79	277.98	169.93	223.71	146.14	0.06	0.11	30.48	108.05	9.47	19.10	1.33	1.35	20.10	4.21	185.12	1.78	4.54	18.32	328326
19	0.42	0.29	1.16	0.84	34.91	15.26	256.62	154.33	221.71	139.07	0.13	0.32	19.65	102.28	8.69	19.33	1.11	1.09	20.89	3.41	178.44	3.00	2.30	17.89	309500
20	0.24	0.22	0.68	0.64	33.11	16.07	172.70	115.00	139.59	98.93	0.02	0.04	17.05	57.71	9.80	24.19	1.11	2.00	28.56	5.40	125.11	3.35	12.67	25.21	370409
21	0.26	0.24	0.73	0.65	25.54	16.41	161.18	118.83	135.64	102.42	0.02	0.07	9.13	42.35	10.90	27.76	1.09	1.30	15.33	6.98	170.53	1.65	2.42	13.68	390003
22	0.25	0.22	0.90	0.83	37.82	17.49	246.69	174.73	208.87	157.25	0.03	0.07	20.33	71.96	13.50	38.17	1.42	2.11	21.58	2.54	150.23	3.13	5.54	18.45	411345
23	0.24	0.17	0.95	0.71	40.66	17.94	230.28	148.02	189.62	130.09	0.07	0.24	22.73	82.26	15.42	37.36	1.52	0.97	26.45	2.13	154.02	3.96	6.59	22.50	449856
24	0.44	0.33	1.11	0.92	25.35	18.29	218.61	170.87	193.26	152.58	0.10	0.19	7.06	47.75	23.46	44.90	3.52	0.63	4.63	1.49	232.51	3.21	7.12	1.41	675130
25	0.36	0.25	1.08	0.81	22.76	14.73	177.14	142.85	154.38	128.12	0.11	0.27	8.03	34.29	22.98	38.76	3.03	0.64	6.79	2.51	159.38	5.43	6.51	1.37	691344
26	0.32	0.21	0.94	0.64	24.14	15.80	185.34	150.52	161.20	134.72	0.11	0.29	8.34	34.82	23.72	41.31	2.76	1.41	5.82	3.21	157.10	4.26	5.82	1.56	592391
27	0.33	0.20	1.05	0.69	42.04	26.30	284.43	224.40	242.39	198.11	0.13	0.37	15.75	60.03	15.40	35.19	1.73	0.83	6.92	1.12	140.74	4.16	3.82	2.76	452108
28	0.25	0.18	0.80	0.65	36.24	23.38	252.41	204.99	216.17	181.62	0.07	0.16	12.86	47.41	11.86	25.23	1.21	0.85	3.72	1.64	125.65	3.25	2.93	0.46	331904
29	0.25	0.17	0.86	0.63	34.48	19.01	241.50	184.42	207.02	165.41	0.08	0.24	15.47	57.08	14.30	29.67	1.17	0.82	3.27	1.33	122.15	2.68	2.94	0.60	411952
30	0.33	0.22	0.83	0.59	31.07	16.66	201.97	152.53	170.90	135.87	0.11	0.25	14.41	49.44	21.55	25.70	1.44	1.44	3.11	1.18	121.31	1.42	6.42	1.69	441654
31	0.19	0.00	0.75	0.43	22.99	12.94	163.05	108.58	140.06	95.65	0.19	0.32	10.06	54.47	12.86	23.43	0.95	0.85	4.40	1.27	121.39	3.71	3.70	0.69	390771
32	0.28	0.27	1.29	1.44	29.92	18.75	251.87	207.56	221.95	188.81	0.01	-0.15	11.17	44.31	12.03	26.13	1.18	2.36	85.28	31.09	91.36	10.95	10.96	74.33	366630
33	0.41	0.27	1.75	2.27	33.42	29.34	272.37	76.50	238.95	47.17	0.14	-0.52	4.08	195.87	27.10	49.49	2.22	1.06	216.11	4.20	117.69	30.17	13.36	185.94	966815
34	0.27	0.22	1.13	1.01	23.61	14.21	188.91	152.43	165.30	138.22	0.05	0.12	9.40	36.47	13.67	25.41	1.13	0.96	65.00	0.68	80.39	11.97	6.51	53.03	490018

35	0.31	0.21	0.94	0.69	46.31	25.77	287.27	204.22	240.96	178.44	0.10	0.25	20.54	83.05	13.77	31.99	1.61	1.56	41.96	5.91	173.13	6.65	11.26	35.31	489 340
36	0.21	0.13	0.62	0.43	26.03	14.27	182.19	113.99	156.16	99.73	0.07	0.20	11.76	68.19	10.34	26.09	1.06	0.49	7.20	1.45	147.55	1.06	4.90	6.14	349 317

Table 7.26 Complete sterol profile table for 36 plasma samples from ICICLE progressive PD patients.
Results expressed in ng/mL.

Chapter 8 Bibliography

2020 Alzheimer's disease facts and figures. (2020a). *Alzheimer's and Dementia*, *16*(3), 391–460. https://doi.org/10.1002/alz.12068

Abdel-Khalik, J., Crick, P. J., Yutuc, E., DeBarber, A. E., Duell, P. B., Steiner, R. D., Laina, I., Wang, Y., & Griffiths, W. J. (2018). Identification of 7α,24-dihydroxy-3-oxocholest-4-en-26-oic and 7α,25-dihydroxy-3-oxocholest-4-en-26-oic acids in human cerebrospinal fluid and plasma. *Biochimie*, *153*, 86–98. https://doi.org/10.1016/j.biochi.2018.06.020

Abdel-Khalik, J., Hearn, T., Dickson, A. L., Crick, P. J., Yutuc, E., Austin-Muttitt, K., Bigger, B. W., Morris, A. A., Shackleton, C. H., Clayton, P. T., Iida, T., Sircar, R., Rohatgi, R., Marschall, H.-U., Sjövall, J., Björkhem, I., Mullins, J. G. L., Griffiths, W. J., & Wang, Y. (2021). Bile acid biosynthesis in Smith-Lemli-Opitz syndrome bypassing cholesterol: Potential importance of pathway intermediates. *The Journal of Steroid Biochemistry and Molecular Biology*, *206*, 105794. https://doi.org/10.1016/j.jsbmb.2020.105794

Abdel-Khalik, J., Yutuc, E., Crick, P. J., Gustafsson, J.-Å., Warner, M., Roman, G., Talbot, K., Gray, E., Griffiths, W. J., Turner, M. R., & Wang, Y. (2017). Defective cholesterol metabolism in amyotrophic lateral sclerosis. *Journal of Lipid Research*, *58*(1), 267–278. https://doi.org/10.1194/jlr.P071639

Abildayeva, K., Jansen, P. J., Hirsch-Reinshagen, V., Bloks, V. W., Bakker, A. H. F., Ramaekers, F. C. S., De Vente, J., Groen, A. K., Wellington, C. L., Kuipers, F., & Mulder, M. (2006). 24(S)-

Hydroxycholesterol Participates in a Liver X Receptor-controlled Pathway in Astrocytes That Regulates Apolipoprotein E-mediated Cholesterol Efflux. *Journal of Biological Chemistry*, *281*(18), 12799–12808. https://doi.org/10.1074/JBC.M601019200

Abrams, M. E., Johnson, K. A., Perelman, S. S., Zhang, L., Endapally, S., Mar, K. B., Thompson, B. M., McDonald, J. G., Schoggins, J. W., Radhakrishnan, A., & Alto, N. M. (2020). Oxysterols provide innate immunity to bacterial infection by mobilizing cell surface accessible cholesterol. *Nature Microbiology*, *5*(7), 929–942. https://doi.org/10.1038/s41564-020-0701-5

Ačimovič, J., & Rozman, D. (2013). Steroidal Triterpenes of Cholesterol Synthesis. *Molecules*, *18*, 4002–4017. https://doi.org/10.3390/molecules18044002

Adibhatla, R. M., & Hatcher, J. F. (2007). Role of lipids in brain injury and diseases. *Future Lipidology*, *2*(4), 403–422. https://doi.org/10.2217/17460875.2.4.403

Agarwal, M., & Khan, S. (2020). Plasma Lipids as Biomarkers for Alzheimer's Disease: A Systematic Review. *Cureus*. https://doi.org/10.7759/cureus.12008

Agatonovic-Kustrin, S., Morton, D. W., Smirnov, V., Petukhov, A., Gegechkori, V., Kuzina, V., Gorpinchenko, N., & Ramenskaya, G. (2019). Analytical strategies in lipidomics for discovery of functional biomarkers from human saliva. In *Disease Markers*. https://doi.org/10.1155/2019/6741518

A-Gonzalez, N., Bensinger, S. J., Hong, C., Beceiro, S., Bradley, M. N., Zelcer, N., Deniz, J., Ramirez, C., Díaz, M., Gallardo, G., Ruiz de Galarreta, C., Salazar, J., Lopez, F., Edwards, P., Parks, J., Andujar, M., Tontonoz, P., & Castrillo, A. (2009). Apoptotic Cells

Promote Their Own Clearance and Immune Tolerance through Activation of the Nuclear Receptor LXR. *Immunity*, *31*(2), 245–258. https://doi.org/10.1016/j.immuni.2009.06.018

Al-Bachari, S., Naish, J. H., Parker, G. J. M., Emsley, H. C. A., & Parkes, L. M. (2020). Blood–Brain Barrier Leakage Is Increased in Parkinson's Disease. *Frontiers in Physiology*, *11*. https://doi.org/10.3389/fphys.2020.593026

Aldana, J., Romero-Otero, A., & Cala, M. P. (2020). Exploring the Lipidome: Current Lipid Extraction Techniques for Mass Spectrometry Analysis. *Metabolites*, *10*(6), 231. https://doi.org/10.3390/metabo10060231

Amran, M. B., Aminah, S., Rusli, H., & Buchari, B. (2020). Bentonite-based functional material as preconcentration system for determination of chromium species in water by flow injection analysis technique. *Heliyon*, *6*(5), e04051. https://doi.org/10.1016/j.heliyon.2020.e04051

Anand, V. S., & Braithwaite, S. P. (2009). LRRK2 in Parkinson's disease: biochemical functions. *FEBS Journal*, *276*(22), 6428–6435. https://doi.org/10.1111/j.1742-4658.2009.07341.x

Angot, E., Steiner, J. A., Hansen, C., Li, J.-Y., & Brundin, P. (2010). Are synucleinopathies prion-like disorders? *The Lancet Neurology*, *9*(11), 1128–1138. https://doi.org/10.1016/S1474-4422(10)70213-1

Apfel, R., Benbrook, D., Lernhardt, E., Ortiz, M. A., Salbert, G., & Pfahl, M. (1994). A novel orphan receptor specific for a subset of thyroid hormone-responsive elements and its interaction with the retinoid/thyroid hormone receptor subfamily. *Molecular and*

Cellular Biology, *14*(10), 7025–7035. https://doi.org/10.1128/mcb.14.10.7025-7035.1994

Aral, T., Aral, H., Ziyadanoğulları, B., & Ziyadanoğulları, R. (2015). Synthesis of a mixed-model stationary phase derived from glutamine for HPLC separation of structurally different biologically active compounds: HILIC and reversed-phase applications. *Talanta*, *131*, 64–73. https://doi.org/10.1016/j.talanta.2014.07.060

Arenas, E. (2022). Parkinson's disease in the single-cell era. In *Nature Neuroscience* (Vol. 25, Issue 5, pp. 536–538). Nature Research. https://doi.org/10.1038/s41593-022-01069-7

Arenas, F., Garcia-Ruiz, C., & Fernandez-Checa, J. C. (2017). Intracellular cholesterol trafficking and impact in neurodegeneration. In *Frontiers in Molecular Neuroscience*. https://doi.org/10.3389/fnmol.2017.00382

Arendt, T., Schindler, C., Brückner, M. K., Eschrich, K., Bigl, V., Zedlick, D., & Marcova, L. (1997). Plastic Neuroneal Remodeling Is Impaired in Patients with Alzheimer's Disease Carrying Apolipoprotein ε4 Allele. *The Journal of Neuroscience*, *17*(2), 516–529. https://doi.org/10.1523/JNEUROSCI.17-02-00516.1997

Arevalo, R., Ni, Z., & Danell, R. M. (2020). Mass spectrometry and planetary exploration: A brief review and future projection. *Journal of Mass Spectrometry*, *55*(1). https://doi.org/10.1002/jms.4454

Arman Qamar, & Deepak L. Bhatt. (2015). Effect of Low Cholesterol on Steroid Hormones and Vitami n E Levels. Just a Theory or Real Concern? *Circulation Research*, *117*, 662–664. https://doi.org/10.1056/NEJMoa040583

Auboeuf, D., Rieusset, J., Fajas, L., Vallier, P., Frering, V., Riou, J. P., Staels, B., Auwerx, J., Laville, M., & Vidal, H. (1997). Tissue Distribution and Quantification of the Expression of mRNAs of Peroxisome Proliferator–Activated Receptors and Liver X Receptor-α in Humans: No Alteration in Adipose Tissue of Obese and NIDDM Patients. *Diabetes*, *46*(8), 1319–1327. https://doi.org/10.2337/diab.46.8.1319

Axelson, M., Aly, A., & Sjövall, J. (1988). Levels of 7α-hydroxy-4-cholesten-3-one in plasma reflect rates of bile acid synthesis in man. *FEBS Letters*, *239*(2), 324–328. https://doi.org/10.1016/0014-5793(88)80944-X

Axelson, M., Björkhem, I., Reihnér, E., & Einarsson, K. (1991). The plasma level of 7α-hydroxy-4-cholesten-3-one reflects the activity of hepatic cholesterol 7α-hydroxylase in man. *FEBS Letters*, *284*(2), 216–218. https://doi.org/10.1016/0014-5793(91)80688-Y

Ayciriex, S., Djelti, F., Alves, S., Regazzetti, A., Gaudin, M., Varin, J., Langui, D., Bièche, I., Hudry, E., Dargère, D., Aubourg, P., Auzeil, N., Laprévote, O., & Cartier, N. (2017). Neuroneal cholesterol accumulation induced by Cyp46a1 down-regulation in mouse hippocampus disrupts brain lipid homeostasis. *Frontiers in Molecular Neuroscience*. https://doi.org/10.3389/fnmol.2017.00211

Bachman, D. L., Wolf, P. A., Linn, R. T., Knoefel, J. E., Cobb, J. L., Belanger, A. J., White, L. R., & D'Agostino, R. B. (1993). Incidence of dementia and probable Alzheimer's disease in a general population: The Framingham Study. *Neurology*, *43*(3, Part 1), 515–515. https://doi.org/10.1212/WNL.43.3_Part_1.515

Bae, E.-J., Kim, D.-K., Kim, C., Mante, M., Adame, A., Rockenstein, E., Ulusoy, A., Klinkenberg, M., Jeong, G. R., Bae, J. R., Lee, C., Lee, H.-J., Lee, B.-D., Di Monte, D. A., Masliah, E., & Lee, S.-J. (2018). LRRK2 kinase regulates α-synuclein propagation via RAB35 phosphorylation. *Nature Communications*, *9*(1), 3465. https://doi.org/10.1038/s41467-018-05958-z

BAE, S.-H., & PAIK, Y.-K. (1997). Cholesterol biosynthesis from lanosterol: development of a novel assay method and characterization of rat liver microsomal lanosterol Δ24-reductase. *Biochemical Journal*, *326*(2), 609–616. https://doi.org/10.1042/bj3260609

Baila-Rueda, L., Cenarro, A., Cofán, M., Orera, I., Barcelo-Batllori, S., Pocoví, M., Ros, E., Civeira, F., Nerín, C., & Domeño, C. (2013). Simultaneous determination of oxysterols, phytosterols and cholesterol precursors by high performance liquid chromatography tandem mass spectrometry in human serum. *Analytical Methods*, *5*(9), 2249. https://doi.org/10.1039/c3ay26395a

Bakeberg, M. C., Gorecki, A. M., Kenna, J. E., Jefferson, A., Byrnes, M., Ghosh, S., Horne, M. K., McGregor, S., Stell, R., Walters, S., Mastaglia, F. L., & Anderton, R. S. (2021). Elevated HDL Levels Linked to Poorer Cognitive Ability in Females With Parkinson's Disease. *Frontiers in Aging Neuroscience*, *13*. https://doi.org/10.3389/fnagi.2021.656623

Balazy, M. (2004). Eicosanomics: targeted lipidomics of eicosanoids in biological systems. *Prostaglandins & Other Lipid Mediators*, *73*(3), 173–180. https://doi.org/10.1016/j.prostaglandins.2004.03.003

Bales, K. R., Verina, T., Cummins, D. J., Du, Y., Dodel, R. C., Saura, J., Fishman, C. E., DeLong, C. A., Piccardo, P., Petegnief, V., Ghetti, B., & Paul, S. M. (1999). Apolipoprotein E is essential for amyloid deposition in the *APP* ^{V717F} transgenic mouse model of Alzheimer's disease. *Proceedings of the National Academy of Sciences*, *96*(26), 15233–15238. https://doi.org/10.1073/pnas.96.26.15233

Bauman, D. R., Bitmansour, A. D., McDonald, J. G., Thompson, B. M., Liang, G., & Russell, D. W. (2009). 25-Hydroxycholesterol secreted by macrophages in response to Toll-like receptor activation suppresses immunoglobulin A production. *Proceedings of the National Academy of Sciences*, *106*(39), 16764–16769. https://doi.org/10.1073/pnas.0909142106

BEAL, S. E. B. and M. F. (2006). Oxidative Damage in Huntington's Disease Pathogenesis. *ANTIOXIDANTS & REDOX SIGNALING*. https://doi.org/10.1089/ars.2006.8.2061

Bell, D. S., Shollenberger, D., & Cramer, H. (2017). Evaluation of retention and selectivity using biphenyl stationary phases. *LC-GC North America*, *35*(6).

Bendor, J. T., Logan, T. P., & Edwards, R. H. (2013). The Function of α-Synuclein. *Neurone*, *79*(6), 1044–1066. https://doi.org/10.1016/j.neurone.2013.09.004

Berg, D., Postuma, R. B., Adler, C. H., Bloem, B. R., Chan, P., Dubois, B., Gasser, T., Goetz, C. G., Halliday, G., Joseph, L., Lang, A. E., Liepelt-Scarfone, I., Litvan, I., Marek, K., Obeso, J., Oertel, W., Olanow, C. W., Poewe, W., Stern, M., & Deuschl, G. (2015). MDS research criteria for prodromal Parkinson's disease. *Movement Disorders*, *30*(12), 1600–1611. https://doi.org/10.1002/mds.26431

Berghoff, S. A., Spieth, L., Sun, T., Hosang, L., Depp, C., Sasmita, A. O., Vasileva, M. H., Scholz, P., Zhao, Y., Krueger-Burg, D., Wichert, S., Brown, E. R., Michail, K., Nave, K.-A., Bonn, S., Odoardi, F., Rossner, M., Ischebeck, T., Edgar, J. M., & Saher, G. (2021). Neuroneal cholesterol synthesis is essential for repair of chronically demyelinated lesions in mice. *Cell Reports*, *37*(4), 109889. https://doi.org/10.1016/j.celrep.2021.109889

Beyea, M. M., Heslop, C. L., Sawyez, C. G., Edwards, J. Y., Markle, J. G., Hegele, R. A., & Huff, M. W. (2007). Selective up-regulation of LXR-regulated genes ABCA1, ABCG1, and APOE in macrophages through increased endogenous synthesis of 24(S),25-epoxycholesterol. *Journal of Biological Chemistry*, *282*(8), 5207–5216. https://doi.org/10.1074/jbc.M611063200

Beyreuther, K., & Masters, C. L. (1991). Amyloid Precursor Protein (APP) and BZA4 Amyloid in the Etiology of Alzheimer's Disease: Precursor-Product Relationships in the Derangement of Neuroneal Function. *Brain Pathology*, *1*(4), 241–251. https://doi.org/10.1111/j.1750-3639.1991.tb00667.x

Bezine, M., Maatoug, S., Ben Khalifa, R., Debbabi, M., Zarrouk, A., Wang, Y., Griffiths, W. J., Nury, T., Samadi, M., Vejux, A., de Sèze, J., Moreau, T., Kharrat, R., El Ayeb, M., & Lizard, G. (2018). Modulation of Kv3.1b potassium channel level and intracellular potassium concentration in 158N murine oligodendrocytes and BV-2 murine microglial cells treated with 7-ketocholesterol, 24S-hydroxycholesterol or tetracosanoic acid (C24:0). *Biochimie*, *153*, 56–69. https://doi.org/10.1016/j.biochi.2018.02.008

Bielska, A. A., Olsen, B. N., Gale, S. E., Mydock-McGrane, L., Krishnan, K., Baker, N. A., Schlesinger, P. H., Covey, D. F., & Ory, D. S. (2014). Side-Chain Oxysterols Modulate Cholesterol Accessibility through Membrane Remodeling. *Biochemistry*, *53*(18), 3042–3051. https://doi.org/10.1021/bi5000096

Bjoandrkhem, I., Heverin, M., Leoni, V., Meaney, S., & Diczfalusy, U. (2006a). Oxysterols and Alzheimer's disease. In *Acta Neurologica Scandinavica* (Vol. 114, Issue SUPPL. 185, pp. 43–49). https://doi.org/10.1111/j.1600-0404.2006.00684.x

Bjoandrkhem, I., Heverin, M., Leoni, V., Meaney, S., & Diczfalusy, U. (2006b). Oxysterols and Alzheimer's disease. In *Acta Neurologica Scandinavica* (Vol. 114, Issue SUPPL. 185, pp. 43–49). https://doi.org/10.1111/j.1600-0404.2006.00684.x

Björkhem, I. (2006a). Crossing the barrier: Oxysterols as cholesterol transporters and metabolic modulators in the brain. In *Journal of Internal Medicine*. https://doi.org/10.1111/j.1365-2796.2006.01725.x

Björkhem, I. (2006b). Crossing the barrier: Oxysterols as cholesterol transporters and metabolic modulators in the brain. In *Journal of Internal Medicine* (Vol. 260, Issue 6, pp. 493–508). https://doi.org/10.1111/j.1365-2796.2006.01725.x

Björkhem, I. (2009). Are side-chain oxidized oxysterols regulators also in vivo? *Journal of Lipid Research*, *50 Suppl*, S213–S218. https://doi.org/10.1194/jlr.R800025-JLR200

Björkhem, I., Andersson, U., Ellis, E., Alvelius, G., Ellegård, L., Diczfalusy, U., Sjövall, J., & Einarsson, C. (2001). From Brain to Bile. *Journal of Biological Chemistry*, *276*(40), 37004–37010. https://doi.org/10.1074/jbc.M103828200

Bjorkhem, I., Heverin, M., Leoni, V., Meaney, S., & Diczfalusy, U. (2006). Oxysterols and Alzheimer's disease. *Acta Neurologica Scandinavica*, *114*(s185), 43–49. https://doi.org/10.1111/j.1600-0404.2006.00684.x

Björkhem, I., Lövgren-Sandblom, A., Leoni, V., Meaney, S., Brodin, L., Salveson, L., Winge, K., Pålhagen, S., & Svenningsson, P. (2013). Oxysterols and Parkinson's disease: Evidence that levels of 24S-hydroxycholesterol in cerebrospinal fluid correlates with the duration of the disease. *Neuroscience Letters*, *555*, 102–105. https://doi.org/10.1016/j.neulet.2013.09.003

Björkhem, I., Patra, K., Boxer, A. L., & Svenningsson, P. (2018). 24S-hydroxycholesterol correlates with tau and is increased in cerebrospinal fluid in Parkinson's disease and corticobasal syndrome. *Frontiers in Neurology*, *9*(SEP). https://doi.org/10.3389/fneur.2018.00756

Blanc, M., Hsieh, W. Y., Robertson, K. A., Kropp, K. A., Forster, T., Shui, G., Lacaze, P., Watterson, S., Griffiths, S. J., Spann, N. J., Meljon, A., Talbot, S., Krishnan, K., Covey, D. F., Wenk, M. R., Craigon, M., Ruzsics, Z., Haas, J., Angulo, A., … Ghazal, P. (2013). The Transcription Factor STAT-1 Couples Macrophage Synthesis of 25-Hydroxycholesterol to the Interferon Antiviral Response. *Immunity*, *38*(1), 106–118. https://doi.org/10.1016/J.IMMUNI.2012.11.004

Blesa, J., Trigo-Damas, I., Quiroga-Varela, A., & Jackson-Lewis, V. R. (2015). Oxidative stress and Parkinson's disease. *Frontiers in Neuroanatomy*, *9*(July), 91. https://doi.org/10.3389/fnana.2015.00091

Bligh, E. G., & Dyer, W. J. (1959). A RAPID METHOD OF TOTAL LIPID EXTRACTION AND PURIFICATION. *Canadian Journal of Biochemistry and Physiology*, *37*(8), 911–917. https://doi.org/10.1139/o59-099

Bloch, K. (1965). *The Biological Synthesis of Cholesterol* (Vol. 06). https://www.science.org

Bodovitz, S., & Klein, W. L. (1996). Cholesterol Modulates α-Secretase Cleavage of Amyloid Precursor Protein. *Journal of Biological Chemistry*, *271*, 4436–4440.

Boer, D. E. C., van Smeden, J., Bouwstra, J. A., & Aerts, J. M. F. G. (2020). Glucocerebrosidase: Functions in and Beyond the Lysosome. *Journal of Clinical Medicine*, *9*(3), 736. https://doi.org/10.3390/jcm9030736

Böhme, D. K. (2016). Ion-molecule reactions in mass spectrometry. In *Encyclopedia of Spectroscopy and Spectrometry* (pp. 338–346). Elsevier. https://doi.org/10.1016/B978-0-12-409547-2.10996-5

Bolam, J. P., & Pissadaki, E. K. (2012). Living on the edge with too many mouths to feed: Why dopamine neuroneneuronees die. *Movement Disorders*, *27*(12), 1478–1483. https://doi.org/10.1002/mds.25135

Bonifati, V., Rizzu, P., van Baren, M. J., Schaap, O., Breedveld, G. J., Krieger, E., Dekker, M. C. J., Squitieri, F., Ibanez, P., Joosse, M., van Dongen, J. W., Vanacore, N., van Swieten, J. C., Brice, A., Meco, G., van Duijn, C. M., Oostra, B. A., & Heutink, P. (2003). Mutations in the *DJ-1* Gene Associated with Autosomal Recessive Early-Onset Parkinsonism. *Science*, *299*(5604), 256–259. https://doi.org/10.1126/science.1077209

Borah, K., Rickman, O. J., Voutsina, N., Ampong, I., Gao, D., Baple, E. L., Dias, I. HK., Crosby, A. H., & Griffiths, H. R. (2020). A quantitative LC-MS/MS method for analysis of mitochondrial - specific oxysterol metabolism. *Redox Biology*, *36*, 101595. https://doi.org/10.1016/j.redox.2020.101595

Bosco, D. A., Fowler, D. M., Zhang, Q., Nieva, J., Powers, E. T., Wentworth, P., Lerner, R. A., & Kelly, J. W. (2006). Elevated levels of oxidized cholesterol metabolites in Lewy body disease brains accelerate α-synuclein fibrilization. *Nature Chemical Biology*, *2*(5), 249–253. https://doi.org/10.1038/nchembio782

Bose, A., & Beal, M. F. (2016). Mitochondrial dysfunction in Parkinson's disease. *Journal of Neurochemistry*, *139*, 216–231. https://doi.org/10.1111/jnc.13731

Bravo-San Pedro, J. M., Niso-Santano, M., Gómez-Sánchez, R., Pizarro-Estrella, E., Aiastui-Pujana, A., Gorostidi, A., Climent, V., López de Maturana, R., Sanchez-Pernaute, R., López de Munain, A., Fuentes, J. M., & González-Polo, R. A. (2013). The LRRK2 G2019S mutant exacerbates basal autophagy through activation of the MEK/ERK pathway. *Cellular and Molecular Life Sciences*, *70*(1), 121–136. https://doi.org/10.1007/s00018-012-1061-y

Brothers, H. M., Gosztyla, M. L., & Robinson, S. R. (2018). The Physiological Roles of Amyloid-β Peptide Hint at New Ways to Treat Alzheimer's Disease. *Frontiers in Aging Neuroscience*, *10*. https://doi.org/10.3389/fnagi.2018.00118

Broughton, R., & Beaudoin, F. (2021). *Analysis of Free and Esterified Sterol Content and Composition in Seeds Using GC and ESI-*

MS/MS (pp. 179–201). https://doi.org/10.1007/978-1-0716-1362-7_11

Brown, A. J., Sharpe, L. J., & Rogers, M. J. (2021). Oxysterols: From physiological tuners to pharmacological opportunities. *British Journal of Pharmacology*, *178*(16), 3089–3103. https://doi.org/10.1111/bph.15073

Brown, J., Theisler, C., Silberman, S., Magnuson, D., Gottardi-Littell, N., Lee, J. M., Yager, D., Crowley, J., Sambamurti, K., Rahman, M. M., Reiss, A. B., Eckman, C. B., & Wolozin, B. (2004). Differential expression of cholesterol hydroxylases in Alzheimer's disease. *The Journal of Biological Chemistry*, *279*(33), 34674–34681. https://doi.org/10.1074/jbc.M402324200

Brown, M. S., & Goldstein, J. L. (1986). A Receptor-Mediated Pathway for Cholesterol Homeostasis. *Science*, *232*(4746), 34–47. https://doi.org/10.1126/science.3513311

Brown, M. S., & Goldstein, J. L. (1997). The SREBP Pathway: Regulation Review of Cholesterol Metabolism by Proteolysis of a Membrane-Bound Transcription Factor. In *Cell* (Vol. 89).

Brown, M. S., Radhakrishnan, A., & Goldstein, J. L. (2018). Retrospective on Cholesterol Homeostasis: The Central Role of Scap. *Annual Review of Biochemistry*, *87*(1), 783–807. https://doi.org/10.1146/annurev-biochem-062917-011852

Browne, S. E., Ferrante, R. J., & Beal, M. F. (2006). Oxidative Stress in Huntington's Disease. *Brain Pathology*. https://doi.org/10.1111/j.1750-3639.1999.tb00216.x

Brügger, B. (2014). Lipidomics: Analysis of the Lipid Composition of Cells and Subcellular Organelles by Electrospray Ionization

Mass Spectrometry. *Annual Review of Biochemistry*. https://doi.org/10.1146/annurev-biochem-060713-035324

Brügger, B., Erben, G., Sandhoff, R., Wieland, F. T., & Lehmann, W. D. (1997). Quantitative analysis of biological membrane lipids at the low picomole level by nano-electrospray ionization tandem mass spectrometry. *Proceedings of the National Academy of Sciences*, *94*(6), 2339–2344. https://doi.org/10.1073/pnas.94.6.2339

Brundin, P., Melki, R., & Kopito, R. (2010). Prion-like transmission of protein aggregates in neurodegenerative diseases. *Nature Reviews Molecular Cell Biology*, *11*(4), 301–307. https://doi.org/10.1038/nrm2873

Brunner, A. M., Lössl, P., Liu, F., Huguet, R., Mullen, C., Yamashita, M., Zabrouskov, V., Makarov, A., Altelaar, A. F. M., & Heck, A. J. R. (2015). Benchmarking Multiple Fragmentation Methods on an Orbitrap Fusion for Top-down Phospho-Proteoform Characterization. *Analytical Chemistry*, *87*(8), 4152–4158. https://doi.org/10.1021/acs.analchem.5b00162

Brzeska, M., Szymczyk, K., & Szterk, A. (2016). Current Knowledge about Oxysterols: A Review. *Journal of Food Science*, *81*(10), R2299–R2308. https://doi.org/10.1111/1750-3841.13423

Burbulla, L. F., Song, P., Mazzulli, J. R., Zampese, E., Wong, Y. C., Jeon, S., Santos, D. P., Blanz, J., Obermaier, C. D., Strojny, C., Savas, J. N., Kiskinis, E., Zhuang, X., Krüger, R., Surmeier, D. J., & Krainc, D. (2017). Dopamine oxidation mediates mitochondrial and lysosomal dysfunction in Parkinson's disease. *Science*. https://doi.org/10.1126/science.aam9080

Burkard, I., Rentsch, K. M., & von Eckardstein, A. (2004). Determination of 24S- and 27-hydroxycholesterol in plasma by high-performance liquid chromatography-mass spectrometry. *Journal of Lipid Research*, *45*(4), 776–781. https://doi.org/10.1194/jlr.D300036-JLR200

Burré, J. (2015). The Synaptic Function of α-Synuclein. *Journal of Parkinson's Disease*, *5*(4), 699–713. https://doi.org/10.3233/JPD-150642

Calvo-Garrido, J., Winn, D., Maffezzini, C., Wedell, A., Freyer, C., Falk, A., & Wredenberg, A. (2021). Protocol for the derivation, culturing, and differentiation of human iPS-cell-derived neuroepithelial stem cells to study neural differentiation in vitro. *STAR Protocols*, *2*(2). https://doi.org/10.1016/j.xpro.2021.100528

Cappiello, A., Termopoli, V., Palma, P., Famiglini, G., Saeed, M., Perry, S., & Navarro, P. (2022). Liquid Chromatography–Electron Capture Negative Ionization–Tandem Mass Spectrometry Detection of Pesticides in a Commercial Formulation. *Journal of the American Society for Mass Spectrometry*, *33*(1), 141–148. https://doi.org/10.1021/jasms.1c00307

Carballo, G. B., Honorato, J. R., De Lopes, G. P. F., & Spohr, T. C. L. D. S. E. (2018). A highlight on Sonic hedgehog pathway. In *Cell Communication and Signaling* (Vol. 16, Issue 1). BioMed Central Ltd. https://doi.org/10.1186/s12964-018-0220-7

Cardenia, V., Rodriguez-Estrada, M. T., Baldacci, E., Savioli, S., & Lercker, G. (2012). Analysis of cholesterol oxidation products by Fast gas chromatography/mass spectrometry. *Journal of*

Separation Science, *35*(3), 424–430. https://doi.org/10.1002/jssc.201100660

Careri, M., Ferretti, D., Manini, P., & Musci, M. (1998). Evaluation of particle beam high-performance liquid chromatography–mass spectrometry for analysis of cholesterol oxides. *Journal of Chromatography A*, *794*(1–2), 253–262. https://doi.org/10.1016/S0021-9673(97)00764-4

Carsana, E. V., Audano, M., Breviario, S., Pedretti, S., Aureli, M., Lunghi, G., & Mitro, N. (2022). Metabolic Profile Variations along the Differentiation of Human-Induced Pluripotent Stem Cells to Dopaminergic NeuroneNeuronees. *Biomedicines*, *10*(9). https://doi.org/10.3390/biomedicines10092069

Cartagena, C. M., Burns, M. P., & Rebeck, G. W. (2010). 24S-hydroxycholesterol effects on lipid metabolism genes are modeled in traumatic brain injury. *Brain Research*, *1319*, 1–12. https://doi.org/10.1016/j.brainres.2009.12.080

Cerqueira, N. M. F. S. A., Oliveira, E. F., Gesto, D. S., Santos-Martins, D., Moreira, C., Moorthy, H. N., Ramos, M. J., & Fernandes, P. A. (2016). Cholesterol Biosynthesis: A Mechanistic Overview. *Biochemistry*, *55*(39), 5483–5506. https://doi.org/10.1021/acs.biochem.6b00342

Cha, S.-H., Choi, Y. R., Heo, C.-H., Kang, S.-J., Joe, E.-H., Jou, I., Kim, H.-M., & Park, S. M. (2015a). Loss of parkin promotes lipid rafts-dependent endocytosis through accumulating caveolin-1: implications for Parkinson's disease. *Molecular Neurodegeneration*, *10*(1), 63. https://doi.org/10.1186/s13024-015-0060-5

Cha, S.-H., Choi, Y. R., Heo, C.-H., Kang, S.-J., Joe, E.-H., Jou, I., Kim, H.-M., & Park, S. M. (2015b). Loss of parkin promotes lipid rafts-dependent endocytosis through accumulating caveolin-1: implications for Parkinson's disease. *Molecular Neurodegeneration*, *10*(1), 63. https://doi.org/10.1186/s13024-015-0060-5

Chambers, C. M., & Ness, G. C. (1997). Translational Regulation of Hepatic HMG-CoA Reductase by Dietary Cholesterol. *Biochemical and Biophysical Research Communications*, *232*(2), 278–281. https://doi.org/10.1006/bbrc.1997.6288

Chambers, C. M., & Ness, G. C. (1998). Dietary Cholesterol Regulates Hepatic 3-Hydroxy-3-methylglutaryl Coenzyme A Reductase Gene Expression in Rats Primarily at the Level of Translation. *Archives of Biochemistry and Biophysics*, *354*(2), 317–322. https://doi.org/10.1006/abbi.1998.0689

Chang, T. Y., Yamauchi, Y., Hasan, M. T., & Chang, C. (2017). Cellular cholesterol homeostasis and Alzheimer's disease. *Journal of Lipid Research*. https://doi.org/10.1194/jlr.R075630

Chaudhuri, K. R., & Schapira, A. H. (2009). Non-motor symptoms of Parkinson's disease: dopaminergic pathophysiology and treatment. *The Lancet Neurology*, *8*(5), 464–474. https://doi.org/10.1016/S1474-4422(09)70068-7

Chelliah, S. S., Bhuvanendran, S., Magalingam, K. B., Kamarudin, M. N. A., & Radhakrishnan, A. K. (2022). Identification of blood-based biomarkers for diagnosis and prognosis of Parkinson's disease: A systematic review of proteomics studies. In *Ageing Research Reviews* (Vol. 73). Elsevier Ireland Ltd. https://doi.org/10.1016/j.arr.2021.101514

Chen, G., Xu, T., Yan, Y., Zhou, Y., Jiang, Y., Melcher, K., & Xu, H. E. (2017). Amyloid beta: structure, biology and structure-based therapeutic development. *Acta Pharmacologica Sinica*, *38*(9), 1205–1235. https://doi.org/10.1038/aps.2017.28

Chen, Y.-Z., Kao, S.-Y., Jian, H.-C., Yu, Y.-M., Li, J.-Y., Wang, W.-H., & Tsai, C.-W. (2015a). Determination of cholesterol and four phytosterols in foods without derivatization by gas chromatography-tandem mass spectrometry. *Journal of Food and Drug Analysis*, *23*(4), 636–644. https://doi.org/10.1016/j.jfda.2015.01.010

Chen, Y.-Z., Kao, S.-Y., Jian, H.-C., Yu, Y.-M., Li, J.-Y., Wang, W.-H., & Tsai, C.-W. (2015b). Determination of cholesterol and four phytosterols in foods without derivatization by gas chromatography-tandem mass spectrometry. *Journal of Food and Drug Analysis*, *23*(4), 636–644. https://doi.org/10.1016/j.jfda.2015.01.010

Cheng, D., Chang, C. C. Y., Qu, X., & Chang, T.-Y. (1995). Activation of Acyl-Coenzyme A:Cholesterol Acyltransferase by Cholesterol or by Oxysterol in a Cell-free System. *Journal of Biological Chemistry*, *270*(2), 685–695. https://doi.org/10.1074/jbc.270.2.685

Chiang, J. Y. L. (1998). Regulation of bile acid synthesis. *Frontiers in Bioscience*, *3*(4), A273. https://doi.org/10.2741/A273

Chu, Y., Dodiya, H., Aebischer, P., Olanow, C. W., & Kordower, J. H. (2009). Alterations in lysosomal and proteasomal markers in Parkinson's disease: Relationship to alpha-synuclein inclusions. *Neurobiology of Disease*, *35*(3), 385–398. https://doi.org/10.1016/j.nbd.2009.05.023

Chu, Y., & Kordower, J. H. (2007). Age-associated increases of α-synuclein in monkeys and humans are associated with nigrostriatal dopamine depletion: Is this the target for Parkinson's disease? *Neurobiology of Disease*, *25*(1), 134–149. https://doi.org/10.1016/j.nbd.2006.08.021

Church, D. A. (1969). Storage-Ring Ion Trap Derived from the Linear Quadrupole Radio-Frequency Mass Filter. *Journal of Applied Physics*, *40*(8), 3127–3134. https://doi.org/10.1063/1.1658153

Cilia, R., Tunesi, S., Marotta, G., Cereda, E., Siri, C., Tesei, S., Zecchinelli, A. L., Canesi, M., Mariani, C. B., Meucci, N., Sacilotto, G., Zini, M., Barichella, M., Magnani, C., Duga, S., Asselta, R., Soldà, G., Seresini, A., Seia, M., … Goldwurm, S. (2016). Survival and dementia in <scp> *GBA* </scp> -associated Parkinson's disease: <scp>T</scp> he mutation matters. *Annals of Neurology*, *80*(5), 662–673. https://doi.org/10.1002/ana.24777

Clark, P. J., Thompson, A. J., Vock, D. M., Kratz, L. E., Tolun, A. A., Muir, A. J., McHutchison, J. G., Subramanian, M., Millington, D. M., Kelley, R. I., & Patel, K. (2012). Hepatitis C virus selectively perturbs the distal cholesterol synthesis pathway in a genotype-specific manner. *Hepatology*, *56*(1), 49–56. https://doi.org/10.1002/hep.25631

Clough, R. L., Dermentzaki, G., & Stefanis, L. (2009). Functional dissection of the α-synuclein promoter: transcriptional regulation by ZSCAN21 and ZNF219. *Journal of Neurochemistry*, *110*(5), 1479–1490. https://doi.org/10.1111/j.1471-4159.2009.06250.x

Cochrane, C. R., Szczepny, A., Watkins, D. N., & Cain, J. E. (2015). Hedgehog signaling in the maintenance of cancer stem cells. In

Cancers (Vol. 7, Issue 3, pp. 1554–1585). https://doi.org/10.3390/cancers7030851

Cossec, J.-C., Simon, A., Marquer, C., Moldrich, R. X., Leterrier, C., Rossier, J., Duyckaerts, C., Lenkei, Z., & Potier, M.-C. (2010). Clathrin-dependent APP endocytosis and Aß secretion are highly sensitive to the level of plasma membrane cholesterol. *Biochimica et Biophysica Acta (BBA) - Molecular and Cell Biology of Lipids*, *1801*(8), 846–852. https://doi.org/10.1016/j.bbalip.2010.05.010

Courtney, R., & Landreth, G. E. (2016). LXR Regulation of Brain Cholesterol: From Development to Disease. *Trends in Endocrinology and Metabolism*, *27*(6), 404–414. https://doi.org/10.1016/j.tem.2016.03.018

Crick, P. J., Yutuc, E., Abdel-Khalik, J., Saeed, A., Betsholtz, C., Genove, G., Björkhem, I., Wang, Y., & Griffiths, W. J. (2019). Formation and metabolism of oxysterols and cholestenoic acids found in the mouse circulation: Lessons learnt from deuterium-enrichment experiments and the CYP46A1 transgenic mouse. *The Journal of Steroid Biochemistry and Molecular Biology*, *195*, 105475. https://doi.org/10.1016/J.JSBMB.2019.105475

CYP46A1 expression . (n.d.). Https://Www.Proteinatlas.Org/ENSG00000036530-CYP46A1/Tissue.

CYP46A1 Human Protein Atlas . (2023, June 21). https://www.proteinatlas.org/ENSG00000036530-CYP46A1/single+cell+type

D. R. Kanpp. (1980). Handbook of analytical derivatization reactions. *Journal of Chromatography*, *194*(104). https://doi.org/10.1016/s0021-9673(00)81058-4

Dabrowski, R., Ripa, R., Latza, C., Annibal, A., & Antebi, A. (2020). Optimization of mass spectrometry settings for steroidomic analysis in young and old killifish. *Analytical and Bioanalytical Chemistry*, *412*(17), 4089–4099. https://doi.org/10.1007/s00216-020-02640-6

Dai, L., Zou, L., Meng, L., Qiang, G., Yan, M., & Zhang, Z. (2021). Cholesterol Metabolism in Neurodegenerative Diseases: Molecular Mechanisms and Therapeutic Targets. *Molecular Neurobiology*, *58*(5), 2183–2201. https://doi.org/10.1007/s12035-020-02232-6

Daneman, R., & Prat, A. (2015). The Blood–Brain Barrier. *Cold Spring Harbor Perspectives in Biology*, *7*(1), a020412. https://doi.org/10.1101/cshperspect.a020412

Dang, E. V., Madhani, H. D., & Vance, R. E. (2020). Cholesterol in quarantine. *Nature Immunology*, *21*(7), 716–717. https://doi.org/10.1038/s41590-020-0712-7

Das, A., Brown, M. S., Anderson, D. D., Goldstein, J. L., & Radhakrishnan, A. (2014). Three pools of plasma membrane cholesterol and their relation to cholesterol homeostasis. *ELife*, *3*. https://doi.org/10.7554/eLife.02882

Daugvilaite, V., Arfelt, K. N., Benned-Jensen, T., Sailer, A. W., & Rosenkilde, M. M. (2014). Oxysterol-EBI2 signaling in immune regulation and viral infection. *European Journal of Immunology*, *44*(7), 1904–1912. https://doi.org/10.1002/eji.201444493

David W. Koppenaal, Charles J. Barinaga, M. Bonner Denton, Roger P. Sperline, Gary M. Hieftje, Gregory D. Schilling, Francisco J. Andrade, & James H. Barnes, I. (2005). MS Detecors. *Analytical Chemistry*, 419A-427A. https://doi.org/https://doi.org/10.1021/ac053495p

Dawkins, E., & Small, D. H. (2014). Insights into the physiological function of the ß-amyloid precursor protein: beyond Alzheimer's disease. *Journal of Neurochemistry*, *129*(5), 756–769. https://doi.org/10.1111/jnc.12675

de Boussac, H., Pommier, A. J., Dufour, J., Trousson, A., Caira, F., Volle, D. H., Baron, S., & Lobaccaro, J.-M. A. (2013). LXR, prostate cancer and cholesterol: the Good, the Bad and the Ugly. *American Journal of Cancer Research*, *3*(1), 58–69. http://www.ncbi.nlm.nih.gov/pmc/articles/PMC3555197/%*(v/v)*5Cnhttp://www.ncbi.nlm.nih.gov/pmc/articles/PMC3555197/pdf/ajcr0003-0058.pdf

de Chaves, E. I. P., Rusiñol, A. E., Vance, D. E., Campenot, R. B., & Vance, J. E. (1997a). Role of Lipoproteins in the Delivery of Lipids to Axons during Axonal Regeneration. *Journal of Biological Chemistry*, *272*(49), 30766–30773. https://doi.org/10.1074/jbc.272.49.30766

de Chaves, E. I. P., Rusiñol, A. E., Vance, D. E., Campenot, R. B., & Vance, J. E. (1997b). Role of Lipoproteins in the Delivery of Lipids to Axons during Axonal Regeneration. *Journal of Biological Chemistry*, *272*(49), 30766–30773. https://doi.org/10.1074/jbc.272.49.30766

de Medina, P., Silvente-Poirot, S., & Poirot, M. (2022). Oxysterols are potential physiological regulators of ageing. In *Ageing Research*

Reviews (Vol. 77). Elsevier Ireland Ltd. https://doi.org/10.1016/j.arr.2022.101615

DeBarber, A. E., Lütjohann, D., Merkens, L., & Steiner, R. D. (2008a). Liquid chromatography–tandem mass spectrometry determination of plasma 24S-hydroxycholesterol with chromatographic separation of 25-hydroxycholesterol. *Analytical Biochemistry*, *381*(1), 151–153. https://doi.org/10.1016/j.ab.2008.05.037

DeBarber, A. E., Lütjohann, D., Merkens, L., & Steiner, R. D. (2008b). Liquid chromatography–tandem mass spectrometry determination of plasma 24S-hydroxycholesterol with chromatographic separation of 25-hydroxycholesterol. *Analytical Biochemistry*, *381*(1), 151–153. https://doi.org/10.1016/j.ab.2008.05.037

DeBarber, A. E., Sandlers, Y., Pappu, A. S., Merkens, L. S., Duell, P. B., Lear, S. R., Erickson, S. K., & Steiner, R. D. (2011). Profiling sterols in cerebrotendinous xanthomatosis: Utility of Girard derivatization and high resolution exact mass LC–ESI-MSn analysis. *Journal of Chromatography B*, *879*(17–18), 1384–1392. https://doi.org/10.1016/j.jchromb.2010.11.019

DeGrella, R. F., & Simoni, R. D. (1982). Intracellular transport of cholesterol to the plasma membrane. *Journal of Biological Chemistry*, *257*(23), 14256–14262. https://doi.org/10.1016/S0021-9258(19)45374-X

Dehay, B., Martinez-Vicente, M., Ramirez, A., Perier, C., Klein, C., Vila, M., & Bezard, E. (2012). Lysosomal dysfunction in Parkinson disease. *Autophagy*, *8*(9), 1389–1391. https://doi.org/10.4161/auto.21011

DeMattos, R. B., Cirrito, J. R., Parsadanian, M., May, P. C., O'Dell, M. A., Taylor, J. W., Harmony, J. A. K., Aronow, B. J., Bales, K. R., Paul, S. M., & Holtzman, D. M. (2004). ApoE and Clusterin Cooperatively Suppress Aβ Levels and Deposition. *Neurone*, *41*(2), 193–202. https://doi.org/10.1016/S0896-6273(03)00850-X

Dennis, E. A., Deems, R. A., Harkewicz, R., Quehenberger, O., Brown, H. A., Milne, S. B., Myers, D. S., Glass, C. K., Hardiman, G., Reichart, D., Merrill, A. H., Sullards, M. C., Wang, E., Murphy, R. C., Raetz, C. R. H., Garrett, T. A., Guan, Z., Ryan, A. C., Russell, D. W., … Subramaniam, S. (2010). A Mouse Macrophage Lipidome. *Journal of Biological Chemistry*, *285*(51), 39976–39985. https://doi.org/10.1074/jbc.M110.182915

Devi, L., Raghavendran, V., Prabhu, B. M., Avadhani, N. G., & Anandatheerthavarada, H. K. (2008). Mitochondrial Import and Accumulation of α-Synuclein Impair Complex I in Human Dopaminergic Neuroneal Cultures and Parkinson Disease Brain. *Journal of Biological Chemistry*, *283*(14), 9089–9100. https://doi.org/10.1074/jbc.M710012200

Di Nottia, M., Masciullo, M., Verrigni, D., Petrillo, S., Modoni, A., Rizzo, V., Di Giuda, D., Rizza, T., Niceta, M., Torraco, A., Bianchi, M., Santoro, M., Bentivoglio, A. R., Bertini, E., Piemonte, F., Carrozzo, R., & Silvestri, G. (2017). DJ-1 modulates mitochondrial response to oxidative stress: clues from a novel diagnosis of PARK7. *Clinical Genetics*, *92*(1), 18–25. https://doi.org/10.1111/cge.12841

Dias, I. H., Borah, K., Amin, B., Griffiths, H. R., Sassi, K., Lizard, G., Iriondo, A., & Martinez-Lage, P. (2019). Localisation of oxysterols at the sub-cellular level and in biological fluids. In *Journal of*

Steroid Biochemistry and Molecular Biology. https://doi.org/10.1016/j.jsbmb.2019.105426

Dias, I. H. K., Wilson, S. R., & Roberg-Larsen, H. (2018). Chromatography of oxysterols. In *Biochimie* (Vol. 153, pp. 3–12). Elsevier B.V. https://doi.org/10.1016/j.biochi.2018.05.004

Dias, V., Junn, E., & Mouradian, M. M. (2013). The Role of Oxidative Stress in Parkinson's Disease. *Journal of Parkinson's Disease*, *3*(4), 461–491. https://doi.org/10.3233/JPD-130230

Dickson, D. W., Braak, H., Duda, J. E., Duyckaerts, C., Gasser, T., Halliday, G. M., Hardy, J., Leverenz, J. B., Del Tredici, K., Wszolek, Z. K., & Litvan, I. (2009). Neuropathological assessment of Parkinson's disease: refining the diagnostic criteria. *The Lancet Neurology*, *8*(12), 1150–1157. https://doi.org/10.1016/S1474-4422(09)70238-8

Diczfalusy, U., Olofsson, K. E., Carlsson, A.-M., Gong, M., Golenbock, D. T., Rooyackers, O., Fläring, U., & Björkbacka, H. (2009). Marked upregulation of cholesterol 25-hydroxylase expression by lipopolysaccharide. *Journal of Lipid Research*, *50*(11), 2258–2264. https://doi.org/10.1194/jlr.M900107-JLR200

Dietschy, J. M., & Turley, S. D. (2004a). *Thematic review series: Brain Lipids.* Cholesterol metabolism in the central nervous system during early development and in the mature animal. *Journal of Lipid Research*, *45*(8), 1375–1397. https://doi.org/10.1194/jlr.R400004-JLR200

Dietschy, J. M., & Turley, S. D. (2004b). Thematic review series: Brain Lipids. Cholesterol metabolism in the central nervous system during early development and in the mature animal.

Journal of Lipid Research, *45*(8), 1375–1397. https://doi.org/10.1194/jlr.R400004-JLR200

Doria, M., Maugest, L., Moreau, T., Lizard, G., & Vejux, A. (2016). Contribution of cholesterol and oxysterols to the pathophysiology of Parkinson's disease. *Free Radical Biology and Medicine*, *101*, 393–400. https://doi.org/10.1016/j.freeradbiomed.2016.10.008

Doxakis, E. (2010). Post-transcriptional Regulation of α-Synuclein Expression by mir-7 and mir-153. *Journal of Biological Chemistry*, *285*(17), 12726–12734. https://doi.org/10.1074/jbc.M109.086827

Drees, J., & Paul, W. (1964). Beschleunigung von Elektronen in einem Plasmabetatron. *Zeitschrift F*[illegible]*r Physik*, *180*(4), 340–361. https://doi.org/10.1007/BF01380519

Du, X., Pham, Y. H., & Brown, A. J. (2004). Effects of 25-Hydroxycholesterol on Cholesterol Esterification and Sterol Regulatory Element-binding Protein Processing Are Dissociable. *Journal of Biological Chemistry*, *279*(45), 47010–47016. https://doi.org/10.1074/jbc.M408690200

Duan, Y., Gong, K., Xu, S., Zhang, F., Meng, X., & Han, J. (2022). *Regulation of cholesterol homeostasis in health and diseases: from mechanisms to targeted therapeutics*. https://doi.org/10.1038/s41392-022-01125-5

Dubois, F., Knochenmuss, R., Zenobi, R., Brunelle, A., Deprun, C., & Le Beyec, Y. (1999). A comparison between ion-to-photon and microchannel plate detectors. *Rapid Communications in Mass Spectrometry*, *13*(9), 786–791. https://doi.org/10.1002/(SICI)1097-0231(19990515)13:9<786::AID-RCM566>3.0.CO;2-3

Duc, D., Vigne, S., & Pot, C. (2019). Oxysterols in Autoimmunity. *International Journal of Molecular Sciences*, *20*(18), 4522. https://doi.org/10.3390/ijms20184522

Duffy, D., & Rader, D. J. (2009). Update on strategies to increase HDL quantity and function. *Nature Reviews Cardiology*, *6*(7), 455–463. https://doi.org/10.1038/nrcardio.2009.94

Dusell, C. D., Umetani, M., Shaul, P. W., Mangelsdorf, D. J., & Mcdonnell, D. P. (2008). *27-Hydroxycholesterol Is an Endogenous Selective Estrogen Receptor Modulator*. https://doi.org/10.1210/me.2007-0383

Duval, C., Touche, V., Tailleux, A., Fruchart, J. C., Fievet, C., Clavey, V., Staels, B., & Lestavel, S. (2006). Niemann-Pick C1 like 1 gene expression is down-regulated by LXR activators in the intestine. *Biochemical and Biophysical Research Communications*, *340*(4), 1259–1263. https://doi.org/10.1016/j.bbrc.2005.12.137

Dzeletovic, S., Breuer, O., Lund, E., & Diczfalusy, U. (1995). Determination of Cholesterol Oxidation Products in Human Plasma by Isotope Dilution-Mass Spectrometry. *Analytical Biochemistry*, *225*(1), 73–80. https://doi.org/10.1006/abio.1995.1110

Eberlé, D., Hegarty, B., Bossard, P., Ferré, P., & Foufelle, F. (2004). SREBP transcription factors: Master regulators of lipid homeostasis. In *Biochimie* (Vol. 86, Issue 11, pp. 839–848). Elsevier B.V. https://doi.org/10.1016/j.biochi.2004.09.018

Edwards, P. A., Kennedy, M. A., & Mak, P. A. (2002). LXRs; *Vascular Pharmacology*, *38*(4), 249–256. https://doi.org/10.1016/S1537-1891(02)00175-1

Ekstrand, M. I., Terzioglu, M., Galter, D., Zhu, S., Hofstetter, C., Lindqvist, E., Thams, S., Bergstrand, A., Hansson, F. S., Trifunovic, A., Hoffer, B., Cullheim, S., Mohammed, A. H., Olson, L., & Larsson, N.-G. (2007). Progressive parkinsonism in mice with respiratory-chain-deficient dopamine neuroneneuronees. *Proceedings of the National Academy of Sciences*, *104*(4), 1325–1330. https://doi.org/10.1073/pnas.0605208103

Emamzadeh, F. N., Aojula, H., McHugh, P. C., & Allsop, D. (2016a). Effects of different isoforms of apoE on aggregation of the α-synuclein protein implicated in Parkinson's disease. *Neuroscience Letters*, *618*, 146–151. https://doi.org/10.1016/j.neulet.2016.02.042

Emamzadeh, F. N., Aojula, H., McHugh, P. C., & Allsop, D. (2016b). Effects of different isoforms of apoE on aggregation of the α-synuclein protein implicated in Parkinson's disease. *Neuroscience Letters*, *618*, 146–151. https://doi.org/10.1016/j.neulet.2016.02.042

Emmanouilidou, E., Stefanis, L., & Vekrellis, K. (2010). Cell-produced α-synuclein oligomers are targeted to, and impair, the 26S proteasome. *Neurobiology of Aging*, *31*(6), 953–968. https://doi.org/10.1016/j.neurobiolaging.2008.07.008

Eschbach, J., von Einem, B., Müller, K., Bayer, H., Scheffold, A., Morrison, B. E., Rudolph, K. L., Thal, D. R., Witting, A., Weydt, P., Otto, M., Fauler, M., Liss, B., McLean, P. J., Spada, A. R. La, Ludolph, A. C., Weishaupt, J. H., & Danzer, K. M. (2015). Mutual exacerbation of peroxisome proliferator-activated receptor γ coactivator 1α deregulation and α-synuclein oligomerization.

Annals of Neurology, *77*(1), 15–32. https://doi.org/10.1002/ana.24294

Espenshade, P. J. (2013). Cholesterol Synthesis and Regulation. In *Encyclopedia of Biological Chemistry* (pp. 516–520). Elsevier. https://doi.org/10.1016/B978-0-12-378630-2.00070-0

Evans, D. A., Bennett, D. A., Wilson, R. S., Bienias, J. L., Morris, M. C., Scherr, P. A., Hebert, L. E., Aggarwal, N., Beckett, L. A., Joglekar, R., Berry-Kravis, E., & Schneider, J. (2003). Incidence of Alzheimer Disease in a Biracial Urban Community. *Archives of Neurology*, *60*(2), 185. https://doi.org/10.1001/archneur.60.2.185

Fahy, E., Subramaniam, S., Brown, H. A., Glass, C. K., Merrill, A. H., Murphy, R. C., Raetz, C. R. H., Russell, D. W., Seyama, Y., Shaw, W., Shimizu, T., Spener, F., van Meer, G., VanNieuwenhze, M. S., White, S. H., Witztum, J. L., & Dennis, E. A. (2005). A comprehensive classification system for lipids. *Journal of Lipid Research*, *46*(5), 839–861. https://doi.org/10.1194/jlr.E400004-JLR200

Fais, M., Dore, A., Galioto, M., Galleri, G., Crosio, C., & Iaccarino, C. (2021). Parkinson's disease-related genes and lipid alteration. In *International Journal of Molecular Sciences* (Vol. 22, Issue 14). MDPI. https://doi.org/10.3390/ijms22147630

Falk, A., Koch, P., Kesavan, J., Takashima, Y., Ladewig, J., Alexander, M., Wiskow, O., Tailor, J., Trotter, M., Pollard, S., Smith, A., & Brüstle, O. (2012). Capture of neuroepithelial-like stem cells from pluripotent stem cells provides a versatile system for in vitro production of human neuroneneuronees. *PLoS ONE*, *7*(1). https://doi.org/10.1371/journal.pone.0029597

Famiglini, G., Palma, P., Termopoli, V., & Cappiello, A. (2021). The history of electron ionization in LC-MS, from the early days to modern technologies: A review. *Analytica Chimica Acta*, *1167*, 338350. https://doi.org/10.1016/j.aca.2021.338350

Fantini, J., Carlus, D., & Yahi, N. (2011). The fusogenic tilted peptide (67–78) of α-synuclein is a cholesterol binding domain. *Biochimica et Biophysica Acta (BBA) - Biomembranes*, *1808*(10), 2343–2351. https://doi.org/10.1016/j.bbamem.2011.06.017

Fassbender, K., Simons, M., Bergmann, C., Stroick, M., Lütjohann, D., Keller, P., Runz, H., Kühl, S., Bertsch, T., von Bergmann, K., Hennerici, M., Beyreuther, K., & Hartmann, T. (2001). Simvastatin strongly reduces levels of Alzheimer's disease ß-amyloid peptides Aß42 and Aß40 *in vitro* and *in vivo*. *Proceedings of the National Academy of Sciences*, *98*(10), 5856–5861. https://doi.org/10.1073/pnas.081620098

Faust, J. R., Luskey, K. L., Chin, D. J., Goldstein, J. L., & Brown, M. S. (1982). Regulation of synthesis and degradation of 3-hydroxy-3-methylglutaryl-coenzyme A reductase by low density lipoprotein and 25-hydroxycholesterol in UT-1 cells. *Proceedings of the National Academy of Sciences*, *79*(17), 5205–5209. https://doi.org/10.1073/pnas.79.17.5205

Feingold, K. R. (2000). *Introduction to Lipids and Lipoproteins*.

Feringa, F. M., & van der Kant, R. (2021). Cholesterol and Alzheimer's Disease; From Risk Genes to Pathological Effects. In *Frontiers in Aging Neuroscience* (Vol. 13). Frontiers Media S.A. https://doi.org/10.3389/fnagi.2021.690372

Fernandes, H. J. R., Hartfield, E. M., Christian, H. C., Emmanoulidou, E., Zheng, Y., Booth, H., Bogetofte, H., Lang, C.,

Ryan, B. J., Sardi, S. P., Badger, J., Vowles, J., Evetts, S., Tofaris, G. K., Vekrellis, K., Talbot, K., Hu, M. T., James, W., Cowley, S. A., & Wade-Martins, R. (2016). ER Stress and Autophagic Perturbations Lead to Elevated Extracellular α-Synuclein in GBA-N370S Parkinson's iPSC-Derived Dopamine NeuroneNeuronees. *Stem Cell Reports*, *6*(3), 342–356. https://doi.org/10.1016/j.stemcr.2016.01.013

Fernandez de la Mora, J. (2000). Electrospray ionization of large multiply charged species proceeds via Dole's charged residue mechanism. *Analytica Chimica Acta*, *406*(1), 93–104. https://doi.org/10.1016/S0003-2670(99)00601-7

Ferrari, A., He, C., Kennelly, J. P., Sandhu, J., Xiao, X., Chi, X., Jiang, H., Young, S. G., & Tontonoz, P. (2020). Aster Proteins Regulate the Accessible Cholesterol Pool in the Plasma Membrane. *Molecular and Cellular Biology*, *40*(19). https://doi.org/10.1128/MCB.00255-20

Ferris, H. A., Perry, R. J., Moreira, G. V., Shulman, G. I., Horton, J. D., & Kahn, C. R. (2017a). Loss of astrocyte cholesterol synthesis disrupts neuroneal function and alters whole-body metabolism. *Proceedings of the National Academy of Sciences*, *114*(5), 1189–1194. https://doi.org/10.1073/pnas.1620506114

Ferris, H. A., Perry, R. J., Moreira, G. V., Shulman, G. I., Horton, J. D., & Kahn, C. R. (2017b). Loss of astrocyte cholesterol synthesis disrupts neuroneal function and alters whole-body metabolism. *Proceedings of the National Academy of Sciences of the United States of America*, *114*(5), 1189–1194. https://doi.org/10.1073/pnas.1620506114

Fester, L., Zhou, L., Bütow, A., Huber, C., von Lossow, R., Prange-Kiel, J., Jarry, H., & Rune, G. M. (2009). Cholesterol-promoted synaptogenesis requires the conversion of cholesterol to estradiol in the hippocampus. *Hippocampus*, *19*(8), 692–705. https://doi.org/10.1002/hipo.20548

Fjeldsted, J. C., & Lee, M. L. (1984). Capillary supercritical fluid chromatography. *Analytical Chemistry*, *56*(4), 619–628. https://doi.org/10.1021/ac00268a004

Folch, J., Lees, M., & Sloane, G. H. (1956). *A SIMPLE METHOD FOR THE ISOLATION AND PURIFICATION OF TOTAL LIPIDES FROM ANIMAL TISSUES**.

Forman, B. M., Ruan, B., Chen, J., Schroepfer, G. J., & Evans, R. M. (1997). The orphan nuclear receptor LXRa is positively and negatively regulated by distinct products of mevalonate metabolism. *Biochemistry*, *94*(20), 10588–10593. https://doi.org/10.1073/pnas.94.20.10588

Fox, B. G., Shanklin, J., Ai, J., Loehr, T. M., & Sanders-Loehr, J. (1994). Resonance Raman Evidence for an Fe-O-Fe Center in Stearoyl-ACP Desaturase. Primary Sequence Identity with Other Diiron-Oxo Proteins. *Biochemistry*, *33*(43), 12776–12786. https://doi.org/10.1021/bi00209a008

FREDRICKSON, D. S., & ONO, K. (1956). The in vitro production of 25- and 26-hydroxycholesterol and their in vivo metabolism. *Biochimica et Biophysica Acta*, *22*(1), 183–184. https://doi.org/10.1016/0006-3002(56)90236-0

Fu, X., Wang, Y., He, X., Li, H., Liu, H., & Zhang, X. (2020). A systematic review and meta-analysis of serum cholesterol and triglyceride levels in patients with Parkinson's disease. In *Lipids*

in Health and Disease (Vol. 19, Issue 1). BioMed Central Ltd. https://doi.org/10.1186/s12944-020-01284-w

Gallego, S. F., Højlund, K., & Ejsing, C. S. (2018). Easy, Fast, and Reproducible Quantification of Cholesterol and Other Lipids in Human Plasma by Combined High Resolution MSX and FTMS Analysis. *Journal of the American Society for Mass Spectrometry*, *29*(1), 34–41. https://doi.org/10.1007/s13361-017-1829-2

Gamba, P., Giannelli, S., Staurenghi, E., Testa, G., Sottero, B., Biasi, F., Poli, G., & Leonarduzzi, G. (2021). The Controversial Role of 24-S-Hydroxycholesterol in Alzheimer's Disease. *Antioxidants*, *10*(5), 740. https://doi.org/10.3390/antiox10050740

Gamba, P., Staurenghi, E., Testa, G., Giannelli, S., Sottero, B., & Leonarduzzi, G. (2019). A crosstalk between brain cholesterol oxidation and glucose metabolism in Alzheimer's disease. *Frontiers in Neuroscience*, *13*(MAY). https://doi.org/10.3389/fnins.2019.00556

Gamba, P., Testa, G., Gargiulo, S., Staurenghi, E., Poli, G., & Leonarduzzi, G. (2015). Oxidized cholesterol as the driving force behind the development of Alzheimer's disease. In *Frontiers in Aging Neuroscience*. https://doi.org/10.3389/fnagi.2015.00119

García-Sanz, P., M.F.G. Aerts, J., & Moratalla, R. (2021). The Role of Cholesterol in α-Synuclein and Lewy Body Pathology in GBA1 Parkinson's Disease. In *Movement Disorders* (Vol. 36, Issue 5, pp. 1070–1085). John Wiley and Sons Inc. https://doi.org/10.1002/mds.28396

García-Sanz, P., Orgaz, L., Bueno-Gil, G., Espadas, I., Rodríguez-Traver, E., Kulisevsky, J., Gutierrez, A., Dávila, J. C., González-

Polo, R. A., Fuentes, J. M., Mir, P., Vicario, C., & Moratalla, R. (2017). N370S -*GBA1* mutation causes lysosomal cholesterol accumulation in Parkinson's disease. *Movement Disorders*, *32*(10), 1409–1422. https://doi.org/10.1002/mds.27119

Genaro-Mattos, T. C., Anderson, A., Allen, L. B., Korade, Z., & Mirnics, K. (2019). Cholesterol Biosynthesis and Uptake in Developing NeuroneNeuronees. *ACS Chemical Neuroscience*, *10*(8), 3671–3681. https://doi.org/10.1021/acschemneuro.9b00248

Geoffrey Ingram Taylor. (1964). Disintegration of water drops in an electric field. *Proceedings of the Royal Society of London. Series A. Mathematical and Physical Sciences*, *280*(1382), 383–397. https://doi.org/10.1098/rspa.1964.0151

Giau, V. Van, Pyun, J.-M., Bagyinszky, E., An, S. S. A., & Kim, S. (2018). A pathogenic PSEN2 p.His169Asn mutation associated with early-onset Alzheimer’s disease. *Clinical Interventions in Aging*, *Volume 13*, 1321–1329. https://doi.org/10.2147/CIA.S170374

Giau, V. Van, Senanarong, V., Bagyinszky, E., Limwongse, C., An, S. S. A., & Kim, S. (2018). Identification of a novel mutation in APP gene in a Thai subject with early-onset Alzheimer's disease. *Neuropsychiatric Disease and Treatment*, *Volume 14*, 3015–3023. https://doi.org/10.2147/NDT.S180174

Girard, A. , and S. G. (1934). *Girard reagents*.

Girard, A., & Sandulesco, G. (1936). Sur une nouvelle série de réactifs du groupe carbonyle, leur utilisation à l'extraction des substances cétoniques et à la caractérisation microchimique des aldéhydes

et cétones. *Helvetica Chimica Acta*, *19*(1), 1095–1107. https://doi.org/10.1002/hlca.193601901148

Glenner, G. G., & Wong, C. W. (1984). Alzheimer's disease: Initial report of the purification and characterization of a novel cerebrovascular amyloid protein. *Biochemical and Biophysical Research Communications*, *120*(3), 885–890. https://doi.org/10.1016/S0006-291X(84)80190-4

Gliozzi, M., Musolino, V., Bosco, F., Scicchitano, M., Scarano, F., Nucera, S., Zito, M. C., Ruga, S., Carresi, C., Macrì, R., Guarnieri, L., Maiuolo, J., Tavernese, A., Coppoletta, A. R., Nicita, C., Mollace, R., Palma, E., Muscoli, C., Belzung, C., & Mollace, V. (2021). Cholesterol homeostasis: Researching a dialogue between the brain and peripheral tissues. In *Pharmacological Research* (Vol. 163). Academic Press. https://doi.org/10.1016/j.phrs.2020.105215

Goate, A., Chartier-Harlin, M.-C., Mullan, M., Brown, J., Crawford, F., Fidani, L., Giuffra, L., Haynes, A., Irving, N., James, L., Mant, R., Newton, P., Rooke, K., Roques, P., Talbot, C., Pericak-Vance, M., Roses, A., Williamson, R., Rossor, M., … Hardy, J. (1991). Segregation of a missense mutation in the amyloid precursor protein gene with familial Alzheimer's disease. *Nature*, *349*(6311), 704–706. https://doi.org/10.1038/349704a0

Goldstein, J. L., DeBose-Boyd, R. A., & Brown, M. S. (2006). Protein Sensors for Membrane Sterols. *Cell*, *124*(1), 35–46. https://doi.org/10.1016/j.cell.2005.12.022

Gong, J.-S., Kobayashi, M., Hayashi, H., Zou, K., Sawamura, N., Fujita, S. C., Yanagisawa, K., & Michikawa, M. (2002). Apolipoprotein E (ApoE) Isoform-dependent Lipid Release from

Astrocytes Prepared from Human ApoE3 and ApoE4 Knock-in Mice. *Journal of Biological Chemistry*, *277*(33), 29919–29926. https://doi.org/10.1074/jbc.M203934200

Gopalan, A. B., van Uden, L., Sprenger, R. R., Fernandez-Novel Marx, N., Bogetofte, H., Neveu, P., Meyer, M., Noh, K.-M., Diz-Muñoz, A., & Ejsing, C. S. (n.d.). *Lipotype acquisition during neural development in vivo is not recapitulated in stem cell-derived neuroneneuronees*. https://doi.org/10.1101/2022.08.31.505694

Goritz, C., Mauch, D. H., & Pfrieger, F. W. (2005a). Multiple mechanisms mediate cholesterol-induced synaptogenesis in a CNS neurone. *Molecular and Cellular Neuroscience*, *29*(2), 190–201. https://doi.org/10.1016/j.mcn.2005.02.006

Goritz, C., Mauch, D. H., & Pfrieger, F. W. (2005b). Multiple mechanisms mediate cholesterol-induced synaptogenesis in a CNS neurone. *Molecular and Cellular Neuroscience*, *29*(2), 190–201. https://doi.org/10.1016/j.mcn.2005.02.006

Götz, J., Streffer, J. R., David, D., Schild, A., Hoerndli, F., Pennanen, L., Kurosinski, P., & Chen, F. (2004). Transgenic animal models of Alzheimer's disease and related disorders: histopathology, behavior and therapy. *Molecular Psychiatry*, *9*(7), 664–683. https://doi.org/10.1038/sj.mp.4001508

Goyal, S., Xiao, Y., Porter, N. A., Xu, L., & Guengerich, F. P. (2014). Oxidation of 7-dehydrocholesterol and desmosterol by human cytochrome P450 46A1. *Journal of Lipid Research*, *55*(9), 1933–1943. https://doi.org/10.1194/jlr.M051508

Griffiths, J. (2008). A brief history of mass spectrometry. In *Analytical Chemistry* (Vol. 80, Issue 15, pp. 5678–5683). https://doi.org/10.1021/ac8013065

Griffiths, W. J., Abdel-Khalik, J., Crick, P. J., Yutuc, E., & Wang, Y. (2016). New methods for analysis of oxysterols and related compounds by LC–MS. *The Journal of Steroid Biochemistry and Molecular Biology*, *162*, 4–26. https://doi.org/10.1016/j.jsbmb.2015.11.017

Griffiths, W. J., Abdel-Khalik, J., Moore, S. F., Wijeyekoon, R. S., Crick, P. J., Yutuc, E., Farrell, K., Breen, D. P., Williams-Gray, C. H., Theofilopoulos, S., Arenas, E., Trupp, M., Barker, R. A., & Wang, Y. (2021a). The Cerebrospinal Fluid Profile of Cholesterol Metabolites in Parkinson's Disease and Their Association With Disease State and Clinical Features. *Frontiers in Aging Neuroscience*, *13*. https://doi.org/10.3389/fnagi.2021.685594

Griffiths, W. J., Abdel-Khalik, J., Moore, S. F., Wijeyekoon, R. S., Crick, P. J., Yutuc, E., Farrell, K., Breen, D. P., Williams-Gray, C. H., Theofilopoulos, S., Arenas, E., Trupp, M., Barker, R. A., & Wang, Y. (2021b). The Cerebrospinal Fluid Profile of Cholesterol Metabolites in Parkinson's Disease and Their Association With Disease State and Clinical Features. *Frontiers in Aging Neuroscience*, *13*. https://doi.org/10.3389/fnagi.2021.685594

Griffiths, W. J., Abdel-Khalik, J., Moore, S. F., Wijeyekoon, R. S., Crick, P. J., Yutuc, E., Farrell, K., Breen, D. P., Williams-Gray, C. H., Theofilopoulos, S., Arenas, E., Trupp, M., Barker, R. A., & Wang, Y. (2021c). The Cerebrospinal Fluid Profile of Cholesterol Metabolites in Parkinson's Disease and Their Association With

Disease State and Clinical Features. *Frontiers in Aging Neuroscience*, *13*. https://doi.org/10.3389/fnagi.2021.685594

Griffiths, W. J., Abdel-Khalik, J., Yutuc, E., Roman, G., Warner, M., Gustafsson, J.-Å., & Wang, Y. (2019). Concentrations of bile acid precursors in cerebrospinal fluid of Alzheimer's disease patients. *Free Radical Biology and Medicine*, *134*, 42–52. https://doi.org/10.1016/j.freeradbiomed.2018.12.020

Griffiths, W. J., Crick, P. J., & Wang, Y. (2013). Methods for oxysterol analysis: Past, present and future. *Biochemical Pharmacology*, *86*(1), 3–14. https://doi.org/10.1016/j.bcp.2013.01.027

Griffiths, W. J., Crick, P. J., Wang, Y., Ogundare, M., Tuschl, K., Morris, A. A., Bigger, B. W., Clayton, P. T., & Wang, Y. (2013). Analytical strategies for characterization of oxysterol lipidomes: Liver X receptor ligands in plasma. In *Free Radical Biology and Medicine* (Vol. 59, pp. 69–84). Elsevier Inc. https://doi.org/10.1016/j.freeradbiomed.2012.07.027

Griffiths, W. J., Gilmore, I., Yutuc, E., Abdel-Khalik, J., Crick, P. J., Hearn, T., Dickson, A., Bigger, B. W., Wu, T. H.-Y., Goenka, A., Ghosh, A., Jones, S. A., & Wang, Y. (2018). Identification of unusual oxysterols and bile acids with 7-oxo or 3β,5α,6β-trihydroxy functions in human plasma by charge-tagging mass spectrometry with multistage fragmentation. *Journal of Lipid Research*, *59*(6), 1058–1070. https://doi.org/10.1194/jlr.D083246

Griffiths, W. J., & Wang, Y. (2018). An update on oxysterol biochemistry: New discoveries in lipidomics. *Biochemical and Biophysical Research Communications*, *504*(3), 617–622. https://doi.org/10.1016/j.bbrc.2018.02.019

Griffiths, W. J., & Wang, Y. (2019a). Sterolomics in biology, biochemistry, medicine. In *TrAC - Trends in Analytical Chemistry* (Vol. 120). Elsevier B.V. https://doi.org/10.1016/j.trac.2018.10.016

Griffiths, W. J., & Wang, Y. (2019b). Sterolomics in biology, biochemistry, medicine. In *TrAC - Trends in Analytical Chemistry* (Vol. 120). Elsevier B.V. https://doi.org/10.1016/j.trac.2018.10.016

Griffiths, W. J., & Wang, Y. (2020). Oxysterols as lipid mediators: Their biosynthetic genes, enzymes and metabolites. *Prostaglandins & Other Lipid Mediators*, *147*, 106381. https://doi.org/10.1016/j.prostaglandins.2019.106381

Griffiths, W. J., & Wang, Y. (2021). Sterols, Oxysterols, and Accessible Cholesterol: Signalling for Homeostasis, in Immunity and During Development. In *Frontiers in Physiology* (Vol. 12). Frontiers Media S.A. https://doi.org/10.3389/fphys.2021.723224

Griffiths, W. J., & Wang, Y. (2022). Cholesterol metabolism: from lipidomics to immunology. In *Journal of Lipid Research* (Vol. 63, Issue 2). American Society for Biochemistry and Molecular Biology Inc. https://doi.org/10.1016/J.JLR.2021.100165

Griffiths, W. J., Wang, Y., Alvelius, G., Liu, S., Bodin, K., & Sjövall, J. (2006). Analysis of oxysterols by electrospray tandem mass spectrometry. *Journal of the American Society for Mass Spectrometry*, *17*(3), 341–362. https://doi.org/10.1016/j.jasms.2005.10.012

Griffiths, W. J., Yutuc, E., Abdel-Khalik, J., Crick, P. J., Hearn, T., Dickson, A., Bigger, B. W., Hoi-Yee Wu, T., Goenka, A., Ghosh, A., Jones, S. A., Covey, D. F., Ory, D. S., & Wang, Y. (2019).

Metabolism of Non-Enzymatically Derived Oxysterols: Clues from sterol metabolic disorders. *Free Radical Biology and Medicine*, *144*, 124–133. https://doi.org/10.1016/J.FREERADBIOMED.2019.04.020

Grigonis, D., Venskutonis, P. R., Sivik, B., Sandahl, M., & Eskilsson, C. S. (2005). Comparison of different extraction techniques for isolation of antioxidants from sweet grass (Hierochloë odorata). *The Journal of Supercritical Fluids*, *33*(3), 223–233. https://doi.org/10.1016/j.supflu.2004.08.006

Grimm, M. O. W., Grimm, H. S., Pätzold, A. J., Zinser, E. G., Halonen, R., Duering, M., Tschäpe, J.-A., Strooper, B. De, Müller, U., Shen, J., & Hartmann, T. (2005). Regulation of cholesterol and sphingomyelin metabolism by amyloid-ß and presenilin. *Nature Cell Biology*, *7*(11), 1118–1123. https://doi.org/10.1038/ncb1313

Grimm, M. O. W., Grimm, H. S., Tomic, I., Beyreuther, K., Hartmann, T., & Bergmann, C. (2008). Independent inhibition of Alzheimer disease ß- and γ-secretase cleavage by lowered cholesterol levels. *Journal of Biological Chemistry*, *283*(17), 11302–11311. https://doi.org/10.1074/jbc.M801520200

Grösgen, S., Grimm, M. O. W., Frieß, P., & Hartmann, T. (2010). Role of amyloid beta in lipid homeostasis. *Biochimica et Biophysica Acta (BBA) - Molecular and Cell Biology of Lipids*, *1801*(8), 966–974. https://doi.org/10.1016/j.bbalip.2010.05.002

Guo, X., Song, W., Chen, K., Chen, X., Zheng, Z., Cao, B., Huang, R., Zhao, B., Wu, Y., & Shang, H.-F. (2015). The serum lipid profile of Parkinson's disease patients: a study from China.

International Journal of Neuroscience, *125*(11), 838–844. https://doi.org/10.3109/00207454.2014.979288

Gupta, S., Takebe, N., & Lorusso, P. (2010). Targeting the Hedgehog pathway in cancer. *Therapeutic Advances in Medical Oncology*, *2*(4), 237–250. https://doi.org/10.1177/1758834010366430

GUZE, S. B. (1995). Diagnostic and Statistical Manual of Mental Disorders, 4th ed. (DSM-IV). *American Journal of Psychiatry*, *152*(8), 1228–1228. https://doi.org/10.1176/ajp.152.8.1228

Guzman, J. N., Sanchez-Padilla, J., Wokosin, D., Kondapalli, J., Ilijic, E., Schumacker, P. T., & Surmeier, D. J. (2010). Oxidant stress evoked by pacemaking in dopaminergic neuroneneuronees is attenuated by DJ-1. *Nature*, *468*(7324), 696–700. https://doi.org/10.1038/nature09536

Haass, C., Koo, E. H., Mellon, A., Hung, A. Y., & Selkoe, D. J. (1992). Targeting of cell-surface ß-amyloid precursor protein to lysosomes: alternative processing into amyloid-bearing fragments. *Nature*, *357*(6378), 500–503. https://doi.org/10.1038/357500a0

Haass, C., Lemere, C. A., Capell, A., Citron, M., Seubert, P., Schenk, D., Lannfelt, L., & Selkoe, D. J. (1995). The Swedish mutation causes early-onset Alzheimer's disease by ß-secretase cleavage within the secretory pathway. *Nature Medicine*, *1*(12), 1291–1296. https://doi.org/10.1038/nm1295-1291

Hailat, I., & Helleur, R. J. (2014). Direct analysis of sterols by derivatization matrix-assisted laser desorption/ionization time-of-flight mass spectrometry and tandem mass spectrometry. *Rapid Communications in Mass Spectrometry*, *28*(2), 149–158. https://doi.org/10.1002/rcm.6766

Han, X., & Gross, R. W. (1994). *Electrospray ionization mass spectroscopic analysis of human erythrocyte plasma membrane phospholipids (plasaogen/mass sectrometry/sph ye l/red blood cell)* (Vol. 91). https://www.pnas.org

Han, X., Yang, J., Cheng, H., Ye, H., & Gross, R. W. (2004). Toward fingerprinting cellular lipidomes directly from biological samples by two-dimensional electrospray ionization mass spectrometry. *Analytical Biochemistry*, *330*(2), 317–331. https://doi.org/10.1016/j.ab.2004.04.004

Hannedouche, S., Zhang, J., Yi, T., Shen, W., Nguyen, D., Pereira, J. P., Guerini, D., Baumgarten, B. U., Roggo, S., Wen, B., Knochenmuss, R., Noël, S., Gessier, F., Kelly, L. M., Vanek, M., Laurent, S., Preuss, I., Miault, C., Christen, I., … Sailer, A. W. (2011). Oxysterols direct immune cell migration via EBI2. *Nature*, *475*(7357), 524–527. https://doi.org/10.1038/nature10280

Hansen, K. B., Yi, F., Perszyk, R. E., Furukawa, H., Wollmuth, L. P., Gibb, A. J., & Traynelis, S. F. (2018). Structure, function, and allosteric modulation of NMDA receptors. *Journal of General Physiology*, *150*(8), 1081–1105. https://doi.org/10.1085/jgp.201812032

Hansson, O., Edelmayer, R. M., Boxer, A. L., Carrillo, M. C., Mielke, M. M., Rabinovici, G. D., Salloway, S., Sperling, R., Zetterberg, H., & Teunissen, C. E. (2022). The Alzheimer's Association appropriate use recommendations for blood biomarkers in Alzheimer's disease. In *Alzheimer's and Dementia* (Vol. 18, Issue 12, pp. 2669–2686). John Wiley and Sons Inc. https://doi.org/10.1002/alz.12756

Hardy, J., Lewis, P., Revesz, T., Lees, A., & Paisan-Ruiz, C. (2009). The genetics of Parkinson's syndromes: a critical review. In *Current Opinion in Genetics and Development* (Vol. 19, Issue 3, pp. 254–265). https://doi.org/10.1016/j.gde.2009.03.008

Harvey, D. J. (2005). Fragmentation of negative ions from carbohydrates: Part 1. Use of nitrate and other anionic adducts for the production of negative ion electrospray spectra from *N*-linked carbohydrates. *Journal of the American Society for Mass Spectrometry*, *16*(5), 622–630. https://doi.org/10.1016/j.jasms.2005.01.004

Hecht, E. S., Scigelova, M., Eliuk, S., & Makarov, A. (2019). Fundamentals and Advances of Orbitrap Mass Spectrometry. In *Encyclopedia of Analytical Chemistry* (pp. 1–40). Wiley. https://doi.org/10.1002/9780470027318.a9309.pub2

Heino, S., Lusa, S., Somerharju, P., Ehnholm, C., Olkkonen, V. M., & Ikonen, E. (2000). Dissecting the role of the Golgi complex and lipid rafts in biosynthetic transport of cholesterol to the cell surface. *Proceedings of the National Academy of Sciences*, *97*(15), 8375–8380. https://doi.org/10.1073/pnas.140218797

Heverin, M., Bogdanovic, N., Lütjohann, D., Bayer, T., Pikuleva, I., Bretillon, L., Diczfalusy, U., Winblad, B., & Björkhem, I. (2004). Changes in the levels of cerebral and extracerebral sterols in the brain of patients with Alzheimer's disease. *Journal of Lipid Research*, *45*(1), 186–193. https://doi.org/10.1194/jlr.M300320-JLR200

Holst, J. P., Soldin, O. P., Guo, T., & Soldin, S. J. (2004). Steroid hormones: Relevance and measurement in the clinical

laboratory. In *Clinics in Laboratory Medicine* (Vol. 24, Issue 1, pp. 105–118). https://doi.org/10.1016/j.cll.2004.01.004

Holtzman, D. M. (2001). ole of apoE/Aβ Interactions in the Pathogenesis of Alzheimer's Disease and Cerebral Amyloid Angiopathy. *Journal of Molecular Neuroscience*, *17*(2), 147–155. https://doi.org/10.1385/JMN:17:2:147

Holtzman, D. M., Bales, K. R., Tenkova, T., Fagan, A. M., Parsadanian, M., Sartorius, L. J., Mackey, B., Olney, J., McKeel, D., Wozniak, D., & Paul, S. M. (2000). Apolipoprotein E isoform-dependent amyloid deposition and neuritic degeneration in a mouse model of Alzheimer's disease. *Proceedings of the National Academy of Sciences*, *97*(6), 2892–2897. https://doi.org/10.1073/pnas.050004797

Holtzman, D. M., Bales, K. R., Wu, S., Bhat, P., Parsadanian, M., Fagan, A. M., Chang, L. K., Sun, Y., & Paul, S. M. (1999). Expression of human apolipoprotein E reduces amyloid-β deposition in a mouse model of Alzheimer's disease. *Journal of Clinical Investigation*, *103*(6), R15–R21. https://doi.org/10.1172/JCI6179

Honda, A., Miyazaki, T., Ikegami, T., Iwamoto, J., Maeda, T., Hirayama, T., Saito, Y., Teramoto, T., & Matsuzaki, Y. (2011). Cholesterol 25-hydroxylation activity of CYP3A. *Journal of Lipid Research*, *52*(8), 1509–1516. https://doi.org/10.1194/jlr.M014084

Honda, A., Miyazaki, T., Ikegami, T., Iwamoto, J., Yamashita, K., Numazawa, M., & Matsuzaki, Y. (2010). Highly sensitive and specific analysis of sterol profiles in biological samples by HPLC–ESI–MS/MS. *The Journal of Steroid Biochemistry and Molecular*

Biology, *121*(3–5), 556–564. https://doi.org/10.1016/j.jsbmb.2010.03.030

Honda, A., Yamashita, K., Hara, T., Ikegami, T., Miyazaki, T., Shirai, M., Xu, G., Numazawa, M., & Matsuzaki, Y. (2009a). Highly sensitive quantification of key regulatory oxysterols in biological samples by LC-ESI-MS/MS. *Journal of Lipid Research*, *50*(2), 350–357. https://doi.org/10.1194/jlr.D800040-JLR200

Honda, A., Yamashita, K., Hara, T., Ikegami, T., Miyazaki, T., Shirai, M., Xu, G., Numazawa, M., & Matsuzaki, Y. (2009b). Highly sensitive quantification of key regulatory oxysterols in biological samples by LC-ESI-MS/MS. *Journal of Lipid Research*, *50*(2), 350–357. https://doi.org/10.1194/jlr.D800040-JLR200

Honda, A., Yamashita, K., Hara, T., Ikegami, T., Miyazaki, T., Shirai, M., Xu, G., Numazawa, M., & Matsuzaki, Y. (2009c). Highly sensitive quantification of key regulatory oxysterols in biological samples by LC-ESI-MS/MS. *Journal of Lipid Research*, *50*(2), 350–357. https://doi.org/10.1194/jlr.D800040-JLR200

Honda, A., Yamashita, K., Miyazaki, H., Shirai, M., Ikegami, T., Xu, G., Numazawa, M., Hara, T., & Matsuzaki, Y. (2008). Highly sensitive analysis of sterol profiles in human serum by LC-ESI-MS/MS. *Journal of Lipid Research*, *49*(9), 2063–2073. https://doi.org/10.1194/jlr.D800017-JLR200

Hoover, B. R., Reed, M. N., Su, J., Penrod, R. D., Kotilinek, L. A., Grant, M. K., Pitstick, R., Carlson, G. A., Lanier, L. M., Yuan, L.-L., Ashe, K. H., & Liao, D. (2010). Tau Mislocalization to Dendritic Spines Mediates Synaptic Dysfunction Independently of Neurodegeneration. *Neurone*, *68*(6), 1067–1081. https://doi.org/10.1016/j.neurone.2010.11.030

Horton, J. D., Goldstein, J. L., & Brown, M. S. (2002a). SREBPs: activators of the complete program of cholesterol and fatty acid synthesis in the liver. *Journal of Clinical Investigation*, *109*(9), 1125–1131. https://doi.org/10.1172/JCI15593

Horton, J. D., Goldstein, J. L., & Brown, M. S. (2002b). SREBPs: activators of the complete program of cholesterol and fatty acid synthesis in the liver. *Journal of Clinical Investigation*, *109*(9), 1125–1131. https://doi.org/10.1172/JCI0215593

Hosseini, E. S., & Heydar, K. T. (2021). Silica modification with 9-methylacridine and 9-undecylacridine as mixed-mode stationary phases in HPLC. *Talanta*, *221*, 121445. https://doi.org/10.1016/j.talanta.2020.121445

Hsiao, J.-H., Halliday, G., & Kim, W. (2017a). α-Synuclein Regulates Neuroneal Cholesterol Efflux. *Molecules*, *22*(10), 1769. https://doi.org/10.3390/molecules22101769

Hsiao, J.-H., Halliday, G., & Kim, W. (2017b). α-Synuclein Regulates Neuroneal Cholesterol Efflux. *Molecules*, *22*(10), 1769. https://doi.org/10.3390/molecules22101769

Hu, G., Antikainen, R., Jousilahti, P., Kivipelto, M., & Tuomilehto, J. (2008). Total cholesterol and the risk of Parkinson disease. *Neurology*, *70*(21), 1972–1979. https://doi.org/10.1212/01.wnl.0000312511.62699.a8

Hu, J., Zhang, Z., Shen, W.-J., & Azhar, S. (2010). Cellular cholesterol delivery, intracellular processing and utilization for biosynthesis of steroid hormones. In *Nutrition & Metabolism* (Vol. 7). http://www.nutritionandmetabolism.com/content/7/1/47

Huang, X., Sterling, N. W., Du, G., Sun, D., Stetter, C., Kong, L., Zhu, Y., Neighbors, J., Lewis, M. M., Chen, H., Hohl, R. J., & Mailman, R. B. (2019). Brain cholesterol metabolism and Parkinson's disease. *Movement Disorders*, *34*(3), 386–395. https://doi.org/10.1002/mds.27609

Huang, Y., Liu, X. Q., Wyss-Coray, T., Brecht, W. J., Sanan, D. A., & Mahley, R. W. (2001). Apolipoprotein E fragments present in Alzheimer's disease brains induce neurofibrillary tangle-like intracellular inclusions in neuroneneuronees. *Proceedings of the National Academy of Sciences*, *98*(15), 8838–8843. https://doi.org/10.1073/pnas.151254698

Husain, M. A., Laurent, B., & Plourde, M. (2021). APOE and Alzheimer's Disease: From Lipid Transport to Physiopathology and Therapeutics. *Frontiers in Neuroscience*, *15*. https://doi.org/10.3389/fnins.2021.630502

Husi, H. (2004). NMDA Receptors, Neural Pathways, and Protein Interaction Databases. *International Review of Neurobiology*, *61*, 49–77. https://doi.org/10.1016/S0074-7742(04)61003-8

Hyuk Yoon, J., Seo, Y., Suk Jo, Y., Lee, S., Cho, E., Cazenave-Gassiot, A., Shin, Y.-S., Hee Moon, M., Joo An, H., Wenk, M. R., & Suh, P.-G. (2022). Brain lipidomics: From functional landscape to clinical significance. In *Sci. Adv* (Vol. 8). https://www.science.org

Ikeda, K., Nakamura, Y., Kiyozuka, T., Aoyagi, J., Hirayama, T., Nagata, R., Ito, H., Iwamoto, K., Murata, K., Yoshii, Y., Kawabe, K., & Iwasaki, Y. (2011). Serological Profiles of Urate, Paraoxonase-1, Ferritin and Lipid in Parkinson's Disease: Changes Linked to Disease Progression. *Neurodegenerative Diseases*, *8*(4), 252–258. https://doi.org/10.1159/000323265

Ikegami, T., Hyogo, H., Honda, A., Miyazaki, T., Tokushige, K., Hashimoto, E., Inui, K., Matsuzaki, Y., & Tazuma, S. (2012). Increased serum liver X receptor ligand oxysterols in patients with non-alcoholic fatty liver disease. *Journal of Gastroenterology*, *47*(11), 1257–1266. https://doi.org/10.1007/s00535-012-0585-0

Ikonen, E., & Parton, R. G. (2000). Caveolins and Cellular Cholesterol Balance. *Traffic*, *1*(3), 212–217. https://doi.org/10.1034/j.1600-0854.2000.010303.x

Infante, R. E., & Radhakrishnan, A. (2017a). Continuous transport of a small fraction of plasma membrane cholesterol to endoplasmic reticulum regulates total cellular cholesterol. *ELife*, *6*. https://doi.org/10.7554/eLife.25466

Infante, R. E., & Radhakrishnan, A. (2017b). Continuous transport of a small fraction of plasma membrane cholesterol to endoplasmic reticulum regulates total cellular cholesterol. *ELife*, *6*. https://doi.org/10.7554/eLife.25466

Ishigami, M., Ogasawara, F., Nagao, K., Hashimoto, H., Kimura, Y., Kioka, N., & Ueda, K. (2018). Temporary sequestration of cholesterol and phosphatidylcholine within extracellular domains of ABCA1 during nascent HDL generation. *Scientific Reports*, *8*(1), 6170. https://doi.org/10.1038/s41598-018-24428-6

Iwatsubo, T. (2004). The γ-secretase complex: machinery for intramembrane proteolysis. *Current Opinion in Neurobiology*, *14*(3), 379–383. https://doi.org/10.1016/j.conb.2004.05.010

Jacob, L., & Lum, L. (2007). Deconstructing the hedgehog pathway in development and disease. *Science (New York, N.Y.)*, *318*(5847), 66–68. https://doi.org/10.1126/science.1147314

Janco, M., Alexander, J. N., Bouvier, E. S. P., & Morrison, D. (2013). Ultra-high performance size-exclusion chromatography of synthetic polymers. *Journal of Separation Science*, *36*(17), 2718–2727. https://doi.org/10.1002/jssc.201300444

Janowski, B. A.; Grogan, M. J.; Jones, S. A.; Wisely, G. B.; Kliewer, S. A.; Corey, E. J.; Mangelsdorf, D. J. (1999). Structural requirements of ligands for the oxysterol liver X receptors LXR ␣ and LXR ␤. *Proc. Natl. Acad. Sci. USA*, *96*, 266–271.

Janowski, B. A., Willy, P. J., Devi, T. R., Falck, J. R., & Mangelsdorf, D. J. (1996). An oxysterol signalling pathway mediated by the nuclear receptor LXRα. *Nature*, *383*(6602), 728–731. https://doi.org/10.1038/383728a0

Janowsky, Bethany A.; Willy, P. J.; Rama Devi, T.; Falck, J. R.; Mangelsdorf, D. J. (1996). An oxysterol signalling pathway mediated by the nuclear receptor LXR. *Nature*, *383*, 728–731.

Janulyte, A., Zerega, Y., Carette, M., Reynard, C., & Andre, J. (2011). Sensitivity and amplitude calibration of a Fourier transform 3D quadrupole ion trap mass spectrometer. *Journal of Mass Spectrometry*, *46*(2), 136–143. https://doi.org/10.1002/jms.1881

Jeon, T.-I., & Osborne, T. F. (2012). SREBPs: metabolic integrators in physiology and metabolism. *Trends in Endocrinology & Metabolism*, *23*(2), 65–72. https://doi.org/10.1016/j.tem.2011.10.004

Jiang, X., Ory, D. S., & Han, X. (2007). Characterization of oxysterols by electrospray ionization tandem mass spectrometry after one-step derivatization with dimethylglycine. *Rapid Communications in Mass Spectrometry*, *21*(2), 141–152. https://doi.org/10.1002/rcm.2820

Jiang, X., Sidhu, R., Porter, F. D., Yanjanin, N. M., Speak, A. O., te Vruchte, D. T., Platt, F. M., Fujiwara, H., Scherrer, D. E., Zhang, J., Dietzen, D. J., Schaffer, J. E., & Ory, D. S. (2011). A sensitive and specific LC-MS/MS method for rapid diagnosis of Niemann-Pick C1 disease from human plasma. *Journal of Lipid Research*, *52*(7), 1435–1445. https://doi.org/10.1194/jlr.D015735

Jin, U., Park, S. J., & Park, S. M. (2019a). Cholesterol metabolism in the brain and its association with Parkinson's disease. In *Experimental Neurobiology* (Vol. 28, Issue 5, pp. 554–567). Korean Society for Neurodegenerative Disease. https://doi.org/10.5607/en.2019.28.5.554

Jin, U., Park, S. J., & Park, S. M. (2019b). Cholesterol metabolism in the brain and its association with Parkinson's disease. *Experimental Neurobiology*, *28*(5), 554–567. https://doi.org/10.5607/en.2019.28.5.554

J.J. Thomson. (1914). Rays of Positive Electricity and Their Application to Chemical Analysis. *Nature*, 549–550.

Jo, Y., & DeBose-Boyd, R. A. (2010). Control of cholesterol synthesis through regulated ER-associated degradation of HMG CoA reductase. *Critical Reviews in Biochemistry and Molecular Biology*, *45*(3), 185–198. https://doi.org/10.3109/10409238.2010.485605

Johnson, D. W., ten Brink, H. J., & Jakobs, C. (2001). A rapid screening procedure for cholesterol and dehydrocholesterol by electrospray ionization tandem mass spectrometry. *Journal of Lipid Research*, *42*(10), 1699–1705. https://doi.org/10.1016/S0022-2275(20)32225-2

Joseph, S. B., Bradley, M. N., Castrillo, A., Bruhn, K. W., Mak, P. A., Pei, L., Hogenesch, J., O'Connell, R. M., Cheng, G., Saez, E., Miller, J. F., & Tontonoz, P. (2004). LXR-Dependent Gene Expression Is Important for Macrophage Survival and the Innate Immune Response. *Cell*, *119*(2), 299–309. https://doi.org/10.1016/j.cell.2004.09.032

Joseph, S. B., Laffitte, B. A., Patel, P. H., Watson, M. A., Matsukuma, K. E., Walczak, R., Collins, J. L., Osborne, T. F., & Tontonoz, P. (2002). Direct and Indirect Mechanisms for Regulation of Fatty Acid Synthase Gene Expression by Liver X Receptors. *Journal of Biological Chemistry*, *277*(13), 11019–11025. https://doi.org/10.1074/jbc.M111041200

Jowaed, A., Schmitt, I., Kaut, O., & Wullner, U. (2010). Methylation Regulates Alpha-Synuclein Expression and Is Decreased in Parkinson's Disease Patients' Brains. *Journal of Neuroscience*, *30*(18), 6355–6359. https://doi.org/10.1523/JNEUROSCI.6119-09.2010

Jp, F. (2006). Biosynthesis of bile acids in mammalian liver. In *EUROPEAN JOURNAL OF DRUG METABOLISM AND PHARMACOKINETICS* (Vol. 31, Issue 3).

Jun, H. J., Hoang, M. H., Yeo, S. K., Jia, Y., & Lee, S. J. (2013). Induction of ABCA1 and ABCG1 expression by the liver X receptor modulator cineole in macrophages. *Bioorganic and Medicinal Chemistry Letters*, *23*(2), 579–583. https://doi.org/10.1016/j.bmcl.2012.11.012

Junn, E., Lee, K.-W., Jeong, B. S., Chan, T. W., Im, J.-Y., & Mouradian, M. M. (2009). Repression of α-synuclein expression and toxicity by microRNA-7. *Proceedings of the National*

Academy of Sciences, *106*(31), 13052–13057. https://doi.org/10.1073/pnas.0906277106

Kainu, T., Kononen, J., Enmark, E., Gustafsson, J.-Å., & Pelto-Huikko, M. (1996). Localization and ontogeny of the orphan receptor OR-1 in the rat brain. *Journal of Molecular Neuroscience*, *7*(1), 29–39. https://doi.org/10.1007/BF02736846

Kandutsch, A. A., Chen, H. W., & Heiniger, H.-J. (1978). Biological Activity of Some Oxygenated Sterols. *Science*, *201*(4355), 498–501. https://doi.org/10.1126/science.663671

Kandutsch, A. A., & Russell, A. E. (1960). Preputial Gland Tumor Sterols: III. A METABOLIC PATHWAY FROM LANOSTEROL TO CHOLESTEROL. *Journal of Biological Chemistry*, *235*(8), 2256–2261. https://doi.org/10.1016/S0021-9258(18)64608-3

Kang, S. S., Ebbert, M. T. W., Baker, K. E., Cook, C., Wang, X., Sens, J. P., Kocher, J.-P., Petrucelli, L., & Fryer, J. D. (2018). Microglial translational profiling reveals a convergent APOE pathway from aging, amyloid, and tau. *Journal of Experimental Medicine*, *215*(9), 2235–2245. https://doi.org/10.1084/jem.20180653

Kapourchali, F. R., Surendiran, G., Goulet, A., & Moghadasian, M. H. (2016). The Role of Dietary Cholesterol in Lipoprotein Metabolism and Related Metabolic Abnormalities: A Mini-review. *Critical Reviews in Food Science and Nutrition*, *56*(14), 2408–2415. https://doi.org/10.1080/10408398.2013.842887

Karasinska, J. M., & Hayden, M. R. (2011). Cholesterol metabolism in Huntington disease. In *Nature Reviews Neurology*. https://doi.org/10.1038/nrneurol.2011.132

Karch, C. M., & Goate, A. M. (2015). Alzheimer's Disease Risk Genes and Mechanisms of Disease Pathogenesis. *Biological Psychiatry*, *77*(1), 43–51. https://doi.org/10.1016/j.biopsych.2014.05.006

Karu, K., Hornshaw, M., Woffendin, G., Bodin, K., Hamberg, M., Alvelius, G., Sjövall, J., Turton, J., Wang, Y., & Griffiths, W. J. (2007). Liquid chromatography-mass spectrometry utilizing multi-stage fragmentation for the identification of oxysterols. *Journal of Lipid Research*, *48*(4), 976–987. https://doi.org/10.1194/jlr.M600497-JLR200

Karu, K., Turton, J., Wang, Y., & Griffiths, W. J. (2011). Nano-liquid chromatography–tandem mass spectrometry analysis of oxysterols in brain: monitoring of cholesterol autoxidation. *Chemistry and Physics of Lipids*, *164*(6), 411–424. https://doi.org/10.1016/j.chemphyslip.2011.04.011

Karuna, R., Christen, I., Sailer, A. W., Bitsch, F., & Zhang, J. (2015). Detection of dihydroxycholesterols in human plasma using HPLC–ESI-MS/MS. *Steroids*, *99*(PB), 131–138. https://doi.org/10.1016/J.STEROIDS.2015.02.002

Katoh, Y., & Katoh, M. (2009). Hedgehog Target Genes: Mechanisms of Carcinogenesis Induced by Aberrant Hedgehog Signaling Activation. *Current Molecular Medicine*, *9*(7), 873–886. https://doi.org/10.2174/156652409789105570

Kaufmann, A. (2020). High-resolution mass spectrometry for bioanalytical applications: Is this the new gold standard? *Journal of Mass Spectrometry*, *55*(9). https://doi.org/10.1002/jms.4533

Kawas, C., Gray, S., Brookmeyer, R., Fozard, J., & Zonderman, A. (2000). Age-specific incidence rates of Alzheimer's disease.

Neurology, *54*(11), 2072–2077. https://doi.org/10.1212/WNL.54.11.2072

Kellner-Weibel, G., Yancey, P. G., Jerome, W. G., Walser, T., Mason, R. P., Phillips, M. C., & Rothblat, G. H. (1999). Crystallization of Free Cholesterol in Model Macrophage Foam Cells. *Arteriosclerosis, Thrombosis, and Vascular Biology*, *19*(8), 1891–1898. https://doi.org/10.1161/01.ATV.19.8.1891

Khosravi-Darani, K. (2010). Research Activities on Supercritical Fluid Science in Food Biotechnology. *Critical Reviews in Food Science and Nutrition*, *50*(6), 479–488. https://doi.org/10.1080/10408390802248759

Kim, C., & Lee, S.-J. (2008). Controlling the mass action of α-synuclein in Parkinson's disease. *Journal of Neurochemistry*, *107*(2), 303–316. https://doi.org/10.1111/j.1471-4159.2008.05612.x

KIM, H.-S. (2000). Carboxyl-terminal fragment of Alzheimer's APP destabilizes calcium homeostasis and renders neuroneal cells vulnerable to excitotoxicity. *The FASEB Journal*, *14*(11), 1508–1517. https://doi.org/10.1096/fj.14.11.1508

Kim, J.-M., Cha, S.-H., Choi, Y. R., Jou, I., Joe, E.-H., & Park, S. M. (2016). DJ-1 deficiency impairs glutamate uptake into astrocytes via the regulation of flotillin-1 and caveolin-1 expression. *Scientific Reports*, *6*(1), 28823. https://doi.org/10.1038/srep28823

Kim, K. S., Kim, J. S., Park, J.-Y., Suh, Y. H., Jou, I., Joe, E.-H., & Park, S. M. (2013). DJ-1 Associates with lipid rafts by palmitoylation and regulates lipid rafts-dependent endocytosis in astrocytes. *Human Molecular Genetics*, *22*(23), 4805–4817. https://doi.org/10.1093/hmg/ddt332

Kim, K.-Y., Stevens, M. V., Akter, M. H., Rusk, S. E., Huang, R. J., Cohen, A., Noguchi, A., Springer, D., Bocharov, A. V., Eggerman, T. L., Suen, D.-F., Youle, R. J., Amar, M., Remaley, A. T., & Sack, M. N. (2011a). Parkin is a lipid-responsive regulator of fat uptake in mice and mutant human cells. *Journal of Clinical Investigation*, *121*(9), 3701–3712. https://doi.org/10.1172/JCI44736

Kim, K.-Y., Stevens, M. V., Akter, M. H., Rusk, S. E., Huang, R. J., Cohen, A., Noguchi, A., Springer, D., Bocharov, A. V., Eggerman, T. L., Suen, D.-F., Youle, R. J., Amar, M., Remaley, A. T., & Sack, M. N. (2011b). Parkin is a lipid-responsive regulator of fat uptake in mice and mutant human cells. *Journal of Clinical Investigation*, *121*(9), 3701–3712. https://doi.org/10.1172/JCI44736

Kim, M.-W., An, B. M., Wang, L., Lee, K. Y., Bang, J., & Joo, B. S. (2020). Effects of Oxysterols on Chondrogenesis of Human Adipose-derived Stem Cells. *Annals of Clinical and Laboratory Science*, *50*(2), 190–198.

Kim, W.-K., Meliton, V., Park, K. W., Hong, C., Tontonoz, P., Niewiadomski, P., Waschek, J. A., Tetradis, S., & Parhami, F. (2009). Negative Regulation of Hedgehog Signaling by Liver X Receptors. *Molecular Endocrinology*, *23*(10), 1532–1543. https://doi.org/10.1210/me.2008-0453

Kingdon, K. H. (1923). A Method for the Neutralization of Electron Space Charge by Positive Ionization at Very Low Gas Pressures. *Physical Review*, *21*(4), 408–418. https://doi.org/10.1103/PhysRev.21.408

Korade, Z., Heffer, M., & Mirnics, K. (2022). Medication effects on developmental sterol biosynthesis. *Molecular Psychiatry*, *27*(1), 490–501. https://doi.org/10.1038/s41380-021-01074-5

Korf, H., Vander Beken, S., Romano, M., Steffensen, K. R., Stijlemans, B., Gustafsson, J.-uke, Grooten, J., & Huygen, K. (2009). Liver X receptors contribute to the protective immune response against Mycobacterium tuberculosis in mice. *Journal of Clinical Investigation*, *119*(6), 1626–1637. https://doi.org/10.1172/JCI35288

Kothencz, R., Nagy, R., Bartha, L., Tóth, J., & Vágó, Á. (2018). Analysis of the interaction between polymer and surfactant in aqueous solutions for chemical-enhanced oil recovery. *Particulate Science and Technology*, *36*(7), 887–890. https://doi.org/10.1080/02726351.2017.1321073

Kovacs, G. G. (2019). Molecular pathology of neurodegenerative diseases: principles and practice. *Journal of Clinical Pathology*, *72*(11), 725–735. https://doi.org/10.1136/jclinpath-2019-205952

Kreilaus, F., Spiro, A. S., McLean, C. A., Garner, B., & Jenner, A. M. (2016). Evidence for altered cholesterol metabolism in Huntington's disease post mortem brain tissue. *Neuropathology and Applied Neurobiology*. https://doi.org/10.1111/nan.12286

Kruve, A., Kaupmees, K., Liigand, J., Oss, M., & Leito, I. (2013). Sodium adduct formation efficiency in ESI source. *Journal of Mass Spectrometry*, *48*(6), 695–702. https://doi.org/10.1002/jms.3218

Kr**ger, R., Menezes Vieira-Saecker, A. M., Kuhn, W., Berg, D., M**ller, T., K**hnl, N., Fuchs, G. A., Storch, A., Hungs, M., Woitalla, D., Przuntek, H., Epplen, J. T., Sch**ls, L., & Riess, O.

(1999). Increased susceptibility to sporadic Parkinson's disease by a certain combined ?-synuclein/apolipoprotein E genotype. *Annals of Neurology*, *45*(5), 611–617. https://doi.org/10.1002/1531-8249(199905)45:5<611::AID-ANA9>3.0.CO;2-X

Kuzu, O. F., Noory, M. A., & Robertson, G. P. (2016). The role of cholesterol in cancer. *Cancer Research*, *76*(8), 2063–2070. https://doi.org/10.1158/0008-5472.CAN-15-2613

Ladislas Wiza, J. (1979). Microchannel plate detectors. *Nuclear Instruments and Methods*, *162*(1–3), 587–601. https://doi.org/10.1016/0029-554X(79)90734-1

Lange, Y., & Steck, T. L. (1997). Quantitation of the Pool of Cholesterol Associated with Acyl-CoA:Cholesterol Acyltransferase in Human Fibroblasts. *Journal of Biological Chemistry*, *272*(20), 13103–13108. https://doi.org/10.1074/jbc.272.20.13103

Lange, Y., Swaisgood, M. H., Ramos, B. V, & Steck, T. L. (1989a). Plasma Membranes Contain Half the Phospholipid and 90*% (v/v)* of the Cholesterol and Sphingomyelin in Cultured Human Fibroblasts. *Journal of Biological Chemistry*, *264*(7), 3786–3793. https://doi.org/10.1016/S0021-9258(19)84918-9

Lange, Y., Swaisgood, M. H., Ramos, B. V, & Steck, T. L. (1989b). Plasma Membranes Contain Half the Phospholipid and 90*% (v/v)* of the Cholesterol and Sphingomyelin in Cultured Human Fibroblasts. *Journal of Biological Chemistry*, *264*(7), 3786–3793. https://doi.org/10.1016/S0021-9258(19)84918-9

Lange, Y., Ye, J., Rigney, M., & Steck, T. L. (1999). Regulation of endoplasmic reticulum cholesterol by plasma membrane cholesterol. *Journal of Lipid Research*, *40*(12), 2264–2270.

Lange, Y., Ye, J., & Strebel, F. (1995). Movement of 25-hydroxycholesterol from the plasma membrane to the rough endoplasmic reticulum in cultured hepatoma cells. *Journal of Lipid Research*, *36*(5), 1092–1097. https://doi.org/10.1016/S0022-2275(20)39867-9

Langness, V. F., van der Kant, R., Das, U., Wang, L., Chaves, R. dos S., & Goldstein, L. S. B. (2021). Cholesterol-lowering drugs reduce APP processing to Aß by inducing APP dimerization. *Molecular Biology of the Cell*, *32*(3), 247–259. https://doi.org/10.1091/mbc.E20-05-0345

Lei, P., Ayton, S., & Bush, A. I. (2021). The essential elements of Alzheimer's disease. In *Journal of Biological Chemistry* (Vol. 296). American Society for Biochemistry and Molecular Biology Inc. https://doi.org/10.1074/jbc.REV120.008207

Lemaire-Ewing, S., Berthier, A., Royer, M. C., Logette, E., Corcos, L., Bouchot, A., Monier, S., Prunet, C., Raveneau, M., Rébé, C., Desrumaux, C., Lizard, G., Néel, D., Raveneau, M., Rébé, : C, & Néel, D. (2009). 7ß-Hydroxycholesterol and 25-hydroxycholesterol-induced interleukin-8 secretion involves a calcium-dependent activation of c-fos via the ERK1/2 signaling pathway in THP-1 cells Oxysterols-induced IL-8 secretion is calcium-dependent. *Cell Biol Toxicol*, *25*, 127–139. https://doi.org/10.1007/s10565-008-9063-0

Leoni, V., & Caccia, C. (2011). Oxysterols as biomarkers in neurodegenerative diseases. *Chemistry and Physics of Lipids*,

164(6), 515–524. https://doi.org/10.1016/j.chemphyslip.2011.04.002

Leoni, V., Long, J. D., Mills, J. A., Di Donato, S., & Paulsen, J. S. (2013). Plasma 24S-hydroxycholesterol correlation with markers of Huntington disease progression. *Neurobiology of Disease*. https://doi.org/10.1016/j.nbd.2013.03.013

Leoni, V., Lütjohann, D., & Masterman, T. (2005). Levels of 7-oxocholesterol in cerebrospinal fluid are more than one thousand times lower than reported in multiple sclerosis. *Journal of Lipid Research*, *46*(2), 191–195. https://doi.org/10.1194/jlr.C400005-JLR200

Leoni, V., Masterman, T., Patel, P., Meaney, S., Diczfalusy, U., & Björkhem, I. (2003). Side chain oxidized oxysterols in cerebrospinal fluid and the integrity of blood-brain and blood-cerebrospinal fluid barriers. *Journal of Lipid Research*, *44*(4), 793–799. https://doi.org/10.1194/jlr.M200434-JLR200

Leoni, V., Solomon, A., Lövgren-Sandblom, A., Minthon, L., Blennow, K., Hansson, O., Wahlund, L.-O., Kivipelto, M., & Björkhem, I. (2013). Diagnostic Power of 24S-Hydroxycholesterol in Cerebrospinal Fluid: Candidate Marker of Brain Health. *Journal of Alzheimer's Disease*, *36*(4), 739–747. https://doi.org/10.3233/JAD-130035

Leslie, P., Carding, P. N., & Wilson, J. A. (2003). Multiple Sclerosis: A Review of the Disease and Treatment Options. *History*, *326*(February), 433–436. https://doi.org/10.1136/bmj.e3056

Li, Y., Lu, W., Marzolo, M. P., & Bu, G. (2001). Differential Functions of Members of the Low Density Lipoprotein Receptor Family Suggested by Their Distinct Endocytosis Rates. *Journal of*

Biological Chemistry, *276*(21), 18000–18006. https://doi.org/10.1074/jbc.M101589200

Liao, F., Yoon, H., & Kim, J. (2017a). Apolipoprotein E metabolism and functions in brain and its role in Alzheimer's disease. *Current Opinion in Lipidology*, *28*(1), 60–67. https://doi.org/10.1097/MOL.0000000000000383

Liao, F., Yoon, H., & Kim, J. (2017b). Apolipoprotein E metabolism and functions in brain and its role in Alzheimer's disease. *Current Opinion in Lipidology*, *28*(1), 60–67. https://doi.org/10.1097/MOL.0000000000000383

Li-Hawkins, J., Lund, E. G., Bronson, A. D., & Russell, D. W. (2000). Expression Cloning of an Oxysterol 7α-Hydroxylase Selective for 24-Hydroxycholesterol. *Journal of Biological Chemistry*, *275*(22), 16543–16549. https://doi.org/10.1074/jbc.M001810200

Lin, T. L., & Matsui, W. (2012). Hedgehog pathway as a drug target: Smoothened inhibitors in development. In *OncoTargets and Therapy* (Vol. 5, pp. 47–58). https://doi.org/10.2147/OTT.S21957

Lin, Y. T., Seo, J., Gao, F., Feldman, H. M., Wen, H. L., Penney, J., Cam, H. P., Gjoneska, E., Raja, W. K., Cheng, J., Rueda, R., Kritskiy, O., Abdurrob, F., Peng, Z., Milo, B., Yu, C. J., Elmsaouri, S., Dey, D., Ko, T., … Tsai, L. H. (2018). APOE4 Causes Widespread Molecular and Cellular Alterations Associated with Alzheimer's Disease Phenotypes in Human iPSC-Derived Brain Cell Types. *Neurone*, *98*(6), 1141-1154.e7. https://doi.org/10.1016/J.NEURONE.2018.05.008

Linder, J., Stenlund, H., & Forsgren, L. (2010). Incidence of Parkinson's disease and parkinsonism in northern Sweden: A

population-based study. *Movement Disorders*, *25*(3), 341–348. https://doi.org/10.1002/mds.22987

Linetti, A., Fratangeli, A., Taverna, E., Valnegri, P., Francolini, M., Cappello, V., Matteoli, M., Passafaro, M., & Rosa, P. (2010a). Cholesterol reduction impairs exocytosis of synaptic vesicles. *Journal of Cell Science*, *123*(4), 595–605. https://doi.org/10.1242/jcs.060681

Linetti, A., Fratangeli, A., Taverna, E., Valnegri, P., Francolini, M., Cappello, V., Matteoli, M., Passafaro, M., & Rosa, P. (2010b). Cholesterol reduction impairs exocytosis of synaptic vesicles. *Journal of Cell Science*, *123*(4), 595–605. https://doi.org/10.1242/jcs.060681

LIPID MAPS® Structure Database (LMSD). (n.d.).

Liu, C., Yang, X. V., Wu, J., Kuei, C., Mani, N. S., Zhang, L., Yu, J., Sutton, S. W., Qin, N., Banie, H., Karlsson, L., Sun, S., & Lovenberg, T. W. (2011a). Oxysterols direct B-cell migration through EBI2. *Nature*, *475*(7357), 519–523. https://doi.org/10.1038/nature10226

Liu, C., Yang, X. V, Wu, J., Kuei, C., Mani, N. S., Zhang, L., Yu, J., Sutton, S. W., Qin, N., Banie, H., Karlsson, L., Sun, S., & Lovenberg, T. W. (2011b). Oxysterols direct B-cell migration through EBI2. *Nature*, *475*(7357), 519–523. https://doi.org/10.1038/nature10226

Liu, G., Boot, B., Locascio, J. J., Jansen, I. E., Winder-Rhodes, S., Eberly, S., Elbaz, A., Brice, A., Ravina, B., van Hilten, J. J., Cormier-Dequaire, F., Corvol, J., Barker, R. A., Heutink, P., Marinus, J., Williams-Gray, C. H., Scherzer, C. R., Scherzer, C., Hyman, B. T., … Nalls, M. A. (2016). Specifically neuropathic

Gaucher's mutations accelerate cognitive decline in Parkinson's. *Annals of Neurology*, *80*(5), 674–685. https://doi.org/10.1002/ana.24781

Liu, Q., Trotter, J., Zhang, J., Peters, M. M., Cheng, H., Bao, J., Han, X., Weeber, E. J., & Bu, G. (2010). Neuroneal LRP1 Knockout in Adult Mice Leads to Impaired Brain Lipid Metabolism and Progressive, Age-Dependent Synapse Loss and Neurodegeneration. *Journal of Neuroscience*, *30*(50), 17068–17078. https://doi.org/10.1523/JNEUROSCI.4067-10.2010

Liu, Q., Zerbinatti, C. V., Zhang, J., Hoe, H.-S., Wang, B., Cole, S. L., Herz, J., Muglia, L., & Bu, G. (2007). Amyloid Precursor Protein Regulates Brain Apolipoprotein E and Cholesterol Metabolism through Lipoprotein Receptor LRP1. *Neurone*, *56*(1), 66–78. https://doi.org/10.1016/j.neurone.2007.08.008

Liu, W., Chakraborty, B., Safi, R., Kazmin, D., Chang, C.-Y., & Mcdonnell, D. P. (n.d.). *Dysregulated cholesterol homeostasis results in resistance to ferroptosis increasing tumorigenicity and metastasis in cancer*. https://doi.org/10.1038/s41467-021-25354-4

Lo Sasso, G., Murzilli, S., Salvatore, L., D'Errico, I., Petruzzelli, M., Conca, P., Jiang, Z. Y., Calabresi, L., Parini, P., & Moschetta, A. (2010). Intestinal specific LXR activation stimulates reverse cholesterol transport and protects from atherosclerosis. *Cell Metabolism*, *12*(2), 187–193. https://doi.org/10.1016/j.cmet.2010.07.002

Loera-Valencia, R., Goikolea, J., Parrado-Fernandez, C., Merino-Serrais, P., & Maioli, S. (2019). Alterations in cholesterol metabolism as a risk factor for developing Alzheimer's disease: Potential novel targets for treatment. In *Journal of Steroid*

Biochemistry and Molecular Biology (Vol. 190, pp. 104–114). Elsevier Ltd. https://doi.org/10.1016/j.jsbmb.2019.03.003

Lordan, S., Mackrill, J. J., & O'Brien, N. M. (2009). Oxysterols and mechanisms of apoptotic signaling: implications in the pathology of degenerative diseases. *The Journal of Nutritional Biochemistry*, *20*(5), 321–336. https://doi.org/10.1016/j.jnutbio.2009.01.001

Lotharius, J., & Brundin, P. (2002). Pathogenesis of parkinson's disease: dopamine, vesicles and α-synuclein. *Nature Reviews Neuroscience*, *3*(12), 932–942. https://doi.org/10.1038/nrn983

Lu, D.-L., Le Cornet, C., Sookthai, D., Johnson, T. S., Kaaks, R., & Fortner, R. T. (2019). Circulating 27-Hydroxycholesterol and Breast Cancer Risk: Results From the EPIC-Heidelberg Cohort. *JNCI: Journal of the National Cancer Institute*, *111*(4), 365–371. https://doi.org/10.1093/jnci/djy115

Lund, E., Andersson, O., Zhang, J., Babiker, A., Ahlborg, G., Diczfalusy, U., Einarsson, K., Sjövall, J., & Björkhem, I. (1996). Importance of a Novel Oxidative Mechanism for Elimination of Intracellular Cholesterol in Humans. *Arteriosclerosis, Thrombosis, and Vascular Biology*, *16*(2), 208–212. https://doi.org/10.1161/01.ATV.16.2.208

Lund, E. G., Guileyardo, J. M., & Russell, D. W. (1999a). cDNA cloning of cholesterol 24-hydroxylase, a mediator of cholesterol homeostasis in the brain. *Proceedings of the National Academy of Sciences*, *96*(13), 7238–7243. https://doi.org/10.1073/pnas.96.13.7238

Lund, E. G., Guileyardo, J. M., & Russell, D. W. (1999b). cDNA cloning of cholesterol 24-hydroxylase, a mediator of cholesterol

homeostasis in the brain. *Proceedings of the National Academy of Sciences*, *96*(13), 7238–7243. https://doi.org/10.1073/pnas.96.13.7238

Lütjohann, D., Breuer, O., Ahlborg, G., Nennesmo, I., Sidén, A., Diczfalusy, U., & Björkhem, I. (1996a). Cholesterol homeostasis in human brain: evidence for an age-dependent flux of 24S-hydroxycholesterol from the brain into the circulation. *Proceedings of the National Academy of Sciences of the United States of America*, *93*(18), 9799–9804. https://doi.org/10.1073/pnas.93.18.9799

Lutjohann, D., Breuer, O., Ahlborg, G., Nennesmo, I., Siden, A., Diczfalusy, U., & Bjorkhem, I. (1996). Cholesterol homeostasis in human brain: evidence for an age-dependent flux of 24S-hydroxycholesterol from the brain into the circulation. *Proceedings of the National Academy of Sciences*. https://doi.org/10.1073/pnas.93.18.9799

Lütjohann, D., Breuer, O., Ahlborg, G., Nennesmo, I., Sidén, A., Diczfalusy, U., & Björkhem, I. (1996b). Cholesterol homeostasis in human brain: evidence for an age-dependent flux of 24S-hydroxycholesterol from the brain into the circulation. *Proceedings of the National Academy of Sciences*, *93*(18), 9799–9804. https://doi.org/10.1073/PNAS.93.18.9799

Lydic, T. A., Busik, J. V., Esselman, W. J., & Reid, G. E. (2009). Complementary precursor ion and neutral loss scan mode tandem mass spectrometry for the analysis of glycerophosphatidylethanolamine lipids from whole rat retina. *Analytical and Bioanalytical Chemistry*, *394*(1), 267–275. https://doi.org/10.1007/s00216-009-2717-9

Ma, Z., Deng, C., Hu, W., Zhou, J., Fan, C., Di, S., Liu, D., Yang, Y., & Wang, D. (2017). Liver X receptors and their agonists: Targeting for cholesterol homeostasis and cardiovascular diseases. *Current Issues in Molecular Biology*, *22*, 41–64. https://doi.org/10.21775/cimb.022.041

Macha, S. F., Mccarley, T. D., & Limbach, P. A. (1999). Influence of ionization energy on charge-transfer ionization in matrix-assisted laser desorption/ionization mass spectrometry. In *Analytica Chimica Acta* (Vol. 397).

Madra, M., & Sturley, S. L. (2010). Niemann–Pick type C pathogenesis and treatment: from statins to sugars. *Clinical Lipidology*, *5*(3), 387–395. https://doi.org/10.2217/clp.10.19

Magalhaes, J., Gegg, M. E., Migdalska-Richards, A., Doherty, M. K., Whitfield, P. D., & Schapira, A. H. V. (2016). Autophagic lysosome reformation dysfunction in glucocerebrosidase deficient cells: relevance to Parkinson disease. *Human Molecular Genetics*, *25*(16), 3432–3445. https://doi.org/10.1093/hmg/ddw185

Makarov, A. (2000). Electrostatic Axially Harmonic Orbital Trapping: A High-Performance Technique of Mass Analysis. *Analytical Chemistry*, *72*(6), 1156–1162. https://doi.org/10.1021/ac991131p

Makarov, A., Denisov, E., Kholomeev, A., Balschun, W., Lange, O., Strupat, K., & Horning, S. (2006a). Performance Evaluation of a Hybrid Linear Ion Trap/Orbitrap Mass Spectrometer. *Analytical Chemistry*, *78*(7), 2113–2120. https://doi.org/10.1021/ac0518811

Makarov, A., Denisov, E., Kholomeev, A., Balschun, W., Lange, O., Strupat, K., & Horning, S. (2006b). Performance Evaluation of a

Hybrid Linear Ion Trap/Orbitrap Mass Spectrometer. *Analytical Chemistry*, *78*(7), 2113–2120. https://doi.org/10.1021/ac0518811

Makrina Daniilidou, Francesca Eroli, Vilma Alanko, Julen Goikolea, Maria Latorre-Leal, Patricia Rodriguez-Rodriguez, William J Griffiths, Yuqin Wang, Manuela Pacciarini, Ann Brinkmalm, Nenad Bogdanovic, Bengt Winblad, Anna Rosenberg, Henrik Zetterberg, Kaj Blennow, Miia Kivipelto, Delphine Ibghi, Angel Cedazo-Minguez, Silvia Maioli, & Anna Sandebring-Matton. (2022). Alzheimer's disease biomarker profiling in a memory clinic cohort without common comorbidities. *BioRxiv*. https://doi.org/10.1101/2022.06.09.495140

Mao, X., Ou, M. T., Karuppagounder, S. S., Kam, T.-I., Yin, X., Xiong, Y., Ge, P., Umanah, G. E., Brahmachari, S., Shin, J.-H., Kang, H. C., Zhang, J., Xu, J., Chen, R., Park, H., Andrabi, S. A., Kang, S. U., Gonçalves, R. A., Liang, Y., … Dawson, T. M. (2016). Pathological α-synuclein transmission initiated by binding lymphocyte-activation gene 3. *Science*, *353*(6307). https://doi.org/10.1126/science.aah3374

Marcello, A., Civra, A., Milan Bonotto, R., Nascimento Alves, L., Rajasekharan, S., Giacobone, C., Caccia, C., Cavalli, R., Adami, M., Brambilla, P., Lembo, D., Poli, G., & Leoni, V. (2020). The cholesterol metabolite 27-hydroxycholesterol inhibits SARS-CoV-2 and is markedly decreased in COVID-19 patients. *Redox Biology*, *36*, 101682. https://doi.org/10.1016/j.redox.2020.101682

Marguet, D., Lenne, P.-F., Rigneault, H., & He, H.-T. (2006). Dynamics in the plasma membrane: how to combine fluidity and order. *The EMBO Journal*, *25*(15), 3446–3457. https://doi.org/10.1038/sj.emboj.7601204

Mariani, E., Polidori, M. C., Cherubini, A., & Mecocci, P. (2005). Oxidative stress in brain aging, neurodegenerative and vascular diseases: An overview. *Journal of Chromatography B*, *827*(1), 65–75. https://doi.org/10.1016/j.jchromb.2005.04.023

Martin, M. G., Pfrieger, F., & Dotti, C. G. (2014). Cholesterol in brain disease: sometimes determinant and frequently implicated. *EMBO Reports*. https://doi.org/10.15252/embr.201439225

Martinez-Vicente, M., Talloczy, Z., Kaushik, S., Massey, A. C., Mazzulli, J., Mosharov, E. V., Hodara, R., Fredenburg, R., Wu, D.-C., Follenzi, A., Dauer, W., Przedborski, S., Ischiropoulos, H., Lansbury, P. T., Sulzer, D., & Cuervo, A. M. (2008). Dopamine-modified α-synuclein blocks chaperone-mediated autophagy. *Journal of Clinical Investigation*. https://doi.org/10.1172/JCI32806

Martins, C. P. B., Bromirski, M., Prieto Conaway, M. C., & Makarov, A. A. (2016). *Orbitrap Mass Spectrometry* (pp. 3–18). https://doi.org/10.1016/bs.coac.2016.01.001

Martins, P. F., de Melo, M. M. R., Sarmento, P., & Silva, C. M. (2016). Supercritical fluid extraction of sterols from Eichhornia crassipes biomass using pure and modified carbon dioxide. Enhancement of stigmasterol yield and extract concentration. *The Journal of Supercritical Fluids*, *107*, 441–449. https://doi.org/10.1016/j.supflu.2015.09.027

Masliah, E., Mallory, M., Ge, N., & Saitoh, T. (1992). Amyloid precursor protein is localized in growing neurites of neonatal rat brain. *Brain Research*, *593*(2), 323–328. https://doi.org/10.1016/0006-8993(92)91329-D

Masters, C. L., Bateman, R., Blennow, K., Rowe, C. C., Sperling, R. A., & Cummings, J. L. (2015a). Alzheimer's disease. *Nature Reviews Disease Primers*, *1*, 15056. https://doi.org/10.1038/nrdp.2015.56

Masters, C. L., Bateman, R., Blennow, K., Rowe, C. C., Sperling, R. A., & Cummings, J. L. (2015b). Alzheimer's disease. In *Nature Reviews Disease Primers* (Vol. 1). Nature Publishing Group. https://doi.org/10.1038/nrdp.2015.56

Mata, I. F., Wedemeyer, W. J., Farrer, M. J., Taylor, J. P., & Gallo, K. A. (2006). LRRK2 in Parkinson's disease: protein domains and functional insights. In *Trends in Neurosciences*. https://doi.org/10.1016/j.tins.2006.03.006

Mattson, M. P., Cutler, R. G., & Jo, D.-G. (2005). Alzheimer peptides perturb lipid-regulating enzymes. *Nature Cell Biology*, *7*(11), 1045–1047. https://doi.org/10.1038/ncb1105-1045

Mauch, D. H., Nägler, K., Schumacher, S., Göritz, C., Müller, E.-C., Otto, A., & Pfrieger, F. W. (2001). CNS Synaptogenesis Promoted by Glia-Derived Cholesterol. *Science*, *294*(5545), 1354–1357. https://doi.org/10.1126/science.294.5545.1354

Maxfield, F. R., & Tabas, I. (2005). Role of cholesterol and lipid organization in disease. *Nature*, *438*(7068), 612–621. https://doi.org/10.1038/nature04399

Mazzulli, J. R., Xu, Y.-H., Sun, Y., Knight, A. L., McLean, P. J., Caldwell, G. A., Sidransky, E., Grabowski, G. A., & Krainc, D. (2011). Gaucher Disease Glucocerebrosidase and α-Synuclein Form a Bidirectional Pathogenic Loop in Synucleinopathies. *Cell*, *146*(1), 37–52. https://doi.org/10.1016/j.cell.2011.06.001

McAlister, G. C., Nusinow, D. P., Jedrychowski, M. P., Wühr, M., Huttlin, E. L., Erickson, B. K., Rad, R., Haas, W., & Gygi, S. P. (2014). MultiNotch MS3 Enables Accurate, Sensitive, and Multiplexed Detection of Differential Expression across Cancer Cell Line Proteomes. *Analytical Chemistry*, *86*(14), 7150–7158. https://doi.org/10.1021/ac502040v

McDonald, J. G., Smith, D. D., Stiles, A. R., & Russell, D. W. (2012a). A comprehensive method for extraction and quantitative analysis of sterols and secosteroids from human plasma. *Journal of Lipid Research*, *53*(7), 1399–1409. https://doi.org/10.1194/jlr.D022285

McDonald, J. G., Smith, D. D., Stiles, A. R., & Russell, D. W. (2012b). A comprehensive method for extraction and quantitative analysis of sterols and secosteroids from human plasma. *Journal of Lipid Research*, *53*(7), 1399–1409. https://doi.org/10.1194/jlr.D022285

McKhann, G., Drachman, D., Folstein, M., Katzman, R., Price, D., & Stadlan, E. M. (1984). Clinical diagnosis of Alzheimer's disease: Report of the NINCDS-ADRDA Work Group* under the auspices of Department of Health and Human Services Task Force on Alzheimer's Disease. *Neurology*, *34*(7), 939–939. https://doi.org/10.1212/WNL.34.7.939

McNamara, D. J. (2013). Cholesterol: Sources, Absorption, Function, and Metabolism. *Encyclopedia of Human Nutrition*, *1–4*, 341–345. https://doi.org/10.1016/B978-0-12-375083-9.00052-0

Meaney, S., Babiker, A., Lütjohann, D., Diczfalusy, U., Axelson, M., & Björkhem, I. (2003). On the origin of the cholestenoic acids in

human circulation. *Steroids*, *68*(7–8), 595–601. https://doi.org/10.1016/S0039-128X(03)00081-3

Meaney, S., Bodin, K., Diczfalusy, U., & Björkhem, I. (2002). On the rate of translocation in vitro and kinetics in vivo of the major oxysterols in human circulation. *Journal of Lipid Research*, *43*(12), 2130–2135. https://doi.org/10.1194/JLR.M200293-JLR200

Meaney, S., Heverin, M., Panzenboeck, U., Ekström, L., Axelsson, M., Andersson, U., Diczfalusy, U., Pikuleva, I., Wahren, J., Sattler, W., & Björkhem, I. (2007). Novel route for elimination of brain oxysterols across the blood-brain barrier: conversion into 7α-hydroxy-3-oxo-4-cholestenoic acid. *Journal of Lipid Research*, *48*(4), 944–951. https://doi.org/10.1194/jlr.M600529-JLR200

Meljon, A., Theofilopoulos, S., Shackleton, C. H. L., Watson, G. L., Javitt, N. B., Knölker, H.-J., Saini, R., Arenas, E., Wang, Y., & Griffiths, W. J. (2012). Analysis of bioactive oxysterols in newborn mouse brain by LC/MS. *Journal of Lipid Research*, *53*(11), 2469–2483. https://doi.org/10.1194/jlr.D028233

Melki, R. (2015). Role of Different Alpha-Synuclein Strains in Synucleinopathies, Similarities with other Neurodegenerative Diseases. *Journal of Parkinson's Disease*, *5*(2), 217–227. https://doi.org/10.3233/JPD-150543

Menon, S., Armstrong, S., Hamzeh, A., Visanji, N. P., Sardi, S. P., & Tandon, A. (2022). Alpha-Synuclein Targeting Therapeutics for Parkinson's Disease and Related Synucleinopathies. *Frontiers in Neurology*, *13*. https://doi.org/10.3389/fneur.2022.852003

Milhiet, P. E., Giocondi, M.-C., & Le Grimellec, C. (2002). Cholesterol Is Not Crucial for the Existence of Microdomains in Kidney

Brush-border Membrane Models. *Journal of Biological Chemistry*, *277*(2), 875–878. https://doi.org/10.1074/jbc.C100654200

Miller, W. L., & Auchus, R. J. (2011). *The Molecular Biology, Biochemistry, and Physiology of Human Steroidogenesis and Its Disorders*. https://doi.org/10.1210/er.2010-0013

Milnerwood, A. J., & Raymond, L. A. (2010). Early synaptic pathophysiology in neurodegeneration: insights from Huntington's disease. *Trends in Neurosciences*, *33*(11), 513–523. https://doi.org/10.1016/j.tins.2010.08.002

Miyake, Y., Sasaki, S., Tanaka, K., Fukushima, W., Kiyohara, C., Tsuboi, Y., Yamada, T., Oeda, T., Miki, T., Kawamura, N., Sakae, N., Fukuyama, H., Hirota, Y., & Nagai, M. (2010). Dietary fat intake and risk of Parkinson's disease: A case-control study in Japan. *Journal of the Neurological Sciences*, *288*(1–2), 117–122. https://doi.org/10.1016/j.jns.2009.09.021

Morley, J. E., Farr, S. A., Banks, W. A., Johnson, S. N., Yamada, K. A., & Xu, L. (2010). A physiological role for amyloid-beta protein:enhancement of learning and memory. *Journal of Alzheimer's Disease : JAD*, *19*(2), 441–449. https://doi.org/10.3233/JAD-2009-1230

Mosharov, E. V., Larsen, K. E., Kanter, E., Phillips, K. A., Wilson, K., Schmitz, Y., Krantz, D. E., Kobayashi, K., Edwards, R. H., & Sulzer, D. (2009). Interplay between Cytosolic Dopamine, Calcium, and α-Synuclein Causes Selective Death of Substantia Nigra NeuroneNeuronees. *Neurone*, *62*(2), 218–229. https://doi.org/10.1016/j.neurone.2009.01.033

Mou, Y., Nandi, G., Mukte, S., Chai, E., Chen, Z., Nielsen, J. E., Nielsen, T. T., Criscuolo, C., Blackstone, C., Fraidakis, M. J., & Li, X. J. (2023). Chenodeoxycholic acid rescues axonal degeneration in induced pluripotent stem cell-derived neuroneneuronees from spastic paraplegia type 5 and cerebrotendinous xanthomatosis patients. *Orphanet Journal of Rare Diseases*, *18*(1), 72. https://doi.org/10.1186/s13023-023-02666-w

Mouritsen, O. G., & Zuckermann, M. J. (2004). What's so special about cholesterol? *Lipids*, *39*(11), 1101–1113. https://doi.org/10.1007/s11745-004-1336-x

Mouzat, K., Raoul, C., Polge, A., Kantar, J., Camu, W., & Lumbroso, S. (2016). Liver X receptors: from cholesterol regulation to neuroprotection—a new barrier against neurodegeneration in amyotrophic lateral sclerosis? In *Cellular and Molecular Life Sciences* (Vol. 73, Issue 20, pp. 3801–3808). https://doi.org/10.1007/s00018-016-2330-y

Mukherjee, S., & Maxfield, F. R. (2004). Lipid and cholesterol trafficking in NPC. *Biochimica et Biophysica Acta (BBA) - Molecular and Cell Biology of Lipids*, *1685*(1), 28–37. https://doi.org/10.1016/j.bbalip.2004.08.009

Munson, B. (2000). Chemical Ionization Mass Spectrometry: Theory and Applications. In *Encyclopedia of Analytical Chemistry*. John Wiley & Sons, Ltd. https://doi.org/10.1002/9780470027318.a6004

Musanti, R., Parati, E., Lamperti, E., & Ghiselli, G. (1993). Decreased Cholesterol Biosynthesis in Fibroblasts from Patients with Parkinson Disease. *Biochemical Medicine and Metabolic Biology*, *49*(2), 133–142. https://doi.org/10.1006/bmmb.1993.1016

Mutemberezi, V., Guillemot-Legris, O., & Muccioli, G. G. (2016a). Oxysterols: From cholesterol metabolites to key mediators. *Progress in Lipid Research*, *64*, 152–169. https://doi.org/10.1016/j.plipres.2016.09.002

Mutemberezi, V., Guillemot-Legris, O., & Muccioli, G. G. (2016b). Oxysterols: From cholesterol metabolites to key mediators. *Progress in Lipid Research*, *64*, 152–169. https://doi.org/10.1016/j.plipres.2016.09.002

Nachtergaele, S.; Mydock, L.; Krishnan, K.; Rammohan, J.; Schlesinger, P. H.; Covey, D. F.; Rohatgi, R. (2012). Oxysterols are allosteric activators of the oncoprotein Smoothened. *Nat. Chem. Biol.*, *8*, 211–220.

Nathan, B. P., Bellosta, S., Sanan, D. A., Weisgraber, K. H., Mahley, R. W., & Pitas, R. E. (1994). Differential Effects of Apolipoproteins E3 and E4 on Neuroneal Growth in Vitro. *Science*, *264*(5160), 850–852. https://doi.org/10.1126/science.8171342

Nathan, B. P., Chang, K.-C., Bellosta, S., Brisch, E., Ge, N., Mahley, R. W., & Pitas, R. E. (1995). The Inhibitory Effect of Apolipoprotein E4 on Neurite Outgrowth Is Associated with Microtubule Depolymerization. *Journal of Biological Chemistry*, *270*(34), 19791–19799. https://doi.org/10.1074/jbc.270.34.19791

Nedelcu, D., Liu, J., Xu, Y., Jao, C., & Salic, A. (2013). Oxysterol binding to the extracellular domain of Smoothened in Hedgehog signaling. *Nature Chemical Biology*, *9*(9), 557–564. https://doi.org/10.1038/nchembio.1290

Nelson, J. A., Steckbeck, S. R., & Spencer, T. A. (1981). Biosynthesis of 24,25-epoxycholesterol from squalene 2,3;22,23-dioxide. *The Journal of Biological Chemistry*, *256*(3), 1067–1068.

Nelson, P. T., Schmitt, F. A., Lin, Y., Abner, E. L., Jicha, G. A., Patel, E., Thomason, P. C., Neltner, J. H., Smith, C. D., Santacruz, K. S., Sonnen, J. A., Poon, L. W., Gearing, M., Green, R. C., Woodard, J. L., Van Eldik, L. J., & Kryscio, R. J. (2011). Hippocampal sclerosis in advanced age: clinical and pathological features. *Brain*, *134*(5), 1506–1518. https://doi.org/10.1093/brain/awr053

Nes, W. D. (2011). Biosynthesis of Cholesterol and Other Sterols. *Chem. Rev*, *111*, 6423–6451. https://doi.org/10.1021/cr200021m

Ness, G. C. (2015). Physiological feedback regulation of cholesterol biosynthesis: Role of translational control of hepatic HMG-CoA reductase and possible involvement of oxylanosterols. In *Biochimica et Biophysica Acta - Molecular and Cell Biology of Lipids* (Vol. 1851, Issue 5, pp. 667–673). Elsevier. https://doi.org/10.1016/j.bbalip.2015.02.008

Nguyen, S., & Fenn, J. B. (2007). Gas-phase ions of solute species from charged droplets of solutions. *Proceedings of the National Academy of Sciences*, *104*(4), 1111–1117. https://doi.org/10.1073/pnas.0609969104

Nieweg, K., Schaller, H., & Pfrieger, F. W. (2009a). Marked differences in cholesterol synthesis between neuroneneuronees and glial cells from postnatal rats. *Journal of Neurochemistry*, *109*(1), 125–134. https://doi.org/10.1111/j.1471-4159.2009.05917.x

Nieweg, K., Schaller, H., & Pfrieger, F. W. (2009b). Marked differences in cholesterol synthesis between neuroneneuronees and glial cells from postnatal rats. *Journal of Neurochemistry*, *109*(1), 125–134. https://doi.org/10.1111/j.1471-4159.2009.05917.x

Nohturfft, A., Brown, M. S., & Goldstein, J. L. (1998). *Topology of SREBP Cleavage-activating Protein, a Polytopic Membrane Protein with a Sterol-sensing Domain**. http://www.jbc.org

Nunan, J., & Small, D. H. (2000). Regulation of APP cleavage by α-, ß- and γ-secretases. *FEBS Letters*, *483*(1), 6–10. https://doi.org/10.1016/S0014-5793(00)02076-7

Obeso, J. A., Stamelou, M., Goetz, C. G., Poewe, W., Lang, A. E., Weintraub, D., Burn, D., Halliday, G. M., Bezard, E., Przedborski, S., Lehericy, S., Brooks, D. J., Rothwell, J. C., Hallett, M., DeLong, M. R., Marras, C., Tanner, C. M., Ross, G. W., Langston, J. W., … Stoessl, A. J. (2017). Past, present, and future of Parkinson's disease: A special essay on the 200th Anniversary of the Shaking Palsy. *Movement Disorders*, *32*(9), 1264–1310. https://doi.org/10.1002/mds.27115

Ogundare, M., Theofilopoulos, S., Lockhart, A., Hall, L. J., Arenas, E., Sjövall, J., Brenton, A. G., Wang, Y., & Griffiths, W. J. (2010a). Cerebrospinal Fluid Steroidomics: Are Bioactive Bile Acids Present in Brain? *Journal of Biological Chemistry*, *285*(7), 4666–4679. https://doi.org/10.1074/jbc.M109.086678

Ogundare, M., Theofilopoulos, S., Lockhart, A., Hall, L. J., Arenas, E., Sjövall, J., Brenton, A. G., Wang, Y., & Griffiths, W. J. (2010b). Cerebrospinal fluid steroidomics: Are bioactive bile acids

present in brain? *Journal of Biological Chemistry*, *285*(7), 4666–4679. https://doi.org/10.1074/jbc.M109.086678

Ohyama, Y., Meaney, S., Heverin, M., Ekström, L., Brafman, A., Shafir, M., Andersson, U., Olin, M., Eggertsen, G., Diczfalusy, U., Feinstein, E., & Björkhem, I. (2006). Studies on the Transcriptional Regulation of Cholesterol 24-Hydroxylase (CYP46A1). *Journal of Biological Chemistry*, *281*(7), 3810–3820. https://doi.org/10.1074/jbc.M505179200

Okwu, A. K., Xu, X. X., Shiratori, Y., & Tabas, I. (1994). Regulation of the threshold for lipoprotein-induced acyl-CoA:cholesterol O-acyltransferase stimulation in macrophages by cellular sphingomyelin content. *Journal of Lipid Research*, *35*(4), 644–655.

Olsen, B. N., Schlesinger, P. H., & Baker, N. A. (2008). Perturbations of Membrane Structure by Cholesterol and Cholesterol Derivatives Are Determined by Sterol Orientation. *JACS*, 4854–4865. https://doi.org/10.1021/ja8095224

Olsson, F., Schmidt, S., Althoff, V., Munter, L. M., Jin, S., Rosqvist, S., Lendahl, U., Multhaup, G., & Lundkvist, J. (2014). Characterization of Intermediate Steps in Amyloid Beta (Aβ) Production under Near-native Conditions. *Journal of Biological Chemistry*, *289*(3), 1540–1550. https://doi.org/10.1074/jbc.M113.498246

Orbitrap IQ-X Tribrid Mass Spectrometer. (n.d.).

Osborne, T. F., Gil, G., Goldstein, J. L., & Brown, M. S. (1988). Operator constitutive mutation of 3-hydroxy-3-methylglutaryl coenzyme A reductase promoter abolishes protein binding to sterol regulatory element. *Journal of Biological Chemistry*,

263(7), 3380–3387. https://doi.org/10.1016/S0021-9258(18)69082-9

Ouimet, M., Barrett, T. J., & Fisher, E. A. (2019). HDL and Reverse Cholesterol Transport. *Circulation Research*, *124*(10), 1505–1518. https://doi.org/10.1161/CIRCRESAHA.119.312617

Owen H. Wheeler. (1968). The Girard Reagents. *Chemical Reviews* , *62*(3), 205–221.

Pandak, W. M., & Kakiyama, G. (2019). The acidic pathway of bile acid synthesis: Not just an alternative pathway. In *Liver Research* (Vol. 3, Issue 2, pp. 88–98). KeAi Communications Co. https://doi.org/10.1016/j.livres.2019.05.001

Pandak, W. M., Ren, S., Marques, D., Hall, E., Redford, K., Mallonee, D., Bohdan, P., Heuman, D., Gill, G., & Hylemon, P. (2002). Transport of cholesterol into mitochondria is rate-limiting for bile acid synthesis via the alternative pathway in primary rat hepatocytes. *Journal of Biological Chemistry*, *277*(50), 48158–48164. https://doi.org/10.1074/jbc.M205244200

Pannu, P. S., Allahverdian, S., & Francis, G. A. (2013). Oxysterol generation and liver X receptor-dependent reverse cholesterol transport: Not all roads lead to Rome. *Molecular and Cellular Endocrinology*, *368*(1–2), 99–107. https://doi.org/10.1016/j.mce.2012.07.013

Park, J., An, S. S. A., Giau, V. Van, Shim, K., Youn, Y. C., Bagyinszky, E., & Kim, S. (2017). Identification of a novel PSEN1 mutation (Leu232Pro) in a Korean patient with early-onset Alzheimer's disease and a family history of dementia. *Neurobiology of Aging*, *56*, 212.e11-212.e17. https://doi.org/10.1016/j.neurobiolaging.2017.04.012

Parrado-Fernández, C., Blennow, K., Hansson, M., Leoni, V., Cedazo-Minguez, A., & Björkhem, I. (2018). Evidence for sex difference in the <scp>CSF</scp> /plasma albumin ratio in ~20 000 patients and 335 healthy volunteers. *Journal of Cellular and Molecular Medicine*, *22*(10), 5151–5154. https://doi.org/10.1111/jcmm.13767

Pataj, Z., Liebisch, G., Schmitz, G., & Matysik, S. (2016). Quantification of oxysterols in human plasma and red blood cells by liquid chromatography high-resolution tandem mass spectrometry. *Journal of Chromatography A*, *1439*, 82–88. https://doi.org/10.1016/j.chroma.2015.11.015

Patterson, C., Feightner, J. W., Garcia, A., Hsiung, G.-Y. R., MacKnight, C., & Sadovnick, A. D. (2008). Diagnosis and treatment of dementia: 1. Risk assessment and primary prevention of Alzheimer disease. *Canadian Medical Association Journal*, *178*(5), 548–556. https://doi.org/10.1503/cmaj.070796

Paul, R., Choudhury, A., Kumar, S., Giri, A., Sandhir, R., & Borah, A. (2017a). Cholesterol contributes to dopamine-neuroneal loss in MPTP mouse model of Parkinson's disease: Involvement of mitochondrial dysfunctions and oxidative stress. *PLOS ONE*, *12*(2), e0171285. https://doi.org/10.1371/journal.pone.0171285

Paul, R., Choudhury, A., Kumar, S., Giri, A., Sandhir, R., & Borah, A. (2017b). Cholesterol contributes to dopamine-neuroneal loss in MPTP mouse model of Parkinson's disease: Involvement of mitochondrial dysfunctions and oxidative stress. *PLOS ONE*, *12*(2), e0171285. https://doi.org/10.1371/journal.pone.0171285

Paul, S. M., Doherty, J. J., Robichaud, A. J., Belfort, G. M., Chow, B. Y., Hammond, R. S., Crawford, D. C., Linsenbardt, A. J., Shu, H.-

J., Izumi, Y., Mennerick, S. J., & Zorumski, C. F. (2013). *The Major Brain Cholesterol Metabolite 24(S)-Hydroxycholesterol Is a Potent Allosteric Modulator of N-Methyl-D-Aspartate Receptors*. https://doi.org/10.1523/JNEUROSCI.2619-13.2013

Peet, D. J., Janowski, B. A., & Mangelsdorf, D. J. (1998). The LXRs: A new class of oxysterol receptors. *Current Opinion in Genetics and Development*, *8*(5), 571–575. https://doi.org/10.1016/S0959-437X(98)80013-0

Peet, D. J., Turley, S. D., Ma, W., Janowski, B. a., Lobaccaro, J. M. a, Hammer, R. E., & Mangelsdorf, D. J. (1998). Cholesterol and bile acid metabolism are impaired in mice lacking the nuclear oxysterol receptor LXR?? *Cell*, *93*(5), 693–704. https://doi.org/10.1016/S0092-8674(00)81432-4

Perez Ortiz, J. M., & Swerdlow, R. H. (2019). Mitochondrial dysfunction in Alzheimer's disease: Role in pathogenesis and novel therapeutic opportunities. In *British Journal of Pharmacology*. https://doi.org/10.1111/bph.14585

Perez-Moral, N., Plankeele, J.-M., Domoney, C., & Warren, F. J. (2018). Ultra-high performance liquid chromatography-size exclusion chromatography (UPLC-SEC) as an efficient tool for the rapid and highly informative characterisation of biopolymers. *Carbohydrate Polymers*, *196*, 422–426. https://doi.org/10.1016/j.carbpol.2018.05.049

Pfrieger, F. W. (2021). Neurodegenerative Diseases and Cholesterol: Seeing the Field Through the Players. In *Frontiers in Aging Neuroscience* (Vol. 13). Frontiers Media S.A. https://doi.org/10.3389/fnagi.2021.766587

Pfrieger, F. W., & Ungerer, N. (2011). Cholesterol metabolism in neuroneneuronees and astrocytes. *Progress in Lipid Research*, *50*(4), 357–371. https://doi.org/10.1016/j.plipres.2011.06.002

Pickrell, A. M., & Youle, R. J. (2015). The Roles of PINK1, Parkin, and Mitochondrial Fidelity in Parkinson's Disease. *Neurone*, *85*(2), 257–273. https://doi.org/10.1016/j.neurone.2014.12.007

Pingale, T. D., & Gupta, G. L. (2021a). Novel therapeutic approaches for Parkinson's disease by targeting brain cholesterol homeostasis. In *Journal of Pharmacy and Pharmacology* (Vol. 73, Issue 7, pp. 862–873). Oxford University Press. https://doi.org/10.1093/jpp/rgaa063

Pingale, T. D., & Gupta, G. L. (2021b). Novel therapeutic approaches for Parkinson's disease by targeting brain cholesterol homeostasis. In *Journal of Pharmacy and Pharmacology* (Vol. 73, Issue 7, pp. 862–873). Oxford University Press. https://doi.org/10.1093/jpp/rgaa063

Pissadaki, E. K., & Bolam, J. P. (2013). The energy cost of action potential propagation in dopamine neuroneneuronees: clues to susceptibility in Parkinson's disease. *Frontiers in Computational Neuroscience*, *7*. https://doi.org/10.3389/fncom.2013.00013

Pizarro, C., Arenzana-Rámila, I., Pérez-del-Notario, N., Pérez-Matute, P., & González-Sáiz, J.-M. (2013). Plasma Lipidomic Profiling Method Based on Ultrasound Extraction and Liquid Chromatography Mass Spectrometry. *Analytical Chemistry*, *85*(24), 12085–12092. https://doi.org/10.1021/ac403181c

Poewe, W., Seppi, K., Tanner, C. M., Halliday, G. M., Brundin, P., Volkmann, J., Schrag, A. E., & Lang, A. E. (2017a). Parkinson

disease. *Nature Reviews Disease Primers*, *3*, 1–21. https://doi.org/10.1038/nrdp.2017.13

Poewe, W., Seppi, K., Tanner, C. M., Halliday, G. M., Brundin, P., Volkmann, J., Schrag, A. E., & Lang, A. E. (2017b). Parkinson disease. *Nature Reviews Disease Primers*, *3*, 1–21. https://doi.org/10.1038/nrdp.2017.13

Poirot, M., & Silvente-Poirot, S. (2013). Cholesterol-5,6-epoxides: Chemistry, biochemistry, metabolic fate and cancer. *Biochimie*, *95*(3), 622–631. https://doi.org/10.1016/J.BIOCHI.2012.05.006

Pokharel, S. M., Shil, N. K., GC, J. B., Colburn, Z. T., Tsai, S.-Y., Segovia, J. A., Chang, T.-H., Bandyopadhyay, S., Natesan, S., Jones, J. C. R., & Bose, S. (2019). Integrin activation by the lipid molecule 25-hydroxycholesterol induces a proinflammatory response. *Nature Communications*, *10*(1), 1482. https://doi.org/10.1038/s41467-019-09453-x

Politis, M., Piccini, P., Pavese, N., Koh, S.-B., & Brooks, D. J. (2008). Evidence of dopamine dysfunction in the hypothalamus of patients with Parkinson's disease: An in vivo 11C-raclopride PET study. *Experimental Neurology*, *214*(1), 112–116. https://doi.org/10.1016/j.expneurol.2008.07.021

Pommier, A. J. C., Alves, G., Viennois, E., Bernard, S., Communal, Y., Sion, B., Marceau, G., Damon, C., Mouzat, K., Caira, F., Baron, S., & Lobaccaro, J. M. A. (2010). Liver X Receptor activation downregulates AKT survival signaling in lipid rafts and induces apoptosis of prostate cancer cells. *Oncogene*, *29*(18), 2712–2723. https://doi.org/10.1038/onc.2010.30

Poole, C. F., & Lenca, N. (2017). Applications of the solvation parameter model in reversed-phase liquid chromatography.

Journal of Chromatography A, *1486*, 2–19. https://doi.org/10.1016/j.chroma.2016.05.099

Pringsheim, T., Jette, N., Frolkis, A., & Steeves, T. D. L. (2014). The prevalence of Parkinson's disease: A systematic review and meta-analysis. In *Movement Disorders* (Vol. 29, Issue 13, pp. 1583–1590). John Wiley and Sons Inc. https://doi.org/10.1002/mds.25945

Prunet, C., Montange, T., Véjux, A., Laubriet, A., Rohmer, J.-F., Riedinger, J.-M., Athias, A., Lemaire-Ewing, S., Néel, D., Petit, J.-M., Steinmetz, E., Brenot, R., Gambert, P., & Lizard, G. (2006). Multiplexed flow cytometric analyses of pro- and anti-inflammatory cytokines in the culture media of oxysterol-treated human monocytic cells and in the sera of atherosclerotic patients. *Cytometry Part A*, *69A*(5), 359–373. https://doi.org/10.1002/cyto.a.20272

Puglielli, L., Tanzi, R. E., & Kovacs, D. M. (2003). Alzheimer's disease: the cholesterol connection. *Nature Neuroscience*, *6*(4), 345–351. https://doi.org/10.1038/nn0403-345

Puzzo, D., Privitera, L., Leznik, E., Fa, M., Staniszewski, A., Palmeri, A., & Arancio, O. (2008). Picomolar Amyloid- Positively Modulates Synaptic Plasticity and Memory in Hippocampus. *Journal of Neuroscience*, *28*(53), 14537–14545. https://doi.org/10.1523/JNEUROSCI.2692-08.2008

Qi, X., Liu, H., Thompson, B., Mcdonald, J., Zhang, C., & Li, X. (2019). *Cryo-EM structure of oxysterol-bound human Smoothened coupled to a heterotrimeric G i*. https://doi.org/10.1038/s41586-019-1286-0

Radhakrishnan, A., Goldstein, J. L., McDonald, J. G., & Brown, M. S. (2008). Switch-like Control of SREBP-2 Transport Triggered by Small Changes in ER Cholesterol: A Delicate Balance. *Cell Metabolism*, *8*(6), 512–521. https://doi.org/10.1016/j.cmet.2008.10.008

Radhakrishnan, A., Ikeda, Y., Joo Kwon, H., Brown, M. S., & Goldstein, J. L. (2007). *Sterol-regulated transport of SREBPs from endoplasmic reticulum to Golgi: Oxysterols block transport by binding to Insig*. www.pnas.org/cgi/content/full/

Raju, A., Jaisankar, P., Borah, A., & Mohanakumar, K. P. (2017). 1-Methyl-4-Phenylpyridinium-Induced Death of Differentiated SH-SY5Y NeuroneNeuronees Is Potentiated by Cholesterol. *Annals of Neurosciences*, *24*(4), 243–251. https://doi.org/10.1159/000481551

Raleigh, D. R., Sever, N., Choksi, P. K., Sigg, M. A., Hines, K. M., Thompson, B. M., Elnatan, D., Jaishankar, P., Bisignano, P., Garcia-Gonzalo, F. R., Krup, A. L., Eberl, M., Byrne, E. F. X., Siebold, C., Wong, S. Y., Renslo, A. R., Grabe, M., McDonald, J. G., Xu, L., … Reiter, J. F. (2018). Cilia-Associated Oxysterols Activate Smoothened. *Molecular Cell*, *72*(2), 316-327.e5. https://doi.org/10.1016/J.MOLCEL.2018.08.034

Ramanan, V. K., & Saykin, A. J. (2013). Pathways to neurodegeneration: Mechanistic insights from GWAS in Alzheimer's disease, Parkinson's disease, and related disorders. In *American Journal of Neurodegenerative Diseases*.

Ramirez, A., Heimbach, A., Gründemann, J., Stiller, B., Hampshire, D., Cid, L. P., Goebel, I., Mubaidin, A. F., Wriekat, A.-L., Roeper, J., Al-Din, A., Hillmer, A. M., Karsak, M., Liss, B., Woods, C. G.,

Behrens, M. I., & Kubisch, C. (2006). Hereditary parkinsonism with dementia is caused by mutations in ATP13A2, encoding a lysosomal type 5 P-type ATPase. *Nature Genetics*, *38*(10), 1184–1191. https://doi.org/10.1038/ng1884

Rawson, R. B., Zelenski, N. G., Nijhawan, D., Ye, J., Sakai, J., Hasan, M. T., Chang, T. Y., Brown, M. S., & Goldstein, J. L. (1997). Complementation Cloning of S2P, a Gene Encoding a Putative Metalloprotease Required for Intramembrane Cleavage of SREBPs. *Molecular Cell*, *1*(1), 47–57. https://doi.org/10.1016/S1097-2765(00)80006-4

Rayleigh L. (1882). On the equilibrium of liquid conducting masses charged with electricity. *The London, Edinburgh, and Dublin Philosophical Magazine and Journal of Science*, *14*(87), 184–186.

Reboldi, A., Dang, E. V., McDonald, J. G., Liang, G., Russell, D. W., & Cyster, J. G. (2014). 25-Hydroxycholesterol suppresses interleukin-1–driven inflammation downstream of type I interferon. *Science*, *345*(6197), 679–684. https://doi.org/10.1126/science.1254790

Reichert, C. O., de Freitas, F. A., Levy, D., & Bydlowski, S. P. (2021). *Oxysterols and mesenchymal stem cell biology* (pp. 409–436). https://doi.org/10.1016/bs.vh.2021.02.004

Repa, J. J., Berge, K. E., Pomajzl, C., Richardson, J. A., Hobbs, H., & Mangelsdorf, D. J. (2002). Regulation of ATP-binding Cassette Sterol Transporters ABCG5 and ABCG8 by the Liver X Receptors α and ß. *Journal of Biological Chemistry*, *277*(21), 18793–18800. https://doi.org/10.1074/jbc.M109927200

Repa, J. J., Turley, S. D., Lobaccaro, J.-M. A., Medina, J., Li, L., Lustig, K., Shan, B., Heyman, R. A., Dietschy, J. M., &

Mangelsdorf, D. J. (2000). Regulation of Absorption and ABC1-Mediated Efflux of Cholesterol by RXR Heterodimers. *Science*, *289*(5484), 1524–1529. https://doi.org/10.1126/science.289.5484.1524

Rideout, H. J., & Stefanis, L. (2014). The Neurobiology of LRRK2 and its Role in the Pathogenesis of Parkinson's Disease. *Neurochemical Research*, *39*(3), 576–592. https://doi.org/10.1007/s11064-013-1073-5

Roberg-Larsen, H., Lund, K., Seterdal, K. E., Solheim, S., Vehus, T., Solberg, N., Krauss, S., Lundanes, E., & Wilson, S. R. (2017). Mass spectrometric detection of 27-hydroxycholesterol in breast cancer exosomes. *The Journal of Steroid Biochemistry and Molecular Biology*, *169*, 22–28. https://doi.org/10.1016/j.jsbmb.2016.02.006

Rocha, E. M., Smith, G. A., Park, E., Cao, H., Brown, E., Hallett, P., & Isacson, O. (2015). Progressive decline of glucocerebrosidase in aging and <scp>P</scp> arkinson's disease. *Annals of Clinical and Translational Neurology*, *2*(4), 433–438. https://doi.org/10.1002/acn3.177

Rogaev, E. I., Sherrington, R., Rogaeva, E. A., Levesque, G., Ikeda, M., Liang, Y., Chi, H., Lin, C., Holman, K., Tsuda, T., Mar, L., Sorbi, S., Nacmias, B., Piacentini, S., Amaducci, L., Chumakov, I., Cohen, D., Lannfelt, L., Fraser, P. E., … George-Hyslop, P. H. S. (1995). Familial Alzheimer's disease in kindreds with missense mutations in a gene on chromosome 1 related to the Alzheimer's disease type 3 gene. *Nature*, *376*(6543), 775–778. https://doi.org/10.1038/376775a0

Rohatgi, R., Milenkovic, L., & Scott, M. P. (2007). Patched1 Regulates Hedgehog Signaling at the Primary Cilium. *Science*, *317*(5836), 372–376. https://doi.org/10.1126/science.1139740

Rozani, V., Gurevich, T., Giladi, N., El-Ad, B., Tsamir, J., Hemo, B., & Peretz, C. (2018). Higher serum cholesterol and decreased Parkinson's disease risk: A statin-free cohort study. *Movement Disorders*, *33*(8), 1298–1305. https://doi.org/10.1002/mds.27413

Russell, D. W., Halford, R. W., Ramirez, D. M. O., Shah, R., & Kotti, T. (2009). Cholesterol 24-Hydroxylase: An Enzyme of Cholesterol Turnover in the Brain. *Annual Review of Biochemistry*, *78*(1), 1017–1040. https://doi.org/10.1146/annurev.biochem.78.072407.103859

Saeed, A. A., Genové, G., Li, T., Lütjohann, D., Olin, M., Mast, N., Pikuleva, I. A., Crick, P., Wang, Y., Griffiths, W., Betsholtz, C., & Björkhem, I. (2014). Effects of a Disrupted Blood-Brain Barrier on Cholesterol Homeostasis in the Brain. *Journal of Biological Chemistry*, *289*(34), 23712–23722. https://doi.org/10.1074/jbc.M114.556159

Sahena, F., Zaidul, I. S. M., Jinap, S., Karim, A. A., Abbas, K. A., Norulaini, N. A. N., & Omar, A. K. M. (2009). Application of supercritical CO2 in lipid extraction – A review. *Journal of Food Engineering*, *95*(2), 240–253. https://doi.org/10.1016/j.jfoodeng.2009.06.026

Saini, R. K., Prasad, P., Shang, X., & Keum, Y. S. (2021). Advances in lipid extraction methods—a review. In *International Journal of Molecular Sciences* (Vol. 22, Issue 24). MDPI. https://doi.org/10.3390/ijms222413643

Sallam, T., Jones, M. C., Gilliland, T., Zhang, L., Wu, X., Eskin, A., Sandhu, J., Casero, D., Vallim, T. Q. de A., Hong, C., Katz, M., Lee, R., Whitelegge, J., & Tontonoz, P. (2016). Feedback modulation of cholesterol metabolism by the lipid-responsive non-coding RNA LeXis. *Nature*, *534*(7605), 124–128. https://doi.org/10.1038/nature17674

Sanderson, J. T. (n.d.). *The Steroid Hormone Biosynthesis Pathway as a Target for Endocrine-Disrupting Chemicals*. https://doi.org/10.1093/toxsci/kfl051

Sandhoff, R., Brügger, B., Jeckel, D., Lehmann, W. D., & Wieland, F. T. (1999). Determination of cholesterol at the low picomole level by nano-electrospray ionization tandem mass spectrometry. *Journal of Lipid Research*, *40*(1), 126–132. https://doi.org/10.1016/S0022-2275(20)33347-2

Sandhu, J., Li, S., Fairall, L., Pfisterer, S. G., Gurnett, J. E., Xiao, X., Weston, T. A., Vashi, D., Ferrari, A., Orozco, J. L., Hartman, C. L., Strugatsky, D., Lee, S. D., He, C., Hong, C., Jiang, H., Bentolila, L. A., Gatta, A. T., Levine, T. P., … Tontonoz, P. (2018). Aster Proteins Facilitate Nonvesicular Plasma Membrane to ER Cholesterol Transport in Mammalian Cells. *Cell*, *175*(2), 514-529.e20. https://doi.org/10.1016/j.cell.2018.08.033

Sarah A. Holstein, & Raymond J. Hohl. (2004). Isoprenoids: Remarkable Diversity of Form and Function. *Lipids*, *39*(4), 293–309. https://doi.org/10.1007/s11745-004-1233-3

Sardi, S. P., Clarke, J., Viel, C., Chan, M., Tamsett, T. J., Treleaven, C. M., Bu, J., Sweet, L., Passini, M. A., Dodge, J. C., Yu, W. H., Sidman, R. L., Cheng, S. H., & Shihabuddin, L. S. (2013). Augmenting CNS glucocerebrosidase activity as a therapeutic

strategy for parkinsonism and other Gaucher-related synucleinopathies. *Proceedings of the National Academy of Sciences*, *110*(9), 3537–3542. https://doi.org/10.1073/pnas.1220464110

Sarkar, S., Davies, J. E., Huang, Z., Tunnacliffe, A., & Rubinsztein, D. C. (2007). Trehalose, a Novel mTOR-independent Autophagy Enhancer, Accelerates the Clearance of Mutant Huntingtin and α-Synuclein. *Journal of Biological Chemistry*, *282*(8), 5641–5652. https://doi.org/10.1074/jbc.M609532200

Sathitnaitham, S., Suttangkakul, A., Wonnapinij, P., McQueen-Mason, S. J., & Vuttipongchaikij, S. (2021). Gel-permeation chromatography–enzyme-linked immunosorbent assay method for systematic mass distribution profiling of plant cell wall matrix polysaccharides. *The Plant Journal*, *106*(6), 1776–1790. https://doi.org/10.1111/tpj.15255

Savinova, T. S., Diep, N. T., Voishvillo, N. E., Andryushina, V. A., Karpova, N. V., Beletskaya, I. P., & Huy, L. D. (2012). Extraction of a mixture of phytosterols from soybean processing by-product and its use in the manufacture of 9α-hydroxyandrost-4-en-3,17-dione. *Pharmaceutical Chemistry Journal*, *46*(3), 183–186. https://doi.org/10.1007/s11094-012-0756-6

Sayre, L. M., Perry, G., & Smith, M. A. (2008). Oxidative stress and neurotoxicity. In *Chemical Research in Toxicology*. https://doi.org/10.1021/tx700210j

Schade, D. S., Shey, L., & Eaton, R. P. (2020). Cholesterol review: A metabolically important molecule. In *Endocrine Practice* (Vol. 26, Issue 12, pp. 1514–1523). American Association of Clinical Endocrinologists. https://doi.org/10.4158/EP-2020-0347

Schapira, A. H. V. (2007). Mitochondrial dysfunction in Parkinson's disease. *Cell Death & Differentiation*, *14*(7), 1261–1266. https://doi.org/10.1038/sj.cdd.4402160

Schiffer, L., Barnard, L., Baranowski, E. S., Gilligan, L. C., Taylor, A. E., Arlt, W., Shackleton, C. H. L., & Storbeck, K.-H. (2019). Human steroid biosynthesis, metabolism and excretion are differentially reflected by serum and urine steroid metabolomes: A comprehensive review. *The Journal of Steroid Biochemistry and Molecular Biology*, *194*, 105439. https://doi.org/10.1016/j.jsbmb.2019.105439

Schöls, L., Rattay, T. W., Martus, P., Meisner, C., Baets, J., Fischer, I., Jägle, C., Fraidakis, M. J., Martinuzzi, A., Saute, J. A., Scarlato, M., Antenora, A., Stendel, C., Höflinger, P., Lourenco, C. M., Abreu, L., Smets, K., Paucar, M., Deconinck, T., … Schüle, R. (2017). Hereditary spastic paraplegia type 5: natural history, biomarkers and a randomized controlled trial. *Brain*, *140*(12), 3112–3127. https://doi.org/10.1093/brain/awx273

Scholsky, K. M. (1989). *Supercritical Phase Transitions at Very High Pressure* (Vol. 66). UTC. https://pubs.acs.org/sharingguidelines

Schönknecht, P., Lütjohann, D., Pantel, J., Bardenheuer, H., Hartmann, T., von Bergmann, K., Beyreuther, K., & Schröder, J. (2002). Cerebrospinal fluid 24S-hydroxycholesterol is increased in patients with Alzheimer's disease compared to healthy controls. *Neuroscience Letters*, *324*(1), 83–85. https://doi.org/10.1016/S0304-3940(02)00164-7

Schroepfer, G. J. (2000a). Oxysterols: modulators of cholesterol metabolism and other processes. *Physiological Reviews*, *80*(1), 361–554. http://www.ncbi.nlm.nih.gov/pubmed/10617772

Schroepfer, G. J. (2000b). *Oxysterols: Modulators of Cholesterol Metabolism and Other Processes*.

Schwudke, D., Oegema, J., Burton, L., Entchev, E., Hannich, J. T., Ejsing, C. S., Kurzchalia, T., & Shevchenko, A. (2006). Lipid Profiling by Multiple Precursor and Neutral Loss Scanning Driven by the Data-Dependent Acquisition. *Analytical Chemistry*, *78*(2), 585–595. https://doi.org/10.1021/ac051605m

Scott, D. A., Tabarean, I., Tang, Y., Cartier, A., Masliah, E., & Roy, S. (2010). A Pathologic Cascade Leading to Synaptic Dysfunction in -Synuclein-Induced Neurodegeneration. *Journal of Neuroscience*, *30*(24), 8083–8095. https://doi.org/10.1523/JNEUROSCI.1091-10.2010

Selkoe, D. J. (2011). Resolving controversies on the path to Alzheimer's therapeutics. *Nature Medicine*, *17*(9), 1060–1065. https://doi.org/10.1038/nm.2460

Selkoe, D. J., & Hardy, J. (2016). The amyloid hypothesis of Alzheimer's disease at 25 years. *EMBO Molecular Medicine*, *8*(6), 595–608. https://doi.org/10.15252/emmm.201606210

Senko, M. W., Remes, P. M., Canterbury, J. D., Mathur, R., Song, Q., Eliuk, S. M., Mullen, C., Earley, L., Hardman, M., Blethrow, J. D., Bui, H., Specht, A., Lange, O., Denisov, E., Makarov, A., Horning, S., & Zabrouskov, V. (2013). Novel Parallelized Quadrupole/Linear Ion Trap/Orbitrap Tribrid Mass Spectrometer Improving Proteome Coverage and Peptide Identification Rates. *Analytical Chemistry*, *85*(24), 11710–11714. https://doi.org/10.1021/ac403115c

Seol, W., Choi, H. S., & Moore, D. D. (1995). Isolation of proteins that interact specifically with the retinoid X receptor: two novel

orphan receptors. *Molecular Endocrinology*, *9*(1), 72–85. https://doi.org/10.1210/mend.9.1.7760852

Sezgin, E., Levental, I., Mayor, S., & Eggeling, C. (2017). The mystery of membrane organization: Composition, regulation and roles of lipid rafts. In *Nature Reviews Molecular Cell Biology*. https://doi.org/10.1038/nrm.2017.16

Shackleton, C. H. L., Chuang, H., Kim, J., de la Torre, X., & Segura, J. (1997). Electrospray mass spectrometry of testosterone esters: Potential for use in doping control. *Steroids*, *62*(7), 523–529. https://doi.org/10.1016/S0039-128X(97)00004-4

Shan, H., Pang, J., Li, S., Chiang, T. B., Wilson, W. K., & Schroepfer, G. J. (2003). Chromatographic behavior of oxygenated derivatives of cholesterol. *Steroids*, *68*(3), 221–233. https://doi.org/10.1016/S0039-128X(02)00185-X

Shen, A., Li, X., Dong, X., Wei, J., Guo, Z., & Liang, X. (2013). Glutathione-based zwitterionic stationary phase for hydrophilic interaction/cation-exchange mixed-mode chromatography. *Journal of Chromatography A*, *1314*, 63–69. https://doi.org/10.1016/j.chroma.2013.09.002

Sherrington, R., Rogaev, E. I., Liang, Y., Rogaeva, E. A., Levesque, G., Ikeda, M., Chi, H., Lin, C., Li, G., Holman, K., Tsuda, T., Mar, L., Foncin, J.-F., Bruni, A. C., Montesi, M. P., Sorbi, S., Rainero, I., Pinessi, L., Nee, L., … St George-Hyslop, P. H. (1995). Cloning of a gene bearing missense mutations in early-onset familial Alzheimer's disease. *Nature*, *375*(6534), 754–760. https://doi.org/10.1038/375754a0

Shi, Q., Chen, J., Zou, X., & Tang, X. (2022). *Intracellular Cholesterol Synthesis and Transport*. https://doi.org/10.3389/fcell.2022.819281

Shibata, M., Yamada, S., Kumar, S. R., Calero, M., Bading, J., Frangione, B., Holtzman, D. M., Miller, C. A., Strickland, D. K., Ghiso, J., & Zlokovic, B. V. (2000). Clearance of Alzheimer's amyloid-ß1-40 peptide from brain by LDL receptor–related protein-1 at the blood-brain barrier. *Journal of Clinical Investigation*, *106*(12), 1489–1499. https://doi.org/10.1172/JCI10498

Shinar, D. M., Endo, N., Rutledge, S. J., Vogel, R., Rodan, G. A., & Schmidt, A. (1994). NER, a new member of the gene family encoding the human steroid hormone nuclear receptor. *Gene*, *147*(2), 273–276. https://doi.org/10.1016/0378-1119(94)90080-9

Sidransky, E., Nalls, M. A., Aasly, J. O., Aharon-Peretz, J., Annesi, G., Barbosa, E. R., Bar-Shira, A., Berg, D., Bras, J., Brice, A., Chen, C.-M., Clark, L. N., Condroyer, C., De Marco, E. V., Dürr, A., Eblan, M. J., Fahn, S., Farrer, M. J., Fung, H.-C., … Ziegler, S. G. (2009). Multicenter Analysis of Glucocerebrosidase Mutations in Parkinson's Disease. *New England Journal of Medicine*, *361*(17), 1651–1661. https://doi.org/10.1056/NEJMoa0901281

Simons, K., & Ehehalt, R. (2002). Cholesterol, lipid rafts, and disease. *Journal of Clinical Investigation*, *110*(5), 597–603. https://doi.org/10.1172/JCI16390

Simons, K., & Ikonen, E. (2000). How cells handle cholesterol. *Science*, *290*(5497), 1721 LP – 1726. https://doi.org/10.1126/science.290.5497.1721

Singh, M., Jain, M., Bose, S., Halder, A., Nag, T. C., Dinda, A. K., & Mohanty, S. (2021). 22(R)-hydroxycholesterol for dopaminergic neuroneal specification of MSCs and amelioration of Parkinsonian symptoms in rats. *Cell Death Discovery*, *7*(1). https://doi.org/10.1038/s41420-020-00351-6

Skibinski, G., Nakamura, K., Cookson, M. R., & Finkbeiner, S. (2014). Mutant LRRK2 Toxicity in NeuroneNeuronees Depends on LRRK2 Levels and Synuclein But Not Kinase Activity or Inclusion Bodies. *Journal of Neuroscience*, *34*(2), 418–433. https://doi.org/10.1523/JNEUROSCI.2712-13.2014

Skubic, C., Vovk, I., Rozman, D., & Križman, M. (2020). Simplified LC-MS Method for Analysis of Sterols in Biological Samples. *Molecules*, *25*(18), 4116. https://doi.org/10.3390/molecules25184116

Sleeman R., & Carter J. F. (2005). Mass Spectrometry. *Encyclopedia of Anlatical Science* , 337–344. https://doi.org/10.1016/b0-12-369397-7/00342-3

Smith, A. D. (n.d.). *Imaging the progression of Alzheimer pathology through the brain*. www.pnas.orgcgidoi10.1073pnas.082107399

Smith, L. C., Pownall, H. J., & Gotto, A. M. (1978). The Plasma Lipoproteins: Structure and Metabolism. *Annual Review of Biochemistry*, *47*(1), 751–777. https://doi.org/10.1146/annurev.bi.47.070178.003535

Smith, L. L. (1987). Cholesterol autoxidation 1981–1986. *Chemistry and Physics of Lipids*, *44*(2–4), 87–125. https://doi.org/10.1016/0009-3084(87)90046-6

Soccio, R. E., & Breslow, J. L. (2004). Intracellular Cholesterol Transport. *Arteriosclerosis, Thrombosis, and Vascular Biology*, *24*(7), 1150–1160. https://doi.org/10.1161/01.ATV.0000131264.66417.d5

Sodero, A. O. (2021a). 24S-hydroxycholesterol: Cellular effects and variations in brain diseases. In *Journal of Neurochemistry* (Vol. 157, Issue 4, pp. 899–918). John Wiley and Sons Inc. https://doi.org/10.1111/jnc.15228

Sodero, A. O. (2021b). 24S-hydroxycholesterol: Cellular effects and variations in brain diseases. In *Journal of Neurochemistry* (Vol. 157, Issue 4, pp. 899–918). John Wiley and Sons Inc. https://doi.org/10.1111/jnc.15228

Sodero, A. O., Weissmann, C., Ledesma, M. D., & Dotti, C. G. (2011). Cellular stress from excitatory neurotransmission contributes to cholesterol loss in hippocampal neuroneneuronees aging in vitro. *Neurobiology of Aging*, *32*(6), 1043–1053. https://doi.org/10.1016/j.neurobiolaging.2010.06.001

SONG, C., HIIPAKKA, R. A., KOKONTIS, J. M., & LIAO, S. (1995). Ubiquitous Receptor: Structures, Immunocytochemical Localization, and Modulation of Gene Activation by Receptors for Retinoic Acids and Thyroid Hormones. *Annals of the New York Academy of Sciences*, *761*(1), 38–49. https://doi.org/10.1111/j.1749-6632.1995.tb31367.x

Song, C., Kokontis, J. M., Hiipakka, R. A., & Liao, S. (1994). Ubiquitous receptor: a receptor that modulates gene activation by retinoic acid and thyroid hormone receptors. *Proceedings of the National Academy of Sciences*, *91*(23), 10809–10813. https://doi.org/10.1073/pnas.91.23.10809

Song, C., & Liao, S. (2000). Cholestenoic Acid Is a Naturally Occurring Ligand for Liver X Receptor α**This work was supported by NIH grants. *Endocrinology*, *141*(11), 4180–4184. https://doi.org/10.1210/endo.141.11.7772

Sossi, V., de la Fuente-Fernández, R., Holden, J. E., Schulzer, M., Ruth, T. J., & Stoessl, J. (2004). Changes of Dopamine Turnover in the Progression of Parkinson's Disease as Measured by Positron Emission Tomography: Their Relation to Disease-Compensatory Mechanisms. *Journal of Cerebral Blood Flow & Metabolism*, *24*(8), 869–876. https://doi.org/10.1097/01.WCB.0000126563.85360.75

Sossi, V., de la Fuente-Fernández, R., Nandhagopal, R., Schulzer, M., McKenzie, J., Ruth, T. J., Aasly, J. O., Farrer, M. J., Wszolek, Z. K., & Stoessl, J. A. (2010). Dopamine turnover increases in asymptomatic *LRRK2* mutations carriers. *Movement Disorders*, *25*(16), 2717–2723. https://doi.org/10.1002/mds.23356

Spann, N. J.; Glass, C. K. (2013). Sterols and oxysterols in immune cell function. *Nature Immunology*, *14*(9), 893–900.

Spencer, T. A., Li, D., Russel, J. S., Collins, J. L., Bledsoe, R. K., Consler, T. G., Moore, L. B., Galardi, C. M., McKee, D. D., Moore, J. T., Watson, M. A., Parks, D. J., Lambert, M. H., & Willson, T. M. (2001). Pharmacophore Analysis of the Nuclear Oxysterol Receptor LXRα. *Journal of Medicinal Chemistry*, *44*(6), 886–897. https://doi.org/10.1021/jm0004749

Staels, B., & Fonseca, V. A. (2009). Bile Acids and Metabolic Regulation. *Diabetes Care*, *32*(suppl_2), S237–S245. https://doi.org/10.2337/dc09-S355

Stafford, G. C., Kelley, P. E., Syka, J. E. P., Reynolds, W. E., & Todd, J. F. J. (1984). Recent improvements in and analytical applications of advanced ion trap technology. *International Journal of Mass Spectrometry and Ion Processes*, *60*(1), 85–98. https://doi.org/10.1016/0168-1176(84)80077-4

Steele, J. W., Ju, S., Lachenmayer, M. L., Liken, J., Stock, A., Kim, S. H., Delgado, L. M., Alfaro, I. E., Bernales, S., Verdile, G., Bharadwaj, P., Gupta, V., Barr, R., Friss, A., Dolios, G., Wang, R., Ringe, D., Protter, A. A., Martins, R. N., … Gandy, S. (2013). Latrepirdine stimulates autophagy and reduces accumulation of α-synuclein in cells and in mouse brain. *Molecular Psychiatry*, *18*(8), 882–888. https://doi.org/10.1038/mp.2012.115

Stelzmann, R. A., Norman Schnitzlein, H., & Reed Murtagh, F. (1995). An english translation of alzheimer's 1907 paper, "über eine eigenartige erkankung der hirnrinde." *Clinical Anatomy*, *8*(6), 429–431. https://doi.org/10.1002/ca.980080612

Sterling, N. W., Lichtenstein, M., Lee, E.-Y., Lewis, M. M., Evans, A., Eslinger, P. J., Du, G., Gao, X., Chen, H., Kong, L., & Huang, X. (2016a). Higher Plasma LDL-Cholesterol is Associated with Preserved Executive and Fine Motor Functions in Parkinson's Disease. *Aging and Disease*, *7*(3), 237. https://doi.org/10.14336/AD.2015.1030

Sterling, N. W., Lichtenstein, M., Lee, E.-Y., Lewis, M. M., Evans, A., Eslinger, P. J., Du, G., Gao, X., Chen, H., Kong, L., & Huang, X. (2016b). Higher Plasma LDL-Cholesterol is Associated with Preserved Executive and Fine Motor Functions in Parkinson's Disease. *Aging and Disease*, *7*(3), 237. https://doi.org/10.14336/AD.2015.1030

Stiles, A. R., Kozlitina, J., Thompson, B. M., McDonald, J. G., King, K. S., & Russell, D. W. (2014a). Genetic, anatomic, and clinical determinants of human serum sterol and vitamin D levels. *Proceedings of the National Academy of Sciences*, *111*(38). https://doi.org/10.1073/pnas.1413561111

Stiles, A. R., Kozlitina, J., Thompson, B. M., McDonald, J. G., King, K. S., & Russell, D. W. (2014b). Genetic, anatomic, and clinical determinants of human serum sterol and vitamin D levels. *Proceedings of the National Academy of Sciences*, *111*(38). https://doi.org/10.1073/pnas.1413561111

Strittmatter, W. J., Saunders, A. M., Schmechel, D., Pericak-Vance, M., Enghild, J., Salvesen, G. S., & Roses, A. D. (1993). Apolipoprotein E: high-avidity binding to beta-amyloid and increased frequency of type 4 allele in late-onset familial Alzheimer disease. *Proceedings of the National Academy of Sciences*, *90*(5), 1977–1981. https://doi.org/10.1073/pnas.90.5.1977

Surmeier, D. J., Guzman, J. N., Sanchez-Padilla, J., & Schumacker, P. T. (2011). The role of calcium and mitochondrial oxidant stress in the loss of substantia nigra pars compacta dopaminergic neuroneneuronees in Parkinson's disease. *Neuroscience*, *198*, 221–231. https://doi.org/10.1016/j.neuroscience.2011.08.045

Surmeier, D. J., Schumacker, P. T., Guzman, J. D., Ilijic, E., Yang, B., & Zampese, E. (2017). Calcium and Parkinson's disease. *Biochemical and Biophysical Research Communications*, *483*(4), 1013–1019. https://doi.org/10.1016/j.bbrc.2016.08.168

Szedlacsek, S. E., Wasowicz, E., Hulea, S. A., Nishida, H. I., Kummerow, F. A., & Nishida, T. (1995a). Esterification of

Oxysterols by Human Plasma Lecithin-Cholesterol Acyltransferase. *Journal of Biological Chemistry*, *270*(20), 11812–11819. https://doi.org/10.1074/JBC.270.20.11812

Szedlacsek, S. E., Wasowicz, E., Hulea, S. A., Nishida, H. I., Kummerow, F. A., & Nishida, T. (1995b). Esterification of Oxysterols by Human Plasma Lecithin-Cholesterol Acyltransferase. *Journal of Biological Chemistry*, *270*(20), 11812–11819. https://doi.org/10.1074/jbc.270.20.11812

Tabas, I. (2002). Consequences of cellular cholesterol accumulation: basic concepts and physiological implications. *Journal of Clinical Investigation*, *110*(7), 905–911. https://doi.org/10.1172/JCI16452

Tahami Monfared, A. A., Byrnes, M. J., White, L. A., & Zhang, Q. (2022). Alzheimer's Disease: Epidemiology and Clinical Progression. In *Neurology and Therapy* (Vol. 11, Issue 2, pp. 553–569). Adis. https://doi.org/10.1007/s40120-022-00338-8

Tall, A. R.; Yvan-Charvet, L. (2015). Cholesterol, inflammation and innate immunity. *Nature Reviews. Immunology*, *15*, 104–116.

Tang, Z., Scherer, P. E., Okamoto, T., Song, K., Chu, C., Kohtz, D. S., Nishimoto, I., Lodish, H. F., & Lisanti, M. P. (1996). Molecular cloning of caveolin-3, a novel member of the caveolin gene family expressed predominantly in muscle. *The Journal of Biological Chemistry*, *271*(4), 2255–2261. https://doi.org/10.1074/jbc.271.4.2255

Tanik, S. A., Schultheiss, C. E., Volpicelli-Daley, L. A., Brunden, K. R., & Lee, V. M. Y. (2013). Lewy Body-like α-Synuclein Aggregates Resist Degradation and Impair Macroautophagy. *Journal of Biological Chemistry*, *288*(21), 15194–15210. https://doi.org/10.1074/jbc.M113.457408

Tcw, J., Liang, S. A., Qian, L., Pipalia, N. H., Chao, M. J., Shi, Y., Bertelsen, S. E., Kapoor, M., Marcora, E., Sikora, E., Holtzman, D. M., Maxfield, F. R., Zhang, B., Wang, M., Poon, W. W., Goate, A. M., & Goate, A. (2019). *Cholesterol and matrisome pathways dysregulated in human APOE ε4 glia*. https://doi.org/10.1101/713362

Teboul, M., Enmark, E., Li, Q., Wikström, A. C., Pelto-Huikko, M., & Gustafsson, J. A. (1995). OR-1, a member of the nuclear receptor superfamily that interacts with the 9-cis-retinoic acid receptor. *Proceedings of the National Academy of Sciences*, *92*(6), 2096–2100. https://doi.org/10.1073/pnas.92.6.2096

Testa, G., Staurenghi, E., Zerbinati, C., Gargiulo, S., Iuliano, L., Giaccone, G., Fantò, F., Poli, G., Leonarduzzi, G., & Gamba, P. (2016a). Changes in brain oxysterols at different stages of Alzheimer's disease: Their involvement in neuroinflammation. *Redox Biology*, *10*, 24–33. https://doi.org/10.1016/j.redox.2016.09.001

Testa, G., Staurenghi, E., Zerbinati, C., Gargiulo, S., Iuliano, L., Giaccone, G., Fantò, F., Poli, G., Leonarduzzi, G., & Gamba, P. (2016b). Changes in brain oxysterols at different stages of Alzheimer's disease: Their involvement in neuroinflammation. *Redox Biology*, *10*, 24–33. https://doi.org/10.1016/j.redox.2016.09.001

Testa, G., Staurenghi, E., Zerbinati, C., Gargiulo, S., Iuliano, L., Giaccone, G., Fantò, F., Poli, G., Leonarduzzi, G., & Gamba, P. (2016c). Changes in brain oxysterols at different stages of Alzheimer's disease: Their involvement in neuroinflammation.

Redox Biology, *10*, 24–33. https://doi.org/10.1016/j.redox.2016.09.001

Theofilopoulos, S., Griffiths, W. J., Crick, P. J., Yang, S., Meljon, A., Ogundare, M., Kitambi, S. S., Lockhart, A., Tuschl, K., Clayton, P. T., Morris, A. A., Martinez, A., Reddy, M. A., Martinuzzi, A., Bassi, M. T., Honda, A., Mizuochi, T., Kimura, A., Nittono, H., … Wang, Y. (2014). Cholestenoic acids regulate motor neurone survival via liver X receptors. *Journal of Clinical Investigation*, *124*(11), 4829–4842. https://doi.org/10.1172/JCI68506

Thomas, M. C., Mitchell, T. W., & Blanksby, S. J. (2005). A comparison of the gas phase acidities of phospholipid headgroups: Experimental and computational studies. *Journal of the American Society for Mass Spectrometry*, *16*(6), 926–939. https://doi.org/10.1016/j.jasms.2005.02.019

Tomasello, D. L., Kim, J. L., Khodour, Y., McCammon, J. M., Mitalipova, M., Jaenisch, R., Futerman, A. H., & Sive, H. (2022). 16pdel lipid changes in iPSC-derived neuroneneuronees and function of FAM57B in lipid metabolism and synaptogenesis. *IScience*, *25*(1). https://doi.org/10.1016/j.isci.2021.103551

Toshimasa Toyo'oka. (1999). *Modern Derivatization Methods for Separation Science* (wiley, Ed.).

Trinh, M. N., Brown, M. S., Goldstein, J. L., Han, J., Vale, G., McDonald, J. G., Seemann, J., Mendell, J. T., & Lu, F. (2020). Last step in the path of LDL cholesterol from lysosome to plasma membrane to ER is governed by phosphatidylserine. *Proceedings of the National Academy of Sciences*, *117*(31), 18521–18529. https://doi.org/10.1073/pnas.2010682117

Trinh, M. N., Brown, M. S., Seemann, J., Vale, G., McDonald, J. G., Goldstein, J. L., & Lu, F. (2022). Interplay between Asters/GRAMD1s and phosphatidylserine in intermembrane transport of LDL cholesterol. *Proceedings of the National Academy of Sciences*, *119*(2). https://doi.org/10.1073/pnas.2120411119

Tswett, M. S. (1905). (On a new category of adsorption phenomena and on its application to biochemical analysis. *Proceedings of the Warsaw Society of Naturalists [i.e., Natural Scientists], Biology Section*, *14*(6), 20–39.

Twelves, D., Perkins, K. S. M., & Counsell, C. (2003). Systematic review of incidence studies of Parkinson's disease. In *Movement Disorders* (Vol. 18, Issue 1, pp. 19–31). https://doi.org/10.1002/mds.10305

Tysnes, O. B., & Storstein, A. (2017). Epidemiology of Parkinson's disease. In *Journal of Neural Transmission*. https://doi.org/10.1007/s00702-017-1686-y

Tyson, T., Steiner, J. A., & Brundin, P. (2016). Sorting out release, uptake and processing of alpha-synuclein during prion-like spread of pathology. *Journal of Neurochemistry*, *139*, 275–289. https://doi.org/10.1111/jnc.13449

Uittenbogaard, A., Everson, W. V., Matveev, S. V., & Smart, E. J. (2002). Cholesteryl Ester Is Transported from Caveolae to Internal Membranes as Part of a Caveolin-Annexin II Lipid-Protein Complex. *Journal of Biological Chemistry*, *277*(7), 4925–4931. https://doi.org/10.1074/jbc.M109278200

Umetani, M., Domoto, H., Gormley, A. K., Yuhanna, I. S., Cummins, C. L., Javitt, N. B., Korach, K. S., Shaul, P. W., & Mangelsdorf,

D. J. (2007). *27-Hydroxycholesterol is an endogenous SERM that inhibits the cardiovascular effects of estrogen*. https://doi.org/10.1038/nm1641

Urbani, L., & Simoni, R. D. (1990). Cholesterol and vesicular stomatitis virus G protein take separate routes from the endoplasmic reticulum to the plasma membrane. *Journal of Biological Chemistry*, *265*(4), 1919–1923. https://doi.org/10.1016/S0021-9258(19)39918-1

Valenza, M., Carroll, J. B., Leoni, V., Bertram, L. N., Björkhem, I., Singaraja, R. R., Di Donato, S., Lutjohann, D., Hayden, M. R., & Cattaneo, E. (2007). Cholesterol biosynthesis pathway is disturbed in YAC128 mice and is modulated by huntingtin mutation. *Human Molecular Genetics*. https://doi.org/10.1093/hmg/ddm170

Valenza, M., Leoni, V., Tarditi, A., Mariotti, C., Björkhem, I., Di Donato, S., & Cattaneo, E. (2007). Progressive dysfunction of the cholesterol biosynthesis pathway in the R6/2 mouse model of Huntington's disease. *Neurobiology of Disease*. https://doi.org/10.1016/j.nbd.2007.07.004

Valitova, J. N., Sulkarnayeva, A. G., & Minibayeva, F. V. (2016). Plant sterols: Diversity, biosynthesis, and physiological functions. In *Biochemistry (Moscow)* (Vol. 81, Issue 8, pp. 819–834). Maik Nauka Publishing / Springer SBM. https://doi.org/10.1134/S0006297916080046

Van Giau, V., Bagyinszky, E., An, S. S., & Kim, S. (2015). Role of apolipoprotein E in neurodegenerative diseases. *Neuropsychiatric Disease and Treatment*, 1723. https://doi.org/10.2147/NDT.S84266

van Maarschalkerweerd, A., Vetri, V., & Vestergaard, B. (2015). Cholesterol facilitates interactions between α-synuclein oligomers and charge-neutral membranes. *FEBS Letters*, *589*(19PartB), 2661–2667. https://doi.org/10.1016/j.febslet.2015.08.013

Varma, V. R., Büşra Lüleci, H., Oommen, A. M., Varma, S., Blackshear, C. T., Griswold, M. E., An, Y., Roberts, J. A., O'Brien, R., Pletnikova, O., Troncoso, J. C., Bennett, D. A., Çakır, T., Legido-Quigley, C., & Thambisetty, M. (2021). Abnormal brain cholesterol homeostasis in Alzheimer's disease—a targeted metabolomic and transcriptomic study. *Npj Aging and Mechanisms of Disease*, *7*(1). https://doi.org/10.1038/s41514-021-00064-9

Vaz, F. M., & Ferdinandusse, S. (2017). Bile acid analysis in human disorders of bile acid biosynthesis. In *Molecular Aspects of Medicine* (Vol. 56, pp. 10–24). Elsevier Ltd. https://doi.org/10.1016/j.mam.2017.03.003

Vehus, T., Roberg-Larsen, H., Waaler, J., Aslaksen, S., Krauss, S., Wilson, S. R., & Lundanes, E. (2016). Versatile, sensitive liquid chromatography mass spectrometry-Implementation of 10 µm OT columns suitable for small molecules, peptides and proteins. *Scientific Reports*, *6*. https://doi.org/10.1038/srep37507

Vejux, A., & Lizard, G. (2009). Cytotoxic effects of oxysterols associated with human diseases: Induction of cell death (apoptosis and/or oncosis), oxidative and inflammatory activities, and phospholipidosis. *Molecular Aspects of Medicine*, *30*(3), 153–170. https://doi.org/10.1016/J.MAM.2009.02.006

Vekrellis, K., Rideout, H. J., & Stefanis, L. (2004). Neurobiology of α-Synuclein. *Molecular Neurobiology*, *30*(1), 001–022. https://doi.org/10.1385/MN:30:1:001

Vekrellis, K., Xilouri, M., Emmanouilidou, E., Rideout, H. J., & Stefanis, L. (2011). Pathological roles of α-synuclein in neurological disorders. *The Lancet Neurology*, *10*(11), 1015–1025. https://doi.org/10.1016/S1474-4422(11)70213-7

Venkateswaran, A., Laffitte, B. A., Joseph, S. B., Mak, P. A., Wilpitz, D. C., Edwards, P. A., & Tontonoz, P. (2000). Control of cellular cholesterol efflux by the nuclear oxysterol receptor LXRalpha. *Proceedings of the National Academy of Sciences*, *97*(22), 12097–12102. https://doi.org/10.1073/pnas.200367697

Vesa M. Olkkonen; Olivier Béaslas; Eija Nissilä. (2012). Oxysterols and Their Cellular Effectors. *Biomolecules*, *2*, 76–103.

Vilariño-Güell, C., Wider, C., Ross, O. A., Dachsel, J. C., Kachergus, J. M., Lincoln, S. J., Soto-Ortolaza, A. I., Cobb, S. A., Wilhoite, G. J., Bacon, J. A., Behrouz, B., Melrose, H. L., Hentati, E., Puschmann, A., Evans, D. M., Conibear, E., Wasserman, W. W., Aasly, J. O., Burkhard, P. R., … Farrer, M. J. (2011). VPS35 Mutations in Parkinson Disease. *The American Journal of Human Genetics*, *89*(1), 162–167. https://doi.org/10.1016/j.ajhg.2011.06.001

Voisin, M., de Medina, P., Mallinger, A., Dalenc, F., Huc-Claustre, E., Leignadier, J., Serhan, N., Soules, R., Ségala, G., Mougel, A., Noguer, E., Mhamdi, L., Bacquié, E., Iuliano, L., Zerbinati, C., Lacroix-Triki, M., Chaltiel, L., Filleron, T., Cavaillès, V., … Silvente-Poirot, S. (2017). Identification of a tumor-promoter cholesterol metabolite in human breast cancers acting through

the glucocorticoid receptor. *Proceedings of the National Academy of Sciences*, *114*(44). https://doi.org/10.1073/pnas.1707965114

Volpicelli-Daley, L. A., Abdelmotilib, H., Liu, Z., Stoyka, L., Daher, J. P. L., Milnerwood, A. J., Unni, V. K., Hirst, W. D., Yue, Z., Zhao, H. T., Fraser, K., Kennedy, R. E., & West, A. B. (2016). G2019S-LRRK2 Expression Augments -Synuclein Sequestration into Inclusions in NeuroneNeuronees. *Journal of Neuroscience*, *36*(28), 7415–7427. https://doi.org/10.1523/JNEUROSCI.3642-15.2016

Vonsattel, J. P. G., Keller, C., & Cortes Ramirez, E. P. (2011). Huntington's disease - neuropathology. In *Handbook of Clinical Neurology*. https://doi.org/10.1016/B978-0-444-52014-2.00004-5

Wales, P., Pinho, R., Lázaro, D. F., & Outeiro, T. F. (2013). Limelight on Alpha-Synuclein: Pathological and Mechanistic Implications in Neurodegeneration. *Journal of Parkinson's Disease*, *3*(4), 415–459. https://doi.org/10.3233/JPD-130216

Wang, H. L., Wang, Y. Y., Liu, X. G., Kuo, S. H., Liu, N., Song, Q. Y., & Wang, M. W. (2016). Cholesterol, 24-Hydroxycholesterol, and 27-Hydroxycholesterol as Surrogate Biomarkers in Cerebrospinal Fluid in Mild Cognitive Impairment and Alzheimer's Disease: A Meta-Analysis. *Journal of Alzheimer's Disease*, *51*(1), 45–55. https://doi.org/10.3233/JAD-150734

Wang, K., Luo, Z., Li, C., Huang, X., Shiroma, E. J., Simonsick, E. M., & Chen, H. (2021). Blood Cholesterol Decreases as Parkinson's Disease Develops and Progresses. *Journal of Parkinson's Disease*, *11*(3), 1177–1186. https://doi.org/10.3233/JPD-212670

Wang, N., Ranalletta, M., Matsuura, F., Peng, F., & Tall, A. R. (2006). LXR-induced redistribution of ABCG1 to plasma membrane in

macrophages enhances cholesterol mass efflux to HDL. *Arteriosclerosis, Thrombosis, and Vascular Biology*, *26*(6), 1310–1316. https://doi.org/10.1161/01.ATV.0000218998.75963.02

Wang, P., Zhang, H., Wang, Y., Zhang, M., & Zhou, Y. (2020). Plasma cholesterol in Alzheimer's disease and frontotemporal dementia. *Translational Neuroscience*, *11*(1), 116–123. https://doi.org/10.1515/tnsci-2020-0098

Wang, Q., Liu, Y., & Zhou, J. (2015). Neuroinflammation in Parkinson's disease and its potential as therapeutic target. In *Translational Neurodegeneration*. https://doi.org/10.1186/s40035-015-0042-0

Wang, S., Li, W., Hui, H., Tiwari, S. K., Zhang, Q., Croker, B. A., Rawlings, S., Smith, D., Carlin, A. F., & Rana, T. M. (2020). Cholesterol 25-Hydroxylase inhibits <scp>SARS</scp> -CoV-2 and other coronaviruses by depleting membrane cholesterol. *The EMBO Journal*, *39*(21). https://doi.org/10.15252/embj.2020106057

Wang, Y., Muneton, S., Sjövall, J., Jovanovic, J. N., & Griffiths, W. J. (2008). The effect of 24S-hydroxycholesterol on cholesterol Homeostasis in neuroneneuronees: Quantitative changes to the cortical neurone proteome. *Journal of Proteome Research*, *7*(4), 1606–1614. https://doi.org/10.1021/pr7006076

Wang, Y., Sousa, K. M., Bodin, K., Theofilopoulos, S., Sacchetti, P., Hornshaw, M., Woffendin, G., Karu, K., Sjo¨vall, J. S., Arenas, E., & Griffiths, W. J. (n.d.). *Targeted lipidomic analysis of oxysterols in the embryonic central nervous systemw*. https://doi.org/10.1039/b819502a

Wang, Y., Sousa, K. M., Bodin, K., Theofilopoulos, S., Sacchetti, P., Hornshaw, M., Woffendin, G., Karu, K., Sjövall, J., Arenas, E., & Griffiths, W. J. (2009). Targeted lipidomic analysis of oxysterols in the embryonic central nervous system. *Molecular BioSystems*, *5*(5), 529. https://doi.org/10.1039/b819502a

Wang, Y., Yutuc, E., & Griffiths, W. J. (2021). Neuro-oxysterols and neuro-sterols as ligands to nuclear receptors, GPCRs, ligand-gated ion channels and other protein receptors. *British Journal of Pharmacology*, *178*(16), 3176–3193. https://doi.org/10.1111/bph.15191

Wang, Y., Yutuc, E., Griffiths, W. J., Griffiths, W. J., & Wang, Y. (2021). Cholesterol metabolism pathways-are the intermediates more important than the products? *FEBS Journal*. https://doi.org/10.1111/febs.15727

Wei, J., Guo, Z., Zhang, P., Zhang, F., Yang, B., & Liang, X. (2012). A new reversed-phase/strong anion-exchange mixed-mode stationary phase based on polar-copolymerized approach and its application in the enrichment of aristolochic acids. *Journal of Chromatography A*, *1246*, 129–136. https://doi.org/10.1016/j.chroma.2012.03.047

Wei, Q., Wang, H., Tian, Y., Xu, F., Chen, X., & Wang, K. (2013). Reduced Serum Levels of Triglyceride, Very Low Density Lipoprotein Cholesterol and Apolipoprotein B in Parkinson's Disease Patients. *PLoS ONE*, *8*(9), e75743. https://doi.org/10.1371/journal.pone.0075743

Weingärtner, O., Laufs, U., Böhm, M., & Lütjohann, D. (2010). An alternative pathway of reverse cholesterol transport: The

oxysterol 27-hydroxycholesterol. *Atherosclerosis*, *209*(1), 39–41. https://doi.org/10.1016/j.atherosclerosis.2009.09.015

Wenk, G. L. (2003). *Neuropathologic Changes in Alzheimer's Disease*.

Whitfield, J. F. (2006). Can statins put the brakes on Alzheimer's disease? *Expert Opinion on Investigational Drugs*, *15*(12), 1479–1485. https://doi.org/10.1517/13543784.15.12.1479

Williams, E. T., Chen, X., & Moore, D. J. (2017). VPS35, the Retromer Complex and Parkinson's Disease. *Journal of Parkinson's Disease*, *7*(2), 219–233. https://doi.org/10.3233/JPD-161020

Willy, P. J., Umesono, K., Ong, E. S., Evans, R. M., Heyman, R. A., & Mangelsdorf, D. J. (1995). LXR, a nuclear receptor that defines a distinct retinoid response pathway. *Genes & Development*, *9*(9), 1033–1045. https://doi.org/10.1101/gad.9.9.1033

Winblad, B., Palmer, K., Kivipelto, M., Jelic, V., Fratiglioni, L., Wahlund, L.-O., Nordberg, A., Backman, L., Albert, M., Almkvist, O., Arai, H., Basun, H., Blennow, K., de Leon, M., DeCarli, C., Erkinjuntti, T., Giacobini, E., Graff, C., Hardy, J., … Petersen, R. C. (2004). Mild cognitive impairment - beyond controversies, towards a consensus: report of the International Working Group on Mild Cognitive Impairment. *Journal of Internal Medicine*, *256*(3), 240–246. https://doi.org/10.1111/j.1365-2796.2004.01380.x

Winslow, A. R., Chen, C.-W., Corrochano, S., Acevedo-Arozena, A., Gordon, D. E., Peden, A. A., Lichtenberg, M., Menzies, F. M., Ravikumar, B., Imarisio, S., Brown, S., O'Kane, C. J., & Rubinsztein, D. C. (2010). α-Synuclein impairs macroautophagy:

implications for Parkinson's disease. *Journal of Cell Biology*, *190*(6), 1023–1037. https://doi.org/10.1083/jcb.201003122

Wójcicka, G., Jamroz-Wiśniewska, A., Horoszewicz, K., & Bełtowski, J. (2007). Liver X receptors (LXRs). Part I: structure, function, regulation of activity, and role in lipid metabolism. *Postpy Higieny i Medycyny Doświadczalnej (Online)*, *61*, 736–759.

Wong, M. W., Braidy, N., Poljak, A., Pickford, R., Thambisetty, M., & Sachdev, P. S. (2017). Dysregulation of lipids in Alzheimer's disease and their role as potential biomarkers. In *Alzheimer's and Dementia*. https://doi.org/10.1016/j.jalz.2017.01.008

Woodward R. B., & Konrad Bloch. (1953). *THE CYCLIZATION OF SQUALENE IN CHOLESTEROL SYNTHESIS*. file:///C:/Users/manue/Downloads/ja01104a535.pdf

Xicoy, H., Wieringa, B., & Martens, G. J. M. (2019). The Role of Lipids in Parkinson's Disease. *Cells*, *8*(1), 27. https://doi.org/10.3390/cells8010027

Xilouri, M., Vogiatzi, T., Vekrellis, K., Park, D., & Stefanis, L. (2009a). Abberant α-Synuclein Confers Toxicity to NeuroneNeuronees in Part through Inhibition of Chaperone-Mediated Autophagy. *PLoS ONE*, *4*(5), e5515. https://doi.org/10.1371/journal.pone.0005515

Xilouri, M., Vogiatzi, T., Vekrellis, K., Park, D., & Stefanis, L. (2009b). Abberant α-Synuclein Confers Toxicity to NeuroneNeuronees in Part through Inhibition of Chaperone-Mediated Autophagy. *PLoS ONE*, *4*(5), e5515. https://doi.org/10.1371/journal.pone.0005515

Xiong, C., Yuan, J., Wang, Z., Wang, S., Yuan, C., & Wang, L. (2018). Preparation and evaluation of a hydrophilic interaction and cation-exchange chromatography stationary phase modified with 2-methacryloyloxyethyl phosphorylcholine. *Journal of Chromatography A*, *1546*, 56–65. https://doi.org/10.1016/j.chroma.2018.02.059

Xu, X., Song, Z., Mao, B., & Xu, G. (2022). Apolipoprotein A1-Related Proteins and Reverse Cholesterol Transport in Antiatherosclerosis Therapy: Recent Progress and Future Perspectives. *Cardiovascular Therapeutics*, *2022*, 1–9. https://doi.org/10.1155/2022/4610834

Xu, Y., Yuan, Y., Smith, L., Edom, R., Weng, N., Mamidi, R., Silva, J., Evans, D. C., & Lim, H.-K. (2013). LC–ESI-MS/MS quantification of 4β-hydroxycholesterol and cholesterol in plasma samples of limited volume. *Journal of Pharmaceutical and Biomedical Analysis*, *85*, 145–154. https://doi.org/10.1016/j.jpba.2013.07.016

Yajima, R., Tokutake, T., Koyama, A., Kasuga, K., Tezuka, T., Nishizawa, M., & Ikeuchi, T. (2015). ApoE-isoform-dependent cellular uptake of amyloid-β is mediated by lipoprotein receptor LR11/SorLA. *Biochemical and Biophysical Research Communications*, *456*(1), 482–488. https://doi.org/10.1016/j.bbrc.2014.11.111

Yamaguchi, S., Yamane, T., Takahashi-Niki, K., Kato, I., Niki, T., Goldberg, M. S., Shen, J., Ishimoto, K., Doi, T., Iguchi-Ariga, S. M. M., & Ariga, H. (2012). Transcriptional Activation of Low-Density Lipoprotein Receptor Gene by DJ-1 and Effect of DJ-1 on

Cholesterol Homeostasis. *PLoS ONE*, *7*(5), e38144. https://doi.org/10.1371/journal.pone.0038144

Yang, H., Yan, F., Wu, D., Huo, M., Li, J., Cao, Y., & Jiang, Y. (2010). Recovery of phytosterols from waste residue of soybean oil deodorizer distillate. *Bioresource Technology*, *101*(5), 1471–1476. https://doi.org/10.1016/j.biortech.2009.09.019

Yang, K., Cheng, H., Gross, R. W., & Han, X. (2009). Automated Lipid Identification and Quantification by Multidimensional Mass Spectrometry-Based Shotgun Lipidomics. *Analytical Chemistry*, *81*(11), 4356–4368. https://doi.org/10.1021/ac900241u

Yasuda, T., Grillot, D., Billheimer, J. T., Briand, F., Delerive, P., Huet, S., & Rader, D. J. (2010). Tissue-specific liver X receptor activation promotes macrophage reverse cholesterol transport in vivo. *Arteriosclerosis, Thrombosis, and Vascular Biology*, *30*(4), 781–786. https://doi.org/10.1161/ATVBAHA.109.195693

Yeagle, P. L. (1991). Modulation of membrane function by cholesterol. *Biochimie*. https://doi.org/10.1016/0300-9084(91)90093-G

Yutuc, E., Angelini, R., Baumert, M., Mast, N., Pikuleva, I., Newton, J., Clench, M. R., Skibinski, D. O. F., Howell, O. W., Wang, Y., & Griffiths, W. J. (2020). Localization of sterols and oxysterols in mouse brain reveals distinct spatial cholesterol metabolism. *Proceedings of the National Academy of Sciences*, *117*(11), 5749–5760. https://doi.org/10.1073/pnas.1917421117

Yutuc, E., Dickson, A. L., Pacciarini, M., Griffiths, L., Baker, P. R. S., Connell, L., Öhman, A., Forsgren, L., Trupp, M., Vilarinho, S., Khalil, Y., Clayton, P. T., Sari, S., Dalgic, B., Höflinger, P., Schöls, L., Griffiths, W. J., & Wang, Y. (2021). Deep mining of oxysterols and cholestenoic acids in human plasma and

cerebrospinal fluid: Quantification using isotope dilution mass spectrometry. *Analytica Chimica Acta*, *1154*, 338259. https://doi.org/10.1016/J.ACA.2021.338259

Zaikin, V. G., & Halket, J. M. (2003). Derivatization in Mass Spectrometry—2. Acylation. *European Journal of Mass Spectrometry*, *9*(5), 421–434. https://doi.org/10.1255/ejms.576

Zang, R., Case, J. B., Yutuc, E., Ma, X., Shen, S., Gomez Castro, M. F., Liu, Z., Zeng, Q., Zhao, H., Son, J., Rothlauf, P. W., Kreutzberger, A. J. B., Hou, G., Zhang, H., Bose, S., Wang, X., Vahey, M. D., Mani, K., Griffiths, W. J., … Ding, S. (2020). Cholesterol 25-hydroxylase suppresses SARS-CoV-2 replication by blocking membrane fusion. *Proceedings of the National Academy of Sciences*, *117*(50), 32105–32113. https://doi.org/10.1073/pnas.2012197117

Zein, A. A., Kaur, R., Hussein, T. O. K., Graf, G. A., & Lee, J.-Y. (2019). ABCG5/G8: a structural view to pathophysiology of the hepatobiliary cholesterol secretion. *Biochemical Society Transactions*, *47*(5), 1259–1268. https://doi.org/10.1042/BST20190130

Zelcer, N., Khanlou, N., Clare, R., Jiang, Q., Reed-Geaghan, E. G., Landreth, G. E., Vinters, H. V, & Tontonoz, P. (2007). Attenuation of neuroinflammation and Alzheimer's disease pathology by liver x receptors. *Proc Natl Acad Sci U S A*, *104*(25), 10601–10606. https://doi.org/0701096104 [pii]\n10.1073/pnas.0701096104

Zerbinati, C., & Iuliano, L. (2017). Cholesterol and related sterols autoxidation. *Free Radical Biology and Medicine*, *111*, 151–155. https://doi.org/10.1016/J.FREERADBIOMED.2017.04.013

Zhang, H., Cao, X., Liu, Y., & Shang, F. (2017). Rapid recovery of high content phytosterols from corn silk. *Chemistry Central Journal*, *11*(1), 108. https://doi.org/10.1186/s13065-017-0277-1

Zhang, J., & Liu, Q. (2015). Cholesterol metabolism and homeostasis in the brain. *Protein & Cell*, *6*(4), 254–264. https://doi.org/10.1007/s13238-014-0131-3

Zhang, J., Zhang, X., Wang, L., & Yang, C. (2017). High performance liquid chromatography-mass spectrometry (LC-MS) based quantitative lipidomics study of ganglioside-NANA-3 plasma to establish its association with Parkinson's disease patients. *Medical Science Monitor*. https://doi.org/10.12659/MSM.904399

Zhang, L., Rajbhandari, P., Priest, C., Sandhu, J., Wu, X., Temel, R., Castrillo, A., de Aguiar Vallim, T. Q., Sallam, T., & Tontonoz, P. (2017). Inhibition of cholesterol biosynthesis through RNF145-dependent ubiquitination of SCAP. *ELife*, *6*. https://doi.org/10.7554/eLife.28766

Zhang, R., Li, Q., Gao, Y., Li, J., Huang, Y., Song, C., Zhou, W., Ma, G., & Su, Z. (2014). Hydrophilic modification gigaporous resins with poly(ethylenimine) for high-throughput proteins ion-exchange chromatography. *Journal of Chromatography A*, *1343*, 109–118. https://doi.org/10.1016/j.chroma.2014.03.064

Zhao, J., Chen, J., Li, M., Chen, M., & Sun, C. (2020). Multifaceted Functions of CH25H and 25HC to Modulate the Lipid Metabolism, Immune Responses, and Broadly Antiviral Activities. In *Viruses* (Vol. 12, Issue 7). MDPI AG. https://doi.org/10.3390/v12070727

Zheng, B., Liao, Z., Locascio, J. J., Lesniak, K. A., Roderick, S. S., Watt, M. L., Eklund, A. C., Zhang-James, Y., Kim, P. D., Hauser,

M. A., Grünblatt, E., Moran, L. B., Mandel, S. A., Riederer, P., Miller, R. M., Federoff, H. J., Wüllner, U., Papapetropoulos, S., Youdim, M. B., … Scherzer, C. R. (2010). *PGC-1* α, A Potential Therapeutic Target for Early Intervention in Parkinson's Disease. *Science Translational Medicine*, *2*(52). https://doi.org/10.1126/scitranslmed.3001059

Zhou, Q. D., Chi, X., Lee, M. S., Hsieh, W. Y., Mkrtchyan, J. J., Feng, A.-C., He, C., York, A. G., Bui, V. L., Kronenberger, E. B., Ferrari, A., Xiao, X., Daly, A. E., Tarling, E. J., Damoiseaux, R., Scumpia, P. O., Smale, S. T., Williams, K. J., Tontonoz, P., & Bensinger, S. J. (2020). Interferon-mediated reprogramming of membrane cholesterol to evade bacterial toxins. *Nature Immunology*, *21*(7), 746–755. https://doi.org/10.1038/s41590-020-0695-4

Zielinski, Z. A. M., & Pratt, D. A. (2016). Cholesterol Autoxidation Revisited: Debunking the Dogma Associated with the Most Vilified of Lipids. *Journal of the American Chemical Society*, *138*(22), 6932–6935. https://doi.org/10.1021/jacs.6b03344

Zimprich, A., Benet-Pagès, A., Struhal, W., Graf, E., Eck, S. H., Offman, M. N., Haubenberger, D., Spielberger, S., Schulte, E. C., Lichtner, P., Rossle, S. C., Klopp, N., Wolf, E., Seppi, K., Pirker, W., Presslauer, S., Mollenhauer, B., Katzenschlager, R., Foki, T., … Strom, T. M. (2011). A Mutation in VPS35, Encoding a Subunit of the Retromer Complex, Causes Late-Onset Parkinson Disease. *The American Journal of Human Genetics*, *89*(1), 168–175. https://doi.org/10.1016/j.ajhg.2011.06.008

Zmysłowski, A., & Szterk, A. (2019). Oxysterols as a biomarker in diseases. In *Clinica Chimica Acta*. https://doi.org/10.1016/j.cca.2019.01.022

Zubarev, R. A., & Makarov, A. (2013). Orbitrap Mass Spectrometry. *Analytical Chemistry*, *85*(11), 5288–5296. https://doi.org/10.1021/ac4001223